

ON FOUR-DIMENSIONAL 2-HANDLEBODIES AND THREE-MANIFOLDS

I. BOBTCHEVA

*Dipartimento di Scienze Matematiche
Università Politecnica delle Marche – Italia*

`bobtchev@dipmat.univpm.it`

R. PIERGALLINI

*Scuola di Scienze e Tecnologie
Università di Camerino – Italia*

`riccardo.piergallini@unicam.it`

Abstract

We show that for any $n \geq 4$ there exists an equivalence functor $\mathcal{S}_n^c \rightarrow Chb^{3+1}$ from the category \mathcal{S}_n^c of n -fold connected simple coverings of $B^3 \times [0, 1]$ branched over ribbon surface tangles up to certain local ribbon moves, and the cobordism category Chb^{3+1} of orientable relative 4-dimensional 2-handlebody cobordisms up to 2-deformations.

As a consequence, we obtain an equivalence theorem for simple coverings of S^3 branched over links, which provides a complete solution to the long-standing Fox-Montesinos covering moves problem. This last result generalizes to coverings of any degree results by the second author and Apostolakis, concerning respectively the case of degree 3 and 4. We also provide an extension of the equivalence theorem to possibly non-simple coverings of S^3 branched over embedded graphs.

Then, we factor the functor above as $\mathcal{S}_n^c \rightarrow \mathcal{H}^r \rightarrow Chb^{3+1}$, where $\mathcal{S}_n^c \rightarrow \mathcal{H}^r$ is an equivalence functor to a universal braided category \mathcal{H}^r freely generated by a Hopf algebra object H . In this way, we get a complete algebraic description of the category Chb^{3+1} . From this we derive an analogous description of the category \widetilde{Cob}^{2+1} of 2-framed relative 3-dimensional cobordisms, which resolves a problem posed by Kerler.

Keywords: 3-manifold, 4-manifold, handlebody, branched covering, ribbon surface, Kirby calculus, braided Hopf algebra, quantum invariant.

AMS Classification: 57M12, 57M27, 57N13, 57R56, 57R65, 16W30, 17B37, 18D35.

Contents

Introduction	3
1. Preliminaries	8
1.1. Links and diagrams	8
1.2. Handlebodies	10
1.3. Ribbon surfaces	15
1.4. Branched coverings	26
1.5. Categories	32
2. 4-dimensional cobordisms and Kirby tangles	36
2.1. The categories of relative handlebody cobordisms Chb_n^{3+1}	36
2.2. Bridged tangles and labeled Kirby tangles	40
2.3. The categories \mathcal{K}_n and the functors \uparrow_k^n and \downarrow_k^n	52
3. Labeled ribbon surface tangles	64
3.1. The category \mathcal{S} of ribbon surface tangles	64
3.2. The categories \mathcal{S}_n and the functors \uparrow_k^n	71
3.3. The functors $\Theta_n : \mathcal{S}_n \rightarrow \mathcal{K}_n$	80
3.4. Fullness of $\Theta_n : \mathcal{S}_n^c \rightarrow \mathcal{K}_n^c$ for $n \geq 3$	90
3.5. The functor $\Xi_n : \mathcal{K}_1 \rightarrow \mathcal{S}_n^c$ for $n \geq 4$	98
3.6. Equivalence between \mathcal{K}_n^c and \mathcal{S}_n^c for $n \geq 4$	111
4. Universal groupoid ribbon Hopf algebra	120
4.1. The universal groupoid Hopf algebras $\mathcal{H}(\mathcal{G})$ and $\mathcal{H}^u(\mathcal{G})$	121
4.2. The universal groupoid ribbon Hopf algebra $\mathcal{H}^r(\mathcal{G})$	131
4.3. The functors $\Phi_n : \mathcal{H}_n^r \rightarrow \mathcal{K}_n$	143
4.4. The adjoint morphisms	146
4.5. The stabilization and reduction functors \uparrow_X and \downarrow_X	165
4.6. The functors $\Psi_n : \mathcal{S}_n \rightarrow \mathcal{H}_n^r$	169
4.7. Equivalence between \mathcal{K}_n^c and $\mathcal{H}_n^{r,c}$	177
5. 3-dimensional cobordisms as boundaries	187
5.1. The categories of relative cobordisms \widetilde{Cob}_n^{2+1} and Cob_n^{2+1}	187
5.2. The quotient categories $\bar{\mathcal{K}}_n, \bar{\bar{\mathcal{K}}}_n, \bar{\mathcal{S}}_n$ and $\bar{\bar{\mathcal{S}}}_n$	188
5.3. Equivalences $\bar{\mathcal{K}}_n^c \cong \bar{\mathcal{S}}_n^c$ and $\bar{\bar{\mathcal{K}}}_n^c \cong \bar{\bar{\mathcal{S}}}_n^c$ for $n \geq 4$	191
5.4. The quotient categories $\bar{\mathcal{H}}_n$ and $\bar{\bar{\mathcal{H}}}_n$	193
5.5. Equivalences $\bar{\mathcal{K}}_n^c \cong \bar{\mathcal{H}}_n^{r,c}$ and $\bar{\bar{\mathcal{K}}}_n^c \cong \bar{\bar{\mathcal{H}}}_n^{r,c}$	196
6. Branched coverings of B^4 and S^3	199
6.1. Covers of B^4 simply branched over ribbon surfaces	199
6.2. Equivalence of branched covers of S^3	206
References	210

Introduction

The present work is based on the preprints [12] and [13] and extends their main results from closed manifolds to the category of cobordisms. In particular, it is the synthesis of years-long search for the answers to the following distinct problems in the topology of 3-manifolds:

PROBLEM A. *Find a finite set of local moves that relate any two labeled links representing the same 3-manifold as a simple branched covering of S^3 .*

PROBLEM B. *Find a universal monoidal braided category freely generated by a Hopf algebra object, which is equivalent to the category $\widetilde{\text{Cob}}^{2+1}$ of 2-framed relative 3-dimensional cobordisms.*

Problem A is an old one, having been formulated by Fox and Montesinos in the seventies. It naturally arose in relation to the Hilden-Hirsch-Montesinos theorem [29, 31, 49], which states that any closed connected oriented 3-manifold can be realized as a 3-fold covering of S^3 branched over a link (actually a knot). Such a covering can be described in terms of its branching link, with each arc labeled by the monodromy of the corresponding meridian (a transposition in the symmetric group Σ_n). Hence, Problem A just expresses the equivalence problem for branched covers in terms of moves for labeled links, usually called covering moves.

In [56], Montesinos conjectured that the two covering moves (M1) and (M2) in Figure 6.2.2 suffice to relate 3-fold simple coverings of S^3 representing the same 3-manifold, up to 4-fold stabilization. This was proved to be true by the second author in [61, 62], where the question was also posed, whether these local moves together with stabilization also suffice for simple coverings of arbitrary degree. In [4] Apostolakis answered this question in the positive for 4-fold coverings, up to 5-fold stabilization.

The complete solution of Problem A is given by Theorem 6.2.3, asserting that labeled isotopy and Montesinos moves suffice to relate any two n -fold branched covering representations of the same 3-manifold, provided that $n \geq 4$. The proof is independent on all the above-mentioned partial results, being based on the branched covering interpretation of the generalized Kirby calculus developed in Chapter 3 and Section 5.3.

We note that this result and its proof were already contained in the preprint [12] (see below for some already published applications). However, the exposition in the present work is adapted to the category of cobordisms, as a preliminary result for answering Problem B.

Problem B was risen by Kerler in [35] (cf. [60, Problem 8-16 (1)]). In that paper, the author considers a universal monoidal braided category \mathcal{Alg} , freely generated by a Hopf algebra object and a full (surjective) functor $\mathcal{Alg} \rightarrow \widetilde{\text{Cob}}^{2+1}$. Moreover, he poses the challenge to find a set of additional relations for \mathcal{Alg} , such that the above functor induces a category equivalence on the quotient of \mathcal{Alg} by the new relations.

This problem is related to the origin of the $(2 + 1)$ -dimensional TQFT's (Topological Quantum Field Theories). We remind that any such theory is a functor from $\widetilde{\text{Cob}}^{2+1}$ to the category of vector spaces Vec_k over a field k . The first constructions of TQFT's were based on semisimple quotients of the representation spaces of quasi-triangular ribbon Hopf algebras (see [65]). Such approach was generalized in [36],

where a TQFT was associated to any modular category with a special braided Hopf algebra in it. The solution to Problem B implies that any TQFT's lives on the representation space of a braided Hopf algebra. Of course, the braided Hopf algebra axioms alone are too weak. Indeed, in the definition of \mathcal{Alg} , Kerler adds the requirement that there exist a ribbon element and a non-degenerate Hopf copairing morphisms, satisfying some extra axioms.

Here, we prove that in order to have that the quotient algebraic category is equivalent to $\widetilde{\mathcal{Cob}}^{2+1}$, two more axioms suffice in addition to the ones presented by Kerler in [35] (cf. Theorem 5.5.4). The first one describes the propagation of the ribbon element through the comultiplication morphism, while the second one relates the copairing and the braiding morphisms. We call the resulting quotient algebra *the universal self-dual ribbon Hopf algebra* and denoted it by $\overline{\mathcal{H}}^r$. The complete list of its relations, including the ones of Kerler, is presented in Tables 4.7.13 and 5.5.3. We note that the algebra $\overline{\mathcal{H}}^r$ (with all its relations) was already defined in the preprint [13]. Moreover, it was shown there that the functor $\overline{\mathcal{H}}^r \rightarrow \widetilde{\mathcal{Cob}}^{2+1}$ induces a bijective map on the closed morphisms. So, the only new point in the present work is the generalization of this result to all morphisms, completing in this way the answer to Problem B.

As it should be clear from the discussion above, Problems A and B originate from different contexts and at first glance they seem quite distant. Yet, an indication that they may be related comes from the very reason for which they are posed. Their solution leads in both cases to a complete diagrammatic language for describing the concerned topological objects. Such languages are respectively based on planar diagrams of links labeled by transpositions in Σ_n , and on planar diagrams of certain decorated uni- and tri-valent graphs describing morphisms in the corresponding Hopf algebra. Both kinds of diagrams are taken modulo a finite set of local moves, i.e. moves which only change a given portion of the diagram inside a disk in a way independent on its outside. The fact that the equivalence moves are finite in number and local in nature, is an important feature in view of the definition of invariants.

Of course, the reason for putting the two results together in the present work is not the philosophical similarity in the statements, but the fact that the proofs are intrinsically related. In both cases, we go up one dimension and discuss the following problems on the cobordism category \mathcal{Chb}^{3+1} of relative 4-dimensional 2-handlebodies up to 2-deformations (handle slidings and creation/cancelation of 1/2-handle pairs).

PROBLEM A'. *Find a finite set of local moves which relate any two labeled ribbon surface tangles representing the same cobordism in \mathcal{Chb}^{3+1} as a simple branched covering of $B^3 \times [0, 1]$.*

PROBLEM B'. *Find a universal monoidal braided category freely generated by a Hopf algebra object, which is equivalent to the cobordisms category \mathcal{Chb}^{3+1} .*

Any cobordism in $\widetilde{\mathcal{Cob}}^{2+1}$ represents the framed boundary of one in \mathcal{Chb}^{3+1} . Moreover, $\widetilde{\mathcal{Cob}}^{2+1}$ is equivalent to the quotient of \mathcal{Chb}^{3+1} modulo 1/2-handle tradings. This allows us to derive the solutions of Problems A and B from those of Problems A' and B' respectively.

If we think of the handlebodies in \mathcal{Chb}^{3+1} as build on a single 0-handle, a standard way of describing them is through Kirby tangles, representing the attaching maps of

the corresponding 1- and 2-handles in the boundary of the 0-handle. Such tangles, modulo isotopy and 1/2-handle moves, form a category \mathcal{K} equivalent to \mathcal{Chb}^{3+1} .

Even if our goal is the description of the morphisms in \mathcal{Chb}^{3+1} , as an intermediate step we will need to work with the category of relative 4-dimensional 2-handlebodies build on n 0-handles. In Section 2.3, we introduce the corresponding category \mathcal{K}_n of generalized admissible Kirby tangles, which describes such handlebodies through the attaching maps of their handles in the boundaries of the n 0-handles. Clearly, \mathcal{K}_n with $n > 1$ is much “bigger” than $\mathcal{K} = \mathcal{K}_1$, but for any $n > k \geq 1$ there exists an injective stabilization functor $\uparrow_k^n : \mathcal{K}_k \rightarrow \mathcal{K}_n$, essentially given by adding canceling pairs of 0/1-handles. The restriction of this functor to the subcategories $\mathcal{K}_k^c \subset \mathcal{K}_k$ and $\mathcal{K}_n^c \subset \mathcal{K}_n$ of “connected” cobordisms is invertible, i.e. there exists a reduction functor $\downarrow_k^n : \mathcal{K}_n^c \rightarrow \mathcal{K}_k^c$ such that $\downarrow_k^n \circ \uparrow_k^n = \text{id}$, while $\uparrow_k^n \circ \downarrow_k^n \simeq \text{id}$ up to natural transformation. In particular, for any $n \geq 2$, the category \mathcal{K}_n^c is equivalent to $\mathcal{K}_1^c = \mathcal{K}_1$.

The reason for considering 4-dimensional 2-handlebodies build on n 0-handles is that they naturally occur when representing handlebodies in \mathcal{Chb}^{3+1} as simple n -fold ($n \geq 2$) coverings of $B^3 \times [0, 1]$ branched over ribbon surfaces. In fact, we will use such branched covering representation of handlebodies in \mathcal{Chb}^{3+1} to solve problems A' and B', according to the following scheme.

In Chapter 3, we construct the category \mathcal{S}_n of ribbon surface tangles, labeled in the symmetric group Σ_n , up to certain labeled isotopy moves, called 1-isotopy moves, and two covering moves. Analogously to \mathcal{K}_n such category describes possibly disconnected cobordisms. Indeed, there is a naturally defined functor $\Theta_n : \mathcal{S}_n \rightarrow \mathcal{K}_n$. Then, we consider the subcategory $\mathcal{S}_n^c \subset \mathcal{S}_n$ which describes connected cobordisms through the restriction $\Theta_n : \mathcal{S}_n^c \rightarrow \mathcal{K}_n^c$. Finally, we define a functor $\Xi_n : \mathcal{K}_1 \rightarrow \mathcal{S}_n^c$ for $n \geq 4$, and show that $\downarrow_1^n \circ \Theta_n$ and Ξ_n are inverse to each other up to natural equivalences. Therefore, we have the following diagram of category equivalences, which solves Problem A'.

$$\begin{array}{ccc}
 \mathcal{S}_n^c & \xleftarrow{\Xi_n} & \mathcal{K}_1 \\
 \Theta_n \searrow & & \nearrow \downarrow_1^n \\
 & \mathcal{K}_n^c &
 \end{array}$$

As a consequence, Theorem 6.1.5 provides local moves (see Figures 6.1.8 and 6.1.9) to relate any two labeled ribbon surfaces representing the same connected oriented 4-dimensional 2-handlebody (up to 2-equivalence) as n -fold simple covering of B^4 , for $n \geq 4$. Based on this result and passing to suitable quotient categories representing the boundary, we obtain the above-mentioned answer to Problem A.

In order to answer Question B, in Chapter 4 we introduce the algebraic analog of the category \mathcal{K}_n , which is the universal ribbon \mathcal{G}_n -Hopf algebra \mathcal{H}_n^r . Here \mathcal{G}_n is the groupoid with the numbers $1, \dots, n$ as the objects and with a unique morphism for each ordered pair of objects. In particular, we define a functor $\Phi_n : \mathcal{H}_n^r \rightarrow \mathcal{K}_n$, which is the analog of Kerler's functor $\mathcal{Alg} \rightarrow \widetilde{\mathcal{Cob}}^{2+1}$ in the context of relative 4-dimensional 2-handlebodies build on multiple 0-handles. Analogously to \mathcal{K}_n , for any $n > k \geq 1$ there exist a stabilization functor $\uparrow_k^n : \mathcal{H}_k^r \rightarrow \mathcal{H}_n^r$, which is invertible (up

to natural transformations) on a subcategory $\mathcal{H}_n^{r,c}$, through the reduction functor $\downarrow_k^n : \mathcal{H}_n^{r,c} \rightarrow \mathcal{H}_k^{r,c}$. In particular, for any $n \geq 2$, the category $\mathcal{H}_n^{r,c}$ is equivalent to $\mathcal{H}_1^{r,c} = \mathcal{H}_1^r$. Moreover, for any $n > k \geq 1$ we have that $\downarrow_k^n \circ \Phi_n = \Phi_k \circ \downarrow_k^n : \mathcal{H}_n^r \rightarrow \mathcal{K}_k$.

Our goal is to show that $\Phi_1 : \mathcal{H}^r \rightarrow \mathcal{K}$ is a category equivalence. We prove this by factoring the functor $\Theta_n : \mathcal{S}_n \rightarrow \mathcal{K}_n$ as $\Phi_n \circ \Psi_n$ with $\Psi_n : \mathcal{S}_n \rightarrow \mathcal{H}_n^{r,c}$, and showing that for any $n \geq 4$ the restriction $\Psi_n : \mathcal{S}_n^c \rightarrow \mathcal{H}_n^{r,c}$ is a category equivalence. This fact and the commutative diagram below imply that the same is true for $\Phi_k : \mathcal{H}_k^{r,c} \rightarrow \mathcal{K}_k^c$ for any $k \geq 1$.

$$\begin{array}{ccccc}
 \mathcal{S}_n^c & \xrightarrow{\Theta_n} & \mathcal{K}_n^c & \xrightarrow{\downarrow_k^n} & \mathcal{K}_k^c \\
 & \searrow \Psi_n & \nearrow \Phi_n & & \nearrow \Phi_k \\
 & & \mathcal{H}_n^{r,c} & \xrightarrow{\quad} & \mathcal{H}_k^{r,c} \\
 & & & \searrow \downarrow_k^n &
 \end{array}$$

In this way, we get a completely algebraic description of the category Chb^{3+1} of connected 4-dimensional 2-handlebodies up to 2-equivalence, as the universal ribbon category $\mathcal{H}^r = \mathcal{H}_1^r$ (cf. Theorem 3.6.4). This solves Problem B'. Then, the answer to Problem B is obtained in Section 5.5, by passing once again to suitable quotient categories \widetilde{Cob}^{2+1} and $\overline{\mathcal{H}}^r$.

We would like to make few comments about applications of the present work.

- a) The solution of Problem A, i.e. the description of 3-dimensional manifolds in terms of labeled links modulo isotopy and covering moves, has already been applied in [27] and [59] to the construction of invariants of 3-manifolds, and in [17] to the construction of convolution algebras of spin networks and spin foams.
- b) The branched covering representation of 4-dimensional 2-handlebodies provided by Theorem 6.1.5 is used in [5], to relate the monodromy descriptions of any two topological Lefschetz fibrations over the disk having 2-equivalent total spaces.
- c) The notion of 2-deformation of 4-dimensional 2-handlebodies is conjectured to be different from the one of diffeomorphism, which in this context is equivalent to 3-deformation (cf. [21, 64] and Section 1.2). The solution of Problem B' associates to any braided ribbon Hopf algebra an invariant of 4-dimensional 2-handlebodies under 2-deformations and implies that, if the conjecture is true, there should exist a braided ribbon Hopf algebra whose invariant distinguishes diffeomorphic but not 2-equivalent handlebodies. The search for such Hopf algebras is a non-trivial challenge, since they have to combine the properties of being unimodular, not self-dual and not semisimple (see the discussion in [11] about the the HKR-type invariants associated to an ordinary ribbon Hopf algebra).
- d) By restricting the map $\downarrow_1^2 \circ \Psi_2$ to double branched covers of B^4 , i.e. to ribbon surfaces labeled with the single permutation $(1\ 2)$, one obtains an invariant of ribbon surfaces under 1-isotopy moves, taking values in \mathcal{H}^r . We remind that the description of all the moves relating isotopic ribbon surfaces is still an open question. We conjecture here (see Remark 6.1.7) that 1-isotopy is weaker than isotopy and that braided ribbon Hopf algebras should detect such a difference.

e) In Chapter 4 we introduce and study the general concept of a groupoid ribbon Hopf algebra, even if it is being used later only in the case of the specific and very simple groupoid \mathcal{G}_n . The reasons for doing this are two. The first one is that working with the general case does not make heavier the algebraic part, actually it makes it easier to follow. The second one is that, in our believe, the group ribbon Hopf algebra (which is another particular case of the construction) should be useful in finding an algebraic description of other types of topological objects, for example the group manifolds studied in [73].

As we already said, the present work is based on the preprints [12] and [13]. The editor suggested to put them together in a single monograph. Moreover, the referee of [13] observed that it should not be too difficult to extend the result there to cobordisms. Indeed, we have been able to achieve such extension by following the main line of the proof in [13] and overcoming some technical obstacles in the definition of the natural transformations. Following the indications of the referee, we have also expanded Section 2 with the definition of the topological category and tried to improve the exposition of the algebraic part. In particular, we have added Section 4.4, where we describe the properties of the adjoint morphisms and express the two new axioms for \mathcal{H}^r in terms of such action. This allows to simplify the proofs in Section 4.5, even if they still remain highly technical.

1. Preliminaries

In this chapter we collect some preliminary definitions and results. Some are known and we just recall them in order to establish terminology and notations. Some others are new and we include them here rather than in a specific chapter, since they are widely used in the following or they seem to have interest in their own right, independently from their application in the present context.

In particular: in Section 1.1 we define the notion of vertically trivial state for a link diagram and prove an elementary property of such states, that makes them much more manageable than arbitrary trivial states; in Section 1.2 we briefly discuss relative handlebodies build on a manifold with boundary; in Section 1.3 we define the 1-isotopy relation for ribbon surfaces and express it in terms of certain moves of planar diagrams; in Section 1.4 we introduce ribbon moves for labeled ribbon surfaces representing simple branched coverings of B^4 .

1.1. Links and diagrams

As usual, we represent a link $L \subset R^3 \subset R^3 \cup \infty \cong S^3$ by a planar *diagram* $D \subset R^2$, consisting of the orthogonal projection of L into R^2 , that can be assumed self-transversal after a suitable horizontal (height preserving) isotopy of L , with a *crossing state* for each double point, telling which arc passes over the other one. Such a diagram D uniquely determines L up to vertical isotopy. On the other hand, link isotopy can be represented in terms of diagrams by crossing preserving isotopy in R^2 and Reidemeister moves.

A link L is called *trivial* if it bounds a disjoint union of disks in R^3 . It is well-known that any link diagram D can be transformed into a diagram D' of a trivial link by suitable crossing changes, that is by inverting the state of some of its crossings. We say that D' is a *trivial state* of D . Actually, any non-trivial link diagram D has many trivial states, but it is not clear at all how they are related to each other. For this reason, we are lead to introduce the more restrictive notions of vertically trivial link and vertically trivial state of a link diagram.

DEFINITION 1.1.1. We say that a link $L \subset R^3$ is *vertically trivial* if it meets any horizontal plane (parallel to R^2) in at most two points belonging to the same component.

If L is a vertically trivial link, then the height function separates the components of L (that is the height intervals of different components are disjoint), so that we can vertically order the components of L according to their height. Moreover, each component can be split into two arcs on which the height function is monotone, assuming the only unique minimum and maximum values at the common endpoints. Then, all the (possibly degenerate) horizontal segments spanned by L in R^3 form a disjoint union of disks bounded by L . This proves that L is a trivial link.

DEFINITION 1.1.2. By a *vertically trivial state* of a link diagram $D \subset R^2$ we mean any trivial state of D which is the diagram of a vertically trivial link.

A vertically trivial state D' of D can be constructed by the usual naive unlinking procedure: 1) number the components of the link L represented by D and fix on each component an orientation and a starting point away from crossings; 2) order

the points of L lexicographically according to the numbering of the components and then to the starting point and the orientation of each component; 3) resolve each double point of D into a crossings of D' by letting the arc which comes first in the order pass under the other one. The link L' represented by D' can be clearly assumed to be vertically trivial, considering on it a height function which preserves the order induced by the vertical bijection with L except for a small arc at the end of each component. Figure 1.1.1 (a) shows how the height function of a component looks like with respect to a parametrization having the starting point and the orientation fixed above. Keeping the parametrization fixed but changing the starting point or the orientation we get different height functions as in Figures 1.1.1 (b) and (c) respectively.

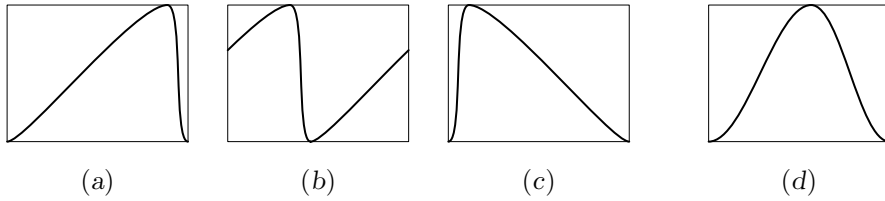


FIGURE 1.1.1. Height functions for vertically trivial knots

Notice that the above unlinking procedure gives us only very special vertically trivial states. While it is clear how to pass from (a) to (b), by moving the starting point along the component, going from (a) to (c) turns out to be quite mysterious without considering generic vertically trivial states. The height function of a component for such a state, with respect to a parametrization starting from the unique minimum point, looks like in Figure 1.1.1 (d), that is apparently an intermediate state between (a) and (c). The following proposition settles the problem of relating different vertically trivial states of the same link diagram.

PROPOSITION 1.1.3. *Any two vertically trivial states D' and D'' of a link diagram D are related by a sequence D_0, D_1, \dots, D_n of vertically trivial states of D , such that $D_0 = D'$, $D_n = D''$ and, for each $i = 1, \dots, n$, D_i is obtained from D_{i-1} by changing all the crossings between two vertically adjacent components or by changing a single self-crossing of one component. Moreover, in the latter case the singular link between D_{i-1} and D_i is trivial, meaning that the unique singular component of it spans a 1-point union of two disks disjoint from all the other components.*

Proof. Since the effect of changing all the crossings between two vertically adjacent components is the transposition of these components in the vertical order, by iterating this kind of modification we can permute as we want the vertical order of all the components. Hence, we only need to address the case of a knot diagram.

Given a knot diagram $D \subset R^2$ with double points $x_1, \dots, x_n \in R^2$, we consider a parametrization $f : S^1 \rightarrow D$ and denote by $t'_i, t''_i \in S^1$ the two values of the parameter such that $f(t'_i) = f(t''_i) = x_i$, for any $i = 1, \dots, n$.

For any smooth knot $K \subset R^3$ which projects to a vertically trivial state of D , let $f_K : S^1 \rightarrow R^3$ be the parametrization of K obtained by lifting f and $h_K : S^1 \rightarrow R$ be the composition of f_K with the height function. Then, h_K is a smooth function with the following properties: 1) h_K has only one minimum and one maximum; 2) $h_K(t'_i) \neq h_K(t''_i)$, for any $i = 1, \dots, n$. In this way, the space of all smooth knots

which project to vertically trivial states of D can be identified with the space of all smooth functions $h : S^1 \rightarrow R$ satisfying properties 1 and 2.

Now, the space \mathcal{S} of all smooth functions $h : S^1 \rightarrow R$ satisfying property 1 is clearly pathwise connected, while the complement $\mathcal{C} \subset \mathcal{S}$ of property 2 is a closed codimension 1 stratified subspace. Therefore, if K' and K'' are knots projecting to the vertically trivial states D' and D'' , then we can join $h_{K'}$ and $h_{K''}$ by a path in \mathcal{S} transversal with respect to \mathcal{C} . This, path gives rise to a finite sequence of self-crossing changes as in the statement, one for each transversal intersection with \mathcal{C} .

The second part of the proposition, follows from [69, Theorem 1.4] but can also be immediately realized by considering the union of all the (possibly degenerate) horizontal segments spanned by the singular component. \square

We emphasize that the property of vertically trivial states given by Proposition 1.1.3 will play a crucial role in the proof of Lemma 3.5.1, and it is far from being shared by all trivial states. For example, Figure 1.1.2 shows a (non-vertically) trivial knot diagram, that is made knotted by any crossing change performed on it.

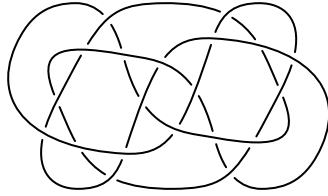


FIGURE 1.1.2.

1.2. Handlebodies

In this section we review some basic definitions and facts about handlebodies, referring to [22] for a detailed discussion of the subject. Our aim here is only to extend the standard general set up given in [22] to the notion of relative handlebody build on a bounded manifold.

Given $0 \leq i \leq d$, a d -dimensional i -handle (or handle of index i) is a copy H^i of $B^i \times B^{d-i}$ attached to a smooth d -manifold W by a smooth embedding $\varphi : S^{i-1} \times B^{d-i} \rightarrow \text{Bd } W$. The map φ and its image $\varphi(S^{i-1} \times B^{d-i}) \subset \text{Bd } W$ are called respectively the *attaching map* and the *attaching region* of H^i .

The two balls $B^i \times \{0\}$ and $\{0\} \times B^{d-i}$ are called respectively the *core* and the *cocore* of H^i , while their boundaries $S^{i-1} \times \{0\}$ and $\{0\} \times S^{d-i-1}$ are called the *attaching sphere* and the *belt sphere* of H^i (this terminology refers to the corresponding subspaces of $W \cup_{\varphi} H^i$ as well). Inside H^i , *longitudinal* means parallel to the core and *transversal* means parallel to the cocore.

By smoothing the corners in a canonical way, $W \cup_{\varphi} H^i$ becomes a smooth d -manifold, which only depends on the isotopy class of the attaching map φ .

We work only with 0- and 1-handles in dimension $d \leq 4$ and with 2-handles in dimension $d = 4$. So, let us have a closer look at these kinds of handles.

The 0-handles are topologically trivial. In fact, attaching a 0-handle H^0 to W is the same as taking the disjoint union $W \sqcup H^0 \cong W \sqcup B^d$.

For a 1-handle H^1 , the attaching map $\varphi : S^0 \times B^d \cong B^d \sqcup B^d \rightarrow \text{Bd} W$, is uniquely determined up to isotopy by the (possibly coinciding) components of $\text{Bd} W$ where the two $(d-1)$ -balls forming the attaching region are located and by the orientations induced by φ on such attaching balls. By reversing the handle H^1 those balls can be interchanged, hence only an unordered pair of components of $\text{Bd} W$ needs to be specified when describing H^1 . Concerning the orientations of the attaching balls, the only relevant information is whether they coincide or not, when the balls are in the same component of $\text{Bd} W$ and this is orientable. If W is orientable, the difference between the two possibilities results in the orientability or non-orientability of $W \cup_{\varphi} H^1$. In dimension 3 and 4 we always assume that W and $W \cup_{\varphi} H^1$ are orientable, which implies that there is essentially only one way to attach H^1 to W for a given pair of components of $\text{Bd} W$.

The case of a 2-handle attached to a 4-manifold W requires some more work. In this case the attaching sphere is a knot $K = \varphi(S^1 \times \{0\})$ in $\text{Bd} W$. Up to reversing the handle H^2 the orientation of K is not relevant. Then H^2 is uniquely determined by the isotopy class of the unoriented knot $K \subset \text{Bd} W$ and by the choice of a framing along K , that means an isotopy class of trivializations of the normal disk bundle νK of K in $\text{Bd} W$. Since we always assume W to be orientable, actually K can be any knot in $\text{Bd} W$. Moreover, the set of all possible framings along K bijectively corresponds to $\pi_1(\text{SO}(2)) \cong \mathbb{Z}$. Unfortunately, unless K is null-homologous in $\text{Bd} W$, there is no canonical way of fixing the zero framing, so in general an explicit description for the framing is needed. This can be given in terms of framed knots in the sense of the following definition.

DEFINITION 1.2.1. Let M be a possibly bounded 3-manifold and $C \subset M$ be regularly embedded smooth curve. Then, a *framed curve* based on C is an embedded smooth band $B \subset M$ with an identification $B \cong C \times [0, 1]$, such that $C \times \{0\}$ coincides with the *base curve* C , $\text{Bd} C \times [0, 1]$ corresponds to $B \cap \text{Bd} M$, while the regularly embedded smooth curve $C_{\text{fr}} \subset M$ corresponding to $C \times \{1\}$ is the *framing curve* which represents the framing along C . In particular, if C is a knot (resp. a link) in $\text{Int} M$ then we call the framed curve a *framed knot* (resp. a *framed link*).

Therefore, to specify a 2-handle attached to a 4-manifold W along a knot $C \subset \text{Bd} W$ with attaching map $\varphi : S^1 \times B^2 \rightarrow \text{Bd} W$, we can use a framed knot based on C by letting the band B in the definition above to be $\varphi(S^1 \times [0, p])$ for an arbitrary point $p \in B^2 - \{0\}$. If C is null-homologous in $\text{Bd} W$, then the framing is determined by the *framing number* $\text{fr}(C) = \text{lk}(C, C_{\text{fr}}) \in \mathbb{Z}$ for C and C_{fr} coherently oriented.

DEFINITION 1.2.2. Let M be a compact smooth $(d-1)$ -manifold with (possibly empty) boundary and let $k \leq d$. A *d-dimensional relative k-handlebody* build on M is a smooth d -manifold W with a given filtration $M \times [0, 1] = W^{-1} \subset W^0 \subset W^1 \subset \dots \subset W^k = W$ of smooth d -submanifolds, such that $W^i = W^{i-1} \cup_{j=1}^{n_i} H_j^i$ is obtained by attaching n_i disjoint i -handles to W^{i-1} , with attaching regions contained in δW^{i-1} , where $\delta W^i = \text{Bd} W^i - (M \times \{0\} \cup \text{Bd} M \times [0, 1])$ for any $0 \leq i \leq k$.

By identifying M with $M \times \{0\} \subset W$, we think of it as a smooth submanifold of $\text{Bd} W$ of dimension $d-1$. Then, the given family of handles forming W starting from $M \times [0, 1]$ is called a *relative k-handlebody decomposition* of the pair (W, M) .

When M is empty, we simply say that W is a *k-handlebody* and call the given family of handles a *k-handlebody decomposition* of W .

We remark that in the usual definition of relative handlebody (cf. Definition 4.2.1 in [22]) the manifold M is taken to be closed. Yet, the cobordisms which we study here are relative handlebodies build on 3-manifolds with boundary, so we need this generalization.

By a well-known result of Cerf [16] (cf. Theorem 4.2.12 in [22], for the case when $\text{Bd } M = \emptyset$), two handlebody decompositions of the same pair (W, M) can be related, up to ambient isotopy of W fixing M , by a finite sequence of the following *handle moves*, all considered for any $i = 1, \dots, d$ (the viceversa trivially holds as well):

- 1) *isotoping the attaching maps* of i -handles $\sqcup_{j=1}^{n_i} H_j^i$ in the submanifold δW^{i-1} of the boundary of the $(i-1)$ -handlebody W^{i-1} ;
- 2) *adding/deleting a pair of canceling handles*, that is an i -handle H^i and an $(i-1)$ -handle H^{i-1} , such that the attaching sphere of H^i intersects the belt sphere of H^{i-1} transversally in a single point;
- 3) *handle sliding* of one i -handle $H_{j_1}^i$ over another one $H_{j_2}^i$, that means changing the attaching map of $H_{j_1}^i$ by an isotopy in the submanifold $\delta W_{j_1}^i$ of the boundary of the i -handlebody $W_{j_1}^i = W^{i-1} \cup_{j \neq j_1} H_j^i \subset W^i$, which pushes attaching sphere of $H_{j_1}^i$ through the belt sphere of $H_{j_2}^i$.

DEFINITION 1.2.3. Let W be a d -dimensional relative k -handlebody W for some $k \leq d$. Then a k -deformation of W consists in a finite sequence of the handle moves described above, such that at each stage we still have a relative k -handlebody, i.e. we never add any canceling i -handle with $i > k$. Two relative k -handlebodies related by a k -deformation will be called k -equivalent.

In the light of this definition, the result of Cerf can be restated by saying that two d -dimensional relative handlebodies (W, M) and (W', M) are diffeomorphic if and only if they are d -equivalent.

For any compact smooth d -manifold W and any (possibly empty) smooth $(d-1)$ -submanifold $M \subset \text{Bd } W$ with (possibly empty) boundary, a relative d -handlebody decomposition of the pair (W, M) can be derived from a suitable Morse function.

Such a decomposition can be assumed to have only one 0-handle in each component disjoint from M and no 0-handles in the other components, and to have only one d -handle in each closed component and no d -handle in the other components. Concerning 0-handles, this can be proved by using handle moves to reduce them to at most one (cf. Proposition 1.2.4), while the case of d -handle is dual (see [22, p. 103] for handlebody duality).

Actually, the reduction of 0-handles and dually of d -handles also applies to deformations, hence something more can be said about them. Namely, if (W, M) and (W', M) are diffeomorphic and have the same number of 0-handles in the corresponding components, then no addition/deletion of canceling 0-handles is needed to deform (W, M) into (W', M) . An analogous dual fact also holds for addition/deletion of d -handles. In particular, if (W, M) and (W', M) are diffeomorphic relative $(d-1)$ -handlebodies, then they are $(d-1)$ -equivalent.

The main focus of this paper is on 2-equivalence of 4-dimensional 2-handlebodies. By the discussion above, two such handlebodies are diffeomorphic if and only if they are 3-equivalent, but whether they are 2-equivalent is an open question, which is

expected to have negative answer (cf. Section I.6 of [38] and Section 5.1 of [22]). A list of 4-dimensional 2-handlebodies which are diffeomorphic, but conjecturally not 2-equivalent can be found in [21].

Lemma 3.3.1 will provide some connection between the notion of 2-deformation of 4-dimensional 2-handlebodies and that of embedded 1-deformation of 2-dimensional 1-handlebodies in B^4 . In a speculative sense, this relates the above mentioned diffeomorphism problem for 4-dimensional 2-handlebodies to the question of whether isotopic ribbon surfaces in B^4 are 1-isotopic, according to the definition we will give in Section 1.3 (cf. Remark 6.1.7).

Since the reduction of 0-handles appears repeatedly and in different contexts in the paper, we state the above-mentioned results in the next proposition and give a sketch of the reduction procedure in the proof. We also consider here the case of k -deformations of relative handlebodies with the minimum number of 0-handles as above, which is essentially the only one occurring in this paper.

PROPOSITION 1.2.4. *Any k -handlebody decomposition of a pair (W, M) can be changed by handle isotopy, 1-handle sliding and deletion of canceling 0/1-handle pairs, in order to leave only one 0-handle in each component disjoint from M and no 0-handles in the other components. Moreover, if (W, M) and (W', M) are k -equivalent relative handlebodies build on the same manifold M , both having only one 0-handle in each component disjoint from M and no 0-handles in the other components, then there is a k -deformation relating them that does not involve any extra 0-handle.*

Proof. We can limit ourselves to the case when W and W' are connected.

Given any k -handlebody decomposition (W, M) , let G be the graph, whose vertices represent the 0-handles and M , if this is non-empty, and whose edges represent the 1-handles (with an edge connecting two vertices for each 1-handle between the corresponding subspaces of W^0). If W is connected then G is connected as well. Consider a maximal tree $T \subset G$ having as root M if this is non-empty, or any 0-handle if M is empty. Then, T contains all the 0-handles of W and we can use deletion of canceling 0/1-handle pairs to reduce all the handles in T to the root.

In order to deal with k -deformations, we first observe that different choices of the maximal tree T used for the 0-handle reduction, produce k -handlebody decompositions that can be related by a k -deformation not involving any extra 0-handle.

Now, given any k -deformation between (W, M) and (W', M) , we can perform the 0-handle reduction described above on all the intermediate handlebodies, in such a way that any 1-handle sliding is performed over a 1-handle in T and any addition/deletion of a canceling 0/1-handle pair corresponds to an edge expansion/contraction of the tree T used for the reduction. This gives a k -deformation between (W, M) and (W', M) without any addition/deletion of canceling 0/1-handle pairs and with some 1-handle sliding turned into attaching map isotopy. \square

We conclude this section by briefly discussing the notion of cobordism between oriented manifolds with boundary and its relation with that of relative handlebody.

By an oriented d -manifold with *marked B -boundary*, we mean any pair (M, β) where M is a compact oriented smooth d -manifold and $\beta : \text{Bd } M \rightarrow B$ is an orientation preserving diffeomorphism, with B a given (possibly empty) closed oriented

smooth $(d - 1)$ -manifold. Due to the existence of a collar of the boundary, we can always consider β up to isotopy.

If (M_0, β_0) and (M_1, β_1) are two oriented d -manifolds with marked B -boundary, then a *relative cobordism* (with corners) between them is a compact oriented smooth $(d + 1)$ -manifold with marked boundary (W, η) , where $\eta : \text{Bd } W \rightarrow -M_0 \cup_{\beta_0 \times \{0\}} (B \times [0, 1]) \cup_{\beta_1 \times \{1\}} M_1$ is an orientation preserving diffeomorphism. We can think of $-M_0$ and M_1 as oriented smooth d -submanifolds of $\text{Bd } W$, by identifying them with their images under η^{-1} .

We say that (M_0, β_0) and (M_1, β_1) are *cobordant* when a relative cobordism as above exists. This gives an equivalence relation on the set of all the compact smooth d -manifolds with marked B -boundary, for a fixed closed smooth $(d - 1)$ -manifold B . In particular, the transitivity is guaranteed by the possibility of composing two relative cobordisms (W_1, η_1) and (W_2, η_2) respectively from (M_0, β_0) to (M_1, β_1) and from (M_1, β_1) to (M_2, β_2) to form a cobordism (W, η) from (M_0, β_0) to (M_2, β_2) , with $W = W_1 \cup_{M_1} W_2$ and η canonically induced in the obvious way by $\eta_1|_{M_0} \cup \eta_2|_{M_2}$.

Any relative cobordism (W, η) between (M_0, β_0) and (M_1, β_1) can be endowed with a structure of relative handlebody build on M_0 with $\delta W = M_1$ (cf. notation introduced in Definition 1.2.2), such that the product $M_0 \times [0, 1] \subset W$ satisfies the condition $\eta|_{\text{Bd } M_0 \times [0, 1]} = \beta_0 \times \text{id}_{[0, 1]}$. Viceversa, any relative handlebody W build on M_0 with $\delta W = M_1$ gives raise to a relative cobordism (W, η) from (M_0, β_0) to (M_1, β_1) , such that $\eta|_{\text{Bd } M_0 \times [0, 1]} = \beta_0 \times \text{id}_{[0, 1]}$. Of course, here the roles of M_0 and M_1 can be exchanged by handlebody duality.

Handlebody decomposition allows us to express any relative cobordism as the composition of elementary cobordisms, meaning cobordisms admitting a relative handlebody structure with only one handle. Namely, for an *elementary cobordism* (W, η) relating (M_0, β_0) to (M_1, β_1) we have $W = M_0 \times [0, 1] \cup_{\varphi} H^i$ and $M_1 = \delta W$. This implies that M_1 can be obtained from M_0 , once this is canonically identified with $M_0 \times \{1\}$, by replacing the attaching region $\varphi(S^{i-1} \times B^{d-i}) \subset \text{Int } M_0$ of H^i with $B^i \times S^{d-i-1} \subset \text{Bd } H^i$ attached to $\text{Cl}(M_0 - \varphi(S^{i-1} \times B^{d-i}))$ through the restriction of φ to $S^{i-1} \times S^{d-i-1}$.

The replacement of a diffeomorphic copy of $S^{i-1} \times B^{d-i}$ in $\text{Int } M_0$ by a diffeomorphic copy of $B^i \times S^{d-i-1}$ attached to the rest of M_0 through a given diffeomorphism between $S^{i-1} \times S^{d-i-1} = \text{Bd}(B^i \times S^{d-i-1})$ and $\text{Bd}(S^{i-1} \times B^{d-i}) \subset \text{Int } M_0$ is usually referred to as a *surgery* of index i (i -surgery in short) on M_0 .

Since surgery takes place in the interior of the manifold and leaves the boundary unchanged, it can be performed on manifolds with marked B -boundary as well. Moreover, the argument above can be reversed to see that if (M_1, β_1) is obtained by i -surgery from (M_0, β_0) , then there is an elementary cobordism from (M_0, β_0) to (M_1, β_1) with only one handle of index i . This allows us to conclude that two oriented manifolds with marked B -boundary are cobordant if and only if they are surgery equivalent, that is they are related by a finite sequence of surgeries.

Now, let $W = M_0 \times [0, 1] \cup_{\varphi} H^i$ be a d -dimensional elementary cobordism from M_0 to $M_1 = \delta W$, with H^i a *trivially attached* i -handle, meaning that the attaching map φ is isotopic to an embedding of $S^{i-1} \times B^{d-i}$ in some smooth $(d - 1)$ -cell $C \subset M_0 \times \{1\}$, which is diffeomorphic to the standard embedding $S^{i-1} \times B^{d-i} \rightarrow B^{d-1}$. In this case, the entire handle H^i can be thought as standardly embedded in a copy of B_+^d

attached to $M_0 \times [0, 1]$ through a diffeomorphism $\rho : B^{d-1} \rightarrow C$. This gives rise, to a cobordism $W' = M_0 \times [0, 1] \cup_\rho B_+^d = M_0 \times [0, 1] \cup_\varphi H^i \cup_\psi H^{i+1}$, obtained by adding to W an $(i+1)$ -handle H^{i+1} that forms a canceling pair with the i -handle H^i . Both W' and its dual handlebody $\overline{W}' = M_0 \times [0, 1] \cup_{\overline{\psi}} \overline{H}^{d-i-1} \cup_{\overline{\varphi}} \overline{H}^{d-i}$ are diffeomorphic to the trivial cobordism $M_0 \times [0, 1]$. Moreover, $\overline{W} = M_0 \times [0, 1] \cup_{\overline{\psi}} \overline{H}^{d-i-1}$ is a new elementary cobordism from M_0 to $M_1 = \delta\overline{W} = \delta W$.

The replacement of the trivially attached i -handle H^i by the trivially attached $(d-i-1)$ -handle \overline{H}^{d-i-1} , converting the cobordism W into the new cobordism \overline{W} between the same manifolds, is called an $i/(d-i-1)$ -handle trading.

Performing such an $i/(d-i-1)$ -handle trading produces the same effect on W as an $(i+1)$ -surgery along the i -sphere given by the union of the core of H^i and a smooth i -cell properly embedded in $M_0 \times [0, 1]$ spanned by the attaching sphere of H^i . Hence, the cobordisms W and \overline{W} turn out to be cobordant.

We observe that under the condition of isotopic triviality of the attaching map of the original handle H^i (or equivalently of the new handle \overline{H}^{d-i-1}), an analogous $i/(d-i-1)$ -handle trading can also be performed on any (possibly non-elementary) cobordism (W, η) between two d -manifolds with B -marked boundary (M_0, β_0) and (M_1, β_1) , with a given handlebody decomposition. The result is a new cobordism (W', η') between (M_0, β_0) and (M_1, β_1) , with a handlebody decomposition obtained from the original one by replacing the trivially attached i -handle H^i with the trivially attached $(d-i-1)$ -handle \overline{H}^{d-i-1} and then reordering the handles.

Actually, handle trading together with handlebody deformation can be proved to generate the cobordism equivalence on the set of all the cobordisms between given manifolds (M_0, β_0) and (M_1, β_1) with marked B -boundary. In other words, two such cobordisms are cobordant if and only if they admit handlebody decompositions that are related by handlebody deformation and handle trading.

The case of interest in this paper is that of $1/2$ -handle trading in dimension 4. In a 4-dimensional cobordism W , for a 1-handle being trivially attached means that both its attaching balls are in the same component of δW^0 (orientability is assumed for cobordisms), while a 2-handle is trivially attached if the attaching map is determined by a trivial knot with trivial framing in δW^1 . Then, given a 4-dimensional relative 2-handlebody decomposition of a relative cobordism, once the reduction described in Proposition 1.2.4 has been performed, we can always trade all the 1-handles for trivially attached 2-handles. This way, we obtain a relative handlebody without 1-handles representing a new relative cobordism between the same manifolds, which is cobordant to the original one.

1.3. Ribbon surfaces

A regularly embedded smooth compact surface $F \subset B^4$ with is called a *ribbon surface* if the Euclidean norm restricts to a Morse function on F with no local maxima in $\text{Int } F$. Assuming $F \subset R_+^4 \subset R_+^4 \cup \{\infty\} \cong B^4$, this property is topologically equivalent to the fact that the fourth Cartesian coordinate restricts to a Morse height function on F with no local minima in $\text{Int } F$. In particular, F has non-empty boundary $\text{Bd } F \subset R^3$ (actually F has no closed components).

DEFINITION 1.3.1. By a *ribbon surface tangle* in $E \times [0, 1] \times [0, 1[$, where $E = [0, 1]^2$ denotes the standard square, we mean a slice $S = F \cap (E \times [0, 1] \times [0, 1[$) of

a ribbon surface $F \subset \text{Int } E \times R \times [0, 1[\subset R_+^4$, such that the intersections $\partial_0 S = F \cap (E \times \{0\} \times [0, 1[)$ and $\partial_1 S = F \cap (E \times \{1\} \times [0, 1[)$ are transversal and project to trivial families of regularly embedded arcs in $E \times [0, 1[$ (trivial means that the arcs are unknotted and unlinked), by the projection forgetting the third coordinate. We call $\partial_0 S$ and $\partial_1 S$ respectively the *lower end* and the *upper end* of S . We also call $\partial S = S \cap (E \times [0, 1] \times \{0\}) = S \cap \text{Bd } F$ the *tangle boundary* of S , while the boundary of S as a surface is $\text{Bd } S = \partial S \cup \partial_0 S \cup \partial_1 S$.

Of course, ribbon surface tangles with empty ends reduce to ribbon surfaces contained in $\text{Int } E \times]0, 1[\times [0, 1[\subset R_+^4$. Then, without loss of generality up to isotopy, we can think of any ribbon surface as a tangle with empty ends. In this way, all the definitions and results given below for ribbon surface tangles specialize to ribbon surfaces.

A ribbon surface tangle $S \subset E \times [0, 1] \times [0, 1[\subset R_+^4$ can be isotoped, through an isotopy preserving the fourth coordinate, to make its projection into $E \times [0, 1] \subset R^3$ a regularly immersed surface, whose self-intersections consist only of disjoint double arcs as in Figure 1.3.1 (a).

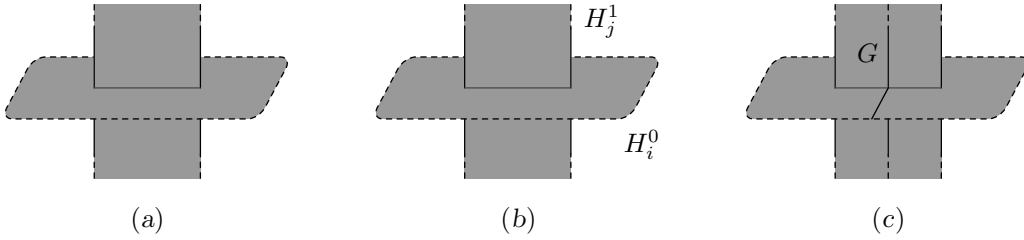


FIGURE 1.3.1. A ribbon intersection

We will refer to such a projection as a 3-dimensional *diagram* of S and use the same notation S for it (the meaning will be clear from the context). Actually, any regularly immersed smooth compact surface $S \subset \text{Int } E \times [0, 1]$ with no closed components and such that all its self-intersections are as above and $S \cap (E \times \{0\})$ and $S \cap (E \times \{1\})$ both consist of trivial regularly embedded arcs, is the diagram of a ribbon surface tangle uniquely determined up to vertical isotopy. This can be obtained by pushing $\text{Int } S$ up inside $\text{Int } R_+^4$ in such a way that all self-intersections disappear.

Since a ribbon surface tangle S is a surface with no closed components, it admits a relative handlebody decomposition $S = C \cup H_1^0 \cup \dots \cup H_r^0 \cup H_1^1 \cup \dots \cup H_s^1$ build on $\partial_0 S \cup \partial_1 S$ with only 0- and 1-handles, where $C \cong (\partial_0 S \cup \partial_1 S) \times [0, 1]$ is a collar of $\partial_0 S \cup \partial_1 S$ in S .

DEFINITION 1.3.2. A relative 1-handlebody decomposition of a ribbon surface tangle S as above is called *adapted* when the following conditions are satisfied:

- (a) each ribbon self-intersection involves an arc contained in the interior of a 0-handle and a proper transversal arc inside a 1-handle as in Figure 1.3.1 (b) (cf. [68] for the case of ribbon surfaces);
- (b) to each component of C is attached a single 1-handle connecting it to a 0-handle or to another component of C itself.

The ribbon surface tangle S endowed with such an adapted 1-handlebody decomposition will be called an *embedded 2-dimensional relative 1-handlebody* (build on $\partial_0 S \cup \partial_1 S$).

According to this definition, the H_i^0 's are disjoint non-singular disks, while the H_j^1 's are non-singular bands attached to C and to the H_i^0 's, which possibly pass through the H_i^0 's as shown in Figure 1.3.1 (b). The handlebody decomposition is induced by the height function, if S is realized as a suitable smooth perturbation of the boundary of $((C \cup H_1^0 \cup \dots \cup H_r^0) \times [0, 2/3]) \cup ((H_1^1 \cup \dots \cup H_s^1) \times [0, 1/3])$ in $E \times [0, 1] \times [0, 1]$.

DEFINITION 1.3.3. We say that two embedded 2-dimensional relative 1-handlebodies build on the same sets of intervals are equivalent up to *embedded 1-deformation*, or briefly that they are *1-equivalent*, if they are related by a finite sequence of the following modifications, all keeping those intervals fixed:

- (a) *adapted isotopy*, that is isotopy of embedded relative 1-handlebodies build on a fixed set of intervals, all adapted except for a finite number of intermediate critical stages, at which one of the modifications described in Figure 1.3.2 takes place (between any two such critical stages, we have isotopy of diagrams in R^3 , preserving ribbon intersections);

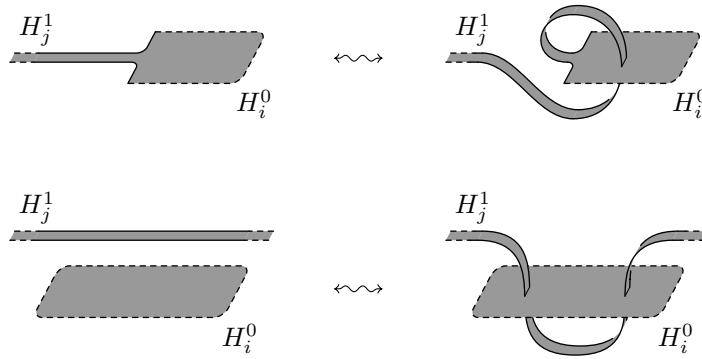


FIGURE 1.3.2. Adapted isotopy moves

- (b) *ribbon intersection sliding*, allowing a ribbon intersection to run along a 1-handle from one 0-handle to another one, as shown in Figure 1.3.3;

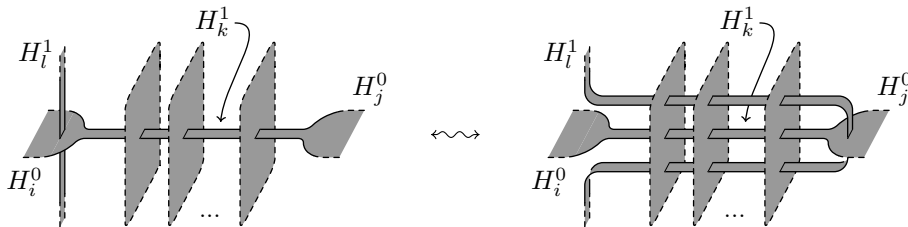


FIGURE 1.3.3. Sliding a ribbon intersection along a 1-handle

- (c) *embedded handles operations*, that is addition/deletion of canceling pairs of 0/1-handles and embedded 1-handle slidings (see Figure 1.3.4).

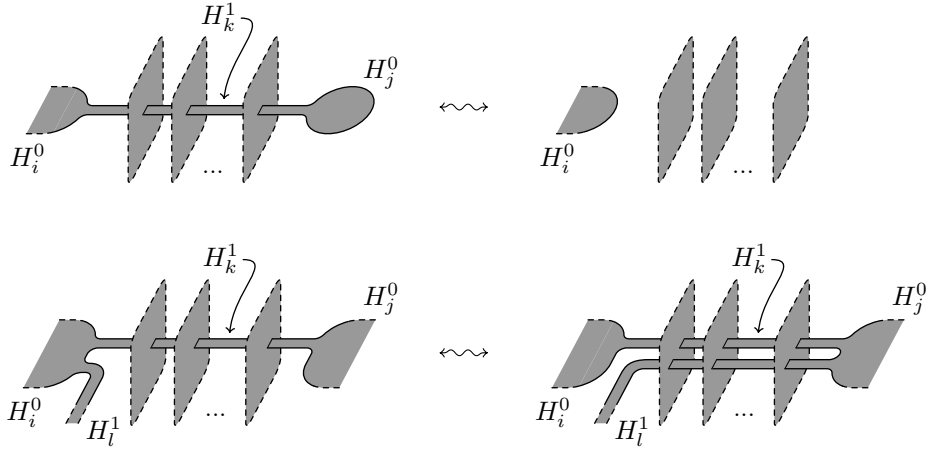


FIGURE 1.3.4. Embedded handle operations

We observe that the second modification of Figure 1.3.2 is actually redundant in presence of the handle operations of Figure 1.3.4 (cf. proof of Proposition 1.3.9). It is also worth noting that the 0-handles H_i^0 and H_j^0 in Figures 1.3.3 and 1.3.4 can be assumed to be distinct in all the cases, up to addition/deletion of canceling pairs of 0/1-handles (where they are always distinct).

PROPOSITION 1.3.4. *All the adapted 1-handlebody decompositions of a ribbon surface tangle S are 1-equivalent as embedded 2-dimensional relative 1-handlebodies. More precisely, up to isotopy inside the 3-dimensional diagram of S , they are related to each other by the special cases without vertical disks of the moves of Figures 1.3.3 and 1.3.4, realized inside S in such a way that S itself is kept invariant.*

Proof. First of all, we observe that the moves specified in the statement allow us to realize the following two modifications: 1) split a 0-handle along any regular arc that avoids ribbon intersections in the diagram, into two 0-handles joined by a new 1-handle, which coincides with a regular neighborhood of the splitting arc; 2) split a 1-handle at any transversal arc that avoids ribbon intersections in the diagram, into two 1-handles, by inserting a new 0-handle given by a regular neighborhood of the splitting arc. We leave the straightforward verification of this to the reader.

Let $S = C \cup H_1^0 \cup \dots \cup H_r^0 \cup H_1^1 \cup \dots \cup H_s^1 = \bar{C} \cup \bar{H}_1^0 \cup \dots \cup \bar{H}_r^0 \cup \bar{H}_1^1 \cup \dots \cup \bar{H}_s^1$ be any two 1-handlebody decompositions of a ribbon surface tangle S , which we denote respectively by H and \bar{H} . Up to isotopy, we can assume $C = \bar{C}$. Moreover, we can suitably split the 1-handles of H and \bar{H} , in such a way that any 1-handle contains at most one ribbon self-intersection of S . Up to isotopy, we can also assume that the 1-handles of H and \bar{H} attached to the same component of C and those forming the same ribbon self-intersection coincide. Let $H_1 = \bar{H}_1, \dots, H_k = \bar{H}_k$ be all these 1-handles. Then, it suffices to see how to transform the remaining 1-handles H_{k+1}^1, \dots, H_s^1 into $\bar{H}_{k+1}^1, \dots, \bar{H}_s^1$, without changing H_1^1, \dots, H_k^1 .

Calling η_i (resp. $\bar{\eta}_j$) the cocore of H_i^1 (resp. \bar{H}_j^1), we have $\eta_1 = \bar{\eta}_1, \dots, \eta_k = \bar{\eta}_k$, while the arcs $\eta_{k+1}, \dots, \eta_s$ can be assumed to be transversal with respect to the arcs $\bar{\eta}_{k+1}, \dots, \bar{\eta}_s$. Up to isotopy, we can think of each 1-handle as a tiny regular neighborhood of its cocore, so that the intersection between $H_{k+1}^1 \cup \dots \cup H_s^1$ and $\bar{H}_{k+1}^1 \cup \dots \cup \bar{H}_s^1$ consists only of a certain number h of small four-sided regions.

We eliminate all these intersection regions in turn, by pushing them outside S along the \bar{H}_j^1 's. This is done by performing on H moves of the types specified in the statement of the proposition, as suggested by the Figure 1.3.5, which concerns the l -th elimination. Namely, in (a) we assume that the intersection is the first one along $\bar{\eta}_j$ starting from the shown end-point in ∂S , then we generate a new 1-handle H_{s+l}^1 by 0-handle splitting to get (b), while (c) is obtained by handle sliding.

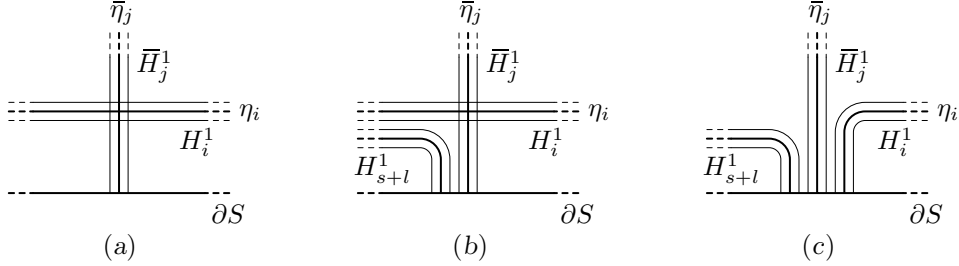


FIGURE 1.3.5. Eliminating intersections of 1-handles of different decompositions

After that, H has been changed into a new handlebody decomposition H' with 1-handles H_1^1, \dots, H_{s+h}^1 , such that H_i^1 is the same as above for $i \leq k$, while it is disjoint from the \bar{H}_j^1 's for $i > k$. Hence, $H_1^1, \dots, H_k^1, H_{k+1}^1, \dots, H_{s+h}^1, \bar{H}_{k+1}^1, \dots, \bar{H}_s^1$ can be considered as the 1-handles of a relative handlebody decomposition of S which can be obtained from both H' and \bar{H} by 0-handle splitting. \square

Forgetting the handlebody structure, 1-equivalence of embedded 2-dimensional relative 1-handlebodies induces an equivalence relation between ribbon surface tangles, which we call 1-isotopy.

DEFINITION 1.3.5. Two ribbon surface tangles are called *1-isotopic* when they admit 1-equivalent adapted relative 1-handlebody decompositions (by the above proposition, this implies that any two such 1-handlebody decompositions of them are 1-equivalent).

Of course 1-isotopy implies isotopy, but the converse is not known and seems to be a delicate question. Actually, also the problem of finding a complete set of moves representing isotopy of ribbon surface tangles is still open, even in the special case of ribbon surfaces.

As we anticipated in Section 1.2, the problem of whether isotopy of ribbon surfaces implies 1-isotopy looks like an embedded lower dimensional analog of the problem of whether diffeomorphism of 4-dimensional 2-handlebodies implies 2-equivalence. In Section 3.3, we will see how this analogy is supported by the connection between the two concepts given in terms of branched coverings.

Now, we want to provide a description of ribbon surface tangles and 1-isotopy in terms of certain planar diagrams and moves between them. A planar diagram of ribbon surface tangle will be based on the projection of a suitable 3-dimensional diagram $S \subset \text{Int } E \times [0, 1]$ into the square $]0, 1[\times [0, 1]$, given by forgetting the second coordinate of $E = [0, 1]^2$.

Since 1-isotopy fixes the ends $\partial_0 S$ and $\partial_1 S$, we will consider only the case when these project regularly into disjoint unions of intervals in $]0, 1[\times \{0\}$ and $]0, 1[\times \{1\}$ respectively. In this case we say that the ribbon surface tangle S has *flat ends*.

We start with the observation that any 3-dimensional diagram of a ribbon surface tangle S with flat ends, considered as a 2-dimensional complex in $\text{Int } E \times [0, 1]$, collapses to a graph G . We can choose G to be the projection of a smooth simple spine P of S (simple means that all the vertices have valence one or three) contained in $S - \partial S$. Moreover, we can assume that G meets at exactly one 1-valent vertex each arc of $\partial_0 S \cup \partial_1 S$ and at exactly one 3- or 4-valent vertex each ribbon intersection arc of S . In this way, G turns out to have vertices of valence 1, 3 and 4.

We call *flat vertices* the 1- or 3-valent vertices of G whose inverse image in P is one vertex with the same valence and *singular vertices* the 3- or 4-valent vertices of G located at the ribbon intersections. The inverse image in P of a singular vertex of G consists of two points along edges of P in the case of valence 4, while it consists of one point along an edge of P and one end point of P in the case of valence 3.

Finally, we assume G to have three distinct tangent lines at each flat 3-valent vertex and two distinct tangent lines at each 3- or 4-valent singular vertex.

Up to horizontal isotopy of $S \bmod \partial_0 S \cup \partial_1 S$, we can contract its diagram to a narrow regular neighborhood of the graph G . Then, by considering a planar diagram of G , we can easily get a planar diagram of S in the sense of the following definition.

DEFINITION 1.3.6. A *planar diagram* of a ribbon surface tangle with flat ends is the planar projection of a 3-dimensional diagram $S \subset \text{Int } E \times [0, 1]$ in the square $]0, 1[\times [0, 1]$ given by forgetting the second coordinate of $E = [0, 1]^2$, decorated consistently with the height function in correspondence of crossings and ribbon intersections, in such a way that it consists of a certain number of copies of the spots (a) to (h) in Figure 1.3.6 and some flat bands connecting pairwise the end arcs of them and those in the projection of $\partial_0 S \cup \partial_1 S$. A planar diagram whose ribbon intersections are all modeled on spot (h) will be called a *special planar diagram*.

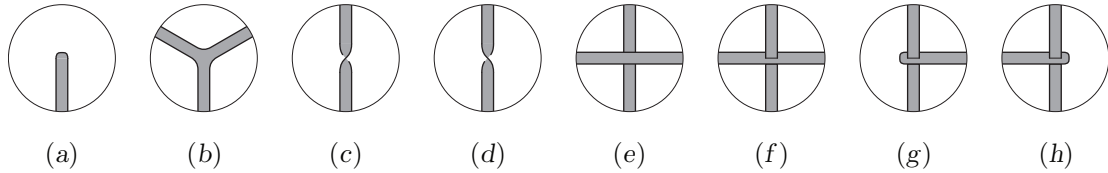


FIGURE 1.3.6. Local models for planar diagrams

As said above, a planar diagram of a ribbon surface tangle with flat ends arises as a diagram of a pair (S, G) where G is a graph in a 3-dimensional diagram S , and this is the right way to think of it.

However, we omit to draw the diagram of the graph G in the pictures of a planar diagram, since it can be trivially recovered, up to diagram isotopy, as the core of the diagram itself. In particular, its singular vertices and diagram crossings are located at the centers of the spots modeled on the three rightmost ones in Figure 1.3.6, while the flat vertices of G are located at the centers of the spots modeled on the two leftmost ones in the same figure.

To be precise, there are two choices in recovering the graph G at a singular vertex, as shown in Figure 1.3.7 for a ribbon intersection of type (h). They give the same graph diagram of each other, but differ for the way the graph is embedded in S . We consider the move depicted in Figure 1.3.7 as an equivalence move for the pair

(S, G) . Up to this move, which does not change the tangle, G is uniquely determined also as a graph in S .

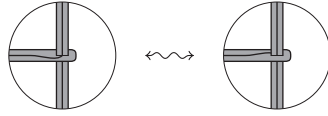


FIGURE 1.3.7. The graph G at a ribbon intersection of type (h)

Like 3-dimensional diagrams, also planar diagrams uniquely determine the ribbon surface tangle S up to vertical isotopy. Here, by vertical isotopy we mean an isotopy that preserves the first and third coordinates. In other words, the 3-dimensional height function (as well as the 4-dimensional one) is left undetermined when presenting S by a planar diagram. Of course, this height function is required to be consistent with the restrictions deriving from the local configurations in Figure 1.3.6.

We remark that any planar diagram can be made special by using the moves $(S1)$ and $(S2)$ depicted in Figure 1.3.8 to remove spots of type (f) and (g) respectively.

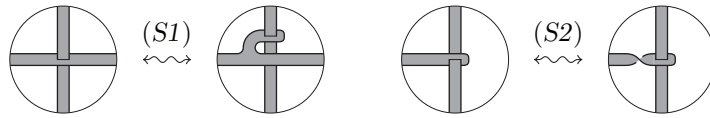


FIGURE 1.3.8. Making ribbon intersections special

PROPOSITION 1.3.7. *Any 3-dimensional diagram of a ribbon surface tangle S with flat ends $\partial_0 S$ and $\partial_1 S$, up to 3-dimensional isotopy mod $\partial_0 S \cup \partial_1 S$, has a (special) planar diagram.*

Proof. Starting from the 3-dimensional diagram S , we can get a special planar diagram by the following steps: 1) contract S to a narrow regular neighborhood N of the graph G ; 2) perturb N to make the planar projection of G into a graph diagram and the projection of N itself regular except for a finite number of half-twists as in Figure 1.3.6 (c) and (d); 3) perform moves $(S1)$ and $(S2)$ at each ribbon intersection of type (f) and (g) respectively. Then, the proposition immediately follows from the observation that all this steps can be realized by 3-dimensional isotopies keeping $\partial_0 S \cup \partial_1 S$ fixed. \square

Figures 1.3.9, 1.3.10 and 1.3.11 show how to interpret the 3-dimensional diagram isotopy in terms of planar diagrams, up to planar isotopy. Actually, moves $(S3)$ and $(S4)$ could be realized by planar isotopy if we think of the planar diagram just as representing the surface S , but this not true if we take into account the graph G .

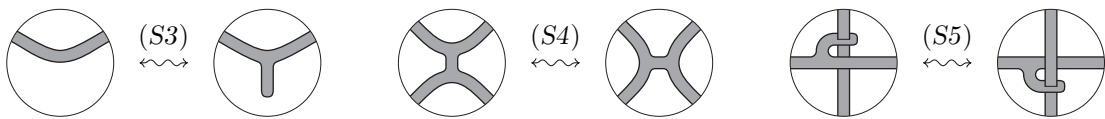


FIGURE 1.3.9. Graph changing moves for special planar diagrams

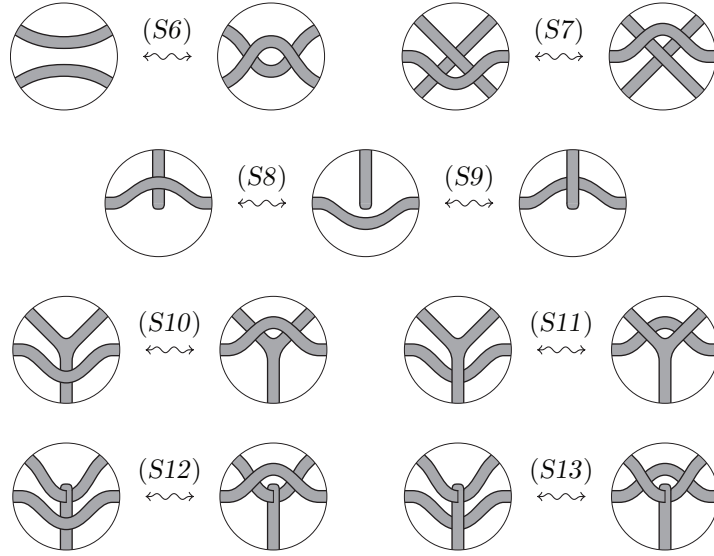


FIGURE 1.3.10. Regular isotopy moves for special planar diagrams

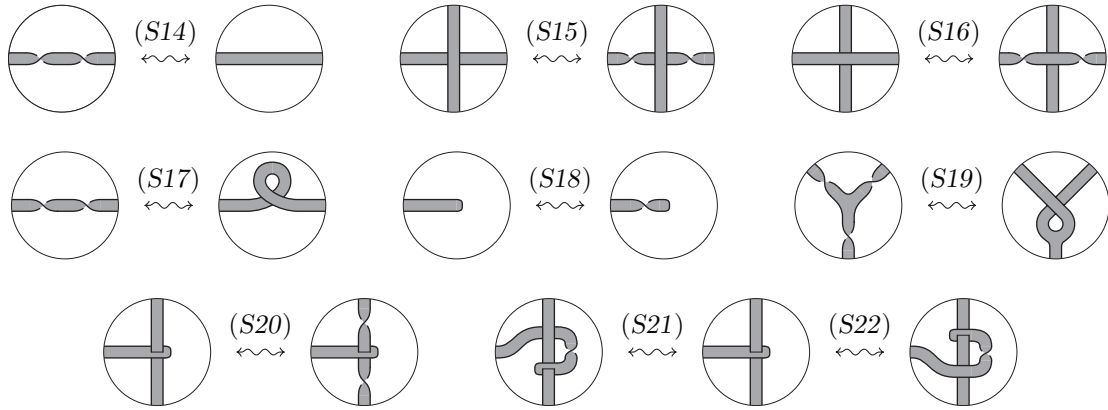


FIGURE 1.3.11. Other 3-dimensional isotopy moves for special planar diagrams

PROPOSITION 1.3.8. *Two planar diagrams represent the same 3-dimensional diagram of a ribbon surface tangle S , up to 3-dimensional isotopy mod $\partial_0 S \cup \partial_1 S$, if and only if they are related by finite sequence of planar isotopies (induced by smooth ambient isotopies of $]0, 1[\times [0, 1]$ mod $]0, 1[\times \{0, 1\}$ in the projection plane) and moves (S1) to (S22) as in Figures 1.3.8, 1.3.9, 1.3.10 and 1.3.11. Moreover, moves (S1) and (S2) are not needed if both the planar diagrams are special.*

Proof. The “if” part is trivial, since all the moves (S1) to (S22) represent special 3-dimensional isotopies of S mod $\partial_0 S \cup \partial_1 S$. To prove the “only if” part, we need to show that these moves do generate any such 3-dimensional isotopy of the 3-dimensional diagrams represented by planar diagrams.

Moves (S1) and (S2) allow us to restrict our attention to special planar diagrams. All the remaining moves (S3) to (S22) only contain terminal ribbon intersections of type (h), hence they can be performed in the context of special planar diagrams. Actually, we will use only them in this special case, proving in this way also the last part of the statement.

Now, consider two special planar diagrams representing ribbon surface tangles S_0 and S_1 as regular neighborhoods of their core graphs G_0 and G_1 , such that there is a 3-dimensional isotopy $H : (S_0, G_0) \times [0, 1] \rightarrow \text{Int } E \times [0, 1]$ taking (S_0, G_0) to (S_1, G_1) , as singular surfaces with ribbon self-intersections, and keeping the tangle ends fixed. Notice that the intermediate pairs $(S_t, G_t) = H((S_0, G_0), t)$ with $0 < t < 1$ do not necessarily project suitably into $]0, 1[\times [0, 1]$ to give planar diagrams.

Of course, we can assume that H is smooth, as a map defined on a pair of smooth stratified spaces, and that the graph G_t regularly projects to a diagram in $]0, 1[\times [0, 1]$ for every $t \in [0, 1]$, except a finite number of t 's corresponding to extended Reidemeister moves for graphs. For such exceptional t 's, the lines tangent to G_t at its vertices are assumed not to be vertical.

We define $\Gamma \subset G_0 \times [0, 1]$ as the subspace of pairs (x, t) for which S_t has a vertical tangency at $x_t = H(x, t)$ (if $x \in G$ is a singular vertex, there are two such tangent planes and we require that one of them is vertical).

We can assume that Γ does not meet $(\partial_0 S_0 \cup \partial_1 S_0) \times [0, 1]$. Moreover, by a standard transversality argument, we can perturb H in such a way that:

- (a) Γ is a graph embedded in $G_0 \times [0, 1]$ as a smooth stratified subspace of constant codimension 1 and the restriction $\eta : \Gamma \rightarrow [0, 1]$ of the height function $(x, t) \mapsto t$ is a Morse function on each edge of Γ ;
- (b) the edges of Γ locally separate regions consisting of points (x, t) for which the projection of S_t into $]0, 1[\times [0, 1]$ has opposite local orientations at x_t ;
- (c) the two planes tangent to any S_t at a singular vertex of G_t are not both vertical, and if one of them is vertical then it does not contain both the lines tangent to G_t at that vertex.

As a consequence of (b), for each flat vertex $x \in G_0$ of valence one (resp. three) there are finitely many points $(x, t) \in \Gamma$, all of which have the same valence one (resp. three) as vertices of Γ . Similarly, as a consequence of (c), for each singular vertex $x \in G_0$ there are finitely many points $(x, t) \in \Gamma$, all of which have valence one or two as vertices of Γ . Moreover, the above-mentioned vertices of Γ of valence one or three are the only vertices of Γ of valence $\neq 2$.

Let $0 < t_1 < \dots < t_k < 1$ be the critical levels t_i at which one of the following facts happens:

- 1) G_{t_i} does not project regularly in R^2 , since there is one point x_i along an edge of G_0 such that the line tangent to G_{t_i} at $H(x_i, t_i)$ is vertical;
- 2) G_{t_i} projects regularly in R^2 , but its projection is not a graph diagram, due to a multiple tangency or crossing;
- 3) there is one point $(x_i, t_i) \in \Gamma$ with x_i a uni-valent or a singular vertex of G_0 ;
- 4) there is one critical point (x_i, t_i) for the function η along an edge of Γ .

Without loss of generality, we assume that only one of the four cases above occurs for each critical level t_i . Notice that the points (x, t) of Γ such that $x \in G_0$ is a flat tri-valent vertex represent a subcase of 2 and for this reason they are not included in case 3.

For $t \in [0, 1] - \{t_1, \dots, t_k\}$, there exists a sufficiently small regular neighborhood N_t of G_t in S_t , such that the pair (N_t, G_t) projects to a special planar diagram, except for the possible presence of some ribbon intersection projecting in the wrong way, as in Figure 1.3.6 (g). We fix this problem by inserting an auxiliary positive

half-twists along the tongues containing those ribbon intersections, as in move (S2). The resulting singular surfaces, still denoted by N_t , projects to a special planar diagram.

Actually, we modify the N_t 's all together to get a new isotopy where no wrong projection of ribbon intersection occurs, so that N_t projects to a special planar diagram for each $t \in [0, 1] - \{t_1, \dots, t_k\}$. Namely, at each critical level when a wrong projection of a ribbon intersection is going to appear in the original isotopy, we insert an auxiliary half-twist, to prevent the projection from becoming wrong. Such half-twist remains close to the ribbon intersection until the first critical level when the projection becomes good again in the original isotopy (remember that 3-dimensional diagram isotopy preserves ribbon intersections). At that critical level we remove the auxiliary half-twist. We remark that the second part of condition (c) is violated when inserting/removing an auxiliary half-twist at critical points of type 2, as it can be seen by looking at moves (S21) and (S22) where this happens.

We observe that the planar diagram of N_t is uniquely determined up to diagram isotopy by that of the graph G_t and by the tangent planes of S_t at G_t . In fact, the half-twists of N_t along the edges of G_t correspond to the transversal intersections of Γ with $G \times \{t\}$ and their signs, depend only on the local behavior of the tangent planes of S_t . In particular, the planar diagrams of (N_0, G_0) and (N_1, G_1) coincide, up to diagram isotopy, with the original ones of (S_0, G_0) and (S_1, G_1) .

If the interval $[t', t'']$ does not contain any critical level t_i , then each single half-twist persists between the levels t' and t'' , and hence the planar isotopy relating the diagrams of $G_{t'}$ and $G_{t''}$ also relate the diagrams of $N_{t'}$ and $N_{t''}$, except for possible slidings of half-twists along ribbons over/under crossings. Therefore the planar diagrams of $(N_{t'}, G_{t'})$ and $(N_{t''}, G_{t''})$, up to diagram isotopy and moves (S14), (S15) and (S16).

On the other hand, if the interval $[t', t'']$ is a sufficiently small neighborhood of a critical level t_i , then the planar diagrams of $N_{t'}$ and $N_{t''}$ are related by the moves in Figures 1.3.10 and 1.3.11, depending on the type of t_i as follows.

If t_i is of type 1, then a positive or negative kink is appearing (resp. disappearing) along an edge of the core graph. When the kink is positive and (x_i, t_i) is a local maximum (resp. minimum) point for η , i.e. two positive half-twists along the ribbon corresponding to the edge are being converted into a kink (resp. viceversa), the diagrams of $N_{t'}$ and $N_{t''}$ are directly related by move (S17). The cases when (x_i, t_i) is not an extremal point for η , that is one or two negative half-twists appear (resp. disappear) together with the positive kink, can be reduced to the previous case by means of move (S14). On the other hand, by using the regular isotopy moves (S6) and (S7) in order to create or delete in the usual way a pair of canceling kinks (without introducing any half-twist) along the ribbon, we can reduce the case of a negative kink to that of a positive one.

If t_i is of type 2, then either a regular isotopy move is occurring between $G_{t'}$ and $G_{t''}$ or two tangent lines at a tri-valent vertex x_i of the graph project to the same line in the plane. In the first case, the regular isotopy move occurring between $G_{t'}$ and $G_{t''}$, trivially extends to one of the moves (S6) to (S13). In the second case, x_i may be either a flat or a singular vertex. If x_i is a flat vertex, then the tangent plane to S_t at $H(x_i, t)$ is vertical for $t = t_i$ and its projection reverses the orientation

when t passes from t' to t'' . Move (S19) (modulo moves (S6) and (S14)) describes the effect on the diagram of such a reversion of the tangent plane. If x_i is a singular vertex, then $N_{t'}$ changes into $N_{t''}$ by one of the moves (S21) or (S21), where auxiliary half-twists are inserted according to what we have said above.

If t_i is of type 3, then either a half-twist is appearing/disappearing at the tip of the tongue of surface corresponding to a uni-valent vertex or one of the two bands at the ribbon intersection corresponding to a singular vertex is being reversed in the planar projection. The first case corresponds to move (S18) (here we have a positive half-twist, for dealing with a negative one we combine this move with (S14)). The second case may happen in two different ways, depending on which band is being reversed. If such band is the one passing through the other in the ribbon intersection, then, we can transform $N_{t'}$ into $N_{t''}$ by applying move (S20), possibly modulo (S14). Otherwise, the projection of the ribbon intersection is changing from good to wrong, and the appearing half-twist is compensated by the auxiliary one up to move (S14).

Finally, if t_i is of type 4, a pair of canceling half-twists is appearing or disappearing along an edge of the graph. This is just move (S14).

At this point, to conclude that moves (S3) to (S22) suffice to realize 3-dimensional isotopy between any two special planar diagrams of a given ribbon surface tangle S , it is left to prove that, given two different core graphs G' and G'' of S as above, the planar diagrams S' and S'' determined respectively by G' and G'' , are related by those moves. This is quite straightforward. In fact, by cutting the 3-dimensional diagram S along the ribbon intersection arcs, we get a new surface \bar{S} with some marked arcs. This operation also makes the graphs G' and G'' into two simple spines P' and P'' of \bar{S} relative to those marked arcs (Figure 1.3.12 shows the effect of the cut at the ribbon intersection in Figure 1.3.7) and to the arcs in $\partial_0 S \cup \partial_1 S$.



FIGURE 1.3.12. Cutting a ribbon surface tangle at a ribbon intersection

From intrinsic point of view, that is considering \bar{S} as an abstract surface and forgetting its inclusion in R^3 , the theory of simple spines tells us that the moves in Figure 1.3.9 suffice to transform P' into P'' . In particular, moves (S3) and (S4) correspond to the well-known moves for simple spines of surfaces, while (S5) relates the different positions of the spine with respect to the marked arcs in the interior of \bar{S} . It remains only to observe that, up to a 3-dimensional diagram isotopy preserving the core graph, hence up to the moves in Figures 1.3.10 and 1.3.11, the portion of the surface involved in each single spine modification can be isolated in the planar diagram. \square

The next proposition says that, up to 3-dimensional diagram isotopy, 1-isotopy of ribbon tangles is generated by the local isotopy moves of Figure 1.3.13.

PROPOSITION 1.3.9. *Two ribbon surface tangles with flat ends are 1-isotopic if and only if their planar diagrams can be related by a finite sequence of 3-dimensional diagram isotopies fixing the tangle ends (cf. Proposition 1.3.8) and moves (S23) to (S26) in Figure 1.3.13.*

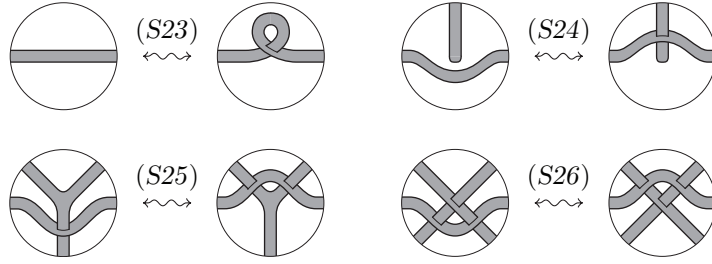


FIGURE 1.3.13. 1-isotopy moves for planar diagrams

Proof. On one hand, we have to realize the modifications of Figures 1.3.2, 1.3.3 and 1.3.4, disregarding the handlebody structure, by moves (S23) to (S26). Proceeding in the order: one move (S23) suffices for the upper part of Figure 1.3.2, while the lower part can be obtained by combining one move (S24) with one move (S25); Figure 1.3.3 requires three moves for each vertical disk, one (S24), one (S25) and one (S26); the upper (resp. lower) part of Figure 1.3.4 can be achieved by one move (S24) (resp. (S25)) for each vertical disk.

On the other hand, the ribbon surfaces of Figure 1.3.13 can be easily provided with adapted handlebody decompositions, so that the relations just described between moves (S23) to (S26) and the above modifications can be reversed. In fact, only the special cases of those modifications with one vertical disk are needed. \square

1.4. Branched coverings

In this section we provide a short account of the theory of branched coverings, with a special emphasis on covering moves in dimension 3 and 4.

Here, we adopt the piecewise-linear approach, which is the most suitable for a unified exposition of the topic in a general context. However, this approach is equivalent to the differentiable one for the special cases we will consider in the next chapters: branched coverings in dimensions 2 and 3 or branched coverings of B^4 whose branching set is a ribbon surface.

DEFINITION 1.4.1. A non-degenerate PL map $p : P \rightarrow Q$ between compact PL manifolds of the same dimension d is called a *branched covering* if there exists an $(d - 2)$ -dimensional subcomplex $B_p \subset Q$, the *branching set* of p , such that the restriction $p|_1 : P - p^{-1}(B_p) \rightarrow Q - B_p$ is an ordinary covering of finite degree n . By the *monodromy* of p we mean the monodromy $\omega_p : \pi_1(Q - B_p, *) \rightarrow \Sigma_n$ of this restriction, which is defined up to conjugation in the permutation group Σ_n , depending on the choice of the base point $*$ and on the numbering of $p^{-1}(*)$. We call p a *simple* branched covering if the monodromy of any meridian loop around a $(d - 2)$ -simplex of B_p is a transposition.

If the subcomplex $B_p \subset Q$ in the definition is minimal with respect to the required property, then we have $B_p = p(S_p)$, where S_p is the *singular set* of p , that is the set of points at which p is not locally injective. In this case, both B_p and S_p , as well as the *pseudo-singular set* $S'_p = \text{Cl}(p^{-1}(B_p) - S_p)$, are (possibly empty) homogeneously $(d - 2)$ -dimensional complexes.

Since p is completely determined, up to PL homeomorphisms, by the ordinary covering $p|_1$ (cf. [19]), we can describe it in terms of the branching set B_p and the

monodromy ω_p . In particular, the monodromies of the meridians around the $(d-2)$ -simplices of B_p determine the structure of the singularities of p . If p is simple, then every point in the interior of a $(d-2)$ -simplex of B_p is the image of one singular point, at which p is topologically equivalent to the complex map $z \mapsto z^2$, and $n-2$ pseudo-singular points.

Starting from $B_p \subset Q$ and ω_p , we can explicitly reconstruct P and p by following steps: 1) choose a $(d-1)$ -dimensional *splitting complex*, that means a subcomplex $C \subset Q - \{*\}$ such that $B_p \subset C$ and the restriction $\omega_{p|_C} : \pi_1(Q - C, *) \rightarrow \Sigma_d$ vanishes; 2) cut Q along C in such a way that each $(d-1)$ -simplex σ of C gives rise to 2 simplices σ^- and σ^+ ; 3) take n copies of the obtained complex (called the *sheets* of the covering) and denote by $\sigma_1^\pm, \dots, \sigma_n^\pm$ the corresponding copies of σ^\pm ; 4) identify in pairs the σ_i^\pm 's according to the monodromy $\rho = \omega_p(\alpha)$ of a loop α meeting C transversally at one point of σ , that is σ_i^- with $\sigma_{\rho(i)}^+$. Up to PL homeomorphisms, P is the result of such identification and p is the map induced by the natural projection of the sheets onto Q .

A convenient representation of p can be given by labeling each $(d-2)$ -simplex of B_p by the monodromy of a preferred meridian around it and each generator (in a finite generating set) of $\pi_1(Q, *)$ by its monodromy, since those loops together generate $\pi_1(Q - B_p, *)$. Of course, only the labels on B_p are needed when Q is simply connected. In any case, with a slight abuse of language if Q is not simply connected, we refer to such a representation as a *labeled branching set*.

DEFINITION 1.4.2. Two branched coverings $p : P \rightarrow Q$ and $p' : P' \rightarrow Q$ are called *equivalent* if and only if there exists PL homeomorphism $h : Q \rightarrow Q$ isotopic to the identity which lifts to a PL homeomorphism $k : P \rightarrow P'$.

By the classical theory of ordinary coverings and [19], such a lifting k of h exists if and only if $h(B_p) = B_{p'}$ and $\omega_{p'}h_* = \omega_p$ up to conjugation in Σ_n , where $h_* : \pi_1(Q - B_p, *) \rightarrow \pi_1(Q - B_{p'}, h(*))$ is the homomorphism induced by h . Therefore, in terms of labeled branching set, the equivalence of branched coverings can be represented by *labeled isotopy*.

Before going on, let us say some further words about the representation through labeled diagrams of the branched coverings in the cases of interest for our purposes. We remark once again that in all those cases PL and smooth are interchangeable.

We represent an n -fold covering $p : P \rightarrow S^3$ (resp. B^3) branched over a link $L \subset S^3$ (resp. a tangle $T \subset B^3$) by a Σ_n -labeled oriented diagram D of L (resp. T), which describes the monodromy of p in terms of the Wirtinger presentation of $\pi_1(S^3 - L)$ (resp. $\pi_1(B^3 - T)$) associated to D . Namely, we label each arc of D by the monodromy of the standard positive meridian around it. Of course, the Wirtinger relations impose constraints on the labeling at crossings, and each Σ_n -labeling of D satisfying such constraints do actually represent an n -fold covering branched over L (resp. T). In this context, labeled isotopy can be realized by means of labeled Reidemeister moves.

For simple coverings, the orientation of D is clearly unnecessary and there are only three possible ways of labeling the arcs at each crossing. These are depicted in Figure 1.4.1. The extension from branching links/tangles to branching embedded

graphs is straightforward. In fact, we only need to take into account extra labeling constraints and labeled moves at the vertices of the graph.

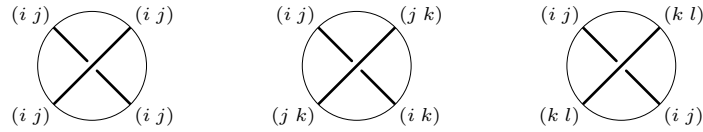


FIGURE 1.4.1. Simple labelings of a link/tangle (i, j, k and l all different)

Now consider an n -fold covering $p : P \rightarrow B^4$ branched over a ribbon surface $S \subset B^4$. We represent it by labeled locally oriented planar diagram of S , where the labels give the monodromy of the meridians in the Wirtinger presentation of $\pi_1(B^4 - S)$ associated to the diagram. Actually, since we will only consider simple coverings, we will never need local orientations.

The same labeling rules as above apply to ribbon intersections as well as to ribbon crossings, these are depicted in Figure 1.4.2. In particular, at a ribbon intersection the label of the band passing through the other gets conjugated by the label of this. Notice that, contrary to what happens for ribbon intersections (in the case of distinct but not disjoint labels), when a ribbon crosses under another one, its label changes only locally (on the undercrossing region).

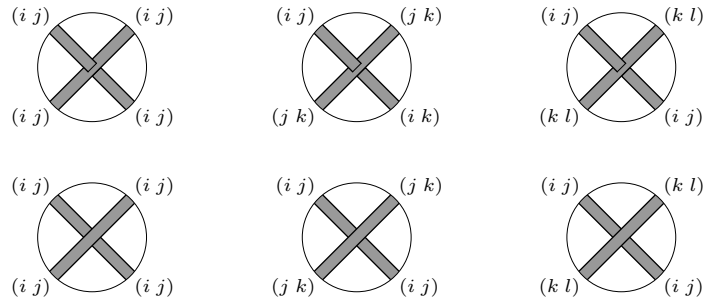


FIGURE 1.4.2. Simple labelings of a ribbon surface (i, j, k and l all different)

We remark that, if $S \subset B^4$ is a labeled ribbon surface representing an n -fold (simple) covering of $p : P \rightarrow B^4$, then $L = S \cap S^3$ is a labeled link representing the restriction $p|_{\text{Bd} P} : \text{Bd} P \rightarrow S^3$. This is still a n -fold (simple) covering, having the diagram of S as a splitting complex.

Labeled ribbon surfaces in B^4 (that is coverings of B^4 simply branched over ribbon surfaces) represent all the 4-dimensional 2-handlebodies. In fact, by Montesinos [52] (cf. Chapter 3), for the connected case it suffices to take labels from the three transpositions of Σ_3 (that is to consider 3-fold simple coverings).

Though labeled isotopy of branching ribbon surfaces preserves the covering manifold P up to diffeomorphisms, we are interested in the (perhaps more restrictive) notion of *labeled 1-isotopy*, which preserves P up to 2-deformations (cf. Lemma 3.3.1). This can be realized by means of labeled diagram isotopy and labeled 1-isotopy moves, that is diagram isotopy and 1-isotopy moves of Figure 1.3.13 suitably labeled according to the rules discussed above.

By a *covering move*, we mean any non-isotopic modification making a labeled branching set representing a branched covering $p : P \rightarrow Q$ into one representing

a different branched covering $p' : P \rightarrow Q$ between the same manifolds (up to PL homeomorphisms). We call such a move *local*, if the modification takes place inside a cell and can be performed whatever is the rest of labeled branching set outside. In the figures depicting local moves, we will draw only the portion of the labeled branching set inside the relevant cell, assuming everything else to be fixed.

As a primary source of covering moves, we consider the following two very general equivalence principles (cf. [63]). Several special cases of these principles have already appeared in the literature and we can think of them as belonging to the “folklore” of branched coverings.

DISJOINT MONODROMIES CROSSING. *Subcomplexes of the branching set of a covering that are labeled with disjoint permutations can be isotoped independently from each other without changing the covering manifold.*

The reason why this principle holds is quite simple. Namely, being the labeling of the subcomplexes disjoint, the sheets non-trivially involved by them do not interact, at least over the region where the isotopy takes place. Hence, the relative position of such subcomplexes is not relevant in determining the covering manifold. Typical applications of this principle are given by the local covering moves (M2), (R2) and (R4) in Figures 1.4.4, 1.4.5 and 1.4.7).

It is worth observing that, abandoning transversality, the disjoint monodromies crossing principle also gives the special case of the next principle when the σ_i 's are disjoint and L is empty.

COHERENT MONODROMIES MERGING. *Let $p : P \rightarrow Q$ be any branched covering with branching set B_p and let $\pi : E \rightarrow K$ be a connected disk bundle embedded in Q , in such a way that: 1) there exists a (possibly empty) subcomplex $L \subset K$ for which $B_p \cap \pi^{-1}(L) = L$ and the restriction of π to $B_p \cap \pi^{-1}(K - L)$ is an unbranched covering of $K - L$; 2) the monodromies $\sigma_1, \dots, \sigma_k$ relative to a fundamental system $\omega_1, \dots, \omega_k$ for the restriction of p over a given disk $D = \pi^{-1}(x)$, with $x \in K - L$, are coherent in the sense that $p^{-1}(D)$ is a disjoint union of disks. Then, by contracting the bundle E fiberwise to K , we get a new branched covering $p' : P \rightarrow Q$, whose branching set $B_{p'}$ is equivalent to B_p , except for the replacement of $B_p \cap \pi^{-1}(K - L)$ by $K - L$, with the labeling uniquely defined by letting the monodromy of the meridian $\omega = \omega_1 \dots \omega_k$ be $\sigma = \sigma_1 \dots \sigma_k$.*

We remark that, by connectedness and property 1, the coherence condition required in 2 actually holds for any $x \in K$. Then, we can prove that p and p' have the same covering manifold, by a straightforward fiberwise application of the Alexander's trick to the components of the bundle $\pi \circ p : p^{-1}(E) \rightarrow K$. A coherence criterion can be immediately derived from Section 1 of [58].

The coherent monodromy merging principle originated from a classical perturbation argument in algebraic geometry and appeared in the literature as a way to deform non-simple coverings between surfaces into simple ones, by going in the opposite direction from p' to p (cf. [8]). In the same way, it can be used in dimension 3, both for achieving simplicity (cf. [25, 26]) and removing singularities from the branching set. We will do that in the proof of Theorem 6.2.4 by means of the moves (G1) and (G2) of Figure 1.4.3, which are straightforward applications of this principle. Actually, similar results could be proved in dimension 4 for labeled singular surfaces

representing possibly non-simple branched coverings, but we will not consider them here.

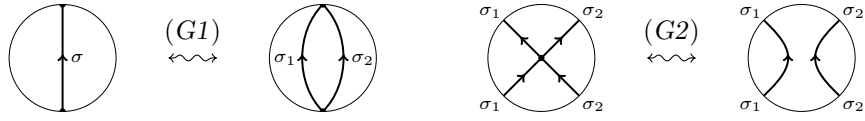


FIGURE 1.4.3. Covering moves for labeled graphs ($\sigma = \sigma_1 \cdot \sigma_2$)

Finally, we consider the notion of stabilization. This is a particular local covering move, which makes sense only for branched coverings of S^m or B^m and, differently from all the previous moves, changes the degree of the covering, increasing it by one.

STABILIZATION. A branched covering $p : P \rightarrow S^d$ (resp. $p : P \rightarrow B^d$) of degree n , can be stabilized to degree $n + 1$ by adding to the labeled branching set a trivial separate $(d - 2)$ -sphere (resp. regularly embedded $(d - 2)$ -disk) labeled with the transposition $(i \ n+1)$, for some $i = 1, \dots, n$.

The covering manifold of such a stabilization is still P , up to PL homeomorphisms. In fact, it turns out to be the connected sum (resp. boundary connected sum) of P itself, consisting of the sheets $1, \dots, n$, with the copy of S^d (resp. B^d) given by the extra trivial sheet $n + 1$.

By *stabilization to degree m* (or *m -stabilization*) of a branched covering $p : P \rightarrow S^d$ (resp. $p : P \rightarrow B^d$) of degree $n \leq m$ we mean the branched covering of degree m obtained from it by performing $m - n$ stabilizations as above. In particular, this leaves p unchanged if $m = n$.

Concerning the cases of interest for this paper, Figure 1.4.4 shows the covering moves introduced by Montesinos (cf. [56]) for labeled links representing simple coverings of S^3 , while in Figure 1.4.5 we introduce new local covering moves for labeled ribbon surfaces representing simple coverings of B^4 , which we call *ribbon moves*.

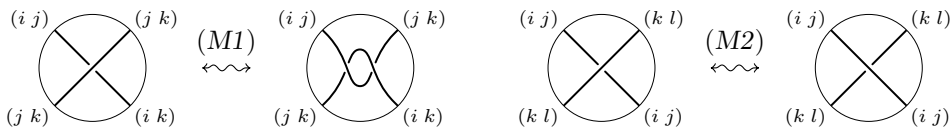


FIGURE 1.4.4. Montesinos moves (i, j, k and l all different)

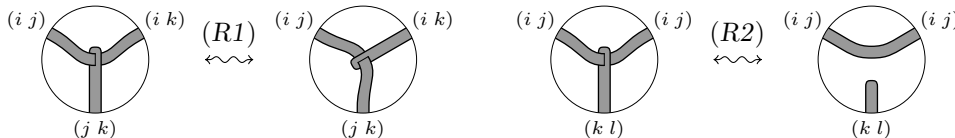


FIGURE 1.4.5. Ribbon moves (i, j, k and l all different)

The coherent monodromy merging principle provides an easy way to verify that $(M1)$ and $(R1)$ are covering moves. This is shown in Figure 1.4.6, where the principle is applied in the first and in the last step for both the moves, the middle step being just labeled isotopy. Moves $(R2)$ and $(M2)$ are nothing else than simple applications of the disjoint monodromies principle, as we observed above.

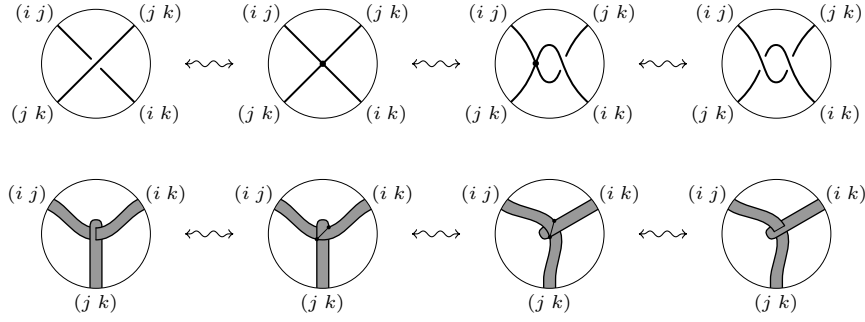


FIGURE 1.4.6. Moves $(M1)$ and $(R1)$ are local covering moves

In the next proposition, we derive from $(R1)$ and $(R2)$ the auxiliary covering moves $(R3)$ to $(R6)$ depicted in Figure 1.4.7, which will be very useful in the following chapters.

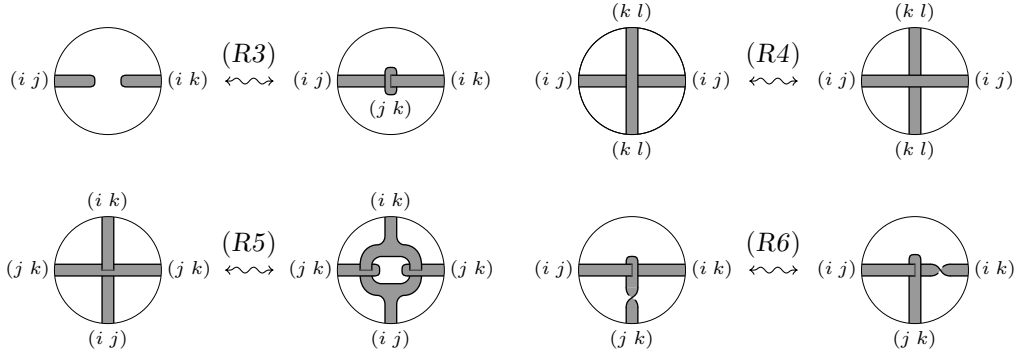


FIGURE 1.4.7. Other moves for labeled ribbon surfaces (i, j, k and l all different)

PROPOSITION 1.4.3. *Up to labeled 1-isotopy, the local moves $(R3)$ to $(R6)$ depicted in Figure 1.4.7 can be generated the ribbon moves $(R1)$ and $(R2)$, hence they are covering moves.*

Proof. Move $(R4)$ can be easily obtained as the composition of two moves $(R2)$. Figures 1.4.8, 1.4.9 and 1.4.10 respectively shows how to get moves $(R3)$, $(R5)$ and $(R6)$ in terms of labeled 1-isotopy and moves $(R1)$.

Here, all the arrows which are not marked by $(R1)$ represent labeled 1-isotopy. Namely, we use the following labeled 1-isotopy moves: $(S24)$ in Figure 1.4.8; $(S1)$, $(S2)$, $(S5)$, $(S21)$ and $(S25)$ in Figure 1.4.9; $(S14)$ and $(S20)$ in Figure 1.4.10. \square

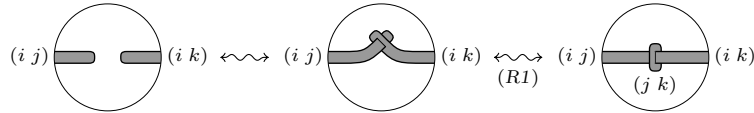


FIGURE 1.4.8. Deriving the covering move $(R3)$

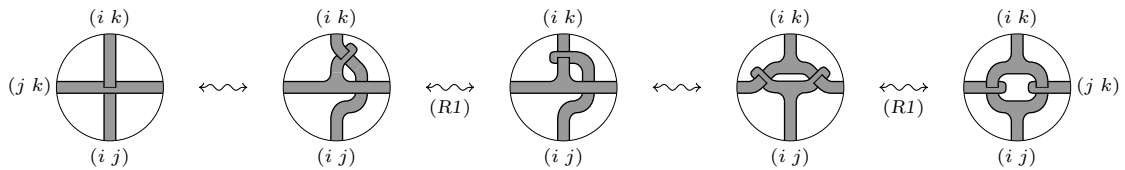


FIGURE 1.4.9. Deriving the covering move $(R5)$

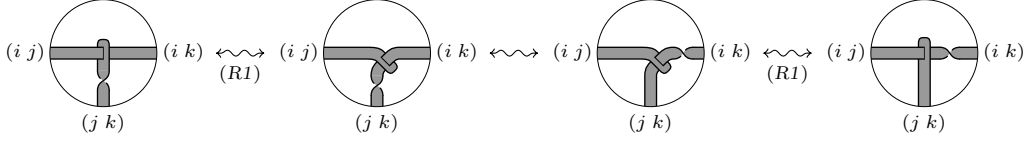


FIGURE 1.4.10. Deriving the covering move (R6)

REMARK 1.4.4. By labeled 1-isotopy and moves above, any n -labeled ribbon surface tangle S can be made orientable under the mild hypothesis that there are enough different labels to generate Σ_n , or equivalently that the covering space represented by S is connected. In fact, twist transfer (R6) allows us to eliminate non-orientable bands as shown in Figure 1.4.11.

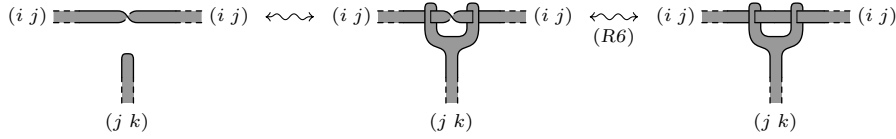


FIGURE 1.4.11. Making labeled ribbon surfaces orientable (i, j and k all different)

1.5. Categories

We list here some basic definitions and statements from the general theory of categories, which are used repeatedly in the paper. A complete reference on the subject is [46].

Given a category \mathcal{C} , we denote by $\text{Obj } \mathcal{C}$ the set of its objects and by $\text{Mor } \mathcal{C}$ the set of morphisms of \mathcal{C} , always assuming that \mathcal{C} is a small category. Moreover, for any $C, C' \in \text{Obj } \mathcal{C}$, the set of morphisms of \mathcal{C} with source C and target C' are denoted by $\text{Mor}_{\mathcal{C}}(C, C')$.

DEFINITION 1.5.1. Given two functors $S, T : \mathcal{C} \rightarrow \mathcal{D}$, a *natural transformation* $\tau : S \rightarrow T$ is a map that assigns to each object $C \in \text{Obj } \mathcal{C}$ a morphism $\tau_C : S(C) \rightarrow T(C)$ of \mathcal{D} , in such a way that for every morphism $f : C \rightarrow C'$ of \mathcal{C} , the following diagram commutes.

$$\begin{array}{ccc} S(C) & \xrightarrow{\tau_C} & T(C) \\ S(f) \downarrow & & \downarrow T(f) \\ S(C') & \xrightarrow{\tau_{C'}} & T(C') \end{array}$$

A natural transformation τ is called *natural equivalence* if τ_C is an isomorphisms for every $C \in \text{Obj } \mathcal{C}$. In this case we write $\tau : S \simeq T$.

DEFINITION 1.5.2. Two categories \mathcal{C} and \mathcal{D} are said to be *equivalent* if there exist functors $T : \mathcal{C} \rightarrow \mathcal{D}$ and $T' : \mathcal{D} \rightarrow \mathcal{C}$, such that $T' \circ T \simeq \text{id}_{\mathcal{C}}$ and $T \circ T' \simeq \text{id}_{\mathcal{D}}$. In this case we call T (and T' as well) an *equivalence of categories*.

We remind that a functor $T : \mathcal{C} \rightarrow \mathcal{D}$ is *faithful* (resp. *full*) if for every $C, C' \in \text{Obj } \mathcal{C}$ the induced map $\text{Mor}_{\mathcal{C}}(C, C') \rightarrow \text{Mor}_{\mathcal{D}}(T(C), T(C'))$ is injective (resp. surjective).

PROPOSITION 1.5.3. *A functor $T : \mathcal{C} \rightarrow \mathcal{D}$ is an equivalence of categories if and only if it is full and faithful and for any object $D \in \text{Obj } \mathcal{D}$ there exists an object $C \in \text{Obj } \mathcal{C}$ and an isomorphism $\sigma_D : D \rightarrow T(C)$.*

Proof. Suppose that T is equivalence of categories. Then there exist a functor $T' : \mathcal{D} \rightarrow \mathcal{C}$ and natural equivalences $\tau : T' \circ T \simeq \text{id}_{\mathcal{C}}$ and $\sigma : T \circ T' \simeq \text{id}_{\mathcal{D}}$. If $T(f_1) = T(f_2)$ for some $f_1, f_2 \in \text{Mor}_{\mathcal{C}}(C, C')$, we have $T'(T(f_1)) = T'(T(f_2))$. Since $T'(T(f_i)) = \tau_{C'}^{-1} \circ f_i \circ \tau_C$ we can conclude that $f_1 = f_2$. Therefore T is faithful, and symmetrically T' is faithful as well. To see that T is full, take $g \in \text{Mor}_{\mathcal{D}}(T(C), T(C'))$ and let $f = \tau_{C'} \circ T'(g) \circ \tau_C^{-1} \in \text{Mor}_{\mathcal{C}}(C, C')$. Then $T'(T(f)) = \tau_{C'}^{-1} \circ f \circ \tau_C = T'(g)$. Since T' is faithful, this implies that $T(f) = g$, which proves that T is full. Moreover, any $D \in \text{Obj } \mathcal{D}$ is isomorphic to $T(T'(D))$ through σ_D . This completes the proof that the condition is necessary.

To see that the condition is sufficient, suppose that $T : \mathcal{C} \rightarrow \mathcal{D}$ is full and faithful and that for any object $D \in \text{Obj } \mathcal{D}$ there exists an object $C \in \text{Obj } \mathcal{C}$ and an isomorphism $\sigma_D : D \rightarrow T(C)$. Then define the functor $T' : \mathcal{D} \rightarrow \mathcal{C}$ as $T'(g) = T^{-1}(\sigma_{D'} \circ g \circ \sigma_D^{-1})$ for any $g \in \text{Mor}_{\mathcal{D}}(D, D')$, and put $\tau_C : T^{-1}(\sigma_{T(C)})$ for any $C \in \text{Obj } \mathcal{C}$. We leave to the reader the rest of the details. \square

We remind that a subcategory $\mathcal{B} \subset \mathcal{C}$ is said to be *full* if $\text{Mor}_{\mathcal{B}}(B, B') = \text{Mor}_{\mathcal{C}}(B, B')$ for any $B, B' \in \mathcal{B}$, in other word if the inclusion functor $\iota : \mathcal{B} \hookrightarrow \mathcal{C}$ is a full functor.

COROLLARY 1.5.4. *Given a subcategory $\mathcal{B} \subset \mathcal{C}$, the inclusion functor $\iota : \mathcal{B} \hookrightarrow \mathcal{C}$ is an equivalence of categories if and only if \mathcal{B} is full and any object of \mathcal{C} is isomorphic to an object of \mathcal{B} .*

DEFINITION 1.5.5. We say that \mathcal{C} is a *strict monoidal category* if there exists an associative bifunctor $\diamond : \mathcal{C} \times \mathcal{C} \rightarrow \mathcal{C}$ and an object $\mathbf{1}$ which is right and left unit for \diamond . Then \diamond is called the *product* on \mathcal{C} and $\text{id}_{\mathbf{1}}$ is called the *unit* of \diamond .

Being more explicit, the bifunctor \diamond consists in two associative binary operations

$$\begin{aligned} \diamond &: \text{Obj}(\mathcal{C}) \times \text{Obj}(\mathcal{C}) \rightarrow \text{Obj}(\mathcal{C}), \\ \diamond &: \text{Mor}_{\mathcal{C}}(A, B) \times \text{Mor}_{\mathcal{C}}(A', B') \rightarrow \text{Mor}_{\mathcal{C}}(A \diamond B, A' \diamond B'), \end{aligned}$$

such that

$$\mathbf{1} \diamond A = A = A \diamond \mathbf{1} \quad \text{and} \quad \text{id}_A \diamond \text{id}_B = \text{id}_{A \diamond B}$$

for any $A, B \in \text{Obj } \mathcal{C}$, while

$$\text{id}_{\mathbf{1}} \diamond f = f = f \diamond \text{id}_{\mathbf{1}} \quad \text{and} \quad (f' \diamond g') \circ (f \diamond g) = (f' \circ f) \diamond (g' \circ g)$$

for any $f \in \text{Mor}_{\mathcal{C}}(A, B), f' \in \text{Mor}_{\mathcal{C}}(B, C), g \in \text{Mor}_{\mathcal{C}}(A', B'), g' \in \text{Mor}_{\mathcal{C}}(B', C')$.

DEFINITION 1.5.6. A strict monoidal category $\mathcal{C} = (\mathcal{C}, \diamond, \mathbf{1})$ is called *braided* if for any $A, B \in \text{Obj}(\mathcal{C})$ there exists natural isomorphism $\gamma_{A,B} : A \diamond B \rightarrow B \diamond A$ such that

$$\gamma_{A, B \diamond C} = (\text{id}_B \diamond \gamma_{A,C}) \circ (\gamma_{A,B} \diamond \text{id}_C) \quad \text{and} \quad \gamma_{A \diamond B, C} = (\gamma_{A,C} \diamond \text{id}_B) \circ (\text{id}_A \diamond \gamma_{B,C}).$$

We recall that a family of morphisms $\nu_A : A \rightarrow B$ is called *natural* if for any morphism $f : A \rightarrow A'$ we have $\nu_{A'} \circ f = f \circ \nu_A$.

DEFINITION 1.5.7. A braided strict monoidal category $\mathcal{C} = (\mathcal{C}, \diamond, \mathbf{1}, \gamma)$ is called *autonomous* (or rigid) (see [70]) if for every $A \in \text{Obj } \mathcal{C}$ it is given a *right dual* object $A^* \in \text{Obj } \mathcal{C}$ and two morphisms

$$\begin{aligned}\Lambda_A &: \mathbf{1} \rightarrow A^* \diamond A \quad (\text{coform}), \\ \lambda_A &: A \diamond A^* \rightarrow \mathbf{1} \quad (\text{form}),\end{aligned}$$

such that the compositions

$$\begin{aligned}A &\longrightarrow A \diamond \mathbf{1} \xrightarrow{\text{id} \diamond \Lambda_A} A \diamond (A^* \diamond A) \longrightarrow (A \diamond A^*) \diamond A \xrightarrow{\lambda_A \diamond \text{id}} \mathbf{1} \diamond A \longrightarrow A, \\ A^* &\longrightarrow \mathbf{1} \diamond A^* \xrightarrow{\Lambda_A \diamond \text{id}} (A^* \diamond A) \diamond A^* \longrightarrow A^* \diamond (A \diamond A^*) \xrightarrow{\text{id} \diamond \lambda_A} A^* \diamond \mathbf{1} \longrightarrow A^*,\end{aligned}$$

are the identities. Then, given any morphism $F : A \rightarrow B$ in \mathcal{C} , we define its *dual* $F^* : B^* \rightarrow A^*$ as follows:

$$F^* = (\text{id}_{A^*} \diamond \lambda_B) \circ (\text{id}_{A^*} \diamond F \diamond \text{id}_{B^*}) \circ (\Lambda_A \diamond \text{id}_{B^*}).$$

DEFINITION 1.5.8. A *twist* in a braided strict monoidal category $\mathcal{C} = (\mathcal{C}, \diamond, \mathbf{1}, \gamma)$ is a family of natural isomorphisms $\theta_A : A \rightarrow A$ with $A \in \text{Obj } \mathcal{C}$, such that $\theta_{\mathbf{1}} = \text{id}_{\mathbf{1}}$ and

$$\theta_{A \diamond B} = \gamma_{B,A} \circ (\theta_B \diamond \theta_A) \circ \gamma_{A,B}$$

for any $A, B \in \text{Obj } \mathcal{C}$.

An autonomous braided strict monoidal category $\mathcal{C} = (\mathcal{C}, \diamond, \mathbf{1}, \gamma, _*, \Lambda, \lambda)$ equipped with a distinguished twist such that $\theta_{A^*} = (\theta_A)^*$ for any object $A \in \text{Obj } \mathcal{C}$ is called *tortile* (the terminology is from [70]).

Many of the categories that we use in the present work are strict monoidal categories generated by certain set of elementary morphisms and relations between those morphisms. We outline here the general construction of such categories (see also section 2 in [70] and the references thereby).

Let S be a (finite) set of *elementary objects*. We denote by $\Pi S = \cup_{m=0}^{\infty} S^m$ the free monoid generated by S , concretely realized as the set of (possibly empty) finite sequences of objects in S , with monoidal product $\diamond : \Pi S \times \Pi S \rightarrow \Pi S$ given by juxtaposition of sequences and unit $\mathbf{1}$ given by the empty sequence (cf. Corollary II.7.2 in [46]). Let also $G(S, E)$ be a directed graph, having ΠS as set of vertices and a finite set E of arrows (oriented edges), which we call *elementary morphisms*. We will always assume that E contains a distinguished loop arrow $\langle \text{id}_s \rangle$ starting and ending at s , for every $s \in S$.

Let now $\bar{G}(S, E)$ be the graph with the same set of vertices ΠS and arrows

$$\sigma \diamond e \diamond \sigma' : \sigma \diamond \sigma_0 \diamond \sigma' \rightarrow \sigma \diamond \sigma_1 \diamond \sigma'$$

for every $e : \sigma_0 \rightarrow \sigma_1 \in E$ and every $\sigma, \sigma' \in \Pi S$. We call any arrow of this form an *expansion* of the elementary morphism e and use the notations $\sigma \diamond e = \sigma \diamond e \diamond \mathbf{1}$ and $e \diamond \sigma' = \mathbf{1} \diamond e \diamond \sigma'$. Moreover, we identify e with $\mathbf{1} \diamond e \diamond \mathbf{1}$ for every $e \in E$, in such a way that $G(S, E) \subset \bar{G}(S, E)$.

Finally, we denote by $F(S, E)$ the free category generated by the graph $\bar{G}(S, E)$. We recall from [46] that set of objects of $F(S, E)$ is ΠS , the set of vertices of the

graph, while the set of morphisms $\text{Mor}_{F(S,E)}(\sigma_0, \sigma_1)$ consists of all paths of consecutive arrows from σ_0 to σ_1 in $\overline{G}(S, E)$. Here, the composition is given by path concatenation and the identity morphisms represented by the paths of length 0.

The notion of expansion can be extended in a unique way to a compositive biaction of ΠS on the morphisms of $F(S, E)$. Explicitly, this is defined by the formulas

$$\begin{aligned}\sigma \diamond (\tau \diamond e \diamond \tau') \diamond \sigma' &= (\sigma \diamond \tau) \diamond e \diamond (\tau' \diamond \sigma'), \\ \sigma \diamond (f_1 \dots f_n) \diamond \sigma' &= (\sigma \diamond f_1 \diamond \sigma') \dots (\sigma \diamond f_n \diamond \sigma'),\end{aligned}$$

for every $e \in E$, every $\sigma, \sigma', \tau, \tau' \in \Pi S$ and every $f_1, \dots, f_n \in \overline{G}(E, S)$ with $n \geq 0$. We still call $\sigma \diamond f \diamond \sigma'$ an *expansion* of f for every $f = f_1 \dots f_n \in \text{Mor } F(S, E)$. In particular, for $n = 0$ we have that identities expand to identities.

PROPOSITION 1.5.9. *Given S and E as above and $R = \{R(\sigma_0, \sigma_1) \mid \sigma_0, \sigma_1 \in \Pi S\}$, with each $R(\sigma_0, \sigma_1)$ being a (possibly empty) relation on $\text{Mor}_{F(S,E)}(\sigma_0, \sigma_1)$, let $C(S, E, R)$ be the quotient category of $F(S, E)$ modulo the equivalence relations generated by:*

- (a) $\langle \text{id}_s \rangle \simeq \text{id}_s$ for every $s \in S$;
- (b) $\sigma \diamond \text{id}_s \diamond \sigma' \simeq \text{id}_{\sigma \diamond s \diamond \sigma'}$ for every $s \in S$ and $\sigma, \sigma' \in \Pi S$;
- (c) $(f \diamond \sigma'_1) \circ (\sigma_0 \diamond f') \simeq (\sigma_1 \diamond f') \circ (f \diamond \sigma'_0)$ for any $f : \sigma_0 \rightarrow \sigma_1, f' : \sigma'_0 \rightarrow \sigma'_1 \in F(S, E)$;
- (d) all the expansions of the relations in R .

Then $C(S, E, R)$ admits a strict monoidal structure defined by

$$f \diamond f' = (f \diamond \sigma'_1) \circ (\sigma_0 \diamond f') = (\sigma_1 \diamond f') \circ (f \diamond \sigma'_0)$$

for any $f : \sigma_0 \rightarrow \sigma_1, f' : \sigma'_0 \rightarrow \sigma'_1 \in C(S, E, R)$, with the unit object $\mathbf{1}$ being the empty set.

Proof. In the light of the definitions, the proof is straightforward. \square

DEFINITION 1.5.10. We call the strict monoidal category $C(S, E, R)$ defined in the previous proposition the *strict monoidal category generated by the set S of elementary objects and the set E of elementary morphisms modulo the set R of elementary relations*. In the case when $R = B \cup A$, where B represents defining axioms of a braided structure in a monoidal category, while E and A represent respectively the basic morphisms and the defining axioms which endow S with a certain algebraic structure, for example braided Hopf algebra, we will refer to the category $C(S, E, R)$ as the *braided strict monoidal category freely generated by the algebraic structure S* (cf. [35], Section 4, Definition 1).

2. 4-dimensional cobordisms and Kirby tangles

In this chapter we introduce 4-dimensional relative 2-handlebody cobordisms between 3-dimensional 1-handlebodies and their representations in terms of bridged tangles and Kirby tangles.

Since we allow handlebodies to have more than one 0-handles and even to be disconnected, we need to generalize the usual notions of bridged tangle and Kirby tangle to include the case of multiple 0-handles. This is done in Section 2.2.

All the handlebodies in this chapter are assumed to be orientable. According to the discussion in Section 1.2, this means that 1-handles can be specified just by the unordered pair of (possibly coinciding) 0-handles where they are attached.

2.1. The categories of relative handlebody cobordisms \mathcal{Chb}_n^{3+1}

Here, we define the category \mathcal{Chb}_n^{3+1} of 4-dimensional relative 2-handlebody cobordisms between 3-dimensional 1-handlebodies with n 0-handles, for any $n \geq 1$.

An object in \mathcal{Chb}_n^{3+1} is a 3-dimensional relative 1-handlebody M build on the disjoint union $\sqcup_{i=1}^n \text{Int } B_i^2$ of n disks, having no 0-handles. With some abuse of notation we write $M = \cup_{i=1}^n H_i^0 \cup_{j=1}^m H_j^1$ and call $H_i^0 = B_i^2 \times [0, 1]$ the i -th 0-handle of M . While the H_j^1 's are the 1-handles whose attaching regions are contained in $\delta M^0 = \sqcup_{i=1}^n \text{Int } B_i^2 \times \{1\}$ (cf. Definition 1.2.2). We define the *front boundary* of M as

$$\partial M = \text{Cl } \delta M = \text{Cl}(\text{Bd } M - \cup_{i=1}^n (B_i^2 \times \{0\}) \cup (\text{Bd } B_i^2 \times [0, 1])).$$

Given two objects $M_0 = \cup_{i=1}^n H_{i,0}^0 \cup_{j=1}^{m_0} H_{j,0}^1$ and $M_1 = \cup_{i=1}^n H_{i,1}^0 \cup_{k=1}^{m_1} H_{k,1}^1$, let $X(M_0, M_1)$ be the 3-dimensional 1-handlebody obtained from $M_0 \sqcup M_1$ by attaching for any $i \leq n$ a single 1-handle $\bar{H}_i^1 \cong B_i^2 \times [0, 1]$ between the i -th 0-handles of M_0 and M_1 , through the identification of $B_i^2 \times \{c\} \subset \bar{H}_i^1$ with $B_i^2 \times \{0\} \subset H_{i,c}^0$ for $c = 0, 1$. Actually, one could cancel the new 1-handles against some of the 0-handles, thinking of $X(M_0, M_1)$ as a 3-dimensional 1-handlebody with n 0-handles of the form $\bar{H}_i^0 = H_{i,0}^0 \cup H_{i,1}^0 \cup \bar{H}_i^1$.

Now, let $Y(M_0, M_1) = \sqcup_{i=1}^n B_i^2 \times [0, 1] \times [0, 1] \cup (M_0 \times [0, 0.1]) \cup (M_1 \times [0.9, 1])$. We identify $X(M_0, M_1) \times [0, 1]$ with $Y(M_0, M_1)$, in such a way that $X(M_0, M_1) \times \{0\}$ is canonically identified with $\sqcup_{i=1}^n B_i^2 \times \{0\} \times [0, 1] \cup (M_0 \times \{0\}) \cup (M_1 \times \{1\}) \subset Y(M_0, M_1)$, while $X(M_0, M_1) \times \{1\}$ corresponds to $\sqcup_{i=1}^n (B_i^2 \times \{1\} \times [0.1, 0.9]) \cup_{j=1}^{m_0} (H_{j,0}^1 \times \{0.1\}) \cup_{k=1}^{m_1} (H_{k,1}^1 \times \{0.9\}) \subset Y(M_0, M_1)$. An example of $X(M_0, M_1)$ and $Y(M_0, M_1)$ is presented in Figure 2.1.1, where all the horizontal segments represent copies of B^2 .

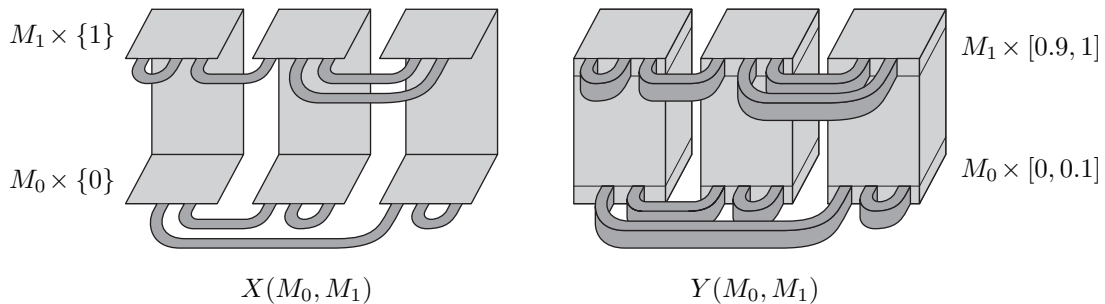


FIGURE 2.1.1. The base space of a relative handlebody cobordism in \mathcal{Chb}_n^{3+1}

A morphism $W : M_0 \rightarrow M_1$ in \mathcal{Chb}_n^{3+1} is a 4-dimensional relative 2-handlebody build on $X(M_0, M_1)$ without 0-handles, considered up to 2-deformation of relative handlebodies (cf. Section 1.2). We remind that W is obtained by attaching 1- and 2- handles to $W^0 = W^{-1} = X(M_0, M_1) \times [0, 1]$. According to the setting above, we identify W^0 with $Y(M_0, M_1)$, in such a way that M_0 and M_1 correspond to $M_0 \times \{0\} \subset Y(M_0, M_1)$ and $M_1 \times \{1\} \subset Y(M_0, M_1)$ respectively. Moreover, we define the *front boundary* of W as the following bounded 3-manifold in $\text{Bd } W$:

$$\partial W = \text{Cl}(\text{Bd } W - (X(M_0, M_1) \times \{0\}) - \cup_{i=1}^n (\text{Bd } B_i^2 \times [0, 1] \times [0, 1])).$$

In particular, if W has no 1- and 2-handles we have:

$$\partial Y(M_0, M_1) \cong (\partial M_0 \times [0, 1]) \cup (X(M_0, M_1) \times \{1\}) \cup (\partial M_1 \times [0, 1]).$$

The composition of two morphisms $W_1 : M_0 \rightarrow M_1$ and $W_2 : M_1 \rightarrow M_2$ in \mathcal{Chb}_n^{3+1} is the morphism $W : M_0 \rightarrow M_2$ defined in the following way. Let $W = W_1 \cup_{M_1} W_2$ be the space obtained from $W_1 \sqcup W_2$ by identifying the target $M_1 \subset W_1$ of W_1 with the source $M_1 \subset W_2$ of W_2 , through the identity. Up to rescaling the last coordinate, we regard the subspace $Y(M_0, M_1) \cup_{M_1} Y(M_1, M_2) \subset W$ as $Y(M_0, M_2)$ with certain 1-handles attached to it on the part of the boundary corresponding to the interior of $X(M_0, M_2) \times \{1\}$. Namely, we have one (4-dimensional) 1-handle $\bar{H}_k^1 = (H_{k,1}^1 \times [0.9, 1]) \cup_{H_{k,1}^1} (H_{k,1}^1 \times [0, 0.1])$ attached to $Y(M_0, M_2)$ for each (3-dimensional) 1-handle $H_{k,1}^1$ of M_1 (see Figure 2.1.2 for an example). Now, all the handles of the relative handlebodies W_1 and W_2 are attached to $Y(M_0, M_1) \cup_{M_1} Y(M_1, M_2) = Y(M_0, M_2) \cup_{k=1}^{m_1} \bar{H}_k^1$, to endow W with a structure of 4-dimensional relative 2-handlebody build on $X(M_0, M_2)$. We notice that $\partial W = \partial W_1 \cup_{\partial M_1} \partial W_2$.

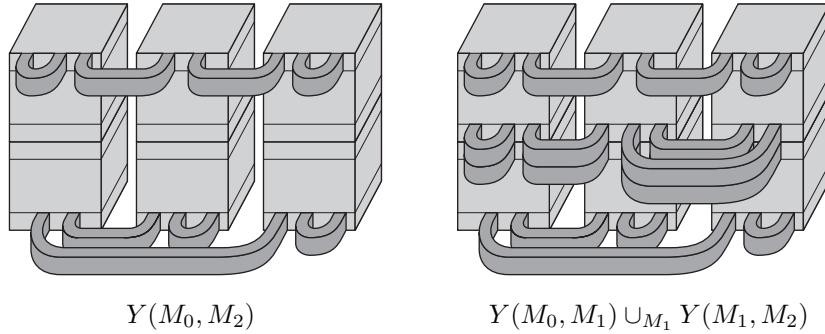


FIGURE 2.1.2. Composing two relative handlebody cobordisms in \mathcal{Chb}_n^{3+1}

The identity id_M of an object $M = \cup_{i=1}^n H_i^0 \cup_{j=1}^m H_j^1$ is represented by the product cobordism $M \times [0, 1]$, whose handlebody structure is given by one 2-handle $H_j^2 = H_j^1 \times [0.1, 0.9] \subset M \times [0, 1]$ for each 1-handle H_j^1 of M (cf. Figure 2.1.3).

Moreover, given any ambient isotopy $\Phi = (\varphi_t)_{t \in [0, 1]}$ of $\cup_{i=1}^n \text{Bd } H_i^0$ fixed outside $\cup_{i=1}^n B_i^2 \times \{1\}$ and constant in the time intervals $[0, 0.1]$ and $[0.9, 1]$, we consider the new object M' which differs from M only for the attaching maps of the 1-handles being isotoped through Φ . In other words, if h_j^1 is the attaching map of the 1-handle H_j^1 in M , then $\varphi_1 \circ h_j^1$ is the attaching map of the same 1-handle in M' . Now, for any

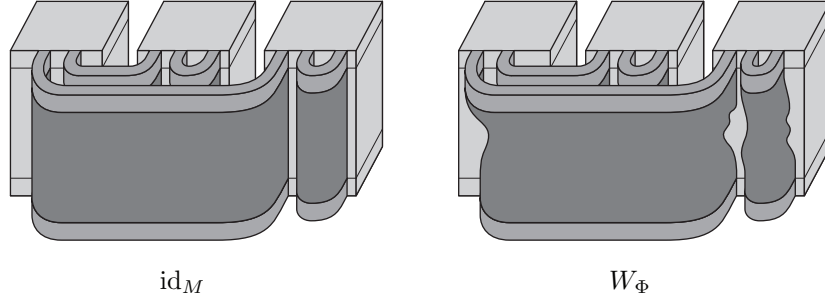


FIGURE 2.1.3. Identity and isotopy cobordisms

$j \leq m$ we attach $H_j^1 \times [0, 1]$ to $\cup_{i=1}^n H_i^0 \times [0, 1]$ by the map $(x, t) \mapsto (\varphi_t(h_j^1(x)), t)$. In this way, we obtain a cobordism W_Φ between M and M' which has a natural structure of 4-dimensional relative 2-handlebody build on $X(M, M')$, with one 2-handle H_j^2 given by $H_j^1 \times [0.1, 0.9] \subset W_\Phi$ for each 1-handle H_j^1 of M (cf. Figure 2.1.3). Then, the morphism $W_\Phi : M \rightarrow M'$ represented by such cobordism is an isomorphism, whose inverse is $W_{\Phi^{-1}} : M' \rightarrow M$ with $\Phi^{-1} = (\varphi_t^{-1})_{t \in [0, 1]}$.

According to Corollary 1.5.4, the fact that there is an isomorphism between any two 3-dimensional handlebodies which are obtained by changing the attaching maps through isotopy, allows us to replace the category \mathcal{Chb}_n^{3+1} with the full subcategory equivalent to it, whose objects are standard handlebodies.

For $n \geq 1$, let $\mathcal{G}_n = \{1, \dots, n\}^2$ be the set of ordered pairs of integers between 1 and n (the reason for this notation is that in Chapter 4 we will consider \mathcal{G}_n as a groupoid) and let $\Pi\mathcal{G}_n = \cup_{m=0}^\infty \mathcal{G}_n^m$ be the set of (possibly empty) finite sequences of pairs in \mathcal{G}_n .

DEFINITION 2.1.1. Given any $\pi = ((i_1, j_1), \dots, (i_m, j_m)) \in \Pi\mathcal{G}_n$ we define the standard 3-dimensional 1-handlebody $M_\pi^n = \cup_{i=1}^n H_i^0 \cup_{j=1}^m H_j^1$ as follows:

- 1) for $1 \leq i \leq n$, let $H_i^0 = E_i \times [0, 1]$ be a copy of $E \times [0, 1]$, with $E = [0, 1]^2$ the standard square;
- 2) if $m \geq 1$, we consider the $2m$ boxes

$$b'_{m,k} = [(k - 0.8)/m, (k - 0.7)/m] \times [0.4, 0.6] \subset E$$

$$b''_{m,k} = [(k - 0.3)/m, (k - 0.2)/m] \times [0.4, 0.6] \subset E$$

with $1 \leq k \leq m$, and let $b'_{m,k,i}$ (resp. $b''_{m,k,i}$) be the copy of $b'_{m,k}$ (resp. $b''_{m,k}$) in E_i ;

- 3) for $1 \leq k \leq m$, let H_k^1 be the 1-handle between the 0-handles $H_{i_k}^0$ and $H_{j_k}^0$ given by the identification of $b'_{m,k,i_k} \times \{1\}$ with $b''_{m,k,j_k} \times \{1\}$ through the map $(x, y, 1) \mapsto (x + 0.5/m, 1 - y, 1)$.

In particular, $M_\emptyset^n = \cup_{i=1}^n H_i^0 = \cup_{i=1}^n E_i \times [0, 1]$ is the disjoint union of n 3-balls.

If $M_{\pi_0}^n$ and $M_{\pi_1}^n$ are two standard 3-dimensional 1-handlebodies with $\pi_0, \pi_1 \in \Pi\mathcal{G}_n$, then $X(M_{\pi_0}^n, M_{\pi_1}^n)$ can be thought as a quotient of $\sqcup_{i=1}^n E_i \times [0, 1]$, up to canonical identifications of $H_{i,0}^0 = E_i \times [0, 1] \cong E_i \times [0, 1] \times \{0\}$ and $H_{i,1}^0 = E_i \times [0, 1] \cong E_i \times [0, 1] \times \{1\}$ respectively with $E_i \times [0, 0.1]$ and $E_i \times [0.9, 1]$.

The standard 3-dimensional 1-handlebodies $M_{\pi_0}^3$ and $M_{\pi_1}^3$ for $\pi_0 = ((1, 3), (1, 2), (2, 2), (3, 3))$ and $\pi_1 = ((1, 1), (1, 2), (2, 3), (2, 3))$, which are respectively isomorphic to M_0 and M_1 of Figure 2.1.1, are shown on the left side of Figure 2.1.4. Here, the

arrows indicate the prescribed identifications. On the right side of the same Figure 2.1.4 is shown a copy of $X(M_{\pi_0}^3, M_{\pi_1}^3)$ described as a quotient of $\sqcup_{i=1}^3 E_i \times [0, 1]$.

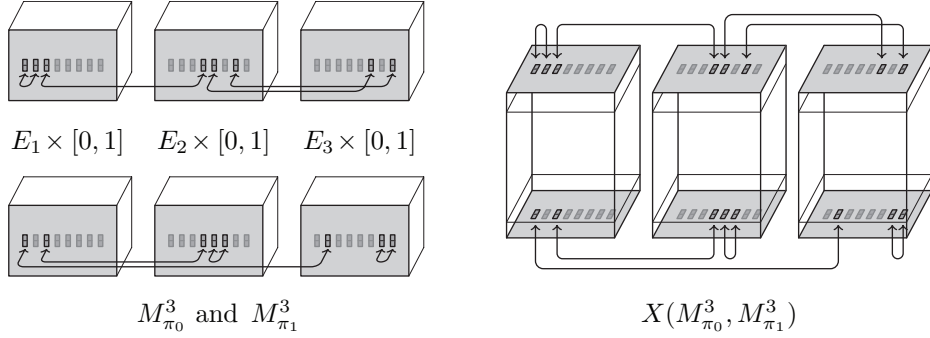


FIGURE 2.1.4. Standard 3-dimensional 1-handlebodies

PROPOSITION 2.1.2. *For any $n \geq 1$, the category \mathcal{Chb}_n^{3+1} is equivalent to its full subcategory, whose objects are the standard 3-dimensional 1-handlebodies M_π^n with $\pi \in \Pi\mathcal{G}_n$, through the inclusion functor.*

Proof. This is an immediate consequence of Corollary 1.5.4. \square

From now on, \mathcal{Chb}_n^{3+1} will denote the full subcategory given in Proposition 2.1.2.

The set $\Pi\mathcal{G}_n$, can be endowed with a monoidal structure, where the product $\pi \diamond \pi'$ is the juxtaposition of π and π' and the unit element is the empty sequence. This induces a monoidal structure on $\text{Obj } \mathcal{Chb}_n^{3+1} = \{M_\pi^n \mid \pi \in \Pi\mathcal{G}_n\}$, which will be denoted in the same way:

$$M_\pi^n \diamond M_{\pi'}^n = M_{\pi \diamond \pi'}^n.$$

We observe that the unit of this product is M_\emptyset^n , the disjoint union of n 3-balls, and that given $\pi = ((i_1, j_1), \dots, (i_m, j_m)) \in \Pi\mathcal{G}_n$ we have:

$$M_\pi^n = M_{(i_1, j_1)}^n \diamond \dots \diamond M_{(i_m, j_m)}^n.$$

Moreover, $M_\pi^n \diamond M_{\pi'}^n$ is the 3-dimensional handlebody obtained from $M_\pi^n \sqcup M_{\pi'}^n$ by glueing the i -th 0-handle of M_π^n to that of $M_{\pi'}^n$ through the map $(1, y, z) \mapsto (0, y, z)$ and then suitably reparametrizing the first coordinate.

Now, we extend the monoidal structure on $\text{Obj } \mathcal{Chb}_n^{3+1}$ to the whole category \mathcal{Chb}_n^{3+1} in the following way. Let $W : M_{\pi_0}^n \rightarrow M_{\pi_1}^n$ and $W' : M_{\pi'_0}^n \rightarrow M_{\pi'_1}^n$ be two morphisms in \mathcal{Chb}_n^{3+1} . Starting from $X(M_{\pi_0}^n, M_{\pi_1}^n) \sqcup X(M_{\pi'_0}^n, M_{\pi'_1}^n)$, we glue the i -th 0-handle of $X(M_{\pi_0}^n, M_{\pi_1}^n)$ (consisting of the i -th 0-handles of $M_{\pi_0}^n$ and $M_{\pi_1}^n$ joined by the 1-handle \overline{H}_i^1) to that of $X(M_{\pi'_0}^n, M_{\pi'_1}^n)$ through the map $(1, y, z) \mapsto (0, y, z)$. Then, we identify the result of the gluing with $X(M_{\pi_0}^n \diamond M_{\pi'_0}^n, M_{\pi_1}^n \diamond M_{\pi'_1}^n)$, by thinking all the three X spaces involved as quotients of $\sqcup_{i=1}^n E_i \times [0, 1]$ and applying a reparametrization of the first coordinate depending on the last one, that is a diffeomorphism $(x, y, z) \mapsto (h^z(x), y, z)$ with h^z an increasing function of x for every z . The same construction crossed by $[0, 1]$, gives $Y(M_{\pi_0}^n \diamond M_{\pi'_0}^n, M_{\pi_1}^n \diamond M_{\pi'_1}^n)$ starting from $Y(M_{\pi_0}^n, M_{\pi_1}^n) \sqcup Y(M_{\pi'_0}^n, M_{\pi'_1}^n)$.

We define the product $W \diamond W'$ to be the 4-dimensional relative 2-handlebody build on $X(M_{\pi_0}^n \diamond M_{\pi'_0}^n, M_{\pi_1}^n \diamond M_{\pi'_1}^n)$ that one obtains by starting from $W \sqcup W'$ and

performing the construction above to the subspace $Y(M_{\pi_0}^n, M_{\pi_1}^n) \sqcup Y(M_{\pi'_0}^n, M_{\pi'_1}^n)$. The handlebody structure on $W \diamond W'$ consists of all the handles of W and W' .

The unit of the product between morphisms is the “empty” relative handlebody $\text{id}_{M_{\emptyset}^n} = Y(M_{\emptyset}^n, M_{\emptyset}^n) : M_{\emptyset}^n \rightarrow M_{\emptyset}^n$ without any handle, that is the disjoint union of n 4-balls.

PROPOSITION 2.1.3. *The product $\diamond : \mathcal{Chb}_n^{3+1} \times \mathcal{Chb}_n^{3+1} \rightarrow \mathcal{Chb}_n^{3+1}$ makes \mathcal{Chb}_n^{3+1} into a strict monoidal category, for any $n \geq 1$.*

Proof. The proof consists into observing that \diamond is associative and verifying the identities which follow the Definition 1.5.5 of a strict monoidal category. This is straightforward and we leave it to the reader. \square

For $n > 1$ the category \mathcal{Chb}_n^{3+1} may have quite complex structure, but what we really want is to understand the category \mathcal{Chb}_1^{3+1} ($n = 1$) of connected cobordisms between connected 3-dimensional handlebodies. In this perspective, the categories with $n > 1$ represent an intermediate step in order to establish in a natural way the connection between the morphisms in \mathcal{Chb}_1^{3+1} and the morphisms of the category of labeled ribbon surfaces coming from the description of the 4-dimensional handlebodies as n -fold branched coverings. In particular, we need a faithful functor (or embedding) from $\mathcal{Chb}_1^{3+1} \rightarrow \mathcal{Chb}_n^{3+1}$ whose image defines a subcategory of \mathcal{Chb}_n^{3+1} equivalent to \mathcal{Chb}_1^{3+1} .

First of all, we have that the inclusion $\Pi\mathcal{G}_k \subset \Pi\mathcal{G}_n$ with $1 \leq k < n$ induces inclusions $M_{\pi}^k \subset M_{\pi}^n$, $X(M_{\pi_0}^k, M_{\pi_1}^k) \subset X(M_{\pi_0}^n, M_{\pi_1}^n)$ and $Y(M_{\pi_0}^k, M_{\pi_1}^k) \subset Y(M_{\pi_0}^n, M_{\pi_1}^n)$, for any $\pi, \pi_0, \pi_1 \in \Pi\mathcal{G}_k$.

Then, we define the faithful functor $\iota_k^n : \mathcal{Chb}_k^{3+1} \subset \mathcal{Chb}_n^{3+1}$, by putting $\iota_k^n(M_{\pi}^k) = M_{\pi}^n$ for any $M_{\pi}^k \in \text{Obj}\mathcal{Chb}_k^{3+1}$ and $\iota_k^n(W) = W \cup_{Y(M_{\pi_0}^k, M_{\pi_1}^k)} Y(M_{\pi_0}^n, M_{\pi_1}^n)$ for any $W : M_{\pi_0}^k \rightarrow M_{\pi_1}^k \in \text{Mor}\mathcal{Chb}_k^{3+1}$.

DEFINITION 2.1.4. Given $n > k \geq 1$, let $\pi_{n \rightarrow k} = ((n, n-1), \dots, (k+1, k))$ and let $\text{id}_{\pi_{n \rightarrow k}}$ be the identity morphism of $M_{\pi_{n \rightarrow k}}^n$. Then, the *stabilization functor* $\uparrow_k^n : \mathcal{Chb}_k^{3+1} \rightarrow \mathcal{Chb}_n^{3+1}$ is defined by:

$$\begin{aligned} \uparrow_k^n M_{\pi}^k &= M_{\pi_{n \rightarrow k}}^n \diamond \iota_k^n(M_{\pi}^k) \text{ for any } M_{\pi}^k \in \text{Obj}\mathcal{Chb}_k^{3+1}, \\ \uparrow_k^n W &= \text{id}_{\pi_{n \rightarrow k}} \diamond \iota_k^n(W) \text{ for any } W \in \text{Mor}\mathcal{Chb}_k^{3+1}. \end{aligned}$$

Moreover, we put $\mathcal{Chb}_n^{3+1, c} = \uparrow_1^n(\mathcal{Chb}_1^{3+1}) \subset \mathcal{Chb}_n^{3+1}$.

We will show in Section 2.3 that the restriction of \uparrow_k^n to $\mathcal{Chb}_k^{3+1, c}$ gives a category equivalence between the $\mathcal{Chb}_k^{3+1, c}$ and $\mathcal{Chb}_n^{3+1, c}$. In particular, $\mathcal{Chb}_1^{3+1} \cong \mathcal{Chb}_n^{3+1, c}$ for any $n \geq 1$. Even if the proof of this will be somewhat technical, the reader should find the statement quite obvious. Indeed $M_{\pi_{n \rightarrow 1}}$ is a 3-ball and therefore the product cobordism $\text{id}_{\sigma_{1 \rightarrow n}}$ is a 4-ball. Hence, we may think of the cobordism $\uparrow_1^n W = \text{id}_{\pi_{n \rightarrow 1}} \diamond \iota_1^n(W)$ as the handlebody obtained by attaching the 1- and 2-handles of W to a single 4-ball.

2.2. Bridged tangles and labeled Kirby tangles

We recall that in the literature can be found two different diagrammatic descriptions of 4-dimensional 2-handlebodies with a single 0-handle: bridged links and Kirby diagrams. Both are based on the representation of the attaching maps of the

1- and 2-handles in the boundary of the 0-handle. In the case of a bridged link (cf. [33, 34]), the 1-handles are represented directly by drawing their attaching regions (disjoint pairs of 3-balls), while in the case of a Kirby diagram (cf. [38, 22]) the 1-handles are represented instead by a “dotted” 0-framed trivial knot.

In [34] bridged tangles are used for describing cobordisms in \mathcal{Chb}_1^{3+1} , while in [35, 36] ribbon tangles, equivalent under Kirby moves, are used to describe the morphisms of the category \mathcal{Cob}_1^{2+1} of 2-framed relative 3-cobordisms which, as explained in Chapter 5, is the “framed boundary” of \mathcal{Chb}_1^{3+1} .

Here we will generalize the notion of bridged tangles and Kirby tangles in order to be able to describe the morphisms of \mathcal{Chb}_n^{3+1} , i.e. 4-dimensional relative 2-handlebodies build on $X(M_{\pi_0}^n, M_{\pi_1}^n)$, where $M_{\pi_0}^n$ and $M_{\pi_1}^n$ are standard 3-dimensional handlebodies with n 0-handles.

DEFINITION 2.2.1. For any $n \geq 1$ and any two finite sequences of ordered pairs $\pi_0 = ((i_1^0, j_1^0), \dots, (i_{m_0}^0, j_{m_0}^0))$ and $\pi_1 = ((i_1^1, j_1^1), \dots, (i_{m_1}^1, j_{m_1}^1))$ in $\Pi\mathcal{G}_n$, a *bridged tangle* from π_0 to π_1 consists of the following data:

- 1) the space $Z_n = \sqcup_{i=1}^n E_i \times [0, 1]$ disjoint union of n numbered copies of $E \times [0, 1]$, where $E = [0, 1]^2$ denotes the standard square, with the subspaces and maps (cf. Definition 2.1.1)

$$\left. \begin{aligned} B'_{\text{in},k} &= b'_{m_0,k,i_k^0} \times [0, 0.1] \subset E_{i_k^0} \times [0, 1] \\ B''_{\text{in},k} &= b''_{m_0,k,j_k^0} \times [0, 0.1] \subset E_{j_k^0} \times [0, 1] \\ \rho_{\text{in},k} : B'_{\text{in},k} &\rightarrow B''_{\text{in},k} \text{ given by } (x, y, z) \mapsto (x + 0.5/m_0, 1 - y, z) \end{aligned} \right\} \text{ for } 1 \leq k \leq m_0,$$

$$\left. \begin{aligned} B'_{\text{out},k} &= b'_{m_1,k,i_k^1} \times [0.9, 1] \subset E_{i_k^1} \times [0, 1] \\ B''_{\text{out},k} &= b''_{m_1,k,j_k^1} \times [0.9, 1] \subset E_{j_k^1} \times [0, 1] \\ \rho_{\text{out},k} : B'_{\text{out},k} &\rightarrow B''_{\text{out},k} \text{ given by } (x, y, z) \mapsto (x + 0.5/m_1, 1 - y, z) \end{aligned} \right\} \text{ for } 1 \leq k \leq m_1;$$

- 2) an orientation preserving embedding $\Phi : P \rightarrow \sqcup_{i=1}^n \text{Int } E_i \times]0.1, 0.9[\subset Z_n$, where $P = \sqcup_{k=1}^r P_k$ with $P_k = P'_k \sqcup P''_k$ a copy of $B^3(0, 0, 2) \sqcup B^3(0, 0, -2) \subset R^3$, the union of the pair of unitary 3-balls with centers $(0, 0, \pm 2)$; we put

$$\left. \begin{aligned} B'_k &= \Phi(P'_k) \\ B''_k &= \Phi(P''_k) \\ \rho_k : B'_k &\rightarrow B''_k \text{ given by } \Phi(x, y, z) \mapsto \Phi(x, y, -z) \end{aligned} \right\} \text{ for } 1 \leq k \leq r;$$

- 3) an embedding $\Psi : Q \rightarrow \sqcup_{i=1}^n \text{Int } E_i \times [0.1, 0.9] - \cup_{k=1}^r (\text{Int } B'_k \sqcup \text{Int } B''_k) \subset Z_n$, with Q the space obtained by cutting the disjoint union $\sqcup_{h=1}^s A_h$ of s copies of the annulus $A = S^1 \times [0, 1]$ along a set of meridian arcs $\alpha_j = \{p_j\} \times [0, 1] \subset A_{h_j}$ for $j = 1, \dots, c$; denoting by α'_j and α''_j the two copies of α_j in $\text{Bd } Q$, we require that: $\Psi(Q)$ meets the boundary of the ambient space transversally in $\cup_{j=1}^c \Psi(\alpha'_j \sqcup \alpha''_j) \subset \cup_{k=1}^r (\text{Bd } B'_k \cup \text{Bd } B''_k) \cup_{k=1}^{m_0} (\text{Bd } B'_{\text{in},k} \cup \text{Bd } B''_{\text{in},k}) \cup_{k=1}^{m_1} (\text{Bd } B'_{\text{out},k} \cup \text{Bd } B''_{\text{out},k})$ and $(\cup_{k=1}^r \rho_k \cup_{k=1}^{m_0} \rho_{\text{in},k} \cup_{k=1}^{m_1} \rho_{\text{out},k})(\Psi(\alpha'_j)) = \Psi(\alpha''_j)$ for any $j = 1, \dots, c$.

We will call $B'_{\text{in},k}$ and $B''_{\text{in},k}$ with $k = 1, \dots, m_0$ (resp. $B'_{\text{out},k}$ and $B''_{\text{out},k}$ with $k = 1, \dots, m_1$) the *in-boxes* (resp. *out-boxes*) of the bridged tangle, while the 3-balls B'_k and B''_k with $k = 1, \dots, r$ will be called *internal balls*.

By a *bridged tangle diagram* we mean the set of the in- and out-boxes together with the images of Φ and Ψ in Z_n . We will use the notation $T(\Phi, \Psi)$ for both the bridged tangle determined by Φ and Ψ and its diagram.

In a bridged tangle diagram we think of $\Psi(Q)$ as a set of framed curves. In the figures, we always represent such a framed curve as a narrow band and draw the base curve C as a thick curve and the framing curve C' as a “parallel” thin curve (cf. Definition 1.2.1). Of course, the choices of the base curve and the framing curve for different components of $\Phi(Q)$ have to be compatible with the map $\cup_{k=1}^r \rho_k \cup_{k=1}^{m_0} \rho_{\text{in},k} \cup_{k=1}^{m_1} \rho_{\text{out},k}$, according to property 3 in Definition 2.2.1.

An example of a bridged tangle diagram is presented in Figure 2.2.1. Here, π_0 and π_1 are as in Figure 2.1.4 and the arrows specify the pairing of boxes and balls.

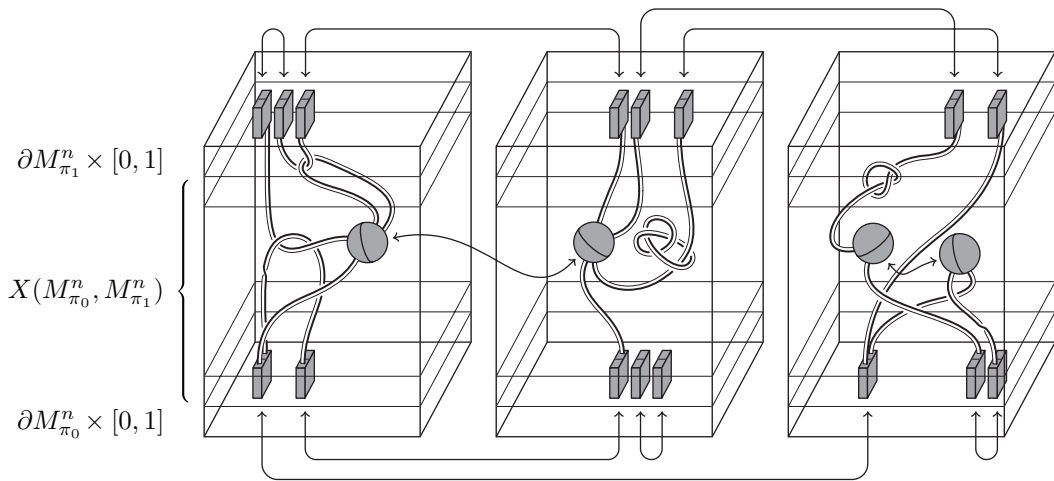


FIGURE 2.2.1. Bridged tangle representation of a cobordism

PROPOSITION 2.2.2. *Given $\pi_0, \pi_1 \in \Pi\mathcal{G}_n$, a bridged tangle $T = T(\Phi, \Psi)$ from π_0 to π_1 specifies a unique 4-dimensional relative 2-handlebody $W_T = W(\Phi, \Psi)$ build on $X(M_{\pi_0}^n, M_{\pi_1}^n)$ without 0-handles. Viceversa, any 4-dimensional relative 2-handlebody build on $X(M_{\pi_0}^n, M_{\pi_1}^n)$ without 0-handles can be specified in this way by a bridged tangle, up to isotopy of the attaching maps of the 2-handles.*

Proof. Given the bridged tangle $T(\Phi, \Psi)$, let Z_n be as in Definition 2.2.1 and let S be the space obtained from Z_n by removing the interiors of all the in-boxes $B'_{\text{in},k}$ and $B''_{\text{in},k}$ and all the out-boxes $B'_{\text{out},k}$ and $B''_{\text{out},k}$ and identifying their boundaries through the maps $\rho_{\text{in},k}$ and $\rho_{\text{out},k}$ respectively. Then S can be identified in a canonical way with $\partial Y(M_{\pi_0}^n, M_{\pi_1}^n)$ (cf. Figure 2.2.1). The subspace $S' \subset S$ coming from $\sqcup_{i=1}^n E_i \times [0.1, 0.9]$ can be canonically identified with $X(M_{\pi_0}^n, M_{\pi_1}^n) \times \{1\}$. Then Φ specifies the attaching maps of r 1-handles H_1^1, \dots, H_r^1 to $X(M_{\pi_0}^n, M_{\pi_1}^n) \times [0, 1]$. The relative 1-handlebody W^1 deriving from attaching these 1-handles, can be realized as the quotient of S' given by the identification of the internal balls B'_k and B''_k through the map ρ_k for $k = 1, \dots, r$. Under this identification Ψ represents the attaching maps of s 2-handles H_1^2, \dots, H_s^2 in the boundary W^1 in terms of framed knots, assuming the attachment longitudinal along each 1-handle (cf. Section 1.2). Observe that the requirements in point 3 of Definition 2.2.1 insure that the

framing of the 2-handles is well-defined. Then, $W(\Phi, \Psi)$ is the relative handlebody $(X(M_{\pi_0}^n, M_{\pi_1}^n) \times [0, 1]) \cup_{k=1}^r H_k^1 \cup_{h=1}^s H_h^2$.

At this point, the second part of the proposition just follows from the fact that the construction above can be reversed starting from any 4-dimensional relative 2-handlebody build on $X(M_{\pi_0}^n, M_{\pi_1}^n)$ without 0-handles, once the attaching maps of the 2-handles have been isotoped to be parallel to the core along each 1-handle. \square

Now we want to interpret 2-equivalence of 4-dimensional relative 2-handlebodies in terms of bridged tangles. To this aim, let us consider the following operations on a bridged tangle $T(\Phi, \Psi)$.

- (a) *Isotopy of Φ and Ψ* , which preserves the intersections of $\Psi(Q)$ with the in- and out-boxes and with the internal balls, as well as the conditions in point 3 of Definition 2.2.1.
- (b) *Pushing through an internal pair of 3-balls* (cf. Figure 2.2.2). Let B'_k and B''_k be a pair of internal balls and put $\Phi'_k = \Phi|_{P'_k}$ and $\Phi''_k = \Phi|_{P''_k}$. Assume that we are given: 1) a 3-ball $B \subset \sqcup_{i=1}^n \text{Int } E_i \times]0.1, 0.9[$, such that $B'_k \subset \text{Int } B$, while $\text{Bd } B$ is disjoint from all the internal balls and meets transversally $\Psi(Q)$ along the image of some meridian arcs like those in point 3 of Definition 2.2.1; 2) a 3-ball $C \subset \text{Int } B''_k$ and an orientation preserving diffeomorphism $\eta : \text{Cl}(B - B'_k) \rightarrow \text{Cl}(B''_k - C)$ such that $\eta|_{\text{Bd } B'_k} = \rho_k|_{\text{Bd } B'_k}$. Then, we modify $T(\Phi, \Psi)$ as follows: replace Φ'_k and Φ''_k with $\bar{\Phi}'_k : P'_k \rightarrow \bar{B}'_k = B$ and $\bar{\Phi}''_k : P''_k \rightarrow \bar{B}''_k = C$ respectively, such that $\eta(\bar{\Phi}'_k(x, y, z)) = \bar{\Phi}''_k(x, y, -z)$ for any $(x, y, z) \in \text{Bd } P'_k$; delete the part of the diagram in $\text{Cl}(B - B'_k)$ and insert its image through η in $\text{Cl}(B''_k - C)$; perform all the consequent modifications on the space Q and the map Ψ . An example is depicted in Figure 2.2.2 (the two balls B'_k and B''_k can lie in two different connected components of Z_n).

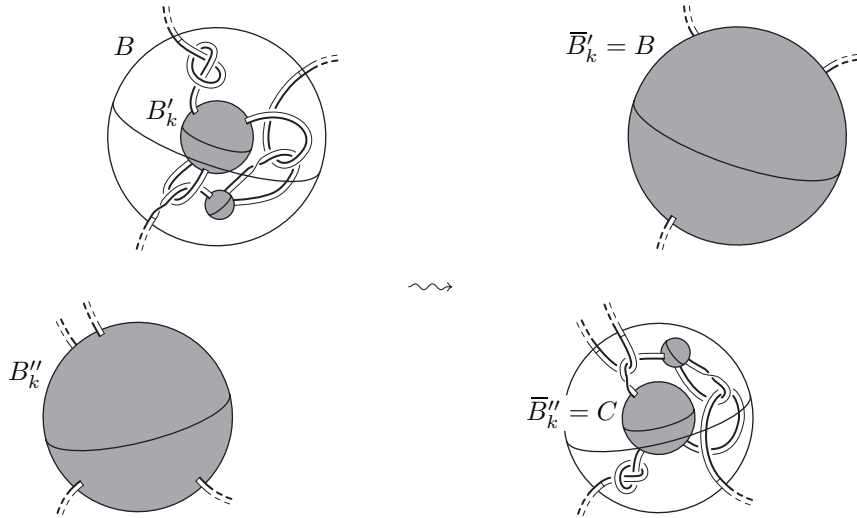


FIGURE 2.2.2. Pushing through an internal pair of 3-balls

- (c) *Pushing through an in/out pair of boxes*. This move is analogous to (b), but instead of 3-balls one works with boxes and, as an additional final step, one has to rescale the new boxes to make them as in point 1 of Definition 2.2.1.

- (d) *2-handle sliding*. Given two different annuli A_i and A_j with $i, j = 1, \dots, s$ as in point 3 of Definition 2.2.1, let Q_i and Q_j the corresponding subspaces of Q . Then the move consists in taking a parallel copy $\Psi(Q_j)^\parallel$ of $\Psi(Q_j)$ in the diagram and replacing $\Psi(Q_i)$ by the band connected sum of it with $\Psi(Q_j)^\parallel$, through a band β connecting any two components of $\Psi(Q_i)$ and $\Psi(Q_j)^\parallel$ contained in the same component of Z_n (cf. Figure 2.2.3).

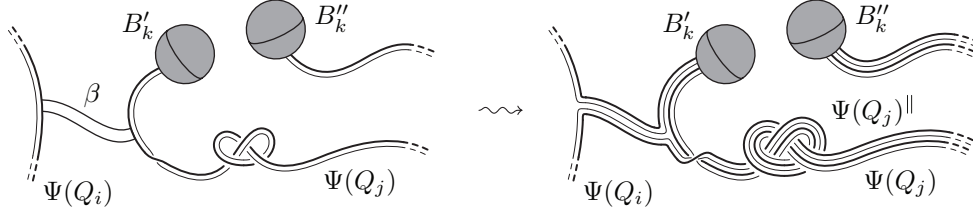


FIGURE 2.2.3. A 2-handle sliding

- (e) *Adding/deleting a canceling 1/2-pair*, that is two internal balls B'_k and B''_k which are joined by a single band and do not intersect elsewhere $\Psi(Q)$ (cf. Figure 2.2.4).

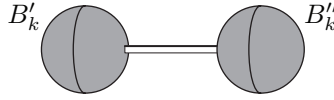


FIGURE 2.2.4. A canceling 1/2-pair

DEFINITION 2.2.3. Two bridged tangles are said to be *2-equivalent* if they are related by a finite sequence of moves of types (a) to (e).

PROPOSITION 2.2.4. Given $\pi_0, \pi_1 \in \Pi\mathcal{G}_n$, two bridged tangles $T(\Phi_1, \Psi_1)$ and $T(\Phi_2, \Psi_2)$ from π_0 to π_1 are 2-equivalent in the sense of the previous definition if and only if the corresponding 4-dimensional relative 2-handlebodies $W(\Phi_1, \Psi_1)$ and $W(\Phi_2, \Psi_2)$ are 2-equivalent as relative handlebodies.

Proof. First of all, we observe that the moves (a) to (e) on a bridged tangle $T(\Phi, \Psi)$ represent 2-deformations of the handlebody $W(\Phi, \Psi)$. In particular, (b) represents isotopy of the attaching maps of the 2-handles and 1-handle slidings over the k -th 1-handle of $W(\Phi, \Psi)$.

Viceversa, assume that $W(\Phi_1, \Psi_1)$ and $W(\Phi_2, \Psi_2)$ are 2-equivalent. Since they are relative handlebodies without 0-handles, there is a 2-deformation relating them that does not involve addition/deletion of canceling pairs of 0- and 1-handles (see Proposition 1.2.4). Such a 2-deformation consists of a finite sequence of the following modifications: isotopies of the attaching maps of the 1-handles and of the 2-handles; addition/deletion of pairs of canceling 1- and 2-handles; sliding of a 1- or 2-handle over another 1- or 2-handle. Isotopy and 1-handle sliding on a handlebody $W(\Phi, \Psi)$ can be represented by moves (a), (b) and (c) on the bridged tangle $T(\Phi, \Psi)$, while the other two modifications just correspond to moves (d) and (e). \square

In the light of Propositions 2.2.2 and 2.2.4, for any $n \geq 1$ we can form a strict monoidal category of bridged tangles \mathcal{T}_n equivalent to $\overline{\mathcal{H}}_n^{3+1}$ through the functor induced by the map $T(\Phi, \Psi) \mapsto W(\Phi, \Psi)$.

The objects of \mathcal{T}_n are the sequences in $\Pi\mathcal{G}_n$. Given two sequences $\pi_0, \pi_1 \in \Pi\mathcal{G}_n$, a morphism in \mathcal{T}_n with source π_0 and target π_1 is a bridged tangle from π_0 to π_1 , considered up to 2-equivalence of bridged tangles.

If $T_1 = T(\Phi_1, \Psi_1) : \pi_0 \rightarrow \pi_1$ and $T_2 = T(\Phi_2, \Psi_2) : \pi_1 \rightarrow \pi_2$ are two morphisms in \mathcal{T}_n , then their composition is the morphism $T = T(\Phi, \Psi) : \pi_0 \rightarrow \pi_2$ defined as follows. Translate T_2 in the space $\bar{Z}_n = \sqcup_{i=1}^n E_i \times [1, 2]$, glue it to T_1 by identifying the two copies of $\sqcup_{i=1}^n E_i \times \{1\}$ in Z_n and \bar{Z}_n , and rescale the third coordinate by the factor $1/2$. In the identification the out-boxes of T_1 are glued to the corresponding in-boxes of T_2 to give a new boxes that, up to smoothing the corners, can be considered as extra internal balls. Then, under the above identification, T is determined by $\Phi = \Phi_1 \sqcup \Phi_2$ extended to include those extra internal balls and by $\Psi = \Psi_1 \sqcup \Psi_2$.

The identity morphism id_π of a sequence $\pi \in \Pi\mathcal{G}_n$ is represented by the bridged tangle from π to π without any internal ball and with a single band connecting any in-box with the corresponding out-box. Notice that the two bands connecting a pair B'_k and B''_k of in-boxes with the corresponding pair of out-boxes, give the attaching map of the 2-handle of $\text{id}_{M_\pi^n}$ between the two copies (in the source a in the target) of the k -th 1-handle of M_π^n .

Finally, \mathcal{T}_n has a strict monoidal structure whose product (which we will denote again by \diamond) is given by juxtaposition on the objects, while on the morphisms $T \diamond T'$ is given by translating T' in the space $Z'_n = \sqcup_{i=1}^n [1, 2] \times [0, 1] \times [0, 1]$, glueing the two tangles by identifying the corresponding copies of $\{1\} \times [0, 1] \times [0, 1]$ in Z_n and Z'_n and then applying a reparametrization of the first coordinate depending on the last one, that is a diffeomorphism $(x, y, z) \mapsto (h^z(x), y, z)$ with h^z increasing function of x for every z . The unit of the product between morphisms is the empty tangle.

Describing the cobordisms in $\mathcal{C}hb_n^{3+1}$ through bridged tangles presents two main difficulties. The first one is that the space Z_n in which lives the tangle diagram is not connected when $n > 1$. The second and most important one is that from a diagrammatic point of view the “pushing through 1-handle” move is highly non-local. Indeed, part of the diagram which is in the neighborhood of one 3-ball appears in the a neighborhood of another 3-ball; moreover, this last ball can even be in a different connected component of the diagram.

Introducing n -labeled Kirby tangles resolves both these problems. Basically the idea is to allow only the use of bridged tangle diagrams in special form. Obviously, this requires a specification of the 2-equivalence moves relating two such special diagrams.

DEFINITION 2.2.5. A bridged tangle $T(\Phi, \Psi)$ will be called a *special bridged tangle* if, using the same notation as in Definition 2.2.1, the following properties are satisfied:

- 1) the map $\text{pr} : Z_n = \sqcup_{i=1}^n E_i \times [0, 1] \rightarrow E \times [0, 1]$ projecting each copy $E_i \times [0, 1]$ onto $E \times [0, 1]$ by the identity is injective on $\Phi(P) \cup \Psi(Q)$;
- 2) $\Psi(Q)$ meets any internal ball B'_k (resp. B''_k) only in the disks $D'_k = \Phi(S_+^2(0, 0, 2)) \subset \text{Bd } B'_k$ (resp. $D''_k = \Phi(S_-^2(0, 0, -2)) \subset \text{Bd } B''_k$) image of the copy in P_k of the upper half-sphere $S_+^2(0, 0, 2) \subset \text{Bd } B^3(0, 0, 2)$ (resp. the lower half-sphere $S_-^2(0, 0, -2) \subset \text{Bd } B^3(0, 0, -2)$); moreover, $\Psi(Q)$ meets each in- or out-box B'_k (resp. B''_k) only in points of the half-space $y > 0$ (resp. $y < 0$);

- 3) an embedding $\bar{\Phi} : C \rightarrow E \times]0.1, 0.9[$ is given, with $C = \sqcup_{k=1}^r C_k$ and C_k the convex hull of P_k , such that $\bar{\Phi}|_P = \text{pr} \circ \Phi$ and $\bar{\Phi}(C) \cap \text{pr}(\Psi(Q)) = \text{pr}(\Phi(P) \cap \Psi(Q))$; we denote by $D_k = \bar{\Phi}(B^2)$ the image of the copy in C_k of the standard disk $B^2 \subset R^2 \subset R^3$ (cf. Figure 2.2.5).

Representing a special bridged tangle diagram is much simpler than a general one. Indeed, thanks to property 1, instead of using n copies of $E \times [0, 1]$, one for each connected component of the diagram, we can draw the diagram directly in $E \times [0, 1]$. Namely, we consider $\text{pr} \circ (\Phi \sqcup \Psi) \subset E \times [0, 1]$ and label each part of the diagram with a number from 1 to n , to keep track of the original component where it lives.

Moreover, by properties 2 (first part) and 3, we can draw only the disk D_k in place of each pair of internal 3-balls $\text{pr}(B'_k)$ and $\text{pr}(B''_k)$, extending the ribbons inside $\bar{\Phi}(C_k)$ by the image of vertical bands under the identification $\bar{\Phi} : C_k \rightarrow \bar{\Phi}(C_k)$, until they intersect it as it is shown on the right side of Figure 2.2.5. As usual, in the diagrams we mark the unknot $\text{Bd} D_k$ by a dot to indicate that it stands for the attaching map of a 1-handle.

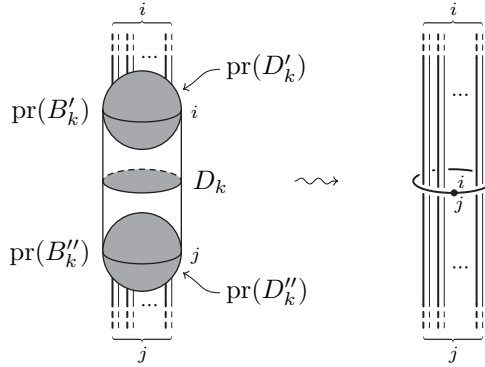


FIGURE 2.2.5. Dot notation for a pair of internal balls in a special bridged tangle

Taking into account the last part of property 2, we do a similar thing for the k -th pair of in-boxes (resp. out-boxes), but adding an extra open framed component. Such extra component passes once through the resulting dotted component and ends in a canonical pair of intervals in $E \times \{0\}$ (resp. $E \times \{1\}$), which represent the k -th element of the source (resp. target) of the tangle (cf. definition below), as shown in Figure 2.2.6. The 3-cell $\bar{\Phi}(C_k)$ and the disk D_k in the above construction, are respectively replaced by the pair of boxes joined by the bent rectangular tube drawn in the figure and by the meridian rectangle of it. The corresponding dotted unknot and the involved framed components has been isotoped in a different standard position

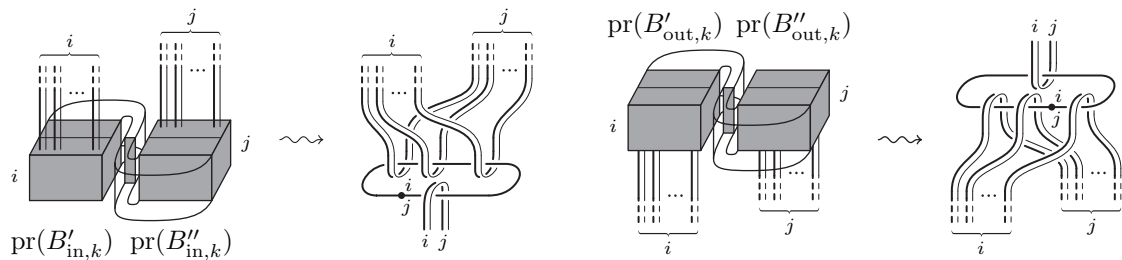


FIGURE 2.2.6. Dot notation for pairs of in/out-boxes in a special bridged tangle

to make the diagram simpler. After such isotopy, the whole configuration is assumed to have the standard form depicted in the figure.

In order to introduce the notion of n -labeled Kirby tangle, we need a preliminary definition. Given any finite sequence $\pi = ((i_1, j_1), \dots, (i_m, j_m)) \in \Pi\mathcal{G}_n$, let $I_\pi = ((a'_{m,1}, a''_{m,1}), \dots, (a'_{m,m}, a''_{m,m}))$ the sequence of pairs of intervals in $E = [0, 1]^2$, each labeled with the corresponding element of π , defined for $1 \leq k \leq m$ by

$$\begin{aligned} a'_{m,k} &= [(k - 0.8)/m, (k - 0.7)/m] \times \{0.5\}, \\ a''_{m,k} &= [(k - 0.3)/m, (k - 0.2)/m] \times \{0.5\}. \end{aligned}$$

DEFINITION 2.2.6. Let $n \geq 1$ and $\pi_0 = ((i_1^0, j_1^0), \dots, (i_{m_0}^0, j_{m_0}^0))$ and $\pi_1 = ((i_1^1, j_1^1), \dots, (i_{m_1}^1, j_{m_1}^1))$ be two sequences of in $\Pi\mathcal{G}_n$. Then an n -labeled (admissible) Kirby tangle in $E \times [0, 1]$ from I_{π_0} to I_{π_1} consists of the following data:

- 1) r dotted unknots spanning disjoint flat disks $D_1, \dots, D_r \subset \text{Int } E \times]0, 1[$;
- 2) a tangle consisting of s framed curves C_1, \dots, C_s (cf. Section 1.2) regularly embedded in $\text{Int } E \times [0, 1]$ and transversal with respect to those disks, such that each open framed curve C_h joins a pair of intervals $(a'_{m_0,k} \times \{0\}, a''_{m_0,k} \times \{0\})$ for some $(a'_{m_0,k}, a''_{m_0,k}) \in I_{\pi_0}$ or $(a'_{m_1,k} \times \{1\}, a''_{m_1,k} \times \{1\})$ for some $(a'_{m_1,k}, a''_{m_1,k}) \in I_{\pi_1}$, with the base curve always ending in the left end-points of the intervals;
- 3) a labeling from $\{1, \dots, n\}$ for each side of the disks D_1, \dots, D_r and each component of the tangle once it has been cut at the intersection with these disks; the labeling must be consistent in the sense that all the framed arcs coming out from one side of a disks (or ending at an interval from I_{π_0} or I_{π_1}) have the same label of that side (or that interval) (cf. Figures 2.2.5 and 2.2.6).

The term ‘‘admissible’’ in the denomination of Kirby tangles refers to the condition in point 2 of the definition, that no framed curve C_k joins an interval of I_{π_0} at level 0 with one of I_{π_1} at level 1 (cf. [48, 36]). However, since we will always work with admissible tangles, we will simply write Kirby tangle to mean an admissible one.

Moreover, the consistency rule in point 3 of the definition makes the labeling redundant and sometimes we will omit the superfluous labels. Observe also that in the case $n = 1$, all labels in the diagram have value 1, so they will be omitted, and we are reduced to an ordinary Kirby tangle.

What we have said after Definition 2.2.5 can be restated by saying that to any special bridged tangle T we can associate a uniquely determined Kirby tangle K_T representing it. This is obtained from T by replacing internal balls and in/out-boxes as described in Figures 2.2.5 and 2.2.6. Notice that the replacement of internal balls depends on the extra structure given by the embedding $\bar{\Phi}$ in point 3 of Definition 2.2.5, hence the construction of K_T cannot be immediately applied to a (non-special) bridged tangle T .

Viceversa, given an n -labeled Kirby tangle K , we can construct a corresponding special bridged tangle, which we will denote by T_K , in the following way: we first convert the dot notation for 1-handles into the ball notation, by reversing the step in Figure 2.2.5; after that we take the disjoint union $Z_n = \sqcup_{i=1}^n E_i \times [0, 1]$ of n copies of $E \times [0, 1]$ and put in the i -th component the portion of the diagram labeled by i ;

eventually, we transform the intervals of I_{π_0} at level 0 into in-boxes and those of I_{π_1} at level 1 into out-boxes.

We observe that the maps $T \mapsto K_T$ and $K \mapsto T_K$ are not exactly the inverse of each other. In particular, T_{K_T} does not coincide with T , but we will see in Proposition 2.2.8 that they are 2-equivalent.

In order to extend the definition of K_T , modulo certain moves, to any bridged tangle T (see proof Proposition 2.2.8) and to interpret the 2-equivalence of bridged tangles in terms of Kirby tangles, we consider the moves depicted in Figure 2.2.7.

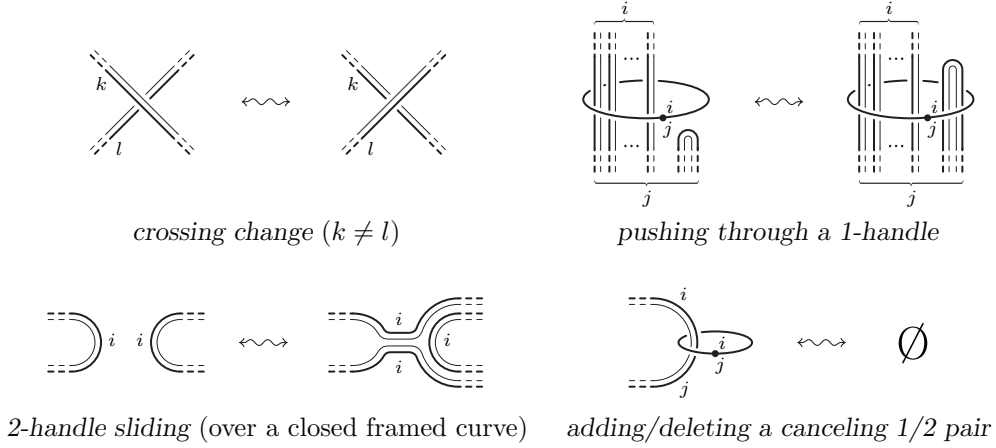


FIGURE 2.2.7. Equivalence moves for n -labeled Kirby tangles

We want to emphasize some facts: 1) crossing change and pushing through a 1-handle are local moves, while 2-handle sliding and adding/deleting a canceling 1/2-pair are global moves; 2) in the 2-handle sliding, we can slide any (possibly open) framed curve, but the framed curve over which the sliding takes place has to be a closed one; 3) for ordinary Kirby tangles, that is for $n = 1$, the crossing change cannot be realized and the other moves are reduced to the usual case, that is for $i = j = 1$.

DEFINITION 2.2.7. Two n -labeled Kirby tangles are said to be *2-equivalent* if they are related by labeled isotopy (preserving the intersections between framed curves and disks) and the moves of Figure 2.2.7.

Before going on, we introduce two auxiliary 2-equivalence moves on Kirby tangles, which will be needed in the proof of the next proposition. These are the 1-handle moves in Figure 2.2.8. They can be derived from the 2-equivalence moves in Figure 2.2.7, as shown in Figure 2.2.9.

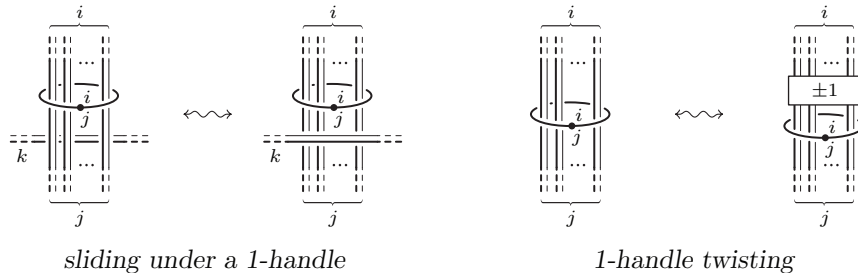


FIGURE 2.2.8. 1-handle moves for n -labeled Kirby tangles

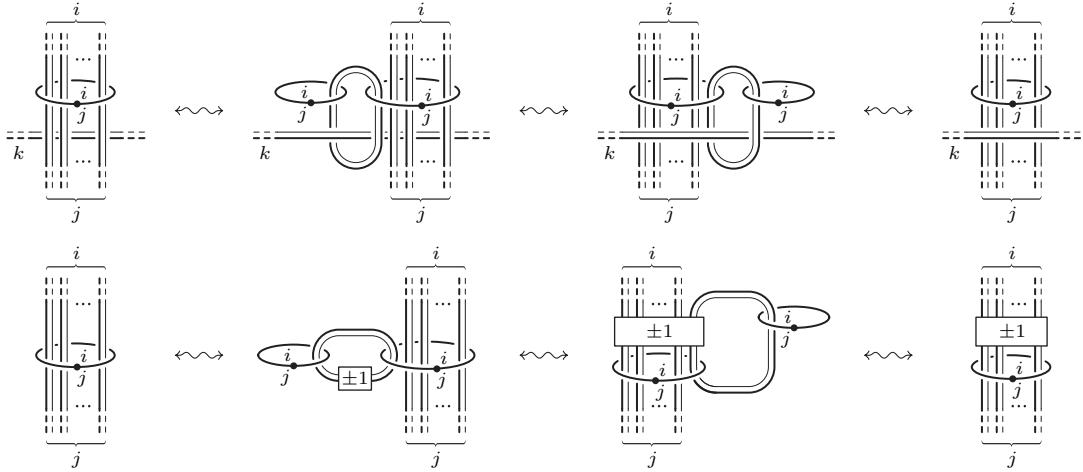


FIGURE 2.2.9. Deriving the 1-handle moves

PROPOSITION 2.2.8. *Any orientable 4-dimensional relative 2-handlebody W build on $X(M_{\pi_0}^n, M_{\pi_1}^n)$, with $\pi_0, \pi_1 \in \Pi\mathcal{G}_n$, can be represented by an n -labeled Kirby tangle K such that $W = W_{T_K}$. Moreover, given two n -labeled Kirby tangles K_1 and K_2 , the 4-dimensional relative 2-handlebodies W_1 and W_2 that they represent are 2-equivalent if and only if K_1 and K_2 are 2-equivalent in the sense of the previous definition.*

Proof. By Proposition 2.2.4 it suffices to show that the map $K \mapsto T_K$ from labeled Kirby tangles to (special) bridged tangles induces a bijection between the equivalence classes of Kirby tangles under isotopy and the moves in Figures 2.2.7 and the 2-equivalence classes of bridged tangles.

First, we observe that the map $K \mapsto T_K$ induces a well-defined map at the level of such equivalence classes, that is changing K through isotopy and the moves in Figures 2.2.7 produces a 2-equivalent bridged tangle. Indeed, any isotopy of K , as well as any crossing change, clearly induces a suitable isotopy of the maps Φ and Ψ determining T_K , while the other three moves in Figure 2.2.7 just induces homonymous moves of bridged tangles (cf. definition starting on page 43).

Now, we want to define the inverse map which associates to the 2-equivalence class of bridged tangle T the 2-equivalence class of a labeled Kirby tangle K_T , based on the construction $T \mapsto K_T$ considered above for T a special bridged tangle.

Any bridged tangle $T = T(\Phi, \Psi)$ can be made into a special one T' by an isotopy of bridged tangles (that is an isotopy of the maps Φ and Ψ , as specified in point (a) on page 43) to achieve properties 1 and 2 in Definition 2.2.5, followed by the extension of Φ to a map $\bar{\Phi}$ as in point 3 of the same definition.

The resulting special bridged tangle T' is not unique, since it depends on the choice of the isotopy and of the extension $\bar{\Phi}$. Nevertheless, we are going to show that the 2-equivalence class of $K_{T'}$ is uniquely determined, depending only on the original bridged tangle T .

Once the isotopy is fixed, different choices of $\bar{\Phi}$ lead to labeled Kirby tangles which can be related by labeled tangle isotopy (preserving the intersections between framed curves and disks) and the two moves in Figure 2.2.8. In fact, it is clear that isotopy of $\bar{\Phi}$ which preserves property 3 of Definition 2.2.5 induces an isotopy of the

corresponding Kirby tangle. Up to such an isotopy, $\bar{\Phi}$ is determined by the set of arcs $\bar{\Phi}(\sqcup_{k=1}^r \gamma_k) \subset E \times]0.1, 0.9[- \text{pr}(\cup_{k=1}^r \text{Int}(B'_k \cup B''_k))$ with $\gamma_k = \{(0, 0)\} \times [0, 1] \subset C_k$ and by the framings along them. Of course, different choices for these arcs are always isotopic keeping their end-points fixed, but during the isotopy they could cross the framed curves of T , and each time this happens K_T changes by a sliding under a 1-handle. While adding a full twist to the framing along any arc induces on T_K a twisting on the corresponding 1-handle.

Concerning the choice of the isotopy, we have that any other special bridged tangle T'' isotopic to T is also isotopic to T' . Moreover, we can assume the isotopy relating T' and T'' to be realized by bridged tangles which satisfy properties 1 and 2 of Definition 2.2.5 at every time, except for a finite number of crossing changes between two framed curves. It follows that the labeled Kirby diagrams $K_{T'}$ and $K_{T''}$ are related by labeled isotopy and crossing changes as in Figure 2.2.7 (remember that the conditions in point 3 of Definition 2.2.1 has to be preserved during the isotopy and this allows us to trivially extend it inside the balls $\bar{\Phi}(C_k)$ when passing to Kirby tangles).

Then, we can define K_T up to 2-equivalence of Kirby tangles for any (possibly non-special) bridged tangle T , just by putting $K_T = K_{T'}$ for some special bridged tangle T' isotopic to T .

At this point, we have to show that if T_1 and T_2 are 2-equivalent bridged tangles, then K_{T_1} and K_{T_2} are equivalent through labeled isotopy and the moves in Figures 2.2.7). If T_1 and T_2 are isotopic bridged tangles, then K_{T_1} and K_{T_2} are equivalent by the argument above.

Concerning the other operations on bridged tangles, we have only to address the pushing through 1-handle operations (b) and (c), since 2-handle sliding and adding/deleting a canceling 1/2-pair are explicitly represented in terms of Kirby diagrams in Figure 2.2.7. Moreover, if a pushing through a 1-handle move involves only pieces of framed tangle and no 3-ball, then it can be realized through labeled isotopy and the top-right move in Figure 2.2.7.

So, we only need to discuss the case when a 3-ball is pushed through a 1-handle (cf. Figure 2.2.10 for an internal pair of balls). The proof that in this case the corresponding Kirby tangle changes through adding/deleting canceling 1/2-pairs and 2-handle slides is presented in Figure 2.2.11.

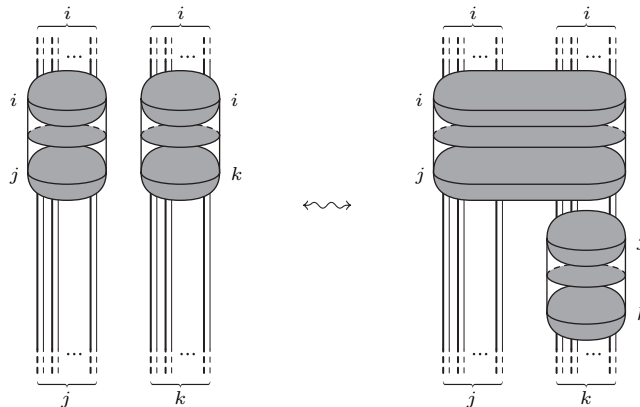


FIGURE 2.2.10. Pushing a 3-ball through a 1-handle

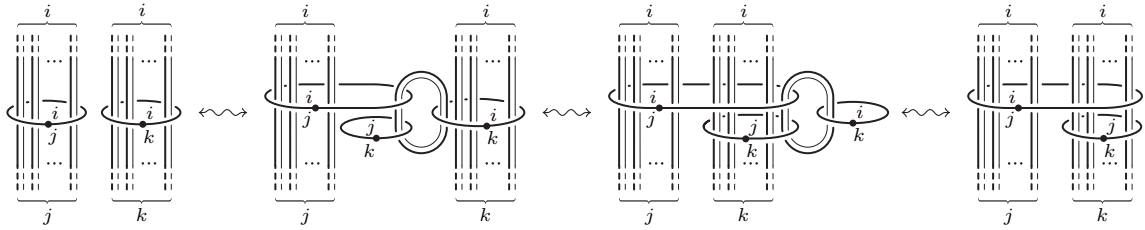


FIGURE 2.2.11. Deriving the 1-handle sliding

To conclude the proof, we observe that the two maps $K \mapsto T_K$ and $T \mapsto K_T$ are inverses to each other on 2-equivalence classes. In other words, K_{T_K} is 2-equivalent to K as a Kirby tangle and T_{K_T} is 2-equivalent to T as a bridged tangle. In both cases, the 2-equivalence is realized by performing the obvious sequence of 2-handle slidings, pushing through a 1-handle and then deletion of a canceling 1/2-pair, in order to remove the extra pair of 1- and 2-handles that arises from each pair of in- and out-boxes as shown in Figure 2.2.6. \square

In the next chapters, labeled Kirby tangles will be always represented through their planar diagrams, so we conclude this section by discussing such representation in some more details.

A labeled Kirby tangle lives in $\text{Int } E \times [0, 1]$ and a *planar diagram* of it is always realized by the projection into the square $]0, 1[\times [0, 1]$ forgetting the second coordinate (in such a way that E projects into $]0, 1[$). As usual, we require that the restriction of the projection to the tangle, including both framed and dotted curves, is regular and that it is injective except for a finite number of transversal double points, which give rise to the crossings.

DEFINITION 2.2.9. A planar diagram of a labeled Kirby tangle K is called *strictly regular*, if the disks D_1, \dots, D_r spanned by the dotted unknots projects bijectively onto disjoint planar disks and the projection of the framed tangle intersects each of such disks as presented on the right side of Figure 2.2.5 (up to planar isotopy).

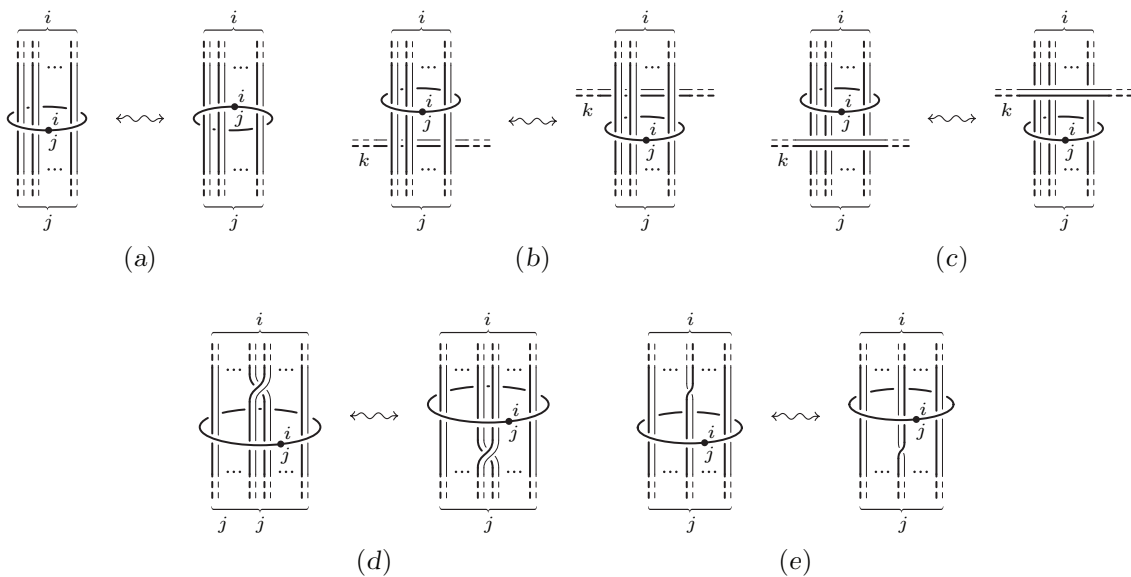


FIGURE 2.2.12. The 1-handle moves for representing isotopy by planar diagrams

Of course, any labeled Kirby tangle admits a strictly regular planar diagram. The proof of the following proposition is quite a standard exercise left to the reader.

PROPOSITION 2.2.10. *Two strictly regular planar diagrams represent isotopic labeled Kirby tangles (where the isotopy is assumed to preserve the intersections between framed curves and disks) if and only if they are related by planar isotopy, labeled framed Reidemeister moves and the moves presented in Figure 2.2.12.*

All the planar diagrams we have drawn until now are strictly regular, but using strictly regular diagrams would make pictures quite heavy for Kirby tangles which are not so simple. In this case, when this does not cause confusion we will draw planar diagrams that are not strictly regular. However, we will always keep the condition that the disks D_1, \dots, D_r project bijectively onto disjoint planar disks.

Sometimes it could be convenient to derogate from the labeling consistency rule for Kirby tangles (cf. point 3 of Definition 2.2.6), by allowing a framed component with label k to cross a disk spanned by a dotted component with labels i and j , provided that $k \notin \{i, j\}$. Clearly, such a crossing does not mean that the framed loop goes over the 1-handle represented by the dotted one, since it originates from the identification of different 0-handles. Figure 2.2.13 shows the way to eliminate it.

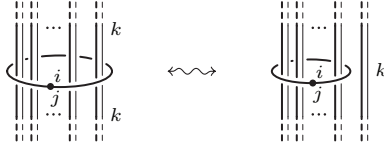


FIGURE 2.2.13. Derogating from the labeling consistency rule for $k \notin \{i, j\}$

2.3. The categories \mathcal{K}_n and the functors \uparrow_k^n and \downarrow_k^n

For any $n \geq 1$, we define the category \mathcal{K}_n of n -labeled Kirby tangles as follows. The objects of \mathcal{K}_n are the sequences of pairs of labeled intervals I_π with $\pi = ((i_1, j_1), \dots, (i_m, j_m)) \in \Pi\mathcal{G}_n$ (cf. the notation introduced just before Definition 2.2.6), while the morphisms of \mathcal{K}_n with source I_{π_0} and target I_{π_1} are the n -labeled Kirby tangles from I_{π_0} to I_{π_1} , considered up to 2-equivalence of Kirby tangles. The composition of two morphisms $K_1 : I_{\pi_0} \rightarrow I_{\pi_1}$ and $K_2 : I_{\pi_1} \rightarrow I_{\pi_2}$ in \mathcal{K}_n is given by translating K_2 on the top of K_1 , glueing the two tangles along I_{π_1} and then rescaling the third coordinate by the factor $1/2$.

On \mathcal{K}_n we also define a strict monoidal structure, whose product, once again denoted by \diamond , is given by $I_\pi \diamond I_{\pi'} = I_{\pi \diamond \pi'}$ on the objects, while on the morphisms $K \diamond K'$ is obtained by translating K' in the space on the right of K and then applying a reparametrization of the first coordinate depending on the last one (cf. definition of the monoidal structure on \mathcal{T}_n given on page 45). The unit of the product is the empty tangle $\text{id}_\emptyset : I_\emptyset \rightarrow I_\emptyset$.

For $\pi = ((i_1, j_1), \dots, (i_m, j_m)) \in \Pi\mathcal{G}_n$, we denote by $\text{id}_\pi : I_\pi \rightarrow I_\pi$ the identity morphism of I_π . It is easy to see that $\text{id}_{(i,j)}$ is given by the tangle presented in Figure 2.3.1, and that $\text{id}_\pi = \text{id}_{(i_1, j_1)} \diamond \dots \diamond \text{id}_{(i_m, j_m)}$. Indeed, if $K : I_{\pi_0} \rightarrow I_{\pi_1}$ is any Kirby tangle, in $K \circ \text{id}_{\pi_0}$ the upper framed components of id_{π_0} get closed and we can slide the lower open components over the closed ones and then cancel them with the dotted components; a symmetric argument works on the top of $\text{id}_{\pi_1} \circ K$.

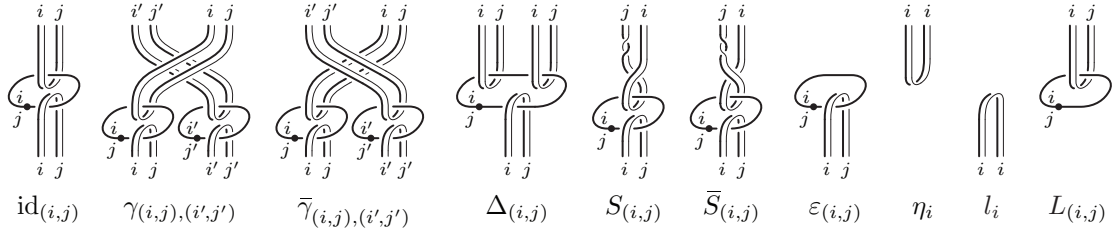


FIGURE 2.3.1. Some morphisms in \mathcal{K}_n

Finally, we endow \mathcal{K}_n with a family of braiding isomorphisms $\gamma_{\pi,\pi'} : I_{\pi \diamond \pi'} \rightarrow I_{\pi' \diamond \pi}$. Namely, $\gamma_{(i,j),(i',j')}$ is presented in Figure 2.3.1 and its inverse is $\gamma_{(i,j),(i',j')}^{-1} = \bar{\gamma}_{(i',j'),(i,j)}$, while the braiding isomorphisms on the other objects are obtained inductively by the relations in Definition 1.5.6 (see Figure 2.3.2 and note that $\gamma_{\pi,\pi'}^{-1} = \bar{\gamma}_{\pi',\pi}$).

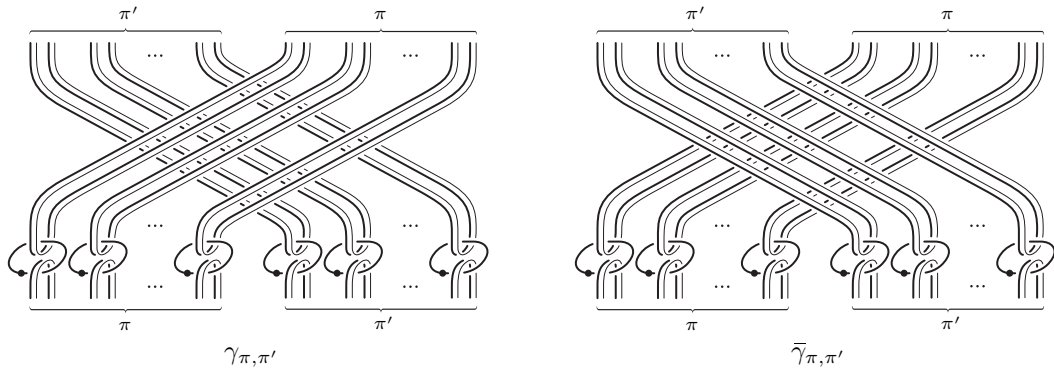


FIGURE 2.3.2. The braiding isomorphisms in \mathcal{K}_n

PROPOSITION 2.3.1. *For any $n \geq 1$, the category \mathcal{K}_n is equivalent as a strict monoidal category to Chb_n^{3+1} , through the functor induced by the map $K \mapsto W_{T_K}$. Moreover, the family of braiding isomorphisms defined above makes \mathcal{K}_n into a braided strict monoidal category.*

Proof. The first part of the statement is nothing else than the categorical version of Proposition 2.2.8. The proof of the second part consists in the straightforward verification of the naturality of the braiding isomorphisms. \square

Before going on, we observe that the Kirby tangles in Figure 2.3.1 represent the elementary morphisms of a braided Hopf algebra structure on \mathcal{K}_n in the sense of Definition 4.1.1. This will be shown in Section 4.3, where we will relate \mathcal{K}_n to the algebraic category \mathcal{H}_n^r . Here, we only need the comultiplication of that structure, in order to introduce reducible Kirby tangles, as discussed below.

For $n > k \geq 1$, we denote by $\iota_k^n : \mathcal{K}_k \subset \mathcal{K}_n$ the faithful functor induced by the inclusion $\mathcal{G}_k \subset \mathcal{G}_n$, which considers any k -labeled Kirby tangle as an n -labeled one. This functor corresponds to the homonymous functor $\iota_k^n : \text{Chb}_k^{3+1} \subset \text{Chb}_n^{3+1}$ through the equivalence of Proposition 2.3.1.

At the end of Section 2.1 we defined the stabilization functor $\uparrow_k^n : \text{Chb}_k^{3+1} \rightarrow \text{Chb}_n^{3+1}$ and the subcategory $\text{Chb}_n^{3+1,c}$ of Chb_n^{3+1} for any $n > k \geq 1$, and we claimed that $\text{Chb}_n^{3+1,c}$ is equivalent to Chb_1^{3+1} through the this functor. Here, we will translate those definitions in terms of Kirby tangles and prove the statement.

DEFINITION 2.3.2. Given $n > k \geq 1$, let $\pi_{n \rightarrow k} = ((n, n-1), \dots, (k+1, k))$ and let $\text{id}_{\pi_{n \rightarrow k}}$ be the identity morphism of $I_{\pi_{n \rightarrow k}}$ in \mathcal{K}_n . Then, the *stabilization functor* $\uparrow_k^n : \mathcal{K}_k \rightarrow \mathcal{K}_n$ is defined by:

$$\begin{aligned} \uparrow_k^n I_\pi &= I_{\pi_{n \rightarrow k}} \diamond \iota_k^n(I_\pi) \text{ for any } I_\pi \in \text{Obj } \mathcal{K}_k, \\ \uparrow_k^n K &= \text{id}_{\pi_{n \rightarrow k}} \diamond \iota_k^n(K) \text{ for any } K \in \text{Mor } \mathcal{K}_k. \end{aligned}$$

From the definition, we immediately see that $\uparrow_k^n = \uparrow_{n-1}^n \circ \dots \circ \uparrow_k^{k+1}$. Figure 2.3.3 shows the stabilization $\uparrow_k^n K$ of a k -labeled Kirby tangle $K \in \mathcal{K}_k$ from π_0 to π_1 .

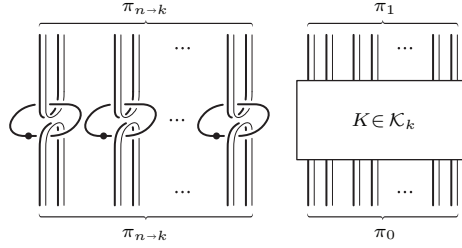


FIGURE 2.3.3. The stabilization $\uparrow_k^n K$ of $K \in \mathcal{K}_k$

Clearly, this stabilization functor corresponds, through the category equivalences given by Proposition 2.3.1, to the stabilization functor $\uparrow_k^n : \mathcal{Chb}_k^{3+1} \rightarrow \mathcal{Chb}_n^{3+1}$ defined at the end of Section 2.1.

Now, let $\Delta_{(i,j)} : I_{(i,j)} \rightarrow I_{(i,j)} \diamond I_{(i,j)}$ be the tangle presented in Figure 2.3.1, for any $(i, j) \in \mathcal{G}_n$. We extend this definition to $\Delta_\pi : I_\pi \rightarrow I_\pi \diamond I_\pi$ for any $\pi \in \Pi \mathcal{G}_n$ (see Figure 2.3.4) by the recursive formula:

$$\Delta_\pi = \Delta_{\pi' \diamond \pi''} = (\text{id}_{\pi'} \diamond \gamma_{\pi', \pi''} \diamond \text{id}_{\pi''}) \circ (\Delta_{\pi'} \diamond \Delta_{\pi''}),$$

which can be easily seen to give always the same result for Δ_π , whatever the decomposition $\pi = \pi' \diamond \pi''$ with $\pi', \pi'' \in \Pi \mathcal{G}_n$.

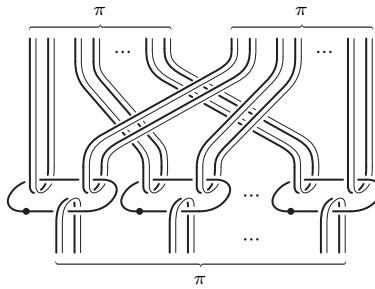


FIGURE 2.3.4. The comultiplication morphism Δ_π in \mathcal{K}_n

According to observation above, the family Δ_π represents the comultiplication in \mathcal{K}_n in sense of Definition 4.1.1. In particular, next proposition states that Δ satisfies the coassociativity property.

PROPOSITION 2.3.3. For any $\pi \in \Pi \mathcal{G}_n$, we have

$$(\Delta_\pi \diamond \text{id}_\pi) \circ \Delta_\pi = (\text{id}_\pi \diamond \Delta_\pi) \circ \Delta_\pi.$$

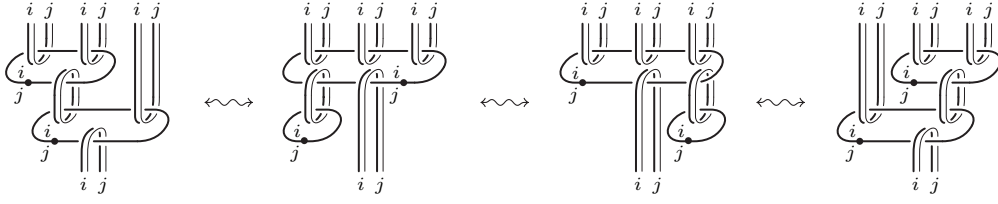


FIGURE 2.3.5. The coassociativity property for $\Delta_{(i,j)}$

Proof. The elementary case of $\pi = (i, j)$ is shown in Figure 2.3.5, while the general case follows from this by induction and tangle isotopy. \square

DEFINITION 2.3.4. Given $n > k \geq 1$ and $\pi_0, \pi_1 \in \Pi\mathcal{G}_n$, we say that an n -labeled Kirby tangle $K \in \mathcal{K}_n$ from $I_{\pi_{n-k}} \diamond I_{\pi_0}$ to $I_{\pi_{n-k}} \diamond I_{\pi_1}$ is k -reducible if it has the form

$$K = (\text{id}_{\pi_{n-k}} \diamond L) \circ (\Delta_{\pi_{n-k}} \diamond \text{id}_{\pi_0}),$$

for some n -labeled Kirby tangle $L \in \mathcal{K}_n$ from $I_{\pi_{n-k}} \diamond I_{\pi_0}$ to I_{π_1} (see Figure 2.3.6).

The composition of two k -reducible Kirby tangles is still k -reducible (by coassociativity) and we denote by \mathcal{K}_{n-k} the subcategory of \mathcal{K}_n , whose objects are $I_{\pi_{n-k}} \diamond I_{\pi}$ with $\pi \in \Pi\mathcal{G}_n$ and whose morphisms are k -reducible n -labeled Kirby tangles. In particular, we denote by \mathcal{K}_n^c the subcategory \mathcal{K}_{n-1} of 1-reducible tangles in \mathcal{K}_n .

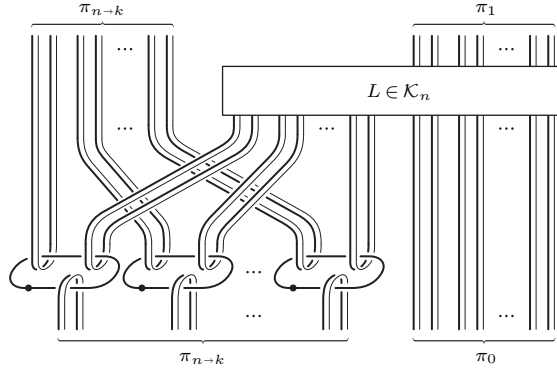


FIGURE 2.3.6. The generic k -reducible morphism $K \in \mathcal{K}_{n-k}$

We observe that the subcategory \mathcal{K}_{n-k} of k -reducible Kirby tangles is not closed with respect to the monoidal product $\diamond : \mathcal{K}_n \times \mathcal{K}_n \rightarrow \mathcal{K}_n$. Nevertheless, we can define a product structure $\boxtimes : \text{Mor}_{\mathcal{K}_{n-k}} \times \text{Mor}_{\mathcal{K}_{n-k}} \rightarrow \text{Mor}_{\mathcal{K}_{n-k}}$ in the following way.

Given two morphisms $K = (\text{id}_{\pi_{n-k}} \diamond L) \circ (\Delta_{\pi_{n-k}} \diamond \text{id}_{\pi_0}) : I_{\pi_{n-k}} \diamond I_{\pi_0} \rightarrow I_{\pi_{n-k}} \diamond I_{\pi_1}$ and $K' = (\text{id}_{\pi_{n-k}} \diamond L') \circ (\Delta_{\pi_{n-k}} \diamond \text{id}_{\pi'_0}) : I_{\pi_{n-k}} \diamond I_{\pi'_0} \rightarrow I_{\pi_{n-k}} \diamond I_{\pi'_1}$ in \mathcal{K}_{n-k} , their product $K \boxtimes K' : I_{\pi_{n-k}} \diamond I_{\pi_0 \diamond \pi'_0} \rightarrow I_{\pi_{n-k}} \diamond I_{\pi_1 \diamond \pi'_1}$ is defined by

$$\begin{aligned} K \boxtimes K' &= K \circ (\text{id}_{\pi_{n-k}} \diamond \gamma_{\pi'_1, \pi_0}) \circ (K' \diamond \text{id}_{\pi_0}) \circ (\text{id}_{\pi_{n-k}} \diamond \gamma_{\pi'_0, \pi_0}^{-1}) \\ &= (\text{id}_{\pi_{n-k}} \diamond L \diamond L') \circ (\Delta_{\pi_{n-k}} \diamond \gamma_{\pi_{n-k}, \pi_0} \diamond \text{id}_{\pi'_0}) \circ (\Delta_{\pi_{n-k}} \diamond \text{id}_{\pi_0 \diamond \pi'_0}). \end{aligned}$$

These two expressions for $K \boxtimes K'$ are related by diagram isotopy, as the reader can easily realize by looking at Figure 2.3.7 that represents the second one. The associativity of \boxtimes is a consequence of the coassociativity property of Δ and its unit is given by $\text{id}_{\pi_{n-k}}$. Observe that \boxtimes does not define a monoidal structure on \mathcal{K}_{n-k}

since in general the product of compositions $(K_2 \circ K_1) \diamond (K'_2 \circ K'_1)$ does not coincide with the composition of products $(K_2 \diamond K'_2) \circ (K_1 \diamond K'_1)$. Yet, we will find the notation a useful tool in describing some identities.

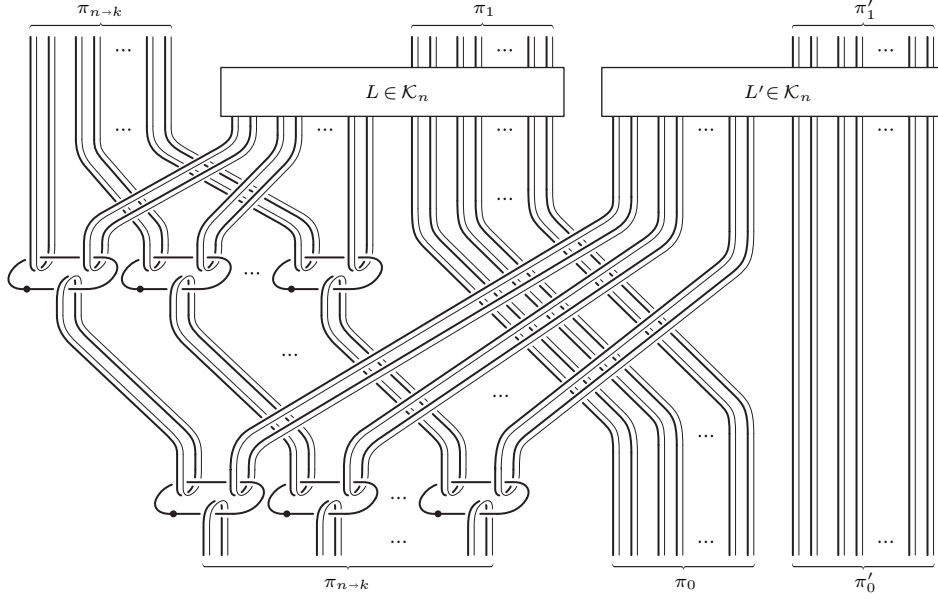


FIGURE 2.3.7. The product $K \diamond K'$ of two morphisms in \mathcal{K}_{n-k}

PROPOSITION 2.3.5. For any $n > k \geq 1$, the image $\uparrow_k^n \mathcal{K}_k$ of the stabilization functor is a subcategory of \mathcal{K}_{n-k} . Moreover, for any two morphisms K and K' in \mathcal{K}_k , we have $\uparrow_k^n (K \diamond K') = (\uparrow_k^n K) \diamond (\uparrow_k^n K')$. Hence, the product \diamond defines a monoidal structure on the subcategory $\uparrow_k^n \mathcal{K}_k$.

Proof. Figure 2.3.8 shows that the n -stabilization of an $(n-1)$ -labeled Kirby tangle is $(n-1)$ -reducible, in other words $\uparrow_{n-1}^n \mathcal{K}_{n-1} \subset \mathcal{K}_{n-(n-1)}$, for any $n \geq 2$. This fact easily implies by induction that $\uparrow_k^n \mathcal{K}_k$ is a subcategory of \mathcal{K}_{n-k} for any $n > k \geq 1$.

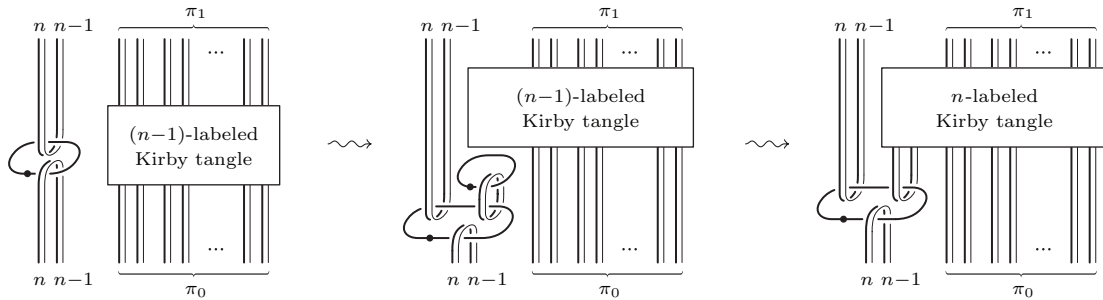


FIGURE 2.3.8. Stabilizations are reducible

The identity $\uparrow_k^n (K \diamond K') = (\uparrow_k^n K) \diamond (\uparrow_k^n K')$ for any K and K' in \mathcal{K}_k , immediately follows from the definition of the product \diamond in \mathcal{K}_{n-k} . \square

Our goal is to prove that $\uparrow_k^n : \mathcal{K}_k \rightarrow \mathcal{K}_{n-k}$ is actually an equivalence of monoidal categories. We will show this by defining a reduction functor $\downarrow_k^n : \mathcal{K}_{n-k} \rightarrow \mathcal{K}_k$, which is the inverse of the stabilization functor up to natural equivalence. Actually,

it is enough to define \downarrow_{n-1}^n and then proceed inductively. The main idea behind the definition of such functor is that, in the presence of a 1-handle with label $(n, n-1)$, we can push the part of diagram contained in the n -th 0-handle through such 1-handle, obtaining in this way a diagram which lives entirely in the first $n-1$ 0-handles. Therefore, as first step we will prove Lemma 2.3.6 below, which formalizes the move of pushing through a 1-handle with generic label (i_0, j_0) . In the present context such formalization may seem excessive, since the statement of the lemma and its proof are quite straightforward. Nevertheless, the proof of its algebraic analog (Proposition 4.4.11) will require a significant amount of work and we hope that seeing how things work out for Kirby tangles will be helpful.

LEMMA 2.3.6. *Given $x = (i_0, j_0) \in \mathcal{G}_n$ and $\pi \in \Pi\mathcal{G}_n$, let π^x be the sequence obtained from π by changing all elements i_0 to j_0 . Then, there exists a monoidal functor ${}_x : \mathcal{K}_n \rightarrow \mathcal{K}_n$ such that $(I_\pi)^x = I_{\pi^x}$ on the set of objects and the following properties hold:*

- (a) *if $i_0 = j_0$, then $K^x = K^{(i_0, i_0)} = K$ for every $K \in \mathcal{K}_n$, that is ${}_x^{(i_0, i_0)} = \text{id}_{\mathcal{K}_n}$;*
- (b) *if $i_0 \neq j_0$, then $K^x = K^{(i_0, j_0)} \in \mathcal{K}_n^{\setminus i_0}$ for every $K \in \mathcal{K}_n$, where $\mathcal{K}_n^{\setminus i_0}$ is the subcategory of \mathcal{K}_n generated by objects and morphisms which do not contain the label i_0 , hence we have a functor ${}_x^{(i_0, j_0)} : \mathcal{K}_n \rightarrow \mathcal{K}_n^{\setminus i_0}$;*
- (c) *given any other $y = (i_0, k_0) \in \Pi\mathcal{G}_n$, there exists a natural equivalence*

$$\xi^{x,y} : \text{id}_{(k_0, j_0)} \diamond {}_x \rightarrow \text{id}_{(k_0, j_0)} \diamond {}_y.$$

In particular, we put $\xi^x = \xi^{x, (i_0, i_0)}$ and denote by $\xi_\pi^x : I_x \diamond I_{\pi^x} \rightarrow I_x \diamond I_\pi$ the relative isomorphism for $\pi \in \Pi\mathcal{G}_n$, in such a way that the following identity holds for any diagram $K \in \mathcal{K}_n$ from I_{π_0} to I_{π_1} :

$$(\text{id}_x \diamond K) \circ \xi_{\pi_0}^x = \xi_{\pi_1}^x \circ (\text{id}_x \diamond K^x).$$

Before proving the lemma, we make a few observations. The natural equivalence ξ^x will be given by a 1-handle of label $x = (i_0, j_0)$ (cf. Figure 2.3.10). Then the last identity implies that the map $K \mapsto K^x$ represents how a Kirby tangle changes when the part of the diagram which lives in the i_0 -th 0-handle is pushed to the j_0 -th 0-handle through such 1-handle. In this perspective, points (a) and (b) of the statement indicate that if $i_0 = j_0$ the tangle can be pushed through without any change, while if $i_0 \neq j_0$ the resulting tangle lives in the other 0-handles different from the i_0 -th. More generally, for $y = (i_0, k_0)$, the natural equivalence $\xi^{x,y}$ in (c) will be given by a 1-handle of label (k_0, j_0) . Then (c) implies that K^y can be obtained from K^x by pushing it through such 1-handle (cf. Figures 2.3.10 and 2.3.12).

Proof of Lemma 2.3.6. Let $K \in \mathcal{K}_n$ be a labeled Kirby tangle from I_{π_0} to I_{π_1} . We define K^x for $x = (i_0, j_0)$ to be the labeled Kirby tangle obtained from any strictly regular plane diagram of K in the following way (see Figure 2.3.9): we first pull all the parts of the diagram with label i_0 on the top of the ones with label $i \neq i_0$, by performing a crossing change (as in Figure 2.2.7) at the crossings where a framed arc labeled i_0 passes under one labeled $i \neq i_0$, and flipping over (as in Figure 2.2.12 (a)) the spanning disks of the dotted unknots with the bottom side labeled i_0 and the top one $i \neq i_0$; then we replace all labels i_0 by j_0 .

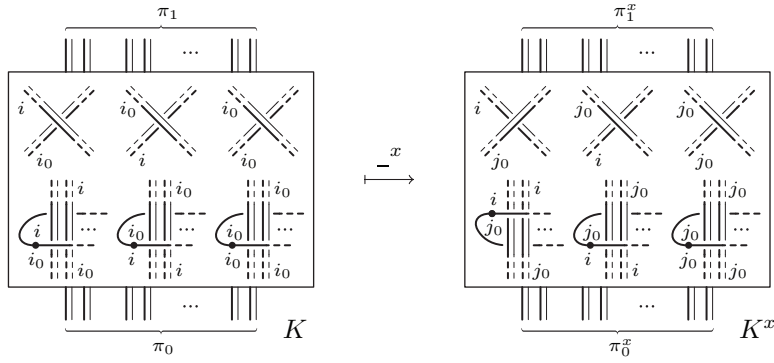


FIGURE 2.3.9. The functorial map $K \mapsto K^x$ ($x = (i_0, j_0)$ and $i \neq i_0$)

As the reader might have understood, the only essential modifications before the label replacement are the crossing changes with $i = j_0 \neq i_0$, being the other crossing changes and the disk flippings reversible after that replacement. Nevertheless, including also these inessential modifications in the definition of K^x , better interprets the geometric idea of pulling all the parts labeled by i_0 on the top and makes more transparent the proof of (c) below.

To see that K^x is well-defined, we first check that it does not depend on the strictly regular diagram of K we started from. Indeed, when changing K by planar isotopy, labeled framed Reidemeister moves and the moves in Figure 2.2.12, K^x changes in the same way, except for some extra crossing changes and an obvious extra sliding under a 1-handle for particular labelings of the moves (b) and (c) in Figure 2.2.12. Namely, the exceptions occur in (b) (resp. (c)) when $k = i_0$ (resp. $k \neq i_0$) and exactly one of i and j coincides with i_0 . Then, we observe that any of the moves in Figure 2.2.7 applied to K , induces an analogous move on K^x . Therefore, the 2-equivalence class of K^x depends only on the 2-equivalence class of K .

At this point, the functoriality and the monoidality of the map $-^x : K \mapsto K^x$, as well as property (b), are immediate. Moreover, if $i_0 = j_0$ no label change occurs and we can undo the crossing changes obtaining $K^x = K$, which gives (a).

It remains to prove (c). Given $x = (i_0, j_0)$ and $y = (i_0, k_0)$ in \mathcal{G}_n , we define $\xi_\pi^{x,y} : I_{(k_0, j_0)} \diamond I_{\pi^x} \rightarrow I_{(k_0, j_0)} \diamond I_{\pi^y}$ to be the tangle presented in Figure 2.3.10, where the largest dotted unknot embraces only the framed strings originally labeled i_0 in I_π . In the same Figure 2.3.10 it is also presented the inverse tangle $(\xi_\pi^{x,y})^{-1}$. The equiv-

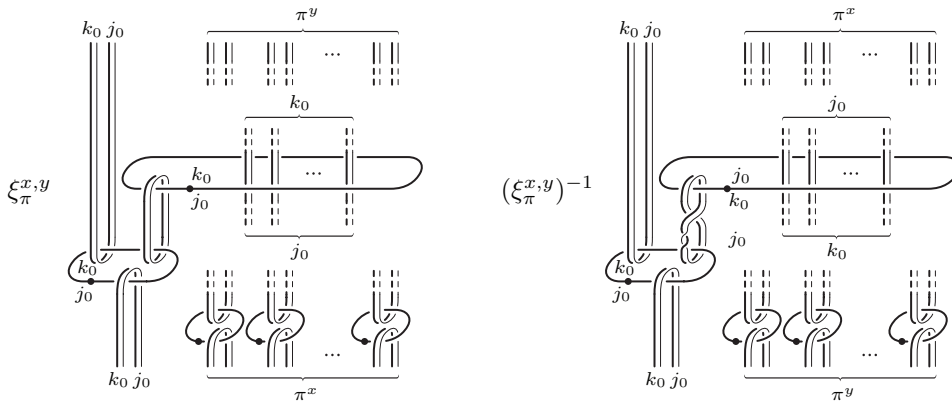


FIGURE 2.3.10. The morphisms $\xi_\pi^{x,y}$ and $(\xi_\pi^{x,y})^{-1}$ ($x = (i_0, j_0)$ and $y = (i_0, k_0)$)

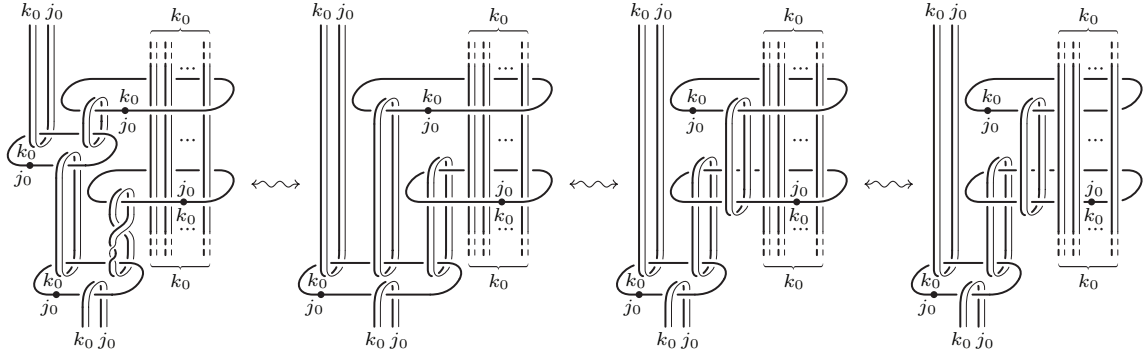


FIGURE 2.3.11. $\xi_{\pi}^{x,y} \circ (\xi_{\pi}^{x,y})^{-1} = \text{id}_{(k_0, j_0) \diamond \pi^y}$ ($x = (i_0, j_0)$ and $y = (i_0, k_0)$)

alence $\xi_{\pi}^{x,y} \circ (\xi_{\pi}^{x,y})^{-1} = \text{id}_{(k_0, j_0) \diamond \pi^y}$ is shown in Figure 2.3.11, where the last step is not drawn and consists in canceling the two framed unknots with the dotted ones. The reader can check in a similar way that $(\xi_{\pi}^{x,y})^{-1} \circ \xi_{\pi}^{x,y} = \text{id}_{(k_0, j_0) \diamond \pi^x}$ as well.

With the above definition of $\xi_{\pi}^{x,y}$, the identity

$$(\text{id}_{(k_0, j_0)} \diamond K^y) \circ \xi_{\pi_0}^{x,y} = \xi_{\pi_1}^{x,y} \circ (\text{id}_{(k_0, j_0)} \diamond K^x)$$

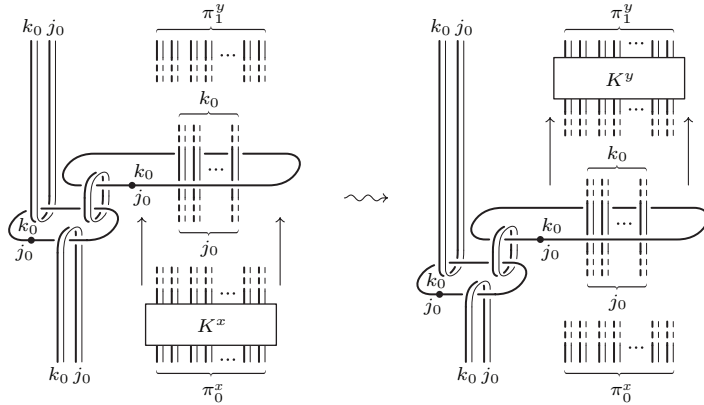


FIGURE 2.3.12. The natural equivalence $\xi^{x,y}$ ($x = (i_0, j_0)$ and $y = (i_0, k_0)$)

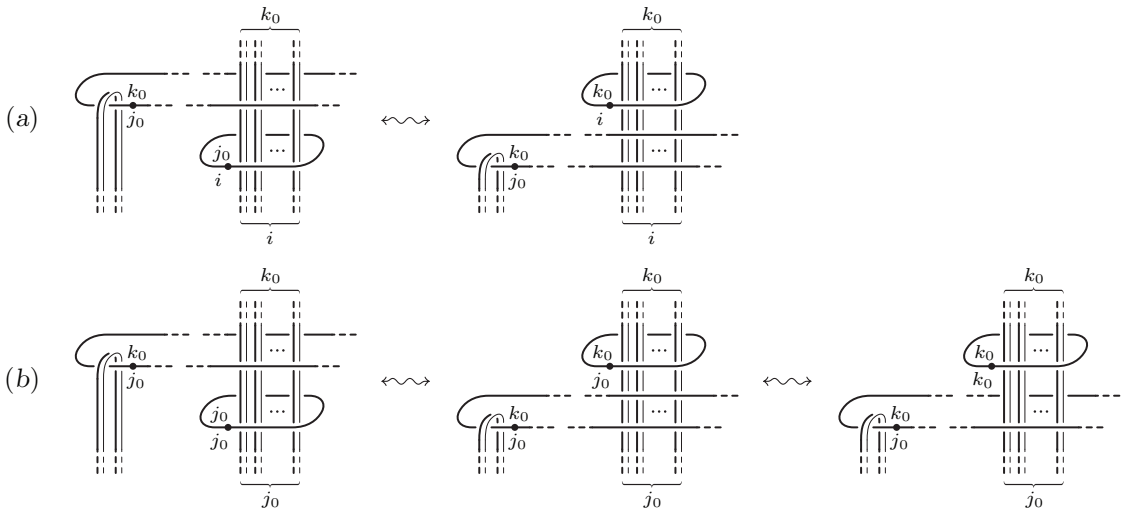


FIGURE 2.3.13. Pushing a dotted unknot through another one ($i \neq j_0$)

corresponding to (c) is obtained by pushing all (and only) the tangle components labeled by j_0 in K^x and originally labeled i_0 in K , through the spanning disk of the dotted unknot of $\xi_{\pi_1^x}^{x,y}$, as indicated by the arrows in Figure 2.3.12. Since those components lie above the rest of the tangle, the pushing through can be realized by Reidemeister moves and the moves (d) and (e) of Figure 2.2.12, until a dotted unknot is encountered, whose spanning disk has one or both sides labeled by j_0 while originally labeled i_0 in K . When this happens we proceed as shown in Figure 2.3.13 (a) or (b) respectively, once the disk has been put in the right position by planar isotopy. In this figure, each step consists in a 1-handle sliding (cf. Figure 2.2.11). \square

Looking at Figure 2.3.1, let us discuss how the functor $_x$ with $x = (i_0, j_0)$ acts on the diagrams drawn there. This will be useful in Section 4.4, when we will relate $_x$ to its algebraic analog (cf. Proposition 4.4.12).

First of all, we observe that all of them but $\Delta_{(i,j)}$ are represented by strictly regular diagrams, therefore the definition directly applies on those diagrams. According to the definition of $_x$ and the subsequent observation about the essential modifications occurring in it, we immediately see that $_x$ only leads to labeling changes for $\text{id}_{(i,j)}$, $\varepsilon_{(i,j)}$, η_i , l_i and $L_{(i,j)}$, while it also involves some crossing changes for $S_{(i,j)}$, $\bar{S}_{(i,j)}$, $\gamma_{(i,j),(i',j')}$ and $\bar{\gamma}_{(i,j),(i',j')}$, in the cases when some of the labels are equal to i_0 . We emphasize once again that not all the involved crossing changes are essential. The only essential ones occur on $S_{(i,j)}$ when $i = j_0$ and $j = i_0$, on $\bar{S}_{(i,j)}$ when $i = i_0$ and $j = j_0$, on $\gamma_{(i,j),(i',j')}$ when $j_0 \in \{i, j\}$ and $i_0 \in \{i', j'\}$, and on $\bar{\gamma}_{(i,j),(i',j')}$ when $i_0 \in \{i, j\}$ and $j_0 \in \{i', j'\}$ (cf. Figures 2.3.14 and 2.3.15).



FIGURE 2.3.14. The tangles $(S_{(j_0, i_0)})^x$ and $(\bar{S}_{(i_0, j_0)})^x$ with $x = (i_0, j_0)$

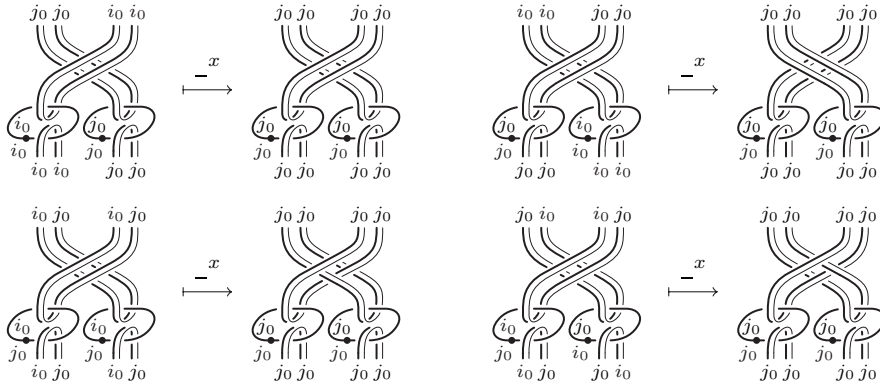


FIGURE 2.3.15. The tangle $(\gamma_{(i,j),(i',j')})^x$ with $x = (i_0, j_0)$ for some particular $(i, j), (i', j') \in \mathcal{G}_n$

Concerning the remaining morphism $\Delta_{(i,j)}$, we have first to put its diagram in strictly regular form. However, also for this morphism the functor $_x$ does not

imply anything more than a labeling change, except in the case when $i \neq i_0$ and $j = i_0$, which is illustrated in Figure 2.3.16. Here, (b) and (c) are the required strictly regular diagrams of the morphism and of its image under $_x$, (d) is just the same as (c) up to diagram isotopy, while a 1-handle twist is needed to get (e). It is worth noticing that the final result is the same as if we had reversed the 1-handle in the original diagram, by using the general reversing procedure described in Figure 3.3.8 of the next chapter, and then performed the prescribed crossing changes and labeling replacement, even without converting the diagram in strictly regular form. Moreover, we observe that the crossing change between (b) and (c) is essential only when $i = j_0$ as above, hence for $i \neq j_0$ we still have $(\Delta_{(i,i_0)})^x = \Delta_{(i,j_0)}$.

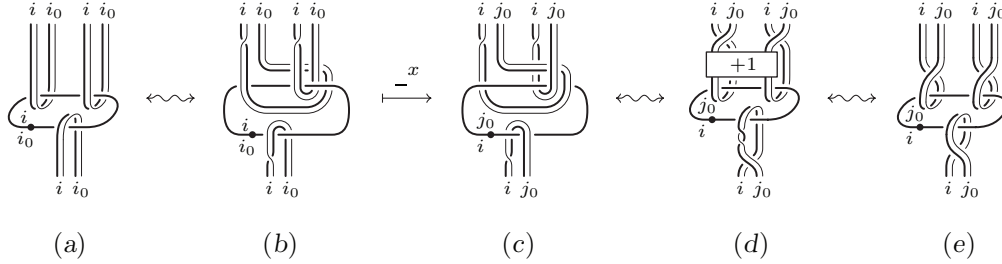


FIGURE 2.3.16. The tangle $(\Delta_{(i,j)})^x$ for $i \neq i_0$ and $j = i_0$

Now we can proceed with the definition of the reduction functor.

DEFINITION 2.3.7. Given $n \geq 2$, we define the *elementary reduction functor* $\downarrow_{n-1}^n : \mathcal{K}_{n \rightarrow (n-1)} \rightarrow \mathcal{K}_{n-1}$ as follows. For any object of $I_{(n,n-1)} \diamond I_\pi$ of $\mathcal{K}_{n \rightarrow (n-1)}$ we put

$$\downarrow_{n-1}^n(I_{(n,n-1)} \diamond I_\pi) = I_{\pi(n,n-1)},$$

while for any morphism $K = (\text{id}_{(n,n-1)} \diamond L) \circ (\Delta_{(n,n-1)} \diamond \text{id}_{\pi_0})$ of $\mathcal{K}_{n \rightarrow (n-1)}$ from $I_{(n,n-1)} \diamond I_{\pi_0}$ to $I_{(n,n-1)} \diamond I_{\pi_1}$ we define (see Figure 2.3.17)

$$\begin{aligned} \downarrow_{n-1}^n K &= (\varepsilon_{(n-1,n-1)} \diamond \text{id}_{\pi_1^{(n,n-1)}}) \circ K^{(n,n-1)} \circ (\eta_{n-1} \diamond \text{id}_{\pi_0^{(n,n-1)}}) \\ &= L^{(n,n-1)} \circ (\eta_{n-1} \diamond \text{id}_{\pi_0^{(n,n-1)}}), \end{aligned}$$

where $\varepsilon_{(n-1,n-1)}$ and η_{n-1} are as in Figure 2.3.1 (for $i = j = n - 1$), $K^{(n,n-1)}$ is defined in Lemma 2.3.6, and the last equality is obtained by 1/2-handle cancellation.

Given $n \geq k \geq 1$, the *reduction functor* $\downarrow_k^n : \mathcal{K}_{n \rightarrow k} \rightarrow \mathcal{K}_k$ is defined as the composition $\downarrow_k^n = \downarrow_k^{k+1} \circ \dots \circ \downarrow_{n-1}^n$ of elementary reduction functors.

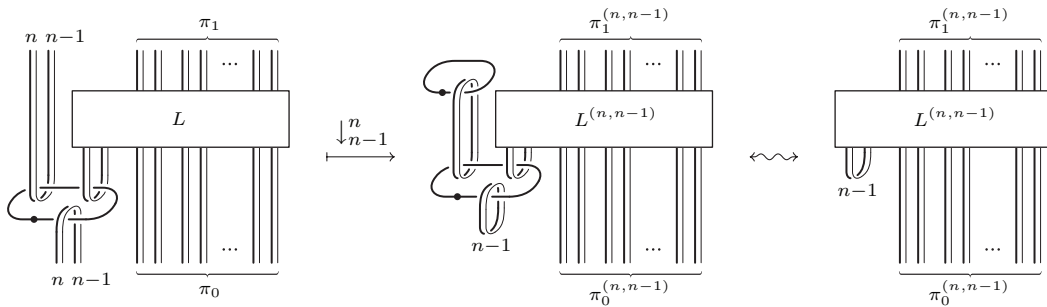


FIGURE 2.3.17. The reduction functor \downarrow_{n-1}^n

LEMMA 2.3.8. For any $n \geq 2$, the reduction $\downarrow_{n-1}^n : \mathcal{K}_{n \rightarrow (n-1)} \rightarrow \mathcal{K}_{n-1}$ is a functor such that $\downarrow_{n-1}^n \circ \uparrow_{n-1}^n = \text{id}_{\mathcal{K}_{n-1}}$, while $\uparrow_{n-1}^n \circ \downarrow_{n-1}^n \simeq \text{id}_{\mathcal{K}_{n \rightarrow (n-1)}}$ up to the natural equivalence $\xi^{(n,n-1)} = \xi^{(n,n-1),(n,n)}$. Therefore, \downarrow_{n-1}^n and \uparrow_{n-1}^n are category equivalences between $\mathcal{K}_{n \rightarrow (n-1)}$ and \mathcal{K}_{n-1} .

Proof. The functoriality of \downarrow_{n-1}^n directly follows from that of the map $K \mapsto K^{(n,n-1)}$ (cf. Lemma 2.3.6). Looking at Figure 2.3.17, we see that $\downarrow_{n-1}^n \circ \uparrow_{n-1}^n = \text{id}_{\mathcal{K}_{n-1}}$. In fact, if the leftmost diagram in the figure comes from the stabilization of an $(n-1)$ -labeled Kirby tangle as on the left in Figure 2.3.8, then $\pi_0^{(n,n-1)} = \pi_0$, $\pi_1^{(n,n-1)} = \pi_1$ and essentially nothing is changed inside the box by the reduction. Hence, we end up with the rightmost diagram that represents the $(n-1)$ -labeled Kirby tangle itself (with an extra canceling 1/2-pair labeled by $n-1$).

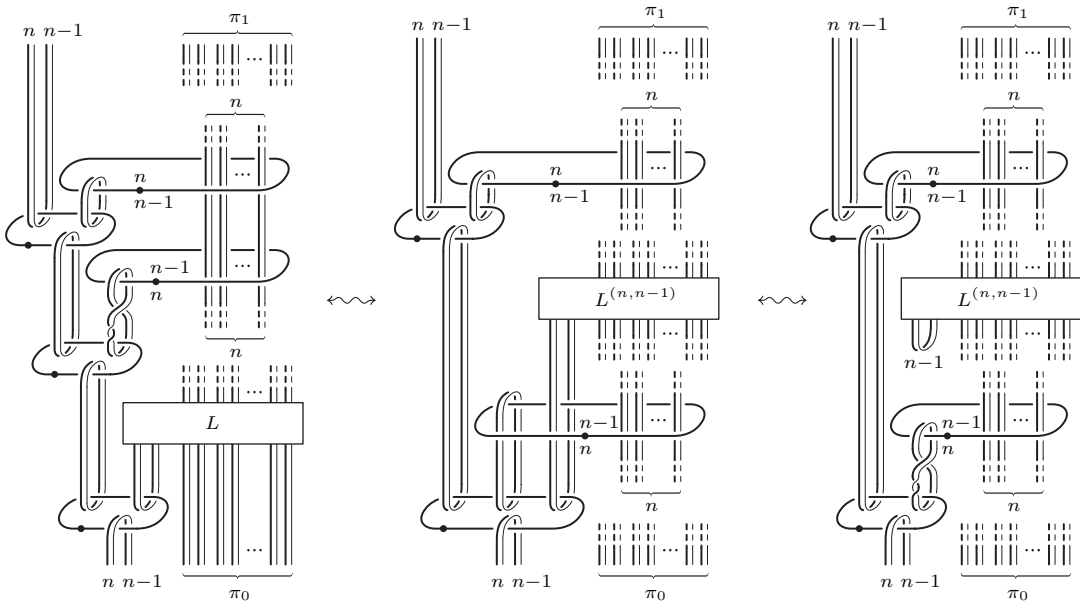


FIGURE 2.3.18. The natural equivalence $\xi^{(n,n-1)} : \uparrow_{n-1}^n \circ \downarrow_{n-1}^n \simeq \text{id}_{\mathcal{K}_{n \rightarrow (n-1)}}$

The proof that $\xi^{(n,n-1)}$ gives a natural equivalence $\text{id}_{\mathcal{K}_{n \rightarrow (n-1)}} \rightarrow \uparrow_{n-1}^n \circ \downarrow_{n-1}^n$ is provided by Figure 2.3.18. Here, the first diagram is equivalent to the $(n-1)$ -reducible tangle $K = (\text{id}_{(n,n-1)} \diamond L) \circ (\Delta_{(n,n-1)} \diamond \text{id}_{\pi_0})$ since $\xi^{(n,n-1)}$ cancels with its inverse, the second tangle is obtained from the first by using Lemma 2.3.6 (c) (cf. Figure 2.3.12 with $x = (n, n-1)$ and $y = (n, n)$), while the third tangle is obtained through 2-handle slidings and isotopy. This completes the proof that \downarrow_{n-1}^n and \uparrow_{n-1}^n are equivalences of monoidal categories. \square

PROPOSITION 2.3.9. For any $n > k \geq 1$, the reduction $\downarrow_k^n : \mathcal{K}_{n \rightarrow k} \rightarrow \mathcal{K}_k$ is a functor such that $\downarrow_k^n \circ \uparrow_k^n = \text{id}_{\mathcal{K}_k}$, while there is a natural equivalence $\xi^{n \rightarrow k} : \uparrow_k^n \circ \downarrow_k^n \simeq \text{id}_{\mathcal{K}_{n \rightarrow k}}$, inductively defined by $\xi^{n \rightarrow (n-1)} = \xi^{(n,n-1)}$ and

$$\xi^{n \rightarrow k} = \xi^{(n,n-1)} \circ (\text{id}_{(n,n-1)} \diamond \xi^{(n-1) \rightarrow k}).$$

Therefore, \downarrow_k^n and \uparrow_k^n are category equivalences between $\mathcal{K}_{n \rightarrow k}$ and \mathcal{K}_k .

Proof. We prove the statement by induction on the difference $n - k$. For $k = n - 1$ it follows from the previous lemma. For $k < n - 1$, taking into account that $\uparrow_k^n = \uparrow_{n-1}^n \circ \uparrow_k^{n-1}$ and $\uparrow_k^n \mathcal{K}_k \subset \mathcal{K}_{n \rightarrow k}$, by the induction hypothesis we have

$$\downarrow_k^n \circ \uparrow_k^n = \downarrow_k^{n-1} \circ \downarrow_{n-1}^n \circ \uparrow_{n-1}^n \circ \uparrow_k^{n-1} = \downarrow_k^{n-1} \circ \uparrow_k^{n-1} = \text{id}_{\mathcal{K}_k}.$$

Moreover, for any $K \in \mathcal{K}_{n \rightarrow k}$ we can write $\uparrow_k^n \downarrow_k^n K = \text{id}_{n, n-1} \diamond (\uparrow_k^{n-1} \downarrow_k^{n-1} \downarrow_{n-1}^n K)$, which induces a natural equivalence $\text{id}_{(n, n-1)} \diamond \xi^{(n-1) \rightarrow k} : \uparrow_k^n \circ \downarrow_k^n \simeq \uparrow_{n-1}^n \circ \downarrow_{n-1}^n$. Then, by composing with $\xi^{(n, n-1)} : \uparrow_{n-1}^n \circ \downarrow_{n-1}^n \simeq \text{id}_{\mathcal{K}_{n \rightarrow (n-1)}}$, we get the natural equivalence $\xi^{n \rightarrow k} : \uparrow_k^n \circ \downarrow_k^n \simeq \text{id}_{\mathcal{K}_{n \rightarrow k}}$. \square

3. Labeled ribbon surface tangles

In Chapter 2 we have seen how to represent 4-dimensional relative 2-handlebody cobordisms between 3-dimensional 1-handlebodies with n 0-handles up to 2-equivalence by means of n -labeled Kirby tangles in $E \times [0, 1]$. These tangles, considered up to isotopy and 2-deformation moves, was encoded as the morphisms of the categories \mathcal{K}_n with $n \geq 1$, equivalent to the categories of cobordisms $\mathcal{C}hb_n^{3+1}$.

The goal of this chapter is to give a different representation of such cobordisms in terms of n -labeled ribbon surface tangles, by describing them as n -fold simple coverings of $E \times [0, 1] \times [0, 1]$ (cf. Sections 1.3 and 1.4). Such ribbon surface tangles, up to labeled 1-isotopy and ribbon moves (cf. Figure 1.4.5), will represent the morphisms of the categories \mathcal{S}_n with $n \geq 2$.

The relation between the two representations of 4-dimensional relative 2-handlebody cobordisms, as Kirby tangles and as labeled ribbon surface tangles, will be established by the functor $\Theta_n : \mathcal{S}_n \rightarrow \mathcal{K}_n$ defined in Section 3.3. The restriction $\Theta_n : \mathcal{S}_n^c \rightarrow \mathcal{K}_n^c$ to a suitable subcategory $\mathcal{S}_n^c \subset \mathcal{S}_n$, representing connected handlebodies, will be proved to be a category equivalence for $n \geq 4$ in Section 3.6.

We emphasize that the same does not hold for $n < 4$. Indeed, it is shown in [52] that all connected 4-dimensional 2-handlebodies are 3-fold (irregular) branched covers of B^4 , but only the symmetric ones are 2-fold (regular) branched covers of B^4 . This implies that Θ_2 cannot be full. Moreover, the result in [7] (cf. also [56]) implies two 3-fold branched covering of B^4 representing the same 4-dimensional 2-handlebody are not necessarily related through 1-isotopy and the ribbon move (R1) (note that move (R2) does not appear when $n \leq 3$). Therefore Θ_3 , as well as Θ_2 , cannot be faithful.

3.1. The category \mathcal{S} of ribbon surface tangles

We define the category \mathcal{S} of ribbon surface tangles as follows. An object of \mathcal{S} is any finite (possibly empty) trivial family A of regularly embedded arcs in $\text{Int } E \times [0, 1[$, with $E = [0, 1]^2$. Given two objects $A_0, A_1 \in \text{Obj } \mathcal{S}$, a morphism of \mathcal{S} with source A_0 and target A_1 is a ribbon surface tangle $S \subset E \times [0, 1] \times [0, 1[$, considered up to 1-isotopy, such that $\partial_0 S = i_0(A_0)$ and $\partial_1 S = i_1(A_1)$, where $i_0, i_1 : E \times [0, 1[\rightarrow E \times [0, 1] \times [0, 1[$ are the inclusions defined $i_0(x, y, t) = (x, y, 0, t)$ and $i_1(x, y, t) = (x, y, 1, t)$ respectively.

The composition of two morphisms $S_1 : A_0 \rightarrow A_1$ and $S_2 : A_1 \rightarrow A_2$ in \mathcal{S} is represented by the ribbon surface tangle obtained by stacking S_2 over S_1 , so that $\partial_0 S_2$ coincides with $\partial_1 S_1$, and then smoothing the union surface and rescaling the third coordinate by $1/2$. Then, the identity morphism $\text{id}_A : A \rightarrow A$ of an object $A \in \mathcal{S}$ is represented by the product ribbon surface tangle $\{(x, y, z, t) \mid (x, y, t) \in A \text{ and } z \in [0, 1]\} \subset E \times [0, 1] \times [0, 1[$.

For any $m \geq 0$ we consider the *standard object* J_m of \mathcal{S} to be the (possibly empty) sequence $J_m = (a_{m,1}, \dots, a_{m,m})$ of regularly embedded arcs in $\text{Int } E \times [0, 1[$ defined as follows. For any $1 \leq k \leq m$, we start with the interval in E

$$a_{m,k} = [(k - 0.8)/m, (k - 0.2)/m] \times \{0.5\},$$

then we push its interior in the interior of $\text{Int } E \times [0, 1[$ to get the regularly embedded arc $a_{m,k}$ (we use the same notation $a_{m,k}$ for both the interval and the arc). All the

arcs forming the J_m 's are assumed to be equivalent up to translations and rescaling of the first coordinate.

We say that a ribbon surface tangle S has *standard ends* if it represents a morphism between standard objects, that is $\partial_0 S = i_0(J_{m_0})$ and $\partial_1 S = i_1(J_{m_1})$ for some $m_0, m_1 \geq 0$. In particular, we denote by $\text{id}_m : J_m \rightarrow J_m$ the identity morphism of J_m for any $m \geq 0$.

We can introduce a strict monoidal structure on the full subcategory of \mathcal{S} with standard objects, in the following way. On the set of standard objects, we consider the product $J_m \diamond J_{m'} = J_{m+m'}$. Then, given two ribbon surface tangles S and S' with standard ends, we define their product $S \diamond S'$, by horizontal juxtaposition of S and S' , followed by a reparametrization of the first coordinate depending only on the third one (that is a diffeomorphism $(x, y, z, t) \mapsto (h^z(x), y, z, t)$ with h^z increasing function of x for every z).

PROPOSITION 3.1.1. *\mathcal{S} is equivalent to its full subcategory whose objects are the standard objects J_m for $m \geq 0$, through the inclusion functor. The product defined above, makes such subcategory into a strict monoidal category, whose unit is represented by the empty tangle $\text{id}_0 : J_0 \rightarrow J_0$.*

Proof. For the first part of the statement, according to Corollary 1.5.4, it suffices to prove that any object of $A \in \mathcal{S}$ consisting of m regularly embedded arcs in $\text{Int } E \times [0, 1[$ is isomorphic to the standard object J_m . In fact, an isomorphism from J_m to A is represented by the ribbon surface tangle (with no ribbon self-intersections) $S = \{(x(p, t), y(p, t), t, z(p, t)) \mid p \in J_m, t \in [0, 1]\}$, with $h_t(p) = (x(p, t), y(p, t), z(p, t))$ any ambient isotopy of $\text{Int } E \times [0, 1[$ such that $h_1(J_m) = A$.

Concerning the strict monoidal structure, the verification of the required properties is straightforward, being the unit of the product the empty morphism, the one represented by the empty ribbon surface tangle. \square

From now on, we will use the notation \mathcal{S} for the strict monoidal category of ribbon surface tangles with standard ends given by Proposition 3.1.1.

The rest of this section will be dedicated to the study of the structure of \mathcal{S} . We will prove that \mathcal{S} is equivalent to a strict monoidal braided category generated by a single object and a set of elementary morphisms and relations in sense of Definition 1.5.10. Moreover, we will show that such category carries also a tortile structure (cf. Definition 1.5.8).

We start with the elementary diagrams in Figure 3.1.1, considered up to isotopy preserving horizontal lines, that is isotopy of the form $((x, y) \mapsto (h_t^y(x), h_t(y)))_{t \in [0, 1]}$ with h_t^y an increasing function of x for every y and t , and h_t increasing function of y for every t . Here, the elementary diagram (a) represents the identity of J_1 .

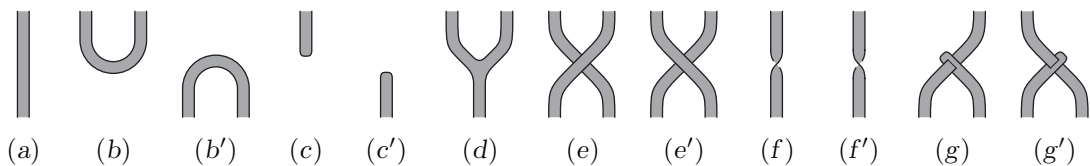


FIGURE 3.1.1. Elementary diagrams in the category \mathcal{S}

Then, also iterated products/compositions of such elementary diagrams, defined by horizontal/vertical juxtaposition and rescaling, turn out to be well-defined up to isotopy preserving horizontal lines.

In this context, the planar isotopy moves in Figure 3.1.2, where the boxes D and D' in $(I1)$ contain any of the elementary diagrams in Figure 3.1.1, can be interpreted as relations between iterated products/compositions of elementary diagrams.

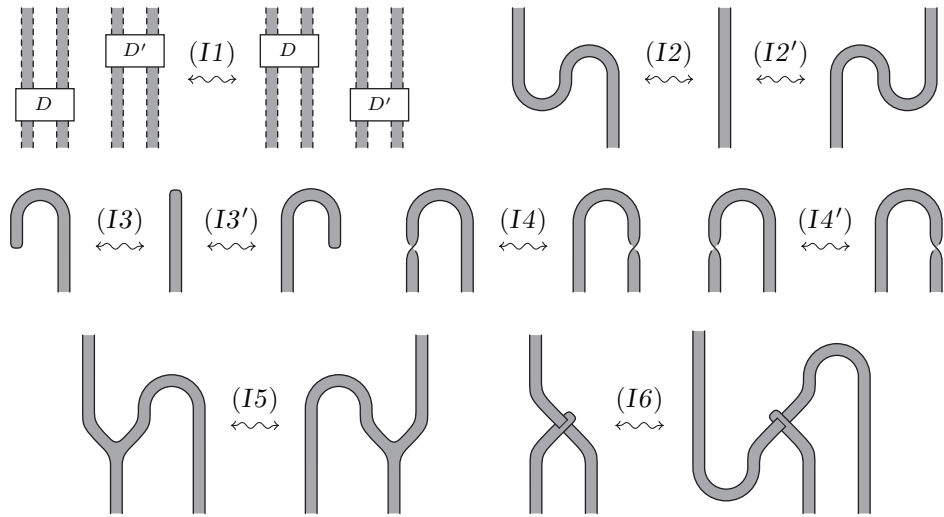


FIGURE 3.1.2. Planar isotopy relations in the category \mathcal{S}

An analogous interpretation of the moves introduced in Figures 1.3.9, 1.3.10 and 1.3.11 to realize 3-dimensional diagram isotopy of ribbon surface tangles, and of the 1-isotopy moves in Figure 1.3.13, leads to the relations depicted in Figures 3.1.3, 3.1.4 and 3.1.5, where the box D in $(I8)$ and $(I9)$ contains any of the elementary diagrams in Figure 3.1.1. In particular, relations $(I7-7')$ and $(I12-12')$ say that (e') and (f') are the inverses of (e) and (f) with respect to the composition.

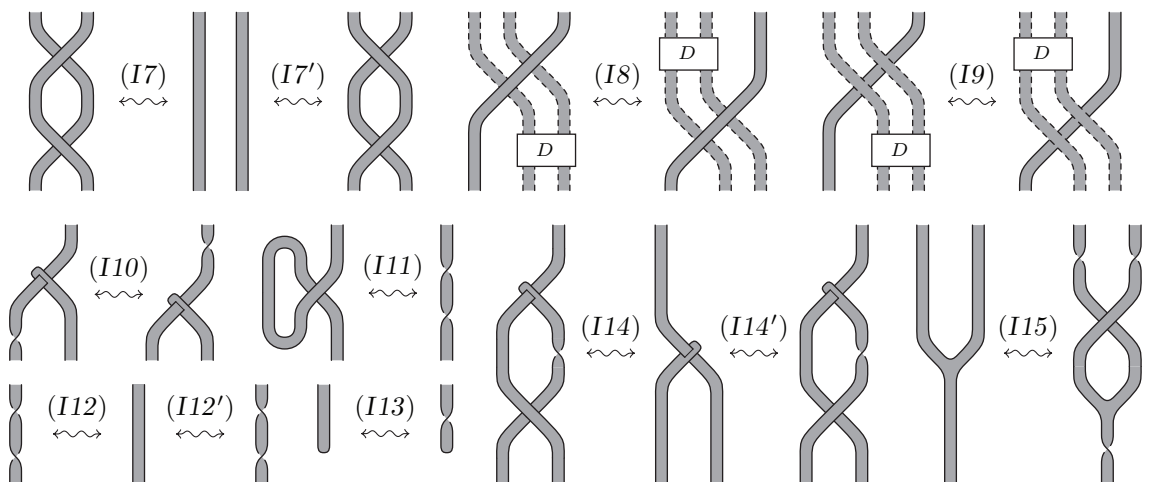


FIGURE 3.1.3. 3-dimensional isotopy relations in the category \mathcal{S}

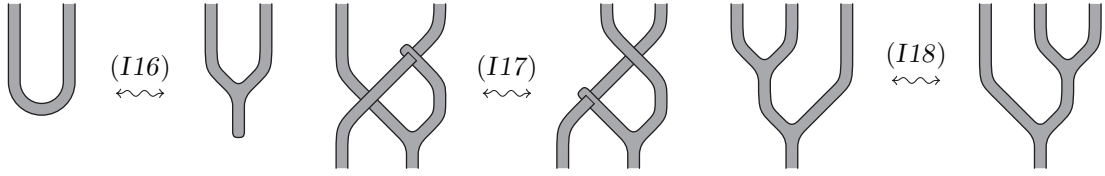


FIGURE 3.1.4. Graph changing relations in the category \mathcal{S}

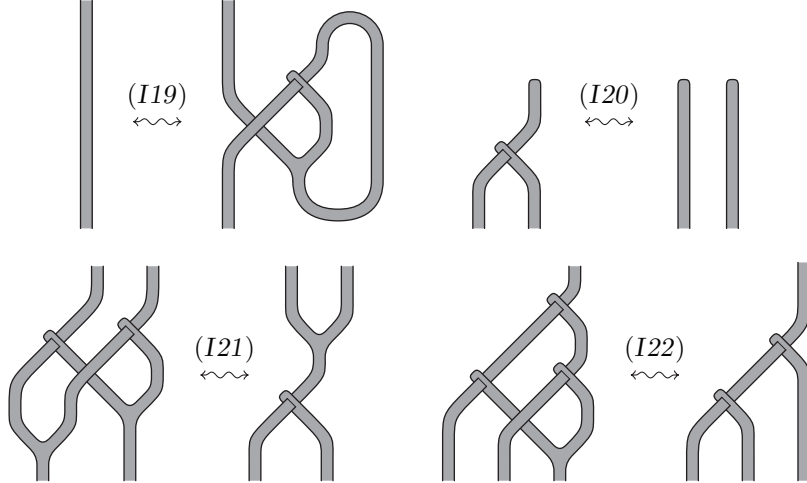


FIGURE 3.1.5. 1-isotopy relations in the category \mathcal{S}

Now, consider the strict monoidal category $C(J_1, E, R)$ generated by the single object J_1 and the set E of elementary morphisms in Figure 3.1.1 modulo the set R of elementary relations (I1) to (I22). Here, the relations (I1) could be omitted, since it is universally valid as requested in point (c) of Proposition 1.5.9.

Remember from Section 1.5 that $\text{Obj } C(J_1, E, R)$ is the free monoid ΠJ_1 generated by J_1 , which can be identified with the set of standard objects $J_m = J_1 \diamond \dots \diamond J_1$ for $m \geq 0$. On the other hand, each iterated product/composition of elements of E can be expressed as a composition of expansions (that is products with identities) of elements of E , that is a morphism of the free category $F(J_1, E)$, which is uniquely determined up to (I1) (and its expansions). Then, all the relations (I2) to (I22) can be seen as relations in the free category $F(J_1, E)$, hence as defining relations for $C(J_1, E, R)$ according to Definition 1.5.10.

PROPOSITION 3.1.2. *\mathcal{S} is equivalent to $C(J_1, E, R)$ as a strict monoidal category, through a monoidal equivalence functor $C(J_1, E, R) \rightarrow \mathcal{S}$, which is the identity on the objects and send each morphism of $C(J_1, E, R)$, represented by a given diagram, to the morphism of \mathcal{S} represented by the corresponding ribbon surface tangle.*

Proof. We consider the map $C(J_1, E, R) \rightarrow \mathcal{S}$ defined by formal propagation over products and compositions of the requirement that elementary diagrams are sent to the corresponding ribbon surface tangle. In other words, any planar diagram given as iterated product/composition of elementary ones is sent to the corresponding ribbon surface tangle as well. Since any morphism in $C(J_1, E, R)$ is represented by a composition of expansions of elements of E , in order to have a well-defined map on the level of morphisms, it suffices to observe the images of the relations in

R are all 1-isotopy moves between the corresponding ribbon surface tangles. Indeed, the relations in Figure 3.1.2 represent planar diagram isotopies, the ones in Figures 3.1.3 correspond to 3-dimensional diagram isotopies, while those in Figures 3.1.4 and 3.1.5 can be realized by the moves in Figures 1.3.9 and 1.3.13 respectively.

Therefore, the map $C(J_1, E, R) \rightarrow \mathcal{S}$ defined as the identity on the objects and as described above on the morphisms is a strict monoidal functor. It remains to see that this functor is full and faithful, hence an equivalence of categories.

The fullness simply means that any morphism of \mathcal{S} can be presented as a composition of expansions of elementary diagrams. First of all, we observe that such a morphism is assumed to have standard ends (after Proposition 3.1.1), hence it can be represented by a special planar diagram thanks to Proposition 1.3.7, since standard ends are flat.

We say that a special planar diagram of a ribbon surface tangle S is in *normal position* with respect to the y -axis if it satisfies the following properties:

- (a) each edge of the core graph G projects to a regular smooth arc immersed in $]0, 1[\times [0, 1]$, such that the y -coordinate restricts to a Morse function on it;
- (b) vertices, half-twists, crossings and local minimum/maximum points for the y -coordinate along the edges of the core graph G have all different y -coordinates (in particular, there are no horizontal tangencies at vertices, half-twists and crossings).

We observe that all the elementary diagrams in Figure 3.1.1 are in normal position with respect to the y -axis, hence this is also true for any composition of expansions of them.

Figure 3.1.6 shows the different ways, up to planar isotopy preserving horizontal lines, to put the spots (a) to (e) and (h) of Figure 1.3.6 in normal position with respect to the y -axis, by planar diagram isotopies which do not introduce any local minimum/maximum for the y -coordinate along the edges of the core graph.

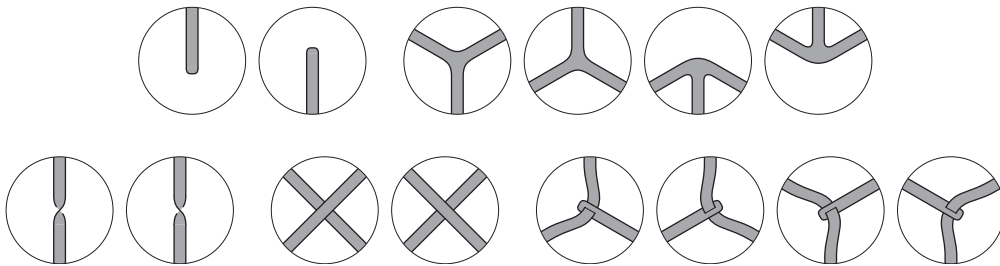


FIGURE 3.1.6. Local models for planar diagrams in normal position

All such local configurations appear among the elementary diagrams in Figure 3.1.1, except for some of those at 3-valent vertices of the core graph. Namely, only the first of those at a flat 3-valent vertex and the first two of those at a singular vertex are considered as elementary diagrams. Up to planar isotopy, the others can be expressed in terms of them as in Figure 3.1.7.

Now, let S be any ribbon surface tangle with standard ends, represented by a special planar diagram, as said above. Then, we can perturb such diagram to get normal position with respect to the y -axis. Finally, the local isotopies described

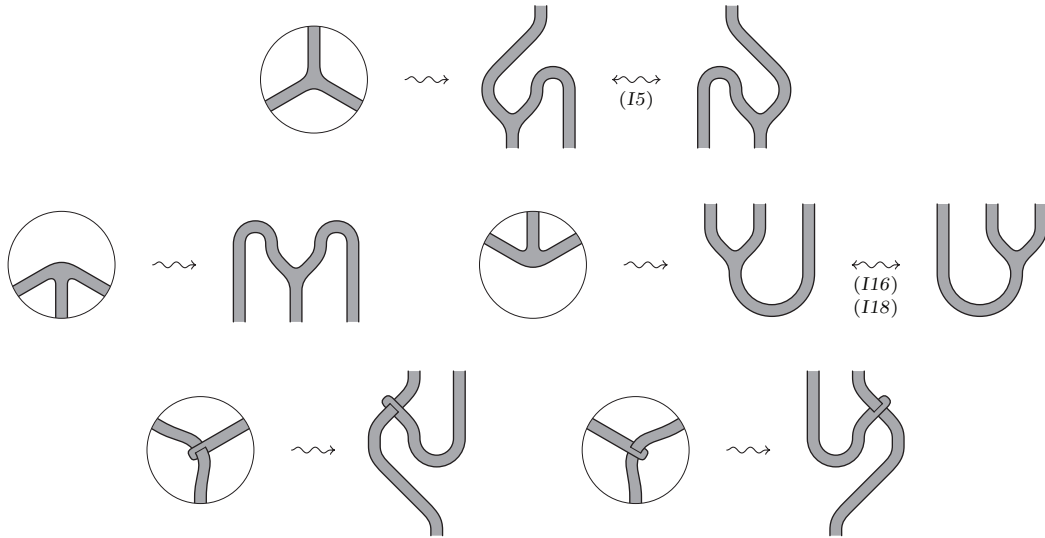


FIGURE 3.1.7. Expressing local models in terms of elementary diagrams

in Figure 3.1.7 can be applied to obtain a presentation of S as composition of expansions of elementary diagrams. This completes the proof of the fullness.

In order to see that the functor is faithful, we have to prove that any two morphisms of \mathcal{S} , expressed as composition of expansions of elementary diagrams, are equivalent up to plane isotopy preserving horizontal lines and the relations (I1) to (I22). In other words, that these relations allow us to interpret any 1-isotopy of ribbon surface tangles with standard ends.

We first focus on planar isotopy, with an argument analogous to that of Proposition 1.3.8. Assume we are given an arbitrary smooth planar isotopy relating any two given presentations of S as above. Denote by \bar{G} the planar graph associated to the planar diagram of the core graph G of S , whose vertices, other than the projections of the vertices of G and the 4-valent vertices at the crossings, also include 2-valent vertices at the half-twists.

We use transversality to perturb the given planar isotopy in such a way there is only a finite number of critical levels where \bar{G} presents exactly one of the following:

- 1) the y -coordinate on one edge is not a Morse function;
- 2) there is a horizontal tangent line at one of the vertices (including half-twists and crossings) ;
- 3) two points among the extremal ones along edges and the vertices (including half-twists and crossings) have the same y -coordinate.

Away from these critical levels the diagram is in normal position with respect to the y -axis and the isotopy can be assumed to preserve horizontal lines.

We will show that the relations in Figures 3.1.2 e 3.1.3 suffice to realize all changes occurring in the diagram when passing through one critical level.

The cases of critical levels of types 1 and 3 are respectively covered by relations (I2-2') and (I1). At critical levels of type 2 the vertex with horizontal tangency is switching from one to another of its normal positions depicted in Figure 3.1.6. At the same time, one extremal point (resp. one pair of canceling extremal points) for the y -coordinate is appearing/disappearing along the edge (resp. the opposite edges) presenting the horizontal tangency. The cases when the vertex we are considering is

a uni-valent flat vertex or a half-twists correspond respectively to relations $(I3-3')$ or $(I4-4')$, modulo $(I1)$ and $(I2-2')$. If the vertex is a crossing, there are four symmetric possibilities and Figure 3.1.8 shows how to realize one them. The other three can be realized in a similar way, by using relations $(I7-7')$, $(I8)$ and $(I9)$. In order to deal with tri-valent vertices, we need to replace the normal positions that are missing in the elementary diagrams as indicated in Figure 3.1.7. After that, modulo $(I1)$ and $(I2-2')$, all the cases reduce to relation $(I6)$ and to the modification described in Figure 3.1.9 for singular vertices, and to relation $(I5)$ for flat vertices.

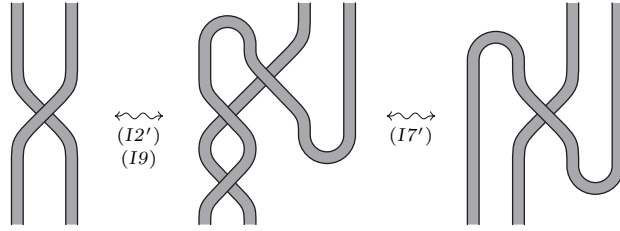


FIGURE 3.1.8. Switching a crossing

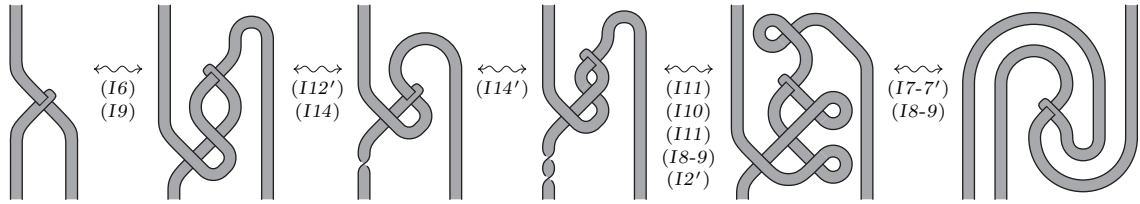


FIGURE 3.1.9. Switching a ribbon intersection

Now we pass to 3-dimensional diagram isotopy. By Proposition 1.3.8, we have to interpret in terms of relations the moves $(S3)$ to $(S22)$ in Figures 1.3.9, 1.3.10 and 1.3.11. Since those moves are defined up to planar isotopy, such interpretation is quite immediate. In particular, we have that: the relations in Figure 3.1.4 give the moves in Figure 1.3.9; the relations in the first line of Figure 3.1.3 give the moves in Figure 1.3.10 and $(S15-16)$; the remaining relations in Figure 3.1.3 give the moves $(S14)$ and $(S17)$ to $(S22)$ in Figure 1.3.11, modulo the previous moves in the case of $(S19)$.

Finally, concerning 1-isotopy moves in 1.3.13 (cf. Proposition 1.3.9), it is enough to observe that, after expressing them in terms of special planar diagrams by using move $(S1)$, they essentially correspond to the relations in Figure 3.1.5. \square

We can use the elementary diagrams in Figure 3.1.1 to define a tortile structure on the category \mathcal{S} (cf. Proposition 3.1.3 below). In particular, we make the following natural choices: (f) for the braiding isomorphism γ_{J_1, J_1} ; (b) and (b') for the form and coform morphisms Λ_{J_1} and λ_{J_1} respectively; the composition $(\lambda_{J_1} \diamond \text{id}_{J_1}) \circ (\text{id}_{J_1} \diamond \gamma_{J_1, J_1}) \circ (\Lambda_{J_1} \diamond \text{id}_{J_1})$ for the twist isomorphism θ_{J_1} (see Figure 3.1.10).

From now on we will write only m instead of J_m in the subscripts of the notation for the morphisms of \mathcal{S} , to keep that notation as simple as possible. For example $\gamma_{1,1}$, λ_1 , Λ_1 and θ_1 will denote the morphisms just mentioned above.

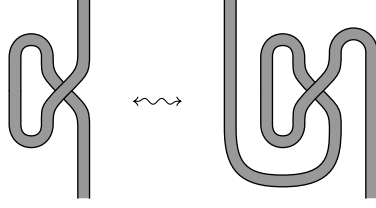


FIGURE 3.1.10. The twist isomorphism θ_1

PROPOSITION 3.1.3. \mathcal{S} is a tortile category, with the tortile structure uniquely determined by $J_m^* = J_m$ for any $m \geq 0$, and by the choices above for $\gamma_{1,1}$, Λ_1 , λ_1 and θ_1 and by the following recursive formulas for $m > 1$:

$$\Lambda_m = (\text{id}_1 \diamond \Lambda_{m-1} \diamond \text{id}_1) \circ \Lambda_1 \quad \text{and} \quad \lambda_m = \lambda_1 \circ (\text{id}_1 \diamond \lambda_{m-1} \diamond \text{id}_1).$$

Proof. The general relations for the braiding isomorphisms (cf. Definition 1.5.6) imply that $\gamma_{0,m} = \gamma_{m,0} = \text{id}_m$ for any $m \geq 0$ and that the recursive formula $\gamma_{m,m'} = (\text{id}_{m'-1} \diamond \gamma_{m,1}) \circ (\gamma_{m,m'-1} \diamond \text{id}_1) = (\gamma_{m-1,m'} \diamond \text{id}_1) \circ (\text{id}_{m-1} \diamond \gamma_{1,m'})$ holds for any $m, m' \geq 1$. Analogously, for the twist isomorphisms (cf. Section 1.5) we have $\theta_0 = \text{id}_0$ and $\theta_m = \gamma_{1,m-1} \circ (\theta_{m-1} \diamond \theta_1) \circ \gamma_{m-1,1}$ for any $m \geq 1$. Then, taking also into account the recursive formulas in the statement, the definitions of $\gamma_{m,m'}$, Λ_m , λ_m and θ_m for any $m, m' \geq 0$, are uniquely determined by the ones of $\gamma_{1,1}$, Λ_1 , λ_1 and θ_1 .

The verification that the families of morphisms we get in this way from our starting choices give a true tortile structure is straightforward. For $m = 1$, the defining properties of forms and cofoms reduce to relations (I1) and (I2-2'), while the self-duality of the twist θ_m follows from relations (I2), (I4) and (I11) (cf. Figure 3.1.10). Then, we can proceed by induction on m , using moves (I7-7'), (I8) and (I9). \square

3.2. The categories \mathcal{S}_n and the functors \uparrow_k^n

As we said at the beginning of the chapter, we want to consider n -fold simple coverings of $E \times [0, 1] \times [0, 1]$, branched over ribbon surface tangles. According to Section 1.4, these can be described in terms of ribbon surface tangles labeled by transpositions in the permutation group Σ_n .

Here, we construct the categories \mathcal{S}_n of such labeled ribbon surface tangles up to certain moves preserving the diffeomorphism type of the covering space for $n \geq 2$. Moreover, we define stabilization functors $\uparrow_k^n : \mathcal{S}_k \rightarrow \mathcal{S}_n$ relating them for any $n > k \geq 2$.

Let $\Gamma_n \subset \Sigma_n$ be the set of all transpositions in the permutation group Σ_n and $\Pi\Gamma_n = \cup_{m=0}^{\infty} \Gamma_n^m$ be the set of (possibly empty) finite sequences of elements of Γ_n . For any sequence $\sigma = ((i_1 j_1), \dots, (i_m j_m)) \in \Pi\Gamma_n$, we denote by J_σ the sequence of intervals $J_m = (a_{m,1}, \dots, a_{m,m})$ (the standard object of \mathcal{S} defined on page 64) with each $a_{m,k}$ labeled by the corresponding transposition $(i_k j_k)$.

DEFINITION 3.2.1. Let $n \geq 2$ and $\sigma_0 = ((i_1^0 j_1^0), \dots, (i_{m_0}^0 j_{m_0}^0))$ and $\sigma_1 = ((i_1^1 j_1^1), \dots, (i_{m_1}^1 j_{m_1}^1))$ be two sequences in $\Pi\Gamma_n$. By an n -labeled ribbon surface tangle from J_{σ_0} to J_{σ_1} we mean a ribbon surface tangle S from J_{m_0} to J_{m_1} with a Γ_n -labeling satisfying the following properties:

- 1) each region in the diagram of S is labeled by a transposition in Γ_n associated to the corresponding meridian, in such a way that the Wirtinger relations in $\pi_1(E \times [0, 1] \times [0, 1] - S)$ are respected (cf. Section 1.4);
- 2) the labels on $\partial_0 S$ and $\partial_1 S$ coincide with those in J_{σ_0} and J_{σ_1} respectively.

We notice that property 1 is the same as requiring that the labeling represents the monodromy homomorphism $\omega_p : \pi_1(E \times [0, 1] \times [0, 1] - S) \rightarrow \Sigma_n$ of an n -fold simple covering of $p : W \rightarrow E \times [0, 1] \times [0, 1]$ branched over S (cf. Section 1.4). By [52] we know that W is a relative 4-dimensional 2-handlebody cobordism between the 3-dimensional 1-handlebodies $M_0 = p^{-1}(E \times \{0\} \times [0, 1])$ and $M_1 = p^{-1}(E \times \{1\} \times [0, 1])$. Moreover, as discussed in Section 1.4, labeled isotopy and the moves (R1) and (R2) in Figure 3.2.1 (cf. Figure 1.4.5) do not change W up to diffeomorphism.

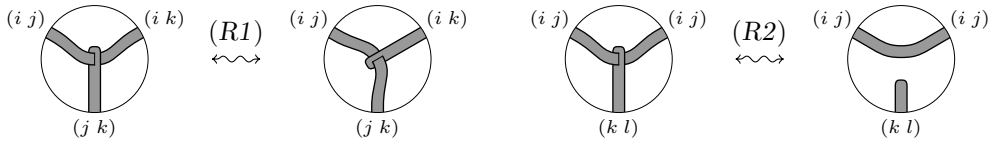


FIGURE 3.2.1. Ribbon moves (i, j, k and l all different)

Actually, in Section 3.3 we will also see that the handlebody structures of M_0 and M_1 are uniquely determined, while that of W is determined only up to 2-equivalence, depending on the choice of an adapted 1-handlebody decomposition of S . We do not know whether labeled isotopy preserves the 2-equivalence class of W , but we will show in Proposition 3.3.2 that labeled 1-isotopy does and that the same holds for moves (R1) and (R2). This is the motivation for the following definition.

DEFINITION 3.2.2. Two n -labeled ribbon surface tangles are said to be *equivalent* if they are related by the labeled version of the 1-isotopy moves (S1) to (S26) in Figures 1.3.8, 1.3.9, 1.3.10, 1.3.11 and 1.3.13, and by the two covering moves (R1) and (R2) in Figure 3.2.1.

Before going on, we recall the auxiliary moves (R3) to (R6) in Figure 3.2.2, which were introduced in Section 1.4 (cf. Figure 1.4.7). These have been shown to derive from the equivalence moves (R1) and (R2) up to 1-isotopy (cf. Proposition 1.4.3), hence they are equivalence moves for labeled ribbon surface tangles as well. Once we will prove that (R1) and (R2) preserve the 2-equivalence class of the covering handlebody W , we will know that the same holds for the moves (R3) to (R6).

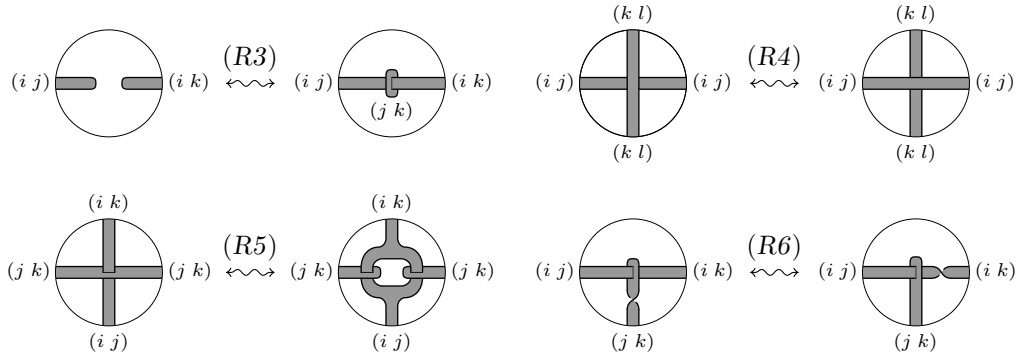


FIGURE 3.2.2. Other moves for labeled ribbon surfaces (i, j, k and l all different)

At this point, we can define the category \mathcal{S}_n of n -labeled ribbon surface tangles for any $n \geq 2$, in the following way. The objects of \mathcal{S}_n are the sequences of labeled intervals J_σ with $\sigma = ((i_1 j_1), \dots, (i_m j_m)) \in \Pi\Gamma_n$ (cf. the notation introduced before Definition 3.2.1), while the morphisms in \mathcal{S}_n with source J_{σ_0} and target J_{σ_1} are the n -labeled ribbon surface tangles from J_{σ_0} to J_{σ_1} , considered up equivalence in the sense of Definition 3.2.2. The composition of morphisms in \mathcal{S}_n is just the labeled version of that in \mathcal{S} . Similarly, we define a strict monoidal structure on \mathcal{S}_n having as the product \diamond the labeled version of that of \mathcal{S} . In particular, $J_\sigma \diamond J_{\sigma'} = J_{\sigma \diamond \sigma'}$ for every $\sigma, \sigma' \in \Pi\Gamma_n$.

The next Propositions 3.2.3 and 3.2.4 generalize Propositions 3.1.2 and 3.1.3 to the categories of labeled ribbon surface tangles \mathcal{S}_n with $n \geq 2$.

Let E_n be the set of the n -labeled versions of the elementary diagrams in Figure 3.1.1, and R_n be the set consisting of the n -labeled versions of relations (I1) to (I22) in Figures 3.1.2, 3.1.3, 3.1.4 and 3.1.5 and of the relations (R1) and (R2) in Figure 3.2.3.

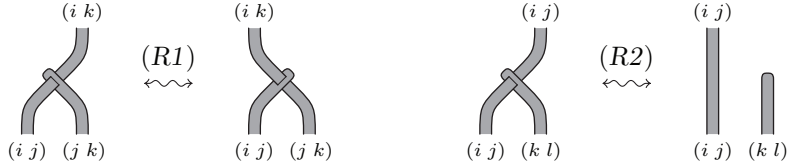


FIGURE 3.2.3. Covering relations in \mathcal{S}_n (i, j, k and l all different)

PROPOSITION 3.2.3. *For any $n \geq 2$, the strict monoidal category \mathcal{S}_n is equivalent to the strict monoidal category $C(\{J_\tau\}_{\tau \in \Gamma_n}, E_n, R_n)$ generated by the objects J_τ with $\tau \in \Gamma_n$ and the set of elementary morphisms E_n modulo the relations R_n , where E_n and R_n are the sets defined above. The equivalence is given by a monoidal functor $C(\{J_\tau\}_{\tau \in \Gamma_n}, E_n, R_n) \rightarrow \mathcal{S}_n$, which is the identity on the objects and sends each morphism of $C(\{J_\tau\}_{\tau \in \Gamma_n}, E_n, R_n) \rightarrow \mathcal{S}_n$ represented by a given n -labeled diagram to the morphism of \mathcal{S} represented by the corresponding n -labeled ribbon surface tangle.*

Proof. We observe that the relations (R1) and (R2) in Figure 3.2.3 express the homonymous covering moves of Figure 3.2.1 in terms of n -labeled elementary diagrams (and their expansions). Then, the statement follows immediately from Proposition 3.1.2 and Definition 3.2.2. \square

Analogously to what we did for \mathcal{S} , we will write σ instead of J_σ in the subscripts of the notation for the morphisms of \mathcal{S}_n . Adopting this convention, Figure 3.2.4 shows some elementary morphisms of \mathcal{S}_n .

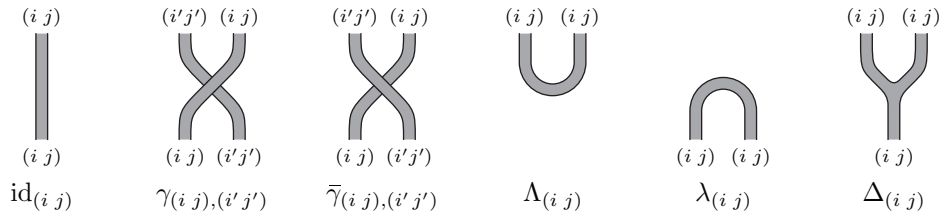


FIGURE 3.2.4. Some elementary morphisms in \mathcal{S}_n

PROPOSITION 3.2.4. For any $n \geq 2$, \mathcal{S}_n is a tortile category, where for σ and σ' sequences in $\Pi\Gamma_n$ of length m and m' respectively: the braiding morphism $\gamma_{\sigma,\sigma'}$ is the braiding morphism $\gamma_{m,m'}$ of \mathcal{S} labeled according to σ and σ' (see Figure 3.2.4 and Figure 3.2.5, and note that $\gamma_{\sigma,\sigma'}^{-1} = \bar{\gamma}_{\sigma',\sigma}$); the dual object of J_σ is $J_\sigma^* = J_{\sigma^*}$, with σ^* the sequence obtained by reversing the order of σ ; the coform, form and twist morphisms Λ_σ , λ_σ and θ_σ are the homologous morphisms Λ_m , λ_m and θ_m of \mathcal{S} labeled according to σ (cf. Figure 3.2.4).

Proof. This is an immediate consequence of Proposition 3.1.3, once we take into account the labeling. \square

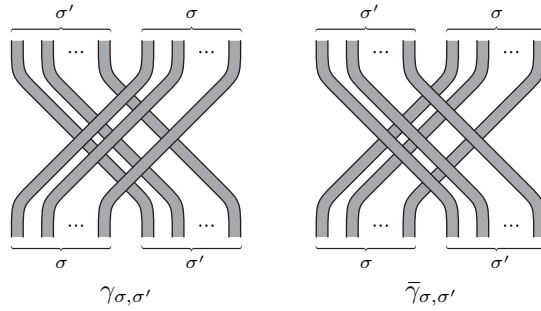


FIGURE 3.2.5. The braiding isomorphisms in \mathcal{S}_n

Now, for any $n > k \geq 2$ we define the stabilization functor $\uparrow_k^n : \mathcal{S}_k \rightarrow \mathcal{S}_n$, which is analogous to the functor $\uparrow_k^n : \mathcal{K}_k \rightarrow \mathcal{K}_n$ introduced in Definition 2.3.2. Similarly to the case of Kirby tangles, we denote by $\iota_k^n : \mathcal{S}_k \rightarrow \mathcal{S}_n$ the faithful functor induced by the inclusion $\Gamma_k \subset \Gamma_n$, which considers any k -labeled ribbon surface tangle as an n -labeled one.

DEFINITION 3.2.5. Given $n > k \geq 1$, let $\sigma_{n \rightarrow k} = ((n \ n-1), \dots, (k+1 \ k))$ and let $\text{id}_{\sigma_{n \rightarrow k}}$ be the identity morphism of $J_{\sigma_{n \rightarrow k}}$ in \mathcal{S}_n . Then, for any $n > k \geq 2$ the stabilization functor $\uparrow_k^n : \mathcal{S}_k \rightarrow \mathcal{S}_n$ is defined by:

$$\begin{aligned} \uparrow_k^n J_\sigma &= J_{\sigma_{n \rightarrow k}} \diamond \iota_k^n(J_\sigma) \text{ for any } J_\sigma \in \text{Obj } \mathcal{S}_k, \\ \uparrow_k^n S &= \text{id}_{\sigma_{n \rightarrow k}} \diamond \iota_k^n(S) \text{ for any } S \in \text{Mor } \mathcal{S}_k. \end{aligned}$$

For any transposition $(i \ j) \in \Gamma_n$, let $\Delta_{(i \ j)} : J_{(i \ j)} \rightarrow J_{(i \ j)} \diamond J_{(i \ j)}$ be the labeled ribbon surface tangle presented in Figure 3.2.4. As shown in Figure 3.2.6, this definition extends inductively to $\Delta_\sigma : J_\sigma \rightarrow J_\sigma \diamond J_\sigma$ for any sequence $\sigma \in \Pi\Gamma_n$, by putting

$$\Delta_\sigma = \Delta_{\sigma' \diamond \sigma''} = (\text{id}_{\sigma'} \diamond \gamma_{\sigma', \sigma''} \diamond \text{id}_{\sigma''}) \circ (\Delta_{\sigma'} \diamond \Delta_{\sigma''}),$$

which turns out to not depend on the decomposition $\sigma = \sigma' \diamond \sigma''$ with $\sigma', \sigma'' \in \Pi\Gamma_n$.

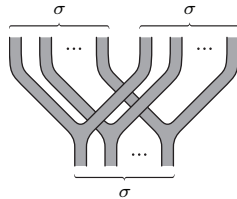


FIGURE 3.2.6. The comultiplication morphism Δ_σ in \mathcal{S}_n

Up to labeled 1-isotopy and move (I18) in Figure 3.1.4, Δ_σ satisfies the coassociativity property, that is:

$$(\Delta_\sigma \diamond \text{id}_\sigma) \circ \Delta_\sigma = (\text{id}_\sigma \diamond \Delta_\sigma) \circ \Delta_\sigma.$$

DEFINITION 3.2.6. Given $n > k \geq 1$, we say that a labeled ribbon surface tangle $S \in \mathcal{S}_n$ from $J_{\sigma_{n-k}} \diamond J_{\sigma_0}$ to $J_{\sigma_{n-k}} \diamond J_{\sigma_1}$ is k -reducible if it is of the form

$$S = (\text{id}_{\sigma_{n-k}} \diamond T) \circ (\Delta_{\sigma_{n-k}} \diamond \text{id}_{\sigma_0}),$$

for some $T : J_{\sigma_{n-k}} \diamond J_{\sigma_0} \rightarrow J_{\sigma_1} \in \mathcal{S}_n$ (see Figure 3.2.7). We will refer to the vertical ribbons forming $\text{id}_{\sigma_{n-k}}$ as the *reduction ribbons* of S .

The composition of two k -reducible labeled tangles is still k -reducible (by coassociativity) and we denote by $\mathcal{S}_{n \rightarrow k}$ the subcategory of \mathcal{S}_n , whose objects are $J_{\sigma_{n-k}} \diamond J_\sigma$ with $\sigma \in \Pi\Gamma_n$ and whose morphisms are k -reducible labeled tangles. In particular, for any $n \geq 2$, we denote by \mathcal{S}_n^c the subcategory $\mathcal{S}_{n \rightarrow 1}$ of 1-reducible labeled tangles in \mathcal{S}_n .

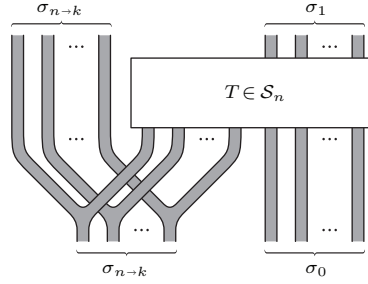


FIGURE 3.2.7. The generic k -reducible morphism $S \in \mathcal{S}_{n \rightarrow k}$

Since the subcategory $\mathcal{S}_{n \rightarrow k}$ of k -reducible ribbon surface tangles is not closed with respect to the product $\diamond : \mathcal{S}_n \times \mathcal{S}_n \rightarrow \mathcal{S}_n$, we endow it with a product structure $\diamond : \text{Mor}_{\mathcal{S}_{n \rightarrow k}} \times \text{Mor}_{\mathcal{S}_{n \rightarrow k}} \rightarrow \text{Mor}_{\mathcal{S}_{n \rightarrow k}}$, similarly to what we have done for k -reducible Kirby tangles. Namely, given two morphisms $S = (\text{id}_{\sigma_{n-k}} \diamond T) \circ (\Delta_{\sigma_{n-k}} \diamond \text{id}_{\sigma_0}) : J_{\sigma_{n-k}} \diamond J_{\sigma_0} \rightarrow J_{\sigma_{n-k}} \diamond J_{\sigma_1}$ and $S' = (\text{id}_{\sigma_{n-k}} \diamond T') \circ (\Delta_{\sigma_{n-k}} \diamond \text{id}_{\sigma'_0}) : J_{\sigma_{n-k}} \diamond J_{\sigma'_0} \rightarrow J_{\sigma_{n-k}} \diamond J_{\sigma'_1}$,

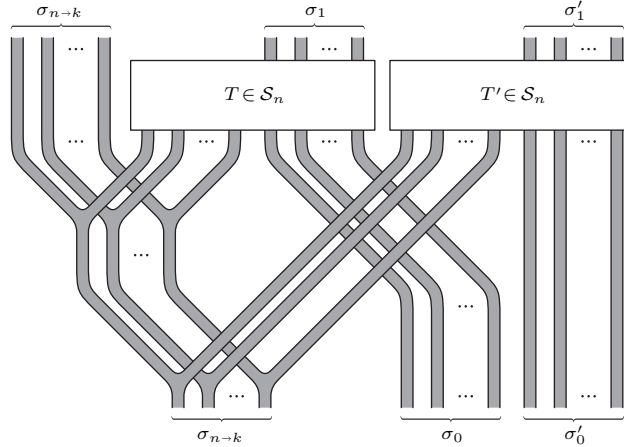


FIGURE 3.2.8. The product $S \diamond S'$ of two morphisms in $\mathcal{S}_{n \rightarrow k}$

in $\mathcal{S}_{n \rightarrow k}$, their product $S \diamond S' : J_{\sigma_{n \rightarrow k}} \diamond J_{\sigma_0 \diamond \sigma'_0} \rightarrow J_{\sigma_{n \rightarrow k}} \diamond J_{\sigma_1 \diamond \sigma'_1}$ is defined by:

$$\begin{aligned} S \diamond S' &= S \circ (\text{id}_{\sigma_{n \rightarrow k}} \diamond \gamma_{\sigma'_1, \sigma_0}) \circ (S' \diamond \text{id}_{\sigma_0}) \circ (\text{id}_{\sigma_{n \rightarrow k}} \diamond \gamma_{\sigma'_0, \sigma_0}^{-1}) \\ &= (\text{id}_{\sigma_{n \rightarrow k}} \diamond T \diamond T') \circ (\Delta_{\sigma_{n \rightarrow k}} \diamond \gamma_{\sigma_{n \rightarrow k}, \sigma_0} \diamond \text{id}_{\sigma'_0}) \circ (\Delta_{\sigma_{n \rightarrow k}} \diamond \text{id}_{\sigma_0 \diamond \sigma'_0}). \end{aligned}$$

These two expressions for $S \diamond S'$ are related by diagram isotopy, as the reader can easily realize by looking at Figure 3.2.8 representing the second one. The associativity of \diamond is a consequence of the coassociativity property of Δ and its unit is given by $\text{id}_{\sigma_{n \rightarrow k}}$. Observe that, as in the case of the category of k -reducible Kirby tangles, \diamond is a useful tool, but it does not define a monoidal structure on $\mathcal{S}_{n \rightarrow k}$, since the product of the compositions of two morphisms, does not coincide with the composition of the corresponding products.

PROPOSITION 3.2.7. *For any $n > k \geq 2$, the image $\uparrow_k^n \mathcal{S}_k$ of the stabilization functor is a subcategory of $\mathcal{S}_{n \rightarrow k}$. Moreover, for any two morphisms S and S' in \mathcal{S}_k , we have $\uparrow_k^n(S \diamond S') = (\uparrow_k^n S) \diamond (\uparrow_k^n S')$. Hence, the product \diamond defines a monoidal structure on the subcategory $\uparrow_k^n \mathcal{S}_k$.*

Proof. Given a ribbon surface tangle S in \mathcal{S}_k , the stabilization $\uparrow_k^n S$ can be put in the form shown in Figure 3.2.7, by expanding a tongue from each stabilization ribbon to the box containing S itself. The identity $\uparrow_k^n(S \diamond S') = (\uparrow_k^n S) \diamond (\uparrow_k^n S')$ for any S and S' in \mathcal{S}_k , immediately follows from the definition of the product \diamond in $\mathcal{S}_{n \rightarrow k}$. \square

We are going to prove that $\mathcal{S}_{n \rightarrow k}$ is equivalent to $\uparrow_{k+2}^n \mathcal{S}_{(k+2) \rightarrow k}$ when $n \geq k+3 \geq 4$. As a consequence, \mathcal{S}_n^c is equivalent to $\uparrow_3^n \mathcal{S}_3^c$ for $n \geq 4$. Actually, the much stronger statement that $\uparrow_4^n : \mathcal{S}_4^c \rightarrow \mathcal{S}_n^c$ is a category equivalence for $n \geq 5$ is also true, as it will follow from Proposition 2.3.9 once Proposition 3.3.4 and Theorem 3.6.4 will be established.

PROPOSITION 3.2.8. *For any $n \geq k+3 \geq 4$, the inclusion of $\uparrow_{k+2}^n \mathcal{S}_{(k+2) \rightarrow k}$ in $\mathcal{S}_{n \rightarrow k}$ is an equivalence of categories.*

Proof. We first prove the statement for $k = n - 3$. More precisely, to any sequence $\sigma \in \text{PII}_n$ we associate a sequence $\sigma' \in \text{PII}_{n-1}$ and a natural isomorphism

$$\zeta_\sigma^{n, n-3} : J_{\sigma_{n \rightarrow (n-3)}} \diamond J_\sigma \rightarrow J_{\sigma_{n \rightarrow (n-3)}} \diamond J_{\sigma'}$$

such that: any labeled ribbon surface tangle

$$\zeta_{\sigma_1}^{n, n-3} \circ (\text{id}_{\sigma_{n \rightarrow (n-3)}} \diamond S) \circ (\Delta_{\sigma_{n \rightarrow (n-3)}} \diamond \text{id}_{\sigma_0}) \circ (\zeta_{\sigma_0}^{n, n-3})^{-1}$$

with $S : J_{\sigma_{n \rightarrow (n-3)}} \diamond J_{\sigma_0} \rightarrow J_{\sigma_1}$ in \mathcal{S}_n , is equivalent to the product of $\text{id}_{(n \ n-1)}$ and an $(n-3)$ -reducible tangle in \mathcal{S}_{n-1} , that is to

$$\text{id}_{(n \ n-1)} \diamond ((\text{id}_{\sigma_{(n-1) \rightarrow (n-3)}} \diamond T) \circ (\Delta_{\sigma_{(n-1) \rightarrow (n-3)}} \diamond \text{id}_{\sigma'_0}))$$

for some $T : J_{\sigma_{(n-1) \rightarrow (n-3)}} \diamond J_{\sigma'_0} \rightarrow J_{\sigma'_1}$ in \mathcal{S}_{n-1} (see Figure 3.2.9). Then Corollary 1.5.4, allows us to conclude that the inclusion of $\uparrow_{n-1}^n \mathcal{S}_{(n-1) \rightarrow (n-3)}$ in $\mathcal{S}_{n \rightarrow (n-3)}$ is an equivalence of monoidal categories.

Given $\sigma = ((i_1 \ j_1), \dots, (i_m \ j_m))$, we let σ' be obtained from σ by replacing any transposition $(i \ n)$ with $(i \ n-1)$ if $i < n-1$ and with $(n-2 \ n-1)$ if $i = n-1$.

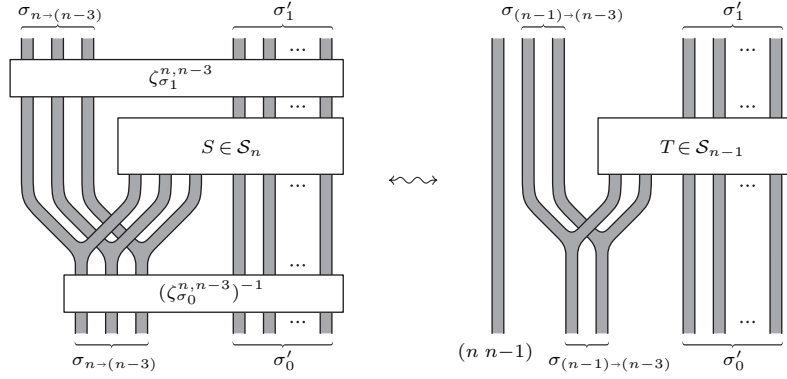


FIGURE 3.2.9. The equivalence between $\mathcal{S}_{n \to (n-3)}$ and $\uparrow_{n-1}^n \mathcal{S}_{(n-1) \to (n-3)}$

Then we define $\zeta_{\sigma}^{n, n-3} = \zeta_{\sigma, m}^{n, n-3} \circ \dots \circ \zeta_{\sigma, 1}^{n, n-3}$, where $\zeta_{\sigma, h}^{n, n-3}$ is the identity if $(i_h j_h) \neq (i n)$ while it is illustrated in Figure 3.2.10 for $(i_h j_h) = (i n)$. Here, the tongue starting from the reduction ribbon of $\text{id}_{(n n-1)}$ passes through the reduction ribbon of $\text{id}_{(n-1 n-2)}$ if $i = n-1$ and in front of all the other ribbons in any case, then it forms a ribbon intersection with the h -th ribbon of id_{σ} . The $\zeta_{\sigma, h}^{n, n-3}$'s are isomorphisms, their inverses being obtained just by vertical reflection. Therefore $\zeta_{\sigma}^{n, n-3}$ is an isomorphism as well.

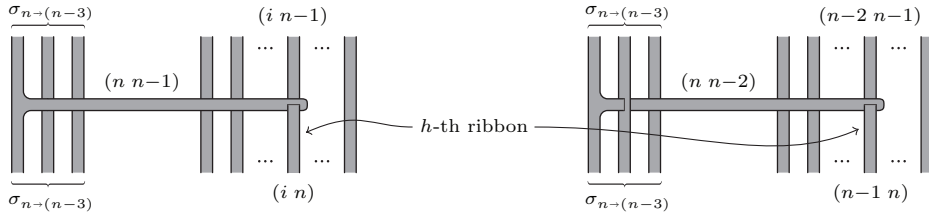


FIGURE 3.2.10. The isomorphism $\zeta_{\sigma, h}^{n, n-3}$ ($i < n-1$)

We observe that $\zeta_{\sigma_1}^{n, n-3} \circ (\text{id}_{\sigma_{n \to (n-3)}} \diamond S) \circ (\Delta_{\sigma_{n \to (n-3)}} \diamond \text{id}_{\sigma_0}) \circ (\zeta_{\sigma_0}^{n, n-3})^{-1}$ factorizes as the composition $P_1 \circ P_2$, where $P_1 = \zeta_{\sigma_1}^{n, n-3} \circ (\text{id}_{\sigma_{n \to (n-3)}} \diamond S) \circ (\zeta_{\sigma_{n \to (n-3)} \diamond \sigma_0}^{n, n-3})^{-1}$ and $P_2 = \zeta_{\sigma_{n \to (n-3)} \diamond \sigma_0}^{n, n-3} \circ (\Delta_{\sigma_{n \to (n-3)}} \diamond \text{id}_{\sigma_0}) \circ (\zeta_{\sigma_0}^{n, n-3})^{-1}$. Then, it will suffice to show that both these factors are equivalent to the product of $\text{id}_{(n n-1)}$ and an $(n-3)$ -reducible tangle in \mathcal{S}_{n-1} .

According to Proposition 1.3.7, we can assume S to be presented by a labeled special planar diagram. Moreover, Figure 3.2.11 shows how S can be transformed through equivalence moves in such a way that:

- (a) at any crossing between two ribbons respectively labeled by $(i n)$ and $(j_1 j_2)$ with $j_1, j_2 < n$, the first ribbon passes in front of the second one;
- (b) there are no crossings between ribbons labeled by $(i n)$ and $(j n)$ with $i \neq j$ (actually, we will need this only for i or j equal to $n-1$);
- (c) there are no ribbon intersections involving the three transpositions $(n-2 n-1)$, $(n-2 n)$ and $(n-1 n)$ as labels.

In particular, to get property (a) we invert any wrong crossing involving the labels $(i n)$ and $(j_1 j_2)$ by applying a move (R4) if $j_1, j_2 \neq i$, and by 1-isotopy (inserting two extra ribbon intersections) as shown in Figure 3.2.11 (a) otherwise.

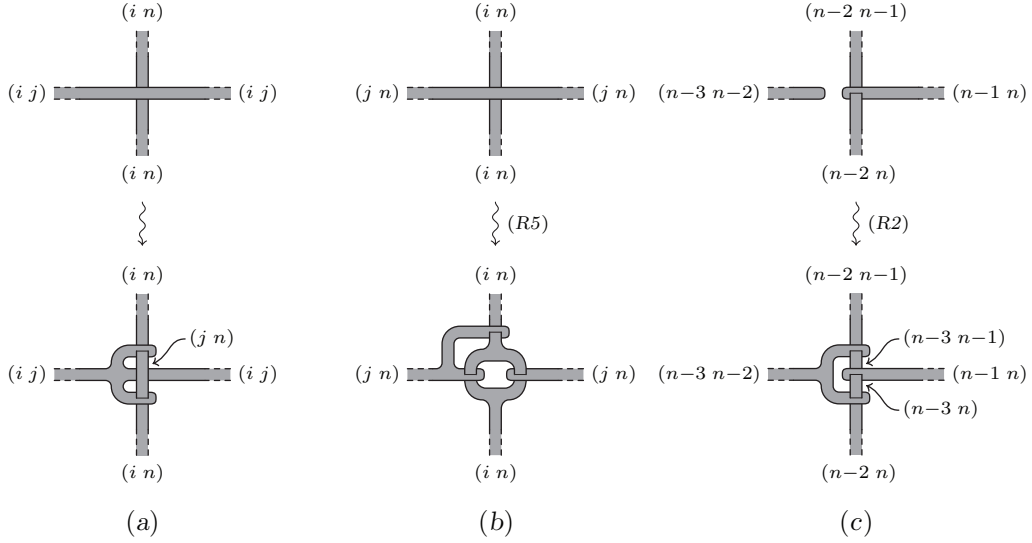


FIGURE 3.2.11.

Then, we proceed as in Figure 3.2.11 (b) to transform all the crossings forbidden by property (b) into ribbon intersections. Finally, in Figure 3.2.11 (c) we see how to get rid of the ribbon intersections forbidden by property (c), possibly after performing move (R1) and/or move (S2) in Figure 1.3.8 to obtain the starting configuration in the figure.

After all those modifications have been performed, we use move (S2) to put the diagram of S again into special form, without losing properties (a), (b) and (c).

Then, we express S as a composition $S_l \circ \dots \circ S_1$, where each S_k is a product of a single labeled elementary tangle (cf. Figure 3.1.1) and some identity ribbons on the left and/or on the right of it. We do that by means of planar isotopy (cf. proof of Proposition 3.1.2). Up to move (R1), we can also assume that each ribbon intersection in the S_k 's is like (g) in Figure 3.1.1. Moreover, if the labels involved in (g) are $(i, n-1)$, (i, n) and $(n-1, n)$ thanks to (c) we have necessarily that $i < n-2$, and up to plane isotopy and move (I14'), we can assume that the target is $J_{(n-1, n)}$

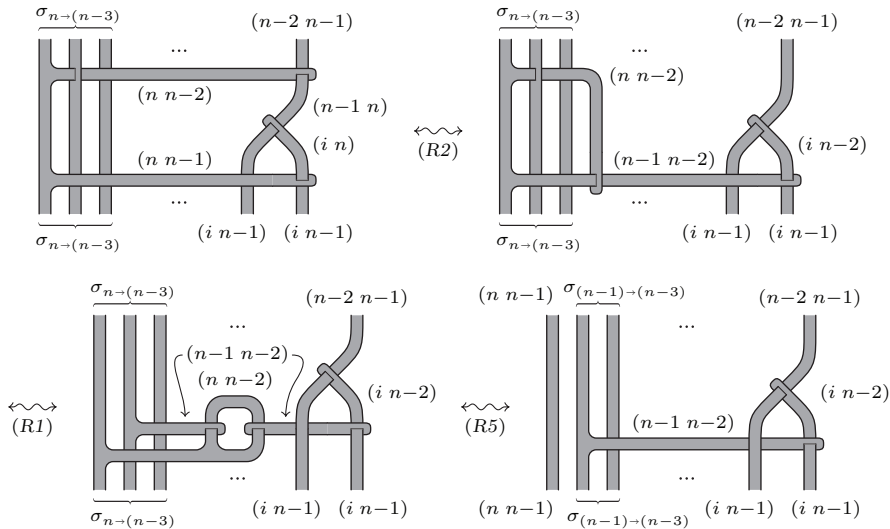


FIGURE 3.2.12. ($i < n-2$)

and the source is $J_{(i\ n-1)} \diamond J_{(i\ n)}$ (cf. the first diagram of Figure 3.2.12). Observe that the resulting plane diagram still satisfies properties (a), (b) and (c).

At this point, in order to prove that P_1 is the product of $\text{id}_{(n\ n-1)}$ with an $(n-3)$ -reducible tangle in \mathcal{S}_{n-1} , we can limit ourselves to consider the case of $\zeta_{\sigma_1}^{n,n-3} \circ (\text{id}_{\sigma_{n \rightarrow (n-3)}} \diamond S) \circ (\zeta_{\sigma_0}^{n,n-3})^{-1}$ with S from σ_0 to σ_1 given by the product of a single labeled elementary tangle and some identity ribbons as above.

If such elementary tangle is not of type (g) with ribbons labeled $(i\ n-1)$, $(i\ n)$ and $(n-1\ n)$, then a straightforward case by case verification shows that $\zeta_{\sigma_1}^{n,n-3} \circ (\text{id}_{\sigma_{n \rightarrow (n-3)}} \diamond S) \circ (\zeta_{\sigma_0}^{n,n-3})^{-1}$ is equivalent up to labeled 1-isotopy to $\text{id}_{\sigma_{n \rightarrow (n-3)}} \diamond S'$, where S' is obtained from S by replacing any transposition $(i\ n)$ with $(i\ n-1)$ if $i < n-1$ and with $(n-2\ n-1)$ if $i = n-1$. In fact, starting from $h = 1$, we can progressively cancel $\zeta_{\sigma_{1,h}}^{n,n-3}$'s with $(\zeta_{\sigma_{0,h}}^{n,n-3})^{-1}$'s on all identity ribbons on the left of the elementary tangle involved. Then, if the resulting tangle is itself the identity, $(f-f')$ or $(e-e')$, we can continue the cancelation until the end. Observe that in the case of the crossings, we can do that only because of conditions (a) and (b). On the other hand, if we reach an elementary tangle of the type $(b-b')$, $(c-c')$ or (d) , before the cancelation some moves (I20) and (I21) must be performed. Finally, if we reach a ribbon intersection with ribbons labeled $(i\ n)$, $(j\ n)$ and $(i\ j)$, where $i \neq n-1 \neq j$, we achieve the cancelation of the ribbons involved in the natural transformation, after performing moves (I22) and (R2).

It remains to consider the case in which the elementary tangle is of type (g) with ribbons labeled $(i\ n-1)$, $(i\ n)$ and $(n-1\ n)$. We start as above by canceling $\zeta_{\sigma_{1,h}}^{n,n-3}$'s and $(\zeta_{\sigma_{0,h}}^{n,n-3})^{-1}$'s, corresponding to the identity ribbons on the left of the

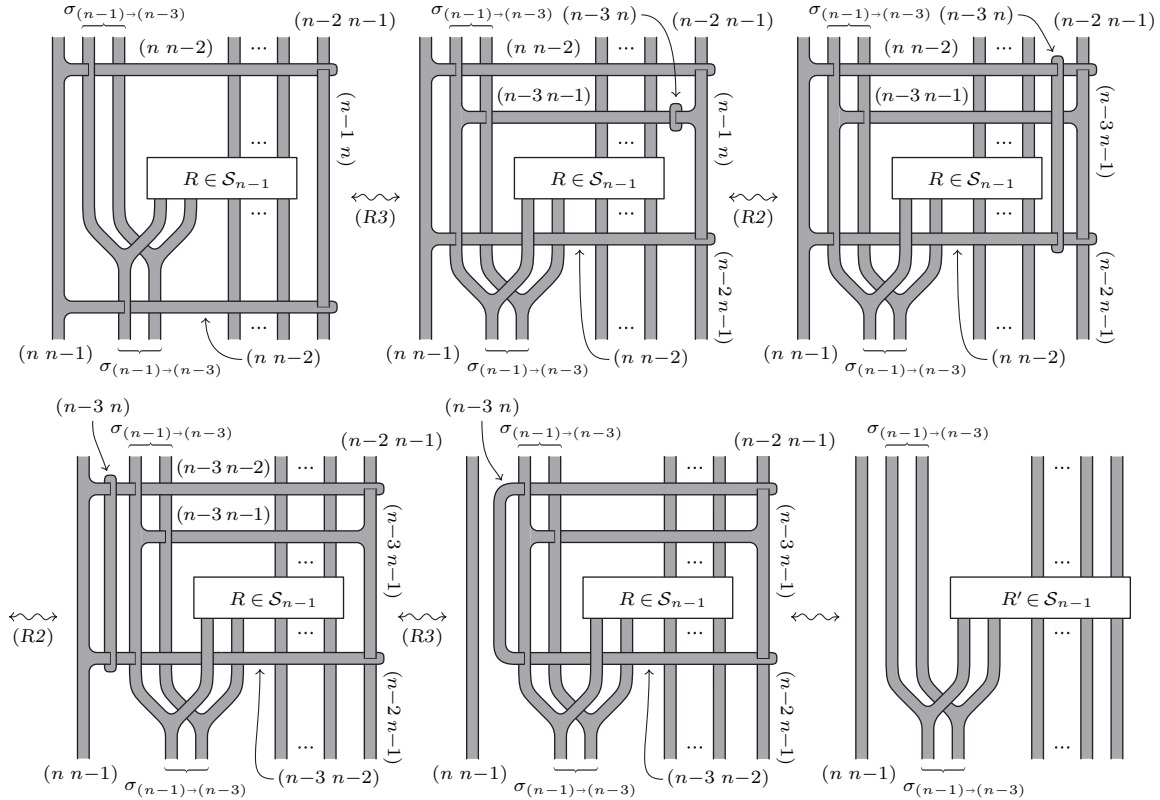


FIGURE 3.2.13.

elementary diagram. Then, we perform the modifications described in Figure 3.2.12 (here the 1-isotopy moves are not indicated). Notice that the final tangle in Figure 3.2.12 is the product of $\text{id}_{(n\ n-1)}$ with an $(n-3)$ -reducible tangle in \mathcal{S}_{n-1} . After that, we proceed by induction on the number of identity ribbons on the right of the elementary diagram. The inductive step consists in forming a new $(n-3)$ -reducible tangle in \mathcal{S}_{n-1} by adding to the previous one a single identity ribbon on the right together with the corresponding $\zeta_{\sigma_1, h}^{n, n-3}$ and $(\zeta_{\sigma_0, h}^{n, n-3})^{-1}$. If the label of the identity ribbon is $(i\ j)$ with $i, j < n$ we are already done, while a trivial 1-isotopy suffices if the label is $(i\ n)$ with $i < n-1$. Figure 3.2.13 shows how to deal the remaining case of label $(n-1\ n)$. This completes the proof that P_1 is equivalent to the product of $\text{id}_{(n\ n-1)}$ and an $(n-3)$ -reducible tangle in \mathcal{S}_{n-1} .

Now, we show that the same holds for the tangle P_2 . We proceed by induction on the difference $n-k$. The starting case is when $n-k=3$, that is $k=n-3$. In this case, modify the horizontal ribbon of $\zeta_{\sigma_{n-(n-3)}}^{n, n-3}$ as described in Figure 3.2.14. Once again, we get the product of $\text{id}_{(n\ n-1)}$ with an $(n-3)$ -reducible tangle in \mathcal{S}_{n-1} . Then, we can conclude by applying the inductive argument in Figure 3.2.13.

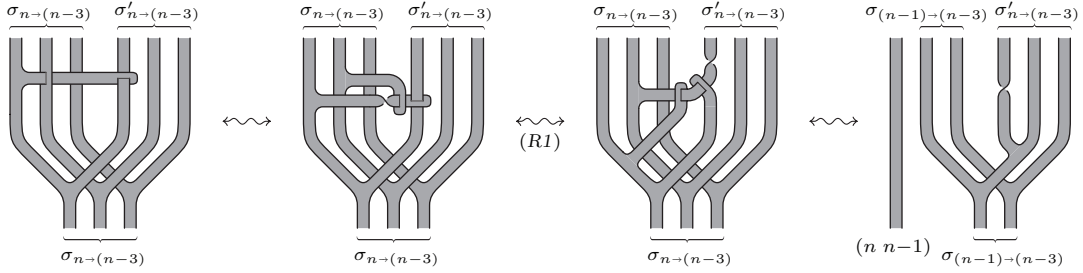


FIGURE 3.2.14.

For $n-k > 3$, the inductive step goes as follows. We define inductively the natural equivalences $\zeta_{\sigma}^{n, k} = (\text{id}_{(n\ n-1)} \diamond \zeta_{\sigma}^{n-1, k}) \circ \zeta_{\sigma}^{n, n-3}$. Then, by applying the result for $k=n-3$ and the inductive hypothesis, we obtain that for any n -labeled ribbon surface tangle S in $\mathcal{S}_{n \rightarrow k}$, the composition $\zeta_{\sigma_1}^{n, k} \circ S \circ (\zeta_{\sigma_0}^{n, k})^{-1}$ is equivalent to a tangle in $\uparrow_{n-1}^n \uparrow_{k+2}^{n-1} \mathcal{S}_{(k+2) \rightarrow k} = \uparrow_{k+2}^n \mathcal{S}_{(k+2) \rightarrow k}$. \square

3.3. The functors $\Theta_n : \mathcal{S}_n \rightarrow \mathcal{K}_n$

The goal of this section is to define the family of functors $\Theta_n : \mathcal{S}_n \rightarrow \mathcal{K}_n$ for $n \geq 2$, which provide the branched covering representation of relative 4-dimensional 2-handlebody cobordisms.

This will be done by exploiting the ideas introduced by Montesinos in [52], to give an effective explicit construction of a generalized Kirby tangle $K_S \in \mathcal{K}_n$ for the branched covering space of $E \times [0, 1] \times [0, 1]$ determined by an n -labeled ribbon surface tangle S with $n \geq 2$.

Before going into details, let us briefly sketch how such construction derives from [52]. Assuming $n \geq 2$, let S be an n -labeled ribbon surface tangle from J_{σ_0} to J_{σ_1} , with $\sigma_0 = ((i_1^0\ j_1^0), \dots, (i_{m_0}^0\ j_{m_0}^0))$ and $\sigma_1 = ((i_1^1\ j_1^1), \dots, (i_{m_1}^1\ j_{m_1}^1))$ sequences in $\Pi\Gamma_n$, and let $p : W \rightarrow E \times [0, 1] \times [0, 1]$ be the simple n -fold branched covering represented by S , according to Section 1.4.

We start with the simple n -fold branched covering of $E \times [0, 1] \times [0, 1]$ represented by the labeled ribbon surface tangle T depicted on the left side of Figure 3.3.1. The corresponding covering space can be easily seen to be $Y(M_{\pi_0}, M_{\pi_1})$, where $\pi_0 = ((i_1^0, j_1^0), \dots, (i_{m_0}^0, j_{m_0}^0))$ and $\pi_1 = ((i_1^1, j_1^1), \dots, (i_{m_1}^1, j_{m_1}^1))$ are determined by assuming $i_h^c > j_h^c$ for any $h = 1, \dots, m_c$ and $c = 0, 1$. In particular, the 3-cell $E \times \{c\} \times [0, 1]$ with the labeled arcs J_{σ_c} represents $M_{\pi_c} \cong M_{\pi_c} \times \{c\} \subset Y(M_{\pi_0}, M_{\pi_1})$ as a n -fold simple branched cover. An n -labeled Kirby tangle for $Y(M_{\pi_0}, M_{\pi_1})$ is given on the right side of the same Figure 3.3.1.

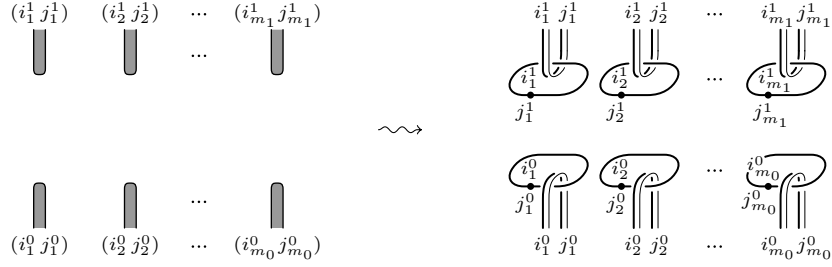


FIGURE 3.3.1. $Y(M_{\pi_0}, M_{\pi_1})$ as a branched cover of $E \times [0, 1] \times [0, 1]$

The ribbon surface tangle S can be obtained from T as follows. First add some regularly embedded disjoint labeled disks D_1, \dots, D_r , and then attach to $S^0 = T \cup D_1 \cup \dots \cup D_r$ some disjoint regularly embedded labeled bands B_1, \dots, B_s , which possibly pass through the disks to form ribbon intersections. In the end, those disks and bands will give an adapted 1-handlebody decomposition of S , considered as a labeled embedded 1-handlebody build on $J_{\sigma_0} \cup J_{\sigma_1}$.

According to [52] (cf. also [23]), each disks D_h with label (i, j) gives raise to a 1-handle H_h^1 attached to $Y(M_{\pi_0}, M_{\pi_1})$ between the sheets i and j of its branched covering representation, while each band B_h gives raise to a 2-handle attached to the covering space represented by S^0 , whose attaching framed knot coincides with the unique annular component of the counterimage of B_h in such covering space. The final result is a relative 2-handlebody decomposition of the space W build on $X(M_{\pi_0}, M_{\pi_1})$.

Now, we want to make the above sketchy recipe into a formal definition of the functor $\Theta_n : \mathcal{S}_n \rightarrow \mathcal{K}_n$ for $n \geq 2$. The non-trivial points here are: 1) the description of the attaching framed knots of the 2-handles; 2) the proof that the 2-deformation class of the 2-handlebody structure of W only depends on the equivalence class of S in the sense of Definition 3.2.2, and in particular it does not depend on the 1-handlebody decomposition of S used in the construction. As we will see, generalized Kirby tangles provide a quite natural way to face the first point, while the second point requires some work.

To define Θ_n on the objects, we consider the map $\Gamma_n \rightarrow \mathcal{G}_n$ given by $(i, j) \mapsto (i, j)$ with $i > j$ and the induced map $\pi : \Pi\Gamma_n \rightarrow \Pi\mathcal{G}_n$ on the sequences. Then, we put $\Theta_n(J_\sigma) = I_{\pi(\sigma)}$ for any $\sigma \in \Pi\Gamma_n$.

The definition of Θ_n on the morphisms is much more involved. Let $S \in \mathcal{S}_n$ be an n -labeled ribbon surface tangle from J_{σ_0} to J_{σ_1} , with $\sigma_0 = ((i_1^0, j_1^0), \dots, (i_{m_0}^0, j_{m_0}^0))$ and $\sigma_1 = ((i_1^1, j_1^1), \dots, (i_{m_1}^1, j_{m_1}^1))$ sequences in $\Pi\Gamma_n$, considered up to 3-dimensional

diagram isotopy. Then we define the generalized Kirby tangle $\Theta_n(S) = K_S$ (well-defined up to 2-equivalence, cf. Lemma 3.3.1 below) by the following steps.

- 1) Start with the n -labeled Kirby tangle on the right side of Figure 3.3.1, where $\pi_0 = \pi(\sigma_0) = ((i_1^0, j_1^0), \dots, (i_{m_0}^0, j_{m_0}^0))$ and $\pi_1 = \pi(\sigma_1) = ((i_1^1, j_1^1), \dots, (i_{m_1}^1, j_{m_1}^1))$.
- 2) Choose an adapted relative 1-handlebody decomposition $S = T \cup D_1 \cup \dots \cup D_r \cup B_1 \cup \dots \cup B_s$ build on $J_{\sigma_0} \cup J_{\sigma_1}$, where: $T = (\cup_{h=1}^{m_0} T_h^0) \cup (\cup_{h=1}^{m_1} T_h^1)$ is a collar of $J_{\sigma_0} \cup J_{\sigma_1}$ in S , with $T_h^c \cong J_{(i_h^c, j_h^c)} \times [0, 1]$ a collar of $J_{(i_h^c, j_h^c)}$ for $h = 1, \dots, m_c$ and $c = 0, 1$; D_1, \dots, D_r are disjoint disks (the 0-handles of the decomposition); B_1, \dots, B_s are disjoint bands attached to $S^0 = T \cup D_1 \cup \dots \cup D_r$ (the 1-handles of the decomposition).
- 3) Add to the starting Kirby tangle a dotted unknot spanning the disk D_h for each $h = 1, \dots, r$; if $(i, j) \in \Gamma_n$ is the label of D_h in S , then choose one of the two possible ways to assign the labels i and j to the faces of D_h (cf. Figure 3.3.2). We call such a choice a *polarization* of the disk D_h .



FIGURE 3.3.2. From 0-handles of S to 1-handles of K_S

- 4) Replace the terminal part of each band attached to any disk D_h by a labeled framed arc consisting of two opposite parallel displacements of it joined together to form a ribbon intersection with D_h as shown in Figure 3.3.3 (a). Do the same for the terminal parts of the bands attached to T , as shown in Figure 3.3.3 (b) and (c). Notice that in all the cases the labeling of the framed arc is uniquely determined by that of the disk spanned by the dotted component.

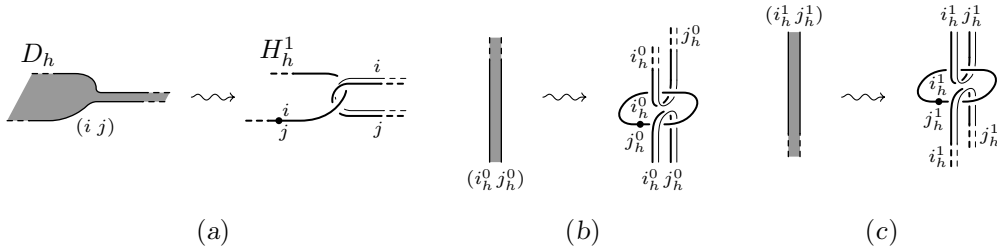


FIGURE 3.3.3. From 1-handles of S to 2-handles of K_S : the ends

- 5) For each ribbon intersection arc in D_h choose a regularly embedded arc $\alpha \subset D_h$ transversally starting from it and ending in $\text{Bd } D_h \cap \text{Bd } S$. All these arcs are chosen to be disjoint from each other and not to meet elsewhere the ribbon intersections in D_h . Moreover, by a 3-dimensional diagram isotopy we can move the relative ribbon intersection inside D_h and contract each arc α in a small neighborhood of its end point in $\text{Bd } D_h$ (cf. Figure 3.3.4).
- 6) Replace a small portion of the band involved in each ribbon intersection in a neighborhood of the corresponding arc α by two labeled framed arcs as shown in Figure 3.3.4 (the four cases depend on how the local labeling of the band is related to the polarization of D_h). Here, the framed arcs are two opposite parallel

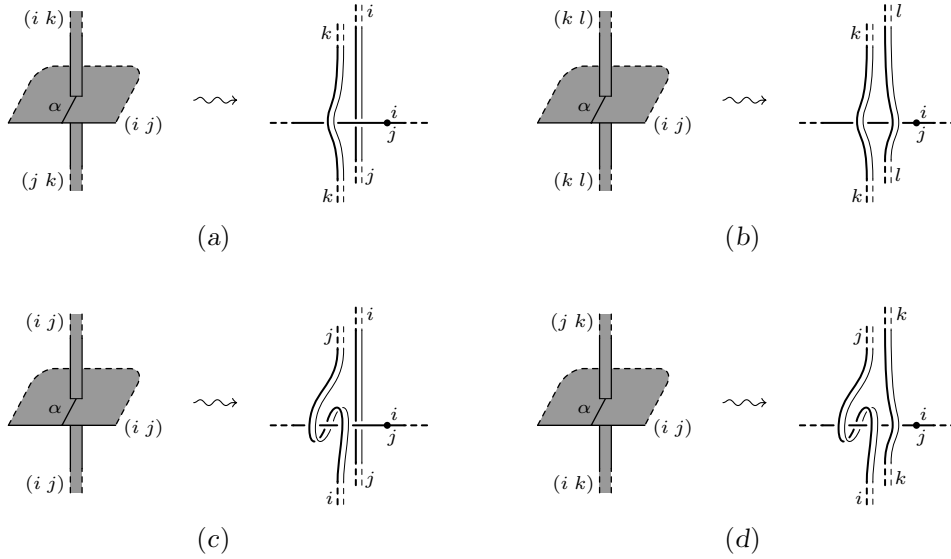


FIGURE 3.3.4. From 1-handles of S to 2-handles of K_S : the ribbon intersections

displacements of the band suitably modified in order to allow labeling compatibility (the opposite choice for the kinks in (c) and (d) would be equivalent up to labeled isotopy) Like in the previous point 4, the labeling of the framed arcs is uniquely determined by the polarization of the disk, with the only exception of case (b) where the labels k and l could be interchanged.

- 7) Finally, replace the remaining part of each band by opposite parallel displacements of it, joining those already inserted in the previous points 4 and 6, inserting one crossover as shown in Figure 3.3.5 (the two possible choices for the crossover are equivalent up to labeled isotopy) where needed to match the labeling.



FIGURE 3.3.5. From 1-handles of S to 2-handles of K_S : the crossovers

We remark that at the end of the construction each band is replaced by a framed knot in the resulting generalized Kirby tangle. By the very definition of generalized Kirby tangle, one could easily check that such framed knot does really represent the unique annular component in the counterimage of the band through the branched covering determined by the labeled ribbon surface tangle $S^0 = T \cup D_1 \cup \dots \cup D_r$, no matter what choices are made at points 3, 5 and 6 (b). Then, it would immediately follow from [52], that K_S represents a relative 2-handlebody structure of W , which only depends on the 1-handlebody decomposition of S chosen at point 2.

Nevertheless, in the next lemma we prove directly that K_S is well-defined up to 2-equivalence (cf. Definition 2.2.7) for a given n -labeled ribbon surface tangle S . Actually, in Proposition 3.3.2 we will see that the 2-equivalence class of K_S is also invariant under 1-isotopy and covering moves of S . In other words, the 2-deformation class of the relative 4-dimensional 2-handlebody represented by K_S does not depend on the choices involved in the above construction of K_S (included the 1-handlebody decomposition of S), in fact it only depends on the equivalence

class of S (cf. Definition 3.2.2). Then, from the results of next Sections (Propositions 3.4.3, 3.5.4 and 3.6.2), it will follow that such 2-deformation class is the same of the relative 2-handlebody structure of W deriving from [52].

LEMMA 3.3.1. *The generalized Kirby tangle K_S constructed above from a given n -labeled ribbon surface tangle S with $n \geq 2$ is well-defined up to 2-equivalence.*

Proof. First of all, we note that the construction of S_K is clearly invariant under labeled 3-dimensional diagram isotopy (preserving ribbon intersections). Then, the relevant choices occurring in it are in the order: the adapted 1-handlebody decomposition of S ; the polarizations of the D_h 's; the arcs α associated to the ribbon intersections; the labeling of the framed arcs in Figure 3.3.4 (b). We prove that K_S does not depend on them up to 2-equivalence, by proceeding in the reversed order and assuming each time that all previous choices are kept fixed.

For the labeling of the framed arcs in Figure 3.3.4 (b), it suffices to observe that switching the labels k and l is compensated up to labeled isotopy by the crossovers inserted in point 7.

Concerning the arcs α , up to labeled 3-dimensional diagram isotopy different choices can be related by a finite sequence of the elementary moves of Figure 3.3.6, where we replace a single arc α by α' . By the invariance under labeled 3-dimensional diagram isotopy, we only need to deal with these elementary moves.

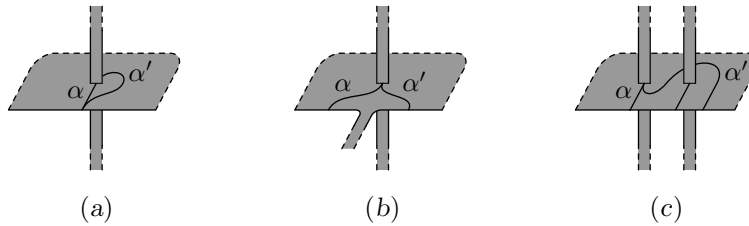


FIGURE 3.3.6. The elementary moves for the arcs α

Move (a) is the same as inserting two opposite half-twists in the vertical band just above and below the ribbon intersection (while leaving α unchanged). But this does not produce any difference on the resulting Kirby tangle, due to the extra crossovers (possibly canceling preexisting ones) needed to keep the labeling consistency. Figure 3.3.7 shows how the insertion of one half-twist along a band only changes the framing of the corresponding framed knot by one full twist of the same sign.



FIGURE 3.3.7. Inserting a half-twist along a band

A simple case by case comparison of the portion of Kirby tangles obtained using α and α' for all the possible labelings in moves (b) and (c), confirms that also these moves change the resulting Kirby tangle by labeled isotopy.

What happens when we invert the polarization of a disk D_h is described in Figure 3.3.8. We start with a given polarization in (a), where we assume that the framed arcs passing through D_h , coming either from bands attached to it or from

ribbon intersection inside it, have been isotoped all together into a canonical position. Then, we isotope upside down the dotted unknot to obtain (b) and use labeled isotopy to make the arcs labeled by i and those labeled by j form separate negative half twists. These two half twists add up to give a unique negative full twist in (c). In the end, we get (d) by performing a positive twist on the 1-handle represented by the dotted unknot (cf. Figures 2.2.8 and 2.2.9). This last diagram, possibly after canceling some of the crossovers appearing in it with preexisting ones or with kinks coming from ribbon intersections (as in Figure 3.3.4 (c) and (d)), is exactly what one gets by choosing the reversed polarization for D_h .

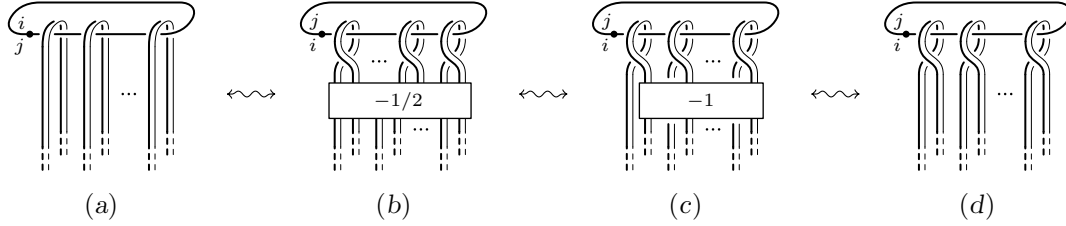


FIGURE 3.3.8. Reversing the polarization of a disk

Finally, the independence of K_S of the adapted 1-handlebody decomposition of S will follow from Proposition 1.3.4, once we prove that performing on S labeled versions of the moves of Figures 1.3.3 and 1.3.4, without vertical disks, corresponds to modifying K_S by certain 2-deformation moves.

In all cases, since H_i^0 and H_j^0 can be assumed to be distinct 0-handles (cf. note after Figure 1.3.4), we can choose the polarizations of them in such a way that no crossover appears along H_k^1 . Then, apparently the two moves of Figure 1.3.4 correspond respectively to addition/deletion of a canceling pair of 1/2-handles and to sliding the 2-handle deriving from H_l^1 over the one deriving from H_k^1 . Similarly, in the case of move of Figure 1.3.3 we have two slidings involving the same 2-handles, one sliding for each of the two parallel copies of H_l^1 forming the framed loop originated from it. We leave to the reader the straightforward verification of this fact for all the four cases of Figure 3.3.4. \square

PROPOSITION 3.3.2. $\Theta_n : \mathcal{S}_n \rightarrow \mathcal{K}_n$, defined by $\Theta_n(J_\sigma) = I_{\pi(\sigma)}$ and $\Theta_n(S) = K_S$ as above, is a braided monoidal functor from the category of n -labeled ribbon surface tangles to the category of n -labeled Kirby tangles, for any $n \geq 2$.

Proof. When thinking of an n -labeled ribbon surface tangle S as a morphism of \mathcal{S}_n , we consider it up to the equivalence relation introduced in Definition 3.2.2. Hence, we have to prove that the 2-equivalence class of K_S is invariant under such equivalence relation. In the light of Proposition 1.3.9 and Lemma 3.3.1, we only need to check the 2-equivalence invariance of K_S when S is changed by the labeled versions of the 1-isotopy moves (S23), (S24), (S24) and (S26) of Figure 1.3.13 and by the covering moves (R1) and (R2) of Figure 3.2.1.

Move (S23) admits a unique labeling up to conjugation in Σ_n . The generalized Kirby diagrams arising from the labeled ribbon surfaces involved in the resulting labeled move are depicted in Figure 3.3.9 (we assume that the surfaces are endowed with the handlebody structures of the corresponding move of Figure 1.3.2). As the reader can easily realize, the two diagrams are related by labeled isotopy.

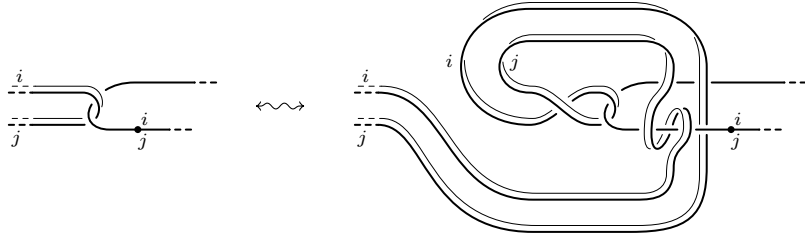


FIGURE 3.3.9. Realizing move (S23)

Moves (S24) and (S25) admit three distinct labelings. Namely, if $(i j)$ is the label of the horizontal component, then the top end of the vertical one can be labeled by $(i j)$, $(j k)$ or $(k l)$.

The first case is considered in Figure 3.3.10 for (S24) and in Figure 3.3.11 for (S25). Looking at these figures, we have that the leftmost and rightmost diagrams correspond respectively to the surfaces on the left and right side of the move with the simplest adapted handlebody structures. The first step in both figures is given by 1/2-handle addition, followed by a 2-handle sliding only in Figure 3.3.11. The next two steps are obtained in turn by a 2-handle sliding and 1/2-handle cancelation. The same figures also apply to the second case, after replacing by k 's all the i 's in the upper half and the j 's in the lower half (except for the labels of the dotted line in the middle). The third case is trivial and we leave it to the reader.

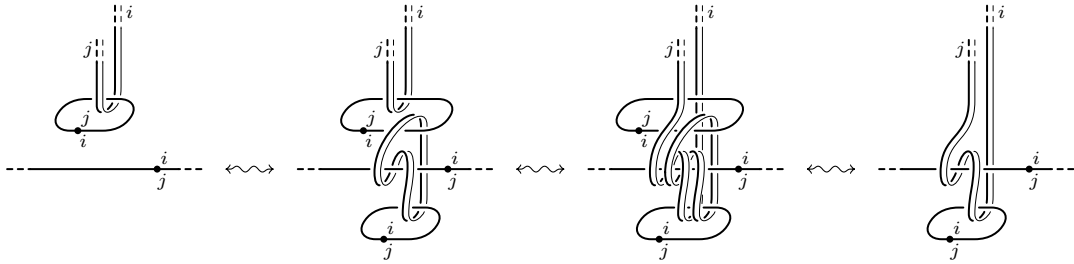


FIGURE 3.3.10. Realizing move (S24)

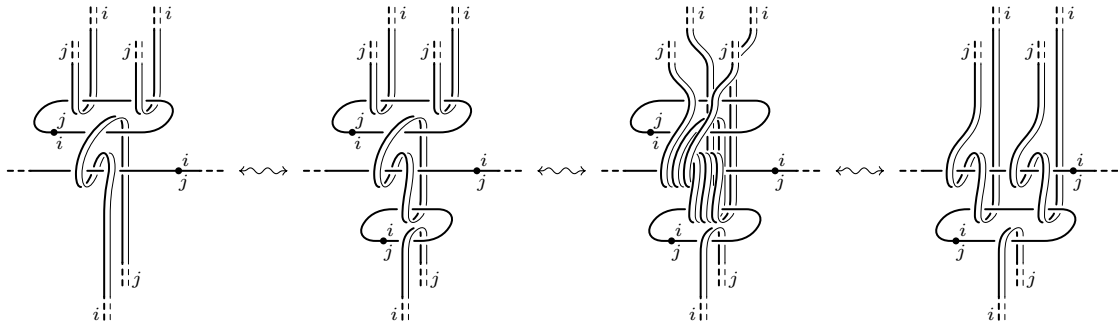


FIGURE 3.3.11. Realizing move (S25)

Finally, let us come to move (S26), which requires a bit more work. As above, let $(i j)$ be the label of the horizontal band. Then, there are eighteen possible ways to label the move, each one determined by the transpositions λ and ρ labeling respectively the left and right bottom ends of the diagonal bands.

By direct inspection we see that, excluding the trivial cases when at least two of the three ribbon intersections involve bands with disjoint monodromies, which are left to the reader, and taking into account the symmetry of the move with respect to its inverse, there are only seven relevant cases: 1) $\lambda = (i j)$ and $\rho = (i j)$; 2) $\lambda = (i j)$ and $\rho = (i k)$; 3) $\lambda = (i k)$ and $\rho = (i j)$; 4) $\lambda = (i k)$ and $\rho = (i k)$; 5) $\lambda = (i k)$ and $\rho = (i l)$; 6) $\lambda = (i k)$ and $\rho = (j l)$; 7) $\lambda = (i k)$ and $\rho = (k l)$.

Figure 3.3.12 regards case 1. Here, the first and last diagrams correspond respectively to the surfaces on the left side and right side of the move with suitable adapted handlebody structures, while the second one is related to the first by two 2-handle slidings and to the third by labeled isotopy. This figure also applies to case 4, after replacing by k 's all the i 's in the upper half and the j 's in the lower half (except for the labels of the dotted line in the middle), as above.

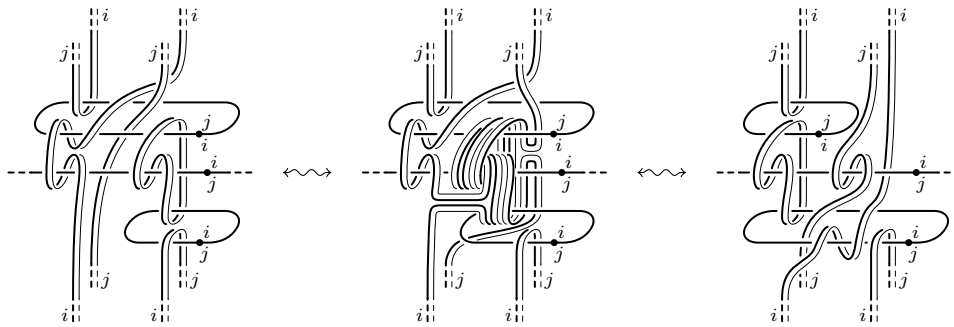


FIGURE 3.3.12. Realizing move (S26) – I

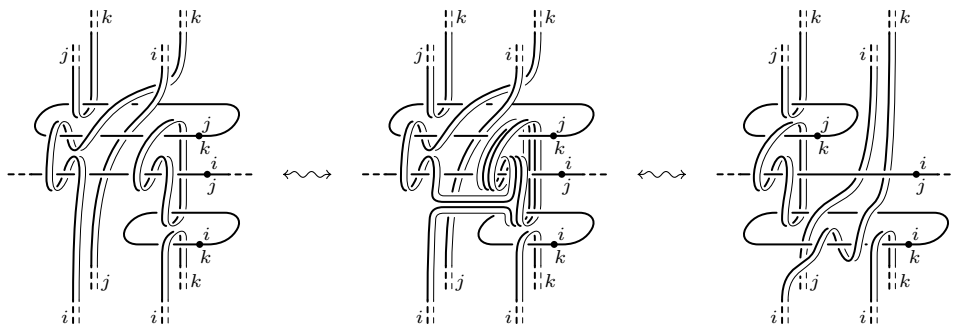


FIGURE 3.3.13. Realizing move (S26) – II

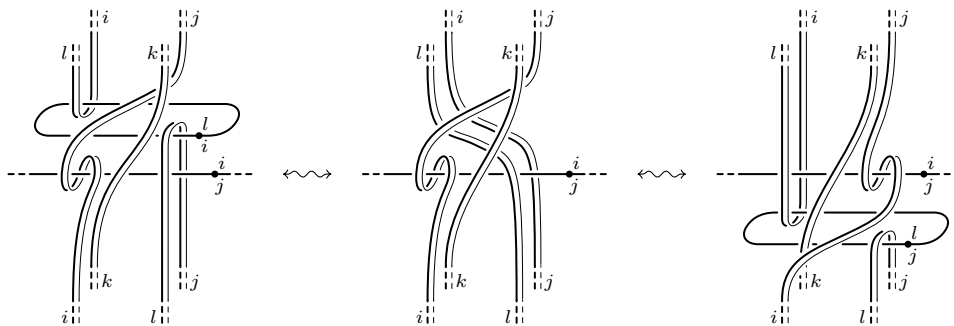


FIGURE 3.3.14. Realizing move (S26) – III

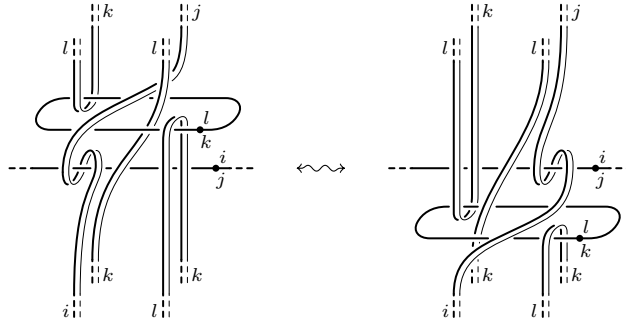


FIGURE 3.3.15. Realizing move (S26) – IV

Similarly, Figure 3.3.13 concerns case 2 and, after the appropriate label replacements, also cases 3 and 5. This time only one 2-handle sliding is needed to relate the first two diagrams. Figures 3.3.14 and 3.3.15 deal with the remaining cases 5 and 7. The three diagrams of Figure 3.3.14 are related by 1/2-handle addition/deletion, while the two diagrams of Figure 3.3.15 by labeled isotopy.

It remains to consider the covering moves (R1) and (R2). If S and S' differ by such a move, then by making the right choices in the construction of $\Theta_n(S)$ and $\Theta_n(S')$ we get the same result up to labeled isotopy. This is shown in Figure 3.3.16 for move (R1), while the analogous easier case of move (R2) is left to the reader.

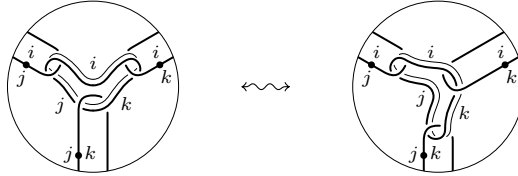


FIGURE 3.3.16. Realizing move (R1)

This completes the proof that Θ_n is well-defined as a functor from \mathcal{S}_n to \mathcal{K}_n , being the identity morphisms and the composition of morphisms clearly preserved by it.

The fact that Θ_n is actually a braided monoidal functor follows from a straightforward verification of the identities $\Theta_n(\gamma_{J_\sigma, J_{\sigma'}}) = \gamma_{I_{\pi(\sigma)}, I_{\pi(\sigma')}}$ for any $\sigma, \sigma' \in \Pi\Gamma_n$ and $\Theta_n(S \diamond S') = \Theta_n(S) \diamond \Theta_n(S')$ for any n -labeled ribbon surface tangles. \square

It is worth remarking that the Theorem 3.3.2 becomes much simpler if we limit ourselves to require that the relative 4-dimensional 2-handlebodies represented by $\Theta_n(S)$ and $\Theta_n(S')$ are diffeomorphic, without insisting that they are 2-equivalent. In fact, labeled isotopy between S and S' (instead of labeled 1-isotopy) suffices for that, since it induces equivalence between the corresponding branched coverings, as recalled in Section 1.4. The relation between isotopy and 1-isotopy of ribbon surfaces in B^4 on one hand and diffeomorphism and 2-equivalence of 4-dimensional 2-handlebodies on the other hand, will be discussed in Remark 6.1.7.

PROPOSITION 3.3.3. *For any $n \geq 2$, Θ_n restricts to a functor $\Theta_n : \mathcal{S}_n^c \rightarrow \mathcal{K}_n^c$, such that $\Theta_n(S \diamond S') = \Theta_n(S) \diamond \Theta_n(S')$ for any two morphisms S and S' in \mathcal{S}_n^c .*

Proof. The proposition follows from the monoidality of Θ_n and from the identities $\Theta_n(\Delta_\sigma) = \Delta_{\pi(\sigma)}$ and $\Theta_n(\gamma_{\sigma, \sigma'}) = \gamma_{\pi(\sigma), \pi(\sigma')}$, which hold for any $\sigma, \sigma' \in \Pi\Gamma_n$. \square

PROPOSITION 3.3.4. For any $n > k \geq 2$ the following diagram commutes.

$$\begin{array}{ccc}
 \mathcal{S}_n & \xrightarrow{\Theta_n} & \mathcal{K}_n \\
 \uparrow_k^n & & \uparrow_k^n \\
 \mathcal{S}_k & \xrightarrow{\Theta_k} & \mathcal{K}_k
 \end{array}$$

Proof. This is a direct consequence of the definitions of the functors involved. \square

In order to have an explicit form of $\Theta_n(S)$ for any $S \in \mathcal{S}_n$, we need to choose a specific adapted 1-handlebody structure on S . By Proposition 3.2.3, it is enough to specify this choice for the elementary morphisms in E_n , represented by the n -labeled versions of the planar diagrams in Figure 3.1.1. Actually, we will consider only the elementary morphisms based on diagrams (a) to (g) in that figure, and use move (I6) in Figure 3.1.2 to reduce those based on (g') to the ones based on (g).

This is done in Figures 3.3.17, 3.3.18 and 3.3.19, where the 0-handles are denoted with lighter gray and the 1-handles with heavier gray color. Notice that there are two types of 0-handles: the ones which are neighborhoods of vertices of the core graph, and the others which divide the ribbons in such a way that none of them contains two boundary arcs. Moreover, since any 1-handle forms at most one ribbon intersection with any disk 0-handle, and in this case the 0-handle has a single band attached to it, the choice of the arcs α is essentially unique up to isotopy, so we omit them.

In the same Figures 3.3.17, 3.3.18 and 3.3.19, we also present the generalized Kirby tangles $\Theta_n(S)$ obtained from the chosen 1-handlebody structures. For later use the image of the elementary morphism in Figure 3.3.19 has been transformed by labeled isotopy and by inverting the polarization of the dotted unknot on the right.

Then, given $S \in \mathcal{S}_n$ as an iterated product/composition of elementary diagrams, we construct $\Theta_n(S)$ as the formal iterated product/composition of the corresponding

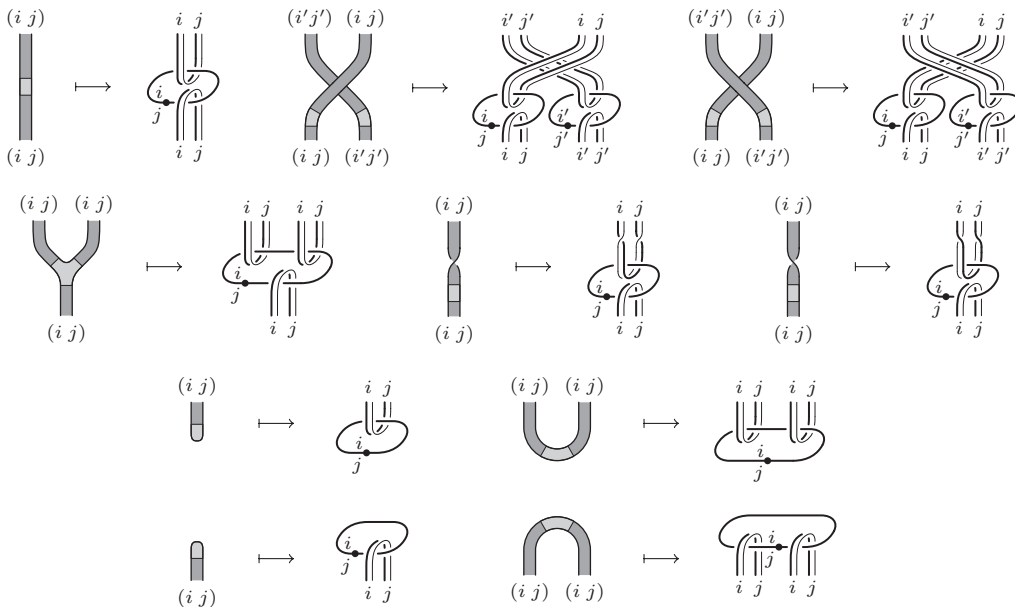


FIGURE 3.3.17. Specifying $\Theta_n - I$ ($i > j$ and $i' > j'$)

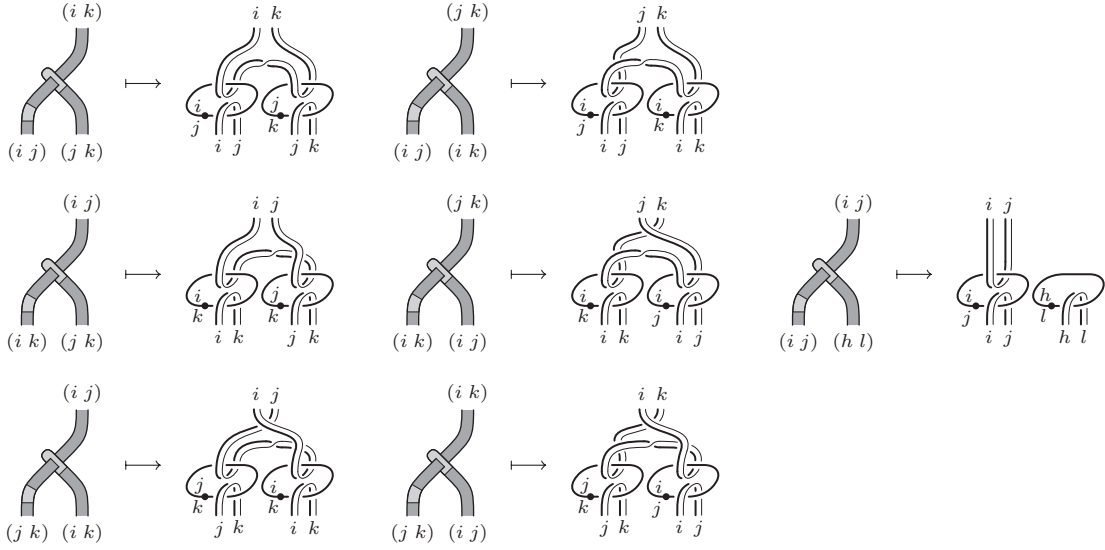


FIGURE 3.3.18. Specifying $\Theta_n - \text{II}$ ($i > j > k, h > l$ and $\{i, j\} \cap \{h, l\} = \emptyset$)

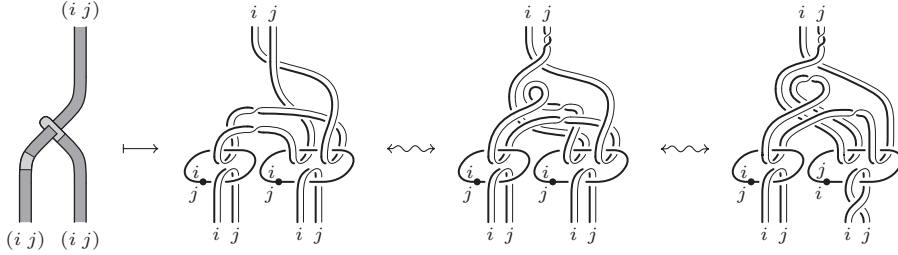


FIGURE 3.3.19. Specifying $\Theta_n - \text{III}$ ($i > j$)

generalized Kirby tangles depicted in those figures. Theorem 3.3.2 assures us that such composition is well-defined as a morphism in K_n .

3.4. Fullness of $\Theta_n : \mathcal{S}_n^c \rightarrow \mathcal{K}_n^c$ for $n \geq 3$

As we will see in Proposition 3.4.4, the fullness of $\Theta_n : \mathcal{S}_n^c \rightarrow \mathcal{K}_n^c$ for any $n \geq 3$ follows from the fullness of $\downarrow_1^3 \circ \Theta_3 : \mathcal{S}_3^c \rightarrow \mathcal{K}_1$. Hence, we focus on the latter.

Given a Kirby tangle $K : I_{m_0} \rightarrow I_{m_1}$ in \mathcal{K}_1 , we will construct a labeled ribbon surface tangle $S_K : J_{\sigma_{3 \rightarrow 1}} \diamond J_{m_0} \rightarrow J_{\sigma_{3 \rightarrow 1}} \diamond J_{m_1}$ in \mathcal{S}_3^c such that $\downarrow_1^3 \Theta_3(S_K) = K$, with all intervals in J_{m_0} and J_{m_1} labeled by $(1\ 2)$.

Actually, the notation S_K is somewhat abusive, since the ribbon surface tangle to which it refers is not uniquely determined by the Kirby tangle K , depending on some choices involved in its construction (at steps 1, 3, 6 and 7). However, in the next sections (cf. Lemma 3.5.1 and Proposition 3.6.3), the uniqueness will be shown to hold for $\uparrow_3^4 S_K$ up to equivalence of ribbon surface tangles.

The global structure of $S_K = Q_{m_1} \circ R_K \circ \bar{Q}_{m_0}$ is illustrated in Figure 3.4.1. Here, $\bar{Q}_{m_0} : J_{\sigma_{3 \rightarrow 1}} \diamond J_{m_0} \rightarrow J_{\sigma_{3 \rightarrow 1}} \diamond J_{2m_0}$ and $Q_{m_1} : J_{\sigma_{3 \rightarrow 1}} \diamond J_{2m_1} \rightarrow J_{\sigma_{3 \rightarrow 1}} \diamond J_{m_1}$ are standard morphisms in $\mathcal{S}_{3 \rightarrow 1}$ that only depend on m_0 and m_1 respectively. On the contrary, the morphism $R_K = \text{id}_{\sigma_{3 \rightarrow 1}} \diamond_{\beta, \gamma, \delta} T_K : J_{\sigma_{3 \rightarrow 1}} \diamond J_{2m_0} \rightarrow J_{\sigma_{3 \rightarrow 1}} \diamond J_{2m_1}$ of $\mathcal{S}_{3 \rightarrow 1}$, which is obtained by attaching to $\text{id}_{\sigma_{3 \rightarrow 1}} \diamond T_K$ certain families of bands β, γ, δ between $\text{id}_{\sigma_{3 \rightarrow 1}}$

and T_K (the horizontal ones on the left of T_K in Figure 3.4.1), depends on the internal structure of K and on the choice of the bands β, γ, δ .

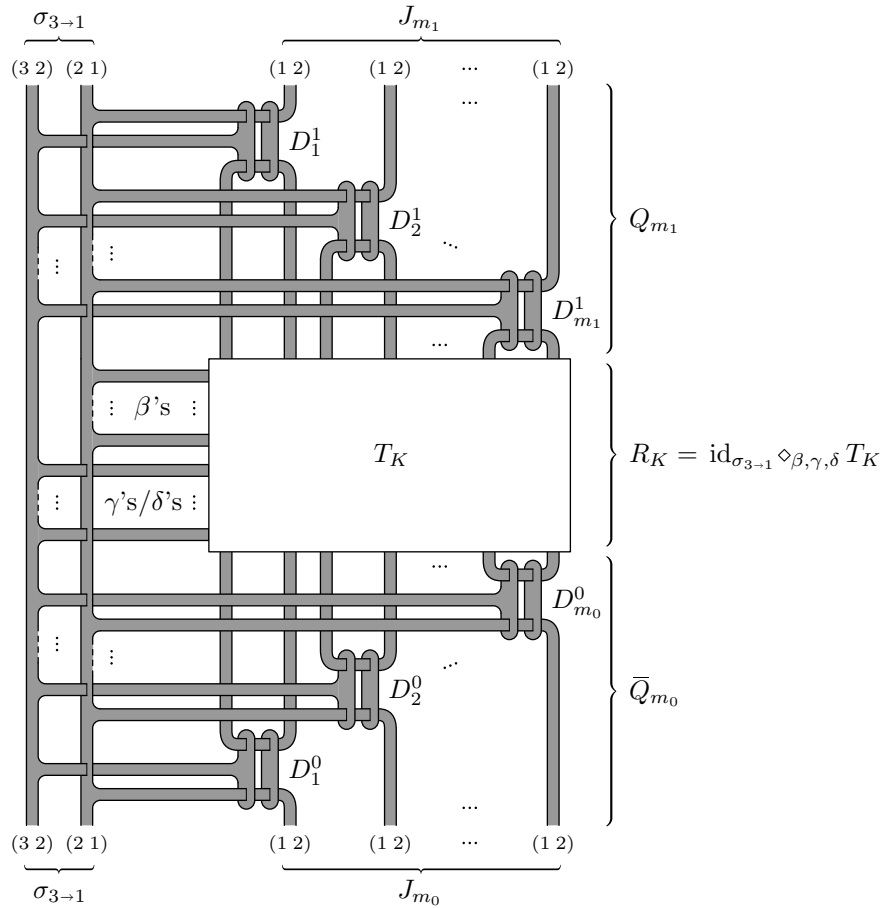


FIGURE 3.4.1. The global structure of S_K

The main steps in the construction of S_K are explained below (namely, step 1 is a preparatory one on K , step 2 concerns \bar{Q}_{m_0} and Q_{m_1} , steps 3 to 5 deal with T_K , steps 6 and 7 regard the families of bands β, γ, δ , step 8 is devoted to the labeling).

- 1) Represent K by a strictly regular planar diagram (see Definition 2.2.9) and break all the open framed components of K , by inserting dotted components

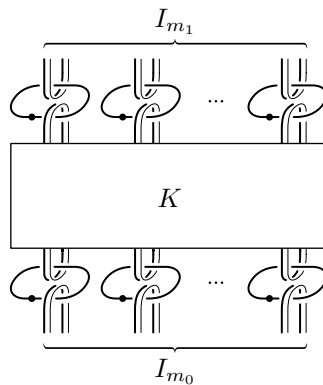


FIGURE 3.4.2. Breaking the open framed components of K

near their ends at I_{m_0} and I_{m_1} , as depicted in Figure 3.4.2. This change is achieved by a 2-deformation, namely by inserting canceling 1/2-pairs and then performing 2-handle slidings, so the resulting Kirby tangle can still be denoted by K . Moreover, denote by $D_1, \dots, D_r \subset E \times [0, 1]$ the disjoint disks spanned by the dotted unknots of the original tangle K (meaning excluded the new ones we have just inserted) and by $L = L_1 \cup \dots \cup L_s$ the framed link formed by the closed framed components of the modified tangle K (corresponding to all the framed curves, both open and closed, of the original K).

- 2) Replace the exterior of the box K in Figure 3.4.2, by the standard ribbon surface tangles \bar{Q}_{m_0} and Q_{m_1} shown in Figure 3.4.1, and extend their reduction ribbons on the left of the box, to compose them into a unique copy of $\text{id}_{\sigma_{3 \rightarrow 1}}$. We observe that \bar{Q}_{m_0} and Q_{m_1} are symmetric to each other (except for the fact that m_0 and m_1 can be different), but they do not represent inverse morphisms (even if $m_0 = m_1$). For future references, we introduce the following notations: $\tilde{\text{id}}_{(2 \ 1)}$ for the union of $\text{id}_{(2 \ 1)}$ with the bands connecting it to J_{m_0} and J_{m_1} in \bar{Q}_{m_0} and Q_{m_1} ; $\tilde{\text{id}}_{(3 \ 2)}$ for the union of $\text{id}_{(3 \ 2)}$ with the parts of \bar{Q}_{m_0} and Q_{m_1} connected to it (the horizontal bands springing from it and the vertical disks where they end); $D_1^0, \dots, D_{m_0}^0$ and $D_1^1, \dots, D_{m_1}^1$ for the remaining vertical disks in \bar{Q}_{m_0} and Q_{m_1} respectively (see Figure 3.4.1).
- 3) Choose a trivial state for the diagram of the unframed link $|L|$ (cf. Section 1.1), and let $L' = L'_1 \cup \dots \cup L'_s$ be the new framed link obtained from L by a regular vertical homotopy, whose corresponding unframed link $|L'|$ is represented by that trivial state. Moreover, assume L' to coincide with L outside $F_1 \cup \dots \cup F_l$, where each F_i is a cylinder projecting onto a small circular neighborhood of a changing crossing. Such a cylinder F_i , together with the relative portion of diagram, is depicted in Figure 3.4.3 (a) and (b), where j and k may or may not be distinct. Here $C_i \subset F_i$ is a regularly embedded disk without vertical tangencies, separating the two bands of $L \cap F_i$ and forming four transversal intersection arcs with L' .

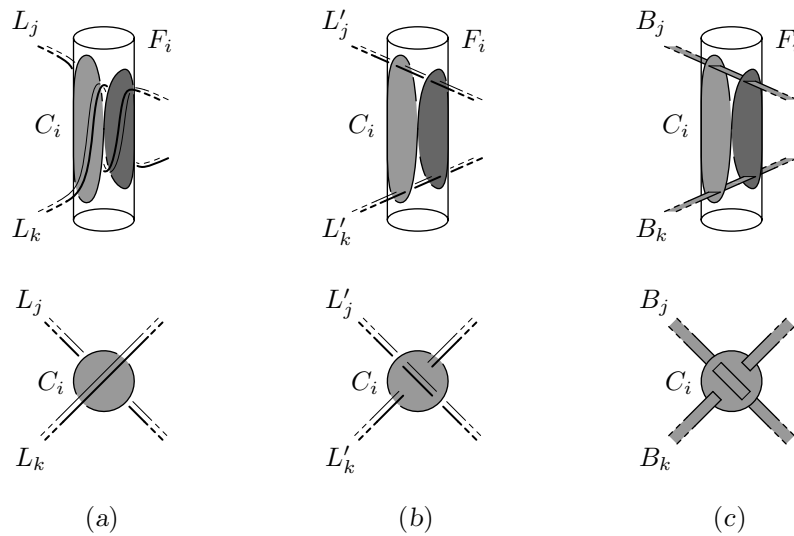


FIGURE 3.4.3. The disk C_i and the framed links L and L' at a changing crossing

- 4) For each disk D_i , take a parallel copy D'_i on one of the two sides of it (see Figure 3.4.4 (b)). Up to 1-isotopy, it does not matter what side of D_i is chosen for D'_i , since the moves in Figure 1.3.13 allow us to push one disk through the other. Denote by G_i the cylinder between D_i and D'_i and assume that $L' \cap G_i = L \cap G_i$ consists of trivial framed arcs as shown in Figure 3.4.4 (b). Of course, the height function of the disks D_i and D'_i varies according to that of such arcs.

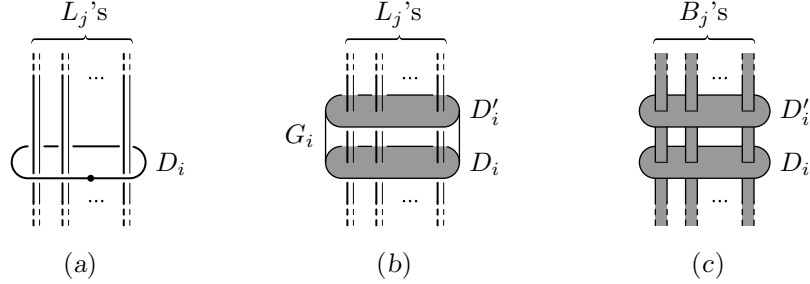


FIGURE 3.4.4. The parallel disks D_i and D'_i for a dotted unknot of K

- 5) For each framed component L_j , consider a (possibly non-orientable) narrow closed band B_j , whose core is the base curve $|L'_j|$ of L'_j and whose framing number is $\text{fr}(L'_j)/2$. In particular, B_j is orientable when $\text{fr}(L'_j)$ is even, while it is non-orientable when $\text{fr}(L'_j)$ is odd. In both cases, $\text{fr}(L'_j)$ coincides with $\text{lk}(L'_j, \text{Bd } B_j)$ if L'_j and $\text{Bd } B_j$ are coherently oriented. The bands B_j are assumed to form with the D_i 's, the D'_i 's and the C_i 's only ribbon intersections, as shown in Figures 3.4.3 (c) and 3.4.4 (c). Furthermore, all the portions of the B_j 's outside of the box K in Figure 3.4.2 are assumed to be blackboard parallel and to coincide with components of \tilde{Q}_{m_0} or Q_{m_1} attached to the box T_K in Figure 3.4.1.
- 6) Connect each band B_j to the boundary component on the right of the reduction ribbon $\text{id}_{(2\ 1)}$ by a narrow band β_j , to get a connected non-singular surface

$$B = \tilde{\text{id}}_{(2\ 1)} \cup \beta_1 \cup \dots \cup \beta_s \cup B_1 \cup \dots \cup B_s.$$

The bands β_1, \dots, β_s are assumed to be disjoint from the F_i 's and the G_i 's defined above and from a given family of disjoint spanning disks $A_1, \dots, A_s \subset E \times [0, 1] - \tilde{\text{id}}_{(2\ 1)}$ for the components $|L'_1|, \dots, |L'_s|$ of the trivial link $|L'|$. The surface B is assumed to be entirely contained in the box T_K , except for $\tilde{\text{id}}_{(2\ 1)}$ and for the portions of the B_j 's mentioned at the end of the previous step 5 and those of the β_j 's coming out from the left side of the box.

- 7) Connect each disk C_i and each disk D'_i to the boundary component on the right of the reduction ribbon $\text{id}_{(3\ 2)}$ by a narrow bands γ_i and δ_i respectively, to get a connected non-singular surface

$$C = \tilde{\text{id}}_{(3\ 2)} \cup \gamma_1 \cup \dots \cup \gamma_l \cup \delta_1 \cup \dots \cup \delta_r \cup C_1 \cup \dots \cup C_l \cup D'_1 \cup \dots \cup D'_r.$$

The bands $\gamma_1, \dots, \gamma_l$ and $\delta_1, \dots, \delta_r$ are assumed to be disjoint from $B \cup D_1 \cup \dots \cup D_r$ and from the interiors of the F_i 's and the G_i 's, except for the ribbon intersections with the reduction ribbon $\text{id}_{(2\ 1)}$ shown in Figure 3.4.1. The surface C is assumed to be entirely contained in the box T_K , except for $\tilde{\text{id}}_{(3\ 2)}$ and for the portions the γ_i 's and δ_i 's coming out from the left side of the box.

8) Finally, define S_K to be the labeled ribbon surface tangle given by the union

$$S_K = B \cup C \cup D_1 \cup \dots \cup D_r \cup D_1^0 \cup \dots \cup D_{m_0}^0 \cup D_1^1 \cup \dots \cup D_{m_1}^1$$

with the unique labeling extending that one we already have at the source and at the target (cf. Figure 3.4.1). In particular, the labeling around the disks C_i and D_i results as in Figure 3.4.5. Then, letting $T_K : J_{2m_0} \rightarrow J_{2m_1}$ be the union of the part of $B_1 \cup \dots \cup B_s$ inside the box in Figure 3.4.1 with the disks $C_1, \dots, C_l, D_1, \dots, D_r$ and D'_1, \dots, D'_r , we have $S_K = Q_{m_1} \circ R_K \circ \bar{Q}_{m_0}$ with $R_K = \text{id}_{\sigma_{3 \rightarrow 1}} \diamond_{\beta, \gamma, \delta} T_K$.

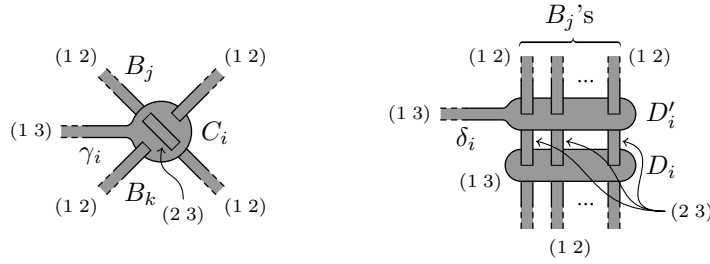


FIGURE 3.4.5. The labeling around the disks C_i and D_i

REMARK 3.4.1. We recall that, up to 2-deformation, any crossing in a Kirby diagram can be inverted by adding a suitable pair of $1/2$ -handles, as in Figure 3.4.6. Actually, up to handle trading this is the trick used in [54] to symmetrize framed links in order to represent closed 3-manifolds as branched covers of S^3 .

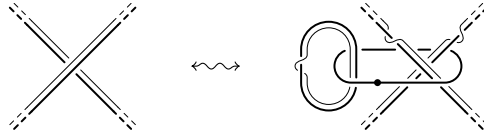


FIGURE 3.4.6. Inverting a crossing up to 2-deformation

Figure 3.4.7 shows, how to interpret in this way the disks C_i we insert at the changing crossings in step 3 of our construction of S_K . Apart from the indicated moves only diagram isotopy is needed for that.

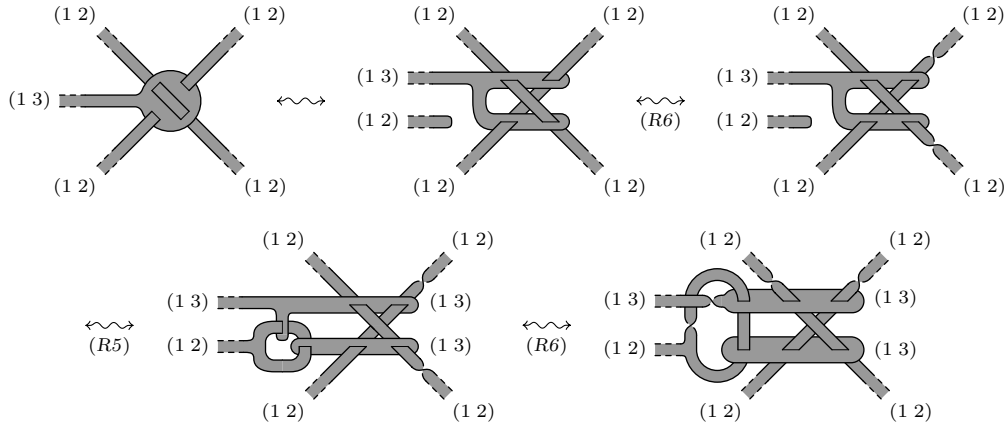


FIGURE 3.4.7. Interpreting the disks C_i in terms as a pair of $1/2$ -handles

REMARK 3.4.2. The definition of S_K does not preserve the corresponding products. The most we can say about it is that, if $K : I_{m_0} \rightarrow I_{m_1}$ and $K' : I_{m'_0} \rightarrow I_{m'_1}$ are two Kirby tangles in \mathcal{K}_1 , then $T_{K \diamond K'} = T_K \diamond T_{K'}$, hence $R_{K \diamond K'} = R_K \diamond R_{K'}$ and $S_{K \diamond K'} = Q_{m_1+m'_1} \circ (R_K \diamond R_{K'}) \circ \bar{Q}_{m_0+m'_0}$ (cf. Figure 3.4.1).

An example of the construction of S_K is presented in Figure 3.4.8. Here, all the framed components in the Kirby tangle K on the left side are blackboard parallel, except for one half-twist needed to satisfy the last requirement in point 2 of Definition 2.2.6. We assume such half-twist to be positive for the two components ending at the top and negative for the component ending at the bottom, in such a way that they cancel with the extra half-twists that appear when closing those components in step 1 of the construction of S_K . Notice the half-twist introduced along the trefoil band in S_K according to step 5 of the construction.

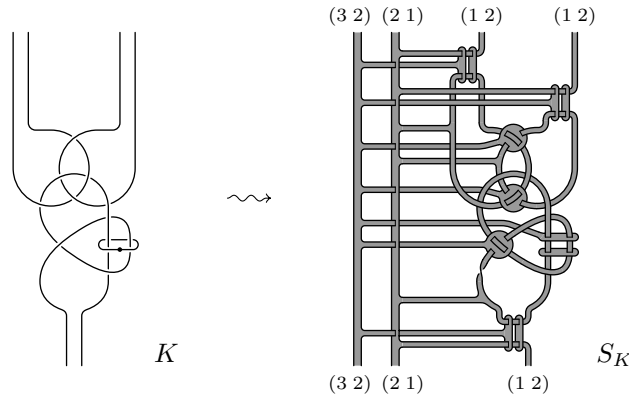


FIGURE 3.4.8. An example of labeled ribbon surface tangle S_K

PROPOSITION 3.4.3. $\downarrow_1^3 \Theta_3(S_K) = K$ for any Kirby tangle $K \in \mathcal{K}_1$.

Proof. Recall that the construction of $\Theta_3(S_K)$ involves some choices. In particular, we need to choose an adapted 1-handlebody decomposition of S_K and a polarization for the 0-handles of such decomposition.

To this aim, we first decompose the reduction ribbons $\text{id}_{(3\ 2)}$ and $\text{id}_{(2\ 1)}$ as a single long 0-handle and two short 1-handles connecting it with the collars of the source and the target. We denote the two 0-handles by $R_{(3\ 2)}^0$ and $R_{(2\ 1)}^0$ and let them contain the attaching arcs of all the horizontal bands attached to the ribbons, including those in \bar{Q}_{m_0} and Q_{m_1} , as well as all the ribbon intersections between such bands and $\text{id}_{(2\ 1)}$.

We also decompose each of the closed bands B_1, \dots, B_s defined in step 5 of the construction of S_K , by putting $B_i = B_i^0 \cup B_i^1$, with B_i^0 a small 0-handle containing the attaching arc of β_i and B_i^1 a 1-handle attached to B_i^0 .

Then, we consider the adapted 1-handlebody structure of S_K , whose 0-handles are $R_{(3\ 2)}^0, R_{(2\ 1)}^0 \cup \beta_1 \cup \dots \cup \beta_s \cup B_1^0 \cup \dots \cup B_s^0$, all the vertical disks in \bar{Q}_{m_0} and Q_{m_1} and the disks $D_1, \dots, D_r, D'_1, \dots, D'_r, C_1, \dots, C_l$ discussed in steps 3 and 4 of the construction of S_K . Consequently, the 1-handles are those in $\text{id}_{(3\ 2)}$ and $\text{id}_{(2\ 1)}$, the bands $\gamma_1, \dots, \gamma_l, \delta_1, \dots, \delta_r$ and all the horizontal bands in \bar{Q}_{m_0} and Q_{m_1} .

Concerning the polarizations, we put the greater label on the top face for all the 0-handles, except in the case of the disks $D_1^0, \dots, D_{m_0}^0$ and $D_1^1, \dots, D_{m_1}^1$ in \bar{Q}_{m_0} and

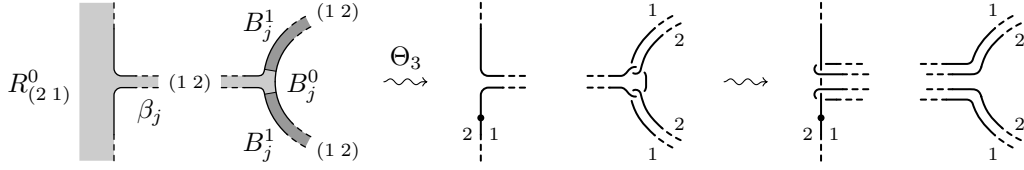


FIGURE 3.4.10. Reducing $\Theta_3(S_K)$ to K : the bands β_j

Figure 3.4.11, and then we eliminate them by 0/1-handle cancellation. We eliminate in the same way one dotted unknot from each pair deriving from a pair of parallel vertical disks in \bar{Q}_{m_0} and Q_{m_1} .

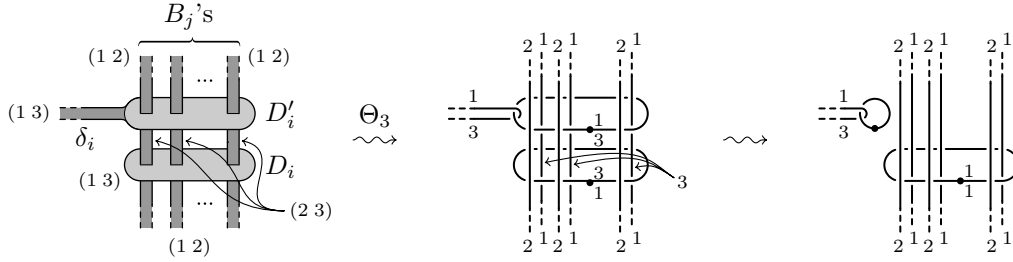


FIGURE 3.4.11. Reducing $\Theta_3(S_K)$ to K : the disks D_i

Moreover, at each band crossing we modify the Kirby diagram by the crossing changes depicted in Figure 3.4.12 and then we use 0/1-handle cancellation once again to eliminate the dotted unknots spanning the disks C_i .

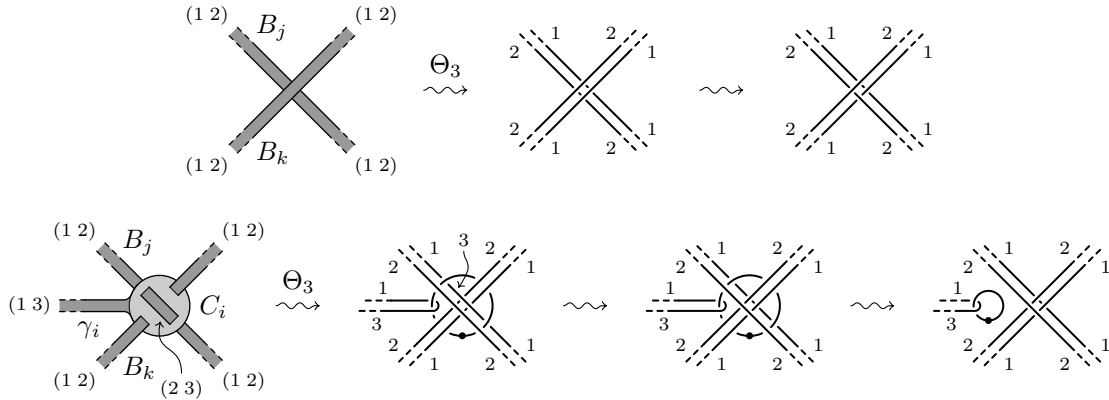


FIGURE 3.4.12. Reducing $\Theta_3(S_K)$ to K : the crossings

At this point, we are left with a generalized Kirby diagram whose framed link \bar{L} is a componentwise band connected sum of the original framed link L , labeled by 1, and a parallel copy L'' of L' , labeled by 2, with a certain number of extra half-twists added to the framing. Namely, each component \bar{L}_j of \bar{L} is the band connected sum of L_j and the parallel copy L''_j of the corresponding component L'_j , through connecting bands running back and forth on the two sides of β_j , with $-2 \text{fr}(L'_j)$ extra half-twists added to the framing (cf. step 5 in the construction of S_K and Figure 3.3.7). Looking at the rightmost diagrams in Figures 3.4.11 and 3.4.12, we see that the part of \bar{L} labeled by 2 has been pulled up over everything else, including the dotted unknots (cf. third diagram in Figure 3.4.9).

Since the unframed link $|L'|$ is trivial and the bands β_i are disjoint from a set of trivializing disks for it, we can isotope $|\bar{L}|$ to get back $|L|$ entirely labeled by 1, without moving the rest of the diagram (cf. fourth diagram in Figure 3.4.9).

We want to show that the last isotopy actually takes the framed link \bar{L} to L , or equivalently that the equality $\text{fr}(\bar{L}_j) = \text{fr}(L_j)$ holds for every $j = 1, \dots, s$. In fact $\text{fr}(\bar{L}_j) = \text{fr}(L_j) + \text{fr}(L''_j) - \text{fr}(L'_j)$, with the last term resulting from the $-2 \text{fr}(L'_j)$ extra half-twists. Then, it suffices to observe that $\text{fr}(L''_j) = \text{fr}(L'_j)$, being L''_j a parallel copy of L'_j .

As it is illustrated by the fifth diagram in Figure 3.4.9, the resulting Kirby tangle is 2-equivalent to $\uparrow_2^3 (\xi^{(2,1)} \circ \uparrow_1^2 K \circ (\xi^{(2,1)})^{-1})$, where $\xi^{(2,1)}$ is the natural equivalence defined in Section 2.3 (see Lemma 2.3.8). Thus, we have $\downarrow_1^3 \Theta_3(S_K) = \downarrow_1^3 \uparrow_2^3 (\xi^{(2,1)} \circ \uparrow_1^2 K \circ (\xi^{(2,1)})^{-1}) = \downarrow_1^3 \uparrow_2^3 \uparrow_1^2 \downarrow_1^2 \uparrow_1^2 K = K$, by Proposition 2.3.9 (cf. last two diagrams in Figure 3.4.9). \square

PROPOSITION 3.4.4. *The functor $\Theta_n : \mathcal{S}_n^c \rightarrow \mathcal{K}_n^c$ is full for any $n \geq 3$.*

Proof. First of all, we observe that $S_K \in \mathcal{S}_3^c$. Indeed, it can be put in the form of Figure 3.2.7 with $n = 3$ and $k = 1$, through a quite obvious labeled isotopy. Then, the fullness of $\Theta_3 : \mathcal{S}_3^c \rightarrow \mathcal{K}_3^c$ follows from Proposition 3.4.3 and the fact that the reduction functor $\downarrow_1^3 : \mathcal{K}_3^c \rightarrow \mathcal{K}_1$ is a category equivalence (Proposition 2.3.9).

For $n > 3$, we have that $\Theta_n(\uparrow_3^n S_K) = \uparrow_3^n \Theta_3(S_K)$ by Proposition 3.3.4. Hence, taking into account that \uparrow_3^n is a category equivalence (Proposition 2.3.9), we can derive the fullness of $\Theta_n : \mathcal{S}_n^c \rightarrow \mathcal{K}_n^c$ from the one of $\Theta_3 : \mathcal{S}_3^c \rightarrow \mathcal{K}_3^c$. \square

3.5. The functor $\Xi_n : \mathcal{K}_1 \rightarrow \mathcal{S}_n^c$ for $n \geq 4$

As discussed at the beginning of the previous section, the ribbon surface tangle S_K does not depend only on the given Kirby diagram K , but also on the various choices involved in its definition. In particular, in step 3 of the construction of S_K we made the choice of a trivial state $|L'|$ of for the diagram of the link $|L|$ contained in a strictly regular diagram of K .

Let \check{S}_K denote any ribbon surface tangle resulting from that construction, under the extra assumption that the trivial state $|L'|$ is vertically trivial.

In this section, we will show that $\uparrow_3^4 \check{S}_K$ is well-defined up to labeled 1-isotopy and moves (R1) and (R2), in other words it does not depend on the choices involved in the construction of \check{S}_K , and that it is invariant under 2-deformations of K .

This will give us a functor $\Xi_4 : \mathcal{K}_1 \rightarrow \mathcal{S}_4^c$ defined by $\Xi_4(K) = \uparrow_3^4 \check{S}_K$, from the category \mathcal{K}_1 of ordinary Kirby tangles to the category $\mathcal{S}_4^c = \mathcal{S}_{4 \rightarrow 1}$ of 1-reducible 4-labeled ribbon surface tangles. Then, by composing with \uparrow_4^n , we will get an analogous functor $\Xi_n : \mathcal{K}_1 \rightarrow \mathcal{S}_n^c$ also for $n > 4$.

Eventually, in the next section we will see that the functor Ξ_4 is full (Proposition 3.6.2), which together with Proposition 3.4.3 implies that $\Xi_4(K) = S_K$, where S_K is constructed using an arbitrary trivial state (Proposition 3.6.3).

LEMMA 3.5.1. *Let K be a given Kirby tangle in \mathcal{K}_1 . Up to labeled 1-isotopy and moves (R1) and (R2), the labeled ribbon surface tangle $\uparrow_3^4 \check{S}_K$ does not depend on the choices of the strictly regular planar diagram of K , of the vertically trivial state of the link $|L|$ and of the bands $\beta_1, \dots, \beta_s, \gamma_1, \dots, \gamma_l$ and $\delta_1, \dots, \delta_r$ involved in the construction of \check{S}_K (cf. steps 1, 3, 6 and 7).*

Proof. First of all, we observe that the spanning disks A_1, \dots, A_s in step 6 of the construction of \check{S}_K can be always assumed to satisfy the following conditions (possibly after a small perturbation of them):

- (a) $A_i \cap B_i$ consists of $|L'_i|$ and a certain number of disjoint clasps connecting $|L'_i|$ with the boundary of A_i , in such a way that $A_i \cup B_i$ collapses to A_i , for every $i = 1, \dots, s$; while $A_i \cap B_j = \emptyset$ for every $i \neq j$;
- (b) $A_1 \cup \dots \cup A_s$ forms with each C_i four clasps and some (possibly none) ribbon intersections, as shown in Figure 3.5.1 (left side);
- (c) $A_1 \cup \dots \cup A_s$ forms with each $D_i \cup D'_i$ two clasps for each intersection point in $|L| \cap D_i = |L'| \cap D_i$ and some (possibly none) ribbon intersections, as shown in Figure 3.5.1 (right side);
- (d) the γ_i 's and the δ_i 's may pass through $A_1 \cup \dots \cup A_s$ forming only ribbon intersections with them.

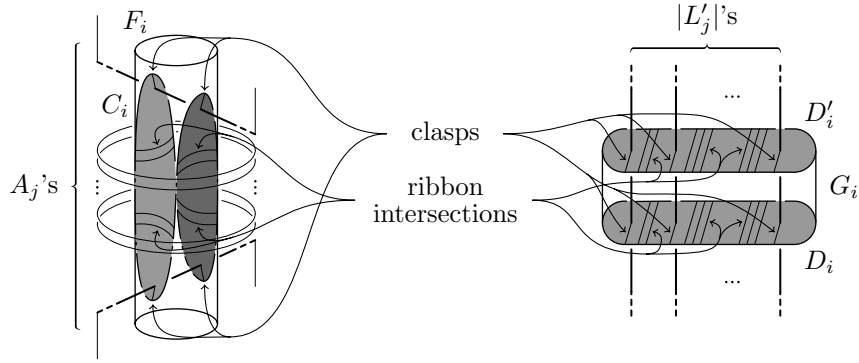


FIGURE 3.5.1. Intersections between $A_1 \cup \dots \cup A_s$ and the disks C_i , D_i and D'_i

At this point we pass to the core of the proof. We prove that \check{S}_K is independent (up to labeled 1-isotopy and moves (R1) and (R2)) on the choices listed in the statement, by proceeding in the reverse order and assuming each time that all previous choices have been fixed. By Proposition 1.4.3, in addition to moves (R1) and (R2), we can use also the moves (R3) to (R6) in Figure 3.2.2.

Concerning the γ_i 's and the δ_i 's, it suffices to prove that labeled 1-isotopy and the moves above enable us to change them one by one.

We start by showing how to replace a band γ_i by a different band γ'_i . Observe that, up to a 3-dimensional isotopy, we can assume γ_i and γ'_i to be disjoint. Then, Figure 3.5.2 illustrates the sequence of moves realizing the replacement. First we modify the diagram in (a) to get the labeled ribbon surface tangle in (c), where both γ_i and γ'_i are attached to C_i , but γ'_i passes through two small disks D and D' labeled (3 4), with D' attached by a narrow band δ to $\text{id}_{(4\ 3)}$. The tangle in (c) is obviously equivalent to \check{S}_K , since we can use move (R3) to cut γ'_i (see diagram (b)), retract the resulting tongue to $\text{id}_{(3\ 2)}$ and then retract the tongue $D' \cup \delta$ to $\text{id}_{(4\ 3)}$. Now, since the label (1 2) of the bands B_j and B_k is disjoint from (3 4), we can move the disks D and D' in turn, to let C_i pass through them by 1-isotopy and four moves (R2), obtaining in this way (d) and then (e). Finally, the same procedure described above to see the equivalence between (a) and (c), but with the roles of γ_i and γ'_i interchanged, gives the equivalence between (e) and (f).

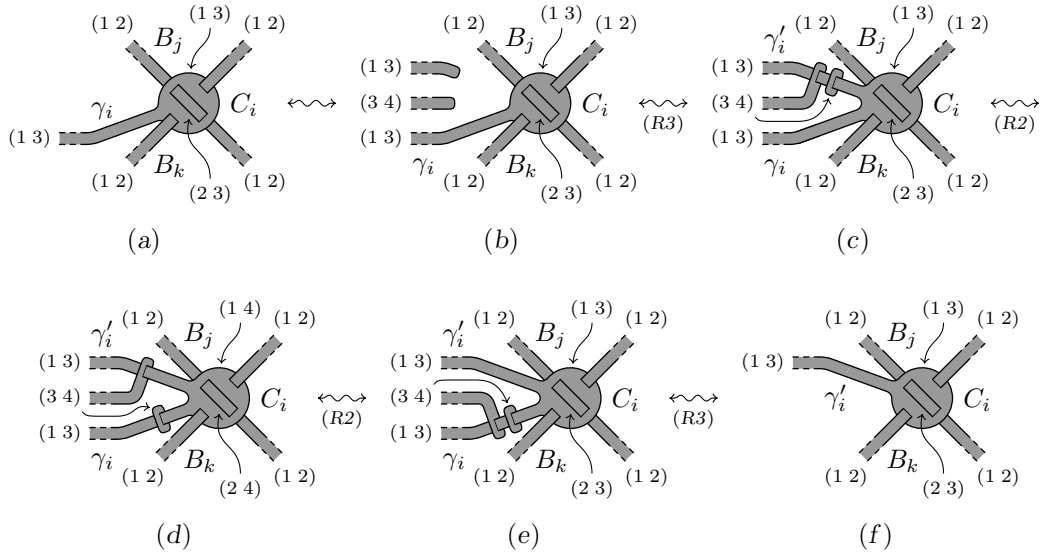


FIGURE 3.5.2. Independence of \tilde{S}_K on the bands γ_i

A similar argument works to change a band δ_i into a different band δ'_i . The process begins and ends like above, with δ_i and δ'_i in place of γ_i and γ'_i , while the central part is illustrated by Figure 3.5.3. In this case, two (R2) moves for each arc passing through D_i are needed in order to move the disks D and D' from δ'_i to δ_i .

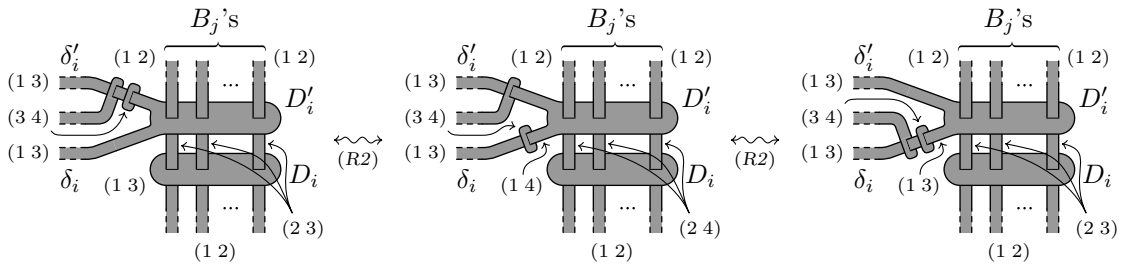


FIGURE 3.5.3. Independence of \tilde{S}_K on the bands δ_i

The proof of the independence of \tilde{S}_K on the β_i 's is more involved, but still based on the same idea. We want to replace certain bands β_1, \dots, β_s with different bands $\beta'_1, \dots, \beta'_s$. According to step 6 in the construction of \tilde{S}_k , there exist two families of disjoint spanning disks A_1, \dots, A_s and A'_1, \dots, A'_s for the link $|L'$ which are disjoint from the β_i 's and from the β'_i 's respectively.

We first consider the special case when $A_i = A'_i$ for every $i = 1, \dots, s$. In this case (but not in general, as we will see) we can replace the bands one by one.

The idea of how a given band β_i can be replaced with a different band β'_i , is presented in Figure 3.5.4, even if that figure is much more sketchy than Figure 3.5.2. In fact, instead of the disk C_i we have here the complex $A_i \cup B_i$ that can be large and complicated, although still collapsible, as it follows from assumption (a) at the beginning of the proof. The first step, to get the labeled ribbon surface tangle in Figure 3.5.4 (a) from \tilde{S}_K , and in particular the disks D and D' , and the last step, to get the final result from the labeled ribbon surface tangle in (e), are once again similar to the above ones. But this time the bands β_i and β'_i in place of γ_i and γ'_i originate from $\text{id}_{(2\ 1)}$ and are labeled (1 2), while the band δ connects the disk D' to

$\text{id}_{(4\ 3)}$ passing through $\text{id}_{(3\ 2)}$ to form a ribbon intersection. We obtain in this way the label $(2\ 4)$ for the disks D and D' , which is disjoint from the label $(1\ 3)$ of the disks D_j , D'_j and the bands γ_j and δ_j . This permits to get (e) from (a) by moving D and D' in turn by 1-isotopy and some moves (R2) and (R4), within a neighborhood of A_i and letting A_i pass through them. In particular, the moves (R2) are needed when the disks cross the clasps that A_i forms with the D_j 's, the D'_j 's and the C_k 's (cf. assumptions (b) and (c) at the beginning of the proof). These clasps always appear in pairs, each pair being formed with one of the C_j 's or with a D_k and the corresponding D'_k or (cf. Figure 3.4.5). Each pair looks like the only one depicted on the right part of the diagrams in Figure 3.5.4. Comparing (b) and (c), we see that the disk D can be pushed beyond such pair by two (R2) moves. On the other hand, the moves (R4) are used in the obvious way to push D beyond each ribbon intersection that the interior of A_i forms with the γ_j 's and the δ_k 's (cf. assumption (d) at the beginning of the proof). Finally, once the disk D has been completely moved from β_i to β'_i (diagram (d) in the figure), we move in the same way the disk D' to get (e) and we are done.

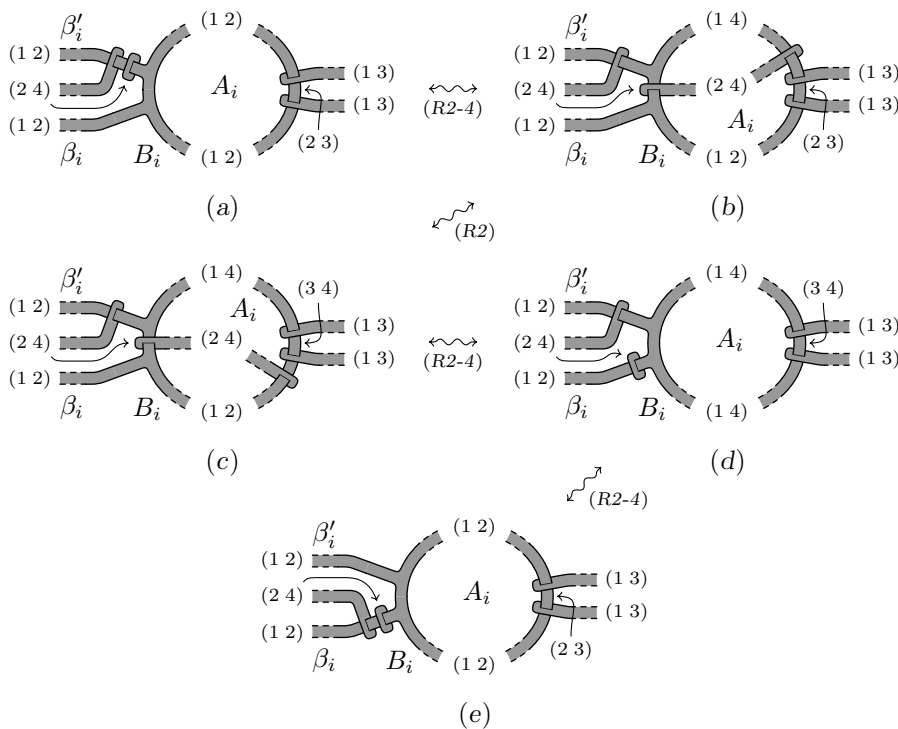


FIGURE 3.5.4. Independence of \check{S}_K on the bands β_i

REMARK. The above argument without any modification except for some extra 1-isotopy moves, proves that, in the special case when $A_1, \dots, A_s = A'_1, \dots, A'_s$, β_i can be replaced by β'_i even if the bands β_1, \dots, β_s and $\beta'_1, \dots, \beta'_s$ form ribbon intersections with the disks A_j with $j \neq i$. The labeled ribbon surface tangles involved are not \check{S}_K 's any more, but we need to extend our argument to such kind of tangles, since they will appear in the following as intermediate stages between genuine \check{S}_K 's.

In order to deal with the case when $A_i \neq A'_i$ for some i , we need a preliminary adjustment. Up to a small isotopy inside a tubular neighborhood of $|L'|$, we separate

the intersection $\text{Int}(A_1 \cup \dots \cup A_s) \cap \text{Int}(A'_1 \cup \dots \cup A'_s)$ from $|L'|$. After that, we put $\text{Int}(A_1 \cup \dots \cup A_s)$ and $\text{Int}(A'_1 \cup \dots \cup A'_s)$ in general position, so that they meet transversally along a finite family of closed curves. Then, we proceed by induction on the number of components of $\text{Int}(A_1 \cup \dots \cup A_s) \cap \text{Int}(A'_1 \cup \dots \cup A'_s)$.

The induction starts from the case when such intersection is empty. In this case, we have pairwise disjoint spheres $S_i = A_i \cup A'_i$ with $i = 1, \dots, s$. Then, there exist new bands β''_i between B_i and $\text{id}_{(2,1)}$, such that: 1) $\beta''_i \cap S_j = \emptyset$ if either $i = j$ or $i \neq j$ and S_i lies in the exterior $E(S_j)$ of S_j ; 2) $\beta''_i \cap S_j$ consists of a single ribbon intersection if $i \neq j$ and S_i lies in the interior $I(S_j)$ of S_j . We choose an indexing such that case 2 possibly happens only for $i > j$. The β''_i 's are not legitimate bands for a genuine \check{S}_K , but according to the remark above about the proof of the special case, we can still apply that argument to change the β_i 's into the β''_i 's one by one, by using the A_i 's, provided we proceed in the order given by the chosen indexing. After that, we can change the β''_i 's into the β'_i in the same way, but using the A'_i 's in place of the A_i 's and proceeding in the reversed order.

We are left with the inductive step. Choose a closed curve C among the components of $\text{Int}(A_1 \cup \dots \cup A_s) \cap \text{Int}(A'_1 \cup \dots \cup A'_s)$, which is contained in $\text{Int} A_i \cap \text{Int} A'_j$ and is an innermost one in $\text{Int} A'_j$ for $i, j \leq s$. We apply the usual cut and paste technique to A_i to remove C from the intersection. Namely, if $D \subset A_i$ and $D' \subset A'_j$ are the subdisks spanned by C , then we replace a subdisk of A_i slightly larger of D with a disk parallel to D' , to get a new spanning disk A''_i . Then, by putting $A''_k = A_k$ for any $k \neq i$, we have a new family A''_1, \dots, A''_s of spanning disks for $|L'|$, whose interiors intersect $\text{Int}(A'_1 \cup \dots \cup A'_s)$ in a smaller number of curves than the original disks A_1, \dots, A_s . Let $\beta''_1, \dots, \beta''_s$ be any family of bands disjoint from the disks A''_1, \dots, A''_s (observe that β_1, \dots, β_s may meet A''_i in D'). Since the disks A''_1, \dots, A''_s can be obviously perturbed to make their interiors disjoint from $\text{Int}(A_1 \cup \dots \cup A_s)$, the starting step of the induction applies to transform the bands β_1, \dots, β_s into $\beta''_1, \dots, \beta''_s$. Finally, these latter can be made into the bands $\beta'_1, \dots, \beta'_s$, by the induction hypothesis. This completes the proof of the independence of \check{S}_K on the β_i 's.

Now we pass to the vertically trivial state $|L'|$. Recall that we are thinking of it as a vertically trivial link, that is a vertically trivial diagram together with a compatible height function. Of course, different choices of the height function, compatible with the same diagram, are related by a vertical diagram isotopy and such an ambient isotopy can be used to relate the resulting labeled ribbon surface tangles.

So, we have only to consider the case of different choices for the vertically trivial state $|L'|$. According to Proposition 1.1.3, any two such choices are related by a sequence of the following two moves: the first one is a single self-crossing change of a given component; the second one is a simultaneous change of all the crossings between two vertically adjacent components.

We first address the second move, which changes the vertical order of two vertically adjacent components. Thanks to what we have already proved, we can choose the disks A_1, \dots, A_s to be perturbations of those generated by the horizontal intervals with endpoints in $|L'|$ (cf. Section 1.1) and the bands β_1, \dots, β_s to satisfy the following conditions:

- 1) the intervals $[a_i, b_i] = h(A_i \cup \beta_i)$, with $i = 1, \dots, s$ and h being the height function in the 3-dimensional space, are pairwise disjoint;

- 2) the planar diagram of the band β_i is disjoint from the projection in the diagram's plane of the corresponding disk A_i , for every $i = 1, \dots, s$.

Assuming that the components of $|L'|$ are numbered according to their vertical order, let $|L'_i|$ and $|L'_{i+1}|$ be the two components involved in the move. We attach to L_i an arbitrary auxiliary band β'_i as in Figure 3.5.4 (a) and then perform the indicated moves which lead to diagram (d) in the same figure. As a result, the labeling of the entire band B_i changes from (1 2) to (1 4), while the labeling of B_{i+1} is left unchanged. This allows us to perform the required crossing changes, bringing B_i on the top of B_{i+1} . Figure 3.5.5 describes the main steps in the realization of such crossing changes in the case when a disk C_j is present in the original crossing. Here, apart from 1-isotopy, we have used one move (R4) relating the second and the third diagram. The other case, when the disk C_j is not present in the original crossing, is obtained by the same steps in the reverse order with the roles of B_i and B_{i+1} (and their labels) exchanged. Once all the crossing changes have been performed, we restore the original labeling of B_i and cancel the auxiliary band β'_i , by reversing the steps from (a) to (d) of Figure 3.5.4. At this point, we are in position to push the disk A_i and the band B_i in the height interval $]b_{i+1}, a_{i+2}[$ through a vertical isotopy (put $a_{i+2} = \infty$ if $i + 1 = s$). We can assume that during this isotopy A_k, B_k and β_k with $k \neq i$ are kept fixed while A_i and B_i are being moved and the necessary vertical deformations are performed on β_i and on those C_j 's, D_j 's and D_j' 's which form ribbon intersections with B_i . The only problem which can arise here, is that after such isotopy β_i could intersect A_{i+1} , so that the resulting labeled ribbon surface tangle would not be a genuine \check{S}_K . To fix this, we can replace the deformed β_i by a legitimate band, thanks to the remark on page 101.

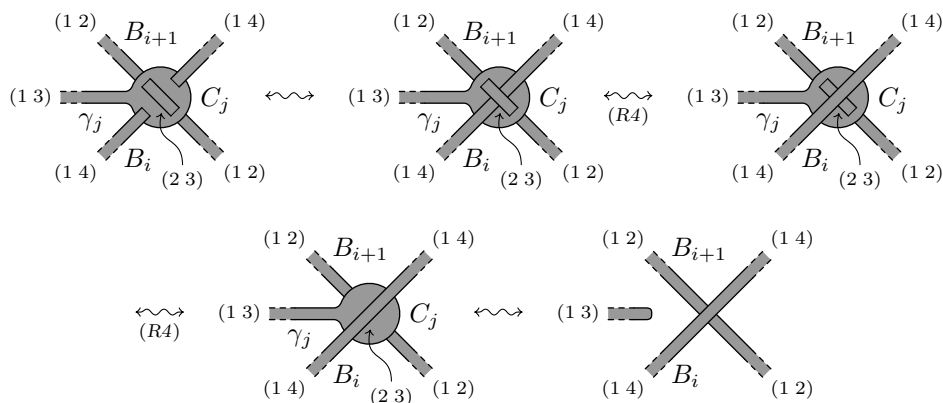


FIGURE 3.5.5. Independence of \check{S}_K on the vertical order of the components of $|L'|$

Concerning a single crossing change making a vertically trivial component $|L'_i|$ into a different vertically trivial state of $|L_i|$, there are four cases to be considered, depending on sign of the crossing and on whether $|L'_i|$ coincides with $|L_i|$ at that crossing or not. In all cases, according to Proposition 1.1.3, there exists a disk A'_i bounded by one of the two arcs of $|L'_i|$ determined by the two points projecting to the changing crossing, and the vertical segment joining these two points. Actually, such a disk can be thought as a perturbation of a subdisk of A_i , in such a way that it does not meet the bands β_1, \dots, β_s . Moreover, we can choose β_i to be attached to B_i in the portion of it corresponding to $|L'_i| - \text{Bd } A'_i$.

Figure 3.5.6 indicates how to realize the crossing change in one of the four cases. For the other three cases it suffices to apply a mirror symmetry to all the stages and/or reverse their order. In step (a), as it was done above, we create a disk D of label $(2\ 4)$ attached to $\text{id}_{(4\ 3)}$ through a narrow band δ passing through $\text{id}_{(3\ 2)}$. Then the disk D is moved within a neighborhood of A'_i to let A'_i pass through it, by 1-isotopy and some moves $(R2)$ and $(R4)$ like in Figure 3.5.4, until diagram (b) is achieved. After that, we get (e) as described in the intermediate steps. At this point, we use move $(R6)$ to transfer the two negative half-twists from D to B_i and we push back D to its original position, by reversing the process from (a) to (b). We remind that the additional negative full twist which appears on B_i compensates the change of crossing (cf. step 5 of the construction of S_K). Indeed, the move changes the framing of L'_i by -2 and therefore the framing of B_i should change by -1 as it does.

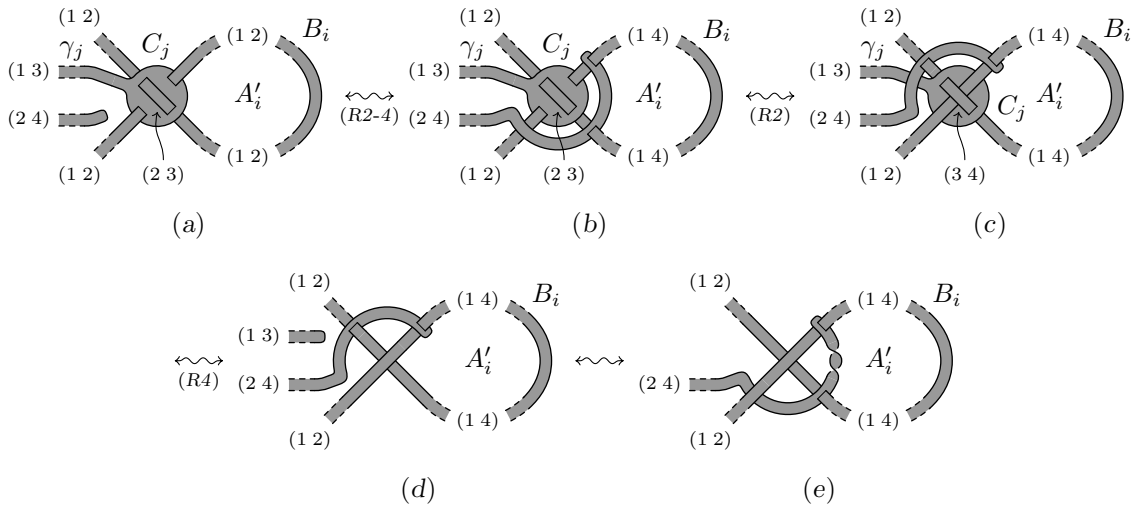


FIGURE 3.5.6. Independence of \check{S}_K on the vertical trivial component $|L'_i|$

Finally, we prove the independence of \check{S}_K on the strictly regular planar diagram of K . We recall that two strictly regular planar diagrams represent isotopic Kirby tangles if they are related through planar isotopy, Reidemeister moves and the moves presented in Figure 2.2.12.

We observe that any Reidemeister move on the link L of closed framed components of K induces the same move on its vertically trivial state L' , and so just a diagram isotopy on \check{S}_K , provided that none of the involved crossings (before and after the move) has been changed when passing from $|L|$ to $|L'|$. The reason is that in this case the two links coincide inside a small 3-cell where the move takes place and such 3-cell is free from the C_i 's. We leave to the reader the straightforward verification that, with the only exception depicted in Figure 3.5.7, a vertically trivial

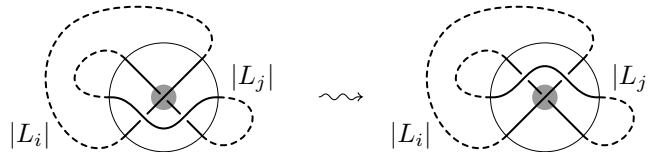


FIGURE 3.5.7. The exceptional Reidemeister move

state $|L'|$ of $|L|$ that satisfies this property can be always achieved by a suitable application of the naive unknotting procedure described in Section 1.1 with height function on each component as in Figure 1.1.1 (a) or (c), depending on the move. In the remaining case of Figure 3.5.7, we need to invert at least one of the two crossings formed by $|L_i|$ and $|L_j|$, in order to get the corresponding components $|L'_i|$ and $|L'_j|$ of the vertically trivial state $|L'|$. Nevertheless, assuming that we invert the crossing inside the shaded circle, the move still induces diagram isotopy on \check{S}_K .

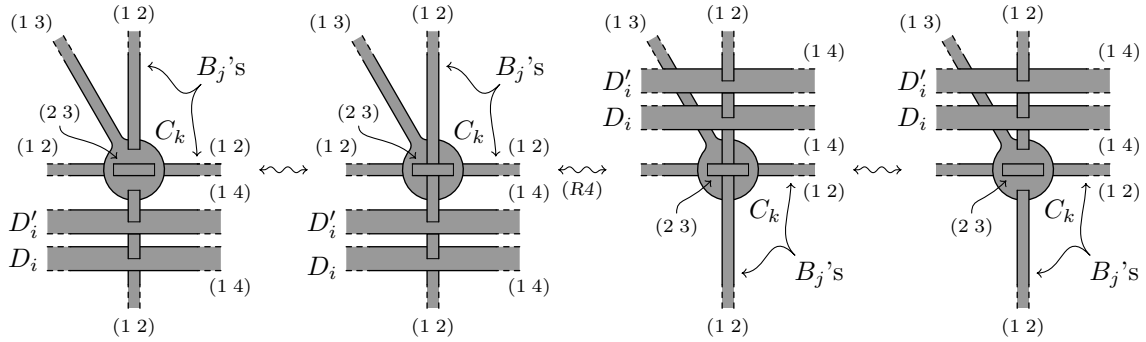


FIGURE 3.5.8. Moving an inverted crossing over/under a pair D_i and D'_i

To complete the proof, we consider the isotopy moves of Figure 2.2.12, which involve the dotted components of K . Moves (a) and (e) in the figure clearly induce labeled diagram isotopy on \check{S}_K . The same is true for move (d) once a suitable vertically trivial state has been chosen leaving unchanged the involved crossing between framed arcs. Also moves (b) and (c) induce labeled diagram isotopy on \check{S}_K when L' coincides with L at all the involved crossings between framed arcs. Otherwise, we perform the first move in Figure 3.5.3 on the disks D_i and D'_i originating from the one handle, changing in this way their labels from (1 3) to (1 4). Then, at any crossing where a disk C_k appears, we proceed as indicated in Figure 3.5.8. Here, four moves (R4) occur in the second step, while labeled 1-isotopy suffices for the other steps. Eventually, we perform backwards the first move in Figure 3.5.3 to restore the original labels of D_i and D'_i . \square

REMARK 3.5.2. The proof of the independence of \check{S}_K on the choice of the bands β , γ and δ in Lemma 3.5.1, works in the following much more general context.

Let S be any labeled ribbon surface tangle in \mathcal{S}_4 whose set of labels is complete, i.e. it generates the whole permutation group Σ_4 . If S contains a band γ_i (resp. δ_i) attached to a local configuration (included the labeling) as in the left (resp. right) side of Figure 3.4.5, then up to equivalence moves, such band can be replaced by any other band γ'_i (resp. δ'_i) attached in the same way to that local configuration. Analogously, if S contains a band β_i attached to a (possibly non-orientable) closed band B_i labeled (1 2) whose core spans a disk A_i as in Figure 3.5.4, and B_i (resp. A_i) forms ribbon intersections only passing through disks (resp. being passed through by bands) of label (1 3), then up equivalence moves, β_i can be replaced by any other band β'_i attached in the same way to B_i .

Indeed, thanks to the completeness of the labeling, we can always create a tongue of label (3 4) (resp. (2 4)) and use it to perform the modification described in Figures 3.5.2 or 3.5.3 (resp. Figure 3.5.4) in order to replace the band γ_i or δ_i (resp. β_i).

We also observe the same argument still works with any labeling obtained from the specific one considered above by conjugation in Σ_4 .

LEMMA 3.5.3. *Up to labeled 1-isotopy and moves (R1) and (R2), the labeled ribbon surface tangle $\uparrow_3^4 \check{S}_K$ is invariant under 2-equivalence of K .*

Proof. According to Definition 2.2.7, in order to prove the invariance of \check{S}_K under 2-equivalence of K , it is enough to consider the moves in Figure 2.2.7, since we have already proved the invariance under isotopy. Moreover, in our case K is an ordinary Kirby tangle and therefore no crossing change is possible, while the other three moves reduce to the ordinary ones without labels. We also recall that in addition to moves (R1) and (R2), we can use the moves (R3) to (R6) introduced in the previous section (cf. Proposition 1.4.3).

A pushing through 1-handle move on K trivially induces labeled isotopy on \check{S}_K . Similarly, the addition/deletion of a canceling 1/2-pair can be easily interpreted in terms of equivalence moves on \check{S}_K . In fact, if the disk D_i and the loop L_j represent a canceling pair in K , then in \check{S}_K the band B_j passes only once through D_i . Thus, by a move (R3) we can remove D_i and break B_j into two tongues. At this point, by labeled 1-isotopy we can retract such tongues to $\text{id}_{(2\ 1)}$ and after that to retract to $\text{id}_{(3\ 2)}$ the tongue $\beta_i \cup D'_i$ and all the $\gamma_k \cup C_k$'s related to crossing changes involving L_j .

The case of a 2-handle sliding requires some preliminaries. First of all, we number the components of L starting from the two ones involved in the sliding, in such a way that L_1 slides over L_2 . In terms of Kirby tangles, this means to replace L_1 with the band connected sum $L_1 \#_\delta \bar{L}_2$, where \bar{L}_2 is a parallel copy of L_2 , and δ is a band connecting L_1 to \bar{L}_2 . Since we have already proved the invariance of \check{S}_K under isotopy, we can isotope K in such a way that in its planar diagram δ is a blackboard parallel band, which does not form any crossing with the L_i 's and lies in a neighborhood of $\text{id}_{(2\ 1)}$ as shown in Figure 3.5.9 (a).

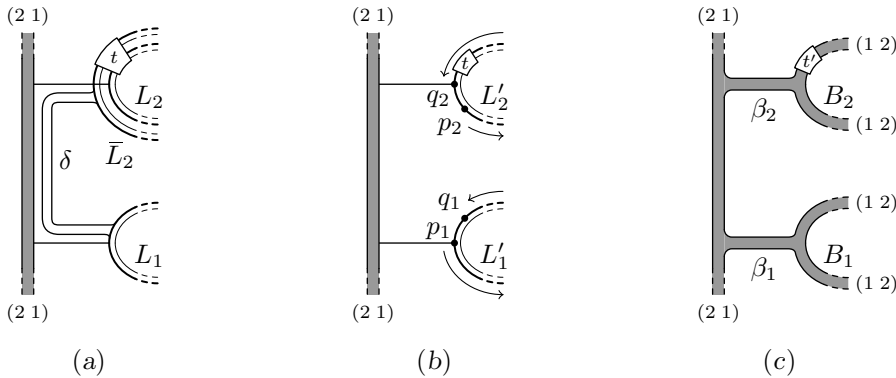


FIGURE 3.5.9. Standard set up for a 2-handle sliding

Then, in the construction of \check{S}_K we choose a vertically trivial state $|L'|$ such that: 1) the vertical order of the components is the one given by the numbering ($|L'_i|$ lies under $|L'_j|$, for $i < j$); 2) the minimum point p_1 (resp. p_2) and the maximum point q_1 (resp. q_2) of the height function h on $|L'_1|$ (resp. $|L'_2|$) coincide with the end points of the attaching arc of δ to L_1 (resp. \bar{L}_2), as in Figure 3.5.9 (b). Here, the arrows indicate the orientations that we will use in the framing computation at the end of the proof, so they are not relevant for the moment. Finally, we choose β_1 and

β_2 to be blackboard parallel bands, such that δ can be thought to run parallel to them and to the part of the boundary of $\text{id}_{(2\ 1)}$ between them, as in Figure 3.5.9 (c). For the sake of convenience, the framed curves L_2 and L'_2 and the ribbon B_2 are assumed to be blackboard parallel outside the twist boxes t and t' in Figure 3.5.9. The reader should be aware that the numbers of twists inside those boxes may differ, accordingly to step 5 of the construction of \check{S}_K .

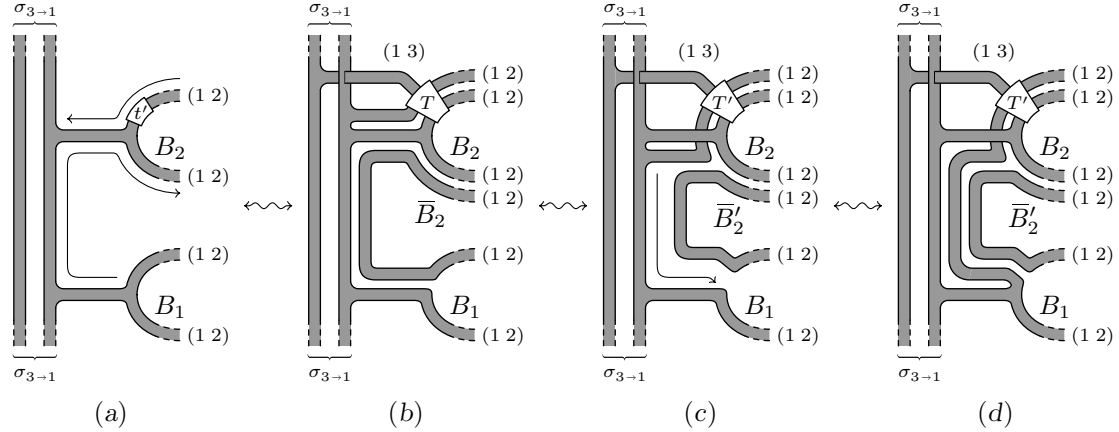


FIGURE 3.5.10. A 2-handle sliding in terms of moves on $\uparrow_3^4 \check{S}_K$

Once it has been set up in this way, the sliding can be interpreted in terms of moves on $\uparrow_3^4 \check{S}_K$, as sketched in Figure 3.5.10. Here, we omit to draw the reduction ribbon $\text{id}_{(4\ 3)}$ that is only implicitly involved in the step from (b) to (c).

We think of B_1 as a 1-handle attached to $\text{id}_{(2\ 1)}$ (like B_j in Figure 3.4.10) and slide one of its attaching arcs as indicated by the arrows in (a), to form a new ribbon \bar{B}_2 parallel to B_2 . Before reaching the twist box t' , this sliding can be entirely realized by labeled diagram isotopy, except for the labeled 1-isotopy moves needed to pass through the D_i 's and C_i 's encountered by B_2 . Each time a disk C_i is passed through, two new ribbon intersections appear as in the first diagram of Figure 3.5.11. Then, we use again 1-isotopy to split C_i into two twin disks similar to the original one, as suggested by the rest of Figure 3.5.11.

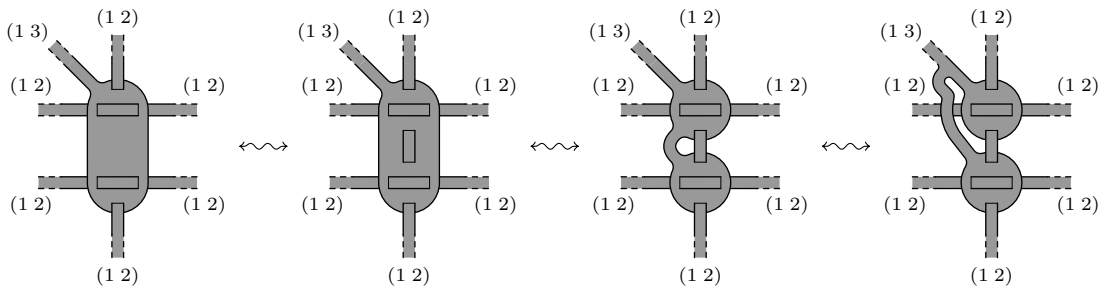


FIGURE 3.5.11.

To get the twist box T in (b), after having followed all the twists of B_2 in the twist box t' , we add some further crossings between B_2 and \bar{B}_2 (together with further C_i 's), in order to make them unlinked. Figure 3.5.12 shows how to add a positive crossing; for a negative one it suffices to mirror the figure. Here, some moves other

than 1-isotopy are needed: one move (R5) in the first step; two opposite moves (R6) in the third; two moves (R1) in the fourth. In particular, we observe that \bar{B}_2 enters and leaves the box T in Figure 3.5.10 (b) on the same side of B_2 .

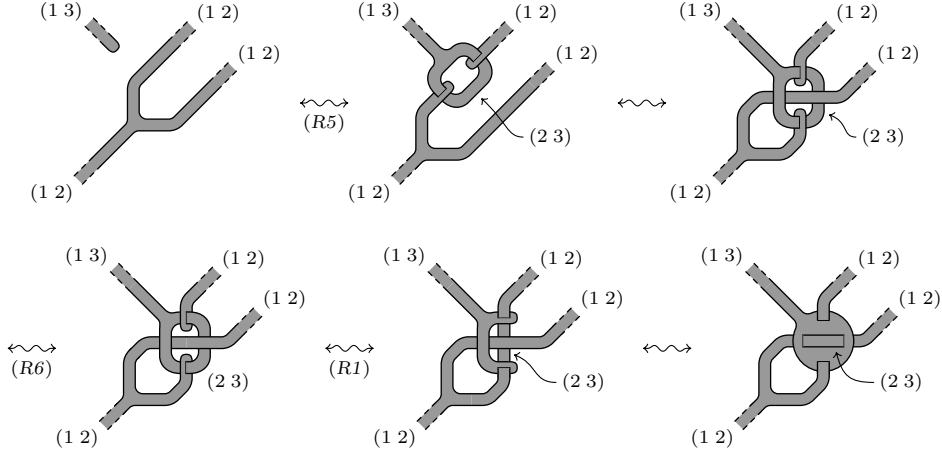


FIGURE 3.5.12.

Now, we consider a disk A_2 spanned by $|L'_2|$ as in step 6 of the construction of \check{S}_K , and perturb it near B_2 in such a way that it becomes disjoint from \bar{B}_2 , while remaining disjoint from all the other B_i 's and continuing to form only clasps and ribbon intersections with the rest of the ribbon surface tangle. Indicating the perturbed disk still by A_2 , we use it to replace the band β_2 in (b) by that in (c) and at the same time pull \bar{B}_2 below B_2 . To do that we first perform steps (a) to (d) in Figure 3.5.4 with $i = 2$, to change the labeling of B_2 from (1 2) to (1 4). Then we change all the crossings where \bar{B}_2 passes over B_2 , by operating as in Figure 3.5.5. Finally, we perform the last step in Figure 3.5.4 obtaining (e) and eventually cut and retract β_2 . In this way, we get the diagram in Figure 3.5.10 (c), where \bar{B}'_2 and T' differ from \bar{B}_2 and T only by the performed crossing changes. Eventually we get (d) by completing the sliding as indicated by the arrow in (c).

We claim that the labeled ribbon surface tangle in Figure 3.5.10 (d) coincides up to 3-dimensional isotopy with $\check{S}_{K'}$, where K' is the ordinary Kirby diagram obtained from K by replacing L_1 with $L_1 \#_\delta \bar{L}_2$.

To prove this claim, let \bar{L}'_2 be the framed unknot whose base curve is the core of the ribbon \bar{B}'_2 and whose framing is the double of that represented by \bar{B}'_2 . Taking into account our starting assumptions on the height function of $|L'|$, the link formed by $|L'_1 \#_\delta \bar{L}'_2|, |L'_2|, \dots, |L'_s|$ is vertically trivial for a suitable height function compatible with the planar diagram in Figure 3.5.10 (d). Moreover, $|L'_1 \#_\delta \bar{L}'_2|$ is the core of the ribbon $B_1 \#_\delta \bar{B}'_2$ and $\text{fr}(L'_1 \#_\delta \bar{L}'_2) = \text{fr}(L'_1) + \text{fr}(\bar{L}'_2)$ is the double of the framing represented by $B_1 \#_\delta \bar{B}'_2$. Therefore, still referring to diagram (d) in Figure 3.5.10, our claim amounts to say that by inverting the crossings marked by the presence of a disk C_i in the framed link formed by $L'_1 \#_\delta \bar{L}'_2, L'_2, \dots, L'_s$, we get the framed link formed by $L_1 \#_\delta \bar{L}_2, L_2, \dots, L_s$, up to diagram isotopy of K . It is clear from the construction that such crossing inversions produce a framed link of components $L_1 \#_\delta \widehat{L}_2, L_2, \dots, L_s$, where \widehat{L}_2 is a framed knot whose base curve $|\widehat{L}_2|$ is parallel to $|L_2|$. Hence, it is left to prove that $\text{lk}(|L_2|, |\widehat{L}_2|) = \text{lk}(|L_2|, |\bar{L}_2|) = \text{fr}(L_2)$ (in other

words, $|\widehat{L}_2|$ and $|\overline{L}_2|$ represent the same framing of $|L_2|$ and $\text{fr}(\widehat{L}_2) = \text{fr}(\overline{L}_2) = \text{fr}(L_2)$, where in both cases the second equality directly derives from the construction.

Since B_2 and \overline{B}'_2 are vertically separated, $\text{lk}(|L'_2|, |\overline{L}'_2|) = 0$ and thus $\text{lk}(|L_2|, |\widehat{L}_2|)$ is the opposite of the signed number of crossings between B_2 and \overline{B}'_2 marked by a C_i in (d). On the other hand, being also B_2 and \overline{B}_2 unlinked, this equals the opposite of the signed number of crossings between B_2 and \overline{B}_2 marked by a C_i in (b). According to the construction of the diagram in (b), there are $-\text{fr}(L'_2)$ such crossings inside the twist box T , while the number of them outside the twist box T is the double of the signed number of the self-crossings of B_2 marked by a C_i in S_K . But this last number is equal to the difference $\text{fr}(L'_2) - \text{fr}(L_2)$, so we can immediately conclude that $\text{lk}(|L_2|, |\widehat{L}_2|) = \text{fr}(L_2)$.

Finally, the equality $\text{fr}(\widehat{L}_2) = \text{fr}(L_2)$ can be derived in a similar way from $\text{fr}(\overline{L}'_2) = 2\text{fr}(\overline{B}'_2) = 2\text{fr}(\overline{B}_2) = 2\text{fr}(B_2) = \text{fr}(L'_2)$, once one observes that the signed number of the self-crossings of \overline{B}'_2 marked by a C_i in (d) coincides with that of the self-crossings of B_2 marked by a C_i in S_K . \square

PROPOSITION 3.5.4. *The map Ξ_4 defined $\Xi_4(I_m) = J_{\sigma_{4+1}} \diamond J_m$ for every $m \geq 0$ and $\Xi_4(K) = \uparrow_3^4 \check{S}_K$ for every Kirby tangle K in \mathcal{K}_1 (cf. Proposition 3.6.3), represents a faithful functor $\Xi_4 : \mathcal{K}_1 \rightarrow \mathcal{S}_4^c$, such that $\Xi_4(\mathcal{K}_1) \subset \mathcal{S}_{4+1}^c$ and $\downarrow_1^4 \circ \Theta_4 \circ \Xi_4 = \text{id}_{\mathcal{K}_1}$. Moreover, for any two morphisms $K : I_{m_0} \rightarrow I_{m_1}$ and $K' : I_{m'_0} \rightarrow I_{m'_1}$ in \mathcal{K}_1 we have $\Xi_4(K \diamond K') = \uparrow_3^4(Q_{m_1+m'_1} \circ (R_K \diamond R_{K'}) \circ \overline{Q}_{m_0 \diamond m'_0})$ (cf. Figure 3.4.1).*

Proof. In the light of the previous Lemmas 3.5.1 and 3.5.3, Ξ_4 is well-defined as a map. To prove that it is a functor, we have to show that it preserves the identity morphisms and the composition of morphisms.

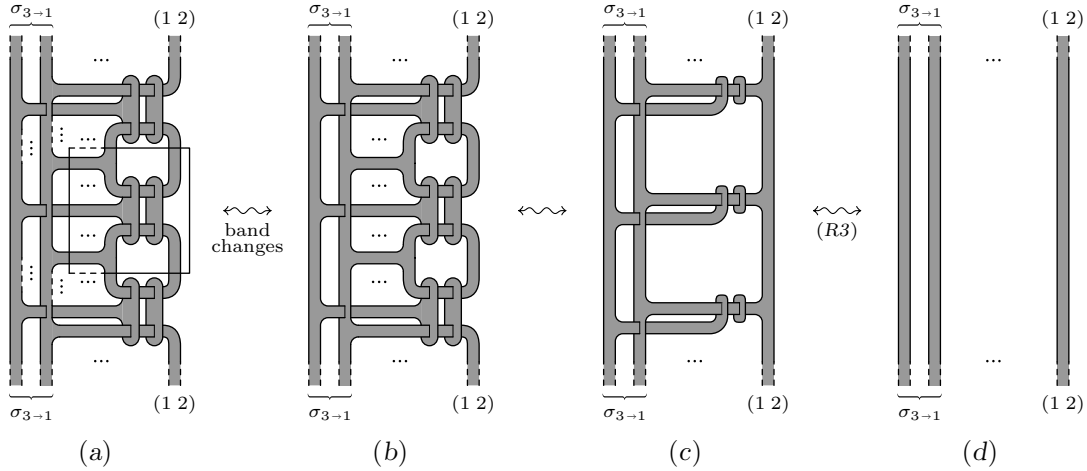


FIGURE 3.5.13. Ξ_4 preserves the identity morphisms

Concerning the identities, we observe that for $K = \text{id}_{I_m}$ the labeled ribbon surface tangle \check{S}_K looks like in Figure 3.5.13 (a), where only the rightmost of the m blocks forming T_K (in the box), Q_m and \overline{Q}_m are drawn. The rest of Figure 3.5.13 outlines how we can reduce this block to a single identity ribbon. Namely, to get (b) we change the β_i 's and the δ_i 's relative to the other blocks and laying between the uppermost and lowermost horizontal bands of label (1 2) in the figure, in such a way that they allow the labeled 1-isotopy from (b) into (c). This can be done by the

same arguments used in the proof of Lemma 3.5.1 thanks to Remark 3.5.2, by using the stabilization ribbon $\text{id}_{(4\ 3)}$ that is there even if not drawn in the figure. Then, we use move (R3) to cut the horizontal bands in (c) and we retract the resulting tongues to get (d). Once the reduction of the rightmost block has been completed, the process can be iterated to reduce one by one, from right to left, also the other $m - 1$ blocks to identity ribbons, hence all $\Xi_4(K)$ to the identity.

Now let us consider the composition. Given two morphisms $K_1 : I_{m_0} \rightarrow I_{m_1}$ and $K_2 : I_{m_1} \rightarrow I_{m_2}$ in \mathcal{K}_1 , we have to prove that $\uparrow_3^4(\check{S}_{K_2} \circ \check{S}_{K_1})$ and $\uparrow_3^4 \check{S}_{K_2 \circ K_1}$ are equivalent up to 1-isotopy and moves (R1) and (R2). This will follow once show that $R_{K_2} \circ \bar{Q}_{m_1} \circ Q_{m_1} \circ R_{K_1}$ is equivalent to $R_{K_2 \circ K_1}$. Apart from the two reduction ribbons on the left, the composition $\bar{Q}_{m_1} \circ Q_{m_1}$ consists of m_1 blocks like the one shown in Figure 3.5.14 (a). Each block contains two arcs labeled (1 2), ending one in the source and the other in the target and originating from two open components in K_1 and K_2 , which create a single closed component in $K_2 \circ K_1$. Figure 3.5.14 describes in a schematic way the transformation of these blocks one by one, starting from the left. Let B_1 and B_2 be the closed bands in R_{K_1} and R_{K_2} to which the two arcs of the block shown in (a) belong. By replacing bands if necessary, we can assume that their attaching bands β_1 and β_2 are the as shown in (b), where we have also slided the two innermost horizontal bands in (a) until they form an extra closed ribbon connected to $\text{id}_{(2\ 1)}$. In the last step from (c) to (d) we first use two (R3) moves to cut and retract the horizontal bands passing through disks, so that in the resulting tangle B_1 and B_2 are replaced with a single closed band attached to $\text{id}_{(1\ 2)}$ by a band β . Then, we change such β in order to allow the iteration of the whole process to the subsequent blocks of $\bar{Q}_{m_1} \circ Q_{m_1}$.

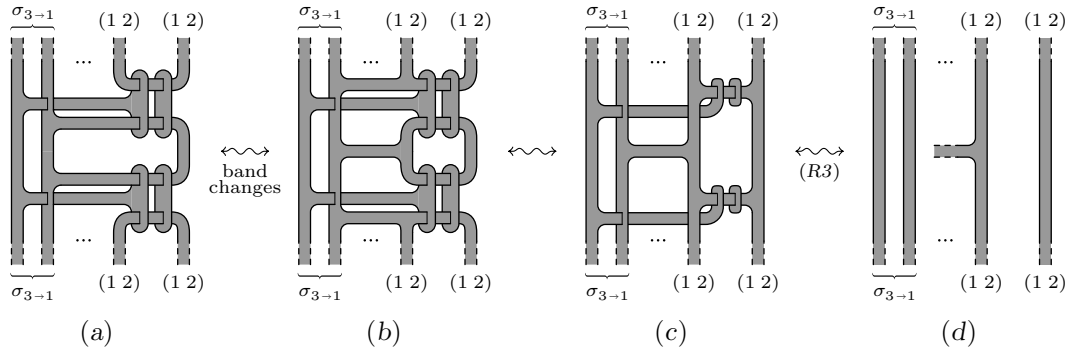


FIGURE 3.5.14. Ξ_4 preserves the composition of morphisms

Finally, the equality $\downarrow_1^4 \Theta_4 \circ \Xi_4 = \text{id}_{\mathcal{K}_1}$ and hence the faithfulness of Ξ_4 immediately follow from Propositions 3.3.4 and 3.4.3, while the second part of the statement is just a reinterpretation of Remark 3.4.2 under the stabilization \uparrow_3^4 . \square

We note that $\Xi_4 : \mathcal{K}_1 \rightarrow \mathcal{S}_4^c$ will be proved to be a category equivalence in the next section (cf. Theorem 3.6.4), and therefore it induces a monoidal structure on \mathcal{S}_4^c , which we do not provide in explicit form.

PROPOSITION 3.5.5. *For any $n \geq 4$, $\Xi_n = \uparrow_4^n \circ \Xi_4 : \mathcal{K}_1 \rightarrow \mathcal{S}_n^c$ is a faithful functor and satisfies the identity $\downarrow_1^n \circ \Theta_n \circ \Xi_n = \text{id}_{\mathcal{K}_1}$.*

Proof. This is a direct consequence of Propositions 3.3.4, 3.4.3 and 3.5.4. \square

3.6. Equivalence between \mathcal{K}_n^c and \mathcal{S}_n^c for $n \geq 4$

We want to prove that the functors $\Theta_n : \mathcal{S}_n^c \rightarrow \mathcal{K}_n^c$ and $\Xi_n : \mathcal{K}_1 \rightarrow \mathcal{S}_n^c$ are equivalences of categories for any $n \geq 4$. Taking into account Propositions 1.5.3 and 3.5.5, to achieve this result it is enough to show that the functor $\Xi_4 : \mathcal{K}_1 \rightarrow \mathcal{S}_4^c$ is full and that any object in \mathcal{S}_n^c is isomorphic to one in its image, i.e. that the inclusion of $\Xi_4(\mathcal{K}_1)$ in \mathcal{S}_4^c is an equivalence of categories.

LEMMA 3.6.1. Any labeled ribbon surface tangle $T : J_{\sigma_{3 \rightarrow 1}} \diamond J_{\sigma_0} \rightarrow J_{\sigma_1}$ in \mathcal{S}_3 is equivalent to a composition $T_l \circ \dots \circ T_1$, where each T_k is an expansion (that is a product with some identity ribbons on the left and/or on the right) of one of the special elementary ribbon surface tangles presented in Figure 3.6.1.

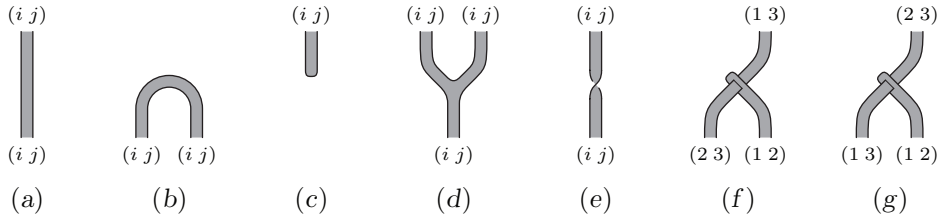


FIGURE 3.6.1. Special elementary morphisms in \mathcal{S}_3 ($(i j) \in \Gamma_3$)

Proof. According to Proposition 1.3.7, we can assume that T is presented by a 3-labeled special planar diagram, that is a planar diagram consisting of some spots like (a) to (e) and (h) in Figure 1.3.6 and some flat bands, with a compatible labeling in Γ_3 . Moreover, we can convert all the negative half-twists occurring in such a diagram into positive ones and crossings, by using labeled versions of the moves (S14) and (S17) in Figure 1.3.11.

Then, we proceed as shown in Figure 3.6.2 to eliminate all the monocromatic ribbon intersections and all the crossings. More precisely, we first eliminate the monocromatic ribbon intersections and crossings by performing the labeled 1-isotopies described in (a) and (b) respectively. Here, the tongues labeled $(i k)$ have

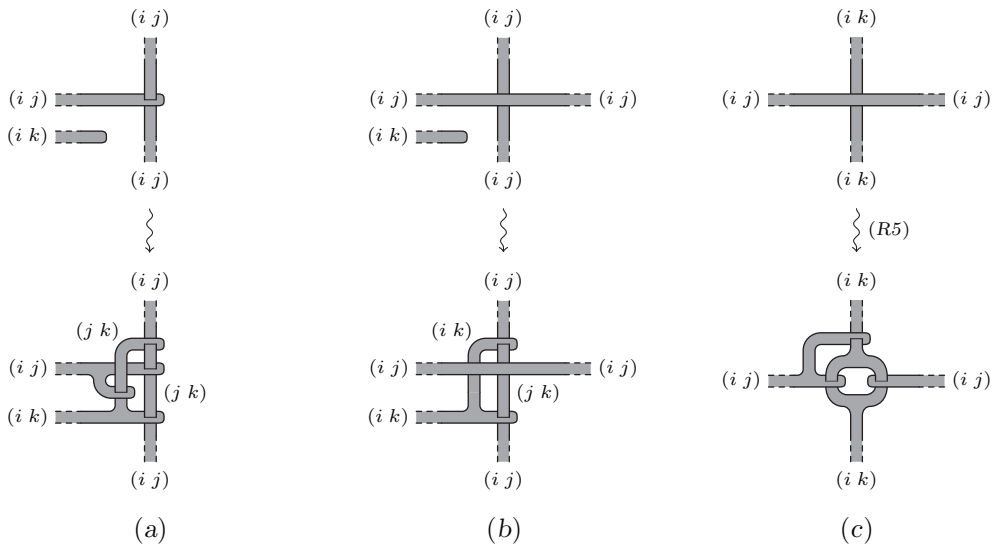


FIGURE 3.6.2.

been pulled out of the closest ribbon with that label. Observe that such ribbon always be created, due to the form of the source. Subsequently, we eliminate all the remaining crossings, including the new ones deriving from (a) and (b), by the moves depicted in (c). Eventually, we put again the diagram into special form by move (S2), which only introduces positive half-twists.

After that, all the three transpositions of Γ_3 are involved in the labeling of any surviving ribbon intersection, so we can use move (R1) to adjust it in such a way that the disk which is passed through is the one with label (1 2).

Finally, by using planar isotopy as in the proof of Proposition 3.1.2, we can express T as $T_l \circ \dots \circ T_1$, where each T_k is an expansion of one of the elementary morphisms of Figure 3.1.1. The previous form of T guarantees that no spot like (e), (e') and (f') occurs. Moreover, we can also eliminate all the spots like (g'), (c') and (b) in the order, by using move (I6), (I3) and (I16) respectively. This leaves us with the required expression of T . \square

PROPOSITION 3.6.2. *The inclusion of $\Xi_4(\mathcal{K}_1)$ in \mathcal{S}_4^c is a category equivalence.*

Proof. We observe that $\Xi_4(\mathcal{K}_1) \subset \uparrow_3^4 \mathcal{S}_3^c$. Moreover, according to Proposition 3.2.8, the inclusion of $\uparrow_3^4 \mathcal{S}_3^c$ in \mathcal{S}_4^c is a category equivalence. Therefore, it suffices to show that the inclusion $\Xi_4(\mathcal{K}_1) \subset \uparrow_3^4 \mathcal{S}_3^c$ is an equivalence as well. By Proposition 1.5.4, this amounts to say that any object in $\uparrow_3^4 \mathcal{S}_3^c$ is isomorphic to one in the image of Ξ_4 and that any morphisms in $\uparrow_3^4 \mathcal{S}_3^c$ between two objects in the image of Ξ_4 is the image of a morphism in \mathcal{K}_1 under Ξ_4 .

About objects, we recall that those in the image of Ξ_4 are given by $J_{\sigma_{4-1}} \diamond J_m$ with $m \geq 0$, where J_m denotes the sequence of m intervals each labeled by (1 2). For any $\sigma = ((i_1 j_1), \dots, (i_m j_m)) \in \Pi\Gamma_3$, we define $\zeta_\sigma : J_{\sigma_{3-1}} \diamond J_\sigma \rightarrow J_{\sigma_{3-1}} \diamond J_m$, as the composition $\zeta_\sigma = \zeta_{\sigma,m} \circ \dots \circ \zeta_{\sigma,1}$, where $\zeta_{\sigma,h}$ is the identity if $(i_h j_h) = (1 2)$, while it is illustrated in Figure 3.6.3 for $(i_h j_h)$ equal to (1 3) and (2 3). Here, the horizontal tongues pass in front of the first $h - 1$ vertical ribbons originating in J_σ , and form ribbon intersections with the h -th one. The $\zeta_{\sigma,h}$'s are isomorphisms, their inverses being obtained by vertical reflection, hence ζ_σ is an isomorphism as well. Then, the desired isomorphism between the generic object $J_{\sigma_{4-1}} \diamond J_\sigma$ in $\uparrow_3^4 \mathcal{S}_3^c$ and an object in the image of Ξ_4 is represented by $\text{id}_{4 \rightarrow 3} \diamond \zeta_\sigma : J_{\sigma_{4-1}} \diamond J_\sigma \rightarrow J_{\sigma_{4-1}} \diamond J_m$.

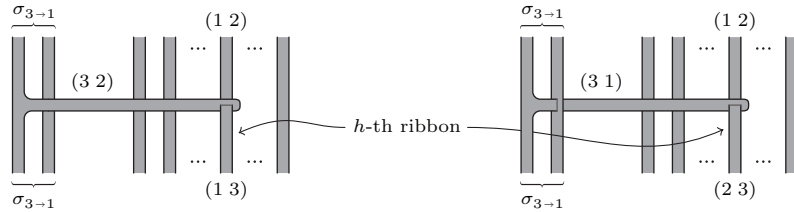


FIGURE 3.6.3. The isomorphism $\zeta_{\sigma,h}$

The proof that any morphism $S : J_{\sigma_{4-1}} \diamond J_{m_0} \rightarrow J_{\sigma_{4-1}} \diamond J_{m_1}$ in $\uparrow_3^4 \mathcal{S}_3^c$ is in the image of Ξ_4 , requires more work. By definition, $S = (\text{id}_{\sigma_{4-1}} \diamond T) \circ (\text{id}_{(4 3)} \diamond \Delta_{\sigma_{3-1}} \diamond \text{id}_{m_0})$ for some $T : J_{\sigma_{3-1}} \diamond J_{m_0} \rightarrow J_{m_1}$ in \mathcal{S}_3 . Then, we have the decomposition

$$S = \text{id}_{(4 3)} \diamond (\zeta_{\sigma_1} \circ (\text{id}_{\sigma_{3-1}} \diamond T) \circ \zeta_{\sigma_{3-1} \diamond \sigma_0}^{-1} \circ \zeta_{\sigma_{3-1} \diamond \sigma_0} \circ (\Delta_{\sigma_{3-1}} \diamond \text{id}_{\sigma_0}) \circ \zeta_{\sigma_0}^{-1}),$$

where ζ_{σ_1} and $\zeta_{\sigma_0}^{-1}$ act as identities, being the elements of J_{m_0} and J_{m_1} all labeled by (1 2). Moreover, by Lemma 3.6.1 we can assume that T is a composition $T_l \circ \dots \circ T_1$, where each $T_k \in \mathcal{S}_3$ is an expansion of one of the special elementary morphisms in Figure 3.6.1. Therefore, if $J_{\sigma_0^k}$ and $J_{\sigma_1^k}$ are respectively the source and the target of T_k , by inserting in $\text{id}_{\sigma_{3 \rightarrow 1}} \diamond T = (\text{id}_{\sigma_{3 \rightarrow 1}} \diamond T_l) \circ \dots \circ (\text{id}_{\sigma_{3 \rightarrow 1}} \diamond T_1)$ the canceling pair $\zeta_{\sigma_0^{k+1}}^{-1} \circ \zeta_{\sigma_1^k}$ between $\text{id}_{\sigma_{3 \rightarrow 1}} \diamond T_{k+1}$ and $\text{id}_{\sigma_{3 \rightarrow 1}} \diamond T_k$ for any $k = 1, \dots, l - 1$, we get

$$\zeta_{\sigma_1} \circ (\text{id}_{\sigma_{3 \rightarrow 1}} \diamond T) \circ \zeta_{\sigma_{3 \rightarrow 1} \diamond \sigma_0}^{-1} = (\zeta_{\sigma_1^l} \circ (\text{id}_{\sigma_{3 \rightarrow 1}} \diamond T_l) \circ \zeta_{\sigma_0^l}^{-1}) \circ \dots \circ (\zeta_{\sigma_1^1} \circ (\text{id}_{\sigma_{3 \rightarrow 1}} \diamond T_1) \circ \zeta_{\sigma_0^1}^{-1}).$$

On the other hand, Figure 3.6.4 shows that $\zeta_{\sigma_{3 \rightarrow 1} \diamond \sigma_0} \circ (\Delta_{\sigma_{3 \rightarrow 1}} \diamond \text{id}_{\sigma_0}) \circ \zeta_{\sigma_0}^{-1}$ is equivalent to the composition of $\text{id}_{(3 \ 2)} \diamond \Delta_{(1 \ 2)} \diamond \text{id}_{\sigma_0}$ and two morphisms having the same form as the $\text{id}_{\sigma_{3 \rightarrow 1}} \diamond T_k$'s above.

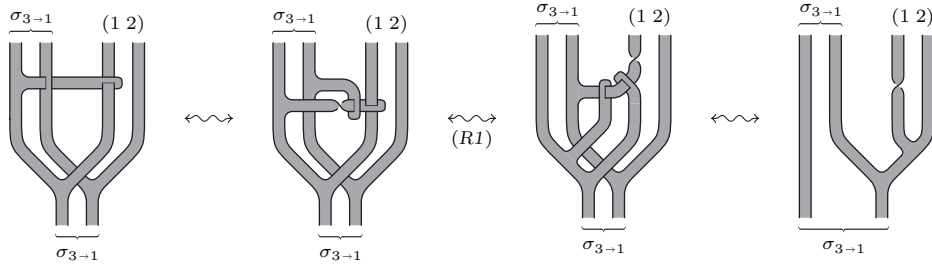


FIGURE 3.6.4.

In conclusion, it is enough to prove that a ribbon surface tangle $S \in \uparrow_1^4 \mathcal{S}_{3 \rightarrow 1}$ is in the image of Ξ_4 in the special cases when $S = \text{id}_{\sigma_{4 \rightarrow 2}} \diamond \Delta_{(1 \ 2)} \diamond \text{id}_m$ for some $m \geq 0$, or $S = \text{id}_{(4 \ 3)} \diamond (\zeta_{\sigma_1} \circ (\text{id}_{\sigma_{3 \rightarrow 1}} \diamond T) \circ \zeta_{\sigma_0}^{-1})$, with $T : J_{\sigma_0} \rightarrow J_{\sigma_1}$ being any expansion in \mathcal{S}_3 of one of the special elementary morphisms in Figure 3.6.1.

We start with the simplest cases when $m = 0$ and T is an elementary morphism. Namely, Figure 3.6.5 shows that $\text{id}_{(4 \ 2)} \diamond \Delta_{(1 \ 2)}$ is equivalent to $\Xi_4(\eta_1)$, where η_1 is a single framed arc (cf. Figure 2.3.1). Here, we first modify the ribbon surface tangle by 1-isotopy and then use move (R3) to eliminate the pair of vertical disks and the horizontal band passing through them.

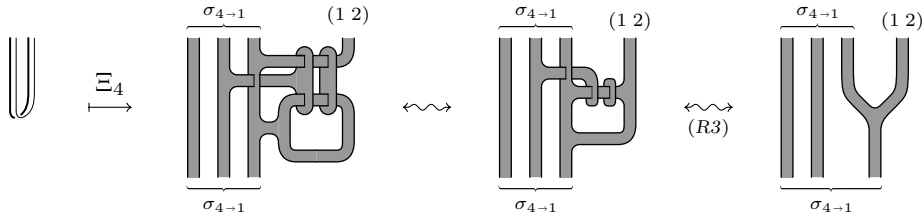


FIGURE 3.6.5.

Concerning $\text{id}_{(4 \ 3)} \diamond (\zeta_{\sigma_1} \circ (\text{id}_{\sigma_{3 \rightarrow 1}} \diamond T) \circ \zeta_{\sigma_0}^{-1})$, we first observe that, if T is one of the tangles (a) to (e) in Figure 3.6.1, then the equality $\text{id}_{(4 \ 3)} \diamond (\zeta_{\sigma_1} \circ (\text{id}_{\sigma_{3 \rightarrow 1}} \diamond T) \circ \zeta_{\sigma_0}^{-1}) = \text{id}_{\sigma_{4 \rightarrow 1}} \diamond T$ can be immediately seen to hold just by using 1-isotopy. So, for those T it is enough to treat the case $(i \ j) = (1 \ 2)$. This has been already done for $T = \text{id}_{(1 \ 2)}$ in the proof of Proposition 3.5.4, while it is done in Figure 3.6.6 for the other T 's, from (b) to (e). This time, the first modification of each ribbon surface tangle consists in the elimination of the pairs of vertical disks on the top and on the bottom

(belonging to the Q_{m_1} 's and the \bar{Q}_{m_0} 's), realized by moves (R3) after suitable 1-isotopy (cf. Figure 3.6.5, where an analogous elimination is detailed into two steps).

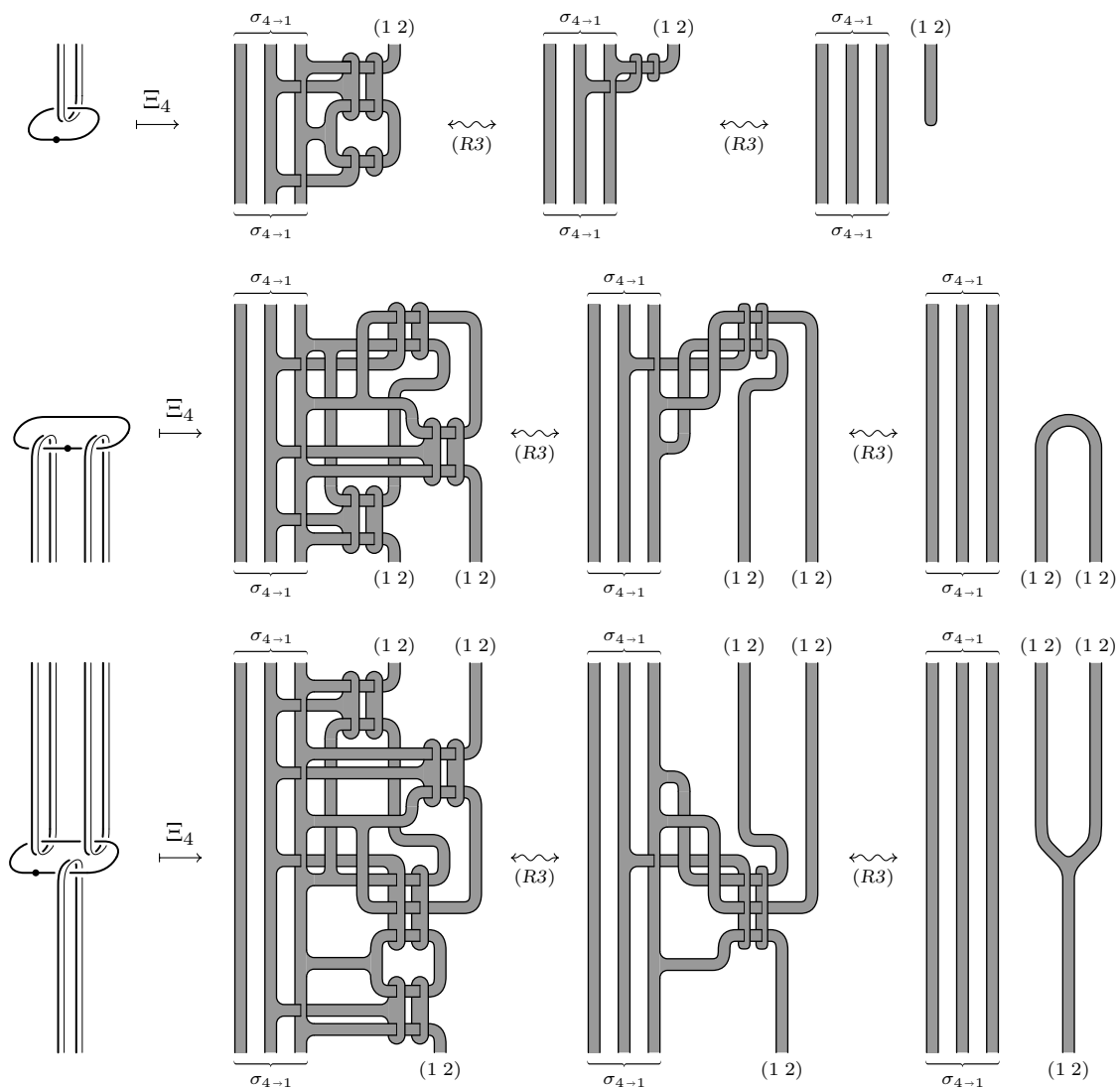


FIGURE 3.6.6.

The cases when T coincides with (f) and (g) are shown in Figure 3.6.7. This figure is more sketchy than the previous ones. In particular, in the starting ribbon surface tangles, the two pairs of vertical disks belonging to \bar{Q}_2 are omitted, assuming that they have been previously eliminated as above. The first step in both cases starts with the further elimination of two of the three pairs of vertical disks, once again by the same procedure as above even if a band replacement is needed in the first case. This is followed by the inversion of some of the ribbon intersection formed by the surviving pair, like in move (S2). The resulting half-twists, together with the preexisting one in the first case, are then canceled with the help of move (R6). At this point, the second step just consists of three (R1) moves and 1-isotopy.

Now, it remains to consider the cases of $\text{id}_{\sigma_{4 \rightarrow 2}} \diamond \Delta_{(1 2)} \diamond \text{id}_m$ with $m > 0$, and $\text{id}_{(4 3)} \diamond (\zeta_{\sigma_1} \circ (\text{id}_{\sigma_{3 \rightarrow 1}} \diamond T) \circ \zeta_{\sigma_0}^{-1})$ with T being a non-trivial expansion in \mathcal{S}_3 of one of the special elementary morphisms in Figure 3.6.1.

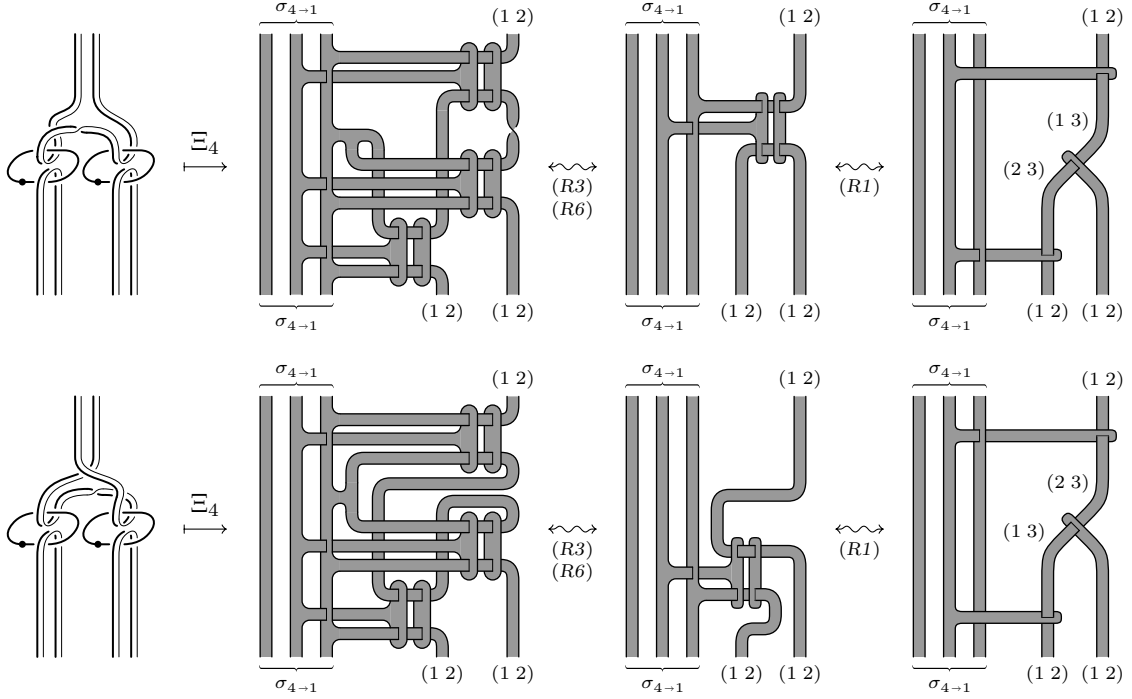


FIGURE 3.6.7.

The following claim allows us to deduce these cases from the spacial ones we have just considered, when $m = 0$ and T is an elementary morphism, by a straightforward inductive argument based on the number of the expansion ribbons.

Given two morphisms K and K' in \mathcal{K}_1 , the claim relates the image of $K \diamond K'$ under Ξ_4 , with the images of K and K' . Unfortunately, we do not have an explicit monoidal structure on $\uparrow_1^4 \mathcal{S}_{3 \rightarrow 1}$, and this makes the statement quite technical. Actually, for the present aim, the claim could be restricted by the assumption that at least one of T and T' is an identity morphism, but this would not make its proof simpler.

CLAIM. Let $T : J_{\sigma_{3 \rightarrow 1}} \diamond J_{\sigma_0} \rightarrow J_{\sigma_{3 \rightarrow 1}} \diamond J_{\sigma_1}$ and $T' : J_{\sigma'_0} \rightarrow J_{\sigma'_1}$ be morphisms in \mathcal{S}_3 , such that $\text{id}_{(4,3)} \diamond (\zeta_{\sigma_1} \circ T \circ \zeta_{\sigma_0}^{-1}) = \Xi_4(K)$ and $\text{id}_{(4,3)} \diamond (\zeta_{\sigma'_1} \circ (\text{id}_{\sigma_{3 \rightarrow 1}} \diamond T') \circ \zeta_{\sigma'_0}^{-1}) = \Xi_4(K')$ for some K and K' in \mathcal{K}_1 . Then

$$\text{id}_{(4,3)} \diamond (\zeta_{\sigma_1 \diamond \sigma'_1} \circ (T \diamond T') \circ \zeta_{\sigma_0 \diamond \sigma'_0}^{-1}) = \Xi_4(B_{\sigma_1, \sigma'_1} \circ (K \diamond K') \circ \bar{B}_{\sigma_0, \sigma'_0}^{-1}).$$

Here, given $\sigma = ((i_1 j_1), \dots, (i_m j_m))$ and $\sigma' = ((i'_1 j'_1), \dots, (i'_{m'} j'_{m'}))$ in $\Pi \Gamma_3$, we denote by $B_{\sigma, \sigma'}$ the framed $2(m + m')$ -braid defined as $B_{\sigma, \sigma'} = b_{m'} \circ \dots \circ b_1$, where b_h is the framed $2(m + m')$ -braid shown in Figure 3.6.8 if $(i'_h j'_h) = (2, 3)$, while it is the identity otherwise.

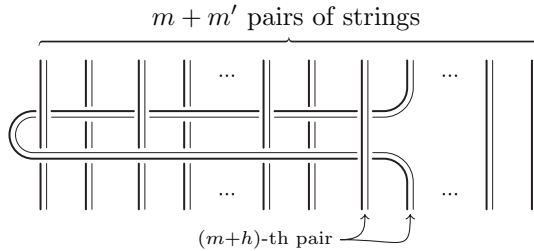


FIGURE 3.6.8. The framed $2(m + m')$ -braid b_h for $(i'_h j'_h) = (2, 3)$

To prove the claim, let us consider $\zeta_{\sigma_1 \diamond \sigma'_1} \circ (T \diamond T') \circ \zeta_{\sigma_0 \diamond \sigma'_0}^{-1}$ and look at Figure 3.6.9, where: m_0, m'_0, m_1, m'_1 denote the lengths of $\sigma_0, \sigma'_0, \sigma_1, \sigma'_1$ respectively. Here once again the reduction ribbon $\text{id}_{(4\ 3)}$ is omitted, being involved only in performing the necessary band replacements as in Remark 3.5.2.

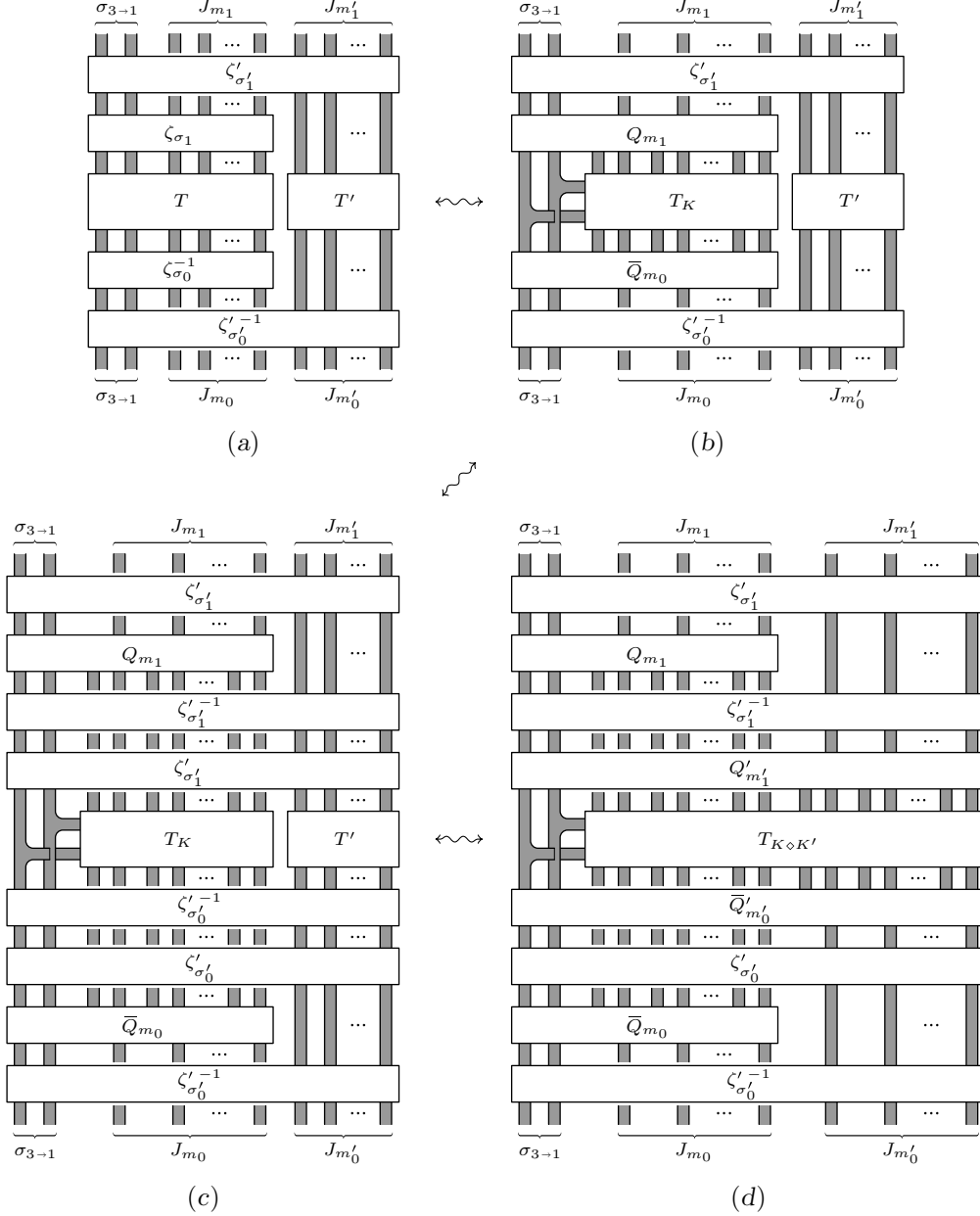


FIGURE 3.6.9.

Diagram (a) in the figure is obtained by decomposing the natural isomorphisms $\zeta_{\sigma_1 \diamond \sigma'_1}$ and $\zeta_{\sigma_0 \diamond \sigma'_0}^{-1}$, according to the identity $\zeta_{\sigma \diamond \sigma'} = \zeta'_{\sigma'} \circ (\zeta_{\sigma} \diamond \text{id}_{\sigma'})$, with

$$\zeta'_{\sigma'} = (\text{id}_{4 \rightarrow 1} \diamond \gamma_{\sigma, \sigma'}) \circ (\zeta_{\sigma'} \diamond \text{id}_{\sigma}) \circ (\text{id}_{4 \rightarrow 1} \diamond \gamma_{\sigma, \sigma'}^{-1}) = \zeta_{\sigma \diamond \sigma', m+m'} \circ \dots \circ \zeta_{\sigma \diamond \sigma', m+1},$$

where m and m' denote the lengths of σ and σ' respectively. Then, we get (b) by using the hypothesis that $\text{id}_{(4\ 3)} \diamond (\zeta_{\sigma_1} \circ T \circ \zeta_{\sigma_0}^{-1}) = \Xi_4(K)$, and (c) just by inserting the canceling pairs $\zeta'_{\sigma'_0} \circ \zeta_{\sigma'_0}$ and $\zeta'_{\sigma'_1} \circ \zeta_{\sigma'_1}$. Here, the horizontal bands forming

the pseudo-products $\diamond_{\beta,\gamma,\delta}$ are fused all together in their terminal parts outside the boxes. In order to get (d), we first change those bands into new ones which pass under $\zeta'_{\sigma'_0}{}^{-1}$ and reach the reduction ribbons $\text{id}_{\sigma_{3 \rightarrow 1}}$ in the region between $\zeta'_{\sigma'_1}{}^{-1}$ and $\zeta'_{\sigma'_0}$ and then apply the hypothesis that $\text{id}_{(4\ 3)} \diamond (\zeta'_{\sigma'_1} \circ (\text{id}_{\sigma_{4 \rightarrow 1}} \diamond T') \circ \zeta'_{\sigma'_0}{}^{-1}) = \Xi_4(K')$ and the fact that $R_K \diamond R_{K'} = R_{K \diamond K'}$ (see Remark 3.4.2). In diagram (d), $Q'_{m'_1} = (\text{id}_{3 \rightarrow 1} \diamond \gamma_{2m'_1, 2m_1}) \circ (Q_{m'_1} \diamond \text{id}_{2m_1}) \circ (\text{id}_{3 \rightarrow 1} \diamond \gamma_{2m'_1, 2m_1}^{-1})$ coincides with the factor of $Q_{m_1+m'_1}$ relative to $J_{m'_1}$ in the decomposition $Q_{m_1+m'_1} = (Q_{m_1} \diamond \text{id}_{m'_1}) \circ Q'_{m'_1}$, while $\bar{Q}'_{m'_0} = (\text{id}_{3 \rightarrow 1} \diamond \gamma_{2m'_0, 2m_0}) \circ (\bar{Q}_{m'_0} \diamond \text{id}_{2m_0}) \circ (\text{id}_{3 \rightarrow 1} \diamond \gamma_{2m'_0, 2m_0}^{-1})$ coincides with the factor of $\bar{Q}_{m_0+m'_0}$ relative to $J_{m'_0}$ in the decomposition $\bar{Q}_{m_0+m'_0} = \bar{Q}'_{m'_0} \circ (\bar{Q}_{m_0} \diamond \text{id}_{m'_0})$.

Now, we want to show that, in the presence of the reduction ribbon $\text{id}_{(4\ 3)}$, the subtangles $\zeta'_{\sigma'_1} \circ (Q_{m_1} \diamond \text{id}_{m'_1}) \circ \zeta'_{\sigma'_1}{}^{-1} \circ Q'_{m'_1}$ and $\bar{Q}'_{m'_0} \circ \zeta'_{\sigma'_0}{}^{-1} \circ (\bar{Q}_{m_0} \diamond \text{id}_{m'_0}) \circ \zeta'_{\sigma'_0}$ in Figure 3.6.9 (d), can be respectively replaced by $Q_{m_1+m'_1} \circ Z_{\sigma_1, \sigma'_1}$ and $Z_{\sigma_0, \sigma'_0}^{-1} \circ \bar{Q}_{m_0+m'_0}$, with the tangles Z defined as follows. Given $\sigma = ((i_1\ j_1), \dots, (i_m\ j_m))$ and $\sigma' = ((i'_1\ j'_1), \dots, (i'_{m'}\ j'_{m'}))$ in $\Pi\Gamma_3$, $Z_{\sigma, \sigma'} = z_{m'} \circ \dots \circ z_1$, where z_h is the tangle shown in Figure 3.6.10 if $(i'_h\ j'_h) = (2\ 3)$, while it is the identity otherwise. Observe that the z_h 's, hence $Z_{\sigma, \sigma'}$ as well, are isomorphisms with their inverses obtained by vertical reflection.

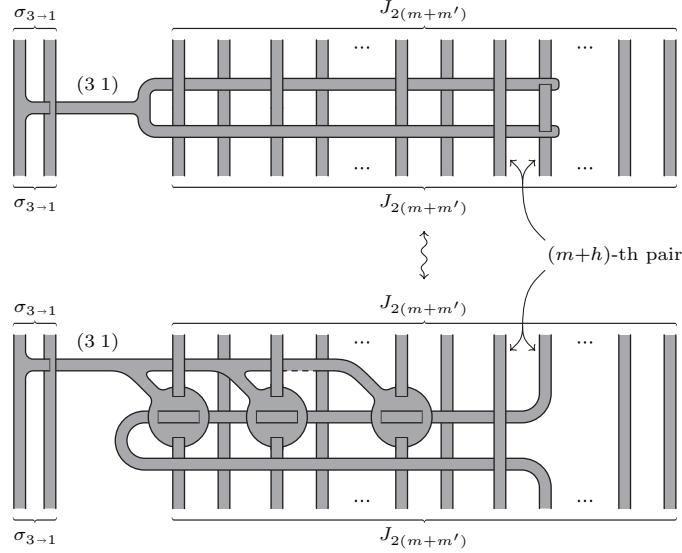


FIGURE 3.6.10. The 3-labeled ribbon surface tangle z_h for $(i'_h\ j'_h) = (2\ 3)$

The proof that $\zeta'_{\sigma'_1} \circ (Q_{m_1} \diamond \text{id}_{m'_1}) \circ \zeta'_{\sigma'_1}{}^{-1} \circ Q'_{m'_1}$ can be replaced by $Q_{m_1+m'_1} \circ Z_{\sigma_1, \sigma'_1}$ goes by induction on the length m'_1 of σ'_1 , starting with the trivial case of $m'_1 = 0$.

The inductive step for $m'_1 \geq 1$ presents some difficulties only when $(i'_{m'_1}\ j'_{m'_1}) = (2\ 3)$. Indeed, if $(i'_{m'_1}\ j'_{m'_1}) = (1\ 2)$, both $\zeta_{\sigma_1 \diamond \sigma'_1, m_1+m'_1}$ and $\zeta_{\sigma_1 \diamond \sigma'_1, m_1+m'_1}^{-1}$ are identities, so there is nothing to prove. While if $(i'_{m'_1}\ j'_{m'_1}) = (1\ 3)$, after a suitable replacement of the bands attached to $\text{id}_{(3\ 2)}$, $\zeta_{\sigma_1 \diamond \sigma'_1, m_1+m'_1}$ and $\zeta_{\sigma_1 \diamond \sigma'_1, m_1+m'_1}^{-1}$ can be moved to be contiguous and then canceled.

The case of $(i'_{m'_1}\ j'_{m'_1}) = (2\ 3)$ is treated in Figure 3.6.11. Here, diagram (a) is obtained by applying the induction hypothesis to the first $m'_1 - 1$ blocks of $Q'_{m'_1}$. In the same diagram, the horizontal bands labeled (3 1) represent $\zeta_{\sigma_1 \diamond \sigma'_1, m_1+m'_1}$ and $\zeta_{\sigma_1 \diamond \sigma'_1, m_1+m'_1}^{-1}$, and all the bands that should be connecting the left side of the box to the reduction ribbon $\text{id}_{(3\ 2)}$ are fused together. To get (b), we first replace the bands

connecting the vertical disks to $\text{id}_{(3\ 2)}$ with new ones, whose attaching arcs in $\text{id}_{(3\ 2)}$ lie over that of $\zeta_{\sigma_1 \diamond \sigma'_1, m_1+m'_1}$, on the top of the diagram. Similarly, we replace the bands coming out from the left side of the box, moving their attaching arcs in $\text{id}_{(3\ 2)}$ under that of $\zeta_{\sigma_1 \diamond \sigma'_1, m_1+m'_1}^{-1}$, on the bottom of the diagram. All those replacements can be done thanks to Remark 3.5.2. The new bands (not drawn in the diagram) can be suitably chosen, in such a way that they allow the slidings we are going to perform in order to get (c). Moreover, we expand a tongue from $\text{id}_{(4\ 3)}$ and move it by 1-isotopy and move (R4) until it reaches the final position in diagram (b). As a consequence, the horizontal bands forming $\zeta_{\sigma_1 \diamond \sigma'_1, m_1+m'_1}$ and $\zeta_{\sigma_1 \diamond \sigma'_1, m_1+m'_1}^{-1}$ acquire labels (4 1). Then, we slide down those bands and the box as suggested by the arrows, up to their new position in (c). In doing that, we use move (R4) to let the

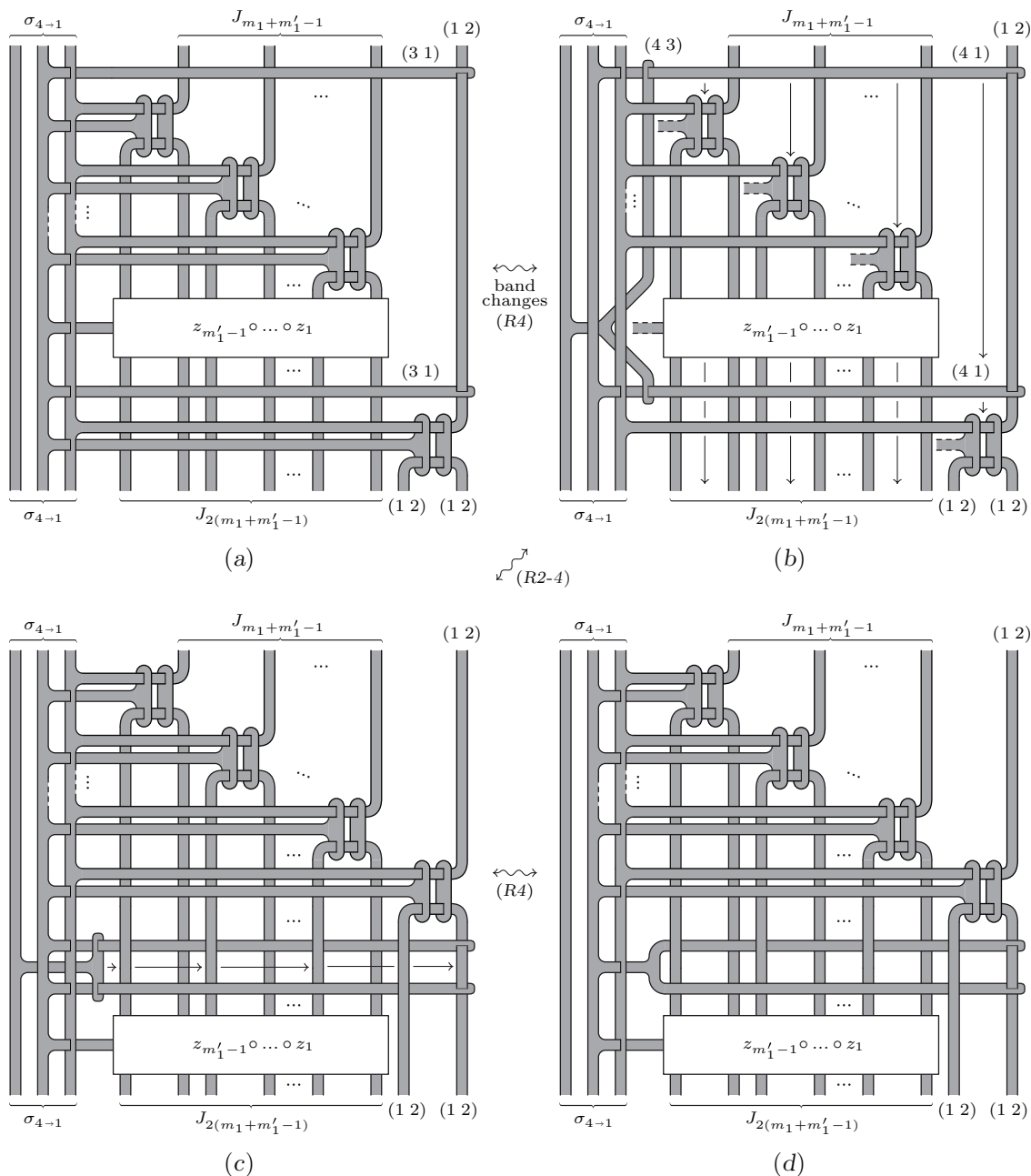


FIGURE 3.6.11.

topmost band pass through the two short bands labeled (2 3) in the middle of each of the first $m_1 + m'_1 - 1$ pairs of vertical disks. While for the $(m_1 + m'_1)$ -th pair, we use move (R2) to let the rightmost vertical disk pass through both the ζ 's. To pass from (c) to (d), we disentangle the vertical disk attached to $\text{id}_{(4\ 3)}$ by moving it to the right, as indicated by the arrow, and use once again move (R4) to let it pass through the vertical bands, and finally we retract the resulting tongue to $\text{id}_{(4\ 3)}$.

This completes the proof that $\zeta'_{\sigma'_1} \circ (Q_{m_1} \diamond \text{id}_{m'_1}) \circ \zeta'^{-1}_{\sigma'_1} \circ Q'_{m'_1}$ can be replaced with $Q_{m_1+m'_1} \circ Z_{\sigma_1, \sigma'_1}$. The replacement of $\bar{Q}'_{m'_0} \circ \zeta'^{-1}_{\sigma'_0} \circ (\bar{Q}_{m_0} \diamond \text{id}_{m'_0}) \circ \zeta'_{\sigma'_0}$ by $Z^{-1}_{\sigma_0, \sigma'_0} \circ \bar{Q}_{m_0+m'_0}$ is symmetric and it is left to the reader.

Once both those replacements have been performed, we are left with $Z_{\sigma_1, \sigma'_1} \circ (\text{id}_{\sigma_{3 \rightarrow 1}} \diamond_{\beta, \gamma, \delta} T_{K \diamond K'}) \circ Z^{-1}_{\sigma_0, \sigma'_0}$, which is equal to $\check{S}_{K''}$ for $K'' = B_{\sigma_1, \sigma'_1} \circ (K \diamond K') \circ B^{-1}_{\sigma_0, \sigma'_0}$ and a suitable choice of the vertically trivial state involved in the construction. \square

Before going on to our main theorem, we want to see the effect of Proposition 3.6.2 on the definition of the functor Ξ_4 itself. In the previous section we defined it by putting $\Xi_4(K) = \uparrow^4_3 \check{S}_K$ for any Kirby tangle $K \in \mathcal{K}_1$, where the check means that the trivial state in point 3 of the construction of the ribbon surface tangle S_K (see Section 3.4) has been actually required to be vertically trivial. As a consequence of Proposition 3.6.2, we can now relax such extra requirement and remove the check from the definition of Ξ_4 . This is the content of the next proposition.

PROPOSITION 3.6.3. *Given a Kirby tangle $K \in \mathcal{K}_1$, the equivalence class of the labeled ribbon surface tangle $\uparrow^4_3 S_K$ does not depend of the choices involved in the construction of S_K . In particular, it does not depend on the choice of the trivial state occurring in point 3 of that construction. Then, we can write $\Xi_4(K) = \uparrow^4_3 S_K$ without requiring any more the vertically triviality of such state.*

Proof. Let K and S_K be as in the statement. Since the equivalence class of $\uparrow^4_3 S_K$ is a morphism between two objects in the image of Ξ_4 , Proposition 3.6.2 tells us that it can be written in the form $\Xi_4(K') = \uparrow^4_3 \check{S}_{K'}$ for some Kirby tangle $K' \in \mathcal{K}_1$. Then, Propositions 2.3.9, 3.3.2, 3.3.4 and 3.4.3, give us the chain of equalities $K = \Theta_3(S_K) = \downarrow^4_1 \Theta_4(\uparrow^4_3 S_K) = \downarrow^4_1 \Theta_4(\uparrow^4_3 \check{S}_{K'}) = \Theta_3(\check{S}_{K'}) = K'$ holding in \mathcal{K}_1 . Moreover, from $K = K'$ in \mathcal{K}_1 we get $\uparrow^4_3 \check{S}_K = \uparrow^4_3 \check{S}_{K'}$ in $\uparrow^4_1 \mathcal{S}_{3 \rightarrow 1}$, thanks to Proposition 3.5.4. Thus, the starting ribbon surface tangle S_K turns out to be equivalent to \check{S}_K . At this point, Lemmas 3.5.1 and 3.5.3 allow us to conclude the proof. \square

Finally, let us state and prove the main equivalence theorem.

THEOREM 3.6.4. *For any $n \geq 4$, the functor $\Xi_n : \mathcal{K}_1 \rightarrow \mathcal{S}_n^c$ and the braided monoidal functor $\Theta_n : \mathcal{S}_n^c \rightarrow \mathcal{K}_n^c$ (cf. Proposition 3.3.2) are category equivalences. Moreover, $\downarrow^n_1 \circ \Theta_n \circ \Xi_n = \text{id}_{\mathcal{K}_1}$, while $\Xi_n \circ \downarrow^n_1 \circ \Theta_n$ is naturally equivalent to $\text{id}_{\mathcal{S}_n^c}$.*

Proof. According to Proposition 3.5.5, $\downarrow^n_1 \circ \Theta_4 \circ \Xi_4 = \text{id}_{\mathcal{K}_1}$, hence $\Xi_4 : \mathcal{K}_1 \rightarrow \mathcal{S}_n^c$ is a faithful functor. Moreover, Proposition 3.6.2 implies that Ξ_4 is full and that any object in \mathcal{S}_n^c is isomorphic to one in its image. Then, Ξ_4 is a category equivalence by Proposition 1.5.3. Since \uparrow^4_1 is also a category equivalence by Proposition 2.3.9, we have that $\Xi_n = \uparrow^4_1 \circ \Xi_4 : \mathcal{K}_1 \rightarrow \mathcal{S}_n^c$ is such for any $n \geq 4$. Since $\downarrow^4_1 \circ \Theta_n \circ \Xi_n = \text{id}_{\mathcal{K}_1}$ by Proposition 3.5.5, $\Theta_n : \mathcal{S}_n^c \rightarrow \mathcal{K}_n^c$ is a category equivalence as well. \square

4. Universal groupoid ribbon Hopf algebra

This chapter is dedicated to the construction and the study of the algebraic categories \mathcal{H}_n^r and of the functors $\Phi_n : \mathcal{H}_n^r \rightarrow \mathcal{K}_n$. For any $n \geq 1$, we will define a suitable subcategory $\mathcal{H}_n^{r,c} \subset \mathcal{H}_n^r$ together with an equivalence reduction functor $\downarrow_1^n : \mathcal{H}_n^{r,c} \rightarrow \mathcal{H}_1^r$, and show that the restriction $\Phi_n : \mathcal{H}_n^{r,c} \rightarrow \mathcal{K}_n^c$ is a category equivalence. In particular, the algebra $\mathcal{H}^r = \mathcal{H}_1^r$ will give an algebraic characterization of the category $\mathcal{C}hb^{3+1} = \mathcal{C}hb_1^{3+1}$ of 4-dimensional relative 2-handlebody cobordisms, in the sense of Kerler ([35]).

The proof is based on the factorization of the category equivalence $\Theta_n : \mathcal{S}_n^c \rightarrow \mathcal{K}_n^c$ defined in Section 3.3, as a composition $\Phi_n \circ \Psi_n$, where for $n \geq 4$ the functor $\Psi_n : \mathcal{S}_n^c \rightarrow \mathcal{H}_n^{r,c}$ is shown to be full. This implies that both Ψ_n and Φ_n are category equivalences. In particular, Ψ_n gives an algebraic interpretation of the simple branched covering representation of 4-dimensional relative 2-handlebody cobordisms.

\mathcal{H}_n^r will be defined as the strict monoidal braided category freely generated by a groupoid Hopf algebra for the groupoid $\mathcal{G}_n = \{1, \dots, n\}^2$, thought with its natural composition given by $(i, j)(j, k) = (i, k)$ for any $1 \leq i, j, k \leq n$.

Before going on, let us see how this groupoid structure of \mathcal{G}_n fits into the picture. As it has been established in [35, 24], $I_{(1,1)} \in \text{Obj } \mathcal{K}_1$ is a braided Hopf algebra object with the comultiplication morphism $\Delta_{(1,1)}$ described in Section 2.3. Actually, by Proposition 2.3.3, $\Delta_{(i,j)} : I_{(i,j)} \rightarrow I_{(i,j)} \diamond I_{(i,j)}$ makes any $I_{(i,j)} \in \text{Obj } \mathcal{K}_n$ into a coalgebra object. From the topological point of view, $\Delta_{(i,j)}$ represents a single 1-handle along which run the attaching maps of three 2-handles. The dual notion of multiplication morphism (see below) corresponds to a 2-handle which runs along exactly three 1-handles. Now, while in \mathcal{K}_1 one can always attach such a 2-handle along any given three 1-handles (since they are all attached on the same 0-handle), the same is not true in \mathcal{K}_n . Here, to be able to close the loop of the attaching sphere, the indices of the 1-handles need to be in the order (i, j) , (j, k) and (i, k) . Then, the algebraic structure of \mathcal{K}_n involves multiplication morphisms $m_{(i,j),(i',j')} : I_{(i,j)} \diamond I_{(i',j')} \rightarrow I_{(i'',j'')}$ defined only for $i' = j$, $i'' = i$ and $j'' = j'$, in other words when (i, j) and (i', j') are composable and $(i, j)(i', j') = (i'', j'')$ in the groupoid \mathcal{G}_n . Moreover, the morphisms $\eta_i : \emptyset \rightarrow I_{(i,i)}$, each given by a 2-handle that cancels against the 1-handle represented by $I_{(i,i)}$, act as units for the multiplication. Therefore, in \mathcal{H}_n^r we will have a family of objects labeled by \mathcal{G}_n and a family of multiplication and unit morphisms between them, which reflects the groupoid structure of \mathcal{G}_n .

Actually, \mathcal{H}_n^r will be introduced as a specialization of the more general notion of universal groupoid ribbon Hopf algebra $\mathcal{H}^r(\mathcal{G})$, with \mathcal{G} being an arbitrary finite groupoid. Disregarding the ribbon structure, the notion of groupoid braided Hopf algebra $\mathcal{H}(\mathcal{G})$ extends the one of group braided Hopf algebra, used in [73, 72] to define TQFT invariants of regular (unbranched) coverings of three manifolds, just because any group can be considered as a groupoid with a single object. The study the algebras $\mathcal{H}(\mathcal{G})$ and $\mathcal{H}^r(\mathcal{G})$ for an arbitrary groupoid \mathcal{G} does not bring to any additional technical difficulties with respect to the one of \mathcal{H}_n^r , allowing on the contrary somewhat simpler notations.

The total list of axioms of a groupoid ribbon Hopf algebra is quite long (11 elementary morphisms and 34 relations between them). Moreover, these axioms have

many important consequences, to which we will refer as properties of the algebra. Of course, a given property usually depends only on a small subset of axioms. So, in order to make more clear the logical structure of such implications, we decided to introduce the axioms in four steps. We start by presenting the axioms of a braided Hopf algebra and showing that the corresponding universal category $\mathcal{H}(\mathcal{G})$ carries an autonomous structure. Then, we require the unimodularity condition, which leads to a tortile category $\mathcal{H}^u(\mathcal{G})$. Here, we require the existence of ribbon morphisms satisfying Kerler's axioms in [35] with the exception of the self-duality condition (we remind that we are looking for an algebra which describes 4-dimensional 2-handlebodies; self-duality will be considered later in Chapter 5, where we study the category of framed 3-dimensional cobordisms). The universal unimodular Hopf algebra with such ribbon morphisms will be called a pre-ribbon Hopf algebra and will be denoted by $\mathcal{H}_v^u(\mathcal{G})$. Finally, the universal ribbon Hopf algebra $\mathcal{H}^r(\mathcal{G})$ is obtained by adding two new axioms which relate the ribbon morphism with the coalgebraic and braided structures.

The diagrammatic language, developed and used in the literature (see for example [24, 35]), will be our main tool in representing the morphisms in the algebraic categories and in the study of the functors between the geometric and the algebraic categories. The next sections contain widespread references to the axioms and properties of the universal ribbon Hopf algebra. In order to simplify the search of such references, we assign a compact name (a letter and a number) to each axiom and property and collect all the corresponding diagrams in few tables.

4.1. The universal groupoid Hopf algebras $\mathcal{H}(\mathcal{G})$ and $\mathcal{H}^u(\mathcal{G})$

Let \mathcal{G} be a groupoid, that is a small category whose morphisms are all invertible. We will denote by \mathcal{G} also the set of the morphisms of \mathcal{G} , endowed with the partial binary operation given by the composition, for which we adopt the multiplicative notation from left to right. The identity of $i \in \text{Obj } \mathcal{G}$ will be denoted by $1_i \in \mathcal{G}$, while the inverse of $g \in \mathcal{G}$ will be denoted by $\bar{g} \in \mathcal{G}$. For $i, j \in \text{Obj } \mathcal{G}$, we denote by $\mathcal{G}(i, j) \subset \mathcal{G}$ the subset of morphisms from i to j . Consequently, if $g \in \mathcal{G}(i, j)$ and $h \in \mathcal{G}(j, k)$ then $gh \in \mathcal{G}(i, k)$. In particular, $g\bar{g} = 1_i$ and $\bar{g}g = 1_j$, and sometimes the identity morphisms will be represented in this way.

A groupoid is called *connected* if $\mathcal{G}(i, j)$ is non-empty for any $i, j \in \text{Obj } \mathcal{G}$. Given two groupoids $\mathcal{G} \subset \mathcal{G}'$, we say that \mathcal{G} is *full* in \mathcal{G}' if \mathcal{G} is a full subcategory of \mathcal{G}' , i.e. $\mathcal{G}(i, j) = \mathcal{G}'(i, j)$ for all $i, j \in \text{Obj } \mathcal{G}$. Moreover, given $k \in \text{Obj } \mathcal{G}$, we denote by $\mathcal{G}^{\setminus k}$ the full subgroupoid of \mathcal{G} with $\text{Obj } \mathcal{G}^{\setminus k} = \text{Obj } \mathcal{G} - \{k\}$

Now, we start with the definition of the notion of Hopf \mathcal{G} -algebra in a braided monoidal category \mathcal{C} . This involves a family $H = \{H_g\}_{g \in \mathcal{G}}$ of objects of \mathcal{C} and certain families of morphisms indexed by (possibly pairs of) such objects.

Here and in the sequel, we will write g instead of H_g in the subscripts of the notation for morphisms of \mathcal{C} . For example, we will use the notations $\text{id}_g = \text{id}_{H_g}$ and $\gamma_{g,h} = \gamma_{H_g, H_h}$. Moreover, based on the MacLane's coherence result for monoidal categories (p. 161 in [45]), we will omit the associativity morphisms since they can be filled in a unique way.

DEFINITION 4.1.1. Given a groupoid \mathcal{G} and a braided monoidal category \mathcal{C} , a Hopf \mathcal{G} -algebra in \mathcal{C} is a family of objects $H = \{H_g\}_{g \in \mathcal{G}}$ in \mathcal{C} , equipped with the families of morphisms in \mathcal{C} described below.

A comultiplication $\Delta = \{\Delta_g : H_g \rightarrow H_g \diamond H_g\}_{g \in \mathcal{G}}$, such that for any $g \in \mathcal{G}$:

$$(\Delta_g \diamond \text{id}_g) \circ \Delta_g = (\text{id}_g \diamond \Delta_g) \circ \Delta_g; \quad (\text{a1})$$

a counit $\varepsilon = \{\varepsilon_g : H_g \rightarrow \mathbf{1}\}_{g \in \mathcal{G}}$, such that for any $g \in \mathcal{G}$:

$$(\varepsilon_g \diamond \text{id}_g) \circ \Delta_g = \text{id}_g = (\text{id}_g \diamond \varepsilon_g) \circ \Delta_g; \quad (\text{a2-2}')$$

a multiplication $m = \{m_{g,h} : H_g \diamond H_h \rightarrow H_{gh}\}_{g,h,gh \in \mathcal{G}}$ (notice that $m_{g,h}$ is defined only when g and h are composable in \mathcal{G}), such that for any $f, g, h, fgh \in \mathcal{G}$:

$$m_{f,g,h} \circ (m_{f,g} \diamond \text{id}_h) = m_{f,gh} \circ (\text{id}_f \diamond m_{g,h}), \quad (\text{a3})$$

$$(m_{g,h} \diamond m_{g,h}) \circ (\text{id}_g \diamond \gamma_{g,h} \diamond \text{id}_h) \circ (\Delta_g \diamond \Delta_h) = \Delta_{gh} \circ m_{g,h}, \quad (\text{a5})$$

$$\varepsilon_{gh} \circ m_{g,h} = \varepsilon_g \diamond \varepsilon_h; \quad (\text{a6})$$

a unit $\eta = \{\eta_i : \mathbf{1} \rightarrow H_{1_i}\}_{i \in \text{Obj } \mathcal{G}}$, such that for any $g \in \mathcal{G}(i, j)$:

$$m_{g,1_j} \circ (\text{id}_g \diamond \eta_j) = \text{id}_g = m_{1_i,g} \circ (\eta_i \diamond \text{id}_g), \quad (\text{a4-4}')$$

$$\Delta_{1_i} \circ \eta_i = \eta_i \diamond \eta_i, \quad (\text{a7})$$

$$\varepsilon_{1_i} \circ \eta_i = \text{id}_{\mathbf{1}}; \quad (\text{a8})$$

an antipode $S = \{S_g : H_g \rightarrow H_{\bar{g}}\}_{g \in \mathcal{G}}$ and its inverse $\bar{S} = \{\bar{S}_g : H_g \rightarrow H_{\bar{g}}\}_{g \in \mathcal{G}}$, such that for any $g \in \mathcal{G}(i, j)$:

$$m_{\bar{g},g} \circ (S_g \diamond \text{id}_{\bar{g}}) \circ \Delta_g = \eta_{1_j} \circ \varepsilon_g, \quad (\text{s1})$$

$$m_{g,\bar{g}} \circ (\text{id}_g \diamond S_{\bar{g}}) \circ \Delta_g = \eta_{1_i} \circ \varepsilon_g, \quad (\text{s1}')$$

$$S_{\bar{g}} \circ \bar{S}_g = \bar{S}_{\bar{g}} \circ S_g = \text{id}_g. \quad (\text{s2-2}')$$

We observe that an ordinary braided Hopf algebra in \mathcal{C} is a Hopf \mathcal{G}_1 -algebra, where \mathcal{G}_1 is the trivial groupoid with a single object and a single morphism. In particular, H_{1_i} is a braided Hopf algebra in \mathcal{C} for any $i \in \text{Obj } \mathcal{G}$.

DEFINITION 4.1.2. Let \mathcal{C} be a braided monoidal category and $H = \{H_g\}_{g \in \mathcal{G}}$ be a Hopf \mathcal{G} -algebra in \mathcal{C} . By a categorical left (resp. right) cointegral of H we mean a family $l = \{l_i : H_{1_i} \rightarrow \mathbf{1}\}_{i \in \text{Obj } \mathcal{G}}$ of morphisms in \mathcal{C} , such that for any $i \in \text{Obj } \mathcal{G}$

$$(\text{id}_{1_i} \diamond l_i) \circ \Delta_{1_i} = \eta_i \circ l_i : H_{1_i} \rightarrow H_{1_i} \quad (\text{i1-1}')$$

$$(\text{resp. } (l_i \diamond \text{id}_{1_i}) \circ \Delta_{1_i} = \eta_i \circ l_i : H_{1_i} \rightarrow H_{1_i}).$$

On the other hand, by categorical right (resp. left) integral of H we mean a family $L = \{L_g : \mathbf{1} \rightarrow H_g\}_{g \in \mathcal{G}}$ of morphisms in \mathcal{C} , such that if $g, h, gh \in \mathcal{G}$ then

$$m_{g,h} \circ (L_g \diamond \text{id}_h) = L_{gh} \circ \varepsilon_h : H_h \rightarrow H_{gh} \quad (\text{i2-2}')$$

$$(\text{resp. } m_{g,h} \circ (\text{id}_g \diamond L_h) = L_{gh} \circ \varepsilon_h : H_g \rightarrow H_{gh}).$$

If l (resp. L) is both right and left categorical cointegral (integral) of H , we call it simply a cointegral (integral) of H .





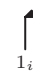





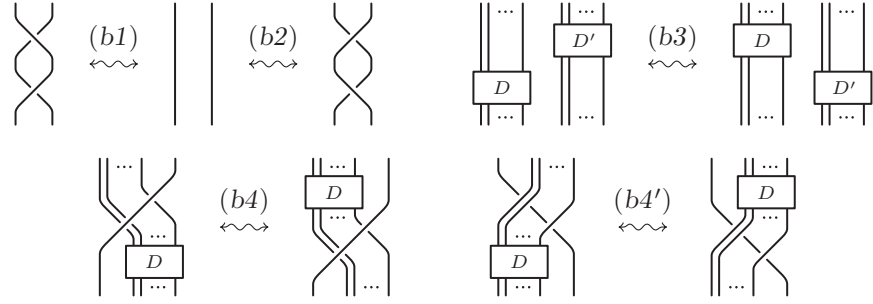
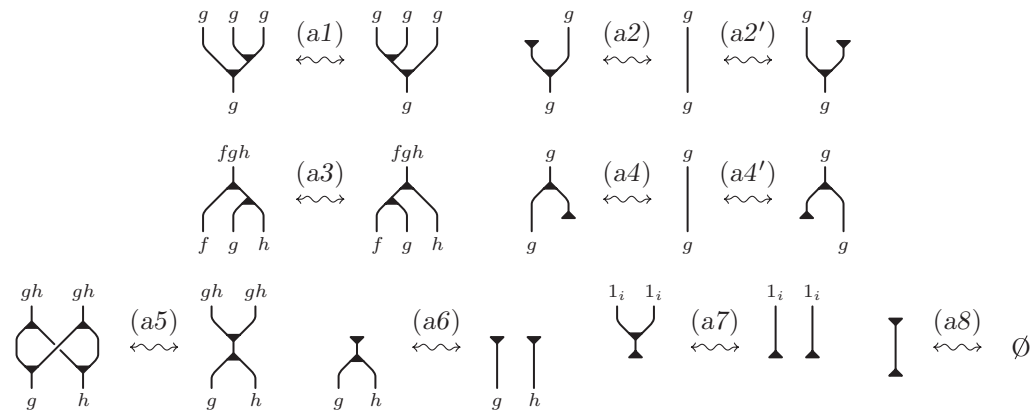
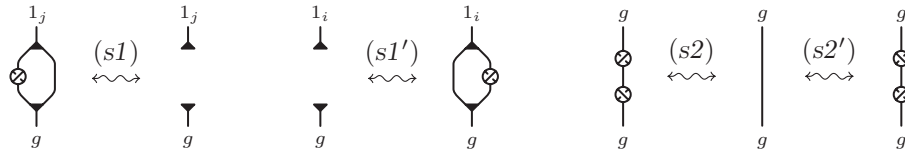
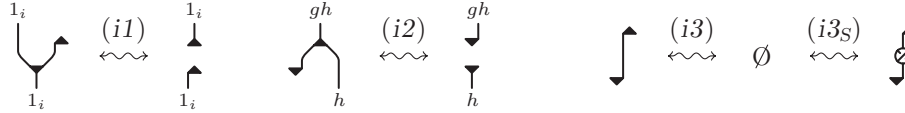
Axioms of the universal braided Hopf algebra $\mathcal{H}(\mathcal{G})$					
$\gamma_{g,h} = $ 	$\Delta_g = $ 	$\varepsilon_g = $ 	$S_g = $ 	$l_i = $ 	
$\bar{\gamma}_{g,h} = $ 	$m_{g,h} = $ 	$\eta_i = $ 	$\bar{S}_g = $ 	$L_g = $ 	
<i>Elementary diagrams</i>					
					
<i>Braid axioms</i>					
					
<i>Bialgebra axioms</i>					
					
<i>Antipode axioms</i>					
					
<i>Integral axioms</i>					

TABLE 4.1.1.

DEFINITION 4.1.3. Given a groupoid \mathcal{G} , the *universal Hopf \mathcal{G} -algebra* $\mathcal{H}(\mathcal{G})$ is the strict braided monoidal category freely generated by a Hopf \mathcal{G} -algebra $H = \{H_g\}_{g \in \mathcal{G}}$ with a left cointegral l and a right integral L , modulo the following additional relations for any $i \in \text{Obj } \mathcal{G}$

$$l_i \circ L_{1_i} = \text{id}_{\mathbf{1}} = l_i \circ S_{1_i} \circ L_{1_i}. \quad (i3-3_S)$$

According to Definition 1.5.10, $\text{Obj } \mathcal{H}(\mathcal{G})$ is the free monoid $\Pi H = \cup_{m=0}^{\infty} H^m$ generated by $H = \{H_g\}_{g \in \mathcal{G}}$ and consisting of all (possibly empty) finite sequences (that is products) of elementary objects. We will use the notation

$$H_\pi = H_{g_1} \diamond \dots \diamond H_{g_m}$$

for the sequence corresponding to $\pi = (g_1, \dots, g_m) \in \Pi \mathcal{G}$, in such a way that H_\emptyset is the unit object and $H_\pi \diamond H_{\pi'} = H_{\pi \circ \pi'}$ for any $\pi, \pi' \in \Pi \mathcal{G}$.

Extending the notational convention made above, we will write π instead of H_π in the subscripts of the notation for morphisms of $\mathcal{H}(\mathcal{G})$. For example, we will use the notations $\text{id}_\pi = \text{id}_{H_\pi}$, $\gamma_{\pi, \pi'} = \gamma_{H_\pi, H_{\pi'}}$, $\bar{\gamma}_{\pi, \pi'} = \bar{\gamma}_{H_\pi, H_{\pi'}}$ for any $\pi, \pi' \in \Pi \mathcal{G}$.

On the other hand, $\text{Mor } \mathcal{H}(\mathcal{G})$ consists of all the compositions of products of identities and one of the elementary morphisms $\gamma_{g,h}, \bar{\gamma}_{g,h}, \Delta_g, \varepsilon_g, m_{g,h}, \eta_i, S_g, \bar{S}_g, L_g, l_i$ as in Definition 4.1.1, modulo the defining axioms for a braided structure and for a Hopf \mathcal{G} -algebra with integrals listed in Definitions 4.1.1 and 4.1.2 (cf. Table 4.1.1).

Moreover, $\mathcal{H}(\mathcal{G})$ satisfies the following universal property: if \mathcal{C} is any braided monoidal category with a Hopf \mathcal{G} -algebra $H' = \{H'_g\}_{g \in \mathcal{G}}$ in it, and H' has a left cointegral and a right integral related by conditions (i3-3_S), then there exists a braided monoidal functor $\mathcal{H}(\mathcal{G}) \rightarrow \mathcal{C}$ sending H_g to H'_g .

Analogously to [35], $\mathcal{H}(\mathcal{G})$ can be described as a category of planar diagrams in $[0, 1] \times [0, 1]$. The objects of $\mathcal{H}(\mathcal{G})$ are sequences of points in $[0, 1]$ labeled by elements in \mathcal{G} , and the morphisms are iterated products and compositions of the elementary diagrams presented in Table 4.1.1, modulo the relations presented in the same figure and plane isotopies which preserve the y -coordinate. We remind that the composition of diagrams $D_2 \circ D_1$ is obtained by stacking D_2 on the top of D_1 and then rescaling, while the product $D_1 \diamond D_2$ is given by the horizontal juxtaposition of D_1 and D_2 and rescaling.

The plane diagrams and the relations between them are going to be our main tool. Observe that the diagrams we use consist in projections of embedded graphs in R^3 with uni-, bi- and tri-valent vertices. The vertices correspond to the defining morphisms in the algebra, and we will call them with the name of the corresponding morphism. For example the bi-valent vertices (which have one incoming and one outgoing edge) will be called antipode vertices. Except the antipode ones, the rest of the vertices are represented by triangles that point up (positively polarized) or point down (negatively polarized). The uni-valent vertices are divided in unit vertices (corresponding to η and ε) and integral vertices (corresponding to l and Λ), while the positively (resp. negatively) polarized tri-valent vertices will be called multiplication (resp. comultiplication) vertices. Observe that the choice of polarization of the vertices is not arbitrary. Indeed, as we will see in Section 4.3, in the category of generalized Kirby tangles \mathcal{K}_n the univalent vertices with same polarization correspond to morphisms with the same handle structure (upside down).

Most of our proofs consist in showing that some morphisms in the universal algebra are equivalent, meaning that the graph diagram of one of them can be obtained from the graph diagram of the other by applying a sequence of the defining relations (moves) of the algebra axioms. We will outline the main steps in this procedure by drawing in sequence some intermediate diagrams, and for each step we will indicate in the corresponding order, the main moves needed to transform the diagram on the left into the one on the right. Actually, some steps can be understood more easily by starting from the diagram on the right and reading the moves in the reverse order. Notice, that the moves represent equivalences of diagrams and we use the same notation for them and their inverses. In the captions of the figures the reader will find (in square brackets) the reference to the pages where those moves are defined. As an example, the reader can see the proof of Proposition 4.1.4, where we have added some additional comments in order to make clearer the interpretation of the figures.

We now proceed with the study of the properties of the category $\mathcal{H}(\mathcal{G})$ listed in Table 4.1.2. Such properties are divided in two sets. The first one generalizes to the case of a groupoid Hopf algebra the well-known properties of the antipode (see [35] and [73] for the case of braided and group Hopf algebras).

PROPOSITION 4.1.4. *The following properties of the antipode in $\mathcal{H}(\mathcal{G})$, hold for any $g, h \in \mathcal{G}$ such that gh is defined, and for any $i \in \mathcal{G}$:*

Properties of the universal braided Hopf algebra $\mathcal{H}(\mathcal{G})$							
<i>Properties of the antipode</i>							
$\Lambda_g =$		$\lambda_g =$					
<i>Existence and properties of coform and form</i>							

TABLE 4.1.2.

$$\Delta_{\bar{g}} \circ S_g = (S_g \diamond S_g) \circ \gamma_{g,g} \circ \Delta_g : H_g \rightarrow H_{\bar{g}} \diamond H_{\bar{g}}, \quad (s3)$$

$$S_{gh} \circ m_{g,h} = m_{\bar{h},\bar{g}} \circ (S_h \diamond S_g) \circ \gamma_{g,h} : H_g \diamond H_h \rightarrow H_{\bar{h}\bar{g}}, \quad (s4)$$

$$\varepsilon_{\bar{g}} \circ S_g = \varepsilon_g, \quad (s5)$$

$$S_{1_i} \circ \eta_i = \eta_i. \quad (s6)$$

Moreover, if $l = \{l_j : H_{1_j} \rightarrow \mathbf{1}\}_{j \in \text{Obj } \mathcal{G}}$ and $L = \{L_g : \mathbf{1} \rightarrow H_g\}_{g \in \mathcal{G}}$ are respectively a left cointegral and a right integral of H , then:

$$l \circ S = \{l_j \circ S_{1_j} : H_{1_j} \rightarrow \mathbf{1}\}_{j \in \text{Obj } \mathcal{G}} \text{ is a right cointegral of } H, \quad (i1')$$

$$S \circ L = \{S_g \circ L_g : \mathbf{1} \rightarrow H_{\bar{g}}\}_{g \in \mathcal{G}} \text{ is a left integral of } H. \quad (i2')$$

Proof. (s3) is proved in Figure 4.1.3. In the first step we obtain the diagram on the left from the one on the right by applying in the order moves (a1-3), move (s1) and (a2-4'). To be precise, before applying (s1) and (a4'), we also use the braid axioms presented in Table 4.1.1, but this in general will not be indicated.

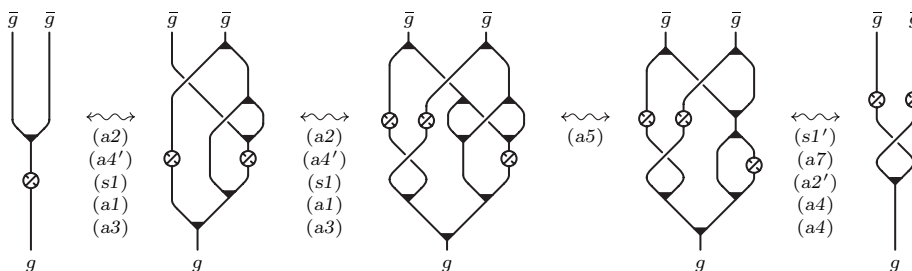


FIGURE 4.1.3. Proof of (s3) [a-s/123]

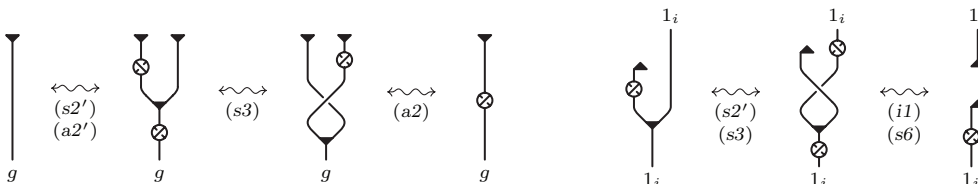


FIGURE 4.1.4. Proof of (s5) and (i1') [a-i/123, s/123-125]

Property (s5) is proved in the left side of Figure 4.1.4. Then (s4) and (s6) are obtained by rotating the diagrams in Figures 4.1.3 and 4.1.4 upside down. Eventually, using (s3) and (s6) one obtains (i1') as shown in the right side of Figure 4.1.4 and (i2') by rotating that figure. \square

The second set of properties in Table 4.1.2 states the existence of an autonomous structure on $\mathcal{H}(\mathcal{G})$ and describes the relation between such structure and the algebraic one. The proposition below proves properties (f1), (f2) and (f3-3'), extending the result in Lemma 7 of [35] to possibly non-unimodular categories.

Note that in the diagrams representing the morphisms of $\mathcal{H}(\mathcal{G})$, it is appropriate to use for the coform and the form the notations (f1) and (f2), presented in Table 4.1.2. In fact, the relations (f3-3') reduce to the standard “pulling the string”, which together with the braid axioms in Table 4.1.1 realize regular isotopy of strings.

PROPOSITION 4.1.5. Given a groupoid \mathcal{G} , the universal Hopf \mathcal{G} -algebra $\mathcal{H}(\mathcal{G})$ is an autonomous category, with $H_\pi^* = H_{\pi^*}$ for every $\pi \in \Pi\mathcal{G}$, where π^* is the sequence obtained by reversing the order of σ . In particular $H_g^* = H_g$ for $g \in \mathcal{G}$, while coform and form are defined by

$$\Lambda_{H_g} = \Lambda_g = \Delta_g \circ L_g, \quad (f1)$$

$$\lambda_{H_g} = \lambda_g = l_{g\bar{g}} \circ m_{g,\bar{g}} \circ (\text{id}_g \diamond S_g), \quad (f2)$$

for any $g \in \mathcal{G}$, and by the following recursive formulas for $\pi = \pi' \diamond \pi'' \in \Pi\mathcal{G}$ (note that the definition is well-posed, giving equivalent results for different decompositions $\pi = \pi' \diamond \pi''$)

$$\Lambda_{H_\pi} = \Lambda_\pi = (\text{id}_{(\pi'')^*} \diamond \Lambda_{\pi'} \diamond \text{id}_{\pi''}) \circ \Lambda_{\pi''},$$

$$\lambda_{H_\pi} = \lambda_\pi = \lambda_{\pi'} \circ (\text{id}_{\pi'} \diamond \lambda_{\pi''} \diamond \text{id}_{(\pi')^*}).$$

Hence, properties (f3-3') in Table 4.1.2 hold in $\mathcal{H}(\mathcal{G})$.

Proof. Figure 4.1.5 shows that Λ_g and λ_g satisfy the relations in the Definition 1.5.7, that is the properties (f3-3'). Then, it suffices to observe that such relations propagate to Λ_π and λ_π for any $\pi \in \mathcal{G}$, by a simple induction on the length of π . \square

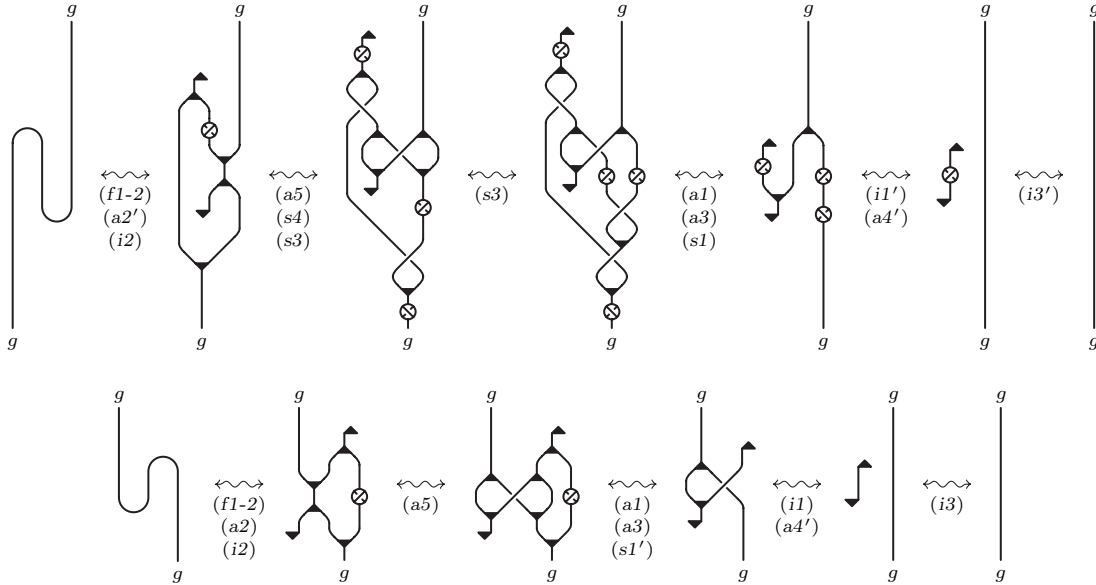


FIGURE 4.1.5. Proof of (f3-3') [a/123, i-s/123-125]

The remaining two properties (f4-4') in Table 4.1.2 can be expressed in terms of the right and left “rotation” maps:

$$\text{rot}_r : \text{Mor}_{\mathcal{H}(\mathcal{G})}(H_{h_0 \diamond \pi_0}, H_{\pi_1 \diamond h_1}) \rightarrow \text{Mor}_{\mathcal{H}(\mathcal{G})}(H_{\pi_0 \diamond h_1}, H_{h_0 \diamond \pi_1}),$$

$$\text{rot}_l : \text{Mor}_{\mathcal{H}(\mathcal{G})}(H_{\pi_0 \diamond h_0}, H_{h_1 \diamond \pi_1}) \rightarrow \text{Mor}_{\mathcal{H}(\mathcal{G})}(H_{h_1 \diamond \pi_0}, H_{\pi_1 \diamond h_0}),$$

defined for any $h_0, h_1 \in \mathcal{G}$ and $\pi_0, \pi_1 \in \Pi\mathcal{G}$ by the identities (see Figure 4.1.6):

$$\text{rot}_r(F) = (\text{id}_{h_0 \diamond \pi_1} \diamond \lambda_{h_1}) \circ (\text{id}_{h_0} \diamond F \diamond \text{id}_{h_1}) \circ (\Lambda_{h_0} \diamond \text{id}_{\pi_0 \diamond h_1}),$$

$$\text{rot}_l(F) = (\lambda_{h_1} \diamond \text{id}_{\pi_1 \diamond h_0}) \circ (\text{id}_{h_1} \diamond F \diamond \text{id}_{h_0}) \circ (\text{id}_{h_1 \diamond \pi_0} \diamond \Lambda_{h_0}).$$

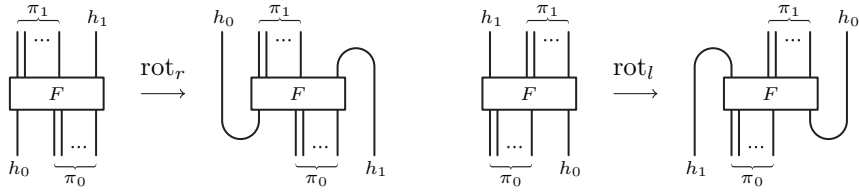


FIGURE 4.1.6. The rotation maps rot_r and rot_l

Proposition 4.1.5 implies that the maps rot_r and rot_l are inverses to each other. Then properties (f4-4') in Table 4.1.2 state that the comultiplication vertices are invariant under such rotation maps. We will see later that the same is not true for the multiplication vertices. The reason for which we study the action of the rotation maps to these types of vertices will become clear in Section 4.6, where the functors Ψ_n will relate them to moves (I5-6) and (R1) in Figures 3.2.1 and 3.1.2 in the category of labeled ribbon surface tangles.

PROPOSITION 4.1.6. In $\mathcal{H}(\mathcal{G})$, for any $g \in \mathcal{G}$ we have

$$\text{rot}_r(\Delta_g) = \text{rot}_l(\Delta_g) = \Delta_g : H_g \rightarrow H_g \diamond H_g, \quad (\text{f4-4}')$$

Proof. (f4) is shown in Figure 4.1.7. (f4') is analogous and left to the reader. \square

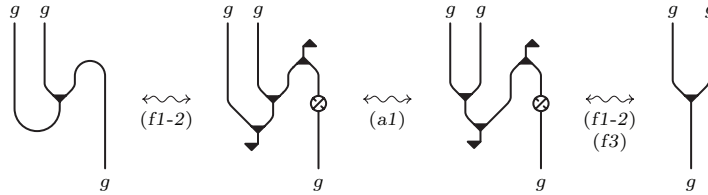


FIGURE 4.1.7. Proof of (f4) [a/123, f/125]

DEFINITION 4.1.7. A Hopf \mathcal{G} -algebra in a braided monoidal category is called *unimodular* if it has S -invariant (2-sided) integral and cointegral, that is:

$$S_g \circ L_g = L_{\bar{g}}, \quad (\text{i4})$$

$$l_{\bar{g}} \circ S_g = l_g. \quad (\text{i5})$$

Then, given a groupoid \mathcal{G} , the *universal unimodular Hopf \mathcal{G} -algebra* $\mathcal{H}^u(\mathcal{G})$ is the quotient of $\mathcal{H}(\mathcal{G})$ modulo the relations (i4) and (i5) above.

The diagrammatic presentation of the relations (i4) and (i5) above can be found in Table 4.1.8. Moreover, as it is indicated there, in $\mathcal{H}^u(\mathcal{G})$ we change the notation for the integral and cointegral vertices by connecting the edge to the middle point of the base of the triangle, to reflect that the corresponding integral is two-sided. In the same Table 4.1.8, we also rewrite the integral axioms (i1-3) (notice that here (i3_S) is redundant) and the properties (i1') and (i2'), as well as the definitions (f1-2) of form and coform, according to the new notation.

Adding the unimodularity condition to the algebra axioms brings to the symmetry of the structure with respect to the rotation around a vertical axis, which inverts the labels in \mathcal{G} and reverse the products of objects and morphisms. In fact, axioms (i4-5) make properties (i1'-2') symmetric to axioms (i1-2), completing the preexisting symmetry of the other axioms. This is the content of next proposition.

Axioms of the universal unimodular braided Hopf algebra $\mathcal{H}^u(\mathcal{G})$ (in addition to the axioms of $\mathcal{H}(\mathcal{G})$)
<p style="text-align: center;">Unimodularity axioms</p>
<p style="text-align: center;">Rewriting the integral axioms</p>
Properties of the universal unimodular braided Hopf algebra $\mathcal{H}^u(\mathcal{G})$
<p style="text-align: center;">Rewriting the properties (i1') and (i2')</p>
<p style="text-align: center;">Rewriting the definition of coform and form</p>
<p style="text-align: center;">Duality of uni-valent vertices with the same polarization</p>
<p style="text-align: center;">Other properties of coform and form</p>

TABLE 4.1.8.

PROPOSITION 4.1.8. *Given a groupoid \mathcal{G} , there is an involutive antimonoidal category equivalence $\text{sym} : \mathcal{H}^u(\mathcal{G}) \rightarrow \mathcal{H}^u(\mathcal{G})$, uniquely determined by the following identities, for any $g, h \in \mathcal{G}$ (composable in the case of $m_{g,h}$), any $H_\pi, H_{\pi'} \in \text{Obj } \mathcal{H}^u(\mathcal{G})$ and any $F, F' \in \text{Mor } \mathcal{H}^u(\mathcal{G})$:*

$$\begin{aligned} \text{sym}(H_g) &= H_{\bar{g}}, \text{sym}(\gamma_{g,h}) = \gamma_{\bar{h},\bar{g}}, \text{sym}(\bar{\gamma}_{g,h}) = \bar{\gamma}_{\bar{h},\bar{g}}, \\ \text{sym}(\Delta_g) &= \Delta_{\bar{g}}, \text{sym}(\varepsilon_g) = \varepsilon_{\bar{g}}, \text{sym}(m_{g,h}) = m_{\bar{h},\bar{g}}, \text{sym}(\eta_i) = \eta_i, \\ \text{sym}(S_g) &= S_{\bar{g}}, \text{sym}(\bar{S}_g) = \bar{S}_{\bar{g}}, \text{sym}(l_i) = l_i, \text{sym}(L_g) = L_{\bar{g}}, \\ \text{sym}(H_\pi \diamond H_{\pi'}) &= \text{sym}(H_{\pi'}) \diamond \text{sym}(H_\pi) \quad \text{and} \quad \text{sym}(F \diamond F') = \text{sym}(F') \diamond \text{sym}(F). \end{aligned}$$

Proof. The universal property of $\mathcal{H}^u(\mathcal{G})$ allows us to define the wanted functor by propagating the identities in the statement over compositions, once we show that this preserves the axioms of $\mathcal{H}^u(\mathcal{G})$. This is indeed the case, being all the axioms invariant or interchanged with their primed versions (possibly up to inversion). That such functor is an involution and hence a category equivalence, follows from its involutive action on the elementary morphisms and products. \square

Some further properties of $\mathcal{H}^u(\mathcal{G})$ are listed in Table 4.1.8. First of all, using the integral axioms (i1) to (i5) and the bialgebra axiom (a8) in Table 4.1.1, it is easy to see that the uni-valent vertices of the same polarization are dual to each other with respect to the form/coform. Moreover, unimodularity leads to the existence of a tortile structure (cf. Definition 1.5.8) with some additional properties, as stated by the next proposition, which is a version of Lemma 8 in [35].

PROPOSITION 4.1.9. *Given a groupoid \mathcal{G} , the universal unimodular Hopf \mathcal{G} -algebra $\mathcal{H}^u(\mathcal{G})$ is a tortile category, with the twist θ_{H_π} defined for any $\pi \in \Pi\mathcal{G}$ by*

$$\theta_{H_\pi} = \theta_\pi = (\lambda_{\pi^*} \diamond \text{id}_\pi) \circ (\text{id}_{\pi^*} \diamond \gamma_{\pi,\pi}) \circ (\Lambda_\pi \diamond \text{id}_\pi).$$

Moreover, the following properties (cf. Table 4.1.8) hold for any $g \in \mathcal{G}$:

$$\theta_g = S_{\bar{g}} \circ S_g = \theta_g^*, \tag{f5-5'}$$

$$(\text{id}_g \diamond S_g) \circ \Lambda_{\bar{g}} = (S_{\bar{g}} \diamond \text{id}_g) \circ \Lambda_g, \tag{f6}$$

$$\lambda_g \circ (\text{id}_g \diamond S_{\bar{g}}) = \lambda_{\bar{g}} \circ (S_g \diamond \text{id}_{\bar{g}}). \tag{f7}$$

Proof. Observe that the definition of θ_π guarantees that $\theta_{\mathbf{1}} = \text{id}_{\mathbf{1}}$ and that the identity $\theta_{\pi \diamond \pi'} = \gamma_{\pi',\pi} \circ (\theta_{\pi'} \diamond \theta_\pi) \circ \gamma_{\pi,\pi'}$ holds, up to isotopy moves, for any $\pi, \pi' \in \Pi\mathcal{G}$. Therefore, in order to see that θ makes $\mathcal{H}^u(\mathcal{G})$ into a tortile category, it is enough to show its naturality and that $\theta_{\pi^*} = \theta_\pi^*$ for any object H_π in $\mathcal{H}^u(\mathcal{G})$.

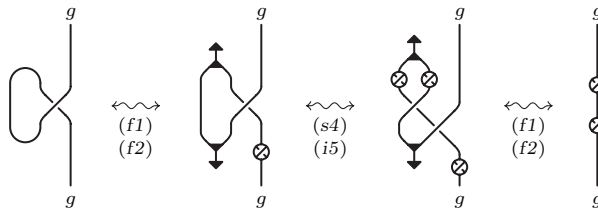


FIGURE 4.1.9. Proof of (f5) [f-i/129, s/125]

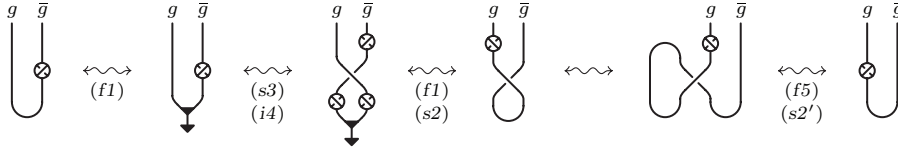


FIGURE 4.1.10. Proof of (f6) [f-i/129, s/123-125]

We will first prove the last identity. Through an induction argument, one can easily see that the general case follows from (f5-5'). Figure 4.1.9 shows that θ_g , represented by the diagram on the left side of (f5), is equivalent to $S_{\bar{g}} \circ S_g$, which proves (f5). Then also θ_g^* , represented up to isotopy moves by the diagram on the right side of (f5'), is equivalent to $S_{\bar{g}} \circ S_g$, being properties (f5) and (f5') symmetric to each other under the category equivalence in Proposition 4.1.8. Moreover, in Figure 4.1.10 we see that (f5) implies (f6), while (f7) immediately follows from (f6) and the properties (f3-3') of the form and coform presented in Table 4.1.2.

It is left to prove the naturality of θ , i.e. that $\theta_{\pi_1} \circ F = F \circ \theta_{\pi_0}$ for any morphism $F : H_{\pi_0} \rightarrow H_{\pi_1}$ in $\mathcal{H}^u(\mathcal{G})$. Since any morphism in $\mathcal{H}^u(\mathcal{G})$ is a composition of expansions (i.e. products with identities) of elementary morphisms, by using the identity $\theta_{\pi \diamond \pi'} = \gamma_{\pi', \pi} \circ (\theta_{\pi'} \diamond \theta_{\pi}) \circ \gamma_{\pi, \pi'}$ and the isotopy moves, we can reduce ourselves to the case when F is any elementary morphism. This case easily follows from (f5) and the properties (s3-6) in Table 4.1.2 and (i4-5) in Table 4.1.8 \square

As we said above, under the right and left rotation maps the multiplication vertices do not remain invariant, but change as described by properties (f8-8') in Figure 4.1.8, which are proved in the next proposition. We observe that (f8) still holds in the non-unimodular case (in $\mathcal{H}(\mathcal{G})$), while (f8') needs the unimodularity axioms.

PROPOSITION 4.1.10. *In $\mathcal{H}^u(\mathcal{G})$, if $g, h, gh \in \mathcal{G}$ (g and h are composable) then*

$$\text{rot}_r(m_{g,h}) = \bar{S}_{\bar{g}} \circ m_{h, \bar{h}\bar{g}} \circ (\text{id}_h \diamond S_{gh}) : H_h \diamond H_{gh} \rightarrow H_g, \quad (f8)$$

$$\text{rot}_l(m_{g,h}) = \bar{S}_{\bar{h}} \circ m_{\bar{h}\bar{g}, g} \circ (S_{gh} \diamond \text{id}_g) : H_h \diamond H_{gh} \rightarrow H_g. \quad (f8')$$

Proof. See Figure 4.1.11 for property (f8). Then property (f8') follows by symmetry, according to Proposition 4.1.8. \square

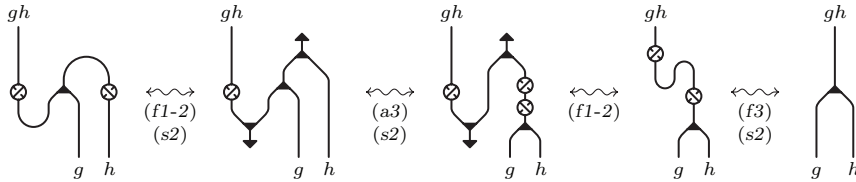


FIGURE 4.1.11. Proof of (f8) [a/123, f/129, s/123]

4.2. The universal groupoid ribbon Hopf algebra $\mathcal{H}^r(\mathcal{G})$

In this section we want to provide the universal unimodular Hopf \mathcal{G} -algebra $\mathcal{H}^u(\mathcal{G})$ with a ribbon structure. The first step in this direction is to postulate the existence of a family of ribbon morphisms, in the sense of the following definition.

DEFINITION 4.2.1. Given a unimodular Hopf \mathcal{G} -algebra H in a braided monoidal category \mathcal{C} , a family of ribbon morphisms of H is a set $v = \{v_g : H_g \rightarrow H_g\}_{g \in \mathcal{G}}$ of invertible morphisms in \mathcal{C} , such that for any $g, h, gh \in \mathcal{G}$:

$$S_g \circ v_g = v_{\bar{g}} \circ S_g, \quad (r3)$$

$$\varepsilon_g \circ v_g = \varepsilon_g, \quad (r4)$$

$$m_{g,h} \circ (v_g \diamond \text{id}_h) = v_{gh} \circ m_{g,h}, \quad (r5)$$

and the family of morphisms $\sigma = \{\sigma_{i,j} : \mathbf{1} \rightarrow H_{1_i} \diamond H_{1_j}\}_{i,j \in \text{Obj } \mathcal{G}}$, defined by

$$\sigma_{i,j} = \begin{cases} (v_{1_i}^{-1} \diamond (v_{1_i}^{-1} \circ S_{1_i})) \circ \Delta_{1_i} \circ v_{1_i} \circ \eta_i & \text{if } i = j, \\ \eta_i \diamond \eta_j & \text{if } i \neq j, \end{cases} \quad (r6)$$

satisfies the following identity for any $i \in \text{Obj } \mathcal{G}$:

$$(\Delta_{1_i} \diamond \text{id}_{1_i}) \circ \sigma_{i,i} = (\text{id}_{1_i} \diamond \text{id}_{1_i} \diamond m_{1_i,1_i}) \circ (\text{id}_{1_i} \diamond \sigma_{i,i} \diamond \text{id}_{1_i}) \circ \sigma_{i,i}. \quad (r7)$$

The axioms above are presented in Table 4.2.1, where we use thinner lines to draw the optional part in the diagram on the righthand side of (r6). Observe that when $i = j$, the thicker units can be deleted by axioms (a4-4') in Table 4.1.1, and therefore $\sigma_{i,i}$ is given just by the thinner diagram.

Axioms for the unimodular braided Hopf algebra $\mathcal{H}_v^u(\mathcal{G})$ (in addition to the axioms of $\mathcal{H}^u(\mathcal{G})$)			
$v_g^n = \begin{array}{c} g \\ \\ n \\ \\ g \end{array}$	$\sigma_{i,j} = \begin{array}{c} 1_i \quad 1_j \\ \quad \\ \text{---} \\ \\ \text{---} \\ \\ 1 \end{array}$	$\begin{array}{c} 1_i \quad 1_j \\ \quad \\ \text{---} \\ \\ \text{---} \\ \\ 1 \end{array}$	$\begin{array}{c} 1_i \quad 1_j \\ \quad \\ \text{---} \\ \\ \text{---} \\ \\ 1 \end{array}$
Additional elementary diagrams			
$\begin{array}{c} g \\ \\ 0 \\ \\ g \end{array} \quad (r1) \quad \begin{array}{c} g \\ \\ g \end{array}$	$\begin{array}{c} g \\ \\ m \\ \\ n \\ \\ g \end{array} \quad (r2) \quad \begin{array}{c} g \\ \\ n+m \\ \\ g \end{array}$	$\begin{array}{c} g \\ \\ \otimes \\ \\ n \\ \\ g \end{array} \quad (r3) \quad \begin{array}{c} g \\ \\ \otimes \\ \\ g \end{array}$	
$\begin{array}{c} \text{---} \\ \\ n \\ \\ g \end{array} \quad (r4) \quad \begin{array}{c} \text{---} \\ \\ g \end{array}$	$\begin{array}{c} gh \\ \\ \text{---} \\ \\ n \quad h \\ \\ g \quad h \end{array} \quad (r5) \quad \begin{array}{c} gh \\ \\ \text{---} \\ \\ n \quad h \\ \\ g \quad h \end{array}$	$\begin{array}{c} 1_i \quad 1_i \quad 1_i \\ \quad \quad \\ \text{---} \\ \\ \text{---} \\ \\ 1 \end{array} \quad (r7) \quad \begin{array}{c} 1_i \quad 1_i \quad 1_i \\ \quad \quad \\ \text{---} \\ \\ \text{---} \\ \\ 1 \end{array}$	
Axioms for the ribbon morphisms			

TABLE 4.2.1.

Usually in the literature (see Section 4 in [35] for the case of a trivial groupoid), instead of ribbon morphisms are introduced ribbon elements, as the ones defined below in the general case of a groupoid Hopf algebra.

DEFINITION 4.2.2. Given a unimodular Hopf \mathcal{G} -algebra H in a braided monoidal category \mathcal{C} , a family of *ribbon elements* of H consists of two sets $V = \{V_i : \mathbf{1} \rightarrow H_{1_i}\}_{i \in \text{Obj } \mathcal{G}}$ and $\bar{V} = \{\bar{V}_i : \mathbf{1} \rightarrow H_{1_i}\}_{i \in \text{Obj } \mathcal{G}}$ of morphisms in \mathcal{C} , such that for any $i \in \text{Obj } \mathcal{G}$ and $g \in \mathcal{G}(i, j)$:

$$S_{1_i} \circ V_i = V_i \quad \text{and} \quad \varepsilon_{1_i} \circ V_i = \mathbf{1},$$

$$m_{1_i, 1_i} \circ (V_i \diamond \bar{V}_i) = \eta_i \quad \text{and} \quad m_{1_i, g} \circ (V_i \diamond \text{id}_g) = m_{g, 1_j} \circ (\text{id}_g \diamond V_j),$$

and the family of morphisms $\sigma = \{\sigma_{i,j} : \mathbf{1} \rightarrow H_{1_i} \diamond H_{1_j}\}_{i,j \in \text{Obj } \mathcal{G}}$, defined by

$$\sigma_{i,j} = \begin{cases} (m_{1_i, 1_i} \diamond m_{1_i, 1_i}) \circ (\bar{V}_i \diamond \text{id}_{1_i} \diamond S_{1_i} \diamond \bar{V}_i) \circ \Delta_{1_i} \circ V_i & \text{if } i = j, \\ \eta_i \diamond \eta_j & \text{if } i \neq j, \end{cases}$$

satisfies the following identity:

$$(\Delta_{1_i} \diamond \text{id}_{1_i}) \circ \sigma_{i,i} = (\text{id}_{1_i} \diamond \text{id}_{1_i} \diamond m_{1_i, 1_i}) \circ (\text{id}_{1_i} \diamond \sigma_{i,i} \diamond \text{id}_{1_i}) \circ \sigma_{i,i}.$$

Actually, next proposition states the equivalence of the two approaches. Moreover, the axioms for ribbon elements can be considered conceptually simpler, in sense that when H is the braiding of an ordinary Hopf algebra \bar{H} the ribbon element is a special central element in \bar{H} (cf. [73]). Nevertheless, as we will discuss below, the approach based on ribbon morphisms seems to be preferable in the present context.

PROPOSITION 4.2.3. *For any unimodular Hopf \mathcal{G} -algebra H in a braided monoidal category \mathcal{C} , there is a bijective correspondence between the set of families of ribbon morphisms and the set of families of ribbon elements of H , given by the map $v \mapsto \{V, \bar{V}\}$ defined by $V_i = v_{1_i} \circ \eta_i$ and $\bar{V}_i = v_{1_i}^{-1} \circ \eta_i$ for every $i \in \text{Obj } \mathcal{G}$, whose inverse $\{V, \bar{V}\} \mapsto v$ is defined by $v_g = m_{1_i, g} \circ (V_i \diamond \text{id}_g)$ for every $g \in \mathcal{G}(i, j)$.*

Proof. The only non-trivial point is to prove the identity $m_{1_i, g} \circ (V_i \diamond \text{id}_g) = m_{g, 1_j} \circ (\text{id}_g \diamond V_j)$, when $V_i = v_{1_i} \circ \eta_i$, $V_j = v_{1_j} \circ \eta_j$ and $g \in \mathcal{G}(i, j)$. This requires the property (r5'), which can be obtained from (r5) by using (s4) (see below). The rest is straightforward and it is left to the reader. \square

As we will see in the next section, the image of the ribbon morphisms/elements in the category \mathcal{K}_n are twists in the attaching map of the corresponding 2-handles. In particular, using ribbon elements, k full twists along the framing of a 2-handle are represented by $m_{1_i} \circ (\text{id}_{1_i} \diamond m_{1_i}) \circ \dots \circ (\text{id}_{1_i} \diamond \dots \diamond \text{id}_{1_i} \diamond m_{1_i}) \circ V_i^{\diamond k}$, and the corresponding graph diagram is quite heavy. On the other hand, using ribbon morphisms, the same k full twists are represented by $v_{1_i}^k \circ \eta_i$, which seems to us much simpler. This is the main reason why we decided to follow this last approach.

DEFINITION 4.2.4. Given a groupoid \mathcal{G} , we define the *universal pre-ribbon Hopf \mathcal{G} -algebra* $\mathcal{H}_v^u(\mathcal{G})$ to be the braided strict monoidal category freely generated by a unimodular Hopf \mathcal{G} -algebra H with a family of ribbon morphisms $v = \{v_g : H_g \rightarrow H_g\}_{g \in \mathcal{G}}$. Then, $\mathcal{H}_v^u(\mathcal{G})$ has the same objects as $\mathcal{H}^u(\mathcal{G})$, while its elementary morphisms are those of $\mathcal{H}^u(\mathcal{G})$ with the addition of the diagrammatic representations of v^n and $\sigma_{i,j}$ shown in Table 4.2.1. Moreover, the defining relations of $\mathcal{H}_v^u(\mathcal{G})$ are the axioms of $\mathcal{H}^u(\mathcal{G})$ (where now in the braid axioms in Table 4.1.1, D can be also a ribbon morphism) plus the axioms for the ribbon morphisms presented in Table 4.2.1.

The category $\mathcal{H}_v^u(\mathcal{G})$ has many important properties presented in Table 4.2.2. Before proving them, we make here few observations about the basic relations of the pre-ribbon algebra and their diagrammatic representation.

- (a) In the diagrams we represent v_g^n by an edge with weight $n \in \mathbb{Z}$. In particular, (r1) states that an edge with weight 0 is the same as an edge without any weight.
- (b) Axiom (r4) says that the weight of an edge attached to a counit vertex can be changed arbitrarily. By property (p1), the same is true for the integral vertex.
- (c) Axiom (r5) and property (r5') imply that the weight of an edge attached to a multiplication vertex can be moved to any other edge attached to that vertex.

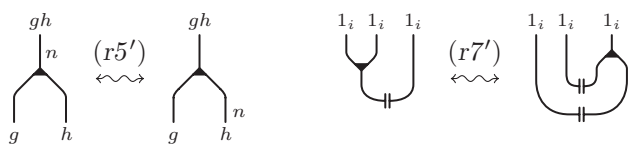
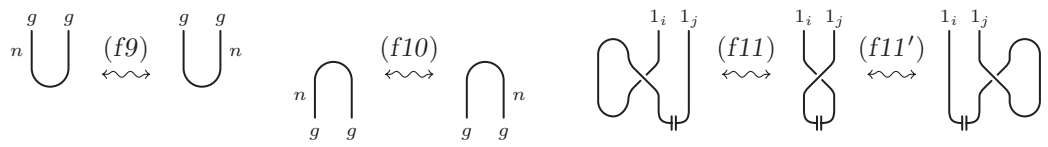
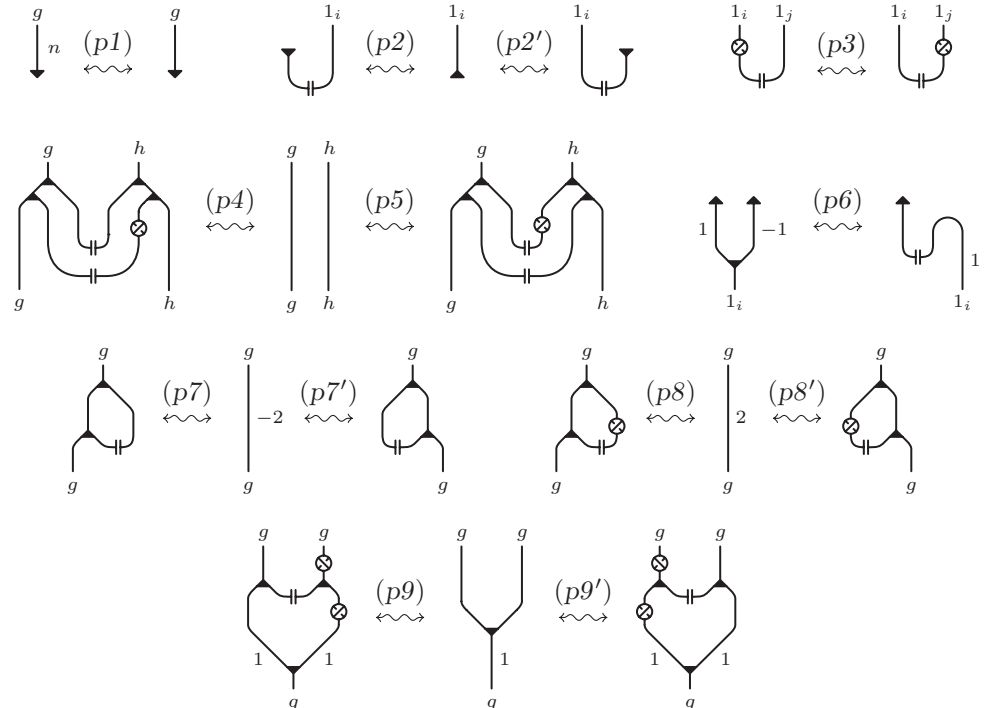
Properties of the unimodular braided Hopf algebra $\mathcal{H}_v^u(\mathcal{G})$		
	$(r5')$	$(r7')$
<i>Relations symmetric to (r5) and (r7)</i>		
	$(f9)$	$(f10)$
<i>Extended isotopy moves</i>		
	$(p1)$	$(p2)$
<i>Other relations</i>		

TABLE 4.2.2.

- (d) We remind that, given two Hopf algebras over the trivial groupoid $(A, m^A, \eta^A, \Delta^A, \varepsilon^A, S^A)$ and $(B, m^B, \eta^B, \Delta^B, \varepsilon^B, S^B)$ in the same braided monoidal category \mathcal{C} , a morphism $\sigma_{A,B} : \mathbf{1} \rightarrow A \diamond B$ is called a *Hopf copairing* if the following conditions are satisfied:

$$\begin{aligned} (\Delta^A \diamond \text{id}_B) \circ \sigma_{A,B} &= (\text{id}_{A \diamond A} \diamond m^B) \circ (\text{id}_A \diamond \sigma_{A,B} \diamond \text{id}_B) \circ \sigma_{A,B}, \\ (\text{id}_A \diamond \Delta^B) \circ \sigma_{A,B} &= (m^A \diamond \text{id}_{B \diamond B}) \circ (\text{id}_A \diamond \sigma_{A,B} \diamond \text{id}_B) \circ \sigma_{A,B}, \\ (\varepsilon^A \diamond \text{id}_B) \circ \sigma_{A,B} &= \eta^B \quad \text{and} \quad (\text{id}_A \diamond \varepsilon^B) \circ \sigma_{A,B} = \eta^A. \end{aligned}$$

Moreover, the Hopf copairing $\sigma_{A,B}$ is called *trivial* if $\sigma_{A,B} = \eta^A \diamond \eta^B$. Therefore, axioms (r6) and (r7) together with properties (r7') and (p2-2'), imply that $\sigma_{i,j} : \mathbf{1} \rightarrow H_{1_i} \diamond H_{1_j}$ is a Hopf pairing, and that such pairing is trivial for $i \neq j$. For this reason we will refer to the morphisms $\sigma_{i,j}$'s as *copairing morphisms* or simply *copairings*.

- (e) Property (p3) tell us that the copairing is symmetric with respect to the rotation around a vertical axis, while properties (r5') and (r7') are the symmetric version of axioms (r5) and (r7). Hence, once those properties will be proved in Proposition 4.2.7, they will imply that the functor $\text{sym} : \mathcal{H}^u(\mathcal{G}) \rightarrow \mathcal{H}^u(\mathcal{G})$ of Proposition 4.1.8 induces an analogous symmetry functor $\text{sym} : \mathcal{H}_v^u(\mathcal{G}) \rightarrow \mathcal{H}_v^u(\mathcal{G})$, which fixes the ribbon morphisms v_g for $g \in \mathcal{G}$.

We now proceed with the proof of the properties of $\mathcal{H}_v^u(\mathcal{G})$ listed in Table 4.2.2, beginning with those which follow directly from the definition (r6) of $\sigma_{i,j}$ and the axioms (r1-5), but do not depend on the copairing property of $\sigma_{i,j}$ (axiom (r7)).

LEMMA 4.2.5. *Properties (r5'), (f9), (f10), (f11-11'), (p1), (p2-2'), (p7-7') and (p9) in Table 4.2.2, hold in $\mathcal{H}_v^u(\mathcal{G})$. Moreover, they can be proved without using axiom (r7).*

Proof. (r5') can be shown to be equivalent to (r5), by using the property (s4) of the antipode (see Table 4.1.2). (f10) is a direct consequence of definition (f2) in Table 4.1.2 and of the relations (r3) and (r5-5').

(f11-11') are trivial when $i \neq j$, due to the definition (r6) and the duality of the corresponding univalent vertices in Table 4.1.2, while the proofs for $i = j$ are presented in Figure 4.2.3. Here, we first prove (f11') in the top line and then we show how it implies (f11) up to isotopy moves in the bottom line.

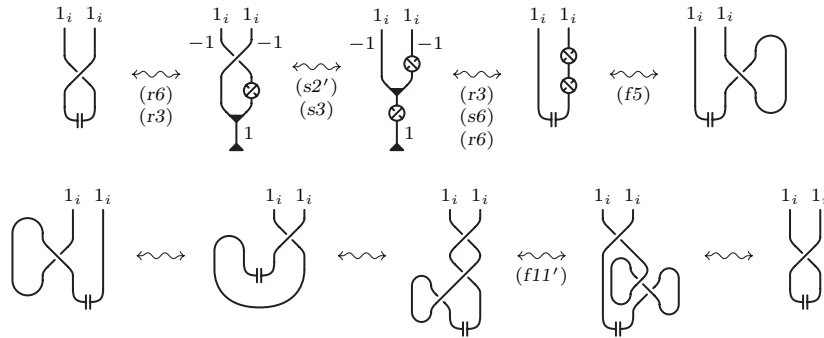


FIGURE 4.2.3. Proof of (f11-11') for $i = j$ [f/129-134, r/132, s/125]

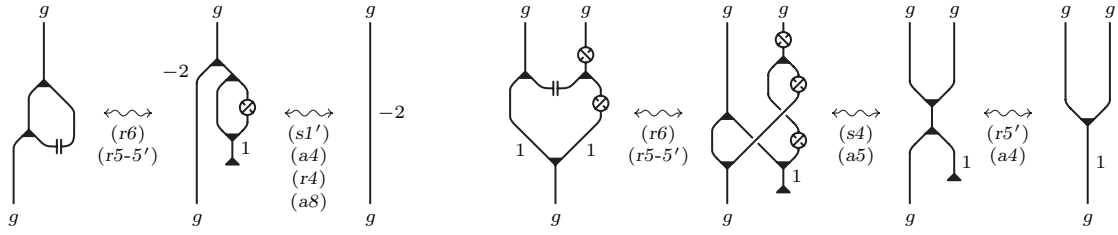


FIGURE 4.2.4. Proof of (p7) and (p9) [a/123, r/132-134, s/123]

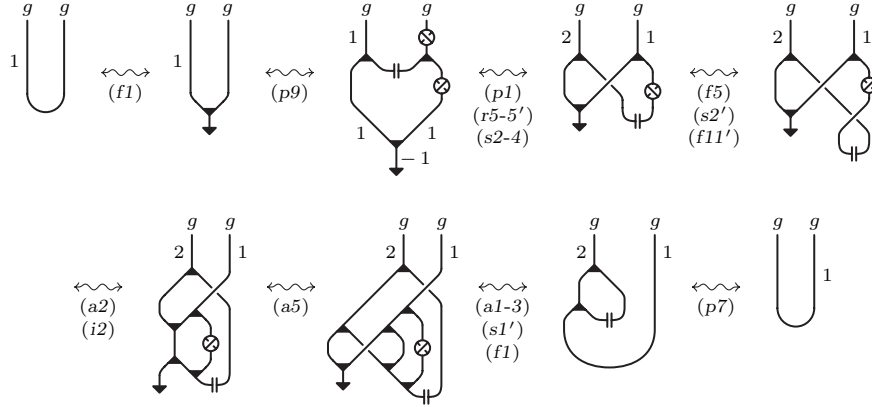


FIGURE 4.2.5. Proof of (f9) [a/123, f/129-134, i/129, p/134, r/132-134, s/123-125]

(p1) can be derived from (r4), by using (r5) and the duality of the negative uni-valent vertices in Table 4.1.2. (p2-2') immediately follow from the definition (r6) of the copairing, the axiom (r2) and the relations (a2-2') and (s5-6) in Tables 4.1.1 and 4.1.2. (p7) and (p9) are proved in Figure 4.2.4. (p7') can be proved in a completely analogous way as (p7). (f9) is proved in Figure 4.2.5. \square

LEMMA 4.2.6. For every $g \in \mathcal{G}(i, j)$ and $h \in \mathcal{G}(j, k)$,

$$\mu_{g,h} = (m_{g,1_i} \diamond m_{1_j,h}) \circ (\text{id}_g \diamond \sigma_{i,j} \diamond \text{id}_h) : H_g \diamond H_h \rightarrow H_g \diamond H_h$$

is an isomorphism in $\mathcal{H}_v^u(\mathcal{G})$, and

$$\mu_{g,h}^{-1} = (m_{g,1_i} \diamond m_{1_j,h}) \circ (\text{id}_g \diamond ((\text{id}_{1_i} \diamond S_{1_j}) \circ \sigma_{i,j}) \diamond \text{id}_h) : H_g \diamond H_h \rightarrow H_g \diamond H_h$$

is its inverse (see Figure 4.2.6). In other words, properties (p4-5) hold in $\mathcal{H}_v^u(\mathcal{G})$.

$$\mu_{g,h} = \begin{array}{c} g \quad h \\ \diagdown \quad \diagup \\ \text{---} \\ \diagup \quad \diagdown \\ g \quad h \end{array} \quad \mu_{g,h}^{-1} = \begin{array}{c} g \quad h \\ \diagdown \quad \diagup \\ \text{---} \\ \diagup \quad \diagdown \\ g \quad h \end{array}$$

FIGURE 4.2.6. The isomorphisms $\mu_{g,h}$ and $\mu_{g,h}^{-1}$

Proof. Property (p4) is proved in Figure 4.2.7. The proof of (p5) is analogous, using (s1) in place of (s1'). \square

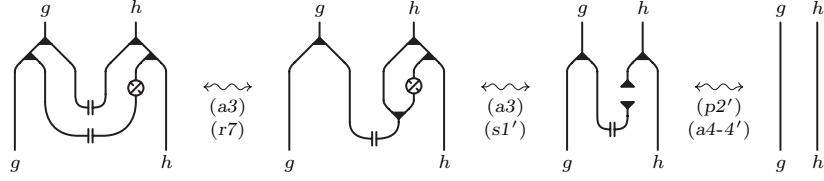


FIGURE 4.2.7. Proof of (p4) [a-s/123, r/134]

PROPOSITION 4.2.7. Given a groupoid \mathcal{G} , all the relations in Table 4.2.2 are satisfied in the universal pre-ribbon Hopf \mathcal{G} -algebra $\mathcal{H}_v^u(\mathcal{G})$. Moreover, there is an involutive antimonoidal category equivalence $\text{sym} : \mathcal{H}_v^u(\mathcal{G}) \rightarrow \mathcal{H}_v^u(\mathcal{G})$ uniquely determined by the identities in Proposition 4.1.8 and by $\text{sym}(v_g) = v_{\bar{g}}$.

Proof. In the light of the previous lemmas, we are left to prove the relations (r7'), (p3), (p6), (p8-8') and (p9').

(r7') is derived from (r7) in Figure 4.2.8, by using the relation (f11'), the braid axioms and the properties of the antipode.

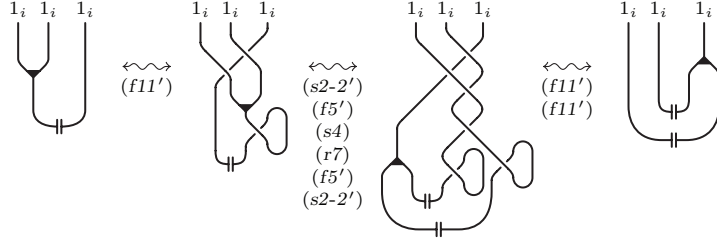


FIGURE 4.2.8. Proof of (r7') [f/129-134, r/134 s/123-125]

To prove (p3), let us consider the morphism

$$\text{sym}(\mu_{g,h}^{-1}) = (m_{g,1_i} \diamond m_{1_j,h}) \circ (\text{id}_g \diamond ((S_{1_i} \diamond \text{id}_{1_j}) \circ \sigma_{i,j}) \diamond \text{id}_h) : H_g \diamond H_h \rightarrow H_g \diamond H_h,$$

where for the moment $\text{sym}(\mu_{g,h}^{-1})$ is just as a notation for the symmetric of $\mu_{g,h}^{-1}$, with the antipode moved to the left side of $\sigma_{i,j}$. Then, by replacing (r7'), (p2') and (s1') in Figure 4.2.7 respectively with (r7), (p2) and (s1), we obtain that (p4) and (p5) are still valid if $\mu_{g,h}^{-1}$ is replaced by $\text{sym}(\mu_{g,h}^{-1})$. Hence $\text{sym}(\mu_{g,h}^{-1})$ and $\mu_{g,h}^{-1}$ are equal, being both two-sided inverses of $\mu_{g,h}$. This gives (p3), by composing with $\eta_g \diamond \eta_h$.

At this point, we are ready to prove that $\text{sym} : \mathcal{H}_v^u(\mathcal{G}) \rightarrow \mathcal{H}_v^u(\mathcal{G})$ defines an involutive antimonoidal category equivalence. According to Proposition 4.1.8, it is enough to check that it preserves the additional ribbon axioms. Indeed, property

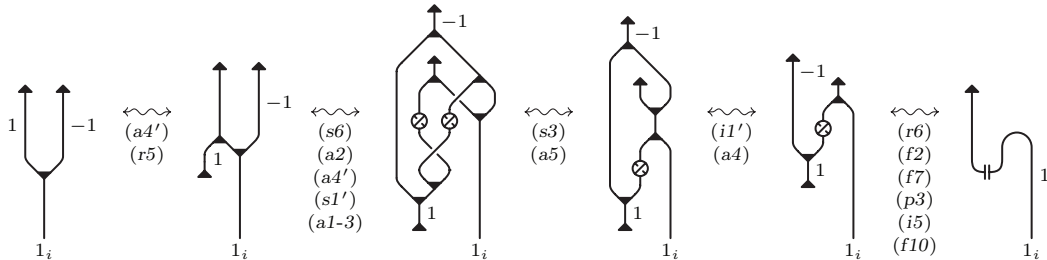


FIGURE 4.2.9. Proof of (p6) [a/123, f/129-134, i/129, p/134, r/132, s/123-125]

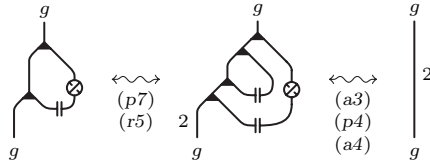


FIGURE 4.2.10. Proof of (p8) [a/123, p/134, r/132]

(p3) implies that the copairing is symmetric, i.e. the antipode which appears in its definition (r6) can be put on either side. Moreover, all ribbon axioms are left invariant by sym with the exceptions of axioms (r5) and (r7), which are mapped to properties (r5') and (r7').

Finally, (p6) and (p8) are proved in Figures 4.2.9 and 4.2.10 respectively, while (p8') and (p9') follow from (p8) and (p9) by symmetry. \square

We observe that the morphisms in $\mathcal{H}_v^u(\mathcal{G})$ are represented by formal graph diagrams, which can be interpreted as plane projection of uni/tri-valent graphs embedded in R^3 . Under this interpretation, some of the equivalence moves between such diagrams correspond to graph isotopies in R^3 . We collect these moves in the following definition.

DEFINITION 4.2.8. Two diagrams representing morphisms in $\mathcal{H}_v^u(\mathcal{G})$, as well as in its quotient $\mathcal{H}^r(\mathcal{G})$ we will define below, will be called *isotopic*, or obtainable from each other through *isotopy*, if they are related by a sequence of moves (b1) to (b4') in Table 4.1.1, (f3-3') in Table 4.1.2, (f5-5') and (f6-7) in Table 4.1.8, (f9), (f10) and (f11-11') in Table 4.2.2.

An example of diagram isotopy is shown in Figure 4.2.11. The reader can check that here only the braid axioms and moves (f11-11') are needed.

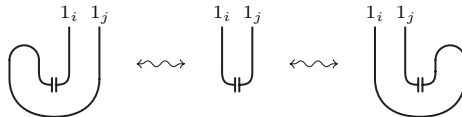


FIGURE 4.2.11. An example of diagram isotopy

Since the application of the isotopy moves will be frequent and quite intuitive, we will usually omit to explicitly indicate them in the diagrammatic proofs.

As we already mentioned, the universal algebra $\mathcal{H}_v^u(\mathcal{G})$ for \mathcal{G} the trivial groupoid is the algebra \mathcal{Alg} introduced by Kerler in [35], without the self-duality axiom, or equivalently without the requirement that the copairing is non-degenerate. We do not impose yet the self-duality, since for now we want to interpret the algebraic structure of cobordisms of relative 4-dimensional 2-handlebodies. Self-duality will be added only later in Chapter 5, when we will study the 3-dimensional boundaries of such handlebodies.

The axioms of $\mathcal{H}_v^u(\mathcal{G}_n)$ are clearly too weak for what we need. In fact, they are compatible with the trivial choice $v_g = \text{id}_g$ of the ribbon morphisms, which brings to trivial copairings. On the contrary, the ribbon morphisms of the Hopf algebra of cobordisms are 2-handles with non-trivial framings and the copairing is the one introduced by Lyubashenko in [44] (see [35] and Section 4.3 below). Therefore,

the universal algebraic category equivalent to such cobordism category necessarily contains additional axioms connecting the ribbon structure to the braiding, in such a way that if the braiding structure of the category is non-trivial, then the ribbon one is forced to be non-trivial as well. Before introducing those axioms, we make the following observation.

PROPOSITION 4.2.9. *Given any any $i \in \text{Obj } \mathcal{G}$ and any $g \in \mathcal{G}(j, k)$, consider the morphisms $\rho_{i,g}$ and $\rho_{g,i} = \text{sym}(\rho_{i,\bar{g}})$ of $\mathcal{H}_v^u(\mathcal{G})$ defined by (see Figure 4.2.12)*

$$\begin{aligned}\rho_{i,g} &= (\text{id}_{1_i} \diamond m_{1_j,g}) \circ (\sigma_{i,j} \diamond \text{id}_g) : H_g \rightarrow H_{1_i} \diamond H_g, \\ \rho_{g,i} &= (m_{g,1_k} \diamond \text{id}_{1_i}) \circ (\text{id}_g \diamond \sigma_{k,i}) : H_g \rightarrow H_g \diamond H_{1_i}.\end{aligned}$$

Then $\rho_{i,g}$ (resp. $\rho_{g,i}$) makes H_g into a left (resp. right) H_{1_i} -comodule.

FIGURE 4.2.12. *The morphisms $\rho_{g,k}$ and $\rho_{k,g}$*

Proof. The proposition is a direct consequence of (p2-2') and (r7-7'). \square

DEFINITION 4.2.10. Given a groupoid \mathcal{G} , a ribbon Hopf \mathcal{G} -algebra in a braided monoidal category \mathcal{C} is a unimodular Hopf \mathcal{G} -algebra H with a family of ribbon morphisms v , which satisfies the two additional conditions (cf. Table 4.2.13):

$$\Delta_g \circ v_g^{-1} = \mu_{g,g} \circ (v_g^{-1} \diamond v_g^{-1}) \circ \bar{\gamma}_{g,g} \circ \Delta_g : H_g \rightarrow H_g \diamond H_g, \quad (r8)$$

$$\begin{aligned}(m_{1_k,h} \diamond m_{g,1_j}) \circ (S_{1_k} \circ (\mu_{h,g} \circ \bar{\gamma}_{g,h} \circ \mu_{g,h}) \diamond S_{1_j}) \circ (\rho_{k,g} \diamond \rho_{h,j}) &= \\ = \gamma_{g,h} : H_g \diamond H_h \rightarrow H_h \diamond H_g, & (r9)\end{aligned}$$

for any $g \in \mathcal{G}(i, j)$ and $h \in \mathcal{G}(k, l)$.

We observe that the relations (r8) and (r9) simplify for some combinations of the labels, because trivial copairings appear. In particular, move (r9) reduces to a crossing change when $g \in \mathcal{G}(i, j)$ and $h \in \mathcal{G}(k, l)$ with $\{i, j\} \cap \{k, l\} = \emptyset$.

Moreover, for a ribbon Hopf algebra whose ribbon (and copairings) morphisms are all trivial the new axioms imply cocommutativity and trivial braiding. This proves the independence of the two new axioms from the rest of the axioms of the algebra. However, the same argument is not valid any more in the presence of the self-duality (see Section 5.4), which is not compatible with the trivial choice for the v_g 's. Therefore, in the self-dual case, which refers to the algebraic description of 3-dimensional framed cobordisms, we do not claim the independence of the axioms (r8) and (r9), even if we are convinced that this is still true.

PROPOSITION 4.2.11. *Modulo the axioms for $\mathcal{H}_v^u(\mathcal{G})$, (r8) is equivalent to either (p10), (p11) or (p12), while (r9) is equivalent to (p13), all these relations being defined in Table 4.2.13.*


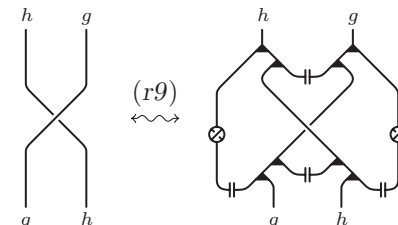


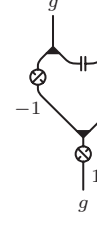
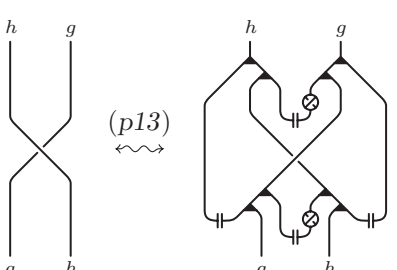




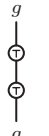

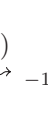


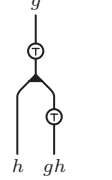
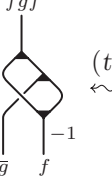
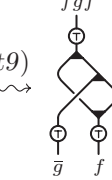
Axioms for the universal ribbon Hopf algebra $\mathcal{H}^r(\mathcal{G})$ (in addition to the axioms of $\mathcal{H}_v^u(\mathcal{G})$)	
	
Properties of the universal ribbon Hopf algebra $\mathcal{H}^r(\mathcal{G})$	
	
	
<p><i>Equivalent forms of the axiom (r8)</i> <i>Equivalent form of the axiom (r9)</i></p>	
	
<p><i>Inverting the antipode through the copairing</i></p>	
	
	
	
	
	
<p><i>Definition and properties of T_g ($f, g \in \mathcal{G}(i, j)$, $h \in \mathcal{G}(j, k)$, $i \neq j \neq k \neq i$)</i></p>	

TABLE 4.2.13.

Proof. The equivalence between (r8) and (p11) derives from (s3) in Table 4.1.2 and (r3) in Table 4.2.1, after having composed both sides of (r8) with v_g on the bottom. (p10) is obtained from (r8) by composing both sides with v_g on the bottom and with the invertible morphism $\gamma_{g,g} \circ \mu_{g,g}^{-1} \circ (v_g \diamond v_g)$ (see Lemma 4.2.6) on the top. Analogously, (p12) is obtained from (p11) by replacing g with \bar{g} and composing both sides with the invertible morphisms $S_g \circ v_g^{-1}$ and $(\bar{S}_g \diamond \bar{S}_g) \circ (v_g \diamond v_g) \circ \mu_{g,g}^{-1}$ respectively on the bottom and on the top.

To see that (r9) implies (p13), it suffices to observe that the diagram on the right side of (p13) can be reduced to the single crossing on the left side, by applying (r9) at the crossing in the middle of it, and then using one move (p3) and four moves (p4-5) to cancel the corresponding copairings. The opposite argument shows that (p13) implies (r9) as well. \square

DEFINITION 4.2.12. Given a groupoid \mathcal{G} , we define the *universal ribbon Hopf \mathcal{G} -algebra* $\mathcal{H}^r(\mathcal{G})$ as the braided strict monoidal category freely generated by a ribbon Hopf \mathcal{G} -algebra H with a family of ribbon morphisms $v = \{v_g : H_g \rightarrow H_g\}_{g \in \mathcal{G}}$. Equivalently, $\mathcal{H}^r(\mathcal{G})$ is the quotient of \mathcal{H}_v^u modulo the relations (r8) and (r9), i.e. the objects and elementary morphisms of $\mathcal{H}^r(\mathcal{G})$ are the same as $\mathcal{H}_v^u(\mathcal{G})$, while the relations are those of $\mathcal{H}_v^u(\mathcal{G})$ plus the additional axioms for the ribbon morphisms (r8) and (r9) in Table 4.2.13.

PROPOSITION 4.2.13. *Given a groupoid \mathcal{G} , all the relations in Table 4.2.13 hold in the universal ribbon Hopf \mathcal{G} -algebra $\mathcal{H}^r(\mathcal{G})$. Moreover, the category equivalence in Proposition 4.2.7 passes to the quotient to give an involutive antimonoidal category equivalence $\text{sym} : \mathcal{H}^r(\mathcal{G}) \rightarrow \mathcal{H}^r(\mathcal{G})$.*

Proof. The existence of the induced involutive antimonoidal category equivalence $\text{sym} : \mathcal{H}^r(\mathcal{G}) \rightarrow \mathcal{H}^r(\mathcal{G})$ is due to the invariance of the axioms (r8) and (r9) under $\text{sym} : \mathcal{H}_v^u(\mathcal{G}) \rightarrow \mathcal{H}_v^u(\mathcal{G})$.

Relations (p10) to (p13) were considered in Proposition 4.2.11. Figure 4.2.14 proves (p15), while (p15') follows by symmetry. Then (p14-14') can be derived from (p15-15') in the same way as (p8) was derived from (p7) (see Figure 4.2.4) and we leave their proof to the reader.

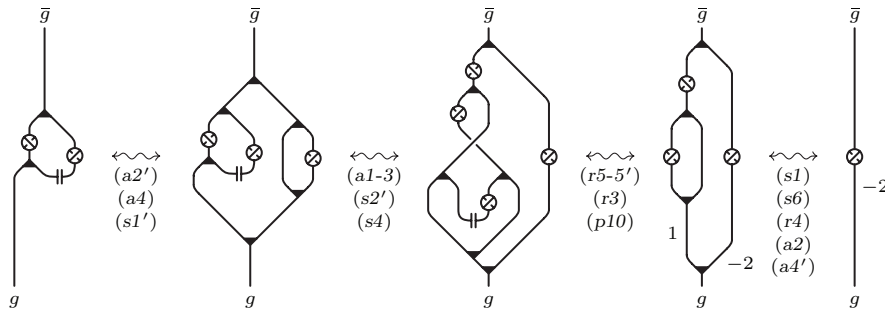


FIGURE 4.2.14. Proof of (p15) [a/123, p/140, r/132-134, s/123-125]

Properties (t2) to (t9) concern the two morphisms

$$T_g = S_g \circ v_g^{-1} \quad \text{and} \quad \bar{T}_g = \bar{S}_g \circ v_g$$

for $g \in \mathcal{G}(i, j)$ with $i \neq j$. Before proving these properties, notice that for an arbitrary $g \in \mathcal{G}$ we have $T_g^{-1} = \bar{T}_g$, while $T_{\bar{g}} \circ T_g$ (resp. $\bar{T}_{\bar{g}} \circ \bar{T}_g$) gives a full positive (resp. negative) twist of an edge with weight -2 (resp. $+2$), as shown in Figure 4.2.15.



FIGURE 4.2.15. $T_{\bar{g}} \circ T_g$ and $\bar{T}_{\bar{g}} \circ \bar{T}_g$ [f/129, r/132]

Now, taking into account the triviality of $\sigma_{i,j}$ for $i \neq j$, we see that (t2-3) immediately follow from relation (p14), (t4-5) rewrite (p11) and (r8) when $g \in \mathcal{G}(i, j)$ with $i \neq j$, and (t6-7) rewrite (f8) and (s4) under the further assumption that $h \in \mathcal{G}(j, k)$ and $j \neq k \neq i$. Finally, (t8-9) are proved in Figure 4.2.16. \square

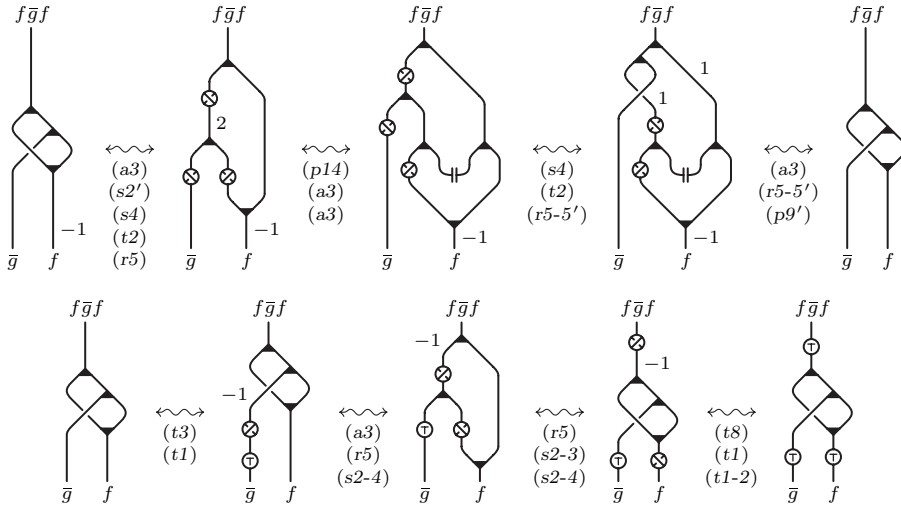


FIGURE 4.2.16. Proof of (t8-9) [a/123, p/134-140, r/132-134, s/125, t/140]

We observe that, thanks to properties (t3-4), when $g \in \mathcal{G}(i, j)$ with $i \neq j$ the morphism T_g is a coalgebra isomorphism, i.e. $\Delta_{\bar{g}} \circ T_g = (T_{\bar{g}} \circ T_g) \circ \Delta_g$.

The next proposition tells us that an inclusion of groupoids $\mathcal{G} \subset \mathcal{G}'$ induces an inclusion between the corresponding universal ribbon Hopf \mathcal{G} -algebras, hence we can write $\mathcal{H}^r(\mathcal{G}) \subset \mathcal{H}^r(\mathcal{G}')$.

PROPOSITION 4.2.14. *Any functor $\varphi : \mathcal{G} \rightarrow \mathcal{G}'$ between groupoids which is injective on the set of objects can be extended to a functor $\Upsilon_\varphi : \mathcal{H}^r(\mathcal{G}) \rightarrow \mathcal{H}^r(\mathcal{G}')$. Moreover, if φ is faithful (an embedding) then Υ_φ is also faithful.*

Proof. We formally define Υ_φ by applying φ to the indices of all the elementary morphisms, that is $\Upsilon_\varphi(\gamma_{g,h}) = \gamma_{\varphi(g),\varphi(h)}$, $\Upsilon_\varphi(\Delta_g) = \Delta_{\varphi(g)}$, $\Upsilon_\varphi(\eta_i) = \eta_{\varphi(i)}$, etc.

To see that Υ_φ is well-defined, we need to check that all relations for $\mathcal{H}^r(\mathcal{G})$ are satisfied in the image. The only problem we might have would be with relations (r8) and (r9) in Table 4.2.13. Those relations will be satisfied if we have that $\Upsilon_\varphi(\sigma_{i,j}) = \sigma_{\varphi(i),\varphi(j)}$, which is always true since φ is injective on objects. This concludes the first part of the proposition since the functoriality of Υ_φ is obvious.

At this point, it is left to show that when φ is injective on morphisms, then Υ_φ is injective on morphisms as well. In this case φ induces an isomorphism of categories $\widehat{\varphi} : \mathcal{G} \rightarrow \varphi(\mathcal{G})$ and $\Upsilon_{\widehat{\varphi}} : \mathcal{H}(\mathcal{G}) \rightarrow \mathcal{H}(\varphi(\mathcal{G}))$ is an isomorphism of categories as well, being $\Upsilon_{\widehat{\varphi}}$ and $\Upsilon_{\widehat{\varphi}^{-1}}$ inverse of each other by construction. Moreover, $\Upsilon_\varphi = \Upsilon_\iota \circ \Upsilon_{\widehat{\varphi}}$ where $\iota : \varphi(\mathcal{G}) \subset \mathcal{G}'$ is the corresponding inclusion. Hence, it suffices to show that the functor Υ_ι is injective on morphisms.

Let $F, F' : A \rightarrow B$ be morphisms of $\mathcal{H}(\varphi(\mathcal{G}))$ with $\Upsilon_\iota(F) = \Upsilon_\iota(F')$. Then, they are represented by diagrams labeled in $\varphi(\mathcal{G})$ and related by a sequence of moves in $\mathcal{H}(\mathcal{G}')$. Now, when we apply a relation move to a diagram representing a morphism of $\mathcal{H}(\mathcal{G}')$, the only new labels that can appear are identities of \mathcal{G}' and products of labels already occurring in it or their inverses. Therefore, since $\varphi(\mathcal{G})$ is a subcategory of \mathcal{G}' , the only labels not belonging to $\varphi(\mathcal{G})$ that can occur in the intermediate diagrams of the sequence are identities 1_i with $i \in \text{Obj } \mathcal{G}' - \text{Obj } \varphi(\mathcal{G})$. The parts of the diagram carrying such labels interact with the rest of the diagram only through move (r9) in Table 4.2.13. Hence, by applying move (r6) to change the trivial copairings into two units, we can disconnect those parts from the rest of the intermediate diagrams. After that, we can delete them to get a new sequence of diagrams between F and F' related by moves in $\mathcal{H}(\varphi(\mathcal{G}))$, which proves that $F = F'$ in $\mathcal{H}(\varphi(\mathcal{G}))$. \square

4.3. The functors $\Phi_n : \mathcal{H}_n^r \rightarrow \mathcal{K}_n$

In the introduction of this chapter we argued that the category of generalized Kirby tangles \mathcal{K}_n contains a ribbon Hopf \mathcal{G}_n -algebra. We will prove this fact here by constructing a functor from the universal ribbon Hopf \mathcal{G}_n -algebra to \mathcal{K}_n . Being this algebra our main object of study we will simplify the notation as follows.

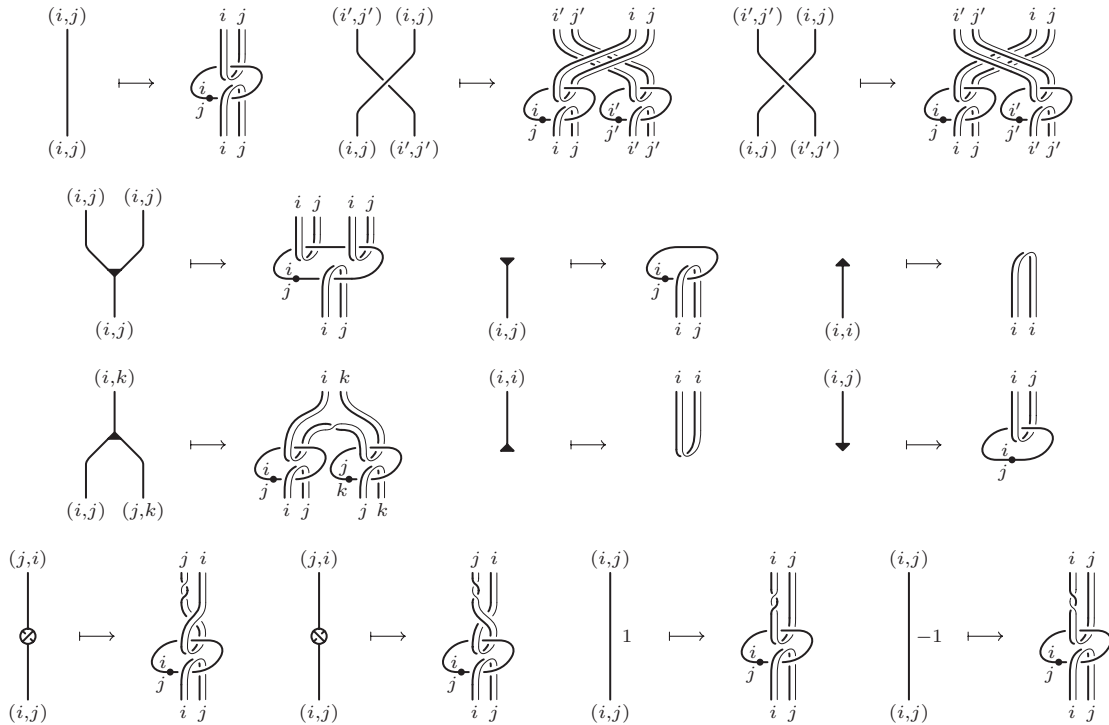


FIGURE 4.2.17. The functor $\Phi_n : \mathcal{H}_n^r \rightarrow \mathcal{K}_n$

For $n \geq 1$, we denote by \mathcal{H}_n^r the universal ribbon Hopf \mathcal{G}_n -algebra $\mathcal{H}^r(\mathcal{G}_n)$ associated to the groupoid \mathcal{G}_n , consisting of the set $\{1, \dots, n\}^2$ with the natural groupoid structure given by $(i, j)(j, k) = (i, k)$ for any $1 \leq i, j, k \leq n$.

The next theorem is an extension of the well-known fact that the category of admissible tangles contains a braided Hopf algebra (see [35, 24]). Indeed, it shows that the categories of generalized Kirby tangles contain groupoid ribbon Hopf algebras.

THEOREM 4.3.1. *There exists a braided monoidal functor $\Phi_n : \mathcal{H}_n^r \rightarrow \mathcal{K}_n$, which sends every object $H_{(i,j)}$ to $I_{(i,j)}$ (defined in Section 2.2) and the elementary morphisms of \mathcal{H}_n^r to the generalized Kirby tangles described in Figure 4.2.17.*

Before proving the theorem, we observe that the images through Φ_n of the form $\lambda_{(i,j)}$, the coform $\Lambda_{(i,j)}$, the copairing $\sigma_{i,j}$ and the morphism $T_{(i,j)}$, are equivalent in \mathcal{K}_n to the tangles presented in Figure 4.3.1. The case of $\sigma_{i,i}$ is shown in Figure 4.3.2, where some 1/2-handle cancelation is understood in the first diagram, while the other cases are easier and left to the reader. Notice that the image of the copairing $\sigma_{i,i}$ is exactly the Lyubashenko's copairing defined in [44].

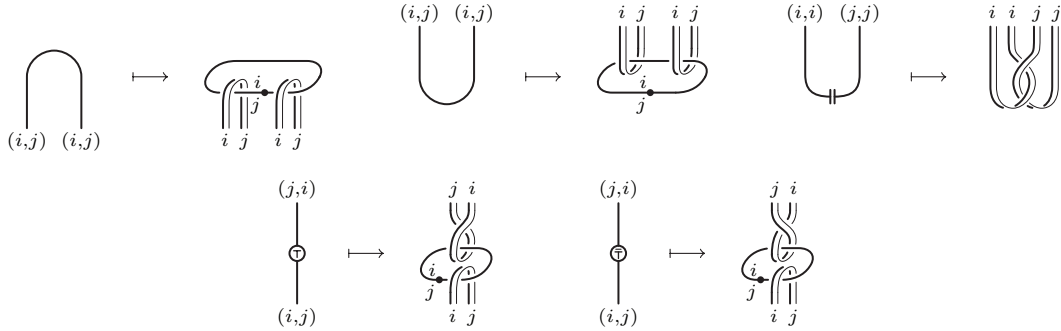


FIGURE 4.3.1. Images under Φ_n of $\lambda_{(i,j)}$, $\Lambda_{(i,j)}$, $\sigma_{i,j}$, $T_{(i,j)}$ and $\bar{T}_{(i,j)}$

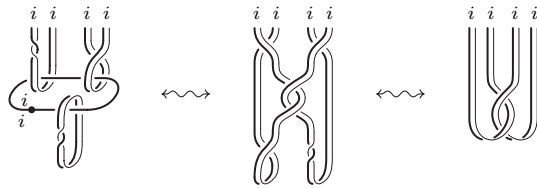


FIGURE 4.3.2. Deriving $\Phi_n(\sigma_{i,i})$ from (r6)

Proof of Theorem 4.3.1. We have to verify that the definition of Φ_n on the elementary morphisms is compatible with the axioms for \mathcal{H}_n^r , namely that it determines equivalent images in \mathcal{K}_n for the two diagrams involved in each of those axioms.

This is easy to check for most of the unimodular braided Hopf algebra axioms in Tables 4.1.1 and 4.1.8. In particular, it reduces to isotopy for the braid axioms and to deletion of canceling 1/2-pairs for the axioms (a2-2'), (a6), (a8), (i3) and (i4), while one needs to make one or two handle slides before deleting for the axioms (a1), (a3), (a4-4'), (a7), (s2-2'), (i1), (i2) and (i5).

Axioms (a5) and (s1) are considered in Figures 4.3.3 and 4.3.4 respectively. Axiom (s1') can be treated similarly to (s1).

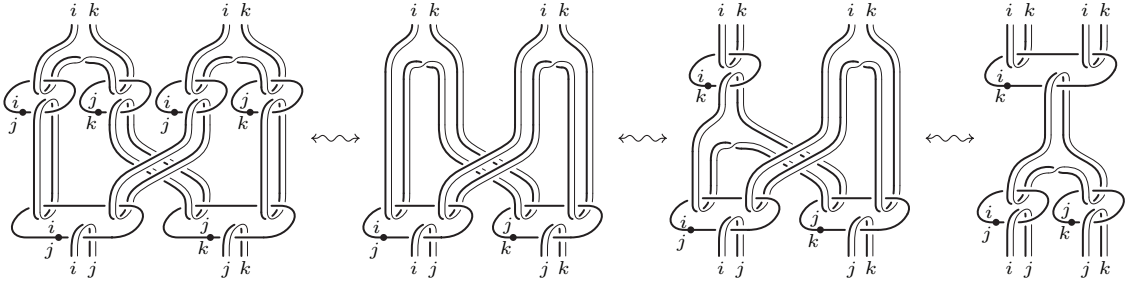


FIGURE 4.3.3. The definition of Φ_n is compatible with (a5)

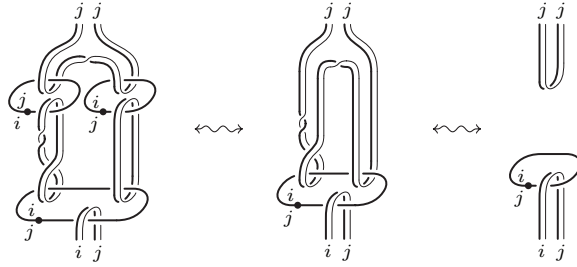


FIGURE 4.3.4. The definition of Φ_n is compatible with (s1)

Now, let us pass to the ribbon axioms in Tables 4.2.1 and 4.2.13. The compatibility with the axioms (r1) to (r5) can be easily proved by applying once again cancelations of 1/2-pairs after suitable handle slidings. The rest of the ribbon axioms are dealt with in Figures 4.3.5, 4.3.6 and 4.3.7. Here, in the rightmost diagrams of the last two figures some cancelations of 1/2-pairs and some crossing changes moves between components with different labels (when they appear) have been performed. \square

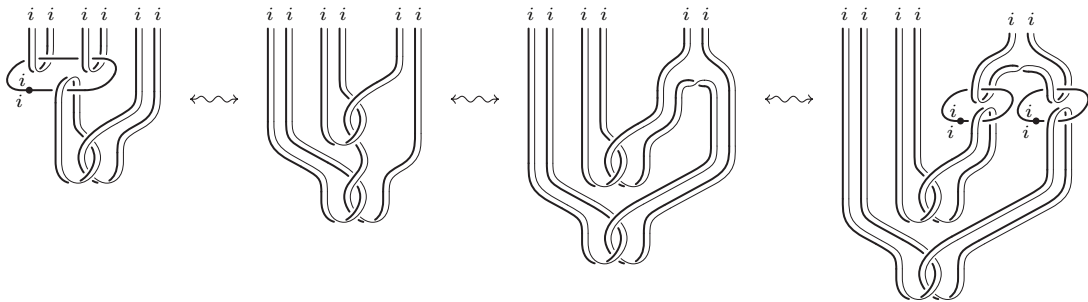


FIGURE 4.3.5. The definition of Φ_n is compatible with (r7)

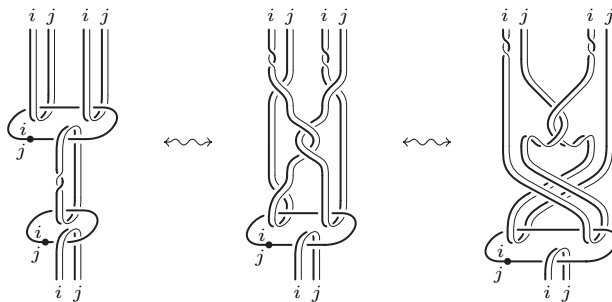


FIGURE 4.3.6. The definition of Φ_n is compatible with (r8)

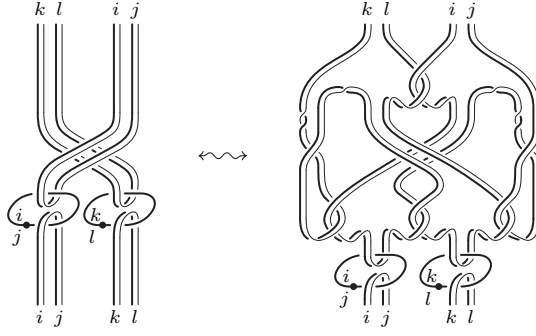


FIGURE 4.3.7. The definition of Φ_n is compatible with (r9)

4.4. The adjoint morphisms

As we have seen in Section 2.3, the *pushing through an 1-handle move* plays an essential role in the definition of the reduction functor $\downarrow_k^n : \mathcal{K}_{n \rightarrow k} \rightarrow \mathcal{K}_k$ for Kirby tangles and in the proof that such functor is a category equivalence.

Now we introduce and study the algebraic analog of such move: the intertwining of a morphism with the adjoint action of the ribbon Hopf algebra on itself. This will be used in Section 4.5 to define the reduction functor between the corresponding algebraic categories.

We remind that the (right) *adjoint action* of a group G on itself is defined by $\text{ad}(x) : g \mapsto g^x = \bar{x}gx$ for any $x, g \in G$. This definition can be extended to an arbitrary groupoid \mathcal{G} just by deleting x and/or \bar{x} from $\bar{x}gx$ when the corresponding composition with g is not defined.

PROPOSITION 4.4.1. *Let \mathcal{G} be a groupoid. Given $x \in \mathcal{G}(i_0, j_0)$, let $_x : \mathcal{G} \rightarrow \mathcal{G}$ be defined on the objects as $i_0^x = j_0$ and $i^x = i$ for $i \neq i_0$, and on the morphisms as*

$$g^x = \begin{cases} \bar{x}gx & \text{if } g \in \mathcal{G}(i_0, i_0), \\ \bar{x}g & \text{if } g \in \mathcal{G}(i_0, j) \text{ with } j \neq i_0, \\ gx & \text{if } g \in \mathcal{G}(i, i_0) \text{ with } i \neq i_0, \\ g & \text{if } g \in \mathcal{G}(i, j) \text{ with } i, j \neq i_0. \end{cases}$$

Denoting by $\mathcal{G}^{\setminus i} \subset \mathcal{G}$ the full subgroupoid of \mathcal{G} with $\text{Obj } \mathcal{G}^{\setminus i} = \text{Obj } \mathcal{G} - \{i\}$ for $i \in \text{Obj } \mathcal{G}$, the following statements hold:

- (a) $_x : \mathcal{G} \rightarrow \mathcal{G}$ is a functor, in particular $(gh)^x = g^x h^x$ and $\overline{g^x} = \bar{g}^x$ for any $g, h \in \mathcal{G}$;
- (b) $(g^x)^y = g^{xy}$ for any $x, y, g \in \mathcal{G}$, that is the functors $_x$ with $x \in \mathcal{G}$ give a right action of \mathcal{G} on itself;
- (c) if $i_0 \neq j_0$, then the image \mathcal{G}^x of $_x$ is the subgroupoid $\mathcal{G}^{\setminus i_0}$ and $_x : \mathcal{G} \rightarrow \mathcal{G}^{\setminus i_0}$ is a left inverse of the inclusion $\mathcal{G}^{\setminus i_0} \subset \mathcal{G}$;
- (d) $_x$ restricts to an equivalence of categories $\mathcal{G}^{\setminus j_0} \rightarrow \mathcal{G}^{\setminus i_0}$, whose inverse $\mathcal{G}^{\setminus i_0} \rightarrow \mathcal{G}^{\setminus j_0}$ is the corresponding restriction of $_{\bar{x}}$ (both are the identity of $\mathcal{G}^{\setminus i_0}$ if $i_0 = j_0$);
- (e) for any $x \in \mathcal{G}(i_0, j_0)$ and $y \in \mathcal{G}(i_0, k_0)$, there exists a natural equivalence $N : _x \rightarrow _y$ such that $N(i_0) = \bar{x}y$ and $N(i) = 1_i$ for $i \neq i_0$.

Proof. All statements are straightforward and left to the reader. \square

Given $x \in \mathcal{G}(i_0, j_0)$, the functor $_x : \mathcal{G} \rightarrow \mathcal{G}$ uniquely extends to a monoidal map $_x : \Pi\mathcal{G} \rightarrow \Pi\mathcal{G}$ given by $\pi^x = (g_1^x, \dots, g_m^x)$ for any $\pi = (g_1, \dots, g_m) \in \Pi\mathcal{G}$, and this in turn induces a monoidal map $_x : \text{Obj } \mathcal{H}^r(\mathcal{G}) \rightarrow \text{Obj } \mathcal{H}^r(\mathcal{G})$, by putting $H_\pi^x = H_{\pi^x}$. Note that the specialization of $_x$ to the case of the groupoid \mathcal{G}_n , coincides the homonymous map defined in Lemma 2.3.6, i.e. given a sequence $\pi \in \Pi\mathcal{G}_n$, π^x is obtained by changing all elements i_0 to j_0 .

The main goal of this section is to construct a monoidal functor $_x : \mathcal{H}^r(\mathcal{G}) \rightarrow \mathcal{H}^r(\mathcal{G})$ which coincides with this map on the objects and it is the algebraic analog of the functor $_x : \mathcal{K}_n \rightarrow \mathcal{K}_n$ defined in Lemma 2.3.6. In particular, we require that the following conditions are satisfied:

- (a) if $x = 1_{i_0}$ then $_x$ is the identity functor;
- (b) given $y \in \mathcal{G}(i_0, k_0)$, there is a natural equivalence

$$\xi^{x,y} : \text{id}_{\bar{y}x} \diamond _x \rightarrow \text{id}_{\bar{y}x} \diamond _y ;$$

that is, to any $\pi \in \Pi\mathcal{G}$ is associated an isomorphism $\xi_\pi^{x,y} : H_{\bar{y}x} \diamond H_\pi^x \rightarrow H_{\bar{y}x} \diamond H_\pi^y$, such that for every morphism $F : H_{\pi_0} \rightarrow H_{\pi_1}$ in $\mathcal{H}^r(\mathcal{G})$ we have

$$(\text{id}_{\bar{y}x} \diamond F^y) \circ \xi_{\pi_0}^{x,y} = \xi_{\pi_1}^{x,y} \circ (\text{id}_{\bar{y}x} \diamond F^x) ;$$

- (c) if $\mathcal{G} = \mathcal{G}_n$, then $\Phi_n(F^x) = \Phi_n(F)^x$ and $\Phi_n(\xi_\pi^{x,y}) = \xi_\pi^{x,y}$ for any $x, y \in \mathcal{G}_n$, $\pi \in \Pi\mathcal{G}_n$ and $F \in \text{Mor } \mathcal{H}_n^r$ (cf. Lemma 2.3.6).

The natural transformation $\xi^{x,y}$ in (b) will be expressed in terms of the categorical generalization of the adjoint action of the ribbon groupoid Hopf algebra on itself. Before introducing this generalization, we remind the definition of the adjoint action in the case of the trivial groupoid.

Let \mathcal{C} be a (strict) braided monoidal category, $(H, m_H, \eta_H, \Delta_H, \varepsilon_H, S_H)$ be a braided Hopf algebra in \mathcal{C} over the trivial groupoid, and A be an algebra in \mathcal{C} with multiplication m_A and unit η_A . We remind that a morphism $\alpha : H \diamond A \rightarrow A$ defines a left action of H on A if the following conditions hold:

$$\alpha \circ (\eta_H \diamond \text{id}_A) = \text{id}_A : A \rightarrow A ;$$

$$\alpha \circ (m_H \circ \text{id}_A) = \alpha \circ (\text{id}_H \diamond \alpha) : H \diamond H \diamond A \rightarrow A ;$$

$$\alpha \circ (\text{id}_H \diamond \eta_A) = \eta_A \circ \varepsilon_H : H \rightarrow A ;$$

$$\alpha \circ (\text{id}_H \diamond m_A) = m_A \circ (\alpha \diamond \alpha) \circ (\text{id}_H \diamond \gamma_{H,A} \diamond \text{id}_A) \circ (\Delta_H \diamond \text{id}_{A \diamond A}) : H \diamond A \diamond A \rightarrow A .$$

The first two conditions express the fact that A is a left H -module, while the last two state that the action intertwines with the multiplication and the unit of A , giving in this way a left H -algebra structure on A (cf. Definition 4.1.2 in [57]). The notion of right action is symmetric and corresponds to a right H -algebra structure on A .

The (left) adjoint action of H on itself is defined as

$$\text{ad}_H = m_H \circ (m_H \diamond S_H) \circ (\text{id}_H \diamond \gamma_{H,H}) \circ (\Delta_H \diamond \text{id}_H) : H \diamond H \rightarrow H .$$

One can introduce analogously the right adjoint action of H on itself, by a symmetric formula with interchanged roles of the two H 's in the source. In the case of a group

algebra and trivial braiding, the formula for the right adjoint action of H on itself coincides with the adjoint action of a group G on itself recalled above.

The fact that these are indeed left and right actions is a classical result and the reader can find the proof in a more general context in Proposition 4.4.3 below. In particular, the adjoint action intertwines with the multiplication and the unit morphisms. On the other hand, in the classical case (trivial braiding) such ac-

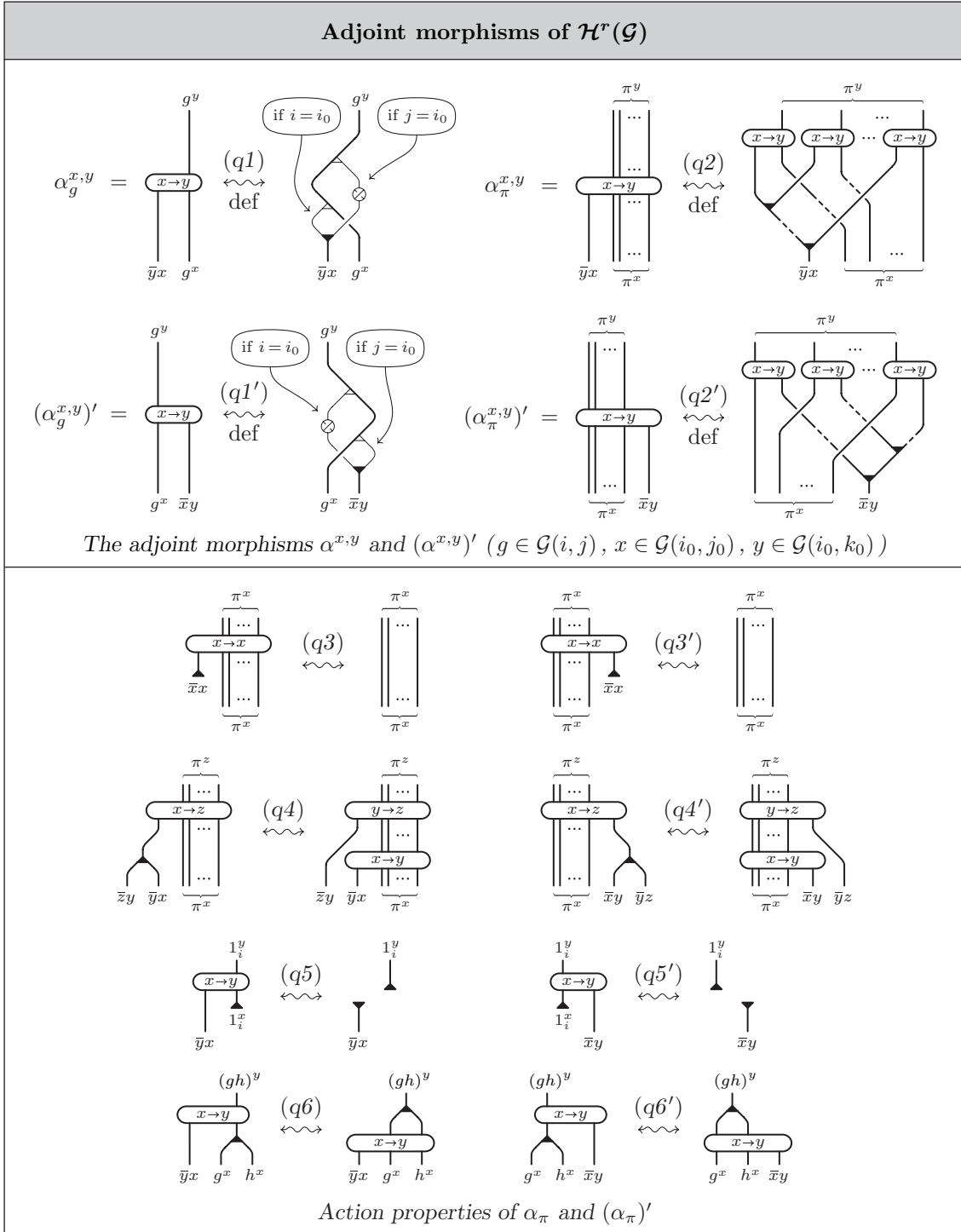


TABLE 4.4.1.

tion is known to intertwine with the comultiplication and the antipode only when the Hopf algebra is cocommutative (see Lemma 5.7.2 in [57]). One of the main results of this section will be that, in the case of a ribbon braided Hopf algebra over the trivial groupoid, the adjoint action intertwines with all elementary morphisms including comultiplication, antipode and braiding (cf. Proposition 4.4.11). Since a ribbon Hopf algebra with non-trivial braiding is not cocommutative, the proof of this fact necessarily makes use of the new ribbon axioms (r8) and (r9) in Table 4.2.13.

Now, we proceed with the generalization of the notion of adjoint action to a groupoid Hopf \mathcal{G} -algebra with a possibly non-trivial groupoid \mathcal{G} .

DEFINITION 4.4.2. Let \mathcal{G} be a groupoid. Given $x \in \mathcal{G}(i_0, j_0)$ and $y \in \mathcal{G}(i_0, k_0)$, for any $\pi \in \Pi\mathcal{G}$ we define the left adjoint morphism $\alpha_\pi^{x,y} : H_{\bar{y}x} \diamond H_\pi^x \rightarrow H_\pi^y$ inductively by the following identities (cf. Table 4.4.1), where $g \in \mathcal{G}(i, j)$ and $\pi = \pi' \diamond \pi''$:

$$\alpha_g^{x,y} = \begin{cases} \varepsilon_{\bar{y}x} \diamond \text{id}_{g^x} & \text{if } i \neq i_0 \neq j, \\ m_{\bar{y}x, g^x} & \text{if } i = i_0 \neq j, \\ m_{g^x, \bar{x}y} \circ (\text{id}_{g^x} \diamond S_{\bar{y}x}) \circ \gamma_{\bar{y}x, g^x} & \text{if } i \neq i_0 = j, \\ m_{\bar{y}x, g^x, \bar{x}y} \circ (m_{\bar{y}x, g^x} \diamond S_{\bar{y}x}) \circ \\ \quad \circ (\text{id}_{\bar{y}x} \diamond \gamma_{\bar{y}x, g^x}) \circ (\Delta_{\bar{y}x} \diamond \text{id}_{g^x}) & \text{if } i = i_0 = j; \end{cases} \quad (q1)$$

$$\alpha_\pi^{x,y} = \alpha_{\pi' \diamond \pi''}^{x,y} = (\alpha_{\pi'}^{x,y} \diamond \alpha_{\pi''}^{x,y}) \circ (\text{id}_{\bar{y}x} \diamond \gamma_{\bar{y}x, \pi'^x} \diamond \text{id}_{\pi''^x}) \circ (\Delta_{\bar{y}x} \diamond \text{id}_{\pi'^x \diamond \pi''^x}). \quad (q2)$$

We also define the symmetric right adjoint morphism $(\alpha_\pi^{x,y})' : H_\pi^x \diamond H_{\bar{x}y} \rightarrow H_\pi^y$ by the following identity (cf. Table 4.4.1), where $\text{sym}(\pi) = \text{sym}(g_1, \dots, g_m) = (\bar{g}_m, \dots, \bar{g}_1)$:

$$(\alpha_\pi^{x,y})' = \text{sym}(\alpha_{\text{sym}(\pi)}^{x,y}).$$

We will use the simplified notation α_π^x and $(\alpha_\pi^y)'$ respectively for $\alpha_\pi^{x, 1_{i_0}} : H_x \diamond H_\pi^x \rightarrow H_\pi$ and $(\alpha_\pi^{1_{i_0}, y})' : H_\pi^y \diamond H_y \rightarrow H_\pi$.

We emphasize that in the definition above H_π^x and H_π^y should not be thought as objects of $\mathcal{H}^r(\mathcal{G})$, but instead as pairs (H_π, x) and (H_π, y) , and similarly π^x and π^y in the corresponding diagrams should not be thought as sequences in $\Pi\mathcal{G}$, but instead as pairs (π, x) and (π, y) . This requires that both the algebraic and the graphical notation keep track of such pairs. Actually, it is enough to specify the target or the source, since one of them determines the other. The only exception to such a rule will be in the case of $x = y = 1_i$, when we will write simply $\alpha_\pi^{1_i} : H_{1_i} \diamond H_\pi \rightarrow H_\pi$ and $(\alpha_\pi^{1_i})' : H_\pi \diamond H_{1_i} \rightarrow H_\pi$, where H_π stays for $H_\pi^{1_i}$. In particular, in the expression $\alpha_\pi^{1_i} : H_{1_i} \diamond H_{\pi^z} \rightarrow H_{\pi^z}$, π^z should be interpreted as an element in $\Pi\mathcal{G}$, and H_{π^z} stays for $H_{\pi^z}^{1_i}$.

PROPOSITION 4.4.3. The adjoint morphisms α and α' defined by the identities (q1) and (q2) above satisfy all the action properties in Table 4.4.1, for any $x \in \mathcal{G}(i_0, j_0)$, $y \in \mathcal{G}(i_0, k_0)$, $z \in \mathcal{G}(i_0, l_0)$ and $\pi \in \Pi\mathcal{G}$, with arbitrary composable $g, h \in \mathcal{G}$ and $i \in \text{Obj}\mathcal{G}$. In particular, $\alpha_\pi^{1_i}$ (resp. $(\alpha_\pi^{1_i})'$) makes H_π into a left (resp. right) H_{1_i} -module, for any $i \in \text{Obj}\mathcal{G}$.

Proof. Up to symmetry, the properties (q3') to (q6') of the morphisms α' are equivalent the corresponding properties (q3) to (q6) of the morphisms α , hence it suffices to prove the latter ones.

Identity (q3) is an immediate consequences of axioms (a4-4') and (a7) in Table 4.1.1 and property (s6) in Table 4.1.2. To prove (q4), we first consider the special case when $\pi = g \in \mathcal{G}$ in Figure 4.4.2. Then, the general case follows by the inductive argument shown in Figure 4.4.3.

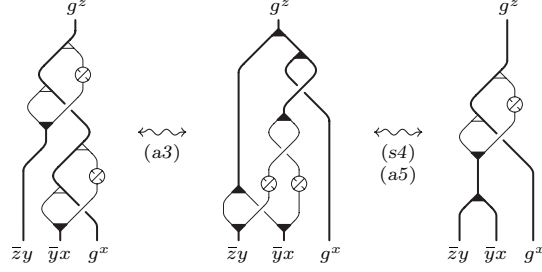


FIGURE 4.4.2. Proof of (q4): the case of $\pi = g \in \mathcal{G}$ [a/123, s/125]

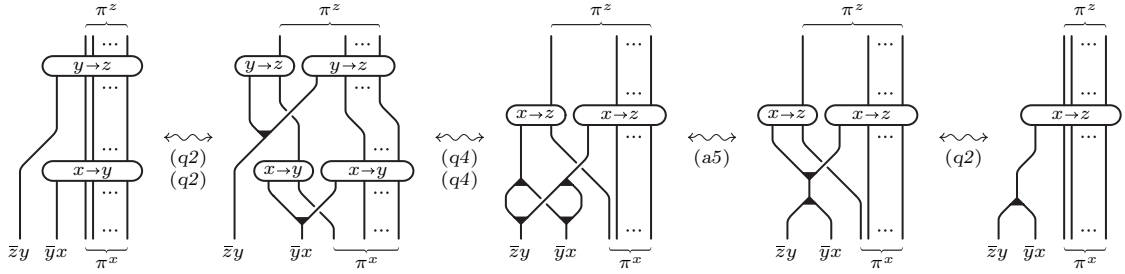


FIGURE 4.4.3. Proof of (q4): the inductive step [a/123, q/148]

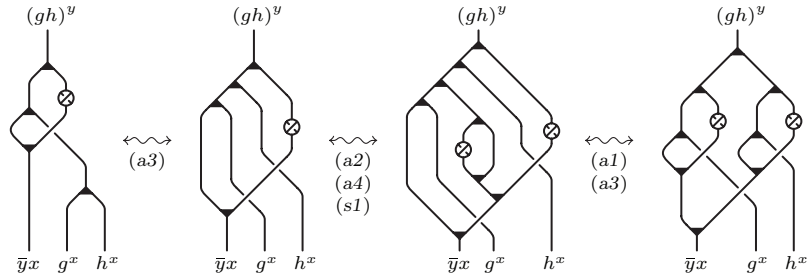


FIGURE 4.4.4. Proof of (q6) for $g, h \in \mathcal{G}(i_0, i_0)$ ($x \in \mathcal{G}(i_0, j_0)$ and $y \in \mathcal{G}(i_0, k_0)$) [a-s/123]

Identity (q5) is trivial for $i \neq i_0$, while it follows from axioms (a4) and (s1') in Table 4.1.1 for $i = i_0$. Finally, identity (q6) is considered in Figure 4.4.4, in the case when $g, h \in \mathcal{G}(i_0, i_0)$. For the other cases, one can just delete the proper edges from the diagrams in that figure. \square

REMARK 4.4.4. In the case when $\mathcal{G} = \mathcal{G}_1$ is the trivial groupoid, the unique left (resp. right) adjoint morphism $\alpha = \alpha_1^{(1,1)}$ (resp. $\alpha' = (\alpha_1^{(1,1)})'$) in Definition 4.4.2 gives the left (resp. right) adjoint action of $H = H_{(1,1)}$ on itself. In the general case, according to what we said after the definition, the left (resp. right) adjoint morphisms $\alpha_g^{x,y}$ (resp. $(\alpha_g^{x,y})'$) can be thought in a certain sense to act on the product $H \times \mathcal{G}$ of the Hopf \mathcal{G} -algebra $H = \{H_g\}_{g \in \mathcal{G}}$ with the groupoid \mathcal{G} itself.

Before going on, we prove the properties of the adjoint morphisms listed in Table 4.4.5. These will be used to define the functor ${}_x : \mathcal{H}^r(\mathcal{G}) \rightarrow \mathcal{H}^r(\mathcal{G})$ and the natural transformation $\xi^{x,y}$ which relates ${}_x$ and ${}_y$ for composable \bar{y} and x .

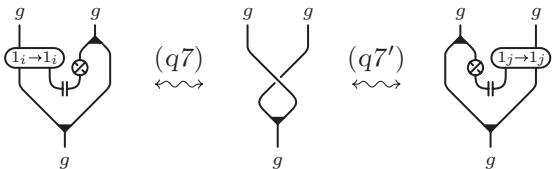
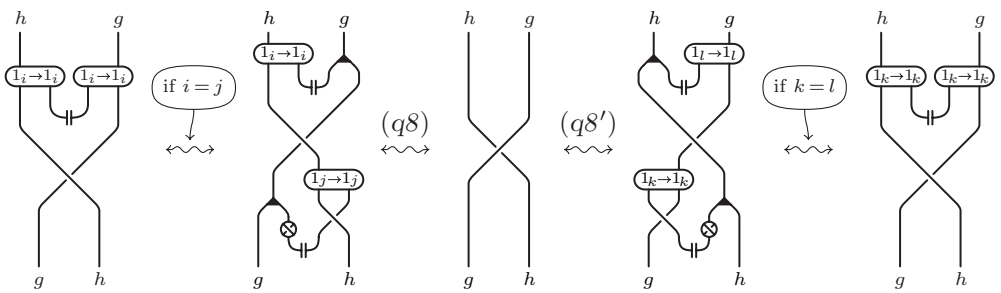
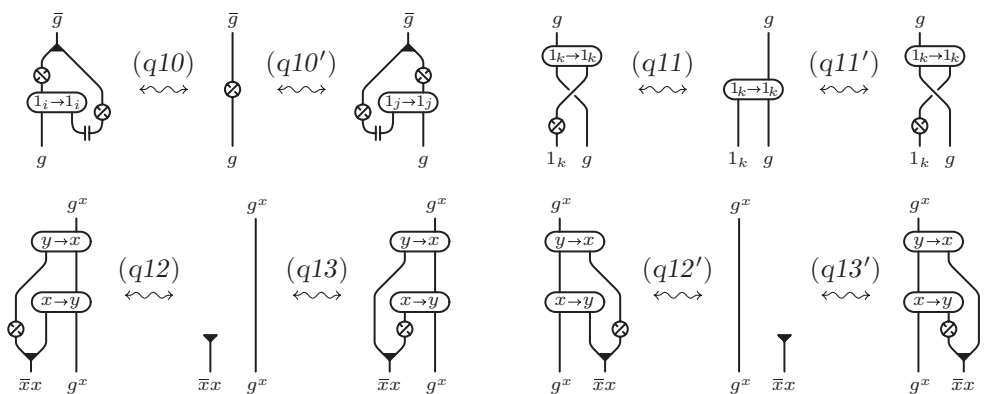
Properties of the adjoint morphisms of $\mathcal{H}^r(\mathcal{G})$				
 <p style="margin: 0;">Equivalent forms of the axiom (r8) ($g \in \mathcal{G}(i, j)$)</p>				
 <p style="margin: 0;">Equivalent forms of the axiom (r9) ($g \in \mathcal{G}(i, j), h \in \mathcal{G}(k, l)$)</p>				
 <p style="margin: 0;">Other relations ($g \in \mathcal{G}(i, j)$)</p>				

TABLE 4.4.5.

PROPOSITION 4.4.5. *The properties in Table 4.4.5 hold in $\mathcal{H}^r(\mathcal{G})$. Moreover, modulo the other axioms of $\mathcal{H}^r(\mathcal{G})$, (r8) is equivalent to either (q7) or (q7'), while (r9) is equivalent to either (q8), (q8'), (q9) or (q9').*

Proof. We can limit ourselves to prove properties (q7) to (q13), since the corresponding primed properties are the symmetric of them under the functor sym . Actually, (q11') becomes the symmetric of (q11) after composition with the isomorphism $\gamma_{g,1_k} \circ S_{1_k}$.

Property (q12) is proved in Figure 4.4.6, and (q13) can be proved in a similar way, by using (s1') instead of (s1). We observe that the proof of (q4), and therefore that of (q12), uses only the axioms of $\mathcal{H}_v^u(\mathcal{G})$.

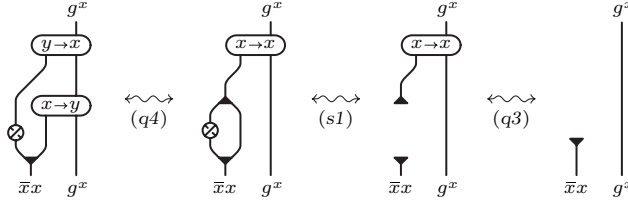


FIGURE 4.4.6. Proof of (q12) [q/148, s/123]

Relation (q7) is obtained in the top line of Figure 4.4.7. The bottom line of the same figure shows that (q7) implies (r8) modulo the relations of $\mathcal{H}_v^u(\mathcal{G})$, including (q13') (see above). Actually, the two moves (r7') in the figure occur only when both the involved copairings are non-trivial, that is when $i = j$.

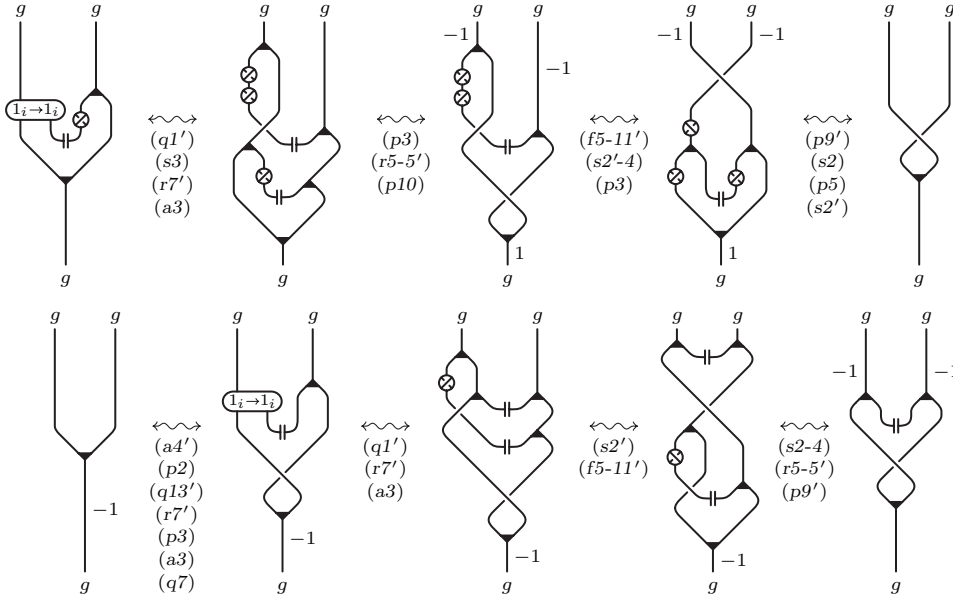


FIGURE 4.4.7. Equivalence between (q7) and (r8) ($g \in \mathcal{G}(i, j)$) [a/123, f/129-134, p/134-140, q/148-151, r/132-134, s/123-125]

Then, we can derive (q11) and (q10) in the order, as described in Figures 4.4.8 and 4.4.9 respectively. In steps four and six of the former figure relation (t2) is used instead of (p14') and (p15') when $i \neq k$, while in the latter it is used instead of (p15) when $i \neq j$.

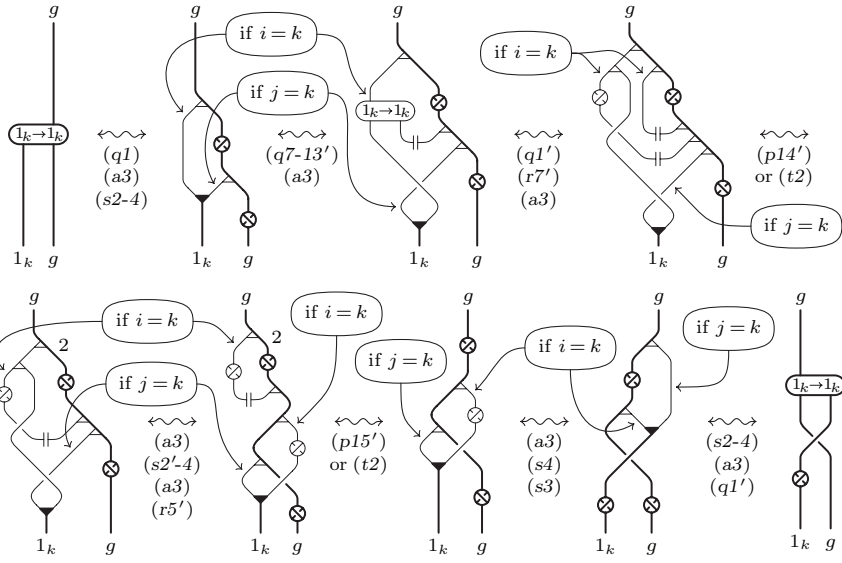


FIGURE 4.4.8. Proof of $(q11)$ ($g \in \mathcal{G}(i, j)$) [a/123, p/140, q/148-151, r/134, s/125, t/140]

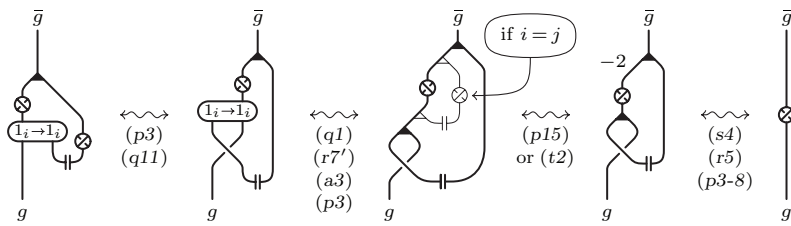


FIGURE 4.4.9. Proof of $(q10)$ ($g \in \mathcal{G}(i, j)$) [a/123, p/134-140, q/148-151, r/132-134, s/125]

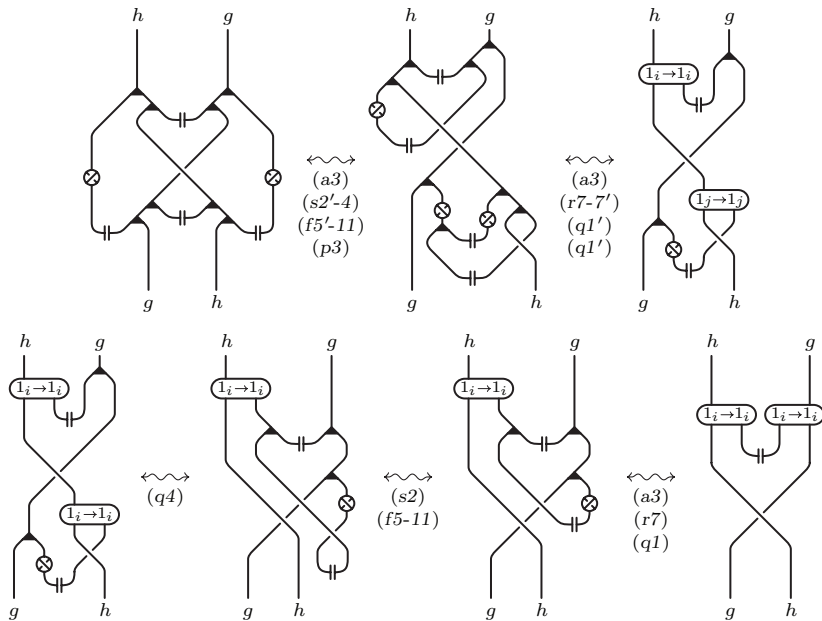


FIGURE 4.4.10. Equivalence between $(r9)$ and $(q8)$ ($g \in \mathcal{G}(i, j)$) [a/123, f/129-134, p/134, q/148-151, r/132-134, s/123-125]

Finally, we are left with (q8) and (q9). A straightforward application of (q12-12') and (q13-13') shows that the diagrams in (q9) represent the inverse morphisms of those represented by the diagrams in (q8), which gives the equivalence between (q8) and (q9). Then, it suffices to verify that (r9) is equivalent to (q8) modulo the axioms of $\mathcal{H}_v^u(\mathcal{G})$. This is done in the top line of Figure 4.4.10. Like above, the moves (r7-7') occur only when both the involved copairings are non-trivial, that is when the corresponding optional edges in the resulting $(\alpha_h^{1i})'$ and $(\alpha_h^{1j})'$ are present. In the bottom line of the same figure we obtain the special form for $i = j$, starting from the last diagram in the top line. \square

Now we will use the left adjoint morphisms to define the algebraic analog of the family of isomorphisms $\xi_\pi^{x,y}$, introduced in Lemma 2.3.6. Like in the case of the category of Kirby tangles, such isomorphisms will eventually define a natural transformation between the functors ${}_x$ and ${}_y$.

DEFINITION 4.4.6. Given $x \in \mathcal{G}(i_0, j_0)$ and $y \in \mathcal{G}(i_0, k_0)$, we define the family of morphisms $\xi_\pi^{x,y} \in \mathcal{H}^r(\mathcal{G})$ for any $\pi \in \Pi\mathcal{G}$ as follows (see Figure 4.4.11):

$$\xi_\pi^{x,y} = (\text{id}_{\bar{y}x} \diamond \alpha_\pi^{x,y}) \circ (\Delta_{\bar{y}x} \diamond \text{id}_{\pi^x}) : H_{\bar{y}x} \diamond H_\pi^x \rightarrow H_{\bar{y}x} \diamond H_\pi^y.$$

We will use the simplified notation ξ_π^x for $\xi_\pi^{x,1_{i_0}} : H_x \diamond H_\pi^x \rightarrow H_x \diamond H_\pi$.

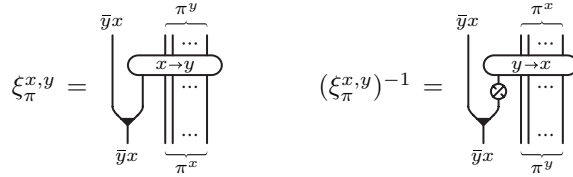


FIGURE 4.4.11.

PROPOSITION 4.4.7. For any $x \in \mathcal{G}(i_0, j_0)$, $y \in \mathcal{G}(i_0, k_0)$ and $\pi \in \Pi\mathcal{G}$ the morphism $\xi_\pi^{x,y}$ is invertible and its inverse is (see Figure 4.4.11):

$$(\xi_\pi^{x,y})^{-1} = (\text{id}_{\bar{y}x} \diamond \alpha_\pi^{y,x}) \circ (\text{id}_{\bar{y}x} \diamond S_{\bar{y}x} \diamond \text{id}_{\pi^y}) \circ (\Delta_{\bar{y}x} \diamond \text{id}_{\pi^y}) : H_{\bar{y}x} \diamond H_\pi^y \rightarrow H_{\bar{y}x} \diamond H_\pi^x.$$

Proof. This is a direct consequence of properties (q12-13) in Table 4.4.5. \square

The next proposition makes into a formal statement the idea that the isomorphisms $\xi_\pi^{x,y} \in \text{Mor } \mathcal{H}_n^r$ given by the above definition for $\mathcal{G} = \mathcal{G}_n$ are nothing else than the algebraic counterpart, under the functors Φ_n defined in Section 4.3, of the homonymous isomorphisms $\xi_\pi^{x,y} \in \text{Mor } \mathcal{K}_n$ introduced in Section 2.3.

PROPOSITION 4.4.8. Given $x = (i_0, j_0)$ and $y = (i_0, k_0)$ in \mathcal{G}_n , for any $\pi \in \Pi\mathcal{G}_n$ we have that $\Phi_n(H_\pi^x) = I_\pi^x$ and $\Phi_n(\xi_\pi^{x,y}) = \xi_\pi^{x,y}$ (cf. Lemma 2.3.6).

Proof. The identity on the objects follows immediately from the definition of Φ_n . For the one on the morphisms, a straightforward verification shows that

$$\xi_{\pi' \diamond \pi''}^{x,y} = (\xi_{\pi'}^{x,y} \diamond \xi_{\pi''}^{x,y}) \circ (\text{id}_{\bar{y}x} \diamond \gamma_{\bar{y}x, \pi'^x} \diamond \text{id}_{\pi''^x}) \circ (\Delta_{\bar{y}x} \diamond \text{id}_{\pi'^x \diamond \pi''^x})$$

holds in both the categories \mathcal{H}_n^r and \mathcal{K}_n . Hence, it suffices to consider the elementary case of $\xi_{(i,j)}^{x,y}$ with $(i, j) \in \mathcal{G}_n$. We leave to the reader to check that $\Phi_n(\xi_{(i,j)}^{x,y}) = \xi_{(i,j)}^{x,y}$ holds for all possible combinations of indices, but Figure 4.4.12 should be helpful. \square

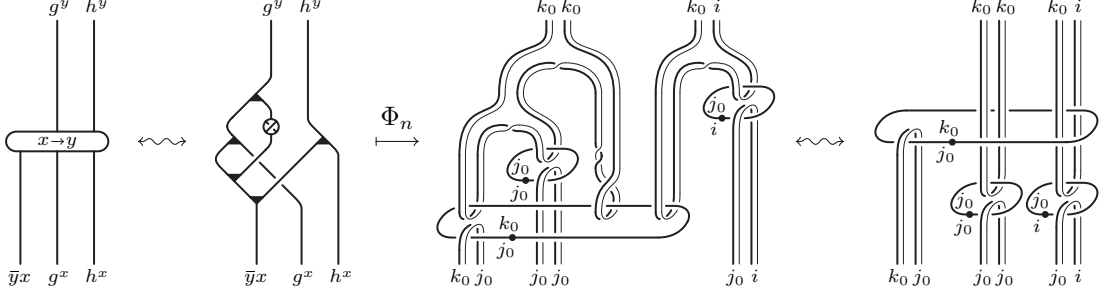


FIGURE 4.4.12. $(x = (i_0, j_0), y = (i_0, k_0), g = (i_0, i_0), h = (i_0, i)$ with $i \neq i_0$)

At this point, we can proceed with the main result of this section, which is the algebraic analog of Lemma 2.3.6.

As the first step, given $x \in \mathcal{G}(i_0, j_0)$, we define F^x for any elementary morphism F of $\mathcal{H}^r(\mathcal{G})$. The most obvious definition, consisting in the formal extension of $_x : \mathcal{G} \rightarrow \mathcal{G}$ with $_x$ acting on the indices, works for $i_0 = j_0$ but it runs into problems for $i_0 \neq j_0$, due to the fact that in the latter case the copairing σ_{i_0, j_0} is trivial, while $\sigma_{i_0^x, j_0^x} = \sigma_{j_0, j_0}$ is not. Thus, some corrections are needed. Since we want to have $\Phi_n(F)^x = \Phi_n(F^x)$ for any morphism F in \mathcal{H}^r_n , the reader can realize the nature of these corrections by looking at the $\Phi_n(F)^x$'s in Figures 2.3.14, 2.3.15 and 2.3.16 (cf. Lemma 2.3.6 and the discussion following it).

DEFINITION 4.4.9. We define $_x$ on the elementary morphisms of $\mathcal{H}^r(\mathcal{G})$ by putting, for any $i, j, k, l \in \text{Obj } \mathcal{G}$, $g \in \mathcal{G}(i, j)$ and $h \in \mathcal{G}(k, l)$, with $j = k$ for $m_{g, h}$:

$$(\eta_i)^x = \eta_{i^x}; \quad (m_{g, h})^x = m_{g^x, h^x}; \quad (\varepsilon_g)^x = \varepsilon_{g^x}; \quad (l_i)^x = l_{i^x}; \quad (L_g)^x = L_{g^x}; \quad (v_g)^x = v_{g^x};$$

$$(\Delta_g)^x = \begin{cases} \mu_{g^x, g^x}^{-1} \circ \Delta_{g^x} = (S_{g^x} \circ v_{g^x}^{-1}) \diamond (S_{g^x} \circ v_{g^x}^{-1}) \circ \Delta_{g^x} \circ \bar{S}_{g^x} \circ v_{g^x} & \text{if } i \neq i_0 = j, \\ \Delta_{g^x} & \text{otherwise;} \end{cases}$$

$$(S_g)^x = \begin{cases} m_{g^x, 1_i} \circ (S_{g^x} \diamond \text{id}_{1_i}) \circ \rho_{g^x, i} = \bar{S}_{g^x} \circ v_{g^x}^2 & \text{if } i \neq i_0 = j, \\ S_{g^x} & \text{otherwise;} \end{cases}$$

$$(\bar{S}_g)^x = \begin{cases} m_{g^x, 1_i} \circ (\bar{S}_{g^x} \diamond S_{1_i}) \circ \rho_{g^x, i} = S_{g^x} \circ v_{g^x}^{-2} & \text{if } i = i_0 \neq j, \\ \bar{S}_{g^x} & \text{otherwise.} \end{cases}$$

$$(\gamma_{g, h})^x = \begin{cases} \gamma_{g^x, h^x} & \text{if } i = i_0 = j, \\ ((\alpha_h^{x, x} \circ \bar{\gamma}_{h^x, 1_{j_0}}) \diamond \text{id}_{g^x}) \circ (\text{id}_{h^x} \diamond \rho_{j_0, g^x}) \circ \gamma_{g^x, h^x} & \text{if } i \neq i_0 = j, \\ \gamma_{g^x, h^x} \circ (\text{id}_{g^x} \diamond (\alpha_h^{x, x} \circ (S_{1_{j_0}} \diamond \text{id}_{h^x}))) \circ (\rho_{g^x, j_0} \diamond \text{id}_{h^x}) & \text{if } i = i_0 \neq j, \\ ((\alpha_h^{x, x} \circ \bar{\gamma}_{h^x, 1_{j_0}}) \diamond \text{id}_{g^x}) \circ (\text{id}_{h^x} \diamond \rho_{j_0, g^x}) \circ \gamma_{g^x, h^x} \circ \\ \circ (\text{id}_{g^x} \diamond (\alpha_h^{x, x} \circ (S_{1_{j_0}} \diamond \text{id}_{h^x}))) \circ (\rho_{g^x, j_0} \diamond \text{id}_{h^x}) & \text{if } i \neq i_0 \neq j; \end{cases}$$

$$(\bar{\gamma}_{g, h})^x = \begin{cases} \bar{\gamma}_{g^x, h^x} & \text{if } i = i_0 = j, \\ (\text{id}_{h^x} \diamond \alpha_g^{x, x}) \circ (\rho_{h^x, j_0} \diamond \text{id}_{g^x}) \circ \bar{\gamma}_{g^x, h^x} & \text{if } i \neq i_0 = j, \\ \bar{\gamma}_{g^x, h^x} \circ ((\alpha_g^{x, x} \circ \bar{\gamma}_{g^x, 1_{j_0}} \circ (\text{id}_{g^x} \diamond \bar{S}_{1_{j_0}})) \diamond \text{id}_{h^x}) \circ (\text{id}_{g^x} \diamond \rho_{j_0, h^x}) & \text{if } i = i_0 \neq j, \\ (\text{id}_{h^x} \diamond \alpha_g^{x, x}) \circ (\rho_{h^x, j_0} \diamond \text{id}_{g^x}) \circ \bar{\gamma}_{g^x, h^x} \circ \\ \circ ((\alpha_g^{x, x} \circ \bar{\gamma}_{g^x, 1_{j_0}} \circ (\text{id}_{g^x} \diamond \bar{S}_{1_{j_0}})) \diamond \text{id}_{h^x}) \circ (\text{id}_{g^x} \diamond \rho_{j_0, h^x}) & \text{if } i \neq i_0 \neq j; \end{cases}$$

Then, according to relation (r6) in Table 4.2.1, we also put:

$$(\sigma_{i,j})^x = \begin{cases} \eta_{j_0} \diamond \eta_{j_0} & \text{if } \{i, j\} = \{i_0, j_0\} \text{ and } i_0 \neq j_0, \\ \sigma_{i^x, j^x} & \text{otherwise.} \end{cases}$$

The diagrams of $(\Delta_g)^x$, $(S_g)^x$ and $(\bar{S}_g)^x$ are presented in Figure 4.4.13, while those of $(\gamma_{g,h})^x$ and $(\bar{\gamma}_{g,h})^x$ are presented in Figure 4.4.14 (here, the antipodes have been moved by (p3) just for pictorial convenience). The equivalences in Figure 4.4.14 can be obtained by moves symmetric to those in the top line of Figure 4.4.10 performed in the reversed order.

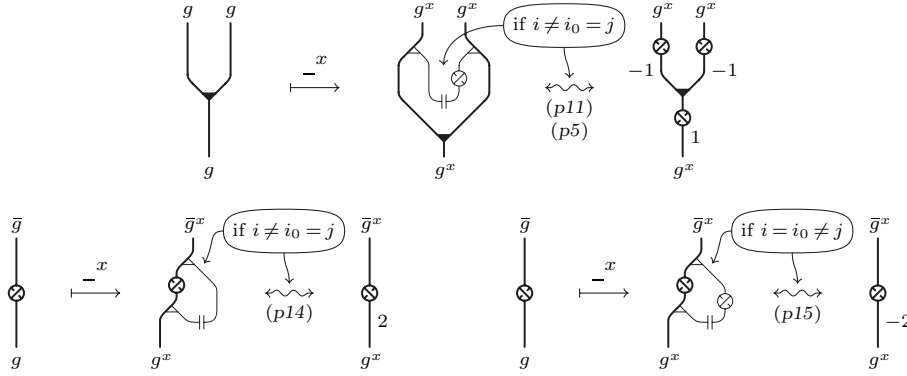


FIGURE 4.4.13. $(\Delta_g)^x$, $(S_g)^x$ and $(\bar{S}_g)^x$ ($g \in \mathcal{G}(i, j)$ and $x \in \mathcal{G}(i_0, j_0)$) [p/134-140]

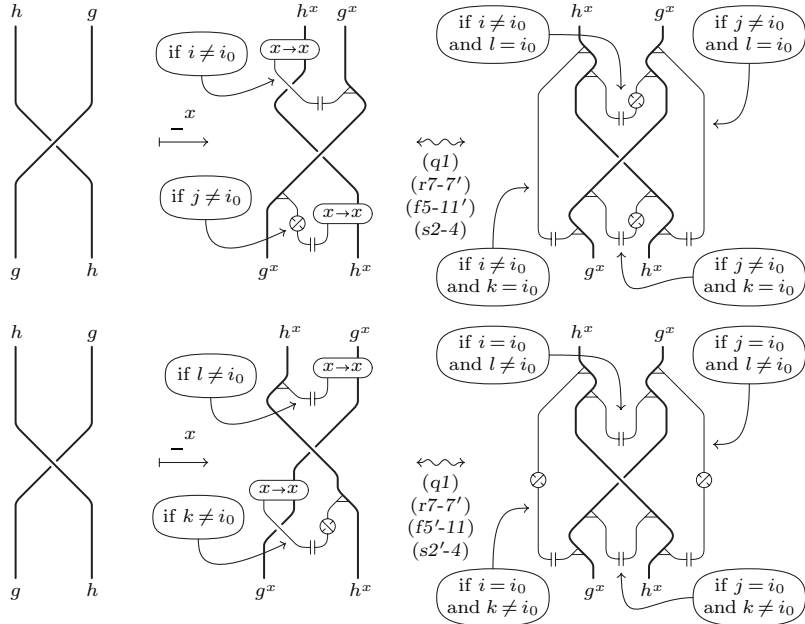


FIGURE 4.4.14. $(\gamma_{g,h})^x$ and $(\bar{\gamma}_{g,h})^x$ ($g \in \mathcal{G}(i, j)$, $h \in \mathcal{G}(k, l)$ and $x \in \mathcal{G}(i_0, j_0)$) [f/129-134, q/148, r/132-134, s/123-125]

We observe that all the corrections to the formal extension of $_x : \mathcal{G} \rightarrow \mathcal{G}$ to the elementary morphisms are inessential when $i_0 = j_0$, being the involved copairings trivial in this case. Moreover, if $i_0 \neq j_0$ then all conditions requiring that certain

index is $\neq i_0$ (resp. $\neq j_0$) can be replaced by $= j_0$ (resp. $= i_0$), because only in that case the copairing involved is non-trivial. The reason for applying the corrections even in some inessential cases, like we did with crossing changes when defining $_x$ for Kirby tangles in Section 2.3, is that this simplifies some proofs in the following. In particular, the proof of property (q15) in Table 4.4.15 below for $i_0 = j_0$, which is far from being trivial in spite of the triviality of $_x$ as a formal extension, will split into subcases of other cases.

It is also worth noticing that the righthand diagrams in Figures 4.4.13 and 4.4.14 are not symmetric, because of the conditions controlling the presence of the optional edges. In other words, our definition of $_x$ on the elementary morphisms does not commute with the symmetry functor sym .

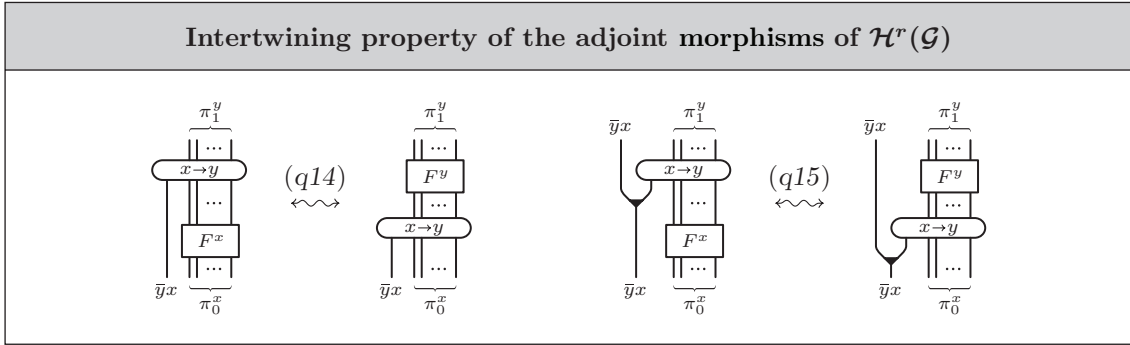


TABLE 4.4.15.

LEMMA 4.4.10. *Given $x \in \mathcal{G}(i_0, j_0)$ and $y \in \mathcal{G}(i_0, k_0)$, the properties (q14) and (q15) shown in Table 4.4.15 hold for F being any elementary morphism of $\mathcal{H}^r(\mathcal{G})$.*

Proof. We can limit ourselves to the proof of (q14), since (q15) can be obtained from it, essentially by composing with $\Delta_{\bar{y}x} \diamond \text{id}_{\pi_0^x}$.

For $F = \eta_i$ and $F = m_{g,h}$ (q14) coincides with action properties (q5) and (q6) respectively, and it was already established in Proposition 4.4.3. Moreover, the identity (q14) for $F = \sigma_{i,j}$ follows from the ones for the other elementary morphisms, being the definition of $(\sigma_{i,j})^x$ based on (r6).

Before considering the rest of the elementary morphisms, we notice that, when F is invertible, the identity (q14) for F implies the one for F^{-1} , once we have checked that $(F^{-1})^x = (F^x)^{-1}$. This is trivially true for $F = S_g$, while it can be easily verified for $F = \gamma_{g,h}$ by using moves (r7-7') and (q12-13) in Tables 4.2.1, 4.2.2 and 4.4.5.

Hence, we are reduced to proving (q14) for $F = l_i, \varepsilon_g, L_g, v_g, \Delta_g, S_g, \gamma_{g,h}$ with $i \in \text{Obj } \mathcal{G}$, $g \in \mathcal{G}(i, j)$ and $h \in \mathcal{G}(k, l)$, and any $x \in \mathcal{G}(i_0, j_0)$ and $y \in \mathcal{G}(i_0, k_0)$.

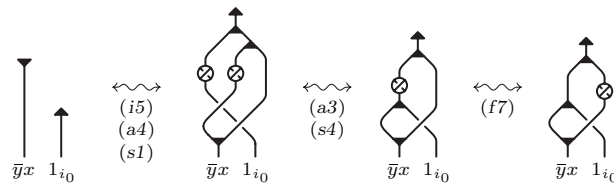


FIGURE 4.4.16. Proof of (q14) for $F = l_{i_0}$ ($x \in \mathcal{G}(k_0, i_0)$ and $y \in \mathcal{G}(j_0, k_0)$)
[a/123, i-f/129, s/123-125]

$F = l_i$. If $i \neq i_0$ there is nothing to prove, being $\xi_{1_i}^{x,y}$ trivial and $F^x = F^y = F$. The case when $i = i_0$ is shown in Figure 4.4.16.

$F = \varepsilon_g, L_g, v_g$. The statements follow respectively from (a6) in Table 4.1.1, (i2-2') in Table 4.1.2 and (r5-5') in Table 4.2.1 and 4.2.2, modulo the relations (a2-2') in Table 4.1.1 and (s5) in Table 4.1.2 in the first two cases.

$F = \Delta_g$. As above, there is nothing to prove for $g \in \mathcal{G}(i, j)$ with $i, j \neq i_0$. For $g \in \mathcal{G}(i_0, j)$ with $j \neq i_0$, the statement essentially reduces to the relation (a5) in Table 4.1.1. The proof for $g \in \mathcal{G}(i, i_0)$ with $i \neq i_0$ is presented in Figure 4.4.17, while the case $g \in \mathcal{G}(i_0, i_0)$ is shown in Figure 4.4.18. The first step of the latter

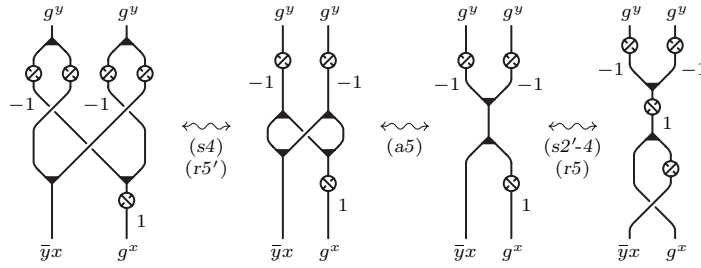


FIGURE 4.4.17. Proof of (q14) for $F = \Delta_g$ with $g \in \mathcal{G}(i, i_0)$ and $i \neq i_0$ ($x \in \mathcal{G}(i_0, j_0)$ and $y \in \mathcal{G}(i_0, k_0)$) [a/123, r/132-134, s/125]

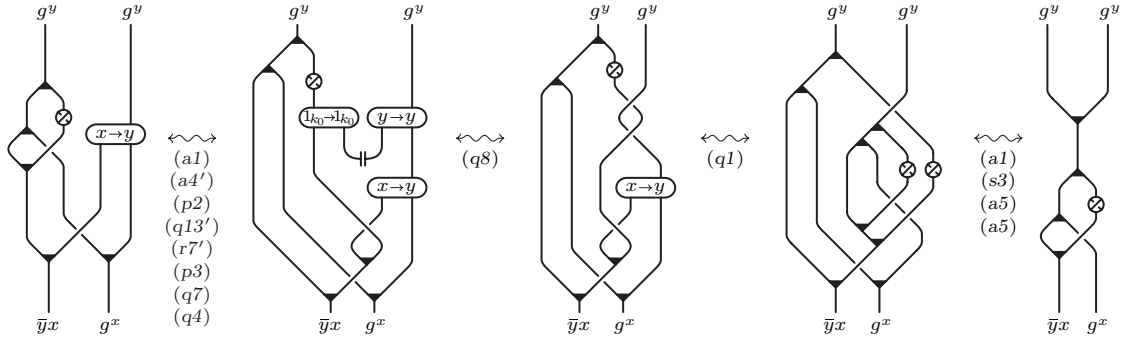


FIGURE 4.4.18. Proof of (q14) for $F = \Delta_g$ with $g \in \mathcal{G}(i_0, i_0)$ ($x \in \mathcal{G}(i_0, j_0)$ and $y \in \mathcal{G}(i_0, k_0)$) [a/123, p/134, q/148-151, s/123-125]

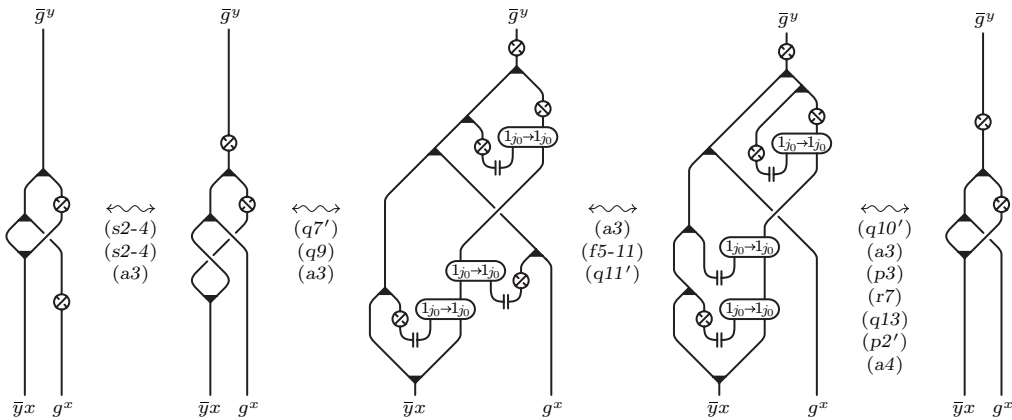


FIGURE 4.4.19. Proof of (q14) for $F = S_g$ with $g \in \mathcal{G}(i_0, i_0)$ ($x \in \mathcal{G}(i_0, j_0)$ and $y \in \mathcal{G}(i_0, k_0)$) [a/123, f/129-134, q/151, s/125]

figure goes like in the first step of the second line of Figure 4.4.7. Moreover, before applying (q8) in the second step, we replace the morphism $\alpha_g^{y,y}$ with the formally identical one $\alpha_g^{1_{k_0}}$.

F = S_g. If $g \in \mathcal{G}(i, j)$ with $i, j \neq i_0$ there is nothing to prove, being $\alpha_g^{x,y}$ trivial and $(S_g)^x = (S_g)^y = S_g$. When $g \in \mathcal{G}(i, i_0)$ with $i \neq i_0$ or $g \in \mathcal{G}(i_0, j)$ with $j \neq i_0$, the statement is equivalent to the property (s4) of the antipode in Table 4.1.2. Figure 4.4.19 addresses the case of $g \in \mathcal{G}(i_0, i_0)$.

F = $\gamma_{g,h}$. We first prove that $(\gamma_{g,h})^x$ and $(\bar{\gamma}_{g,h})^x$ can be represented by the diagrams depicted in Figure 4.4.20. Since these diagrams can be easily seen to be inverse to one another by using the relations (r7'), (q4) and (q12-13) in Tables 4.2.2, 4.4.1 and 4.4.5, it suffices to consider $(\gamma_{g,h})^x$.

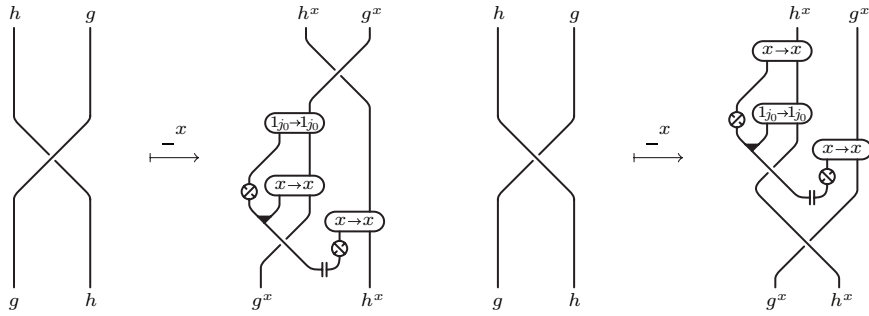


FIGURE 4.4.20. Equivalent forms of $(\gamma_{g,h})^x$ and $(\bar{\gamma}_{g,h})^x$ ($x \in \mathcal{G}(i_0, j_0)$)

Look at the diagram corresponding to $(\gamma_{g,h})^x$ in Figure 4.4.20. When $i_0 = j_0$, we can substitute $\alpha_{g^x}^{1_{j_0}}$ with $\alpha_g^{x,x}$ and cancel this with the preexisting one by move (q12) in Table 4.4.5. After that also $\alpha_h^{x,x}$ can be deleted to get γ_{g^x,h^x} , which in this case is equal to $(\gamma_{h,g})^x$ as we noticed above.

Now assume $i_0 \neq j_0$. We have already observed that in this case the condition $i \neq i_0$ (resp. $j \neq i_0$) in the definition of $(\gamma_{g,h})^x$ (cf. Figure 4.4.14) is equivalent to $i = j_0$ (resp. $j = j_0$). Then, Figures 4.4.21 and 4.4.22 deal with the cases $g \in \mathcal{G}(i_0, j)$ and $g \in \mathcal{G}(j_0, j)$ respectively. For $g \in \mathcal{G}(i, j)$ with $i \neq i_0, j_0$, we refer again to Figure 4.4.21, noting that the second diagram in the figure is directly isotopic to the fourth one, once the edges marked with an asterisk in the expansions of the α 's are deleted.

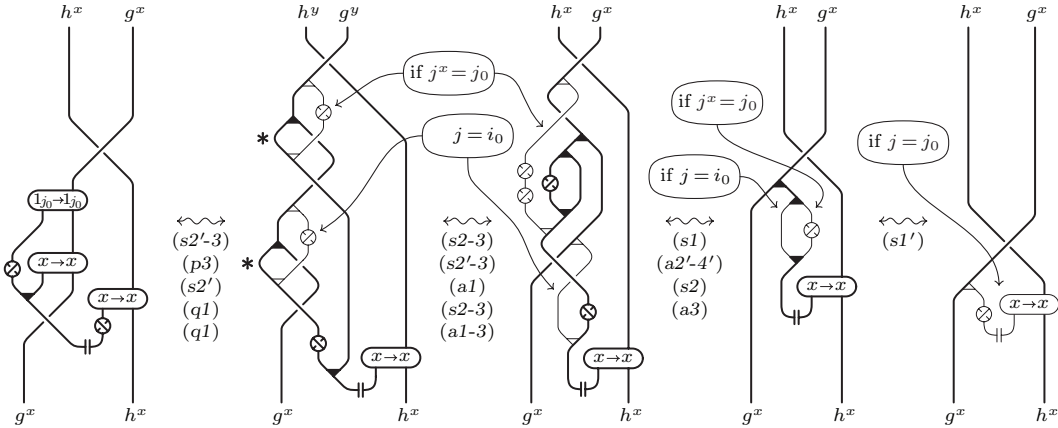


FIGURE 4.4.21. ($g \in \mathcal{G}(i_0, j)$ and $x \in \mathcal{G}(i_0, j_0)$) [a/123, q/148, s/123-125]

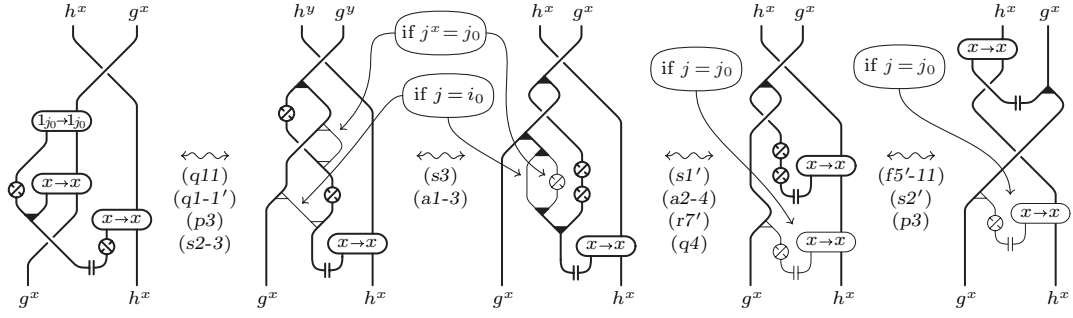


FIGURE 4.4.22. ($g \in \mathcal{G}(j_0, j)$ and $x \in \mathcal{G}(i_0, j_0)$) [a/123, f/129-134, p/134, q/148-151, r/134, s/123-125]

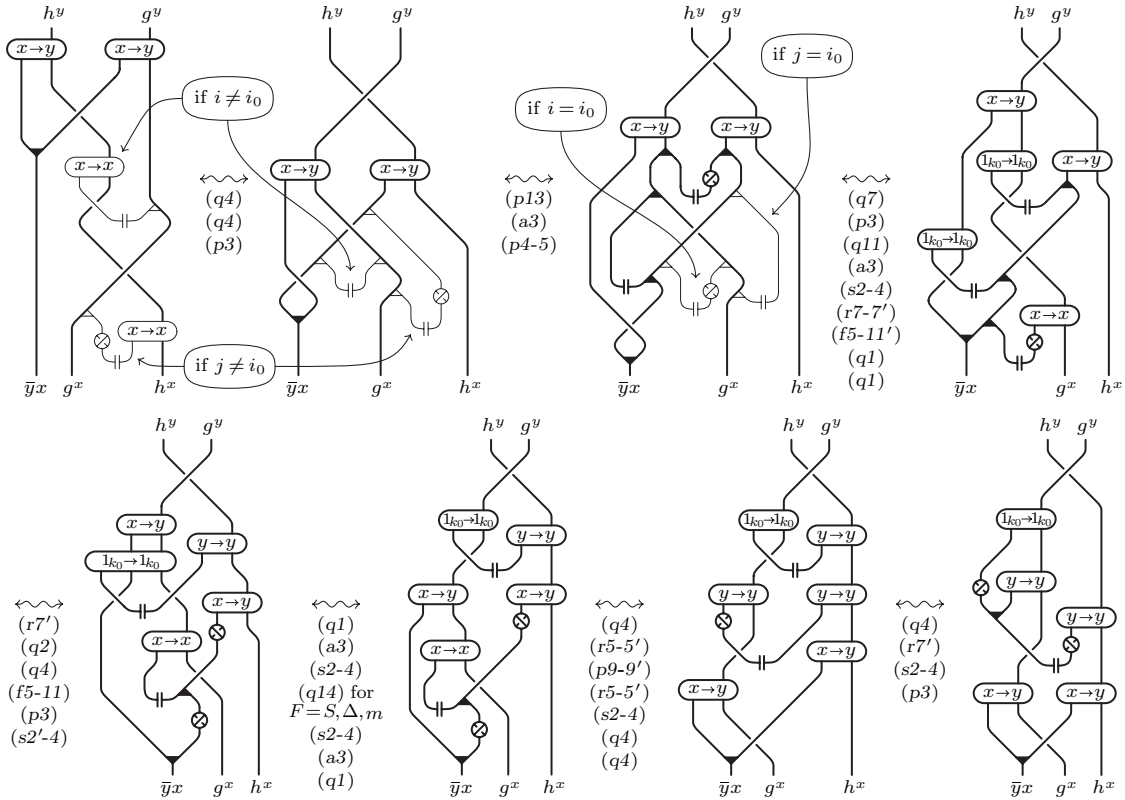


FIGURE 4.4.23. Proof of (q14) for $\gamma_{g,h}$ ($x \in \mathcal{G}(i_0, j_0)$ and $y \in \mathcal{G}(i_0, k_0)$) [a/123, f/129-134, p/134-140, q/148-151-157, r/132-134, s/123-125]

At this point, identity (q14) for $\gamma_{g,h}$ is proved in Figure 4.4.23, where $(\gamma_{g,h})^x$ in the first diagram has the original form, while $(\gamma_{g,h})^y$ in the last diagram has the equivalent form given above. We note that the top line ends with two applications of (q1) to get $\alpha_g^{x,x}$ and $\alpha_{g^{k_0}}^1$ in the fourth diagram. The conditions of the corresponding optional edges in the third diagram are explicitly indicated for $\alpha_g^{x,x}$, while they are implicitly provided by the copairings occurring in them for $\alpha_{g^{k_0}}^1$. Moreover, we observe that the second diagram in the bottom line is obtained from the first one, by moving $\alpha_g^{x,y}$ down and letting it pass through $\alpha_{\bar{y}^{k_0}}^1$. This can be done thanks to the identity (q14) we have already proved for the elementary morphisms S , Δ and m , once $\alpha_g^{x,y}$ has been transformed as in the first step of Figure 4.4.8. \square

Below, \mathcal{G}^i denotes the full subgroupoid of \mathcal{G} with $\text{Obj } \mathcal{G}^i = \text{Obj } \mathcal{G} - \{i\}$ (cf. Proposition 4.4.1) and $\mathcal{H}^r(\mathcal{G}^i) \subset \mathcal{H}^r(\mathcal{G})$ is the universal ribbon Hopf algebra constructed on \mathcal{G}^i , with the inclusion given by Proposition 4.2.14.

PROPOSITION 4.4.11. *Let \mathcal{G} be a groupoid. For any $x \in \mathcal{G}(i_0, j_0)$ the map $\bar{_}^x : \text{Obj } \mathcal{H}^r(\mathcal{G}) \rightarrow \text{Obj } \mathcal{H}^r(\mathcal{G})$ defined after Proposition 4.4.1 extends to a monoidal functor*

$$\bar{_}^x : \mathcal{H}^r(\mathcal{G}) \rightarrow \mathcal{H}^r(\mathcal{G}),$$

which transforms the elementary morphisms according to in Definition 4.4.9, and satisfies the following properties:

(a) if $i_0 \neq j_0$ then $(\mathcal{H}^r(\mathcal{G}))^x \subset \mathcal{H}^r(\mathcal{G}^{\setminus i_0})$, hence there is an induced functor

$$\bar{_}^x : \mathcal{H}^r(\mathcal{G}) \rightarrow \mathcal{H}^r(\mathcal{G}^{\setminus i_0});$$

(b) $\bar{_}^x$ restricts to the identity on $\mathcal{H}^r(\mathcal{G}^{\setminus i_0})$ and to an equivalence of categories $\mathcal{H}^r(\mathcal{G}^{\setminus j_0}) \rightarrow \mathcal{H}^r(\mathcal{G}^{\setminus i_0})$, whose inverse is given by the restriction of $\bar{_}^x$ to $\mathcal{H}^r(\mathcal{G}^{\setminus i_0})$;

(c) for any other $y \in \mathcal{G}(i_0, k_0)$, the isomorphisms $\xi_\pi^{x,y}$ introduced in Definition 4.4.6 (cf. Proposition 4.4.7) give a natural equivalence

$$\xi^{x,y} : \text{id}_{\bar{y}x} \diamond \bar{_}^x \rightarrow \text{id}_{\bar{y}x} \diamond \bar{_}^y,$$

i.e. for any morphism $F : H_{\pi_0} \rightarrow H_{\pi_1}$ in $\mathcal{H}^r(\mathcal{G})$ we have (cf. Table 4.4.15):

$$\xi_{\pi_1}^{x,y} \circ (\text{id}_{\bar{y}x} \diamond F^x) = (\text{id}_{\bar{y}x} \diamond F^y) \circ \xi_{\pi_0}^{x,y}. \quad (q15)$$

Proof. We want to show that the propagation of the definition of $\bar{_}^x$ over products and compositions is well-defined, i.e. it preserves all the axioms relating the elementary morphisms in $\mathcal{H}^r(\mathcal{G})$ presented in Tables 4.1.1, 4.1.8, 4.2.1 and 4.2.13. This will give us the functor $\bar{_}^x : \mathcal{H}^r(\mathcal{G}) \rightarrow \mathcal{H}^r(\mathcal{G})$.

We only need to consider the case $i_0 \neq j_0$, since for $i_0 = j_0$ the map $\bar{_}^x$ acts as identity on the elementary morphisms.

Let us begin with the braid axioms in Table 4.1.1. The preservation of (b1) and (b2) is equivalent to the identity $(\gamma_{g,h}^{-1})^x = ((\gamma_{g,h})^x)^{-1}$, which was already discussed at the beginning of the proof of Lemma 4.4.10. Move (b3) is trivially preserved.

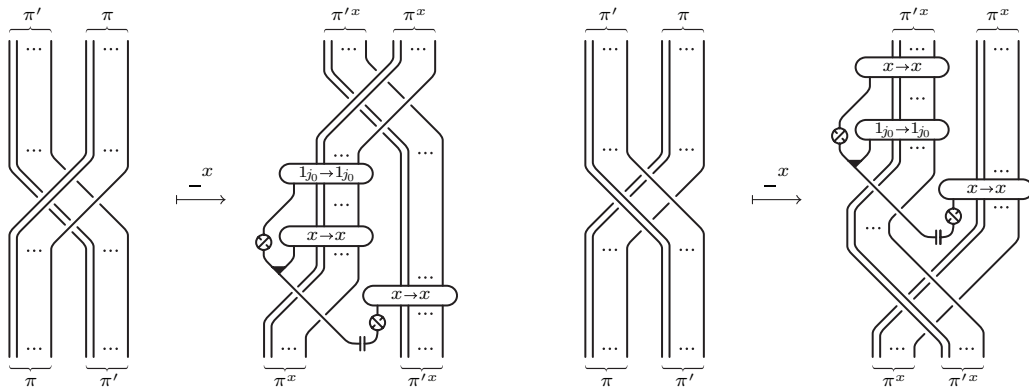


FIGURE 4.4.24. $(\gamma_{\pi, \pi'})^x$ and $(\bar{\gamma}_{\pi, \pi'})^x$ ($x \in \mathcal{G}(i_0, j_0)$)

To deal with moves $(b4-4')$, we first prove that the alternative form provided in Figure 4.4.20 for $(\gamma_{g,h})^x$ and $(\bar{\gamma}_{g,h})^x$ can be generalized to $(\gamma_{\pi,\pi'})^x$ and $(\bar{\gamma}_{\pi,\pi'})^x$ for any $\pi, \pi' \in \Pi\mathcal{G}$, as shown in Figure 4.4.24. Actually, only the cases when $\pi = (g_1, g_2)$ and $\pi' = h$ or $\pi = g$ and $\pi' = (h_1, h_2)$ are needed for our purposes. We derive these cases for $(\bar{\gamma}_{\pi,\pi'})^x$ in Figures 4.4.25 and 4.4.26 respectively, while leaving to the reader to see that the same argument also allows to prove the general case, by a double induction on the lengths of π and π' . Then, the expression for $(\gamma_{\pi,\pi'})^x$ follows, being the inverse of that for $(\bar{\gamma}_{\pi,\pi'})^x$.

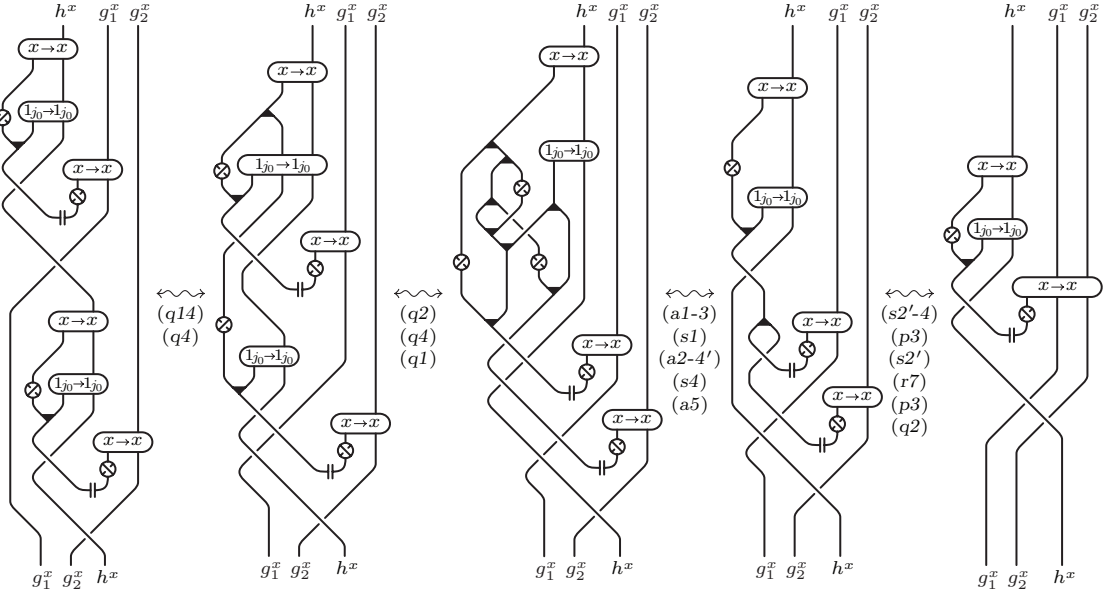


FIGURE 4.4.25. Deriving $(\bar{\gamma}_{(g_1, g_2), h})^x$ ($x \in \mathcal{G}(i_0, j_0)$) [a/123, p/134, q/148-157, r/132, s/123-125]

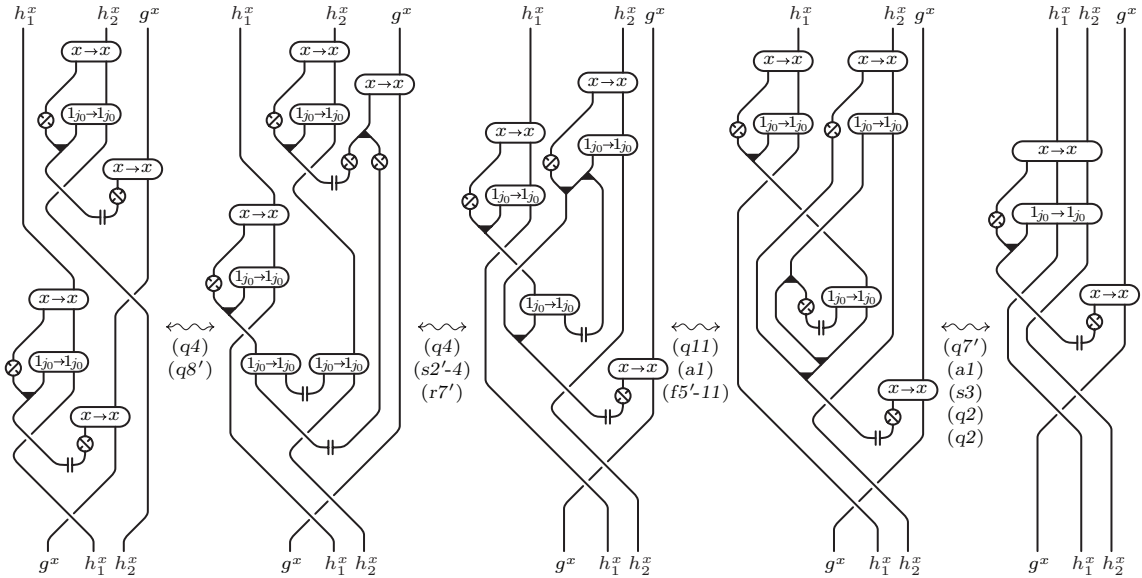


FIGURE 4.4.26. Deriving $(\bar{\gamma}_{g, (h_1, h_2)})^x$ ($x \in \mathcal{G}(i_0, j_0)$) [a/123, f/129-134 q/148-151, r/134, s/123-125]

Now, using the form of $(\gamma_{\pi,\pi'})^x$ in Figure 4.4.24, the preservation of (b4-4') follows from the special cases of (q14) for $\alpha^{x,x}$ and α^{1j_0} .

We continue with the bi-algebra axioms in Table 4.1.1. The only non-trivial ones are (a1), (a2) and (a5) when g or h are in $\mathcal{G}(j_0, i_0)$. In this case, (a1) and (a2) follow directly from the definition of $(\Delta_g)^x$ in the rightmost diagram in Figure 4.4.13. The proof of (a5) for $g \in \mathcal{G}(j_0, i_0)$ and $h \in \mathcal{G}(i_0, i_0)$ is presented in Figure 4.4.27. For different choices of g and h we have analogous or simpler proofs.

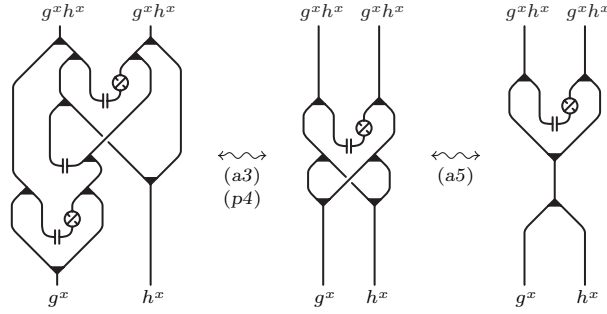


FIGURE 4.4.27. $-^x$ preserves (a5) for $g \in \mathcal{G}(j_0, i_0)$ and $h \in \mathcal{G}(i_0, i_0)$ ($x \in \mathcal{G}(i_0, j_0)$) [a/123, p/134]

From the antipode axioms in Table 4.1.1 the only non-trivial ones are (s1) and (s1') for $g \in \mathcal{G}(j_0, i_0)$. Figure 4.4.28 proves the preservation of (s1) in this case, while the proof for (s1') is obtained by symmetry.

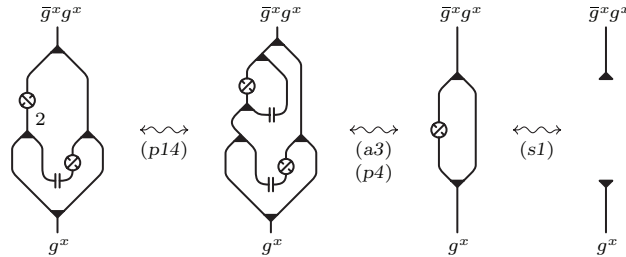


FIGURE 4.4.28. $-^x$ preserves (s1) for $g \in \mathcal{G}(j_0, i_0)$ ($x \in \mathcal{G}(i_0, j_0)$) [a/123, p/134-140, s/123]

The integral axioms in Table 4.1.8 are trivially preserved because $(m_{g,h})^x = m_{g^x,h^x}$ and $(\Delta_{1_i})^x = \Delta_{1_i^x}$.

Also the ribbon axioms in Table 4.2.1 are trivially preserved, while the only non-trivial cases in Table 4.2.13 are (r8) when $g \in \mathcal{G}(j_0, i_0)$ and (r9) with $g \in \mathcal{G}(i, j)$ and $h \in \mathcal{G}(k, l)$ such that some of i, j are equal to i_0 and some of k, l are equal to j_0 or vice versa. Figure 4.4.29 deals with the above-mentioned case of (r8). Some of the cases of (r9) are presented in Figure 4.4.30 (cf. expression of $(\sigma_{i,j})^x$ on page 156) and the others are analogous. This concludes the proof of the functoriality of $-^x$.

At this point, thanks to the functoriality of $-^x$, the validity of identity (q15), already known from Lemma 4.4.10 for F being an elementary morphism, extends to any other morphism F . This gives the naturality of $\xi^{x,y}$ stated in point (c).

Finally, we observe that the definition $-^x$ on the elementary morphisms of $\mathcal{H}^r(\mathcal{G})$ which do not involve i_0 or j_0 coincides with the formal extension of $-^x$ (cf. Figures

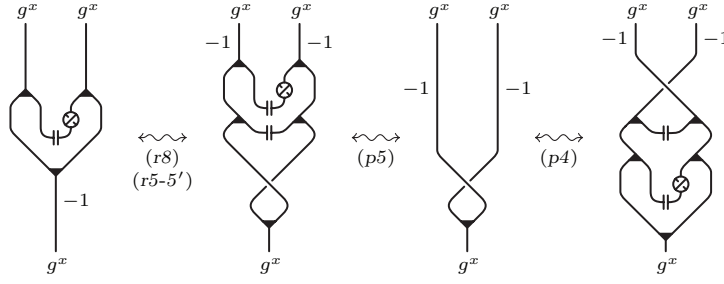


FIGURE 4.4.29. $_x$ preserves (r8) when $g \in \mathcal{G}(j_0, i_0)$ ($x \in \mathcal{G}(i_0, j_0)$) [p/134, r/132-134-140]

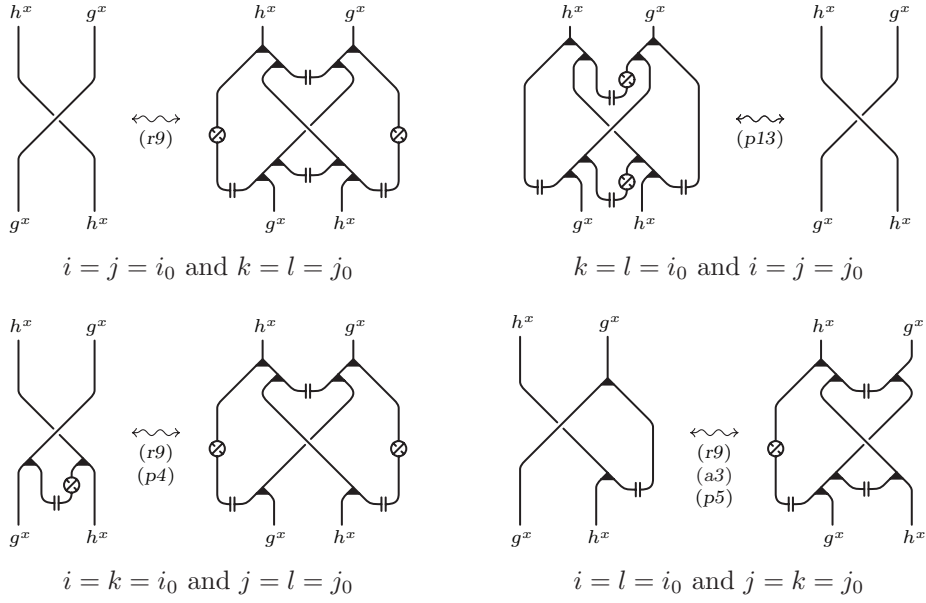


FIGURE 4.4.30. $_x$ preserves (r9) ($g \in \mathcal{G}(i, j)$, $h \in \mathcal{G}(k, l)$, $x \in \mathcal{G}(i_0, j_0)$) [p/134-140, r/140]

4.4.13 and 4.4.14). This fact together with Proposition 4.4.1 (d) imply points (a) and (b) of the statement. \square

PROPOSITION 4.4.12. For $x = (i_0, j_0) \in \mathcal{G}_n$, the following diagram commutes.

$$\begin{array}{ccc}
 \mathcal{H}_n^r & \xrightarrow{\Phi_n} & \mathcal{K}_n \\
 _x \downarrow & & \downarrow _x \\
 \mathcal{H}_n^r & \xrightarrow{\Phi_n} & \mathcal{K}_n
 \end{array}$$

Proof. We remind that both functors $_x : \mathcal{K}_n \rightarrow \mathcal{K}_n$ and $_x : \mathcal{H}_n^r \rightarrow \mathcal{H}_n^r$ are the identities when $i_0 = j_0$. Moreover, when $i_0 \neq j_0$, they still leave unchanged diagrams and Kirby tangles where no label i_0 occurs, while they just replace any label i_0 with j_0 in the diagrams and Kirby tangles where no label j_0 occurs.

This shows that $\Phi_n(F^x) = \Phi_n(F)^x$ when $x = (i_0, i_0)$ or $F \in \mathcal{H}_n^r$ is an elementary morphism which does not contain at least one of the labels i_0 or j_0 . Therefore, it

remains to check such identity for elementary morphisms $F \in \mathcal{H}_n^r$ that contain both i_0 and j_0 with $i_0 \neq j_0$.

The cases $F = \Delta_{(j_0, i_0)}, S_{(j_0, i_0)}, \bar{S}_{(i_0, j_0)}$ can be checked directly by comparing the $\Phi_n(F)^x$'s in Figures 2.3.14 and 2.3.16 with the definitions of $(\Delta_{(j_0, i_0)})^x, (S_{(j_0, i_0)})^x$ and $(\bar{S}_{(i_0, j_0)})^x$ (see Definition 4.4.9 and Figure 4.4.13).

When $F = \gamma_{(i, j), (k, l)}$ or $F = \bar{\gamma}_{(k, l), (i, j)}$ with some of k, l equal to i_0 , we observe that the copairings which appear in F^x (see Definition 4.4.9 and Figure 4.4.14) have the effect of pulling the strings labeled i_0 above the ones labeled j_0 in $\Phi_n(F)$ (cf. Figure 4.3.7), obtaining this way $\Phi_n(F)^x$. For example, Figure 2.3.15 depicts the $\Phi_n(F)^x$'s corresponding to the F^x 's on the left of the arrows in Figure 4.4.30.

In all the other cases, no corrections occur in Definition 4.4.9 of F^x and also $\Phi_n(F)^x$ differs from $\Phi_n(F)$ only for the replacement of labels i_0 with j_0 , since $\Phi_n(F)$ admits a strictly regular planar diagram where the paths labeled i_0 pass over the ones of label j_0 . \square

4.5. The stabilization and reduction functors \uparrow_X and \downarrow_X

Based on the results of the previous section, we are now ready to define the reduction functors in the context of the universal algebraic categories. This will be done in a way completely analogous to what we did in Section 2.3 for Kirby tangles, even if we will continue to work in the more general framework of Hopf algebras over an arbitrary groupoid.

We remind that to any (small) category we can associate an oriented graph whose vertices are the objects of the category and whose edges are its morphisms/arrows. We will use the same notation for the category and its graph.

DEFINITION 4.5.1. Let $\mathcal{G} \subset \mathcal{G}'$ be a (strict) full inclusion of groupoids such that the quotient \mathcal{G}'/\mathcal{G} of the graph of \mathcal{G}' by the one of \mathcal{G} is connected. Then a sequence $X = (x_n, \dots, x_1) \in \Pi(\mathcal{G}' - \mathcal{G})$ will be called a *spanning sequence* for the pair $(\mathcal{G}', \mathcal{G})$ if its image $(x_n, \dots, x_1)/\mathcal{G} \subset \mathcal{G}'/\mathcal{G}$ forms a spanning tree for \mathcal{G}'/\mathcal{G} with all edges oriented towards the root and $(x_i, \dots, x_1)/\mathcal{G} \subset \mathcal{G}'/\mathcal{G}$ is still a tree for each $i < n$.

Given a full inclusion of groupoids $\iota : \mathcal{G} \rightarrow \mathcal{G}'$ and a spanning sequence X for $(\mathcal{G}', \mathcal{G})$, let $\Upsilon_X = \Upsilon_\iota : \mathcal{H}^r(\mathcal{G}) \rightarrow \mathcal{H}^r(\mathcal{G}')$ denote the faithful functor induced by ι (cf. Proposition 4.2.14).

PROPOSITION 4.5.2. Let $\mathcal{G} \subset \mathcal{G}'$ be a full inclusion of groupoids and $X = (x_n, \dots, x_1)$ be a spanning sequence for $(\mathcal{G}', \mathcal{G})$. Then, the map:

$$\uparrow_X H_\pi = H_X \diamond H_\pi \text{ for any } H_\pi \in \text{Obj } \mathcal{H}^r(\mathcal{G}),$$

$$\uparrow_X F = \text{id}_X \diamond \Upsilon_X(F) \text{ for any } F \in \text{Mor } \mathcal{H}^r(\mathcal{G}),$$

defines a functor $\uparrow_X : \mathcal{H}^r(\mathcal{G}) \rightarrow \mathcal{H}^r(\mathcal{G}')$, called the *X-stabilization functor*. Moreover, if $\mathcal{G}' \subset \mathcal{G}''$ is another full inclusion of groupoids and $Y = (y_m, \dots, y_1)$ is a spanning sequence for $(\mathcal{G}'', \mathcal{G}')$, then $\uparrow_Y \circ \uparrow_X = \uparrow_{Y \cup X}$, where $Y \cup X = (y_m, \dots, y_1, x_n, \dots, x_1)$ is a spanning sequence for $(\mathcal{G}'', \mathcal{G})$.

Proof. All statements are straightforward. \square

We remind that the definition of the comultiplication can be extended to $\Delta_\pi : H_\pi \rightarrow H_\pi \diamond H_\pi$ for any $\pi \in \Pi\mathcal{G}$ (see Figure 4.5.1) in the following way:

$$\Delta_\pi = \Delta_{\pi' \diamond \pi''} = (\text{id}_{\pi'} \diamond \gamma_{\pi', \pi''} \diamond \text{id}_{\pi''}) \circ (\Delta_{\pi'} \diamond \Delta_{\pi''}).$$

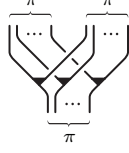


FIGURE 4.5.1. The comultiplication morphism Δ_π in $\mathcal{H}^r(\mathcal{G})$

DEFINITION 4.5.3. Given a full inclusion of groupoids $\mathcal{G} \subset \mathcal{G}'$ and a spanning sequence $X = (x_n, \dots, x_1)$ for $(\mathcal{G}', \mathcal{G})$, we say that a morphism $F : H_X \diamond H_{\pi_0} \rightarrow H_X \diamond H_{\pi_1}$ in $\mathcal{H}^r(\mathcal{G})$ is *X-reducible* if it is equivalent to one in the form

$$F = (\text{id}_X \diamond G) \circ (\Delta_X \diamond \text{id}_{\pi_0}),$$

for some morphism $G : H_X \diamond H_{\pi_0} \rightarrow H_{\pi_1}$ in $\mathcal{H}^r(\mathcal{G}')$ (see Figure 4.5.2).

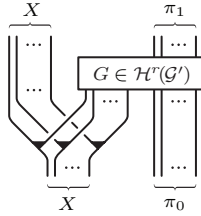


FIGURE 4.5.2. The generic *X*-reducible morphism $F \in \mathcal{H}_X^r(\mathcal{G}')$

The composition of two *X*-reducible morphisms is still *X*-reducible (by the coassociativity) and we denote by $\mathcal{H}_X^r(\mathcal{G}')$ the subcategory of $\mathcal{H}^r(\mathcal{G}')$, whose objects are $H_X \diamond H_\pi$ with $H_\pi \in \text{Obj } \mathcal{H}^r(\mathcal{G}')$ and whose morphisms are *X*-reducible morphisms.

Analogously to the categories of reducible Kirby tangles and reducible ribbon surface tangles, also $\text{Mor}_{\mathcal{H}_X^r(\mathcal{G}')}$ can be endowed with a product structure $\diamond : \text{Mor}_{\mathcal{H}_X^r(\mathcal{G}')} \times \text{Mor}_{\mathcal{H}_X^r(\mathcal{G}')} \rightarrow \text{Mor}_{\mathcal{H}_X^r(\mathcal{G}')}$ as follows. The product of two morphisms $F = (\text{id}_X \diamond G) \circ (\Delta_X \diamond \text{id}_{\pi_0})$ and $F' = (\text{id}_X \diamond G') \circ (\Delta_X \diamond \text{id}_{\pi'_0})$ of $\mathcal{H}_X^r(\mathcal{G}')$ is defined by (see Figure 4.5.3)

$$\begin{aligned} F \diamond F' &= F \circ (\text{id}_X \diamond \gamma_{\pi'_1, \pi_0}) \circ (F' \diamond \text{id}_{\pi_0}) \circ (\text{id}_X \diamond \gamma_{\pi'_0, \pi_0}^{-1}) \\ &= (\text{id}_X \diamond G \diamond G') \circ (\Delta_X \diamond \gamma_{X, \pi_0} \diamond \text{id}_{\pi'_0}) \circ (\Delta_X \diamond \text{id}_{\pi_0 \diamond \pi'_0}). \end{aligned}$$

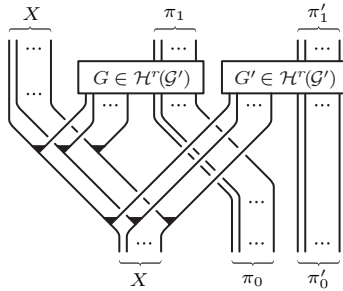


FIGURE 4.5.3. The product $F \diamond F'$ of two morphisms in $\mathcal{H}_X^r(\mathcal{G}')$

The coassociativity property of Δ implies the associativity of \diamond , while id_X is its unit. Observe also that \diamond does not define a monoidal structure on $\mathcal{H}_X^r(\mathcal{G}')$, since it does not intertwine with the composition.

PROPOSITION 4.5.4. *Given a full inclusion of groupoids $\mathcal{G} \subset \mathcal{G}'$ and a spanning sequence X for $(\mathcal{G}', \mathcal{G})$, we have $\uparrow_X \mathcal{H}^r(\mathcal{G}) \subset \mathcal{H}_X^r(\mathcal{G}')$. Moreover, for any two morphisms $F, F' \in \mathcal{H}^r(\mathcal{G})$, we have $\uparrow_X(F \diamond F') = \uparrow_X F \diamond \uparrow_X F'$. In particular, \diamond induces a monoidal structure on $\uparrow_X \mathcal{H}^r(\mathcal{G})$.*

Proof. Figure 4.5.4 shows that the X -stabilization of a morphism $F \in \mathcal{H}^r(\mathcal{G})$ is X -reducible, in other words $\uparrow_X \mathcal{H}^r(\mathcal{G})$ is a subcategory of $\mathcal{H}_X^r(\mathcal{G}')$. The rest of the statement is straightforward. \square

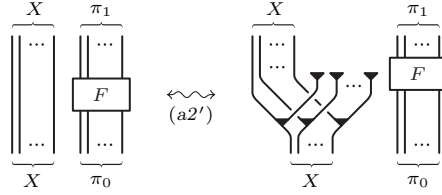


FIGURE 4.5.4. Stabilizations are reducible [a/123]

Our goal is to prove that $\uparrow_X : \mathcal{H}^r(\mathcal{G}) \rightarrow \mathcal{H}_X^r(\mathcal{G}')$ is actually an equivalence of categories. Like we did in Section 2.3 for Kirby tangles, we will show this by defining a reduction functor $\downarrow_X : \mathcal{H}_X^r(\mathcal{G}') \rightarrow \mathcal{H}^r(\mathcal{G})$ which, up to natural equivalence, is the inverse of the stabilization functor. We first consider the case when the spanning sequence X consists of a single element $x \in \mathcal{G}'$, that is $X = (x)$. In this case, we use the simplified notations $\mathcal{H}_x^r(\mathcal{G}') = \mathcal{H}_{(x)}^r(\mathcal{G}')$, $\uparrow_x = \uparrow_{(x)}$ and $\downarrow_x = \downarrow_{(x)}$.

DEFINITION 4.5.5. Let \mathcal{G} be a groupoid. Given $x \in \mathcal{G}(i_0, j_0)$ with $i_0 \neq j_0$, considered as a spanning sequence for $(\mathcal{G}, \mathcal{G}^{\setminus i_0})$, we define the *elementary reduction functor* $\downarrow_x : \mathcal{H}_x^r(\mathcal{G}) \rightarrow \mathcal{H}^r(\mathcal{G}^{\setminus i_0})$, by putting

$$\downarrow_x(H_x \diamond H_\pi) = H_{\pi^x}$$

for any object $H_x \diamond H_\pi$ of $\mathcal{H}_x^r(\mathcal{G})$, and (see Figure 4.5.5)

$$\downarrow_x F = (\varepsilon_{1_{j_0}} \diamond \text{id}_{\pi_1^x}) \circ F^x \circ (\eta_{j_0} \diamond \text{id}_{\pi_0^x}) = G^x \circ (\eta_{j_0} \diamond \text{id}_{\pi_0^x})$$

for any morphism $F = (\text{id}_x \diamond G) \circ (\Delta_x \diamond \text{id}_{\pi_0}) : H_x \diamond H_{\pi_0} \rightarrow H_x \diamond H_{\pi_1}$. Here, $_{}^x : \mathcal{H}_x^r(\mathcal{G}) \rightarrow \mathcal{H}^r(\mathcal{G}^{\setminus i_0})$ is the restriction of the functor defined in Proposition 4.4.11.

Given a full inclusion $\mathcal{G} \subset \mathcal{G}'$ of groupoids and a spanning sequence $X = (x_n, \dots, x_1)$ for $(\mathcal{G}', \mathcal{G})$, the *reduction functor* $\downarrow_X : \mathcal{H}_X^r(\mathcal{G}') \rightarrow \mathcal{H}^r(\mathcal{G})$ is defined as the composition $\downarrow_X = \downarrow_{x_1} \circ \dots \circ \downarrow_{x_n}$ of elementary reduction functors. Observe that the composition is well-defined, since if $x_n \in \mathcal{G}(i_n, j_n)$ then (x_{n-1}, \dots, x_1) forms a spanning tree for $(\mathcal{G}')^{\setminus i_n}$.

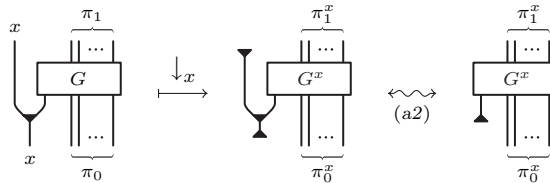


FIGURE 4.5.5. The reduction functor \downarrow_x [a/123]

LEMMA 4.5.6. For any $x \in \mathcal{G}(i_0, j_0)$, the reduction $\downarrow_x : \mathcal{H}_x^r(\mathcal{G}) \rightarrow \mathcal{H}^r(\mathcal{G}^{\setminus i_0})$ is a functor such that $\downarrow_x \circ \uparrow_x = \text{id}_{\mathcal{H}^r(\mathcal{G}^{\setminus i_0})}$, while $\uparrow_x \circ \downarrow_x \simeq \text{id}_{\mathcal{H}_x^r(\mathcal{G})}$ up to the natural equivalence $\xi^x = \xi^{x, i_0}$. Therefore, \downarrow_x and \uparrow_x are category equivalences between $\mathcal{H}_x^r(\mathcal{G})$ and $\mathcal{H}^r(\mathcal{G}^{\setminus i_0})$.

Proof. That \downarrow_x is well-defined functor follows from the identity

$$(\varepsilon_{1_{j_0}} \diamond \text{id}_{j_0} \diamond \text{id}_{j_0}) \circ (\Delta_{1_{j_0}} \diamond \text{id}_{j_0}) \circ \Delta_{1_{j_0}} \circ \eta_{j_0} = \eta_{j_0} \diamond \eta_{j_0}$$

and from the functoriality of the map $_x$.

Looking at Figure 4.5.5, we see that $\downarrow_x \circ \uparrow_x = \text{id}_{\mathcal{H}^r(\mathcal{G}^{\setminus i_0})}$. Indeed, if the leftmost diagram in the figure comes from the stabilization of a morphism in $\mathcal{H}^r(\mathcal{G}^{\setminus i_0})$ as in Figure 4.5.4, we have $\pi_0^x = \pi_0$, $\pi_1^x = \pi_1$ and $G^x = G$ by Theorem 4.4.11 (b). Hence, we end up with the rightmost diagram that represents $(\varepsilon_{1_{j_0}} \circ \eta_{j_0}) \diamond G = G$ by (a8) in Table 4.1.1. Finally, Figure 4.5.6 shows that ξ^x gives a natural equivalence $\uparrow_x \circ \downarrow_x \simeq \text{id}_{\mathcal{H}_x^r(\mathcal{G})}$. \square

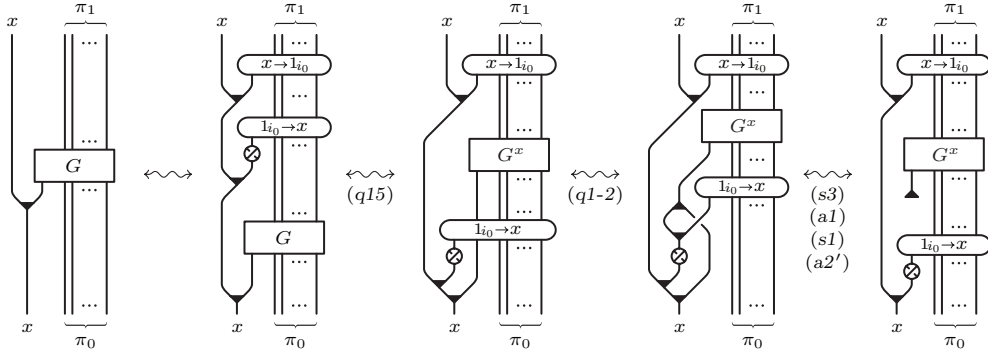


FIGURE 4.5.6. The natural equivalence $\xi^x : \uparrow_x \circ \downarrow_x \simeq \text{id}_{\mathcal{H}_x^r(\mathcal{G})}$ ($x \in \mathcal{G}(i_0, j_0)$)
[a/123, s/123-125, q/148-157]

PROPOSITION 4.5.7. Given a full inclusion of groupoids $\mathcal{G} \subset \mathcal{G}'$ and a spanning sequence $X = (x_n, \dots, x_1)$ for $(\mathcal{G}', \mathcal{G})$, the reduction $\downarrow_X : \mathcal{H}_X^r(\mathcal{G}') \rightarrow \mathcal{H}^r(\mathcal{G})$ is a functor such that $\downarrow_X \circ \uparrow_X = \text{id}_{\mathcal{H}^r(\mathcal{G})}$, while there is a natural equivalence $\xi^X : \uparrow_X \circ \downarrow_X \simeq \text{id}_{\mathcal{H}_X^r(\mathcal{G})}$, inductively defined by $\xi^{(x_1)} = \xi^{x_1}$ and

$$\xi^X = \xi^{x_n} \circ (\text{id}_{x_n} \diamond \xi^Y)$$

with $Y = (x_{n-1}, \dots, x_1)$. Therefore, \downarrow_X and \uparrow_X are category equivalences between $\mathcal{H}_X^r(\mathcal{G}')$ and $\mathcal{H}^r(\mathcal{G})$.

Proof. We proceed by induction on n . For $n = 1$ the statement follows from the previous lemma. For $n > 1$, we have $\uparrow_X = \uparrow_{x_n} \circ \uparrow_Y$ and $\downarrow_X = \downarrow_Y \circ \downarrow_{x_n}$ with $Y = (x_1, \dots, x_{n-1})$. Then, taking into account that $\uparrow_X \mathcal{H}^r(\mathcal{G}) \subset \mathcal{H}_X^r(\mathcal{G}')$, by the induction hypothesis we have

$$\downarrow_X \circ \uparrow_X = \downarrow_Y \circ \downarrow_{x_n} \circ \uparrow_{x_n} \circ \uparrow_Y = \downarrow_Y \circ \uparrow_Y = \text{id}_{\mathcal{H}^r(\mathcal{G})}.$$

Moreover, for any $F \in \mathcal{H}_X^r(\mathcal{G})$ we can write $\uparrow_X \downarrow_X F = \text{id}_{x_n} \diamond (\uparrow_Y \downarrow_Y (\downarrow_{x_n} F))$, which induces a natural equivalence $\text{id}_{x_n} \diamond \xi^Y : \uparrow_X \circ \downarrow_X \simeq \uparrow_{x_n} \circ \downarrow_{x_n}$. Then, by composing with $\xi^{x_n} : \uparrow_{x_n} \circ \downarrow_{x_n} \simeq \text{id}_{\mathcal{H}_{x_n}^r(\mathcal{G})}$, we get the natural equivalence $\xi^X : \uparrow_X \circ \downarrow_X \simeq \text{id}_{\mathcal{H}_X^r(\mathcal{G})}$. \square

Next proposition specializes the results above to the case when $\mathcal{G} = \mathcal{G}_k$, $\mathcal{G}' = \mathcal{G}_n$ and $X = \pi_{n \rightarrow k} = ((n, n-1), \dots, (k+1, k))$, with $n > k \geq 1$. In this case, we will use a notation analogous to the one introduced in the context of the categories of Kirby tangles. In particular, we put $\uparrow_k^n = \uparrow_{\pi_{n \rightarrow k}}$, $\downarrow_k^n = \downarrow_{\pi_{n \rightarrow k}}$, $\xi^{n \rightarrow k} = \xi^{\pi_{n \rightarrow k}}$ and $\mathcal{H}_{n \rightarrow k}^r = \mathcal{H}_{\pi_{n \rightarrow k}}^r(\mathcal{G}_n)$. Then we have the stabilization and reduction functors:

$$\uparrow_k^n = \uparrow_{n-1}^n \circ \dots \circ \uparrow_k^{k+1} : \mathcal{H}_k^r \rightarrow \mathcal{H}_n^r \quad \text{and} \quad \downarrow_k^n = \downarrow_k^{k+1} \circ \dots \circ \downarrow_{n-1}^n : \mathcal{H}_{n \rightarrow k}^r \rightarrow \mathcal{H}_k^r.$$

PROPOSITION 4.5.8. *For any $n > k \geq 1$, the reduction $\downarrow_k^n : \mathcal{H}_{n \rightarrow k}^r \rightarrow \mathcal{H}_k^r$ and the restriction of the stabilization $\uparrow_k^n : \mathcal{H}_k^r \rightarrow \mathcal{H}_{n \rightarrow k}^r$ are category equivalences such that $\downarrow_k^n \circ \uparrow_k^n = \text{id}_{\mathcal{H}_k^r}$ and $\xi^{n \rightarrow k} : \uparrow_k^n \circ \downarrow_k^n \simeq \text{id}_{\mathcal{H}_{n \rightarrow k}^r}$ is a natural equivalence. Moreover, we have the following commutative diagrams.*

$$\begin{array}{ccc} \mathcal{H}_n^r & \xrightarrow{\Phi_n} & \mathcal{K}_n \\ \uparrow_k^n \uparrow & & \uparrow \uparrow_k^n \\ \mathcal{H}_k^r & \xrightarrow{\Phi_k} & \mathcal{K}_k \end{array} \quad \begin{array}{ccc} \mathcal{H}_{n \rightarrow k}^r & \xrightarrow{\Phi_n} & \mathcal{K}_{n \rightarrow k} \\ \downarrow_k^n \downarrow & & \downarrow \downarrow_k^n \\ \mathcal{H}_k^r & \xrightarrow{\Phi_k} & \mathcal{K}_k \end{array}$$

Proof. The first part of the statement is just a special case of Propositions 4.5.4 and 4.5.7. The commutativity of the diagrams immediately follows from the definitions of the stabilization and reduction functors on both categories and Proposition 4.4.12. \square

4.6. The functors $\Psi_n : \mathcal{S}_n \rightarrow \mathcal{H}_n^r$

We remind that in Section 3.3 it was defined a functor $\Theta_n : \mathcal{S}_n \rightarrow \mathcal{K}_n$ from n -labeled ribbon surface tangles to n -labeled Kirby tangles. The goal of this section is to show that Θ_n factorizes through the functor $\Phi_n : \mathcal{H}_n^r \rightarrow \mathcal{K}_n$ introduced in Section 4.3. Namely, we will construct a functor $\Psi_n : \mathcal{S}_n \rightarrow \mathcal{H}_n^r$ such that $\Theta_n = \Phi_n \circ \Psi_n$. Moreover, we will show that the restriction $\Psi_n : \mathcal{S}_n^c \rightarrow \mathcal{H}_n^{r,c}$ is well-defined and full for any $n \geq 4$. This fact will allow us to prove the equivalence of the categories \mathcal{S}_n^c , \mathcal{K}_n^c and $\mathcal{H}_n^{r,c}$ for any $n \geq 4$ and the equivalence between \mathcal{K}_n^c and $\mathcal{H}_n^{r,c}$ for any $n \geq 1$.

First of all, we observe that the objects of \mathcal{S}_n correspond to sequences of transpositions in Γ_n , i.e. unordered pairs of different indices, while the objects of \mathcal{H}_n^r correspond to sequences of morphisms in \mathcal{G}_n , i.e. ordered pairs of indices. Hence, any functor $\mathcal{S}_n \rightarrow \mathcal{H}_n^r$ would require a choice of an ordering of the indices.

THEOREM 4.6.1. *For any strict total order \prec on the set of objects of \mathcal{G}_n with $n \geq 2$, there exists a braided monoidal functor $\Psi_n^\prec : \mathcal{S}_n \rightarrow \mathcal{H}_n^r$, such that:*

- (a) Ψ_n^\prec restricts to a monoidal functor $\Psi_n^\prec : \mathcal{S}_{n \rightarrow k} \rightarrow \mathcal{H}_{n \rightarrow k}^r$ for any $1 \leq k < n$;
- (b) if \prec' is another strict total order on the set of objects of \mathcal{G}_n , there is a natural equivalence $\tau : \Psi_n^\prec \rightarrow \Psi_n^{\prec'}$, which is identity on the empty set;

(c) the following diagram commutes

$$\begin{array}{ccc}
 \mathcal{S}_n & \xrightarrow{\Theta_n} & \mathcal{K}_n \\
 & \searrow \Psi_n & \nearrow \Phi_n \\
 & & \mathcal{H}_n^r
 \end{array}$$

where $\Psi_n = \Psi_n^<$ with $<$ being the natural order on $\text{Obj } \mathcal{G}_n$.

Proof. Given a strict total order \prec on $\text{Obj } \mathcal{G}_n$, we define inductively $\Psi_n^{\prec} : \mathcal{S}_n \rightarrow \mathcal{H}_n^r$ on the objects according to the identities:

$$\Psi_n^{\prec}(J_{(i,j)}) = H_{(i,j)} \text{ for any } i, j \in \text{Obj } \mathcal{G}_n \text{ with } i \succ j,$$

$$\Psi_n^{\prec}(J_{\sigma}) = \Psi_n^{\prec}(J_{\sigma'}) \diamond \Psi_n^{\prec}(J_{\sigma''}) \text{ for any } \sigma = \sigma' \diamond \sigma'' \in \Pi\Gamma_n.$$

Moreover, given another order \prec' on $\text{Obj } \mathcal{G}_n$, we consider the invertible morphisms $\tau_{\sigma} : \Psi^{\prec}(J_{\sigma}) \rightarrow \Psi^{\prec'}(J_{\sigma})$ with $\sigma \in \Pi\Gamma_n$ uniquely determined by:

$$\tau_{(i,j)} = \begin{cases} \text{id}_{(i,j)} : H_{(i,j)} \rightarrow H_{(i,j)} & \text{if } i \succ j \text{ and } i \succ' j \\ T_{(i,j)} : H_{(i,j)} \rightarrow H_{(j,i)} & \text{if } i \succ j \text{ and } j \succ' i \end{cases}$$

$$\tau_{\sigma} = \tau_{\sigma'} \diamond \tau_{\sigma''} \text{ for any } \sigma = \sigma' \diamond \sigma'' \in \Pi\Gamma_n.$$

On the morphisms of \mathcal{S}_n we define Ψ_n^{\prec} as follows. Figures 4.6.1 and 4.6.2 describe the images under Ψ_n^{\prec} of any labeling of the elementary morphisms from (a) to (g) in Figure 3.1.1, while the image of any labeling of the ribbon surface tangle (g') in the same Figure 3.1.1 is defined through relation (I6) in Figure 3.1.2.

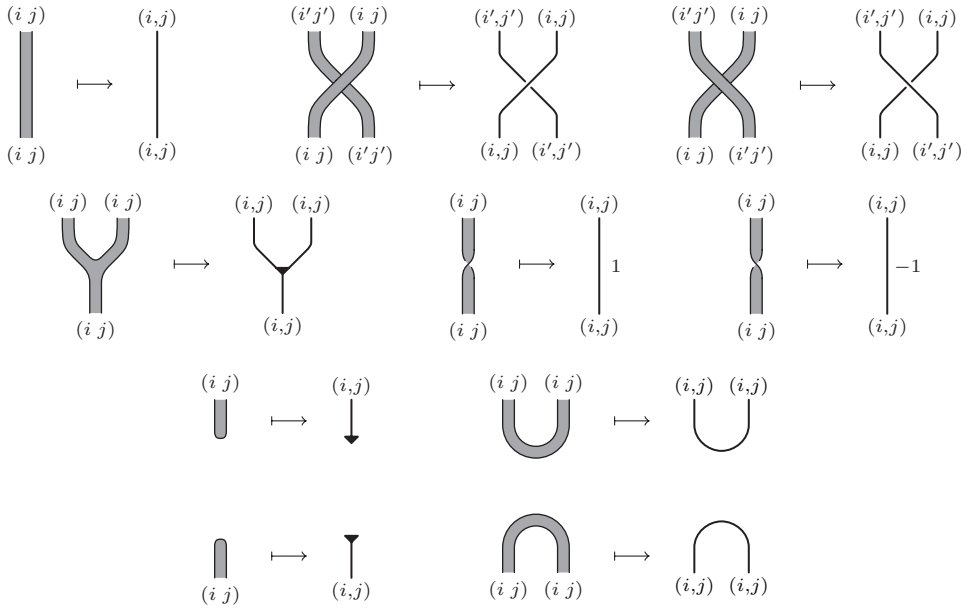


FIGURE 4.6.1. The functor $\Psi_n^{\prec} - I$ ($i \succ j, i' \succ j'$)

($f3-3'$), ($f4-4'$) and ($f1$) in Table 4.1.2; ($I3-3'$) rewrite the bottom-left duality moves in Table 4.1.8; ($I4-4'$) follow from ($f10$) in Table 4.2.2; ($I10$), ($I12-12'$) and ($I13$) follow from ($r2$), ($r5$) and ($p1$) in Tables 4.2.1 and 4.2.2; ($I11$) follows from ($f5$) and ($t1-3$) in Tables 4.1.8 and 4.2.13; ($I15$) follows from ($t5$) in Table 4.2.13; ($I20$) follows from ($a6$), ($s6$) and ($r4$) in Tables 4.1.1, 4.1.2 and 4.2.1; ($R1$) follows from ($t3$) and ($t6$) in Table 4.2.13, taking into account that T propagates through the form and the coform, due to ($f6-7$) in Table 4.1.8 and ($f9-10$) in Table 4.2.2.

Below we indicate how the verification goes for the remaining moves.

We start with ($I19$) in Figure 4.6.3. The labeling of this move is unique up to reordering the indices, while the labelings of other moves present different cases, depending on the labels at the ribbon intersections. We will call a ribbon intersection uni-, bi- or tri-labeled according to the number of different labels that occur in it.

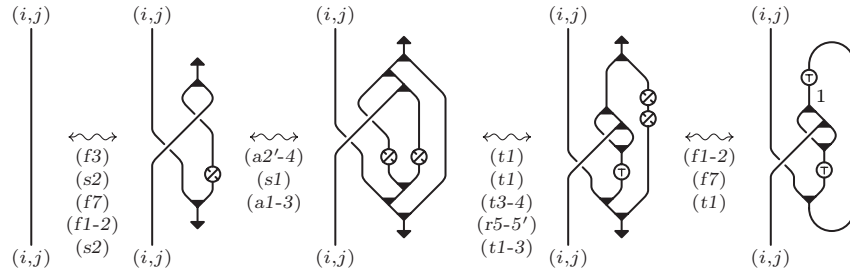


FIGURE 4.6.3. Preservation of ($I19$) ($i \succ j$) [$a/123$, $f/125-129$, $r/132-134$, $s/123$, $t/140$]

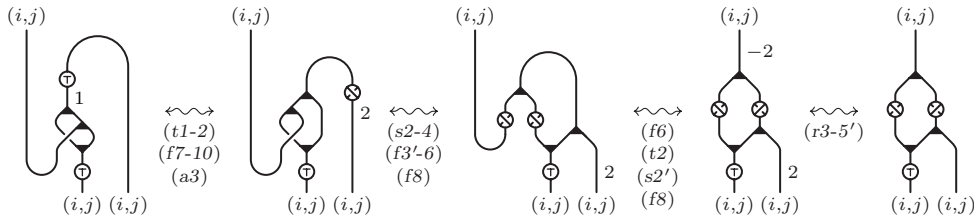


FIGURE 4.6.4. Preservation of ($I14-14'$) in the uni-labeled case - I ($i \succ j$) [$a/123$, $f/125-129-134$, $r/132-134$, $s/123-125$, $t/140$]

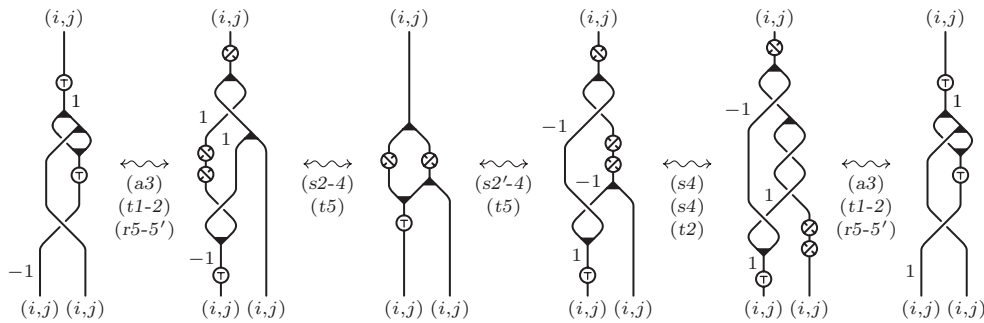


FIGURE 4.6.5. Preservation of ($I14-14'$) in the uni-labeled case - II ($i \succ j$) [$a/123$, $r/132-134$, $s/123-125$, $t/140$]

(*I14-14'*) for a bi-labeled ribbon intersection are trivial, since they follow from the braid axioms. For a tri-labeled ribbon intersection they follow directly from (*t3-6*) and (*t7*) in Table 4.2.13. Figures 4.6.4 and 4.6.5 deal with the uni-labeled case. More precisely, Figure 4.6.4 shows that the image under $\Psi_n^<$ of the labeled ribbon surface tangle in the middle of (*I14-14'*) is equivalent to the third graph diagram in Figure 4.6.5.

(*I17*) for a bi-labeled ribbon intersection reduces to a crossing change, so it follows from axioms (*r9*) in Table 4.2.13. The tri- and uni-labeled cases are presented in Figures 4.6.6 and Figure 4.6.7 respectively.

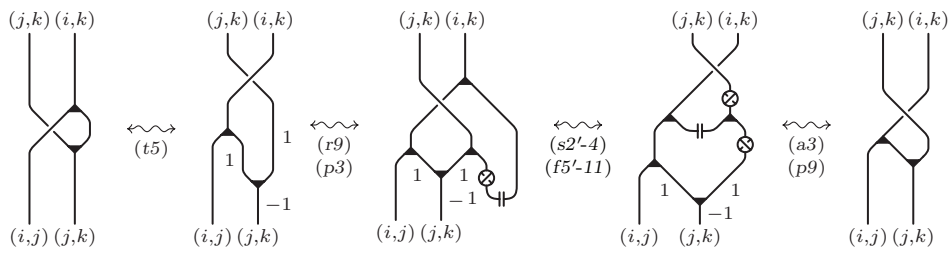


FIGURE 4.6.6. Preservation of (*I17*) in the tri-labeled case ($i \succ j \succ k$) [*a*/123, *f-p*/134, *r*/140, *s*/123-125, *t*/140]

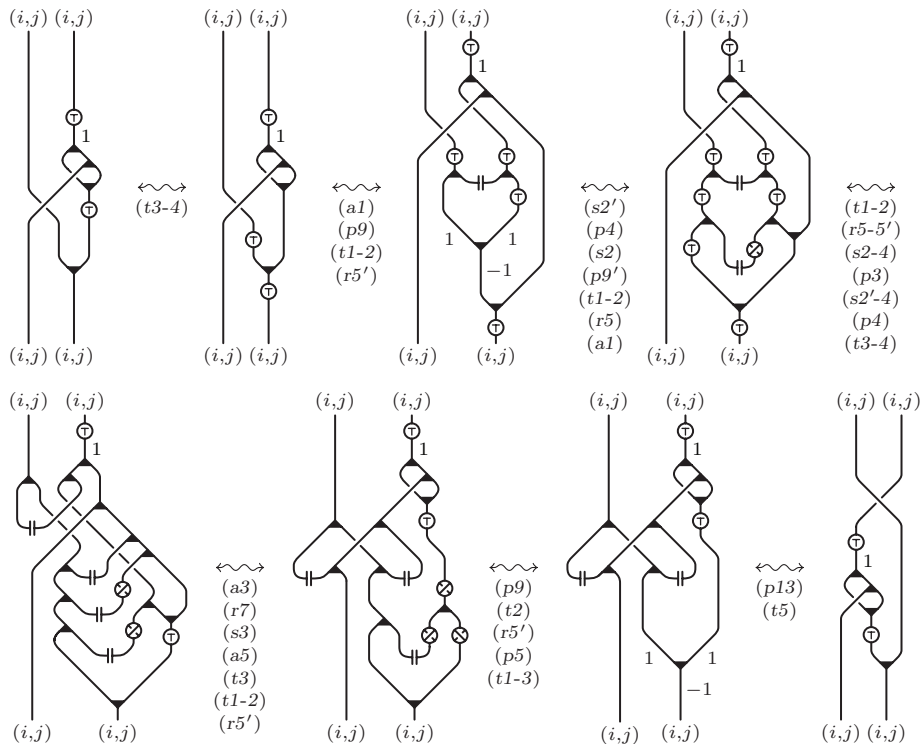


FIGURE 4.6.7. Preservation of (*I17*) in the uni-labeled case ($i \succ j$) [*a*/123, *p*/134-140, *r*/132-134, *s*/123-125, *t*/140]

(*I21*) for bi-labeled ribbon intersection is trivial, while for tri-labeled ribbon intersection, with the proper choice of the order \prec , it corresponds to the bi-algebra axiom (*a5*) in Table 4.1.1. The uni-labeled case is treated in Figure 4.6.8.

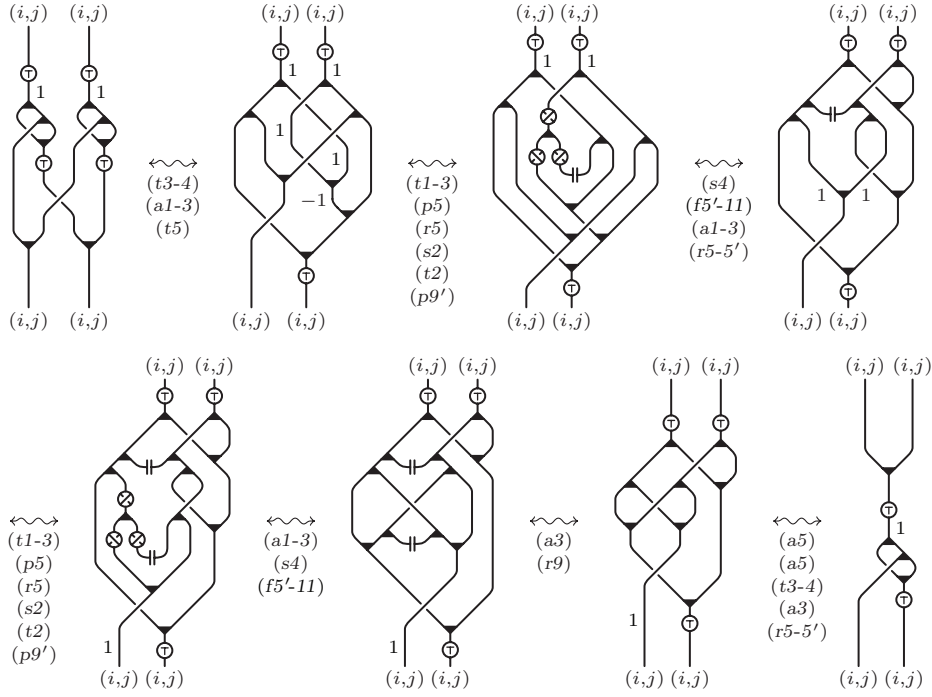


FIGURE 4.6.8. Preservation of $(I21)$ in the uni-labeled case ($i \succ j$) [a/123, f/129-134, p/134, r/132-134-140, s/123-125, t/140]

$(I22)$ is the most complicated relation to deal with, since the source of the involved morphisms consists of three intervals which can be labeled independently from each other, so there are many different cases. First of all, we observe that the presence of disjoint labels allows us to simplify the relation by using move $(R2)$ in Figure 3.2.3 to remove the bi-labeled ribbon intersections. In particular, when one of those labels is disjoint from both the other two, such simplification reduce $(I22)$ to $(I16)$ and $(I20)$ modulo $(I2-2')$, $(I3-3')$, $(I5)$ and $(I8)$. Up to conjugation, the only remaining labelings of the three intervals that include a pair of disjoint labels, are given by the sequences $((i j), (i k), (k l))$ and $((i j), (k l), (i k))$ where i, j, k, l are

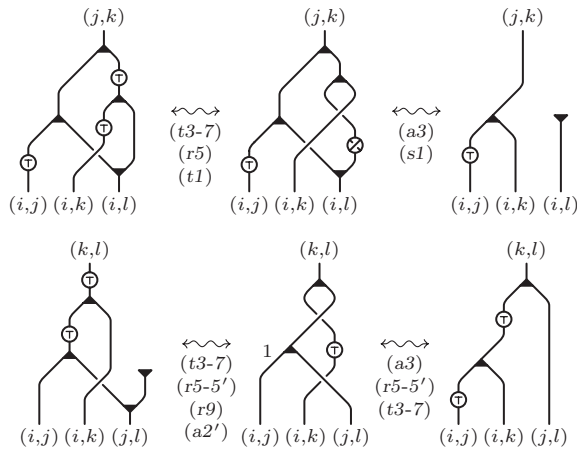


FIGURE 4.6.9. Preservation of $(I22)$ in the non-trivial cases when a bi-labeled ribbon intersection occurs, ($i \succ j \succ k \succ l$) [a/123, r/132-134-140, s/123, t/140]

all distinct. Assuming $i \succ j \succ k \succ l$, after simplification the first case corresponds to the bi-algebra axiom (a3) in Table 4.1.1, while the second one reduces to (I16) and (I20) as above. Figure 4.6.9 concerns the two remaining cases when a bi-labeled ribbon intersection occurs (even if there is no pair of disjoint labels in the source). The rest of the cases are presented in Figures 4.6.10, 4.6.11 and 4.6.12 respectively, depending on the number of uni-labeled ribbon intersections.

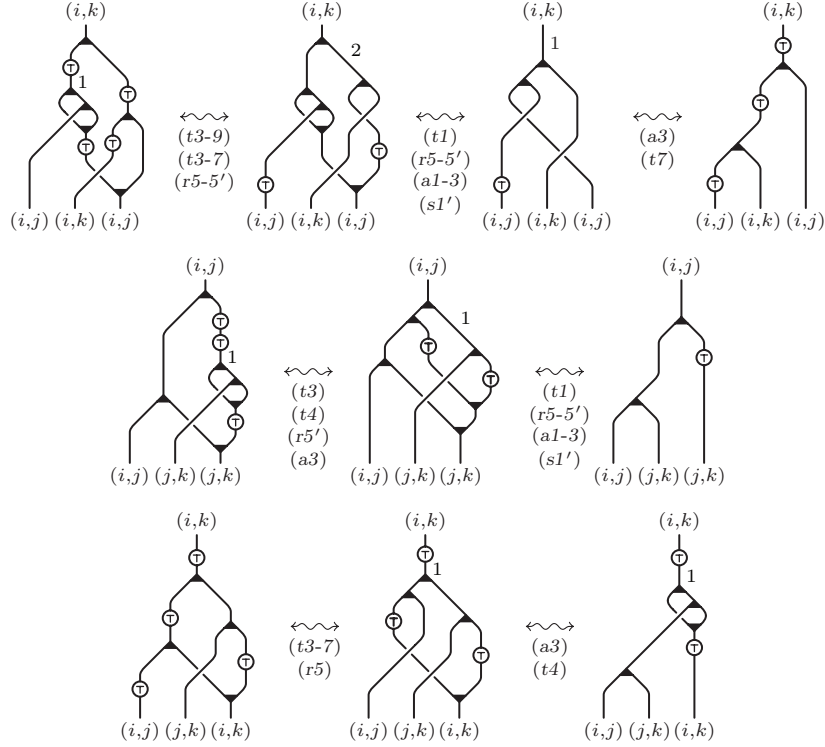


FIGURE 4.6.10. Preservation of (I22) in the cases when one uni-labeled ribbon intersection occurs ($i \succ j \succ k$) [a/123, r/132-134, s/123, t/140]

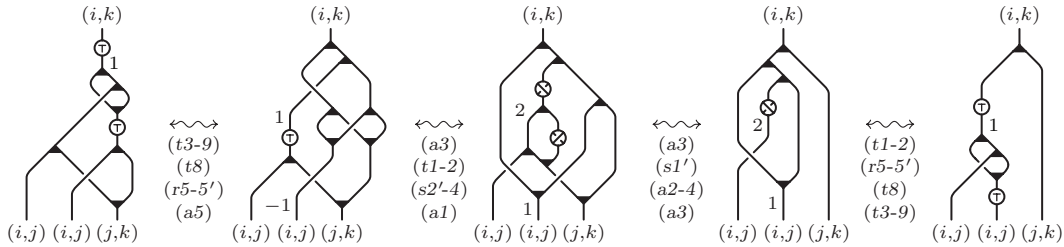


FIGURE 4.6.11. Preservation of (I22) in the cases when two uni-labeled ribbon intersections occur ($i \succ j \succ k$) [a/123, r/132-134, s/123-125, t/140]

This completes the proof that Ψ_n^\prec is a well-defined functor. Then, its monoidality is trivial while the desired natural equivalence τ in (b) was defined in the beginning. Moreover, property (a) directly derives from the fact that the image of the elementary morphism $\Delta_{(i,j)}$ in Figure 3.2.4 is exactly $\Delta_{(i,j)}$ for $i \succ j$. Finally, the commutativity of the diagram in (c) can be seen by comparing the definitions of Φ_n

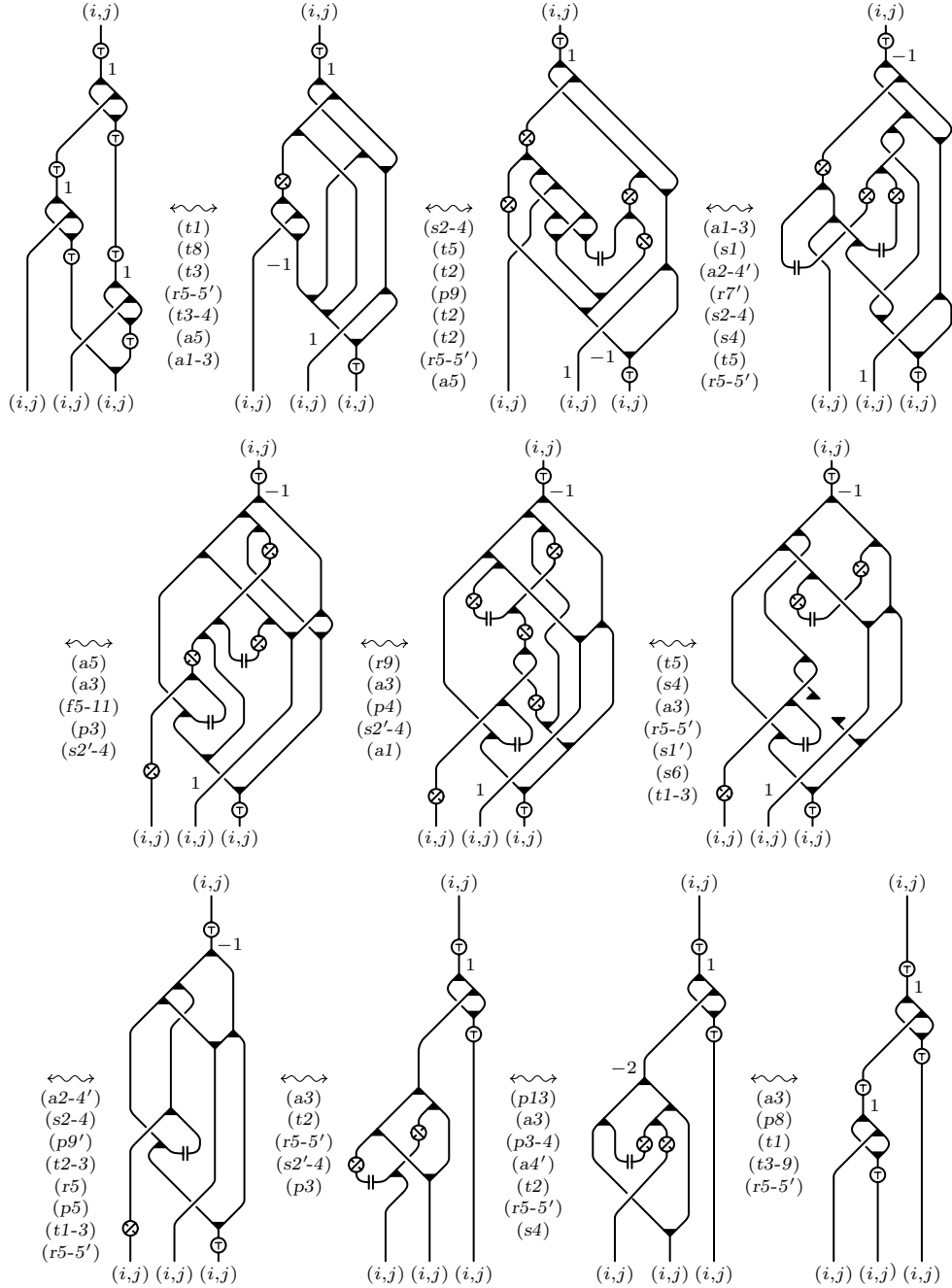


FIGURE 4.6.12. Preservation of $(I22)$ in the uni-labeled case ($i > j$) [$a/123$, $f/129-134$, $p/134-140$, $r/132-134-140$, $s/123-125$, $t/140$]

in Section 4.3 (cf. Figures 4.2.17 and 4.3.1) and Ψ_n (cf. Figures 4.6.1 and 4.6.2) with the definition of Θ_n in Section 3.3 (cf. Figures 3.3.17, 3.3.18 and 3.3.19). \square

Theorem 4.6.1 with $n = 2$ and Proposition 4.5.8 imply that there exists a functor from the category of 1-isotopy equivalence classes of (unlabeled) ribbon surface tangles \mathcal{S} (cf. Section 3) to the universal ribbon Hopf algebra $\mathcal{H}^r = \mathcal{H}_1^r$ (over the trivial groupoid). Observe that the two categories are obviously not equivalent, but the corollary below allows us to associate to any braided unimodular ribbon Hopf algebra an invariant of ribbon surface tangles under 1-isotopy moves.

COROLLARY 4.6.2. *There exists a monoidal functor $\Psi : \mathcal{S} \rightarrow \mathcal{H}^r$, defined by $\Psi(J_m) = H^{\diamond m}$ on the objects and by Figure 4.6.13 on the elementary morphisms.*

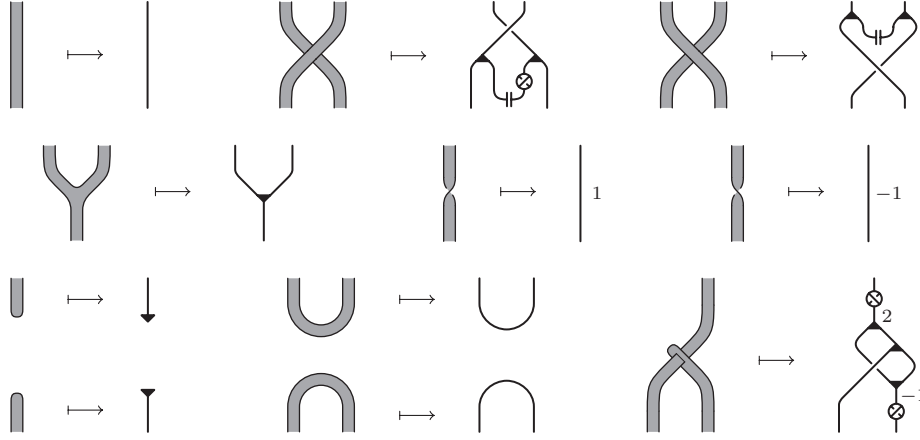


FIGURE 4.6.13. The functor $\Psi : \mathcal{S} \rightarrow \mathcal{H}^r$

Proof. Comparing the presentation of the category \mathcal{S} in Proposition 3.1.2 with the one of the category \mathcal{S}_n in Proposition 3.2.3, we observe that the the relations of \mathcal{S}_2 are just the labeled versions of the relations of \mathcal{S} (see Figure 3.2.3). In fact, the extra relations (R1) and (R2) do not appear in \mathcal{S}_2 since they involve at least three different labels. Therefore, the category \mathcal{S} is equivalent to \mathcal{S}_2 , where the equivalence functor is given by labeling the whole surface by the transposition (1 2). Then, we put $\Psi = \downarrow_1^2 \circ \Psi_2$ and the statement follows from Theorem 4.6.1, Proposition 4.5.8 and the identity in Figure 4.6.14. \square

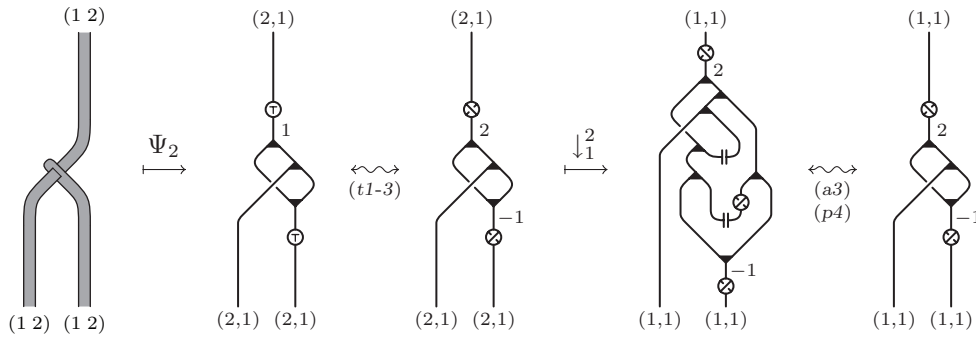


FIGURE 4.6.14. [a/123, p/134, t/140]

4.7. Equivalence between \mathcal{K}_n^c and $\mathcal{H}_n^{r,c}$

According to point (a) of Theorem 4.6.1, we know that the functor $\Psi_n : \mathcal{S}_n \rightarrow \mathcal{H}_n$ restricts to a well-defined functor $\Psi_n : \mathcal{S}_n^c \rightarrow \mathcal{H}_n^{r,c}$, where we use the notation $\mathcal{S}_n^{r,c} = \mathcal{S}_{n \rightarrow 1}^r$ and $\mathcal{H}_n^{r,c} = \mathcal{H}_{n \rightarrow 1}^r$. Now we will show that for $n \geq 3$ such restriction is full (cf. Proposition 4.7.3) and this will allow us to complete the proof of the equivalence of the categories \mathcal{S}_n^c , $\mathcal{H}_n^{r,c}$ and \mathcal{K}_n^c with $n \geq 4$ (cf. Theorem 4.7.4).

We first need two technical lemmas.

LEMMA 4.7.1. Given $(i, j) \in \mathcal{G}_n$ with $i \neq j$, the identity $\text{id}_{\pi_{n \rightarrow 1}}$ as a morphism of $\mathcal{H}_n^{r,c}$ can be represented by a diagram containing a counit vertex $\varepsilon_{(i,j)}$ and no edge labeled (k, k) with $1 \leq k \leq n$.

Proof. Since $\text{id}_{\pi_{n \rightarrow 1}}$ contains $\text{id}_{\pi_{i \rightarrow j}}$ for $n \geq i \geq j \geq 1$, it suffices to prove that $\text{id}_{\pi_{i \rightarrow j}}$ can be represented by two diagrams containing $\varepsilon_{(i,j)}$ and $\varepsilon_{(j,i)}$ respectively and no edge labeled (k, k) . This is done in Figure 4.7.1. \square

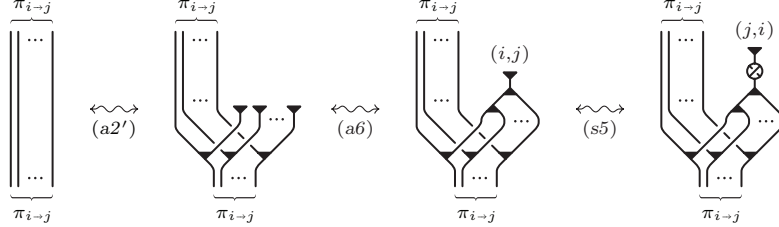


FIGURE 4.7.1. ($i > j$) [a/123, s/125]

LEMMA 4.7.2. Let F be any morphism of $\mathcal{H}_n^{r,c}$ whose source and target are in $\Psi_n(\text{Obj } \mathcal{S}_n^c)$, i.e. they have the form $H_{\pi_{n \rightarrow 1}} \diamond H_\pi$, with $\pi = ((i_1, j_1), \dots, (i_m, j_m)) \in \Pi \mathcal{G}_n$ such that $i_h > j_h$ for $h = 1, \dots, m$. If F is given by a composition of products of the elementary diagrams presented in Figure 4.7.2 with $i \neq j \neq k \neq i$ and $i' \neq j'$, then it is in the image of Ψ_n .

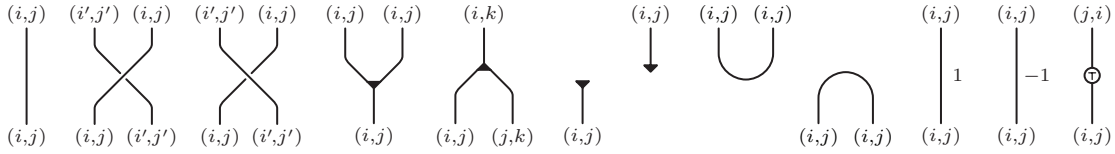


FIGURE 4.7.2. ($i \neq j \neq k \neq i, i' \neq j'$)

Proof. Consider a morphism F as in the statement. We call a label (i, j) in the diagram *good* if $i > j$ and *bad* if $i < j$. We also call a vertex of the diagram *good* if all the labels of the edges attached to it are good and *bad* otherwise. Observe that we can transform any comultiplication, counit and any integral vertex into a good one by applying to it, if necessary, the moves in Figure 4.7.3. Therefore, we can assume that any bad vertex of the diagram is a multiplication vertex.

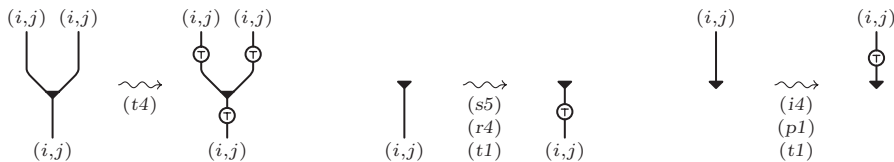


FIGURE 4.7.3. ($i < j$) [i/129, p/134, r/132, s/125, t/140]

Now, consider the diagram of F as a planar diagram of a graph in which each edge e is weighted by an integer and decorated by a certain number $n(e)$ of T 's. We observe that the T 's can be slid along the edges by using the braid axioms in Table 4.1.1 and the moves in Figure 4.7.4. Then, we can always assume $n(e) = 0, 1$, since move $(t3)$ in Table 4.2.13 allows us to eliminate any two T 's along the same

edge, once they are slid next to each other. If both the ends of an edge e have good (resp. bad) labels, then $n(e) = 0$ and the entire edge e has a good (resp. bad) label. In the bad case, we insert two T 's along e by (t3) and slide them near to the ends of e . On the contrary, if the labels at the ends of an edge are one good and the other bad, then there is exactly one T along e and we slide it near to the badly labeled end.

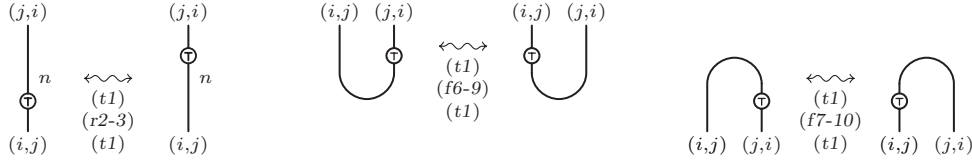


FIGURE 4.7.4. ($i \neq j$) [f/129-134, r/132, t/140]

After that, any bad label in the diagram is confined to a small arc between a T and a bad multiplication vertex. Taking into account the definition of Ψ_n in Figures 4.6.1 and 4.6.2, we see that such a diagram is a composition of products of diagrams each of which is the image of an elementary morphism under the monoidal functor Ψ_n . Therefore, F itself is in the image of Ψ_n . \square

PROPOSITION 4.7.3. *The functor $\Psi_n : \mathcal{S}_n^c \rightarrow \mathcal{H}_n^{r,c}$ is full for any $n \geq 3$.*

Proof. Let F be a morphism of $\mathcal{H}_n^{r,c}$ whose source and target are in $\Psi_n(\text{Obj } \mathcal{S}_n^c)$. We represent F by a diagram which does not use the copairing and form/coform notation. This is possible, since those morphisms are defined in terms of the other elementary morphisms.

Then an edge of the diagram will be called an i -edge, $1 \leq i \leq n$, if it is labeled (i, i) and if it does not join a multiplication and a cointegral vertex (cf. Figure 4.7.5). Moreover, a vertex will be called an i -vertex if it is not cointegral vertex and all edges attached to it are labeled (i, i) . In the figures below we will indicate i -edges by thinner lines and i -vertices by empty triangles.

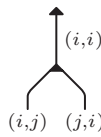


FIGURE 4.7.5. Not an i -edge

As a preliminary step, we will show how to transform the diagram representing F into an equivalent one, where no i -vertices and i -edges appear for any $1 \leq i \leq n$. Actually, the figures below deal only with edges of zero weight and not containing antipodes, but the generalization to other weights or to the presence of the antipodes is straightforward. Observe also that since $n \geq 2$, according to Lemma 4.7.1 we may assume that the diagram of F contains a counit $\varepsilon_{(i,j)}$ with $j \neq i$. Moreover, through isotopy moves such counit can be moved near any given i -edge.

We start by eliminating all uni-valent i -vertices as described in Figure 4.7.6. Then by applying, if necessary, the edge breaking shown in Figure 4.7.7, we obtain a diagram where all i -edges connect two tri-valent vertices such that at most one of them is an i -vertex. In particular, no i -edge connects two comultiplication vertices.

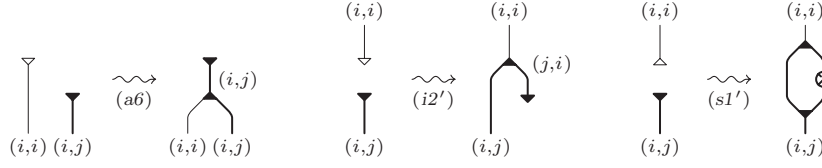


FIGURE 4.7.6. Eliminating the uni-valent i -vertices ($i \neq j$) [a-s/123, i/129]

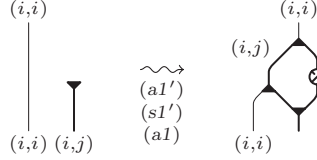


FIGURE 4.7.7. Breaking an i -edge ($i \neq j$) [a-s/123]

We proceed by eliminating the tri-valent i -vertices, first the comultiplication ones by the leftmost move in Figure 4.7.8 and then the multiplication ones by using the two other moves in the same figure (or their vertical reflections).

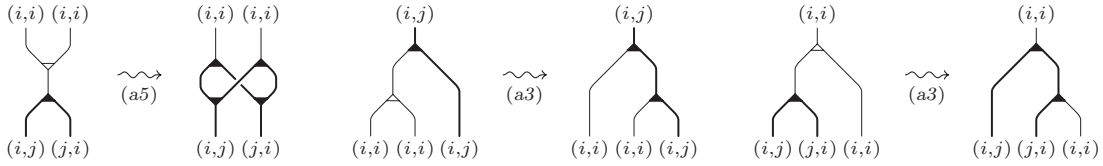


FIGURE 4.7.8. Eliminating tri-valent i -vertices ($i \neq j$) [a/123]

At this point the only remaining i -edges connect two multiplication tri-valent vertices none of which is an i -vertex. Such edges are eliminated through the moves shown in Figure 4.7.9 (or their vertical reflections). For the move on the right side, by applying Lemma 4.7.1 in the case $n \geq 3$, we assume that there is close by a count of label (j, k) with $i \neq j \neq k \neq i$.

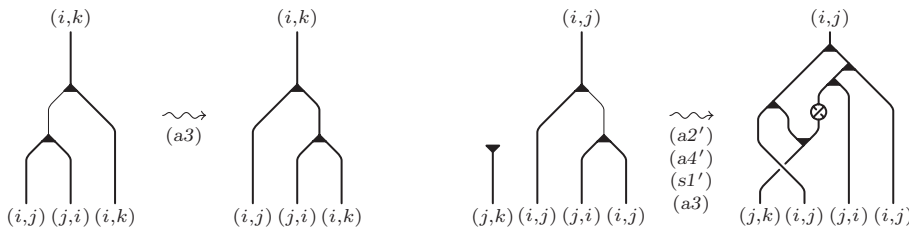


FIGURE 4.7.9. Eliminating i -edges between two tri-valent vertices none of which is an i -vertex ($i \neq j \neq k \neq i$) [a-s/123]

This gives a diagram, where any edge labeled (i, i) is attached to one multiplication tri-valent and one cointegral vertex as in Figure 4.7.5 where $i \neq j$. By using the form notation (f2) in Table 4.1.8, we can eliminate those exceptional edges as well, leaving only labels of the type (i, j) with $i \neq j$. Finally, we express all antipodes in terms of T 's and ribbon morphisms through the moves (t1-2) in Table 4.2.13.

In the end, the resulting diagram of F is a composition of products of the diagrams in Figure 4.7.2 and the proposition follows from Lemma 4.7.2.

We note that the images of the uni-labeled ribbon intersections do not appear. This is because any ribbon surface tangle is equivalent to one which does not contain such ribbon intersection. \square

THEOREM 4.7.4. *For any $n \geq 4$, we have the following commutative diagram of equivalence functors:*

$$\begin{array}{ccc}
 \mathcal{S}_n^c & \xrightarrow{\Theta_n} & \mathcal{K}_n^c \\
 \searrow \Psi_n & & \nearrow \Phi_n \\
 & \mathcal{H}_n^{r,c} &
 \end{array}$$

Proof. Observe that the commutativity of the diagram has already been established in Theorem 4.6.1 (c). Moreover, Theorem 3.6.4 tells us that Θ_n is a category equivalence for $n \geq 4$. Then, for $n \geq 4$ the functor Ψ_n is faithful. On the other hand, it is also full, by Proposition 4.7.3.

Therefore, according to Proposition 1.5.3, to conclude that Ψ_n is a category equivalence, and hence so is Φ_n , it is enough to prove that for any object $H_{\pi_{n-1}} \diamond H_{\pi} \in \text{Obj } \mathcal{H}_n^{r,c}$ with $\pi = ((i_1, j_1), \dots, (i_m, j_m)) \in \Pi \mathcal{G}_n$ an arbitrary sequence, there exists an isomorphism $\varphi_{\pi} : H_{\pi_{n-1}} \diamond H_{\pi} \rightarrow H_{\pi_{n-1}} \diamond H_{\pi'}$ with $H_{\pi_{n-1}} \diamond H_{\pi'} \in \Psi_n(\text{Obj } \mathcal{S}_n^c)$, that is $i'_k > j'_k$ for $k = 1, \dots, m$.

We call an element $(i_l, j_l) \in \pi$ *bad* if $i_l \leq j_l$. Then, we proceed by induction on the number of bad elements of π . The inductive step is provided by the following claim: if the number of bad elements in π is $s > 0$, then there is an isomorphism $\varphi_{\pi} : H_{\pi_{n-1}} \diamond H_{\pi} \rightarrow H_{\pi_{n-1}} \diamond H_{\pi'}$, where the number of bad elements in π' is $s - 1$.

To prove the claim, suppose that $m > 1$ and that the first bad element in π is (i_k, j_k) . If $i_k < j_k$ the desired isomorphism φ_{π} is given by the product of identity

FIGURE 4.7.10. Definition of φ_{π} when $i_k = j_k < n$

FIGURE 4.7.11. Definition of φ_{π} when $i_k = j_k = n$.

morphisms and the antipode applied on the k -th string of H_π . If $i_k = j_k < n$ the isomorphism φ_π and its inverse φ_π^{-1} are presented in Figure 4.7.10, while if $i_k = j_k = n$ they are presented in Figure 4.7.11. The identities $\varphi_\pi^{-1} \circ \varphi_\pi = \text{id}_\pi$ and $\varphi_\pi \circ \varphi_\pi^{-1} = \text{id}_{\pi'}$ directly follow from the axioms (s1-1') in Table 4.1.1. \square

We are ready now to state the main theorem of this section, proving that the universal algebraic category $\mathcal{H}^r = \mathcal{H}_1^r = \mathcal{H}_1^{r,c}$ is equivalent to the category of relative cobordisms of 4-dimensional 2-handlebodies. The elementary diagrams and defining relations of \mathcal{H}^r are collected in Tables 4.7.12 and 4.7.13. Of course, they are simply the specializations of the ones in Tables 4.1.1, 4.1.8, 4.2.1 and 4.2.13 to the case of the trivial groupoid \mathcal{G}_1 . In this case, all labels are equal to $(1, 1)$, and are therefore omitted. Moreover, we remind that in this case the adjoint morphisms $\alpha : H \diamond H \rightarrow H$ (resp. $\alpha' : H \diamond H \rightarrow H$) define the left (resp. right) adjoint action of H on itself, and the two addition ribbon axioms (r8) and (r9) can be equivalently expressed in terms of such action as shown in Table 4.7.14 (cf. Proposition 4.4.5).

THEOREM 4.7.5. *The functor $\Phi_n : \mathcal{H}_n^{r,c} \rightarrow \mathcal{K}_n^c$ is a category equivalence for any $n \geq 1$. In particular, the universal ribbon Hopf algebra \mathcal{H}^r is equivalent to the category $\mathcal{C}hb^{3+1}$ of relative cobordisms of 4-dimensional 2-handlebodies.*

Proof. According to Theorem 4.7.4, Φ_n is a category equivalence for any $n \geq 4$. Then, for any $1 \leq n \leq 3$ the commutative diagram in Proposition 4.5.8, implies that $\Phi_n \circ \downarrow_n^4 = \downarrow_n^4 \circ \Phi_4$, where the reduction functors are known to be category equivalences by Propositions 2.3.9 and 4.5.7. Therefore Φ_n is a category equivalence as well. In particular, for $n = 1$ we obtain that $\Phi_1 : \mathcal{H}^r = \mathcal{H}_1^r \rightarrow \mathcal{K} = \mathcal{K}_1$ is a category equivalence. But according to Theorem 2.3.1, \mathcal{K} is equivalent to $\mathcal{C}hb^{3+1}$, hence \mathcal{H}^r is equivalent to $\mathcal{C}hb^{3+1}$ as well. \square











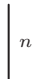

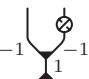
Elementary diagrams for the universal ribbon Hopf algebra $\mathcal{H}^r = \mathcal{H}_1^r$				
$\gamma =$ 	$\Delta =$ 	$\varepsilon =$ 	$S =$ 	$l =$ 
$\bar{\gamma} =$ 	$m =$ 	$\eta =$ 	$\bar{S} =$ 	$L =$ 
$v^n =$ 	$\sigma =$ 	$\xleftrightarrow{\text{def}} \text{(r6)}$ 		

TABLE 4.7.12.

REMARK 4.7.6. The category equivalence established in Theorem 4.7.5 implies that one can use braided ribbon Hopf algebras to construct sensitive invariants of 4-dimensional 2-handlebodies. Of course, in order to be able to calculate such invariants, given a Kirby tangle $K : I_{m_0} \rightarrow I_{m_1}$ in $\mathcal{K} = \mathcal{K}_1$, we need an explicit form for the morphism F_K in \mathcal{H}^r such that $\Phi_1(F_K) = K$. One such form is given by $F_K = \downarrow_1^3 \Psi(S_K)$, where S_K was constructed in Section 3.4, while Ψ_n and \downarrow_1^3 were defined respectively in Section 4.6 and Section 4.5. Of course, such approach requires a good understanding of all functors used in it, and it is quite long in practice.

Axioms for the universal ribbon Hopf algebra $\mathcal{H}^r = \mathcal{H}_1^r$	
<p style="text-align: center;">Braid axioms</p>	
<p style="text-align: center;">Bialgebra axioms</p>	
<p style="text-align: center;">Antipode axioms</p>	
<p style="text-align: center;">Integral axioms</p>	
<p style="text-align: center;">Ribbon axioms</p>	

TABLE 4.7.13.

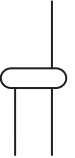

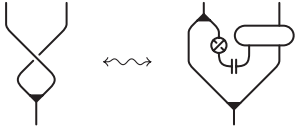
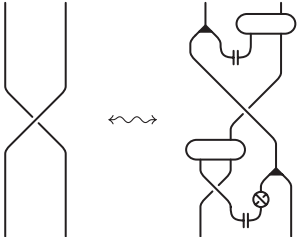
Left adjoint action in $\mathcal{H}^r = \mathcal{H}_1^r$	
$\alpha = $  $\stackrel{\text{def}}{\sim}$ 	
 <i>Equivalent form of the axiom (r8)</i>	 <i>Equivalent form of the axiom (r9)</i>

TABLE 4.7.14.

We will outline here a simpler procedure for constructing F_K , which is less explicit but works quite well in many concrete examples.

We start by representing K by a strictly regular planar diagram and use the following objects (and notations) from the indicated steps of the construction of the surface S_K in Section 3.4:

- 1) the disks D_1, \dots, D_r spanned by the dotted unknots of K and the framed link $L = L_1 \cup \dots \cup L_s$ introduced in step 1;
- 2) a trivial state for the diagram of the unframed link $|L|$ and the framed link $L' = L'_1 \cup \dots \cup L'_s$, whose corresponding unframed link $|L'|$ is represented by that trivial state, together with the family of cylinders F_1, \dots, F_l inside which the trivializing crossing changes take place, all considered in step 3;
- 3) a family A_1, \dots, A_s of disjoint spanning disks for the components $|L'_1|, \dots, |L'_s|$ of the trivial link $|L'|$, as in step 6.

The A_j 's can be assumed to intersect each cylinder F_i as depicted in the left side of Figure 3.5.1 (disregard the disk C_i). Then, we can extend them by introducing one clasp inside each F_i , to give a family $\widehat{A}_1, \dots, \widehat{A}_s$ of spanning disks for the original link $|L|$. Actually, in doing that we possibly introduce other singularities, which consist of two double arcs meeting at a triple point along the clasp intersection for each horizontal subdisk of the A_j 's inside the F_i 's. By suitable finger moves at the interior of the disks, we can eliminate all the triple points to leave only ribbon intersections, and then transform each ribbon intersection into a pair of new clasps.

Moreover, we can assume that the \widehat{A}_j 's form with the D_i 's only clasp and ribbon intersections, like in the right side of Figure 3.5.1. Also in this case, each ribbon intersection can be transformed into a pair of new clasps, by a finger move as above.

Finally, if L_j is the closure of an open framed component in K joining a'_{m_c, i_j} to a''_{m_c, i_j} with $c = 0, 1$, then we assume that the portion of \widehat{A}_j outside the box \widehat{K} in Figure 3.4.2 is flat and cut it off (cf. Figure 4.7.15 (a)).

We still denote by D_1, \dots, D_r and $\widehat{A}_1, \dots, \widehat{A}_s$ the disks resulting after the above modifications, which form only clasp singularities as the ones in Figure 4.7.15 (b).

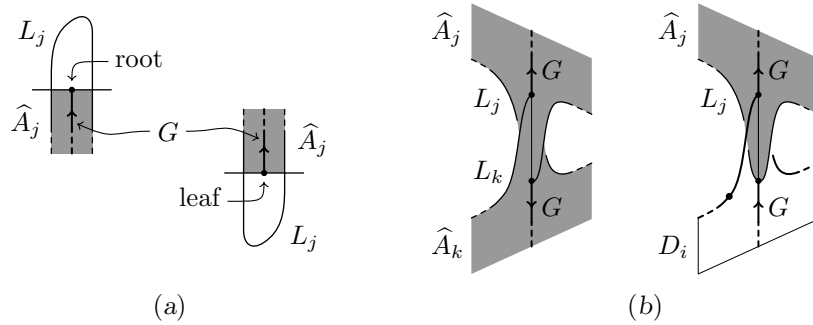


FIGURE 4.7.15.

Now, we consider an oriented graph G consisting of a rooted uni/tri-valent tree embedded in each of such disks. For the tree T inside any disk, we require that (cf. Figure 4.7.15): the root of T belongs to the boundary of the disk and coincides the middle point of the segment at the target level if such segment exists (in the case of a disk A_j); the leaves of T include all the end points of the clasp arcs in the interior of the disk and the middle point of the segment at the source level if such segment exists (in the case of a disk A_j); T does not meet the boundary of the disk and the clasp arcs at any point other than those already mentioned. Moreover, we orient the edges of T towards the leaves in the case of a disk D_i and towards the root in the case of a disk \widehat{A}_j .

Let \overline{G} be the oriented graph obtained by adding to G all the clasp arcs as new oriented edges. The orientation of each new edge goes from the tree of D_i to that of \widehat{A}_j if the corresponding clasp involves such disks, while it is arbitrary otherwise (if the clasp involves two A_j 's).

At this point, a suitable ambient isotopy of $E \times [0, 1]$ fixing $E \times \{0, 1\}$ allows us to put the oriented graph \overline{G} in regular position with respect to the projection plane, in such a way that y -coordinate is increasing along the projection of each oriented edge, and then to deform the union $D_1 \cup \dots \cup D_r \cup \widehat{A}_1 \cup \dots \cup \widehat{A}_s$ to a narrow regular neighborhood N of \overline{G} in it.

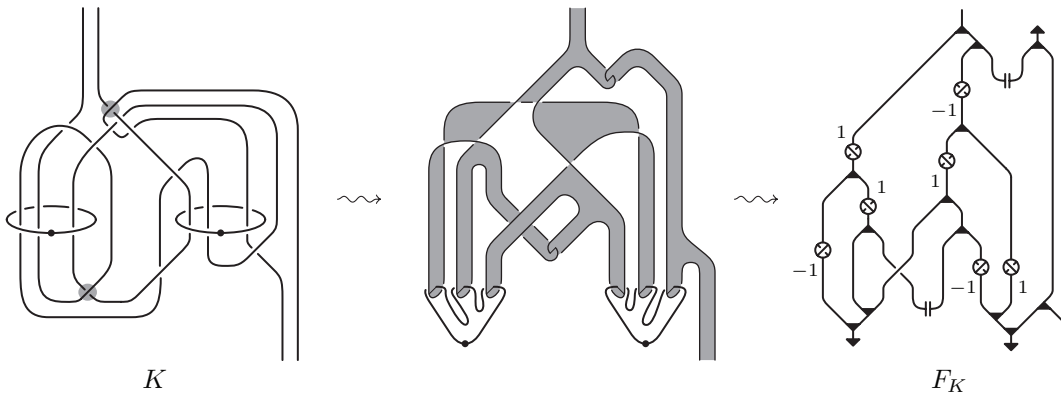


FIGURE 4.7.16.

As a result of such ambient isotopy, the original planar diagram of K is transformed into an equivalent planar diagram, which can be easily expressed as a composition of expansions of Kirby tangles as in Figures 4.2.17 and 4.3.1, after insertion of canceling pairs of $1/2$ -handles.

Then, the morphism F_K is given by the analogous product of expansions of the corresponding elementary morphisms of \mathcal{H}_1^r in the same figures, whose images under Φ_1 are those Kirby tangles. In particular, each clasp intersections between two A_j 's gives rise to a copairing morphism in F_K .

Figure 4.7.16 shows the morphism F_K for a very simple Kirby tangle K . This is represented by the leftmost diagram, where the trivializing crossings are encircled by a small gray disk. The intermediate diagram represents the regular neighborhood N of the graph G in the construction above.

5. 3-dimensional cobordisms as boundaries

This chapter is mainly aimed to prove the Kerler's conjecture (stated in [35]), that the category of 2-framed 3-dimensional relative cobordisms $\widetilde{\mathcal{C}ob}^{2+1}$ admits a purely algebraic characterization in terms of a universal algebraic category generated by a Hopf algebra object.

Here, we think of $\widetilde{\mathcal{C}ob}^{2+1}$ as the quotient category of $\mathcal{C}hb_1^{3+1}$ modulo 1/2-handle trading. This point of view provides a canonical monoidal functor $\mathcal{C}hb_1^{3+1} \rightarrow \widetilde{\mathcal{C}ob}^{2+1}$, through which we will derive the proof of the Kerler's conjecture from the results of the previous chapter.

An analogous algebraic characterization will be also given for the category of 3-dimensional relative cobordisms $\mathcal{C}ob^{2+1}$, as the further quotient of $\widetilde{\mathcal{C}ob}^{2+1}$ modulo blowing down/ups.

5.1. The categories of relative cobordisms $\widetilde{\mathcal{C}ob}_n^{2+1}$ and $\mathcal{C}ob_n^{2+1}$

We recall from Section 2.1 that the objects of $\mathcal{C}hb_n^{3+1}$ have been restricted to be the standard 3-dimensional 1-handlebodies M_π^n described in Definition 2.1.1, where n is the number of 0-handles and $\pi \in \Pi\mathcal{G}_n$. To such an M_π^n is associated its front boundary $F_\pi^n = \partial M_\pi^n$, which is a standard compact oriented surface with marked $(S_1^1 \sqcup \dots \sqcup S_n^1)$ -boundary. In fact, $\text{Bd } F_\pi^n$ has n components, one for each 0-handle of M_π^n , and the given numbering of these 0-handles induces the marking of $\text{Bd } F_\pi^n$ (which depends only on n and not on π).

Moreover, for any morphism $W : M_0 \rightarrow M_1$ in $\mathcal{C}hb_n^{3+1}$, which is a 4-dimensional relative 2-handlebody build on $X(M_0, M_1)$, the front boundary ∂W can be seen as a 3-dimensional relative cobordism $\partial W : \partial M_0 \rightarrow \partial M_1$ between surfaces with marked boundary. Actually, $X(M_0, M_1)$ itself can be seen as such a 3-dimensional cobordism, and W represents a relative cobordism, build up with only 1- and 2-handles, between $X(M_0, M_1)$ and ∂W as oriented 3-manifolds with marked boundary.

Now, consider the handle trading and blowing up/down moves on W , whose description in terms of n -labeled Kirby tangle is given in Figure 5.1.1. These are nothing else than the labeled versions of the well-known Kirby calculus moves and like them preserve the boundary of W . In particular, they preserve the 3-dimensional relative cobordism $\partial W : \partial M_0 \rightarrow \partial M_1$.

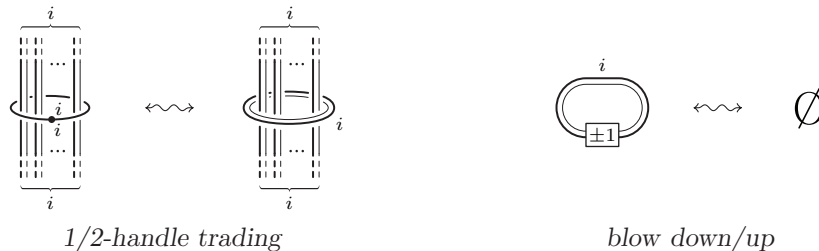


FIGURE 5.1.1. Kirby calculus moves

As discussed in Section 1.2, a 1/2-handle trading changes W into a new 4-dimensional relative 2-handlebody \overline{W} , which is related to W by a relative 5-dimensional cobordism of 4-manifolds with marked boundary. Then, 1/2-handle trading also

preserves the signature of W , i.e. $\sigma(\overline{W}) = \sigma(W)$. According to [6] (cf. [74, 34, 36]), the extra information given by $\sigma(W)$ can be interpreted as a 2-framing on ∂W , i.e. a homotopy class of trivializations of $TM \oplus TM$ as a $\text{Spin}(6)$ bundle. So, we can say that 1/2-handle trading preserves ∂W as a 2-framed 3-dimensional relative cobordism. On the contrary, a blowing up transforms W into the connected sum with $W \# \pm CP^2$, hence it changes the signature by ± 1 .

In the light of the above considerations, for any $n \geq 1$ we define the category of 2-framed 3-dimensional relative cobordisms $\widetilde{\mathcal{C}ob}_n^{2+1}$ and the category of 3-dimensional relative cobordisms \mathcal{Cob}_n^{2+1} , directly as quotients of \mathcal{Chb}_n^{3+1} .

Namely, the objects of both the categories $\widetilde{\mathcal{C}ob}_n^{2+1}$ and \mathcal{Cob}_n^{2+1} are those of \mathcal{Chb}_n^{3+1} . The morphisms of $\widetilde{\mathcal{C}ob}_n^{2+1}$ are equivalence classes of morphisms of \mathcal{Chb}_n^{3+1} under the equivalence relation generated by 1/2-handle trading, while the morphisms of \mathcal{Cob}_n^{2+1} are equivalence classes of morphisms of \mathcal{Chb}_n^{3+1} under the equivalence relation generated by 1/2-handle trading and blowing down/up.

Notice that composition and product of cobordisms are preserved by 1/2-handle trading and blow down/up moves, since these take place in the interior leaving the boundary unchanged. Therefore, $\widetilde{\mathcal{C}ob}_n^{2+1}$ and \mathcal{Cob}_n^{2+1} inherit from \mathcal{Chb}_n^{3+1} a strict monoidal structure, whose product will be still denoted by \diamond , and we have monoidal quotient functors

$$\mathcal{Chb}_n^{3+1} \rightarrow \widetilde{\mathcal{C}ob}_n^{2+1} \rightarrow \mathcal{Cob}_n^{2+1}.$$

In particular, the categories $\widetilde{\mathcal{C}ob}_1^{2+1} = \widetilde{\mathcal{C}ob}_1^{2+1}$ and $\mathcal{Cob}^{2+1} = \mathcal{Cob}_1^{2+1}$ are respectively equivalent to the categories $\widetilde{\mathcal{C}ob}$ and \mathcal{Cob} introduced in [36], admitting the same presentations in terms of elementary morphisms and relations given for those categories in Chapter 4 of [36] (cf. [35], where the notation \mathbf{Cob} is used for $\widetilde{\mathcal{C}ob}^{2+1}$).

The definitions of $\widetilde{\mathcal{C}ob}_n^{2+1}$ and \mathcal{Cob}_n^{2+1} as quotients of \mathcal{Cob}_n^{3+1} are enough for our present aim to prove the equivalence of $\widetilde{\mathcal{C}ob}^{2+1}$ and \mathcal{H}^r .

Such definitions are motivated by the fact that the classical Lickorish-Rohlin-Wallace's theorem [41, 66, 75] asserting that any closed oriented 3-manifold is the boundary of a 4-dimensional 2-handlebody, and the Kirby calculus [37] relating any two such handlebodies with diffeomorphic boundaries, can be adapted to the context of the 4-dimensional relative 2-handlebody cobordisms in \mathcal{Cob}_n^{3+1} . As a consequence, $\widetilde{\mathcal{C}ob}_n^{2+1}$ and \mathcal{Cob}_n^{2+1} can be identified as the categories of all the (2-framed) 3-dimensional cobordisms between surfaces with n -component marked boundary and given 3-dimensional filling, up to diffeomorphisms preserving (the 2-framing and) the fillings. In fact, the case of $n = 1$ is treated in [36] (cf. comment 1. in 0.4.1 on page 8 of the same reference for $n > 1$).

5.2. The quotient categories $\overline{\mathcal{K}}_n$, $\overline{\overline{\mathcal{K}}}_n$, $\overline{\mathcal{S}}_n$ and $\overline{\overline{\mathcal{S}}}_n$

We want to define the quotient categories $\overline{\mathcal{K}}_n$ and $\overline{\overline{\mathcal{K}}}_n$ of \mathcal{K}_n corresponding to $\widetilde{\mathcal{C}ob}_n^{2+1}$ and \mathcal{Cob}_n^{2+1} respectively. Before doing that, we see how to eliminate some redundancy in the 1/2-handle trading and blow down/up moves.

LEMMA 5.2.1. *Modulo 2-handle sliding, any 1/2-handle trading can be reduced to one where the involved 1-handle is a canceling one, as in Figure 5.2.2 (a). Modulo 2-handle sliding and 1/2-handle trading, positive and negative blow down/up are inverse to one another.*

Proof. See Figure 5.2.1. \square

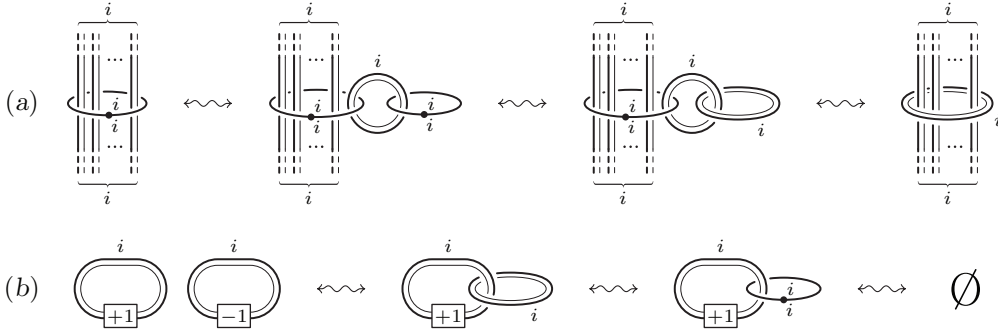


FIGURE 5.2.1. Proof of Lemma 5.2.1

According to the previous lemma, we define $\bar{\mathcal{K}}_n$ and $\overline{\bar{\mathcal{K}}}_n$ as follows. The objects of both $\bar{\mathcal{K}}_n$ and $\overline{\bar{\mathcal{K}}}_n$ coincide with those of \mathcal{K}_n . The morphisms of $\bar{\mathcal{K}}_n$ are equivalence classes of morphisms of \mathcal{K}_n modulo the move in Figure 5.2.2 (a), while the morphisms of $\overline{\bar{\mathcal{K}}}_n$ are equivalence classes of morphisms of \mathcal{K}_n modulo both moves in the same Figure 5.2.2.

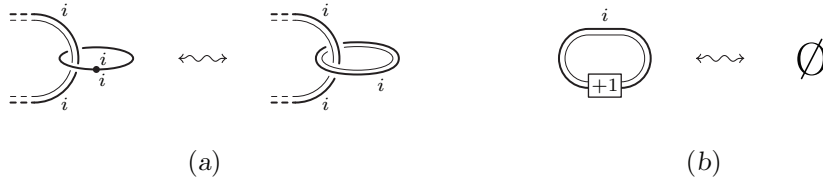


FIGURE 5.2.2. Additional moves in $\bar{\mathcal{K}}_n$ and $\overline{\bar{\mathcal{K}}}_n$

Since the moves in Figure 5.2.2 involve only closed components of the diagram, they preserve composition and product of n -labeled Kirby tangles. Hence, $\bar{\mathcal{K}}_n$ and $\overline{\bar{\mathcal{K}}}_n$ inherit from \mathcal{K}_n a strict monoidal structure, whose product will be still denoted by \diamond , and we have monoidal quotient functors

$$\mathcal{K}_n \rightarrow \bar{\mathcal{K}}_n \rightarrow \overline{\bar{\mathcal{K}}}_n.$$

PROPOSITION 5.2.2. *The equivalence of monoidal categories $\mathcal{K}_n \cong Chb_n^{3+1}$ given by Proposition 2.3.1 induces equivalences of monoidal categories on the quotients $\bar{\mathcal{K}}_n \cong \widetilde{Cob}_n^{2+1}$ and $\overline{\bar{\mathcal{K}}}_n \cong Cob_n^{2+1}$.*

Proof. This is an immediate consequence of Proposition 2.3.1 and Lemma 5.2.1, taking into account that the labeled Kirby tangle moves in Figures 5.2.1 and 5.2.2 already interpret 1/2-handle trading and blow down/up under the equivalence of \mathcal{K}_n and Chb_n^{3+1} in Proposition 2.3.1. \square

Given $n > k \geq 1$, we define the subcategories $\bar{\mathcal{K}}_{n \rightarrow k} \subset \bar{\mathcal{K}}_n$ and $\overline{\bar{\mathcal{K}}}_{n \rightarrow k} \subset \overline{\bar{\mathcal{K}}}_n$ to be the images of $\mathcal{K}_{n \rightarrow k} \subset \mathcal{K}_n$ under the quotient functors. Since the additional moves in Figure 5.2.2 involve only uni-labeled components, when applied to a reducible Kirby tangle K as in Figure 2.3.6, they essentially take place inside the box L .

Then, $\bar{\mathcal{K}}_{n \rightarrow k}$ and $\bar{\bar{\mathcal{K}}}_{n \rightarrow k}$ can also be thought as quotients of $\mathcal{K}_{n \rightarrow k}$, and we have the following commutative diagram of inclusion and quotient functors.

$$\begin{array}{ccccc} \mathcal{K}_{n \rightarrow k} & \rightarrow & \bar{\mathcal{K}}_{n \rightarrow k} & \rightarrow & \bar{\bar{\mathcal{K}}}_{n \rightarrow k} \\ \cap & & \cap & & \cap \\ \mathcal{K}_n & \rightarrow & \bar{\mathcal{K}}_n & \rightarrow & \bar{\bar{\mathcal{K}}}_n \end{array}$$

PROPOSITION 5.2.3. *For any $n > k \geq 1$, the category equivalences $\uparrow_k^n : \mathcal{K}_k \rightarrow \mathcal{K}_{n \rightarrow k}$ and $\downarrow_k^n : \mathcal{K}_{n \rightarrow k} \rightarrow \mathcal{K}_k$ given by the stabilization and reduction functors induce well-defined functors on the quotient categories*

$$\begin{aligned} \uparrow_k^n : \bar{\mathcal{K}}_k &\rightarrow \bar{\mathcal{K}}_{n \rightarrow k} \quad \text{and} \quad \uparrow_k^n : \bar{\bar{\mathcal{K}}}_k &\rightarrow \bar{\bar{\mathcal{K}}}_{n \rightarrow k}, \\ \downarrow_k^n : \bar{\mathcal{K}}_{n \rightarrow k} &\rightarrow \bar{\mathcal{K}}_k \quad \text{and} \quad \downarrow_k^n : \bar{\bar{\mathcal{K}}}_{n \rightarrow k} &\rightarrow \bar{\bar{\mathcal{K}}}_k. \end{aligned}$$

Moreover, $\downarrow_k^n \circ \uparrow_k^n$ is equal to $\text{id}_{\bar{\mathcal{K}}_k}$ (resp. $\text{id}_{\bar{\bar{\mathcal{K}}}_k}$) while $\uparrow_k^n \circ \downarrow_k^n$ is naturally equivalent to $\text{id}_{\bar{\mathcal{K}}_{n \rightarrow k}}$ (resp. $\text{id}_{\bar{\bar{\mathcal{K}}}_{n \rightarrow k}}$). Then, \uparrow_k^n and \downarrow_k^n are category equivalence.

Proof. By Proposition 2.3.9, $\downarrow_k^n \circ \uparrow_k^n = \text{id}_{\mathcal{K}_k}$ while $\uparrow_k^n \circ \downarrow_k^n$ is naturally equivalent to $\text{id}_{\mathcal{K}_{n \rightarrow k}}$. Therefore, the statement will follow once we show that \uparrow_k^n and \downarrow_k^n are well defined on the quotient categories.

That the stabilization functor \uparrow_k^n is well defined on the quotients is straightforward, since by definition $\uparrow_k^n K = \text{id}_{n \rightarrow k} \diamond K$ for any $K \in \mathcal{K}_k$.

Concerning the reduction functor \downarrow_k^n , it has been defined as composition of elementary reduction functors (cf. Definition 2.3.7). Then, it is enough to consider the case of \downarrow_{n-1}^n . In this case, for any $K \in \mathcal{K}_{n \rightarrow (n-1)}$ we have by definition:

$$\downarrow_{n-1}^n K = (\varepsilon_{(n-1, n-1)} \diamond \text{id}_{\pi_1^{(n, n-1)}}) \circ K^{(n, n-1)} \circ (\eta_{n-1} \diamond \text{id}_{\pi_0^{(n, n-1)}}),$$

where $K^{(n, n-1)}$ is obtained from K by pulling all tangle components labeled n above the ones labeled $n-1$ and then changing the label n with $n-1$ (cf. proof of Lemma 2.3.6). Since both the additional relations in $\bar{\mathcal{K}}_k$ and $\bar{\bar{\mathcal{K}}}_k$ involve only uni-labeled sub-tangles, they are obviously preserved by the map $K \mapsto K^{(n, n-1)}$, hence $\downarrow_{n-1}^n K$ is well defined, being the composition of $K^{(n, n-1)}$ with fixed tangles. \square

Now we define the quotient categories $\bar{\mathcal{S}}_n$ and $\bar{\bar{\mathcal{S}}}_n$ of the category \mathcal{S}_n of n -labeled ribbon surface tangles, and make some considerations about them analogous to those made above for $\bar{\mathcal{K}}_n$ and $\bar{\bar{\mathcal{K}}}_n$. In the next section, we will establish the relation between $\bar{\mathcal{S}}_n$ (resp. $\bar{\bar{\mathcal{S}}}_n$) and $\bar{\mathcal{K}}_n$ (resp. $\bar{\bar{\mathcal{K}}}_n$).

Once again, the objects of $\bar{\mathcal{S}}_n$ and $\bar{\bar{\mathcal{S}}}_n$ are those of \mathcal{S}_n . The morphisms of $\bar{\mathcal{S}}_n$ are equivalence classes of morphisms of \mathcal{S}_n modulo the relation (T) in Figure 5.2.3, while the morphisms of $\bar{\bar{\mathcal{S}}}_n$ are equivalence classes of morphisms of \mathcal{S}_n modulo both the relations (T) and (P) in the same Figure 5.2.3. Notice that such moves do not change the boundary of the ribbon surface tangle up to isotopy.

The moves in Figure 5.2.3 clearly preserve composition and product of n -labeled ribbon surface tangles, being local in nature. Hence, $\bar{\mathcal{S}}_n$ and $\bar{\bar{\mathcal{S}}}_n$ inherit from \mathcal{S}_n a strict monoidal structure, whose product will be still denoted by \diamond , and we have monoidal quotient functors

$$\mathcal{S}_n \rightarrow \bar{\mathcal{S}}_n \rightarrow \bar{\bar{\mathcal{S}}}_n.$$

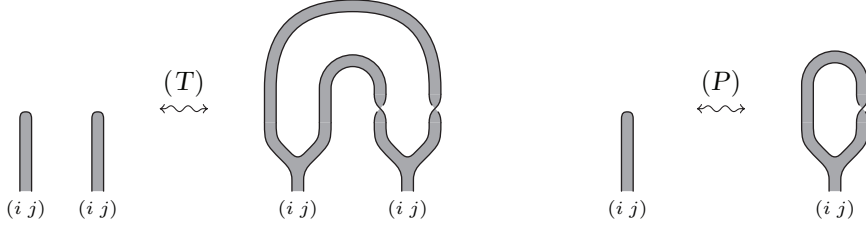


FIGURE 5.2.3. Additional relations in $\bar{\mathcal{S}}_n$ and $\bar{\bar{\mathcal{S}}}_n$

Given $n > k \geq 1$, we define the subcategories $\bar{\mathcal{S}}_{n \rightarrow k} \subset \bar{\mathcal{S}}_n$ and $\bar{\bar{\mathcal{S}}}_{n \rightarrow k} \subset \bar{\bar{\mathcal{S}}}_n$ to be the images of $\mathcal{S}_{n \rightarrow k} \subset \mathcal{S}_n$ under the quotient functors. Thus, we have quotient functors

$$\mathcal{S}_{n \rightarrow k} \rightarrow \bar{\mathcal{S}}_{n \rightarrow k} \rightarrow \bar{\bar{\mathcal{S}}}_{n \rightarrow k}$$

PROPOSITION 5.2.4. *For any $n > k \geq 2$ the functor $\uparrow_k^n : \mathcal{S}_k \rightarrow \mathcal{S}_n$ induces well-defined functors on the quotient categories, for which we use the same notation:*

$$\uparrow_k^n : \bar{\mathcal{S}}_k \rightarrow \bar{\mathcal{S}}_n \quad \text{and} \quad \uparrow_k^n : \bar{\bar{\mathcal{S}}}_k \rightarrow \bar{\bar{\mathcal{S}}}_n.$$

Proof. The statement is straightforward. \square

5.3. Equivalences $\bar{\mathcal{K}}_n^c \cong \bar{\mathcal{S}}_n^c$ and $\bar{\bar{\mathcal{K}}}_n^c \cong \bar{\bar{\mathcal{S}}}_n^c$ for $n \geq 4$

According to the notation introduced in Sections 2.3 and 3.2, we put $\bar{\mathcal{K}}_n^c = \bar{\mathcal{K}}_{n \rightarrow 1}^c$, $\bar{\bar{\mathcal{K}}}_n^c = \bar{\bar{\mathcal{K}}}_{n \rightarrow 1}^c$, $\bar{\mathcal{S}}_n^c = \bar{\mathcal{S}}_{n \rightarrow 1}^c$ and $\bar{\bar{\mathcal{S}}}_n^c = \bar{\bar{\mathcal{S}}}_{n \rightarrow 1}^c$.

In Section 3.3 we defined the functor $\Theta_n : \mathcal{S}_n \rightarrow \mathcal{K}_n$, whose restriction $\Theta_n : \mathcal{S}_n^c \rightarrow \mathcal{K}_n^c$ was shown to be a category equivalence for every $n \geq 4$ in Section 3.6 (see Theorem 3.6.4). The goal of this section is to prove an analogous fact for the quotients introduced in the previous section.

PROPOSITION 5.3.1. *For any $n \geq 2$ the functor $\Theta_n : \mathcal{S}_n \rightarrow \mathcal{K}_n$ induces well-defined braided monoidal functors on the quotient categories:*

$$\begin{aligned} \bar{\Theta}_n : \bar{\mathcal{S}}_n &\rightarrow \bar{\mathcal{K}}_n \quad \text{and} \quad \bar{\Theta}_n : \bar{\mathcal{S}}_n^c \rightarrow \bar{\mathcal{K}}_n^c, \\ \bar{\bar{\Theta}}_n : \bar{\bar{\mathcal{S}}}_n &\rightarrow \bar{\bar{\mathcal{K}}}_n \quad \text{and} \quad \bar{\bar{\Theta}}_n : \bar{\bar{\mathcal{S}}}_n^c \rightarrow \bar{\bar{\mathcal{K}}}_n^c. \end{aligned}$$

Proof. Thanks to Propositions 3.3.2 and 3.3.3, it is enough to prove that if two ribbon surface tangles S and S' in \mathcal{S}_n are related by a (T) move, then their images $\Theta_n(S)$ and $\Theta_n(S')$ in \mathcal{K}_n are related by a handle trading, while if S and S' are related by a (P) move, then $\Theta_n(S)$ and $\Theta_n(S')$ are related by a blow down/up.

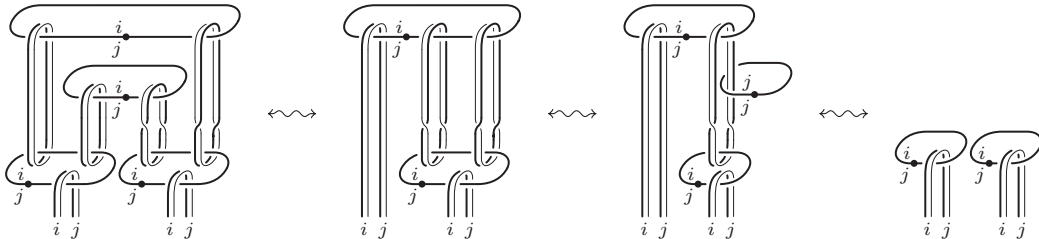


FIGURE 5.3.1. The image of move (T) under the functor Θ_n

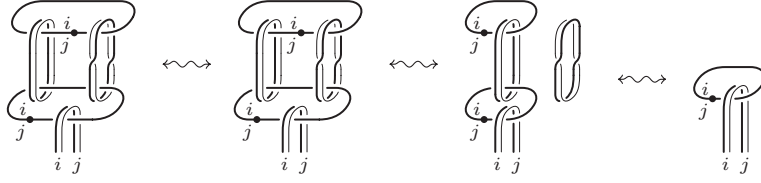


FIGURE 5.3.2. The image of move (P) under the functor Θ_n

These facts are shown in Figures 5.3.1 and 5.3.2 respectively. In particular, the second equivalence in Figure 5.3.1 consists in a handle sliding followed by a $1/2$ -handle trading, while a blow down is performed in the last step of Figure 5.3.2. \square

PROPOSITION 5.3.2. *For any $n \geq 4$, the functor $\Xi_n : \mathcal{K}_1 \rightarrow \mathcal{S}_n^c$ induces well-defined functors on the quotient categories:*

$$\bar{\Xi}_n : \bar{\mathcal{K}}_1 \rightarrow \bar{\mathcal{S}}_n^c \quad \text{and} \quad \bar{\Xi}_n : \bar{\mathcal{K}}_1 \rightarrow \bar{\mathcal{S}}_n^c.$$

Proof. Taking into account the defining identity $\Xi_n = \uparrow_4^n \circ \Xi_4$ (cf. Proposition 3.5.5) and Proposition 5.2.4, it suffices to show that if two Kirby tangles K and K' in \mathcal{K}_1 are related by a $1/2$ -handle trading as in Figure 5.2.2 (a), then their images $\Xi_4(K)$ and $\Xi_4(K')$ in \mathcal{S}_4^c are related by a (T) move, while if K and K' are related by blowing down/up as in Figure 5.2.2 (b), then $\Xi_4(K)$ and $\Xi_4(K')$ are related by a (P) move.

In the light of the construction of the surface S_K in Section 3.4, the latter fact is essentially trivial, since the unknot with frame $+1$ involved in the blow down/up

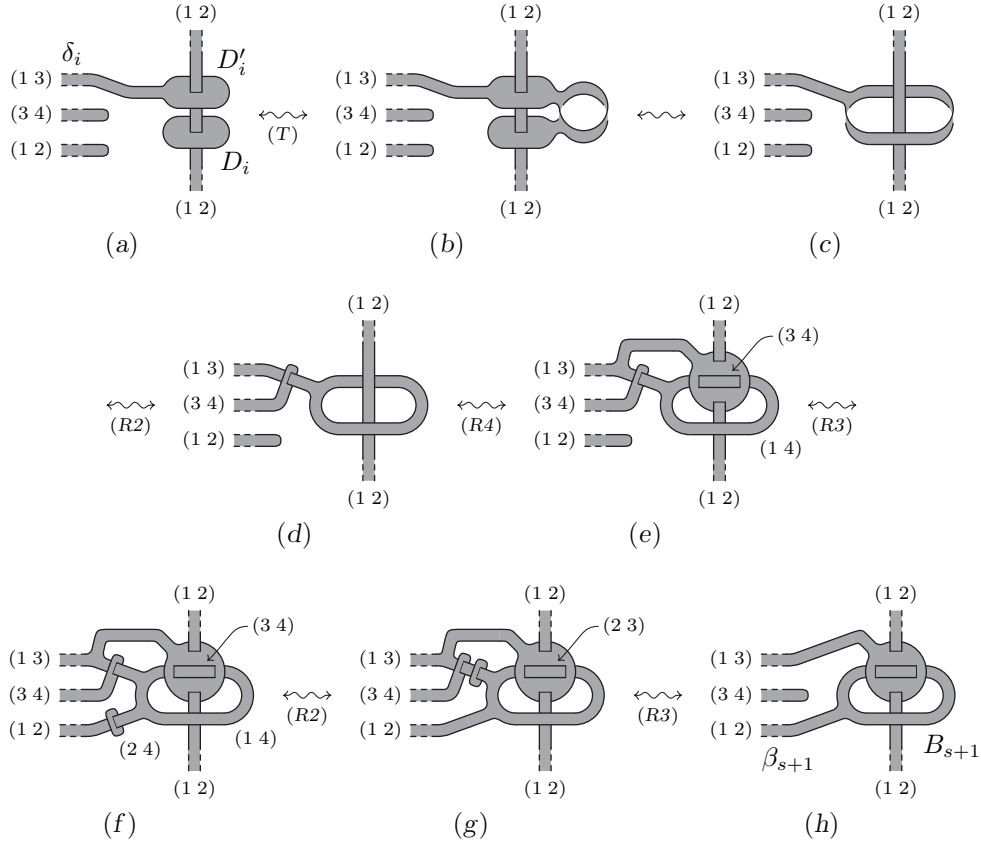


FIGURE 5.3.3.

corresponds in S_K exactly to a positively half twisted closed band as the one in the right-hand side of the move (P). The former fact is proved in Figure 5.3.3. This figure shows the sequence of moves needed to replace the disks D_i and D'_i in diagram (a), corresponding to a canceling 1-handle of K , with the new ribbon B_{s+1} in diagram (h), corresponding to the new 2-handle of K' deriving from the trading. The two bands labeled (1 2) and (3 4) in (a) are assumed to have been expanded from the stabilization ones. The first band will give rise to the band β_{s+1} , the second one is only an auxiliary band, which has to be retracted back in (h). \square

THEOREM 5.3.3. *For any $n \geq 4$, the restriction functor $\bar{\Theta}_n : \bar{\mathcal{S}}_n^c \rightarrow \bar{\mathcal{K}}_n^c$ (resp. $\bar{\Theta}_n : \bar{\mathcal{S}}_n^c \rightarrow \bar{\mathcal{K}}_n^c$) and the functor $\bar{\Xi}_n : \bar{\mathcal{K}}_1 \rightarrow \bar{\mathcal{S}}_n^c$ (resp. $\bar{\Xi}_n : \bar{\mathcal{K}}_1 \rightarrow \bar{\mathcal{S}}_n^c$) are category equivalences. Moreover, $\downarrow_1^n \circ \bar{\Theta}_n \circ \bar{\Xi}_n$ (resp. $\downarrow_1^n \circ \bar{\Theta}_n \circ \bar{\Xi}_n$) is equal to $\text{id}_{\bar{\mathcal{K}}_1}$ (resp. $\text{id}_{\bar{\mathcal{K}}_1}$), while $\bar{\Xi}_n \circ \downarrow_1^n \circ \bar{\Theta}_n$ (resp. $\bar{\Xi}_n \circ \downarrow_1^n \circ \bar{\Theta}_n$) is naturally equivalent to $\text{id}_{\bar{\mathcal{S}}_n^c}$ (resp. $\text{id}_{\bar{\mathcal{S}}_n^c}$).*

Proof. It follows immediately by Theorem 3.6.4 and the propositions above. \square

5.4. The quotient categories $\bar{\mathcal{H}}_n$ and $\bar{\bar{\mathcal{H}}}_n$

Analogously to what was done for the categories of Kirby and ribbon surface tangles, we introduce the quotients of the universal groupoid ribbon Hopf algebra $\mathcal{H}^r(\mathcal{G})$ by two additional relations. The first relation states the duality of the algebra integral and cointegral with respect to the copairing. The second one is a kind of normalization telling that a specific closed morphism equals the empty morphism id_1 . In particular, the corresponding quotients of $\mathcal{H}_n^{r,c} \subset \mathcal{H}_n^r$ will be shown to be equivalent to $\bar{\mathcal{K}}_n^c$ and $\bar{\bar{\mathcal{K}}}_n^c$ in the next section.

DEFINITION 5.4.1. Given a groupoid \mathcal{G} , a ribbon Hopf \mathcal{G} -algebra H in a braided monoidal category \mathcal{C} is called *self-dual* if the following identity (cf. Table 5.4.1) holds for every $i \in \mathcal{G}$:

$$(l_i \diamond \text{id}_{1_i}) \circ \sigma_{i,i} = L_{1_i}. \quad (d)$$

Moreover, a self-dual ribbon Hopf \mathcal{G} -algebra H is called *boundary* if the following normalization identity (cf. Table 5.4.2) holds for every $i \in \mathcal{G}$:

$$l_i \circ v_{1_i} \circ \eta_i = \text{id}_1. \quad (n)$$

We define the *universal self-dual ribbon Hopf algebra* $\bar{\mathcal{H}}^r(\mathcal{G})$ to be the quotient category of $\mathcal{H}^r(\mathcal{G})$ modulo the relations (d) presented in Table 5.4.1, and the *universal boundary ribbon Hopf algebra* $\bar{\bar{\mathcal{H}}}^r(\mathcal{G})$ to be the quotient category of $\bar{\mathcal{H}}^r(\mathcal{G})$ modulo the relations (n) presented in Tables 5.4.2.

Like for the categories of tangles, the quotients $\bar{\mathcal{H}}^r(\mathcal{G})$ and $\bar{\bar{\mathcal{H}}}^r(\mathcal{G})$ inherit from $\mathcal{H}^r(\mathcal{G})$ a strict monoidal structure, whose product will be still denoted by \diamond , and we have monoidal quotient functors

$$\mathcal{H}^r(\mathcal{G}) \rightarrow \bar{\mathcal{H}}^r(\mathcal{G}) \rightarrow \bar{\bar{\mathcal{H}}}^r(\mathcal{G}).$$

It is well-known (cf. [35]) that the relation (d) in Table 5.4.1 implies the symmetric relation (d') and also the non-degeneracy of the copairing and the duality of the multiplication and comultiplication morphisms in $\bar{\mathcal{H}}^r(\mathcal{G})$. For the sake of completeness we present the result below.

Axiom for the universal self-dual ribbon Hopf algebra $\overline{\mathcal{H}}^r(\mathcal{G})$ (in addition to the axioms of $\mathcal{H}^r(\mathcal{G})$)
Properties of the universal self-dual ribbon Hopf algebra $\overline{\mathcal{H}}^r(\mathcal{G})$
<p style="text-align: center;">Relation symmetric to (d)</p>
<div style="display: flex; justify-content: space-around; align-items: flex-start;"> <div style="text-align: center;"> $\bar{\sigma}_{i,j} =$ <p>(d1) def</p> </div> <div style="text-align: center;"> <p>(d2)</p> </div> <div style="text-align: center;"> <p>(d2')</p> </div> </div> <div style="display: flex; justify-content: space-around; align-items: center; margin-top: 10px;"> <div style="text-align: center;"> <p>(d3)</p> </div> <div style="text-align: center;"> <p>(d3')</p> </div> </div> <p style="text-align: center;">Definition and properties of the pairing</p>

TABLE 5.4.1.

Axiom for the universal boundary ribbon Hopf algebra $\overline{\overline{\mathcal{H}}}^r(\mathcal{G})$ (in addition to the axioms of $\overline{\mathcal{H}}^r(\mathcal{G})$)
Property of the universal boundary ribbon Hopf algebra $\overline{\overline{\mathcal{H}}}^r(\mathcal{G})$
<p style="text-align: center;">Relation symmetric to (n)</p>

TABLE 5.4.2.

PROPOSITION 5.4.2. *Let \mathcal{G} be any groupoid. Then, the following relation holds in $\overline{\mathcal{H}}^r(\mathcal{G})$ for every $i \in \mathcal{G}$ (cf. Table 5.4.1):*

$$(\text{id}_{1_i} \diamond l_i) \circ \sigma_{i,i} = L_{1_i}, \quad (d')$$

Moreover, the pairing morphisms $\bar{\sigma}_{i,j} : H_{1_i} \diamond H_{1_j} \rightarrow \mathbf{1}$ in $\overline{\mathcal{H}}^r(\mathcal{G})$ defined by

$$\bar{\sigma}_{i,j} = (\Lambda_{1_i} \diamond \Lambda_{1_j}) \circ (\text{id}_{1_i} \diamond \sigma_{i,j} \diamond S_{1_j}^{-1}) \quad (d1)$$

for every $i, j \in \mathcal{G}$, satisfy the following identities (d2-2') and (d3-3') in Table 5.4.1.

Proof. Relation (d') is equivalent to (d) modulo (i5) and (f5-11) in Tables 4.1.8 and 4.2.2. Identity (d2) is proved in Figure 5.4.3, and then (d2') follows by symmetry. Finally, by using (d2-2'), one can easily derive (d3-3') from (r7-7') in Tables 4.2.1 and 4.2.2. \square

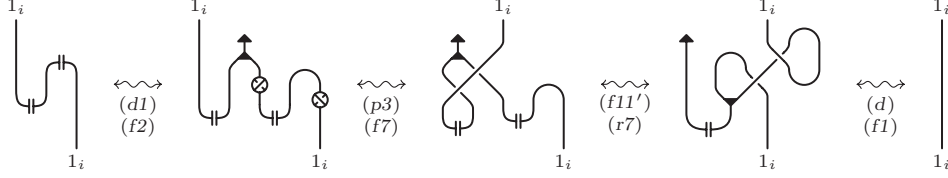


FIGURE 5.4.3. Deriving relation (d2) in $\bar{\mathcal{H}}^r(\mathcal{G})$ [d/194, f/129-134, p/134, r/132]

PROPOSITION 5.4.3. *Given a groupoid \mathcal{G} , the following relation holds in $\bar{\mathcal{H}}_n^r$ for every $i \in \mathcal{G}$ (see Table 5.4.2):*

$$l_i \circ v_{1_i}^{-1} \circ \eta_i = \text{id}_{1_i}. \quad (n')$$

Proof. See Figure 5.4.4. \square

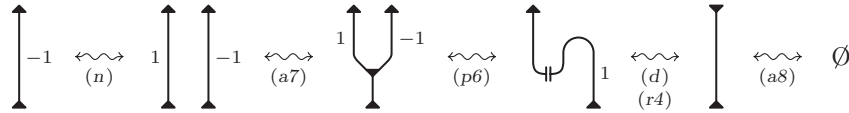


FIGURE 5.4.4. Deriving relation (n') in $\bar{\mathcal{H}}^r(\mathcal{G})$ [a/123, d/194, n/194, p/134, r/132]

Given a full inclusion of groupoids $\mathcal{G} \subset \mathcal{G}'$ and a spanning sequence $X = (x_n, \dots, x_1)$ for the pair $(\mathcal{G}', \mathcal{G})$, we define the subcategories $\bar{\mathcal{H}}_X^r(\mathcal{G}) \subset \bar{\mathcal{H}}^r(\mathcal{G})$ and $\bar{\mathcal{H}}_X^r(\mathcal{G}') \subset \bar{\mathcal{H}}^r(\mathcal{G}')$ to be the images of $\mathcal{H}_X^r(\mathcal{G}) \subset \mathcal{H}^r(\mathcal{G})$ under the quotient functors. As for Kirby tangles, we have the following commutative diagram of inclusion and quotient functors

$$\begin{array}{ccccc} \mathcal{H}_X^r(\mathcal{G}) & \rightarrow & \bar{\mathcal{H}}_X^r(\mathcal{G}) & \rightarrow & \bar{\bar{\mathcal{H}}}_X^r(\mathcal{G}) \\ \cap & & \cap & & \cap \\ \mathcal{H}^r(\mathcal{G}) & \rightarrow & \bar{\mathcal{H}}^r(\mathcal{G}) & \rightarrow & \bar{\bar{\mathcal{H}}}^r(\mathcal{G}) \end{array}$$

PROPOSITION 5.4.4. *For any full inclusion of groupoids $\mathcal{G} \subset \mathcal{G}'$ and spanning sequence $X = (x_n, \dots, x_1)$ for the pair $(\mathcal{G}', \mathcal{G})$, the stabilization functor $\uparrow_X : \mathcal{H}^r(\mathcal{G}) \rightarrow \mathcal{H}_X^r(\mathcal{G}')$ and the reduction functor $\downarrow_X : \mathcal{H}_X^r(\mathcal{G}') \rightarrow \mathcal{H}^r(\mathcal{G})$ induce well-defined functors on the quotient categories*

$$\begin{array}{l} \uparrow_X : \bar{\mathcal{H}}^r(\mathcal{G}) \rightarrow \bar{\mathcal{H}}_X^r(\mathcal{G}') \quad \text{and} \quad \downarrow_X : \bar{\mathcal{H}}_X^r(\mathcal{G}') \rightarrow \bar{\mathcal{H}}^r(\mathcal{G}), \\ \uparrow_X : \bar{\bar{\mathcal{H}}}^r(\mathcal{G}) \rightarrow \bar{\bar{\mathcal{H}}}_X^r(\mathcal{G}') \quad \text{and} \quad \downarrow_X : \bar{\bar{\mathcal{H}}}_X^r(\mathcal{G}') \rightarrow \bar{\bar{\mathcal{H}}}^r(\mathcal{G}). \end{array}$$

Moreover, $\downarrow_X \circ \uparrow_X = \text{id}_{\bar{\mathcal{H}}^r(\mathcal{G})}$ (resp. $\downarrow_X \circ \uparrow_X = \text{id}_{\bar{\bar{\mathcal{H}}}^r(\mathcal{G})}$), while $\uparrow_X \circ \downarrow_X$ is naturally equivalent to $\text{id}_{\bar{\mathcal{H}}_X^r(\mathcal{G}')}$ (resp. $\text{id}_{\bar{\bar{\mathcal{H}}}_X^r(\mathcal{G}')}$). In particular, \downarrow_X and \uparrow_X are equivalences of categories.

Proof. The last part of the statement will follow immediately from Theorem 4.5.7, once we prove that \uparrow_X and \downarrow_X induce well-defined functors between the quotient categories. This fact is obvious for the stabilization functor \uparrow_X . Concerning the reduction \downarrow_X , we recall from Definition 4.5.5 that $\downarrow_X = \downarrow_{x_1} \circ \dots \circ \downarrow_{x_n}$. Then, it is enough to consider the case of an elementary reduction $\downarrow_x : H_x^r(\mathcal{G}) \rightarrow H^r(\mathcal{G}^{\setminus i_0})$ for $x \in \mathcal{G}(i_0, j_0)$. On the other hand, still referring to Definition 4.5.5, we have $\downarrow_x F = (\varepsilon_{1_{j_0}} \diamond \text{id}_{\pi_1^x}) \circ F^x \circ (\eta_{j_0} \diamond \text{id}_{\pi_0^x})$ for any $F : H_x \diamond H_{\pi_0} \rightarrow H_x \diamond H_{\pi_1}$ in $\mathcal{H}_x^r(\mathcal{G})$. Hence, we are reduced to proving that the functor $_x : \mathcal{H}^r(\mathcal{G}) \rightarrow \mathcal{H}^r(\mathcal{G}^{\setminus i_0})$ defined in Proposition 4.4.11 passes to the quotient, giving well-defined functors

$$_x : \bar{\mathcal{H}}^r(\mathcal{G}) \rightarrow \bar{\mathcal{H}}^r(\mathcal{G}) \quad \text{and} \quad _x : \bar{\bar{\mathcal{H}}}^r(\mathcal{G}) \rightarrow \bar{\bar{\mathcal{H}}}^r(\mathcal{G}).$$

This follows from the fact that the additional axioms (d) and (n) defining the quotient categories $\bar{\mathcal{H}}^r(\mathcal{G})$ and $\bar{\bar{\mathcal{H}}}^r(\mathcal{G})$ have the form $F_1 = F_2$, where all labels occurring in F_1 and F_2 are equal to 1_i for some $i \in \mathcal{G}$. Then, by Definition 4.4.9 F_1^x and F_2^x have the same graph diagrams as F_1 and F_2 , but label 1_{i_x} instead of 1_i . In particular, F_1^x and F_2^x satisfy the same relation as F_1 and F_2 . \square

5.5. Equivalences $\bar{\mathcal{K}}_n^c \cong \bar{\mathcal{H}}_n^{r,c}$ and $\bar{\bar{\mathcal{K}}}_n^c \cong \bar{\bar{\mathcal{H}}}_n^{r,c}$

Now we want to prove that the commutative diagram in Theorem 4.7.4 induces analogous commutative diagrams of equivalence functors between the quotient categories. This will imply the equivalence of $\widetilde{\mathcal{C}ob}^{2+1}$ (resp. $\mathcal{C}ob^{2+1}$) and $\bar{\mathcal{H}}^r = \bar{\mathcal{H}}_1^r$ (resp. $\bar{\bar{\mathcal{H}}}^r = \bar{\bar{\mathcal{H}}}_1^r$).

Analogously to what was done in Sections 4.5 and 4.7, when $\mathcal{G} = \mathcal{G}_k$, $\mathcal{G}' = \mathcal{G}_n$ and $X = \pi_{n \rightarrow k} = ((n, n-1), \dots, (k+1, k))$ with $n > k \geq 1$, we adopt the notation $\bar{\mathcal{H}}_{\pi_{n \rightarrow k}}^r = \bar{\mathcal{H}}_{n \rightarrow k}^r$ and $\bar{\bar{\mathcal{H}}}_{\pi_{n \rightarrow k}}^r = \bar{\bar{\mathcal{H}}}_{n \rightarrow k}^r$, and we put $\bar{\mathcal{H}}_n^{r,c} = \bar{\mathcal{H}}_{n-1}^r(\mathcal{G}_n)$ and $\bar{\bar{\mathcal{H}}}_n^{r,c} = \bar{\bar{\mathcal{H}}}_{n-1}^r(\mathcal{G}_n)$.

PROPOSITION 5.5.1. *For any $n \geq 1$, the functor $\Phi_n : \mathcal{H}_n \rightarrow \mathcal{K}_n$ induces well-defined monoidal functors on the quotient categories*

$$\bar{\Phi}_n : \bar{\mathcal{H}}_n^r \rightarrow \bar{\mathcal{K}}_n \quad \text{and} \quad \bar{\bar{\Phi}}_n : \bar{\bar{\mathcal{H}}}_n^r \rightarrow \bar{\bar{\mathcal{K}}}_n.$$

Moreover, for any $n > k \geq 1$ we have the following commutative diagrams.

$$\begin{array}{ccc} \bar{\mathcal{H}}_{n \rightarrow k}^r & \xrightarrow{\bar{\Phi}_n} & \bar{\mathcal{K}}_{n \rightarrow k} \\ \downarrow \downarrow_k^n & & \downarrow \downarrow_k^n \\ \bar{\mathcal{H}}_k^r & \xrightarrow{\bar{\Phi}_k} & \bar{\mathcal{K}}_k \end{array} \quad \begin{array}{ccc} \bar{\bar{\mathcal{H}}}_{n \rightarrow k}^r & \xrightarrow{\bar{\bar{\Phi}}_n} & \bar{\bar{\mathcal{K}}}_{n \rightarrow k} \\ \downarrow \downarrow_k^n & & \downarrow \downarrow_k^n \\ \bar{\bar{\mathcal{H}}}_k^r & \xrightarrow{\bar{\bar{\Phi}}_k} & \bar{\bar{\mathcal{K}}}_k \end{array}$$

Proof. For the first part of the statement, it suffices to observe that, under the functor $\Phi_n : \mathcal{H}_n \rightarrow \mathcal{K}_n$ defined in Theorem 4.3.1, the relations (d) and (n) in Tables 5.4.1 and 5.4.2 translate directly in the moves (a) and (b) in Figure 5.2.2. Then, the commutative diagrams are obtained just by quotienting the second diagram in Proposition 4.5.8. \square

PROPOSITION 5.5.2. For any $n \geq 4$, the functor $\Psi_n : \mathcal{S}_n \rightarrow \mathcal{H}_n^r$ induces well-defined braided monoidal functors between the quotient categories:

$$\begin{aligned} \bar{\Psi}_n : \bar{\mathcal{S}}_n &\rightarrow \bar{\mathcal{H}}_n^r \quad \text{and} \quad \bar{\bar{\Psi}}_n : \bar{\bar{\mathcal{S}}}_n \rightarrow \bar{\bar{\mathcal{H}}}_n^r, \\ \bar{\Psi}_n : \bar{\mathcal{S}}_n^c &\rightarrow \bar{\mathcal{H}}_n^{r,c} \quad \text{and} \quad \bar{\bar{\Psi}}_n : \bar{\bar{\mathcal{S}}}_n^c \rightarrow \bar{\bar{\mathcal{H}}}_n^{r,c}. \end{aligned}$$

Proof. Figure 5.5.1 (resp. 5.5.2) shows that the images under $\Psi_n : \mathcal{S}_n \rightarrow \mathcal{H}_n^r$ of the two sides of the relation (T) (resp. (P)) in Figure 5.2.3 are equivalent in $\bar{\mathcal{H}}_n^r$ (resp. $\bar{\bar{\mathcal{H}}}_n^r$). Therefore, Ψ_n induces well-defined functors between the quotient categories. \square

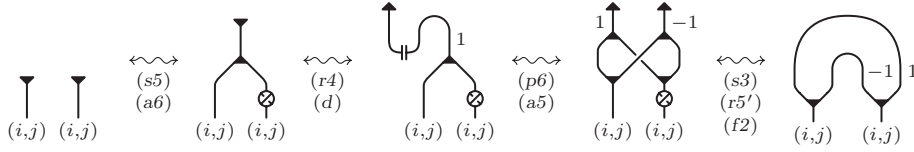


FIGURE 5.5.1. The image of move (T) in $\bar{\mathcal{H}}_n^r$ ($i > j$) [a/123, f/129, d/194, p/134, r/132-134, s/125]

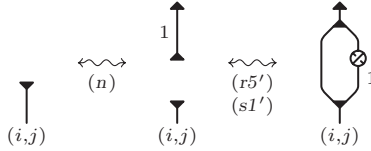


FIGURE 5.5.2. The image of move (P) in $\bar{\bar{\mathcal{H}}}_n^r$ ($i > j$) [n/194, r/134, s/123]

THEOREM 5.5.3. For any $n \geq 4$, we have the following commutative diagrams of equivalence functors:

$$\begin{array}{ccc} \bar{\mathcal{S}}_n^c & \xrightarrow{\bar{\Theta}_n} & \bar{\mathcal{K}}_n^c \\ \bar{\Psi}_n \searrow & & \nearrow \bar{\Phi}_n \\ & \bar{\mathcal{H}}_n^{r,c} & \end{array} \quad \begin{array}{ccc} \bar{\bar{\mathcal{S}}}_n^c & \xrightarrow{\bar{\bar{\Theta}}_n} & \bar{\bar{\mathcal{K}}}_n^c \\ \bar{\bar{\Psi}}_n \searrow & & \nearrow \bar{\bar{\Phi}}_n \\ & \bar{\bar{\mathcal{H}}}_n^{r,c} & \end{array}$$

Proof. The existence of the functors has been already established in Propositions 5.3.1, 5.5.1 and 5.5.2. The commutativity of the diagrams follows from that of the diagram in Theorem 4.7.4 by taking the respective quotients. According to Theorem 5.3.3, for $n \geq 4$ the functors $\bar{\Theta}_n$ and $\bar{\bar{\Theta}}_n$ are category equivalences, which implies that in this case $\bar{\Psi}_n$ and $\bar{\bar{\Psi}}_n$ are faithful. Now, since Ψ_n is a category equivalence, it is full and any object in \mathcal{H}_n^r is isomorphic to one in its image. Then, the same holds for its quotients $\bar{\Psi}_n$ and $\bar{\bar{\Psi}}_n$, which implies that these are category equivalences as well, and by the commutativity of the diagram, so are $\bar{\Phi}_n$ and $\bar{\bar{\Phi}}_n$. \square

At this point, we are ready to give the announced algebraic description of the category of (2-framed) 3-dimensional relative codordisms in terms of the categories $\bar{\mathcal{H}}^r = \bar{\mathcal{H}}_1^r$ (in the 2-framed case) and $\bar{\bar{\mathcal{H}}}^r = \bar{\bar{\mathcal{H}}}_1^r$. The elementary morphisms and defining axioms of such algebraic categories are listed in Tables 4.7.12 and 4.7.13

and Table 5.5.3. Observe that axiom (d) in the last table expresses the integral L in terms of the cointegral λ and the copairing σ , and by substituting such expression in axioms (i2-3) in 4.7.13, we can cancel both, L from the list of the elementary diagrams in Tables 4.7.12, and (d) from the list of the axioms.

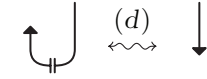

Axioms for the universal Hopf algebras $\overline{\mathcal{H}}^r = \overline{\mathcal{H}}_1^r$ and $\overline{\overline{\mathcal{H}}}^r = \overline{\overline{\mathcal{H}}}_1^r$ (in addition to the axioms of $\mathcal{H}^r = \mathcal{H}_1^r$)	
 <p style="margin-top: 10px;">Additional axiom for $\overline{\mathcal{H}}^r = \overline{\mathcal{H}}_1^r$</p>	 <p style="margin-top: 10px;">Additional axioms for $\overline{\mathcal{H}}^r = \overline{\mathcal{H}}_1^r$</p>

TABLE 5.5.3.

THEOREM 5.5.4. *The functors $\overline{\Phi}_n : \overline{\mathcal{H}}_n^{r,c} \rightarrow \overline{\mathcal{K}}_n^c$ and $\overline{\overline{\Phi}}_n : \overline{\overline{\mathcal{H}}}_n^{r,c} \rightarrow \overline{\overline{\mathcal{K}}}_n^c$ are category equivalences for any $n \geq 1$. In particular, the universal self-dual ribbon Hopf algebra $\overline{\mathcal{H}}^r = \overline{\mathcal{H}}_1^r$ is equivalent to the category of 2-framed 3-dimensional relative cobordisms $\widetilde{\mathcal{C}ob}^{2+1} = \widetilde{\mathcal{C}ob}_1^{2+1}$, while universal boundary ribbon Hopf algebra $\overline{\overline{\mathcal{H}}}^r = \overline{\overline{\mathcal{H}}}_1^r$ is equivalent to the category of 3-dimensional relative cobordisms $\mathcal{C}ob^{2+1} = \mathcal{C}ob_1^{2+1}$.*

Proof. According to Theorem 5.5.3, $\overline{\Phi}_n$ is a category equivalence for any $n \geq 4$. For any $1 \leq n \leq 3$, the commutative diagrams in Proposition 5.5.1 imply that $\overline{\Phi}_n \circ \downarrow_n^4 = \downarrow_n^4 \circ \overline{\Phi}_4$ (resp. $\overline{\overline{\Phi}}_n \circ \downarrow_n^4 = \downarrow_n^4 \circ \overline{\overline{\Phi}}_4$). By Propositions 5.2.3 and 5.4.4, the reduction functors involved in this identity are category equivalences and therefore, $\overline{\Phi}_n$ (resp. $\overline{\overline{\Phi}}_n$) is a category equivalence as well. In particular, for $n = 1$ we obtain that $\overline{\Phi}_1 : \overline{\mathcal{H}}_1^r \rightarrow \overline{\mathcal{K}}_1$ (resp. $\overline{\overline{\Phi}}_1 : \overline{\overline{\mathcal{H}}}_1^r \rightarrow \overline{\overline{\mathcal{K}}}_1$) is a category equivalence. Then, the second part of the statement follows from Proposition 5.2.2 with $n = 1$. \square

6. Branched coverings of B^4 and S^3

In this chapter we apply the previous results to the covering moves problem for branched coverings of B^4 and S^3 .

In particular, Section 6.1 concerns the representation of 4-dimensional 2-handlebodies as simple coverings of B^4 branched over ribbon surfaces. Here, we will derive from the results of Chapters 2 and 3 an effective way to convert any Kirby diagram into a 3-labeled ribbon surface providing such a representation, and a 2-equivalence criterion in terms of moves for labeled ribbon surface.

Then, in Section 6.2, by adding the further moves introduced in Section 5.2 and restricting all the moves to the boundary, we obtain a complete solution of the Fox-Montesinos covering moves problem for simple coverings of S^3 branched over links. Finally, we extend such result to arbitrary coverings of S^3 branched over graphs.

6.1. Covers of B^4 simply branched over ribbon surfaces

Recalling the definitions in Sections 2.1, we have that the 2-equivalence classes of connected 4-dimensional 2-handlebodies bijectively correspond to the morphisms $W : M_\emptyset^1 \rightarrow M_\emptyset^1$ in \mathcal{Chb}_1^{3+1} , or equivalently, in terms of Kirby diagrams, to the morphisms $K : I_\emptyset \rightarrow I_\emptyset$ in \mathcal{K}_1 (cf. Proposition 2.3.1). This follows from Proposition 1.2.4, by taking into account that such a morphism W is a relative 4-dimensional 2-handlebody build on the unique 0-handle $H^0 = Y(M_\emptyset^1, M_\emptyset^1) \cong B^4$, considered up to 2-deformations that fix H^0 and do not introduce any extra 0-handle.

On the other hand, an n -fold covering of B^4 simply branched over a ribbon surface, is represented by an n -labeled ribbon surface in B^4 , which is nothing else than a morphism $S : J_\emptyset \rightarrow J_\emptyset$ in \mathcal{S}_n . Moreover, the functor $\Theta_n : \mathcal{S}_n \rightarrow \mathcal{K}_n$ introduced in Section 3.3 sends S to a n -labeled Kirby diagram $K_S : I_\emptyset \rightarrow I_\emptyset$ in \mathcal{K}_n . This in turn represents a relative 4-dimensional 2-handlebody $W_S : M_\emptyset^n \rightarrow M_\emptyset^n$ build on the n 0-handles $H_1^0 \sqcup \dots \sqcup H_n^0 = Y(M_\emptyset^n, M_\emptyset^n) \cong B^4 \sqcup \dots \sqcup B^4$, considered up to 2-equivalence modulo the 0-handles.

Then, the restriction of Θ_n from n -labeled ribbon surfaces (i.e. ribbon surface tangles with empty source and target) to n -labeled Kirby diagrams (i.e. Kirby tangles with empty source and target), exactly encodes the realization of 4-dimensional 2-handlebodies up to 2-equivalence as simple branched coverings of B^4 given by Montesinos in [52]. In fact, according to the discussion at the beginning of Section 3.3, if $S \subset B^4$ is an n -labeled ribbon surface representing a simple branched covering $p : W \rightarrow B^4$, any adapted 1-handlebody decomposition of S induces a 2-handlebody decomposition of W with n 0-handles, whose 1-handles (resp. 2-handles) correspond to the 0-handles (resp. 1-handles) of S . Moreover, Lemma 3.3.1 says that 1-deformations in S induce 2-deformations in W , hence the 2-handlebody structure of W turns out to be well-defined up to 2-equivalence by Propositions 1.3.4.

The main result of Montesinos [52] is that any connected oriented 4-dimensional 2-handlebody W has a 3-fold branched covering representation as above. Actually, the ribbon surface S can always be made orientable (cf. Remark 1.4.4 or [42, 63] for other constructions giving directly orientable branching surfaces). In that paper the labeled ribbon surface S is obtained from a Kirby diagram of W , after it has been suitably symmetrized with respect to a standard 3-fold simple covering representation of the 1-handlebody W^1 .

A simpler and more effective construction of a labeled ribbon surface S representing W , similar to that of labeled links given in [54] for 3-manifolds (cf. Remark 3.4.1), can be derived from Proposition 3.4.3. This is the content of Proposition 6.1.2 below.

But first we need the following definition. Let us denote by \mathcal{K}_n^\emptyset the set of all n -labeled Kirby diagrams $K : I_\emptyset \rightarrow I_\emptyset$ in \mathcal{K}_n and by \mathcal{S}_n^\emptyset the set of all n -labeled ribbon surfaces $S : J_\emptyset \rightarrow J_\emptyset$ in \mathcal{S}_n .

DEFINITION 6.1.1. Given any Kirby tangle $K : I_{\pi_0} \rightarrow I_{\pi_1}$ in \mathcal{K}_n with $\pi_0 = ((i_1^0, j_1^0), \dots, (i_{m_0}^0, j_{m_0}^0))$ and $\pi_1 = ((i_1^1, j_1^1), \dots, (i_{m_1}^1, j_{m_1}^1))$, we define the *closure* of K to be the Kirby diagram $\widehat{K} = (\varepsilon_{(i_1^1, j_1^1)} \diamond \dots \diamond \varepsilon_{(i_{m_1}^1, j_{m_1}^1)}) \circ K \circ (L_{(i_1^0, j_1^0)} \diamond \dots \diamond L_{(i_{m_0}^0, j_{m_0}^0)})$ in \mathcal{K}_n^\emptyset (see Figure 6.1.1). Similarly, given a ribbon surface tangle $S : J_{\sigma_0} \rightarrow J_{\sigma_1}$ in \mathcal{S}_n , we define the *closure* of S to be the ribbon surface \widehat{S} in \mathcal{S}_n^\emptyset shown in Figure 6.1.2.

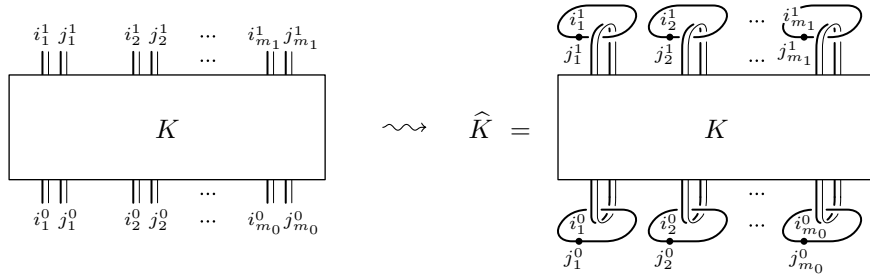


FIGURE 6.1.1. The closure \widehat{K} of a Kirby tangle K in \mathcal{K}_n

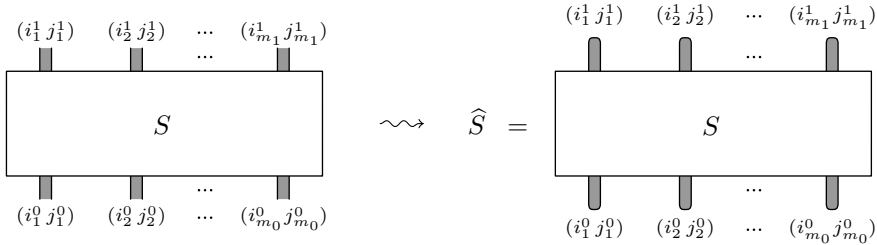


FIGURE 6.1.2. The closure \widehat{S} of a ribbon surface tangle S in \mathcal{S}_n

It is clear from the definitions (cf. Figure 3.3.17) that the functor $\Theta_n : \mathcal{S}_n \rightarrow \mathcal{K}_n$ preserves closures, i.e. if $\Theta_n(S) = K$ then $\Theta_n(\widehat{S}) = \widehat{K}$.

We also observe that the stabilization $\uparrow_k^n K$ of a k -labeled Kirby diagram K is an n -labeled Kirby tangle with non-empty source and target $I_{\pi_{n-k}}$. But the closure of $\uparrow_k^n K$ is an n -labeled Kirby diagram and the corresponding 4-dimensional 2-handlebody is 2-equivalent to the one given by K (see Figure 6.1.3 for $k = n - 1$). Such 2-equivalence consists in the deletion of canceling pairs of 1/2-handles and then 0/1-handles (in the rightmost diagram of Figure 6.1.3, the n -th 0-handle can be canceled against the 1-handle connecting it to the $(n - 1)$ -th 0-handle, since K lives in the other 0-handles).

Analogously, the closure of the stabilization $\uparrow_k^n S$ of a k -labeled ribbon surface S corresponds to an n -fold stabilization of the k -fold branched covering represented by S , as defined in Section 1.4 (see Figure 6.1.4 for $k = n - 1$).

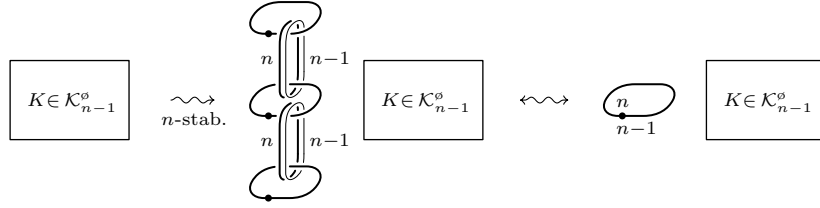


FIGURE 6.1.3. n -stabilization of an $(n - 1)$ -labeled Kirby diagram

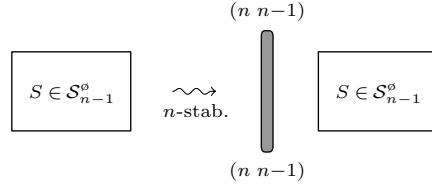


FIGURE 6.1.4. n -stabilization of an $(n - 1)$ -labeled ribbon surface

PROPOSITION 6.1.2. *Let W be a connected 4-dimensional 2-handlebody and K be any uni-labeled Kirby diagram of it. Then, the closure \widehat{S}_K of the ribbon tangle S_K defined in Section 3.4 is a 3-labeled ribbon surface such that the 4-dimensional 2-handlebody described by the 3-labeled Kirby diagram $\Theta_3(\widehat{S}_K)$ is 2-equivalent to W . In other words, \widehat{S}_K represents W up to 2-equivalence as a 3-fold branched covering of B^4 . The global structure of \widehat{S}_K is depicted in Figure 6.1.5 (see Section 3.4 for the definition of T_K).*

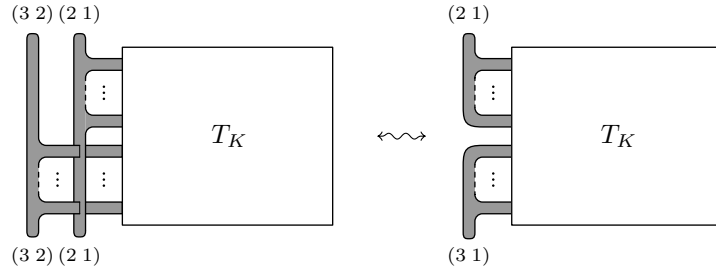


FIGURE 6.1.5. The global structure of the ribbon surface \widehat{S}_K

Proof. The same argument of the proof of Proposition 3.4.3 still works here, except for the absence of all the components relative to the ribbon surface tangles \overline{Q}_{m_0} and Q_{m_1} , which are empty in the present context, and for the use of handle cancelation in place of the reduction functor \downarrow_1^3 in the end. Namely, we start with the adapted 1-handlebody decomposition of \widehat{S}_K having the same handles as the one of S_K in the proof of Proposition 3.4.3, apart from the fact that the collars of the source and the target are now considered as 0-handles. Then, we consider the corresponding 3-labeled Kirby diagram $\Theta_3(\widehat{S}_K)$ and perform on it the slidings and the crossing changes described in the Figures 3.4.10, 3.4.11 and 3.4.12. After that, we can isotope the resulting diagram to the separate union of two chains of handles on the left, like those in the first diagram of Figure 6.1.3 for $n = 3$ and $n = 2$ respectively, and a copy of the original K labeled by 1. This is just a 3-stabilization of K , hence it can be reduced to K by canceling all the handles carrying the labels 3 and 2 in the order as shown in Figure 6.1.3. \square

Our first covering moves theorem concerns the 2-equivalence of 4-dimensional 2-handlebodies represented by labeled ribbon surfaces in B^4 , as described above in terms of the Θ_n 's. Its proof will make use of the next two lemmas.

LEMMA 6.1.3. *For any k -reducible Kirby tangle $K \in \mathcal{K}_{n \rightarrow k}$, the 4-dimensional 2-handlebodies represented by the Kirby diagrams $\downarrow_k^n \widehat{K}$ and \widehat{K} are 2-equivalent.*

Proof. The case of $k = n - 1$ is shown in Figure 6.1.6, while the general case follows by induction on the difference $n - k$. Starting from \widehat{K} with $K = (\text{id}_{(n,n-1)} \diamond L) \circ (\Delta_{(n,n-1)} \diamond \text{id}_{\pi_0}) \in \mathcal{K}_{n \rightarrow k}$, the first step in the figure is just a 1/2-handle cancelation, the second one is based on Lemma 2.3.6 like the first step in Figure 2.3.18, the third one consists in a 2-handle sliding. Finally, the last diagram is the closure of $\uparrow_{n-1}^n \downarrow_{n-1}^n K$, hence it can be reduced to the closure of $\downarrow_{n-1}^n K$ as said above (cf. Figure 6.1.3). \square

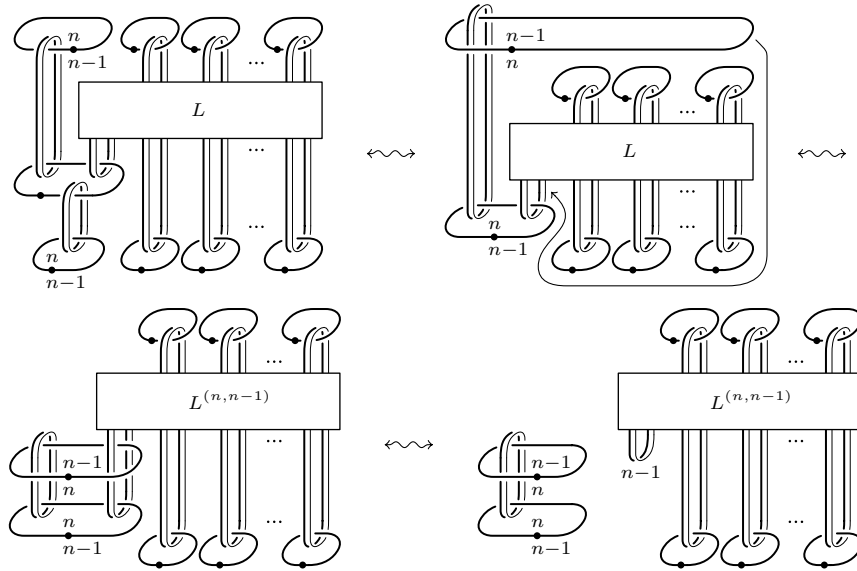


FIGURE 6.1.6. Proof of Lemma 6.1.3

LEMMA 6.1.4. *Up to labeled 1-isotopy, any n -labeled ribbon surface S representing a connected branched covering of B^4 is the closure \widehat{R} of a 1-reducible ribbon surface tangle $R = (\text{id}_{\sigma_{n-1}} \diamond T) \circ \Delta_{\sigma_{n-1}} : I_{\sigma_{n-1}} \rightarrow I_{\sigma_{n-1}}$ in \mathcal{S}_n^c (cf. Figure 6.1.7).*

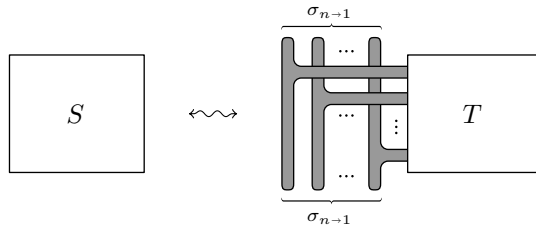


FIGURE 6.1.7. Connected coverings are given by 1-reducible ribbon surfaces

Proof. The connectedness of the covering implies that the transpositions which appear as labels of S generate a transitive subgroup of the symmetric group Σ_n .

This is trivially equivalent to say that they generate all Σ_n . Then, we can use the labeled 1-isotopy move (S24) in Figure 1.3.13 to expand from S a tongue which, after a suitable sequence of ribbon intersections, is labeled with any given transposition $\tau \in \Sigma_n$ on its tip. In particular, in this way we can expand from S the reduction bands making it the closure of a 1-reducible n -labeled ribbon surface tangle, as in Figure 6.1.7. \square

THEOREM 6.1.5. *Two connected simple coverings of B^4 branched over ribbon surfaces represent 2-equivalent 4-dimensional 2-handlebodies if and only if, after stabilization to the same degree ≥ 4 , their labeled branching surfaces can be related by labeled 1-isotopy, i.e. labeled 3-dimensional diagram isotopy and the labeled versions of the 1-isotopy moves in figure Figure 1.3.13 (cf. Proposition 1.3.9), and the ribbon moves (R1) and (R2) in Figure 1.4.5. For the reader convenience those moves are reproduced in Figures 6.1.8 and 6.1.9 below.*

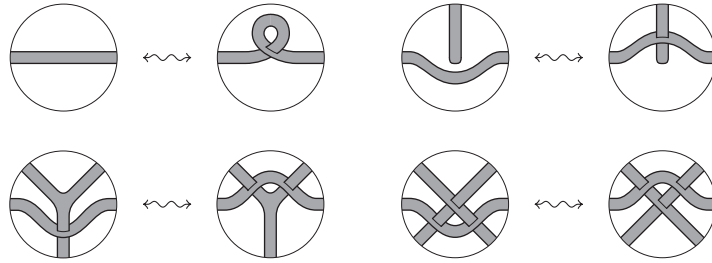


FIGURE 6.1.8. Labeled 1-isotopy moves (with any labeling)

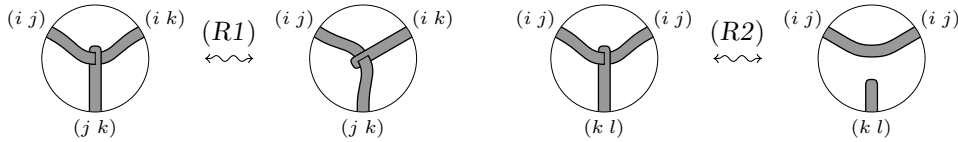


FIGURE 6.1.9. Ribbon moves (i, j, k and l all different)

Proof. Let $\mathcal{K}_n^{c,\emptyset}$ be the set of morphisms $K : I_{\pi_{n-1}} \rightarrow I_{\pi_{n-1}}$ in \mathcal{K}_n^c , and $\mathcal{S}_n^{c,\emptyset}$ be the set of morphisms $S : J_{\sigma_{n-1}} \rightarrow J_{\sigma_{n-1}}$ in \mathcal{S}_n^c . Moreover, consider the subsets $\widehat{\mathcal{K}}_n^{c,\emptyset} \subset \widehat{\mathcal{K}}_n^\emptyset$ and $\widehat{\mathcal{S}}_n^{c,\emptyset} \subset \widehat{\mathcal{S}}_n^\emptyset$ consisting of the closures of the morphisms in $\mathcal{K}_n^{c,\emptyset}$ and $\mathcal{S}_n^{c,\emptyset}$ respectively. Then, by the above discussion of the closure and Lemma 6.1.3, we have the following commutative diagram.

$$\begin{array}{ccccc}
 \mathcal{S}_n^{c,\emptyset} & \xrightarrow{\Theta_n} & \mathcal{K}_n^{c,\emptyset} & \xrightarrow{\downarrow_1^n} & \mathcal{K}_1^\emptyset \\
 \searrow \text{closure} & & \searrow \text{closure} & & \nearrow \text{2-equiv.} \\
 & & \widehat{\mathcal{S}}_n^{c,\emptyset} & \xrightarrow{\Theta_n} & \widehat{\mathcal{K}}_n^{c,\emptyset}
 \end{array}$$

We observe the 1-reduction $\downarrow_1^n K$ of a Kirby tangle $K \in \mathcal{K}_n^{c,\emptyset}$ is already a Kirby diagram, hence we have $\widehat{\downarrow_1^n K} = \downarrow_1^n K$. Then, the 2-equivalence arrow is given by Lemma 6.1.3 and it consists in the reduction to only one 0-handle as described in the proof of that lemma.

By Lemma 6.1.4, any n -labeled ribbon surface that represents a connected branched covering of B^4 can be seen as a representative of an element of $\widehat{\mathcal{S}}_n^{c,\emptyset}$. Then, according to the discussion at the beginning of the section, the branched covering representation of 4-dimensional 2-handlebodies in the statement coincides with the composition of $\Theta_n : \widehat{\mathcal{S}}_n^{c,\emptyset} \rightarrow \widehat{\mathcal{K}}_n^{c,\emptyset}$ and the 2-equivalence map $\widehat{\mathcal{K}}_n^{c,\emptyset} \rightarrow \mathcal{K}_1^\emptyset$.

Now, the “if” part of the statement just says that such composition is well-defined, which is known from Propositions 3.3.2 and 3.3.4 for any $n \geq 2$. While the “only if” part says that it is injective for $n \geq 4$. This immediately follows from the surjectivity of the closure map $\mathcal{S}_n^{c,\emptyset} \rightarrow \widehat{\mathcal{S}}_n^{c,\emptyset}$ and the bijectivity of $\downarrow_1^n \circ \Theta_n : \mathcal{S}_n^{c,\emptyset} \rightarrow \mathcal{K}_1^\emptyset$, guaranteed by Theorem 3.6.4 for any $n \geq 4$. \square

Before of going on, let us make a pair of remarks on the above results about the representation of 4-dimensional 2-handlebodies as branched coverings of B^4 .

REMARK 6.1.6. Both Proposition 6.1.2 and Theorem 6.1.5 concern connected handlebodies. However, their generalization to more connected components is straightforward, being different components independent from each other. Of course, to represent 4-dimensional 2-handlebodies with c connected components in general are needed coverings of degree $3c$. While coverings of degree $3c + 1$ are involved in relating two covering representations of 2-equivalent handlebodies (degree $4c$ is needed if the stabilizations are required to be performed once for all at the beginning). Moreover, in contrast with the connected case, also labeling conjugation has to be allowed, in order to get the same set of labels for the sheets of the two coverings contained in corresponding components.

REMARK 6.1.7. We recall that 1-isotopy of ribbon surfaces in B^4 was derived from embedded 1-deformation of embedded 2-dimensional 1-handlebodies in B^4 , by forgetting the handlebody structure. On the other hand, isotopy is related in a similar way to a suitable notion of embedded 2-deformation. In this perspective, isotopy differs from 1-isotopy just for allowing also addition/deletion of embedded canceling pairs of 1/2-handles and 2-handle isotopy (which may involve non-ribbon intersections in the diagram, such as double loops and triple points).

Analogously, diffeomorphic 4-dimensional 2-handlebodies are 3-equivalent (cf. Section 1.2). Hence, the notion of diffeomorphism between 4-dimensional 2-handlebodies differs from that of 2-equivalence for allowing also addition/deletion of canceling pairs of 2/3-handles and 3-handle isotopy.

Now, the connection between labeled 1-isotopy of ribbon surfaces in B^4 and 2-equivalence of 4-dimensional 2-handlebodies, established in the proofs of Lemma 3.3.1 and Proposition 3.3.2 (cf. also Lemma 3.5.3 for the opposite direction) through branched coverings and covering moves, can be at least partially extended. More precisely, attaching a labeled 2-handle to the branching surface $S \subset B^4$ of a simple branched covering $p : W \rightarrow B^4$ corresponds to attaching a 3-handle to the covering 4-dimensional handlebody W , in such a way that a canceling pair of labeled 1/2-handles in S corresponds to a canceling pair of 2/3-handles in W .

This suggests a possible approach towards the study of the difference between 2-deformation and diffeomorphism of 4-dimensional 2-handlebodies, by relating it to the difference between 1-isotopy and isotopy of ribbon surfaces. Good test examples could be the Akbulut-Kirby 4-balls Δ_n (see figure 6.1.10 for the case of $n = 3$),

which were proved to be diffeomorphic to B^4 in [21], but are not known to be 2-equivalent to B^4 . In fact, the proof of the diffeomorphism $\Delta_n \cong B^4$ is based on the cleaver addition of a canceling pair of 2/3-handles, followed by an isotopy of the attaching map of the 3-handle and eventually by the cancellation of it against another 2-handle. It would be interesting to see whether this process corresponds to changing the branching ribbon surface by labeled isotopy.

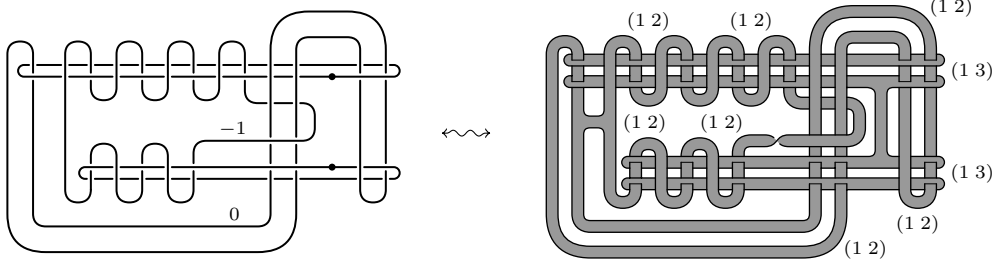


FIGURE 6.1.10. The Akbulut-Kirby 4-ball Δ_3

We conclude the section with the following theorem concerning 4-dimensional 2-handlebodies having diffeomorphic boundaries. This will be applied in the next section to obtain covering moves theorems for 3-manifolds.

THEOREM 6.1.8. *Two connected simple coverings of B^4 branched over ribbon surfaces represent 4-dimensional 2-handlebodies with diffeomorphic oriented boundaries if and only if, after stabilization to the same degree ≥ 4 , their labeled branching surfaces can be related by labeled 1-isotopy, the ribbon moves (R1) and (R2), and the moves (P) and (T) in Figure 6.1.11 (cf. Figure 5.2.3).*

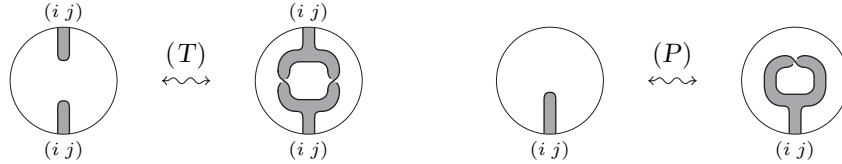


FIGURE 6.1.11. Ribbon moves (i, j, k and l all different)

Proof. In the light of Propositions 5.2.3 and 5.3.1, the commutative diagram in the proof of Theorem 6.1.5 induces the following one under the quotient functors $\mathcal{S}_n \rightarrow \overline{\overline{\mathcal{S}}}_n$ and $\mathcal{K}_n \rightarrow \overline{\overline{\mathcal{K}}}_n$. Here, the double bar denotes the image in the quotient of the corresponding set in the original diagram.

$$\begin{array}{ccccc}
 \overline{\overline{\mathcal{S}}}_n^{c,\emptyset} & \xrightarrow{\overline{\overline{\Theta}}_n} & \overline{\overline{\mathcal{K}}}_n^{c,\emptyset} & \xrightarrow{\downarrow^n} & \overline{\overline{\mathcal{K}}}_1^\emptyset \\
 \searrow \text{closure} & & \searrow \text{closure} & & \nearrow \text{2-equiv.} \\
 & & \widehat{\widehat{\mathcal{S}}}_n^{c,\emptyset} & \xrightarrow{\overline{\overline{\Theta}}_n} & \widehat{\widehat{\mathcal{K}}}_n^{c,\emptyset}
 \end{array}$$

Up to planar isotopy the moves (T) and (P) in Figure 6.1.11 are the same as the homonymous additional relations defining the quotient category $\overline{\overline{\mathcal{S}}}_n$. On the

other hand, we know that two uni-labeled Kirby diagrams represent 4-dimensional 2-handlebodies with diffeomorphic boundaries if and only if they are equivalent in $\overline{\overline{\mathcal{K}}}_1^\emptyset$ (this is just the classical Kirby's theorem).

Then, the theorem can be rephrased by saying that the composition of $\overline{\overline{\mathcal{O}}}_n : \overline{\overline{\mathcal{S}}}_n^{c,\emptyset} \rightarrow \overline{\overline{\mathcal{K}}}_n^{c,\emptyset}$ with the 2-equivalence arrow is a well-defined injective map. This can be proved by arguing on the commutative diagram as in the proof of Theorem 6.1.5, thanks to Proposition 5.3.1 and Theorem 5.3.3. \square

6.2. Equivalence of branched covers of S^3

Our last goal is to derive from Theorem 6.1.8 the announced general solution of the covering moves problem for branched coverings of S^3 .

As a preliminary step, we show that any simply labeled link in S^3 can be transformed through the Montesinos moves in Figure 1.4.4 into the boundary of a labeled ribbon surface in B^4 (see Proposition 6.2.2). This follows quite directly from Theorem B of [58] about liftable braids, which we state here as Lemma 6.2.1 after having recalled a couple of definitions.

A simply labeled braid is called a *liftable braid* when the two labelings at its ends coincide. By an *interval* we mean any braid that is conjugate to a standard generator in the braid group. Actually, to make both the terms “liftable” and “interval” meaningful, one should think of braids as self-homeomorphisms of the disk in the usual way (see [9] or [58]), but this is not relevant in the present context.

Of course, a labeled interval, as well as a standard generator, may or may not be liftable depending on the labeling. We say that a labeled interval x is of *type i* if x^i is the first positive power of x which is liftable. It is not difficult to realize that conjugation preserves interval types and that each interval is of type 1, 2 or 3 (cf. Lemma 2.4 of [9] or Lemma 2.3 of [58]).

The labeled intervals x , y and z , whose first liftable positive powers are depicted in Figure 6.2.1, are the standard models for the three types above. Namely, any labeled interval of type 1, 2 or 3 is respectively a conjugate of $x^{\pm 1}$, $y^{\pm 1}$ or $z^{\pm 1}$. Evidently, in the figure only the two non-trivial strings of each labeled braid are drawn, the other ones being just horizontal arcs with arbitrary labels. Moreover, in the labeling of each single braid, we assume that i , j , k and l are all different.

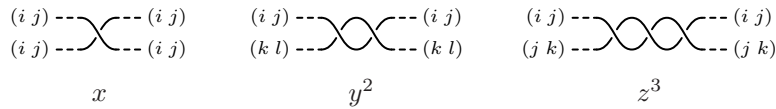


FIGURE 6.2.1.

The main result of [58] is the following.

LEMMA 6.2.1. *Any liftable braid is a product liftable powers of intervals.*

We emphasize that the lemma holds without restrictions on the degree n of the labeling. However, it is worth observing that the case of $n = 2$ is trivial (every braid is liftable in this case), while the case of $n = 3$ differs from the general one for the absence of intervals of type 2. This special case was previously proved in [9] (cf. also [10]), but the proof of Lemma 6.2.1 given in [58] does not depend on [9].

The relevant consequence of Lemma 6.2.1 in the present context is the following branched covering counterpart of the vanishing of the oriented cobordism group Ω_3 .

PROPOSITION 6.2.2. *Any labeled link $L \subset S^3$ representing a (possibly disconnected) n -fold simple branched covering of S^3 is equivalent, up to labeled isotopy and moves (M1) and (M2) in Figure 1.4.4, to the boundary of labeled ribbon surface $S \subset B^4$ representing an n -fold simple branched covering of B^4 .*

Proof. Up to labeled isotopy, we can assume that the link L is the closure \widehat{B} of simply labeled braid B (for example, we can use the labeled version of the well-known Alexander’s braiding procedure). Of course B is a liftable braid. Then, Lemma 6.2.1 tells us that, up to labeled isotopy, we can think of B a product of conjugates of braids like $x^{\pm 1}$, $y^{\pm 2}$ or $z^{\pm 3}$ (see Figure 6.2.1). Since braids $y^{\pm 2}$ and $z^{\pm 3}$ can be obviously trivialized respectively by moves (M2) and (M1), we can reduce ourselves to the case when B is a product of liftable intervals.

In this case, a simply labeled ribbon surface $S \subset B^4$ bounded by L can be easily constructed from the band presentation of B (see [67, 68]) determined by its factorization into liftable intervals. Namely, we start with a disjoint union of labeled trivial disks in B^4 , spanned by the labeled trivial braid obtained from B by trivializing all the terms $x^{\pm 1}$ appearing in the factorization. Then, we attach to these disks a labeled half-twisted band for each such term. The 3-dimensional diagram of S may or may not form ribbon intersection, depending on the conjugating braids of the liftable intervals in the factorization of B (cf. [67, 68]). The labeling consistency when attaching the bands is always ensured by the liftability of the intervals. \square

Now we can prove our equivalence theorem for simply labeled links in S^3 .

THEOREM 6.2.3. *Two connected simple coverings of S^3 branched over links represent diffeomorphic oriented 3-manifolds if and only if, after stabilization to the same degree ≥ 4 , their labeled branching links can be related by labeled isotopy and the Montesinos moves (M1) and (M2) in Figure 6.2.2 (cf. Figure 1.4.4).*

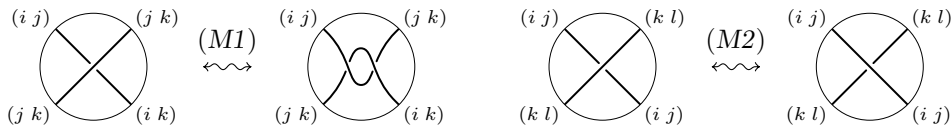


FIGURE 6.2.2. Montesinos moves (i, j, k and l all different)

Proof. As mentioned in Section 1.4, it has been known for a long time, since the early work of Montesinos, that moves (M1) and (M2) are covering moves. That is they, as well as labeled isotopy and stabilization, do not change the covering manifold up to diffeomorphism (see Figure 1.4.6 for a proof of this fact). Therefore, nothing more has to be added about the “if” part of the theorem.

The “only if” part follows from Proposition 6.2.2 and Theorem 6.1.8, taking into account that moves (T) and (P) preserve the boundary up to labeled isotopy, while the restriction of moves (R1) and (R2) to the boundary can be realized by moves (M1) and (M2) respectively. The last fact is trivial for move (R2) and it is shown in Figure 6.2.3 for move (R1). \square

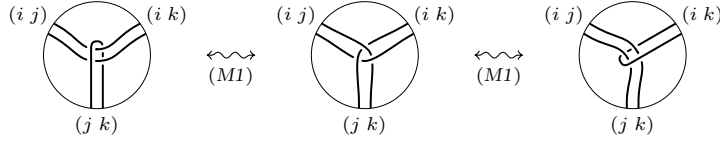


FIGURE 6.2.3.

Finally, we want to extend Theorem 6.2.3 to arbitrary connected branched coverings of S^3 , by adding the extra moves (G1) and (G2) in Figure 6.2.4 (cf. Figure 1.4.3), where the local orientations of the branching set is only needed to specify the monodromy. The further extension to disconnected branched coverings is left to the reader (cf. Remark 6.1.6).

THEOREM 6.2.4. *Two connected coverings of S^3 branched over a graph represent diffeomorphic oriented 3-manifolds if and only if, after stabilization to the same degree ≥ 4 , their branching graphs can be related by labeled isotopy and the moves (M1), (M2), (G1) and (G2) in Figures 6.2.2 and 6.2.4.*

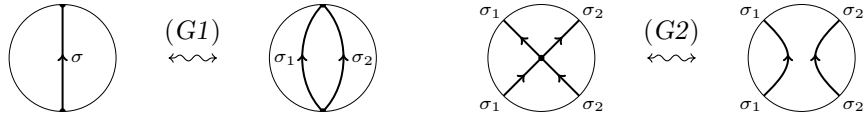


FIGURE 6.2.4. Covering moves for labeled graphs ($\sigma = \sigma_1 \cdot \sigma_2$)

Proof. We have already observed in Section 1.4 that moves (G1) and (G2) are covering moves, as they are applications of the coherent monodromies merging principle. In the light of Theorem 6.2.3, we have only to show that they allow us to transform any labeled graph into a simply labeled link. We proceed in two steps: first we make the labeling simple, by performing moves (G1) on the edges; then we make the graph into a link, by performing moves (G2) on the vertices.

Let $G \subset R^3$ be a labeled embedded graph, endowed with a given graph structure without loops (that is every edge has distinct endpoints). We make the labeling simple, by operating on the edges of G one by one. Each time, we assume, up to labeled isotopy, that the edge e under consideration is not involved in any crossing. Denoting by $\sigma \in \Sigma_n$ the label of e , we consider a coherent factorizations $\sigma = \tau_1 \dots \tau_k$ into transpositions (any minimal factorization of σ is coherent). Then, we split e into k edges e_1, \dots, e_k with the same endpoints, such that e_i is labeled by τ_i , for each $i = 1, \dots, k$. To do that, we perform $k - 1$ moves (G1), which progressively isolate the transpositions τ_i as labels of new edges. Once all edges of G have been managed in this way, we are left with a simply labeled graph that we still denote by G .

Now, we operate on the vertices of G one by one, in order to make G into a link. Let v be a vertex of G and e_1, \dots, e_h be the edges of G having v as an endpoint, numbered according to the counterclockwise order in which they appear around v in the planar diagram of G . Since the total monodromy $\tau_1 \dots \tau_h$ around v must be trivial, h must be even and the edges around v , can be reordered, up to labeled isotopy, in such a way that $\tau_i = \tau_{h-i+1}$, for every $i = 1, \dots, h/2$. This immediately follows from the well-known classification of the branched coverings of S^2 , if one looks at a small 2-sphere around v transversal to G (cf. [8] or [58]). Then, by $h/2 - 1$ applications

of move (G2), we replace the vertex v by $h/2$ non-singular vertices $v_1, \dots, v_{h/2}$, such that v_i is a common endpoint of e_i and e_{h-i+1} , for each $i = 1, \dots, h/2$. We leave to the reader to verify that the sequence $\tau_1, \dots, \tau_{h/2}$ is coherent and that this suffices for the needed moves (G2) to be performable. Obviously, after all the singular vertices of G have been replaced by non-singular ones, we are done. \square

References

- [1] S. Akbulut, *An exotic 4-manifold*, J. Diff. Geom. **33** (1991), 357–361.
- [2] S. Akbulut and R. Kirby, *Branched covers of surfaces in 4-manifolds*, Math. Ann. **252** (1980), 111–131.
- [3] J.W. Alexander, *Note on Riemann spaces*, Bull. Amer. Math. Soc. **26** (1920), 370–373.
- [4] N. Apostolakis, *On 4-fold covering moves*, Algebraic & Geometric Topology **3** (2003), 117–145.
- [5] N. Apostolakis, R. Piergallini and D. Zuddas, *Lefschetz fibration over the disk*, preprint arXiv:1104.4536 (2011).
- [6] S. Atiyah, *On framings of 3-manifolds*, Topology **29** (1990), 1–7.
- [7] I. Bernstein and A.L. Edmonds, *The degree and branch set of a branched covering*, Invent. math. **45** (1978), 213–220.
- [8] I. Bernstein and A.L. Edmonds, *On the construction of branched coverings of low-dimensional manifolds*, Trans. Amer. Math. Soc. **247** (1979), 87–124.
- [9] J.S. Birman and B. Wajnryb, *3-fold branched coverings and the mappings class group of a surface*, in “Geometry and Topology”, Lecture Notes in Math. **1167**, Springer-Verlag 1985, 24–46.
- [10] J. S. Birman and B. Wajnryb, *Presentations of the mapping class group. Errata: “3-fold branched coverings and the mapping class group of a surface” and “A simple presentation of the mapping class group of an orientable surface”*, Israel J. Math. **88** (1994), 425–427.
- [11] I. Bobtcheva and M.G. Messia, *HKR-type invariants of 4-thickenings of 2-dimensional CW-complexes*, Algebraic and Geometric Topology **3** (2003), 33–87.
- [12] I. Bobtcheva and R. Piergallini, *Covering Moves and Kirby Calculus*, preprint arXiv:math.GT/0407032 (2004).
- [13] I. Bobtcheva and R. Piergallini, *A universal invariant of four-dimensional 2-handlebodies and three-manifolds*, preprint arXiv:math.GT/0612806 (2006).
- [14] I. Bobtcheva and F. Quinn, *The reduction of quantum invariants of 4-thickenings*, Fundamenta Mathematicae **188** (2005), 21–43.
- [15] Y. Bespalov, T. Kerler, V. Lyubashenko and V. Turaev, *Integrals for braided Hopf algebras*, J. Pure Appl. Algebra **148** (2000), 113–164.
- [16] J. Cerf, *La stratification naturelle des espaces fonction différentiables réelles et la théorème de la pseudo-isotopie*, Publ. Math. I.H.E.S. **39** (1970).
- [17] D. Denicola, M. Marcolli and A.Z. al-Yasry, *Spin foams and noncommutative geometry*, Class. Quantum Grav. **27** (2010), 205025.
- [18] R. Fenn and C. Rourke, *On Kirby’s calculus of links*, Topology **18** (1979), 1–15.
- [19] R.H. Fox, *Covering spaces with singularities*, in “Algebraic Geometry and Topology, A symposium in honour of S. Lefschetz”, Princeton University Press 1957, 243–257.

- [20] C.A. Giller, *Towards a classical knot theory for surfaces in R^4* , Illinois J. Math. **26** (1982), 591–631.
- [21] R.E. Gompf, *Killing the Akbulut-Kirby 4-sphere, with relevance to the Andrews-Curtis and Schoenflies problems*, Topology **30** (1991), 97–115.
- [22] R.E. Gompf and A.I. Stipsicz, *4-manifolds and Kirby calculus*, Grad. Studies in Math. **20**, Amer. Math. Soc. 1999.
- [23] M. Iori and R. Piergallini, *4-manifolds as covers of S^4 branched over non-singular surfaces*, Geometry & Topology **6** (2002), 393–401.
- [24] K. Habiro, *Claspers and finite type invariants of links*, Geometry & Topology, **4** (2000), 1–83.
- [25] F. Harou, *Description chirurgicale des revêtements triples simples de S^3 ramifiés le long d’un entrelacs*, Ann. Inst. Fourier **51** (2001), 1229–1242.
- [26] F. Harou, *Description en terme de revêtements simples de revêtements ramifiés de la sphère*, preprint 2002.
- [27] E. Hatakenaka, *Invariants of 3-manifolds derived from covering presentations*, Math. Proc. Camb. Philos. Soc. **149** (2010), 263–295.
- [28] M. Hennings, *Invariants from links and 3-manifolds obtained from Hopf algebras*, J. London Math. Soc. (2) **54** (1996), 594–624.
- [29] H.M. Hilden, *Every closed orientable 3-manifold is a 3-fold branched covering space of S^3* , Bull. Amer. Math. Soc. **80** (1974), 1243–1244.
- [30] H.M. Hilden, *Three-fold branched coverings of S^3* , Bull. Amer. J. Math. **98** (1976), 989–997.
- [31] U. Hirsch, *Über offene Abbildungen auf die 3-Sphäre*, Math. Z. **140** (1974), 203–230.
- [32] T. Kerler, *Genealogy of nonperturbative quantum invariants of 3-manifolds – The surgical family*, in “Geometry and Physics”, Lecture Notes in Pure and Applied Physics **184**, Marchel Dekker 1997, 503–547.
- [33] T. Kerler, *Equivalence of bridged links calculus and Kirby’s calculus on links on nonsimply connected 3-manifolds*, Topology and its Appl. **87**, (1998), 155–162.
- [34] T. Kerler, *Bridged links and tangle presentations of cobordism categories*, Adv. Math **141** (1999), 207–281.
- [35] T. Kerler, *Towards an algebraic characterization of 3-dimensional cobordisms*, Contemporary Mathematics **318** (2003), 141–173.
- [36] T. Kerler and V.V. Lyubashenko, *Non-semisimple topological quantum field theories for 3-manifolds with corners*, Lecture Notes in Mathematics **1765**, Springer-Verlag 2001.
- [37] R. Kirby, *A calculus for framed links in S^3* , Invent. math. **45** (1978), 36–56.
- [38] R. Kirby, *The topology of 4-manifolds*, Lecture Notes in Mathematics **1374**, Springer-Verlag 1989.

- [39] G. Kuperberg, *Non-involutive Hopf algebras and 3-manifold invariants*, Duke Math. J. **84** (1996), 83–129.
- [40] F. Laudenbach and V. Poenaru, *A note on 4-dimensional handlebodies*, Bull. Soc. Math. France **100** (1972), 337–344.
- [41] W.R.B. Lickorish, *A representation of orientable, combinatorial 3-manifolds*, Ann. Math. **76** (1962), 531–540.
- [42] A. Loi and R. Piergallini, *Compact Stein surfaces with boundary as branched covers of S^4* , Invent. math. **143** (2001), 325–348.
- [43] G. Lusztig, *Introduction to quantum groups*, Progress in Mathematics **110**, Birkhäuser 1993.
- [44] V.V. Lyubashenko, *Modular transformations for tensor categories*, J. Pure Appl. Algebra **98**,(1998), 279–327.
- [45] S. MacLane, *Natural associativities and commutativities*, Rice Univ. Studies **49** (1963), 28–46.
- [46] S. MacLane, *Categories for the working Mathematicians*, Graduate Texts in Mathematics **5**, Springer-Verlag 1971.
- [47] S. Matveev, *Algorithmic topology and classification of 3-manifolds*, Algorithms and Computation in Mathematics **9**, Springer 2003.
- [48] S. Matveev and M. Polyak, *A geometrical presentation of the surface mapping class group and surgery*, Comm. Math. Phys. **160** (1994), 537–550.
- [49] J.M. Montesinos, *A representation of closed, orientable 3-manifolds as 3-fold branched coverings of S^3* , Bull. Amer. Math. Soc. **80** (1974), 845–846.
- [50] J.M. Montesinos, *Sobre la representacion de variedades tridimensionales*, unpublished preprint (1975).
- [51] J.M. Montesinos, *Three-manifolds as 3-fold branched covers of S^3* , Quart. J. Math. Oxford (2) **27** (1976), 85–94.
- [52] J.M. Montesinos, *4-manifolds, 3-fold covering spaces and ribbons*, Trans. Amer. Math. Soc. **245** (1978), 453–467.
- [53] J.M. Montesinos, *Heegaard diagrams for closed 4-manifolds*, in “Geometric Topology”, J.C. Cantrell ed., Academic Press 1979, 219–237.
- [54] J.M. Montesinos, *A note on 3-fold branched coverings of S^3* , Math. Proc. Camb. Phil. Soc. **88** (1980), 321–325.
- [55] J.M. Montesinos, *Representing 3-manifolds by a universal branching set*, Proc. Camb. Phil. Soc. **94** (1983), 109–123.
- [56] J.M. Montesinos, *A note on moves and irregular coverings of S^4* , Contemp. Math. **44** (1985), 345–349.
- [57] S. Montgomery, *Hopf algebras and their action on rings*, CBMS Regional Conference Series in Mathematics **82**, Amer. Math. Soc. 1993.
- [58] M. Mulazzani and R. Piergallini, *Lifting braids*, Rend. Ist. Mat. Univ. Trieste **XXXII** (2001), Suppl. 1, 193–219.

- [59] T. Nosaka, *4-fold symmetric quandle invariants of 3-manifolds*, Algebraic & Geometric Topology **11** (2011), 1601–1648.
- [60] T. Ohtsuki, *Problems on invariants of knots and 3-manifolds*, Geom. Topol. Monogr. **4**, in “Invariants of knots and 3-manifolds (Kyoto, 2001)”, Geom. Topol. Publ. 2002, 377–572.
- [61] R. Piergallini, *Covering Moves*, Trans Amer. Math. Soc. **325** (1991), 903–920.
- [62] R. Piergallini, *Four-manifolds as 4-fold branched covers of S^4* , Topology **34** (1995), 497–508.
- [63] R. Piergallini and D. Zuddas, *A universal ribbon surface in B^4* , Proc. London Math. Soc. **90** (2005), 763–782.
- [64] F. Quinn, *Lectures on Axiomatic Topological Quantum Field Theory*, IAS/Park City Mathematical Series **1**, Amer. Math. Soc. 1995.
- [65] N.Yu. Reshetikhin and V.G. Turaev, *Invariants of 3-manifolds via link polynomials and quantum groups*, Invent. Math. **103** (1991), 547–597.
- [66] V.A. Rohlin, *A three dimensional manifold is the boundary of a four dimensional one*, Dokl. Akad. Nauk. SSSR **114** (1951), 355–357.
- [67] L. Rudolph, *Braided surfaces and Seifert ribbons for closed braids*, Comment. Math. Helvetici **58** (1983), 1–37.
- [68] L. Rudolph, *Special position for surfaces bounded by closed braids*, Rev. Mat. Ibero-Americana **1** (1985), 93–133; revised version: preprint 2000.
- [69] M. Scharlemann and A. Thompson, *Link genus and Conway moves*, Comment. Math. Helvetici **64** (1989), 527–535.
- [70] M.C. Shum, *Tortile tensor categories*, Journal of Pure and Applied Algebra **93** (1994), 57–110.
- [71] T. Standford, *Finite type invariants of knots, links and graphs*, Topology **35** (1996), 1027–1050.
- [72] V. Turaev, *Homotopy field theory in dimension 3 and crossed group-categories*, eprint arXiv:math/0005291 (2000).
- [73] A. Virelizier, *Algèbres de Hopf graduées et fibrés plats sur les 3-variétés*, PhD thesis, Institut de recherche mathématique avancée, Université Louis Pasteur et CNRS 2001.
- [74] K. Walker, *On Witten’s 3-manifold invariants*, preprint 1991.
- [75] A.H. Wallace, *Modifications and cobounding manifolds*, Canad. J. Math. **12** (1960), 503–528.